

Profiling the Abiotic Stress Responsive MicroRNA Landscape in *Arabidopsis thaliana*

Supervisors

**Dr. Christopher Lambrides, Professor Robert Furbank,
Professor Christopher Grof and Dr. Andrew Eamens**

Joseph Leigh Pegler
B.Biotech (Hons)

*This research was supported by an Australian Government Research Training Program
(RTP) Scholarship.*

A thesis submitted in fulfilment of the requirements for the
degree of Doctor of Philosophy in Biological Science
School of Environmental and Life Sciences
The University of Newcastle
New South Wales, Australia
July, 2020

DECLARATION

STATEMENT OF ORIGINALITY

I hereby certify that the work embodied in the thesis is my own work, conducted under normal supervision. The thesis contains no material which has been accepted, or is being examined, for the award of any other degree or diploma in any university or other tertiary institution and, to the best of my knowledge and belief, contains no material previously published or written by another person, except where due reference has been made. I give consent to the final version of my thesis being made available worldwide when deposited in the University's Digital Repository, subject to the provisions of the Copyright Act 1968 and any approved embargo.

.....

Joseph L. Pegler

ACKNOWLEDGMENT OF AUTHORSHIP

I hereby certify that the work embodied in this thesis contains published work of which I am a joint author. I have included as part of the thesis a written declaration endorsed in writing by my supervisor, attesting to my contribution to the joint publications.

By signing below I confirm that Joseph Pegler contributed greater than 95% of data collection and analyses required for the manuscript preparations of each of the publications included in this thesis. The authorship and final approval of each manuscript was jointly undertaken by each co-author listed for each respective publication.

.....

Dr. Andrew L. Eamens

Dedicated to my Mother and Father,
Debbie and David

ACKNOWLEDGEMENTS

First and foremost, I would like to thank my supervisors Andy and Chris. My journey from the completion of honours to the submission of this thesis would simply not have been achievable nor would it have been enjoyable if it were not for both of you. The unwavering guidance, support and friendship throughout my candidature is something I will forever be grateful for. I would also like to thank my external supervisors Bob and Chris (L) who were instrumental in guiding the development of my original PhD project in *Setaria*, a project that unfortunately could not be completed due the demolition of the entire UON glasshouse facility (R.I.P). Throughout my candidature I have been very fortunate to have many people who have provided extremely constructive feedback, guidance and provide me additional opportunities and for that I am thankful to: Dr Quan Nguyen, Emeritus Professor John Patrick, Conjoint Professor Christina Offler, Associate Professor David McCurdy, Associate Professor David Collings, Professor Brett Neilan, Dr Geoffrey De Iuliis and Chris Brown. I have been lucky enough and extremely grateful to have made many great friendships that I will cherish for many years to come. To Jackson Oultram, Tayla Corocher, Sadia Ahammed, and Simon Wheeler if it were not for your friendship and support throughout what has been a very challenging endeavour, I simply would have not made it this far. Mum, Dad, Shannon, Dylan and Pop, the endless encouragement and love you have always shown me has made monumental tasks like this one, seem very achievable. Without your love and support any success I have had or will have in my life would not have been possible. Last but not least, Zoe, for the best part of four years you have been on the frontlines of tolerating me when I return home from the long grind in the lab or the office. Your love, kindness and patience has been unwavering. I can only imagine the difficulties of standing by a PhD student but as promised the end has arrived and importantly the next step.

TABLE OF CONTENTS

DECLARATION.....	i
ACKNOWLEDGEMENT OF AUTHORSHIP	ii
ACKNOWLEDGEMENTS.....	iv
TABLE OF CONTENTS	v
FIGURES AND TABLES	xii
PUBLICATIONS FROM THESIS RESEARCH	xvi
ABSTRACT	xvii
UNITS OF MEASUREMENT	xviii
ABBREVIATIONS	xix

CHAPTER I: Introduction	1
1.1 The Plant MicroRNA Pathway: The Production and Action Stages	2
1.2 The <i>Arabidopsis</i> DOUBLE-STRANDED RNA BINDING (DRB) Protein Family	2
1.3 The Impact of Heat, Drought and Salt Stress on American and Australian Agriculture.....	4
1.3.1 Heat Stress	4
1.3.2 Drought and Salt Stress	5
1.4 The Role of Plant microRNAs in Mitigating the Impact of Heat, Drought and Salt Stress on Global Agriculture.	5
1.5 Aims.....	6

CHAPTER II: Phenotypic and Molecular Analysis of Abiotically Stressed <i>Arabidopsis</i> Plant Lines.....	9
2.1 Chapter Overview/ Rationale	10
2.2 Introduction.....	12
2.3 Material and Methods	14
2.3.1 Plant Growth Conditions.....	14
2.3.1.1 <i>Arabidopsis thaliana</i> Plant Lines.....	14
2.3.1.2 Heat, Mannitol and Salt Stress Treatment of <i>Arabidopsis</i> Plant Lines	14
2.3.2 Phenotypic Analysis of Col-0, <i>drb1</i> , <i>drb2</i> and <i>drb4</i> Plant Lines.....	15
2.3.2.1 Plant Fresh Weight Assessment.....	15
2.3.2.2 Rosette Area Determination	15

2.3.2.3	Assessment of Primary Root Length	15
2.3.2.4	Anthocyanin Content Determination	16
2.3.2.5	Determination of Chlorophyll <i>a</i> and <i>b</i> Content	16
2.3.3	<i>Assessment of MicroRNA and Gene Transcript Abundance in Abiotically Stressed Arabidopsis thaliana</i>	17
2.4	Results.....	18
2.4.1	The Phenotypic Response of Wild-Type <i>Arabidopsis</i> Plants and the <i>drb</i> Knockout Mutant Lines to Heat, Mannitol and Salt Stress	18
2.4.1.1	Fresh Weight.....	20
2.4.1.2	Rosette Area	22
2.4.1.3	Primary Root Length	24
2.4.1.4	Anthocyanin Accumulation	26
2.4.1.5	Chlorophyll <i>a</i> and <i>b</i> Content.....	28
2.4.2	The Molecular Response of Wild-Type <i>Arabidopsis</i> Plants and the <i>drb</i> Knockout Mutant Lines to Heat, Mannitol and Salt Stress	30
2.4.2.1	Quantification of the Expression of $\Delta 1$ -PYRROLINE-5-CARBOXYLATE SYNTHETASE1 (<i>P5CS1</i>).....	30
2.4.2.2	The Use of High Throughput Sequencing to Determine the Contribution of <i>DRB1</i> , <i>DRB2</i> and <i>DRB4</i> to the MicroRNA Landscape of <i>Arabidopsis thaliana</i>	32
2.4.2.3	The Use of High Throughput Sequencing to Profile the MicroRNA Landscape of Heat, Mannitol and Salt Stressed Col-0, <i>drb1</i> , <i>drb2</i> and <i>drb4</i> Plants	34
2.4.2.4	RT-qPCR analysis of <i>DCL1</i> , <i>DRB1</i> , <i>DRB2</i> and <i>DRB4</i> expression in Heat, Mannitol and Salt Stressed Col-0, <i>drb1</i> , <i>drb2</i> and <i>drb4</i> Plants	36
2.4.2.5	Experimental Validation of Altered MicroRNA Abundance in Control and Abiotically Stressed Wild-Type <i>Arabidopsis</i> Whole Seedlings	40
2.4.2.6	Molecular Profiling of the miR396 Regulatory Module in Heat, Mannitol and Salt Stressed Col-0, <i>drb1</i> , <i>drb2</i> and <i>drb4</i> Whole Seedlings	41
2.4.2.7	Molecular Profiling of the miR399 Regulatory Module in Heat, Mannitol and Salt Stressed Col-0, <i>drb1</i> , <i>drb2</i> and <i>drb4</i> Whole Seedlings	44

2.4.2.8	Molecular Profiling of the miR408 Regulatory Module in Heat, Mannitol and Salt Stressed Col-0, <i>drb1</i> , <i>drb2</i> and <i>drb4</i> Whole Seedlings	47
2.5	Discussion	51
2.5.1	The Phenotypic and Physiological Consequences of a Heat Stress Growth Regime	53
2.5.2	Mannitol and Salt Stress Growth Conditions Elicit Similar Phenotypic and Physiological Consequences.....	55
2.5.3	Anthocyanin Production is Defective in <i>drb1</i> Seedlings	57
2.5.4	Molecular Confirmation of Abiotic Stress	58
2.5.5	DRB1, DRB2 and DRB4 are Required for MicroRNA Production	59
2.5.6	Small RNA Sequencing Identified MicroRNAs Central to the Adaptive Response of <i>Arabidopsis</i> to Heat, Mannitol and Salt Stress	61
2.5.7	The Nuclear-Localised <i>DRB</i> Hierarchy and <i>DCL1</i> Expression Profile in Response to Heat, Mannitol and Salt Stress	63
2.5.8	The miR396 Regulatory Module in Response to Heat, Mannitol and Salt Stress	65
2.5.9	The miR399 Regulatory Module in Response to Heat, Mannitol and Salt Stress	68
2.5.10	The miR408 Regulatory Module in Response to Heat, Mannitol and Salt Stress	70
CHAPTER III: The Phenotypic and Molecular Consequence of Manipulating the miR396 Regulatory Module in <i>Arabidopsis</i>		73
3.1	Chapter Overview/ Rationale	74
3.2	Introduction.....	76
3.2.1	Improved Phosphate Use Efficiency Equates to Improved Crop Production.....	76
3.2.2	The MicroRNA396 Regulatory Module	77
3.3	Material and Methods.....	81
3.3.1	Preparation and storage of bacterial competent cells	81
3.3.1.1	<i>Escherichia coli</i> (<i>DH5α</i>).....	81
3.3.1.2	<i>Agrobacterium tumefaciens</i> (<i>AGL1</i>)	81
3.3.2	Cloning.....	81
3.3.2.1	Transgene Sequence Amplification or Synthesis.....	81
3.3.2.2	A-tailing of Transgene Insertion Fragments	82

3.3.2.3	Bacterial Plasmid DNA Purification.....	82
3.3.2.4	Restriction Digest and Fragment Purification.....	82
3.3.2.5	DNA Ligation	82
3.3.2.6	Heat Shock Transformation of <i>DH5α</i> Competent Cells and the Identification of Insert Positive Bacterial Clones via PCR.....	83
3.3.2.7	DNA Sequencing for Insert Confirmation	83
3.3.2.8	Electroporation.....	83
3.3.2.9	Floral Dip Transformation and Screening for Putative Transformant Lines.	84
3.3.3	Plant Growth Conditions.....	85
3.3.4	Phenotypic Analyses of Transformed Col-0 Seedlings	85
3.3.5	Molecular Analyses of Transformed Col-0 Seedlings	86
3.4	Results.....	87
3.4.1	The Requirement of <i>DRB1</i> , <i>DRB2</i> and <i>DRB4</i> in Appropriate Regulation of the Phosphate Responsive, miR396/ <i>GRF7</i> Regulatory Module in <i>Arabidopsis</i>	87
3.4.2	The Phenotypic Response of <i>Arabidopsis</i> miR396 Molecularly Modified Plant Lines to Phosphate Deficiency and Salt Stress	89
3.4.2.1	Fresh Weight.....	91
3.4.2.2	Rosette Area	93
3.4.2.3	Primary Root Length	95
3.4.2.4	Anthocyanin Accumulation	97
3.4.2.5	Chlorophyll <i>a</i> and <i>b</i> Content.....	99
3.4.3	The Molecular Response of <i>Arabidopsis</i> Plant Lines With Molecularly Altered miR396 Abundance to Phosphate Deficiency and Salt Stress	102
3.5	Discussion	106
3.5.1	The Impact of Phosphate Deficiency on the miR396 Regulatory Module	106
3.5.2	Manipulation of the miR396/ <i>GRF</i> Regulatory Module Results in Altered Growth and Development and the Response of <i>Arabidopsis</i> to Abiotic Stress	107
3.5.2.1	Molecularly Modified miR396 Abundance Provides <i>Arabidopsis</i> Seedlings with Superior Phenotypic Traits Under Non-Stress Growth Conditions.....	108

3.5.2.2	Molecularly Modified miR396 Abundance Alters the Tolerance of <i>Arabidopsis</i> Seedlings to P Deficiency and Salt stress	110
----------------	--	-----

CHAPTER IV: The Phenotypic and Molecular Consequence of Manipulating the miR399 Regulatory Module in *Arabidopsis* 114

4.1	Chapter Overview/ Rationale	115
4.2	Introduction	116
4.2.1	The microRNA399/ <i>PHOSPHATE2</i> Regulatory Module in the Plant Development and Abiotic Stress Response	116
4.3	Material and Methods	118
4.4	Results.....	119
4.4.1	The Requirement of <i>DRB1</i> , <i>DRB2</i> and <i>DRB4</i> in Appropriate Regulation of the Phosphate Responsive, miR399/ <i>PHO2</i> Regulatory Module in <i>Arabidopsis</i>	119
4.4.2	The Phenotypic Response of <i>Arabidopsis</i> miR399 Molecularly Modified Plant Lines to Phosphate Deficiency and Salt Stress	120
4.4.2.1	Fresh Weight.....	122
4.4.2.2	Rosette Area	124
4.4.2.3	Primary Root Length	126
4.4.2.4	Anthocyanin Accumulation	128
4.4.2.5	Chlorophyll <i>a</i> and <i>b</i> Content	130
4.4.3	The Molecular Response of <i>Arabidopsis</i> Plant Lines With Molecularly Altered miR399 Abundance to Phosphate Deficiency and Salt Stress	133
4.5	Discussion	135
4.5.1	The Requirement of <i>DRB1</i> , <i>DRB2</i> and <i>DRB4</i> for Appropriate Regulation of the miR399/ <i>PHO2</i> Regulatory Module in <i>Arabidopsis</i>	135
4.5.2	Manipulation of the miR399/ <i>PHO2</i> Regulatory Module Results in Altered Growth and Development and the Response of <i>Arabidopsis</i> to Abiotic Stress	135
4.5.2.1	Molecularly Modified miR399 Abundance Provides <i>Arabidopsis</i> Seedlings with Superior Phenotypic Traits Under Non-Stress Growth Conditions.....	136
4.5.2.2	Molecularly Modified miR399 Abundance Alters the	

	Tolerance of <i>Arabidopsis</i> Seedlings to P Deficiency and Salt Stress.....	138
CHAPTER V: Summary and Future Directions		142
5.1	Summary of Key Results.....	143
5.1.1	Generation of a Heat, Mannitol and Salt Stress Responsive MicroRNA Dataset.....	143
5.1.2	The Contribution of the Nuclear-Localised DRB Proteins to the <i>Arabidopsis</i> MicroRNA Landscape	143
5.1.3	Characterisation of the <i>Arabidopsis</i> miR396 Regulatory Module	144
5.1.4	Characterisation of the <i>Arabidopsis</i> miR399 Regulatory Module	145
5.2	Future Directions.....	146
5.2.1	Selection of Heat, Mannitol and Salt Responsive MicroRNAs for Further Characterisation	146
5.2.2	Western Blot Analysis to Demonstrate Translational Repression as a Mechanism of Regulation of miRNA Target Gene Expression.....	146
APPENDICES 1-6		148
A.1	Appendix 1: Publications.....	148
A.1.1	Publication One: The Plant microRNA Pathway: The Production and Action Stages.....	149
A.1.2	Publication Two: Profiling of the Differential Abundance of Drought and Salt Stress- Responsive MicroRNAs across Grass Crop and Genetic Model Plant Species.....	174
A.1.3	Publication Three: Profiling the Abiotic Stress Responsive microRNA Landscape of <i>Arabidopsis thaliana</i>	193
A.1.4	Publication Four: DRB1, DRB2 and DRB4 Are Required for Appropriate Regulation of the microRNA399/ <i>PHOSPHATE2</i> Expression Module in <i>Arabidopsis thaliana</i>	211
A.2	Appendix 2: Solutions and Mediums	237
A.2.1	Solutions.....	238
A.2.1.1	MS Macro (20X).....	238
A.2.1.2	MS Micro (100X)	238
A.2.1.3	MS Vitamins (100X)	238
A.2.1.4	MS Iron + EDTA (200X)	239
A.2.1.5	0.5 M EDTA (pH 8.0).....	239

	A.2.1.6	10X TBE.....	239
	A.2.1.7	0.1M CaCl ₂ (*or 0.1M CaCl ₂ +15% glycerol).....	239
	A.2.1.8	Tris-EDTA (TE) buffer (1X).....	239
A.2.2		Mediums.....	240
	A.2.2.1	Murashige and Skoog (MS) Plant Growth Medium..	240
	A.2.2.2	Luria-Bertani (LB) Liquid Medium.....	240
	A.2.2.3	Yeast Extract Peptone (YEP) Liquid Medium.....	240
	A.2.2.4	Super Optimal Broth with Catabolite Repression (SOC) Liquid Medium.....	241
A.3		Appendix 3: Standardised Reaction Programs.....	242
	A.3.1	PCR and qPCR Cycling Conditions.....	243
		A.3.1.1 Genotyping PCR.....	243
		A.3.1.2 cDNA Synthesis.....	243
		A.3.1.3 miRNA-Specific cDNA Synthesis.....	243
		A.3.1.4 quantitative PCR.....	244
		A.3.1.5 Colony PCR Screen.....	244
		A.3.1.6 Amplification of Gene Fragments PCR.....	244
A.4		Appendix 4: Primer Sequences.....	245
	A.4.1	Primer Sequences.....	245
		A.4.1.1 Genotyping Related Primers.....	246
		A.4.1.2 Cloning Related Primers.....	246
		A.4.1.3 qPCR Related miRNA Primers.....	247
		A.4.1.4 qPCR Related miRNA Target Gene Primers.....	248
A.5		Appendix 5: Bacterial Cloning Material.....	250
	A.5.1	Transgene Sequences.....	251
	A.5.2	Competent Cells.....	251
	A.5.3	Plasmid DNA Vectors.....	251
	A.5.4	Antibiotics and Herbicides.....	252
A.6		Appendix 6: Additional Results.....	253
	A.6.1	RT-PCR Based Genotyping of DRB Knockout Plant Lines.....	254
	A.6.2	sRNA Sequencing Raw Read Count.....	255
	A.6.3	Developmental and Reproductive Phenotype of Col-0 Plants, and miR396 and miR399 Altered Plants.....	269
		REFERENCES.....	270

FIGURES AND TABLES

CHAPTER II: Phenotypic and molecular analysis of abiotic stressed *Arabidopsis* plant lines

- Figure 2.1** *Arabidopsis* developmental and physiological processes under miRNA regulation.
- Figure 2.2** Phenotypic and physiological consequence of a heat, mannitol or salt stress treatment on 15 d old wild-type *Arabidopsis* (Col-0) and DRB-knockout mutant lines *drb1*, *drb2* and *drb4*.
- Figure 2.3** Whole seedling fresh weight of heat, mannitol and salt stressed *Arabidopsis* Col-0 and DRB-knockout mutant lines, *drb1*, *drb2* and *drb4*, compared to their non-stressed counterparts of the same age.
- Figure 2.4** Rosette area of heat, mannitol and salt stressed *Arabidopsis* Col-0 and DRB-knockout mutant lines, *drb1*, *drb2* and *drb4*, compared to their non-stressed counterparts of the same age.
- Figure 2.5** Primary root length of heat, mannitol and salt stressed *Arabidopsis* Col-0 and DRB-knockout mutant lines, *drb1*, *drb2* and *drb4*, compared to their non-stressed counterparts of the same age.
- Figure 2.6** Anthocyanin accumulation of heat, mannitol and salt stressed *Arabidopsis* Col-0 and DRB-knockout mutant lines, *drb1*, *drb2* and *drb4*, compared to their non-stressed counterparts of the same age.
- Figure 2.7** Chlorophyll *a* (A) and *b* (B) content of heat, mannitol and salt stressed *Arabidopsis* Col-0 and DRB-knockout mutant lines, *drb1*, *drb2* and *drb4*, compared to their non-stressed counterparts of the same age.
- Figure 2.8** RT-qPCR analysis of *P5CS1* expression in heat, mannitol and salt stressed *Arabidopsis* Col-0 and DRB-knockout mutant lines, *drb1*, *drb2* and *drb4*, compared to their non-stressed counterparts of the same age.
- Figure 2.9** Heat map of miRNA accumulation in the *Arabidopsis* DRB mutants, *drb1*, *drb2* and *drb4*.
- Figure 2.10** Small-RNA sequencing analysis of the miRNA accumulation profiles of 15 d old *Arabidopsis* Col-0 seedlings and DRB-knockout mutants, *drb1*, *drb2* and *drb4* seedlings exposed to heat, mannitol or salt stress, relative to non-stressed control counterparts.

- Figure 2.11** RT-qPCR assessment of *DCL1*, *DRB1*, *DRB2* and *DRB4* in non-stressed and stress treated *Arabidopsis* plant lines.
- Figure 2.12** Molecular analysis of the miR396/*GRF7* regulatory module in 15 d old *Arabidopsis* Col-0 seedlings and DRB-knockout mutants, *drb1*, *drb2* and *drb4* exposed to heat, mannitol or salt stress, relative to untreated (control) seedlings.
- Figure 2.13** Molecular analysis of the miR399/*PHO2* regulatory module in 15 d old *Arabidopsis* Col-0 seedlings and DRB-knockout mutants, *drb1*, *drb2* and *drb4* exposed to heat, mannitol or salt stress, relative to untreated (control) seedlings.
- Figure 2.14** Molecular analysis of the miR408/*LAC3* regulatory module in 15 d old *Arabidopsis* Col-0 seedlings and DRB-knockout mutants, *drb1*, *drb2* and *drb4* exposed to heat, mannitol or salt stress, relative to untreated (control) seedlings.

CHAPTER III: The Phenotypic and Molecular Consequence of Manipulating the miR396 Regulatory Module in *Arabidopsis*

- Figure 3.1** Conservation of GRF N-terminal domain between *Arabidopsis* and grass crops.
- Figure 3.2** Molecular analysis of the miR396/*GRF7* regulatory module in the shoot tissue of 15 d old *Arabidopsis* Col-0 seedlings and DRB-knockout mutants, *drb1*, *drb2* and *drb4* exposed to P deficiency, relative to untreated (control) seedlings.
- Figure 3.3** Phenotypic and physiological consequence of a P deficiency or salt stress treatment on 15 d old wild-type *Arabidopsis* (Col-0), *MIM396* and *MIR396*.
- Figure 3.4** Whole seedling fresh weight of P⁻ and salt stressed *Arabidopsis* Col-0 and miR396 altered lines, *MIM396* and *MIR396*, relative to non-stressed Col-0 seedlings.
- Figure 3.5** Rosette area of P⁻ and salt stressed *Arabidopsis* Col-0 and miR396 altered lines, *MIM396* and *MIR396*, compared to non-stressed Col-0 seedlings.
- Figure 3.6** Primary root length of P⁻ and salt stressed *Arabidopsis* Col-0 and miR396 altered lines, *MIM396* and *MIR396*, compared to non-stressed Col-0 seedlings.
- Figure 3.7** Anthocyanin accumulation of P⁻ and salt stressed *Arabidopsis* Col-0 and miR396 altered lines, *MIM396* and *MIR396*, compared to non-stressed Col-0 seedlings.

Figure 3.8 Chlorophyll a (A) and b (B) content of P⁻ and salt stressed *Arabidopsis* Col-0 and miR396 altered lines, *MIM396* and *MIR396*, compared to non-stressed Col-0 seedlings.

Figure 3.9 RT-qPCR assessment of miR396 and miR396 targeted *GRFs*, *GRF1-3*; 7-9 in non-stressed and stress treated *Arabidopsis* plant lines.

CHAPTER IV: The Phenotypic and Molecular Consequence of Manipulating the miR399 Regulatory Module in *Arabidopsis*

Figure 4.1 The *Arabidopsis* miR399/*PHO2* pathway under phosphate (Pi) deficient growth conditions.

Figure 4.2 Phenotypic and physiological consequence of a P deficiency or salt stress treatment on 15 d old wild-type *Arabidopsis* (Col-0), *MIM399* and *MIR399*.

Figure 4.3 Whole seedling fresh weight of P⁻ and salt stressed *Arabidopsis* Col-0 and miR399 altered lines, *MIM399* and *MIR399*, compared to non-stressed Col-0 seedlings.

Figure 4.4 Rosette area of P⁻ and salt stressed *Arabidopsis* Col-0 and miR399 altered lines, *MIM399* and *MIR399*, compared to non-stressed Col-0 seedlings.

Figure 4.5 Primary root length of P⁻ and salt stressed *Arabidopsis* Col-0 and miR399 altered lines, *MIM399* and *MIR399*, compared to non-stressed Col-0 seedlings.

Figure 4.6 Anthocyanin accumulation of P⁻ and salt stressed *Arabidopsis* Col-0 and miR399 altered lines, *MIM399* and *MIR399*, compared to non-stressed Col-0 seedlings.

Figure 4.7 Chlorophyll a (A) and b (B) content of P⁻ and salt stressed *Arabidopsis* Col-0 and miR399 altered lines, *MIM399* and *MIR399*, compared to non-stressed Col-0 seedlings.

Figure 4.8 RT-qPCR assessment of *miR399* and miR399 target gene, *PHO2*, in non-stressed and stress treated *Arabidopsis* plant lines.

APPENDICES 1-6

- Table A.3.1** PCR cycling conditions used for genotyping PCRs.
- Table A.3.2** PCR cycling conditions used to synthesis cDNA.
- Table A.3.3** PCR cycling conditions used to synthesis miRNA-specific cDNA.
- Table A.3.4** qPCR cycling condition.
- Table A.3.5** PCR cycling conditions for screening for +/- bacterial colonies.
- Table A.3.6** PCR cycling conditions used for amplifying gene fragments for cloning.
- Table A.4.1** The nucleotide sequence of all primers used in this study pertaining to the genotyping of *Arabidopsis* DRB-KO mutant plant lines investigated.
- Table A.4.2** The nucleotide sequence of all primers utilised in the molecular cloning methodologies of this study.
- Table A.4.3** The nucleotide sequence of all primers used in this study pertaining to SL-RT-qPCR analyses of miRNAs.
- Table A.4.4** The nucleotide sequence of all primers used in this study pertaining to RT-qPCR analyses of target gene mRNAs and miRNA production machinery investigated.
- Table A.5.1** Transgene sequences used in this study.
- Table A.5.2** Competent cell host lines used in this study.
- Table A.5.3** Plasmid DNA vectors used in this study.
- Table A.5.4** Working antibiotic concentration.
- Table A.5.5** Working herbicide concentration.
- Figure A.6.1** Genotyping of wild-type *Arabidopsis* plants and *drb* knockout insertion mutant lines.
- Table A.6.1** Raw miRNA reads and the Log₂ fold change in abundance of each *Arabidopsis* miRNA sRNA detected via high throughput sRNA sequencing.
- Figure A.6.2** Developmental and reproductive phenotype of Col-0 plants, and miR396 and miR399 altered plants.

PUBLICATIONS FROM THESIS RESEARCH

Journal Articles

- **Pegler, J. L., Oultram, J. M., Grof, C. P., and Eamens, A. L.** (2019). DRB1, DRB2 and DRB4 Are Required for Appropriate Regulation of the microRNA399/PHOSPHATE2 Expression Module in *Arabidopsis thaliana*. *Plants*, **8**(5), 124.
- **Pegler, J. L., Oultram, J. M., Grof, C. P., and Eamens, A. L.** (2019). Profiling the Abiotic Stress Responsive microRNA Landscape of *Arabidopsis thaliana*. *Plants*, **8**(3), 58.
- **Pegler, J., Grof, C., and Eamens, A.** (2018). Profiling of the Differential Abundance of Drought and Salt Stress-Responsive MicroRNAs Across Grass Crop and Genetic Model Plant Species. *Agronomy*, **8**(7), 118.

Book Chapters

- **Pegler, J. L., Grof, C. P., and Eamens, A. L.** (2019). The Plant microRNA Pathway: The Production and Action Stages. In *Plant MicroRNAs* (pp. 15-39). Humana Press, New York, NY.

ABSTRACT

There is overwhelming scientific consensus that anthropogenically driven global warming and the burgeoning global population are having, and will increasingly have, detrimental impacts on natural ecosystems and human health. One such pressing issue is the ability to provide food security for a growing human population with a largely insufficient global crop yield to land capability ratio, together with the increasing prevalence of unfavourable plant growth conditions associated with global warming. It has been evident in recent decades that the unsustainable practise of clearing ecosystems rich in biodiversity for the cultivation of additional food crops must be replaced with an alternate approach, such as a molecular modification approach that targets crop yield improvement: with crop yield one of the traits of a plant that is extremely susceptible to climate change. MicroRNAs, a class of small (21 to 24 nucleotide (nt)) regulatory RNA, are well documented to act as '*master regulators*' of plant development as well as demonstrated to play an additional role in plant adaption to abiotic stress. Therefore, the molecular modification of such abiotic responsive miRNAs provides an attractive alternate avenue for the generation of plant lines that display tolerance to abiotic stress. As a first step to achieving this goal, this study utilised a high throughput small RNA sequencing (sRNA-seq) approach to profile the miRNA landscape of wild-type *Arabidopsis thaliana* (*Arabidopsis*) plants exposed to heat, drought and salt stress. sRNA-seq identified large miRNA cohorts responsive to each applied stress, with 121, 123 and 118 miRNAs determined to have a greater than 2.0-fold change in abundance post heat, drought and salt stress treatment of *Arabidopsis* plants, respectively. From this large number of potential targets for future molecular modification, the miRNAs, miR396 and miR399, and their respective regulatory modules, were selected for further characterisation. A transgenesis approach was used to generate miRNA knockdown and overexpression plant lines for the miR396 and miR399 sRNA. This approach revealed that the molecular manipulation of miR396 and miR399 sRNA abundance impacted on numerous aspects of the growth and development of *Arabidopsis* plants; either under standard growth conditions, or when exposed to a 7 day stress regime of either phosphate deficiency or salt stress. The information presented in this research thesis provides a foundation for the selection of crucial abiotic stress responsive miRNAs whose molecular manipulation provides the modified plant lines with a degree of tolerance to the imposed stress. This research thesis additionally provides further extensive molecular evidence of the essential regulatory role that DRB1, DRB2 and DRB4 play in miRNA production, both in non-stressed *Arabidopsis* plants, and in *Arabidopsis* plants post their exposure to heat, mannitol and salt stress, or when *Arabidopsis* is cultivated in the absence of phosphate.

UNIT OF MEASUREMENT

Concentration

M	molar
mM	millimolar (10^{-3} M)
pmol	picomolar (10^{-12} M)
v/v	volume for volume
w/v	weight for volume

Length

cm	centimetre (10^{-2} metre)
mm	millimetre (10^{-3} metre)
µm	micrometre (10^{-6} metre)
nm	nanometre (10^{-9} metre)

Light

µmol m⁻² s⁻¹	micromole of photons per square metre per second
---	--

Mass

g	gram
ng	nanogram (10^{-9} g)

Other

g	acceleration due to gravity
Kb	kilobases
pH	potens hydrogen ($\log_{10}[\text{H}^+]$)

Temperature

°C	degrees Celsius
RT	room temperature ($\approx 20^\circ\text{C}$)

Time

d	day
h	hour
min	minute
s	seconds

Volume

mL	millilitre (10^{-3} litre)
µL	microliter (10^{-6} litre)

ABBREVIATIONS

A	adenosine	NaCl	sodium chloride (salt)
AGO	ARGONAUTE	natsiRNA	natural antisense short interfering RNA
AGRF	Australian Genome Research Facility	NADP+	nicotinamide adenine dinucleotide phosphate
<i>Arabidopsis</i>	<i>Arabidopsis thaliana</i>	OE	overexpression
CaMV	cauliflower mosaic virus	P5CS1	Δ 1-PYRROLINE-5-CARBOXYLATE SYNTHETASE1
CO₂	carbon dioxide	P5CS	Δ 1-PYRROLINE-5-CARBOXYLATE SYNTHETASE
Col-0	Columbia-0 ecotype	P	phosphate
DCL	DICER-LIKE	P⁻	phosphate deficiency
MQ-H₂O	Milli-Q water	Pi	inorganic phosphorous
DRB	DOUBLE STRANDED RNA BINDING	PHO2	PHOSPHATE2
dsRBM	double-stranded RNA binding motifs	pre-miRNA	precursor miRNA
dsRNA	Double-stranded RNA	pri-miRNA	primary miRNA
FAO	Food and Agriculture Organization	RISC	RNA INDUCED SILENCING COMPLEX
GAEZ	Global Agro-Ecological Zones	RuBisCO	Ribulose-1, 5-bisphosphate carboxylase/oxygenase
GIF	GROWTH INTERACTING FACTOR	ROS	reactive oxygen species
GRF	GROWTH REGULATING FACTOR	RNA	ribonucleic acid
IIASA	International Institute for Applied Systems Analysis	SAM	shoot apical meristem
IPCC	Intergovernmental Panel on Climate Change	SD	standard deviation
KD	knockdown	sRNA	small RNA
KO	knockout	sRNA-seq	sRNA sequencing
LAC	LACCASE	tasiRNA	trans-acting small interfering RNA
LB	Luria-Bertani	UV-B	ultraviolet B
LN₂	liquid nitrogen	YEP	Yeast Extract Peptone
miRNA	microRNA		
MS	Murashige and Skoog		
mRNA	messenger RNA		

CHAPTER I

Introduction

1.1 The Plant MicroRNA Pathway: The Production and Action Stages

The contents of this section of the thesis can be found in the following publication:

Pegler, J. L., Grof, C. P., and Eamens, A. L. (2019). The Plant microRNA Pathway: The Production and Action Stages. *Plant MicroRNAs* (pp. 15-39). Humana Press, New York, NY.

https://link.springer.com/protocol/10.1007/978-1-4939-9042-9_2

A copy of this publication can be found in **Appendix 1 (A.1.1)** of this thesis, pages 149-173.

1.2 The *Arabidopsis* DOUBLE-STRANDED RNA BINDING (DRB) Protein Family

DOUBLE-STRANDED RNA BINDING (DRB) proteins have been reported for many eukaryote species and demonstrated to mediate central roles in a range of RNA-directed pathways (Curtin *et al.*, 2008; Kim *et al.*, 2009). However, most DRB proteins characterised to date have been demonstrated to be involved in either small RNA (sRNA) production or sRNA target gene expression regulation (Curtin *et al.*, 2008; Hiraguri *et al.*, 2005; Masliah *et al.*, 2013). In *Arabidopsis thaliana* (*Arabidopsis*), five DRB proteins (DRB1 to DRB5) have been identified and demonstrated to mediate varying roles in the parallel RNA silencing pathways of this model plant species (Curtin *et al.*, 2008; Eamens *et al.*, 2012b; Hiraguri *et al.*, 2005). All five *Arabidopsis* DRB proteins harbour two amino-terminal located double-stranded (ds) RNA-binding motifs (dsRBMs) that mediate interaction with either; i) a specifically structured dsRNA substrate, or; ii) their preferred protein partner(s), namely mediating DRB/DICER-LIKE (DCL) functional associations (Curtin *et al.*, 2008; Eamens *et al.*, 2011).

As previously described, DCL1 is the primary DCL protein responsible for processing miRNA precursor transcripts in *Arabidopsis* (see **Section 1.1**). However, in order for DCL1 to function as an efficient endonuclease in this process (accurate dsRNA cleavage), DCL1 must form a functional partnership with DRB1 (Curtin *et al.*, 2008). DRB1 ensures that both nucleus localised DCL1-catalysed precursor transcript processing steps required for miRNA maturation are executed at highly specific positions on the precursor transcript (Eamens *et al.*, 2009; Eamens *et al.*, 2011). Eamens and colleagues (2009) further demonstrated an additional role for DRB1 in the *Arabidopsis* miRNA pathway; correct orientation of the miRNA/miRNA* duplex into the ARGONAUTE1 (AGO1) endonuclease to ensure removal of the miRNA* passenger strand, and RNA Induced Silencing Complex (RISC) incorporation of

the miRNA guide strand to direct efficient miRNA target gene expression repression (Eamens *et al.*, 2009).

The DRB1/DCL1 functional partnership is closely mirrored by the DRB4/DCL4 interaction. The DRB4/DCL4 functional partnership is essential for efficient and accurate production of 'young' or 'newly-evolved' miRNAs, *trans*-acting small interfering RNAs (tasiRNAs), and natural antisense siRNAs (natsiRNA) in *Arabidopsis* (Gascioli *et al.*, 2005; Nakazawa *et al.*, 2007; Xie *et al.*, 2005). Recent research has demonstrated that DRB2 is also required for the production of specific miRNA and tasiRNA species in developmentally important tissues of *Arabidopsis* (Eamens *et al.*, 2012a; Eamens *et al.*, 2012b; Pélissier *et al.*, 2011; Reis *et al.*, 2015). Collectively, these findings suggest that DRB2 is functionally distinct to DRB1 and DRB4, in that DRB2 can; i) recognise and bind to structurally distinct molecules of dsRNA (both perfectly (siRNA precursors) and imperfectly (miRNA precursors) dsRNA), and; ii) form functional partnerships with either DCL1 or DCL4 (Eamens *et al.*, 2012a; Eamens *et al.*, 2012b; Pélissier *et al.*, 2011; Reis *et al.*, 2015). Reis *et al.*, (2015) further demonstrated that in *Arabidopsis* tissues where *DRB1* and *DRB2* expression overlaps, DRB2 represses *DRB1* gene expression. This is presumed to allow for promotion of the less favoured DRB2/DCL1 interaction in these tissues, compared to the canonical and preferential DRB1/DCL1 interaction, to broaden the role of DRB2 in the miRNA pathway. This research also revealed that DRB1 and DRB2 determine the silencing fate of an individual *Arabidopsis* miRNA, that is; i) a miRNA that requires the DRB1/DCL1 partnership for its production regulates the expression of its targeted genes via the canonical messenger RNA (mRNA) cleavage-based mechanism of RNA silencing, whereas; ii) a miRNA that is generated by the DRB2/DCL1 partnership regulates the expression of its targeted genes via a translational inhibition mode of RNA silencing (Reis *et al.*, 2015). Pélissier *et al.*, (2011) further showed that DRB2 is also antagonistic to the DRB4/DCL4 functional partnership in tasiRNA production from *TAS3* precursor transcripts and Eamens *et al.*, (2009) demonstrated that DRB2 is synergistic to this partnership for the production of newly-evolved miRNAs, miRNAs that are processed from precursors that fold to form near perfectly structured dsRNA stem-loops.

Unlike DRB1, DRB2 and DRB4, DRB3 and DRB5 are localised to the cytoplasm (Eamens *et al.*, 2012a). Localisation to this alternate cellular compartment strongly suggests that neither DRB3 nor DRB5 play a role in sRNA production, a process that predominantly occurs in the plant cell nucleus (Curtin *et al.*, 2008; Eamens *et al.*, 2012a). Eamens and colleagues (2012b) largely confirmed this by demonstrating that DRB3 and DRB5 play little to no role in dsRNA processing, but found evidence that strongly suggests that both of these DRB family members are involved in the formation of an alternative RISC complex in the

cytoplasm. More specifically, using a transgene-based approach, Eamens *et al.* (2012b) demonstrated that DRB3 and DRB5 are required to mediate a translational inhibition mode of RNA silencing to repress the expression of target genes of DRB2-dependent miRNAs (Eamens *et al.*, 2012b).

1.3 The Impact of Heat, Drought and Salt Stress on American and Australian Agriculture

1.3.1 Heat Stress

In the current age of climate change, driven by ever-increasing greenhouse gas emissions, the world is faced with the reality of ambient temperatures that continue to rise (Christidis *et al.*, 2011; Donat *et al.*, 2013; Min *et al.*, 2011; Perkins *et al.*, 2012; Rahmstorf and Coumou, 2011). The danger of increasing ambient temperatures to both the global health system and agricultural production is becoming increasingly clear. Most notably, in 2018, at the request of the United Nations Climate Change Conference (2015), the Intergovernmental Panel on Climate Change (IPCC) released their '*Special Report on Global Warming of 1.5°C*', created by authors from 40 countries. The report, which sourced over 6,000 scientific publications, highlighted the inevitable, detrimental global environmental effects of a 1.5°C and a 2.0°C increase in temperature, urging for immediate action from policy and "unprecedented changes in all aspects of society" (IPCC, 2018).

Focusing on the impact of elevated temperatures on agriculture, with a specific focus on crop yield, many research groups have implemented prediction based modelling to determine the severity of yield loss on major global food crops resulting from climate change induced events of heat stress over the next century (Donat *et al.*, 2013; Fischer and Knutti, 2015; Semenov and Shewry, 2011; Teixeira *et al.*, 2013; Zhao *et al.*, 2017). Prediction based modelling utilised by Semenov and Shewry (2011), investigated the effect of heat stress on European wheat cultivars, and suggested that the heat stress that accompanies climate change poses an even greater threat to crop yield than the associated drought stress, a finding that strongly identifies the need to develop heat tolerant cultivars for each of the world's major cropping species (Semenov and Shewry, 2011). Moreover, Teixeira and colleagues (2013), used the Food and Agriculture Organization/International Institute for Applied Systems Analysis (FAO/IIASA) Global Agro-Ecological Zones (GAEZ) Model to investigate the global risk of increasing heat stress on key crops; maize (*Zea mays*), rice (*Oryza sativa*), soybean (*Glycine max*) and wheat (*Triticum aestivum*). This study generated findings that indicate that

in future growing seasons, large cropping areas in Asia, North America and North India, have a high risk of yield damage due to the effects of heat stress (Teixeria *et al.*, 2013).

1.3.2 Drought and Salt stress

The contents of this section of the thesis can be found in the following publication:

Pegler, J.L., Grof, C.P.L., and Eamens, A.L. (2018). Profiling of the Differential Abundance of Drought and Salt Stress-Responsive MicroRNAs Across Grass Crop and Genetic Model Plant Species. *Agronomy*, 8(7), 118.

<https://www.mdpi.com/2073-4395/8/7/118>

A copy of this publication can be found in **Appendix 1 (A.1.2)** of this thesis, pages 174-192. Please refer to the section titled '2. *The Impact of Drought and Salt Stress on American and Australian Agriculture*', pages 176-178.

1.4 The Role of Plant microRNAs in Mitigating the Impact of Heat, Drought and Salt Stress on Global Agriculture.

The introduction to this section and contents pertaining to drought and salt stress can be found in the following publication:

Pegler, J.L., Grof, C.P.L., and Eamens, A.L. (2018). Profiling of the Differential Abundance of Drought and Salt Stress-Responsive MicroRNAs Across Grass Crop and Genetic Model Plant Species. *Agronomy*, 8(7), 118.

<https://www.mdpi.com/2073-4395/8/7/118>

A copy of this publication can be found in **Appendix 1 (A.1.2)** of this thesis, pages 174-192. Please refer to the section titled '3. *The Role of Plant microRNAs in Response to Drought and Salt Stress*, pages 178-179.

Similar to drought and salt stress, the elevated ambient temperatures that accompany anthropogenic driven climate change are propelling plant biologists to investigate molecular avenues that could potentially lead to the development of modified crops that have the improved heat tolerance to that of their non-molecularly modified counterparts, particularly

with respect to crop yield (Hasanuzzaman *et al.*, 2013; Wahid *et al.*, 2007). Again, the miRNA class of sRNA has been identified as an ideal candidate for a molecular modification based approach with studies across the grain crop species, barley (*Hordeum vulgare*), wheat and rice, identifying and/or characterising miRNAs, or the target genes of these miRNAs, responsive to heat stress (Kruszka *et al.*, 2014; Mittal *et al.*, 2012; Xin *et al.*, 2010). Further, the analyses of Xin and colleagues (2010) that employed a high-throughput sequencing approach to profile the sRNA landscape of wheat identified a cohort of 12 miRNAs responsive to elevated temperature. Similarly, Mittal *et al.*, (2012) demonstrated that when rice was exposed to heat stress, 12 miRNAs were differentially expressed (> 2.0-fold), compared to their abundance in rice plants cultivated under standard growth conditions.

1.5 Aims

The aim of this research was to molecularly dissect the miRNA/miRNA target gene regulatory modules that potentially underpin the ability of *Arabidopsis* to tolerate exposure to the abiotic stresses, of heat, drought (induced by mannitol due to the *in vitro* nature of this study) and salinity. This body of research contains four overarching aims:

Aim 1: To phenotypically characterise the consequence of a 7 day (d) heat, mannitol (to simulate drought) or salt stress treatment of wild-type *Arabidopsis* seedlings (ecotype Columbia-0; Col-0) and the *DRB* knockout mutant plant lines, *drb1*, *drb2* and *drb4* (**Chapter II**).

Given the key roles that the nuclear localised DRB proteins, DRB1, DRB2 and DRB4, play in the production stage of the *Arabidopsis* miRNA pathway (Eamens *et al.*, 2011; Eamens *et al.*, 2012a; Hiraguri *et al.*, 2005; Pouch- Pélissier *et al.*, 2008), the first experimental aim of this project was to characterise the phenotypic response of 15 d old Col-0, *drb1*, *drb2* and *drb4* seedlings post a 7 d period of heat, mannitol or salt stress. In conjunction with the visual inspection for the expression of phenotypic and/or physiological stress markers, quantitative assessments were collected, including; (1) fresh weight; (2) rosette area; (3) primary root length; (4) anthocyanin content, and; (5) chlorophyll *a* and *b* content. In addition to the outlined phenotypic assessments, quantitative RT-PCR (RT-qPCR) was employed to determine the transcript abundance of the known *Arabidopsis* stress responsive gene, $\Delta 1$ -PYRROLINE-5-CARBOXYLATE SYNTHETASE1 (*P5CS1*; Ashraf and Foolad, 2007; Szabados and Savoure, 2010).

Aim 2 To molecularly profile the consequence of a 7 d heat, mannitol and salt stress treatment period on 15 d old Col-0, *drb1*, *drb2* and *drb4* seedlings (**Chapter II**).

To identify a miRNA-mediated molecular response to the imposed 7 d heat, mannitol or salt stress treatment period, RNA-sequencing (RNA-seq) of the sRNA fraction (sRNA-seq) of Col-0, *drb1*, *drb2* and *drb4* plants was employed. Subsequent to sRNA-seq, RT-qPCR was utilised to experimentally validate the abundance trends of a subset of miRNAs identified by sRNA-seq. Stemming from this molecular profiling exercise, three miRNAs, including miR396, miR399 and miR408, were subsequently selected for further analysis. The selection of these miRNAs was based on; (1) sRNA-seq identification and RT-qPCR confirmation that each miRNA was responsive to heat, mannitol and salt stress, and; (2) the functional role of the target gene(s) of each miRNA according to the literature. In addition to miRNA quantification, an RT-qPCR based approach was further used to determine whether the regulatory module of each selected miRNA was also responsive to the imposed stress: this was achieved via target gene expression quantification.

Aim 3 Stemming from the results generated by **Aim 2**, *Arabidopsis* transformant lines harbouring a miR396 knockdown or an overexpression construct were generated. These plant lines were subsequently profiled at both the phenotypic and molecular level to determine whether the introduced modifications altered the sensitivity of each plant line to salt stress or phosphate deficiency (**Chapter III**).

Based on the results of '**Aim 2**', miRNA knockdown (*MIM396*) and overexpression (*MIR396*) plant expression vectors were developed for miR396. This miRNA was selected for further experimental characterisation based on; (1) being demonstrated responsive to heat, mannitol and salt stress (**Figure 2.10 and Figure 2.12**); (2) the documented role of the miR396 regulatory module in either *Arabidopsis* development, and/or the response of *Arabidopsis* to abiotic stress (Omidbakhshfard *et al.*, 2015), and; (3) the miR396 being a highly conserved sRNA across the plant kingdom (Axtell and Meyers, 2018). Given the well-known P responsive miRNA, miR399, being demonstrated highly responsive to each of the abiotic stress conditions elicited in this study (**Figure 2.10**), investigating the response of miR396, a miRNA shown to also be highly responsive to heat, mannitol and salt stress (**Figure 2.10**), to P deficient conditions was also investigated. Therefore, the newly generated miR396 plant lines, *MIM396* and *MIR396*, were exposed to the abiotic stress growth regimes of salt stress (150 mM NaCl) and P deficiency for a 7 d period. Post the stress treatments, the 15 d old plants were then

phenotypically and molecularly analysed in parallel to Col-0 seedlings to determine if either plant line displayed an elevated or reduced tolerance to the imposed stress. Additionally, identifying the role of DRB1, DRB2 and DRB4 in the appropriate regulation of the miR396/*GRF7* regulatory module under a phosphate deficient (P⁻) stress growth regime was central to the phenotypic and molecular analyses.

Aim 4 Stemming from the results generated in **Aim 2**, *Arabidopsis* transformant lines harbouring a miR399 knockdown or overexpression plant expression vector were generated. These plant lines were subsequently profiled at both the phenotypic and molecular level to determine whether the introduced modifications altered the sensitivity of either plant line to salt stress or phosphate deficiency (**Chapter IV**).

Identical to the approach used for miR396 and again based of the results of **Aim 2**, miR399 knockdown (*MIM399*) and overexpression (*MIR399*) plant expression vectors were developed. The miR399 sRNA was selected for further experimental characterisation on the same basis as miR396, specifically; (1) miR399 being demonstrated responsive to heat, mannitol and salt stress (**Figure 2.10 and Figure 2.12**); (2) the documented role of the miR399 expression module in either *Arabidopsis* development, and/or the adaptive response of *Arabidopsis* to abiotic stress (Bari *et al.*, 2006; Fujii *et al.*, 2005; Hsieh *et al.*, 2009; Lin *et al.*, 2008), and; (3) miR399 being a highly conserved sRNA across the plant kingdom (Axtell and Meyers, 2018). As miR399 is a well know P responsive miRNA, the newly generated *MIM399* and *MIR399* plant lines were exposed to the abiotic stress growth regimes of salt stress and P deficiency for a 7 d period. Post the imposed stress treatment, 15 d old plants were phenotypically and molecularly analysed in parallel to Col-0 seedlings to determine if either plant line displayed an elevated or reduced tolerance to either stress. In addition, identifying the role of DRB1, DRB2 and DRB4 in the appropriate regulation of the miR399 expression module under a salt stress or P deficient growth regime was central to the conducted analyses.

Collectively the results of the four experimental aims of this project provided further insight into the molecular regulation that occurs in *Arabidopsis* during periods of exposure to abiotic stresses, including heat, mannitol and salt stress, and phosphate deficiency. The sRNA-seq dataset (**Aim 2**) and the complementary molecular modification approach (**Aim 3 and 4**) lay a promising foundation for future research to identify molecular solutions to develop plant lines that can tolerate stress yet demonstrate growth in a challenging environment.

Chapter II

Phenotypic and Molecular Analysis
of Abiotically Stressed *Arabidopsis*
Plant Lines

2.1 Chapter Overview / Rationale

Over a decade ago, Curtin and colleagues (2008) reported on the initial characterisation of all five members of the *Arabidopsis* DRB protein (1-5) family via an insertional knockout mutant approach. Specifically, the authors noted the distinct developmental and molecular phenotypes displayed by the *drb1*, *drb2* and *drb4* loss-of-function mutants: plant lines that we now know are defective in the activity of the three nucleus localised DRB family members demonstrated to be required for miRNA production. As central machinery proteins required for accurate and efficient DCL-catalysed processing of dsRNA precursor molecules to produce a mature miRNA sRNA, DRB1, DRB2 and DRB4 are crucial to the global sRNA profile of *Arabidopsis* (Eamens *et al.*, 2011; Eamens *et al.*, 2012a; Fukudome *et al.*, 2011; Hiraguri *et al.*, 2005; Pélissier *et al.*, 2011; Pouch-Pélissier *et al.*, 2008). Each miRNA sRNA is liberated from a precursor transcript of distinct secondary structure, either an; (1) imperfectly dsRNA hairpin, or a (2) hairpin of near-perfect dsRNA structure with respect to the stems of the overall stem loop dsRNA structure. The structure of each miRNA precursor determines the protein machinery recruited for its subsequent processing, namely the recruitment of a specific DRB/DCL protein partnership. This initial selective recruitment is thought to subsequently determine the mechanism of target gene expression repression directed by each miRNA sRNA upon its maturation, namely either; (1) target transcript cleavage, or; (2) translational repression (Eamens *et al.*, 2012b; Reis *et al.*, 2015).

Given the demonstrated antagonism between DRB2, and DRB1 and DRB4, during their respective DCL1 and DCL4 involvement in the production stage of the *Arabidopsis* miRNA pathway (Eamens *et al.*, 2012a; Pélissier *et al.*, 2011), assessing the phenotypic response of Col-0 seedlings and of the single knockout mutant lines, *drb1*, *drb2* and *drb4*, to the abiotic stresses of heat, mannitol and salt stress, presents a novel avenue of investigation. To date, many studies in *Arabidopsis* have demonstrated the abiotic stress responsiveness of large miRNAs cohorts (Khraiwesh *et al.*, 2012; Liu *et al.*, 2008; Sunkar *et al.*, 2012; Sunkar and Zhu, 2004), miRNAs which have the ability to regulate a variety of phenotypic and physiological responses that result in elevated tolerance to abiotic stress conditions. Given the specific degree of defect to miRNA production that each *drb* mutant plant harbours, it is highly likely that each *Arabidopsis* plant line will have a unique molecular response, and therefore a unique phenotypic/physiological response, to each of the applied stresses. The continued optimisation of high-throughput sequencing technology and its ever-increasing application, and therefore affordability, provides contemporary molecular biologists with an effective avenue to rapidly profile the sRNA landscape of a specific tissue or organ, at a specific stage of development, and post cultivation of a plant under a specific growth regime.

Therefore, high throughput sequencing provides a powerful molecular tool that a plant biologist can use to identify, and compare, the sRNA landscapes that underpin; (1) a standard plant phenotype or developmental response when a plant is cultivated under standard non-stressed (control) conditions, or; (2) the '*stress induced*' phenotype displayed by the same plant line post its exposure to an abiotic stress treatment. Therefore, the use of a high throughput sequencing approach to profile the sRNA landscapes of wild-type (Col-0) *Arabidopsis* plants, and those of the mutant lines, *drb1*, *drb2* and *drb4*, presents itself as an effective technique to further establish the role each DRB plays in contributing to the overall miRNA profile of *Arabidopsis* under standard growth conditions and post exposure to the stress regimes of heat, mannitol or salt stress. More specifically, it was expected that documenting miRNA abundance changes in Col-0, *drb1*, *drb2* and *drb4* plants post their exposure to heat, mannitol and salt treatment would shed some additional light onto the miRNA-mediated molecular mechanisms that underpin the distinct phenotypic and physiological response that each of these four plant lines display to each assessed stress.

2.2 Introduction

The frequency and intensity of a range of abiotic stresses has increased in recent decades either as a direct or indirect result of anthropogenically driven climate change. Due to the sessile nature of a plant, the ability to physically relocate due to the prevalence and/or severity of an abiotic stress is an unachievable mechanism for a plant to employ for stress avoidance. Instead, a plant must utilise a molecular approach to alter its phenotype and/or physiology in order to adapt to the exposed stress. One such molecular mechanism a plant will employ is miRNA-directed regulation of target gene expression, genes which underpin the regulation of a phenotypic or physiological characteristic required for a plant to mount an adaptive response to the abiotic stress (Khraiwesh *et al.*, 2012). At a phenotypic and physiological level, and in an attempt to tolerate and/or adapt to abiotic stress a plant can modify; (1) the rate at which it transitions between developmental phases; (2) leaf structure and/or architecture; (3) the degree of ROS scavenging; (4) nutrient uptake and homeostasis, and; (5) root architecture. In *Arabidopsis*, miRNAs have been shown to regulate the expression of key target genes within each one of these pathways (see **Figure 2.1**).

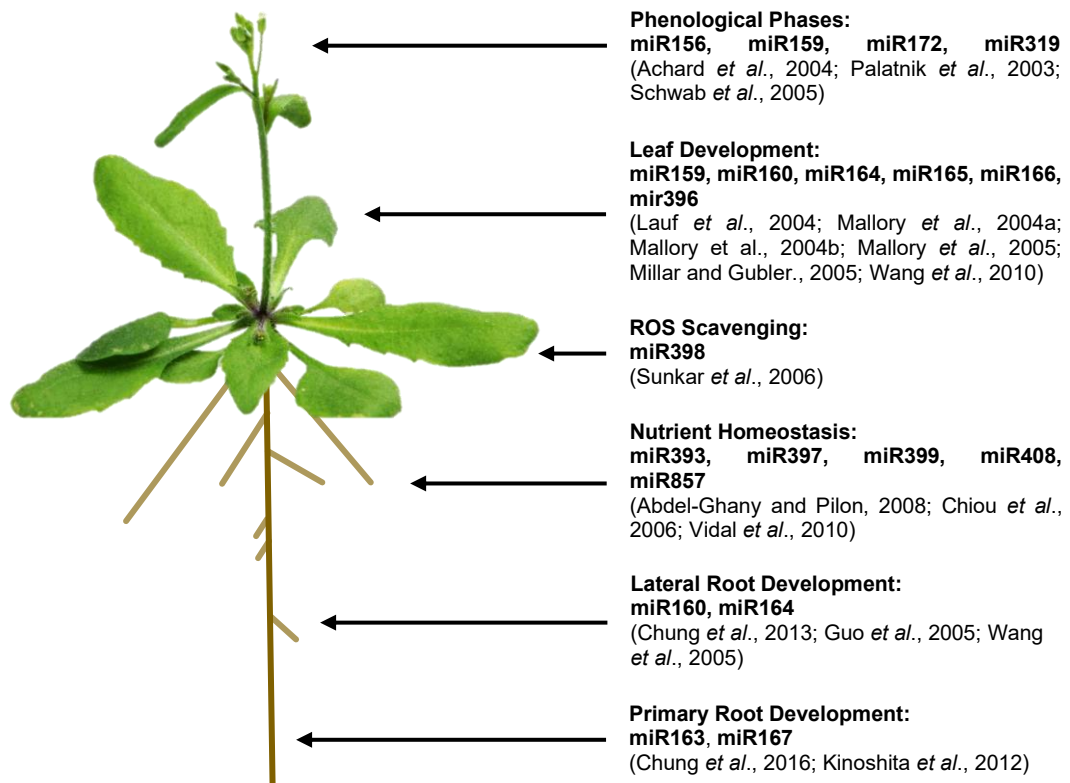


Figure 2.1 *Arabidopsis* developmental and physiological processes under miRNA regulation. Six key *Arabidopsis* developmental and physiological processes are indicated, namely, (1) phenological phases, (2) leaf development, (3) ROS scavenging, (4) nutrient homeostasis, (5) lateral root development, and (6) primary root development. Based on previous literature, miRNAs that have been shown to be involved in the regulation of each of the processes are listed. The photo of the *Arabidopsis* seedling was previously taken by Dr Eric Belfield.

Due to the regulatory role held by miRNAs, these molecules of sRNA form ideal targets for molecular modification as part of the development of plants with an enhanced ability to tolerate abiotic stress. Moreover, previous studies in *Arabidopsis*, have utilised such an approach, with transgenesis studies altering miRNAs abundance to increase the tolerance or sensitivity of the plant to conditions of heat (Guan *et al.*, 2013; Lin *et al.*, 2018), mannitol (Kim *et al.*, 2010a; Kim *et al.*, 2010b) and salt (Denver and Ullah, 2019; Kim *et al.*, 2010a; Kim *et al.*, 2010b; Song *et al.*, 2013) stress. However, given that large miRNA cohorts have previously been shown to be responsive to abiotic stresses in multiple plant species, it is safe to assume many more miRNAs are required for a plant to coordinate a phenotypic response that would allow for an elevated tolerance to an imposed abiotic stress (Liu *et al.*, 2008; Shen *et al.*, 2010; Xin *et al.*, 2010). Therefore, identification of the entire cohort of miRNAs responsive to heat, mannitol or salt stress in *Arabidopsis* is of high interest. Additionally, the loss of essential miRNA production machinery proteins, such as DRB1, DRB2 and DRB4, will alter the ability of *Arabidopsis* to molecularly, and therefore phenotypically/physiologically respond, to each abiotic stress, with these mutant plant lines harbouring an altered miRNA landscapes.

2.3 Material and Methods

2.3.1 Plant Growth Conditions.

2.3.1.1 *Arabidopsis thaliana* Plant Lines

The plant lines used in this study included wild-type *Arabidopsis* (ecotype Columbia-0; Col-0) and the previously described T-DNA insertion knockout mutant lines, *drb1* (SALK_064863), *drb2* (GABI_348A09) and *drb4* (SALK_000736) (Curtin *et al.*, 2008), with each of these three *drb* mutant lines maintained in the Col-0 background. Homozygosity for the T-DNA insertion in the *DRB1*, *DRB2* and *DRB4* loci was confirmed via PCR-based genotyping (see **Appendix A.6.1**, page 254) using the primers listed in **Appendix A.4.1** (page 246). For each plant line, seeds were surface sterilised in 1.5 mL microfuge tubes via a 90 minute (min) room temperature (RT) treatment with chloride gas. Post sterilisation, tubes were immediately capped and transferred to a sterilised Biosafety cabinet. In the Biosafety cabinet, and under aseptic conditions, the sterilised *Arabidopsis* seeds were transferred to petri dishes that contained standard Murashige and Skoog (MS) plant growth media (Gamborg *et al.*, 1976). Post sowing, plates were sealed with sterile surgical tape, and then stratified in the dark at 4°C for 48 hours (h) (stratification breaks seed dormancy to ensure even germination). Following stratification, the plates were transferred to a temperature controlled growth cabinet (A1000 Growth Chamber, Conviron®, Australia). For seed germination, and subsequent cultivation to the desired stage of plant development (in this study, 8 day (d) old *Arabidopsis* seedlings were determined to be at the desired developmental stage for abiotic stress treatments), a standard growth regime of 16 h of light and 8 h of dark, and a 22°C/18°C day/night temperature was applied.

2.3.1.2 Heat, Mannitol and Salt Stress Treatment of *Arabidopsis* Plant Lines

Following an 8 d cultivation period under the standard growth regime outlined above, Col-0, *drb1*, *drb2* and *drb4* seedlings, were transferred to either a 'non-stressed' or 'stressed' growth environment. Prior to sterilising the plant growth media via autoclaving, for the salt stress and mannitol stress regimes, 2.12 grams (g) of sodium chloride (NaCl) and 9.11 g of mannitol was added to 250 millilitres (mL) of liquid MS media to obtain final concentrations of 150 mM NaCl and 200 mM mannitol, respectively. Under aseptic conditions in a sterilised Biosafety cabinet, 8 d old seedlings were either transferred to fresh standard MS growth media (to be used for the non-stressed controls and the heat-stressed samples, respectively), or onto MS growth media supplemented with either 150 mM NaCl (salt stress samples) or 200 mM mannitol (drought stress samples). Post seedling transfer, each growth media plate was again sealed with sterile surgical tape and the sealed plates immediately returned to the temperature

controlled growth cabinets for an additional 7 d period of cultivation under standard growth conditions. For the heat stress treatment, 8 d old Col-0, *drb1*, *drb2* and *drb4* seedlings were again transferred to new standard MS media (to replicate the seedling transferral process of the salt and mannitol stress treatments) and post transfer, seedling plates were transferred to a separate temperature controlled growth cabinet with an alternate growth regime of 32°C for the 16 h light period and 28°C for the 8 h period of darkness.

2.3.2 Phenotypic Analysis of the Col-0, *drb1*, *drb2* and *drb4* Arabidopsis Lines

2.3.2.1 Plant Fresh Weight Assessment

Plant weight was initially assessed for 15 d old seedlings following the 7 d cultivation period under a standard growth regime and on either standard MS media (non-stressed controls), or on the MS media supplemented with either 150 mM NaCl, or with 200 mM mannitol. The fresh weight of the 15 d old heat-stressed *Arabidopsis* lines was assessed in parallel. Specifically, 4 replicates of 6, 15 d old seedlings were transferred to each pre-labelled and pre-weighed 1.5 mL microfuge tube, per plant line and growth regime. Post seedling transfer, each tube was capped, and the final weights determined on a standard set of laboratory scales.

2.3.2.2 Rosette Area Determination

Prior to transferral of 15 d old seedlings to 1.5 mL microfuge tubes for plant fresh weight determination, each plate for each plant line, and growth regime, was photographed from directly above and at a set distance of 30 cm. The resulting images were analysed using the image processing program, ImageJ®, to determine rosette area.

2.3.2.3 Assessment of Primary Root Length

Eight day old Col-0, *drb1*, *drb2* and *drb4* seedlings that had been germinated and cultivated on standard MS growth media (**Section 2.3.1.1**) were transferred to 6 standard MS plates (3 plates were used as the non-stressed controls and the other 3 plates used for the heat stress analyses), or to 3 MS growth media plates supplemented with either 150 mM NaCl or 200 mM mannitol plates (seedlings transfer was conducted under aseptic conditions in a surface sterilised Biosafety cabinet). The 8 seedlings that were transferred to each plate for each plant line, and growth regime, were placed at 1.0 cm intervals across a horizontal line that had been manually drawn at a set point on the bottom side of each media plate. Plates were then sealed with sterilised surgical tape and transferred to the temperature controlled

growth cabinet, orientated vertically, and cultivated for an additional 7 d period under a standard growth regime (for the controls and the salt stress and mannitol stress treatments). The heat stress treatment plates were also orientated for 7 d of vertical growth under the elevated temperature regime outlined in **Section 2.3.1.2**. At the conclusion of the 7 d treatment period, a photograph was taken of each vertically orientated plate, per plant line and growth regime. Root architecture was assessed using the image processing program, ImageJ®.

2.3.2.4 *Anthocyanin Content Determination*

Post determination of the weight of each 1.5 mL microfuge tube, four *Arabidopsis* plants from each plant line (performed in triplicate; 3 x 4 = 12 plants per plant line), and growth regime, were transferred to a corresponding tube. Tubes were capped, re-weighed and immediately frozen in liquid nitrogen (LN₂). Under LN₂, each sample was ground into a fine powder using a LN₂-chilled micro pestle in its microfuge tube. Five hundred microlitres (µL) of 99:1 methanol/HCl (v/v) was added to each tube immediately following the grinding process. Post processing of each sample, the tube was capped, and immediately stored in the dark at RT to allow each sample to completely thaw. Once all samples had been processed, each tube was thoroughly vortexed and then 330 µL of Milli-Q water (MQ-H₂O) was added. Tubes were capped, thoroughly vortexed, and then 500 µL of chloroform added. Tubes were capped and shaken vigorously by hand for 15 seconds (s) before being centrifuged at RT for 5 minutes (min) at 4,000·g . Post centrifugation, 500 µL of the upper aqueous phase was immediately transferred to a new, labelled 1.5 mL microfuge tube. Tubes were transferred in the dark to a spectrophotometer (BioMate™ 3S Spectrophotometer, Thermo Scientific, Australia) and the absorbance of each sample was determined at wavelength 535 nm (A_{535}), using 99:1 methanol/HCl as the blanking solution. Absorbance per milligram (A_{535}/mg) of fresh weight was then calculated.

2.3.2.5 *Determination of Chlorophyll a and b Content*

As described for the determination of anthocyanin content (**Section 2.3.2.4**), 4 plants of each *Arabidopsis* line and growth regime were transferred in triplicate to pre-weighed and labelled 1.5 mL microfuge tubes. Post seedling transfer, tubes were capped, reweighed and immediately frozen in LN₂. The plant material was ground into a fine powder using a LN₂-chilled micro pestle, and once the plant material was completely homogenised, 500 µL of 80% (v/v) acetone was immediately added to the tube. Tubes were then capped and incubated at RT in the dark until the sample had completely thawed and/or, all samples had been processed. The samples were then centrifuged at RT for 5 min at 4,000·g, before 500 µL of the resulting supernatant from each sample was transferred to a new, labelled 1.5 mL

microfuge tube. Sample tubes were transferred in the dark to the spectrophotometer and the absorbance of each sample assessed at wavelengths, 647 and 664nm, to obtain chlorophyll *a* and *b* absorbance, respectively. Absorbance per mg of plant fresh weight (A_{647}/mg and A_{664}/mg) was then determined for the chlorophyll *a* and *b* content of each plant line and growth regime. Total chlorophyll *a* and *b* content was subsequently determined using the Lichtenthaler equations (Lichtenthaler and Wellburn, 1983).

2.3.3 Assessment of MicroRNA and Gene Transcript Abundance in Abiotically Stressed *Arabidopsis thaliana*

For all material and methods utilised for the preparation and analysis of *Arabidopsis* Col-0, *drb1*, *drb2* and *drb4* samples for small RNA sequencing and RT-qPCR-based expression analyses, please refer to the following publication:

Pegler, J. L., Oultram, J. M., Grof, C. P., and Eamens, A. L. (2019). Profiling the Abiotic Stress Responsive microRNA Landscape of *Arabidopsis thaliana*. *Plants*, 8(3), 58. <https://www.mdpi.com/2223-7747/8/3/58>

A copy of this publication can be found in **Appendix 1 (A.1.3)** of this thesis, pages 193-210. The relevant experimental methodologies are detailed in sections; '*Total RNA extraction and high throughput sequencing of the small RNA fraction*', page 206, '*Bioinformatic assessment of the microRNA landscape of Arabidopsis whole seedlings*', page 206, and '*Quantitative reverse transcriptase polymerase chain reaction analyses*', page 207.

2.4 Results

2.4.1 ***The Phenotypic Response of Wild-Type Arabidopsis Plants and the drb Knockout Mutant Lines to Heat, Mannitol and Salt Stress***

All phenotypic and molecular results in this section pertaining to *Arabidopsis* (ecotype Columbia-0 (Col-0)) seedlings can be found in the publication:

Pegler, J. L., Oultram, J. M., Grof, C. P., and Eamens, A. L. (2019). Profiling the Abiotic Stress Responsive microRNA Landscape of *Arabidopsis thaliana*. *Plants*, 8(3), 58.

<https://www.mdpi.com/2223-7747/8/3/58>

A copy of this publication can be found in **Appendix 1 (A.1.3)** of this thesis, pages 193-210.

Post germination and cultivation on standard MS growth media, 8 d old *Arabidopsis* seedlings (Col-0, *drb1*, *drb2*, and *drb4* plant lines) were exposed to a 7 d treatment period of either heat, mannitol or salt stress. The distinct phenotypic response of each plant line to each growth regime, namely, non-stress (control), heat, mannitol or salt stress is presented in **Figure 2.2**. Compared to the non-stress control seedlings of each plant line, stressed Col-0, *drb1*, *drb2*, and *drb4* plants each displayed a unique 'stress induced' phenotype when exposed to a 7 d heat, mannitol or salt stress treatment. Phenotypic markers of stress presented in **Figure 2.2**, include leaf curling and differences in leaf pigmentation (either chlorosis or anthocyanin accumulation). To quantify the phenotypic response of each plant line to each stress treatment, assessments of; (1) fresh weight (**Figure 2.3**); (2) rosette area (**Figure 2.4**); (3) primary root length (**Figure 2.5**); (4) anthocyanin accumulation (**Figure 2.6**), and; (5) chlorophyll *a* and *b* content (**Figure 2.7A-B**) were conducted. It is important to note here that for each phenotypic assessment presented in this Chapter, the response of each plant line to each imposed stress is presented as a percentage of the corresponding measurement determined for the non-stress control counterparts of each plant line (i.e., comparison to non-stress 15 d old Col-0, *drb1*, *drb2* and *drb4* seedlings). In addition, and to further confirm that the phenotypic changes displayed by each *Arabidopsis* line is an accurate reflection that each abiotic stress growth regime elicited a molecular response, the expression level of the well characterised, stress response gene, *P5CS1* (Strizhov *et al.*, 1997; Urano *et al.*, 2009; Yoshida *et al.*, 1999), was assessed via a standard RT-qPCR (**Figure 2.8**).

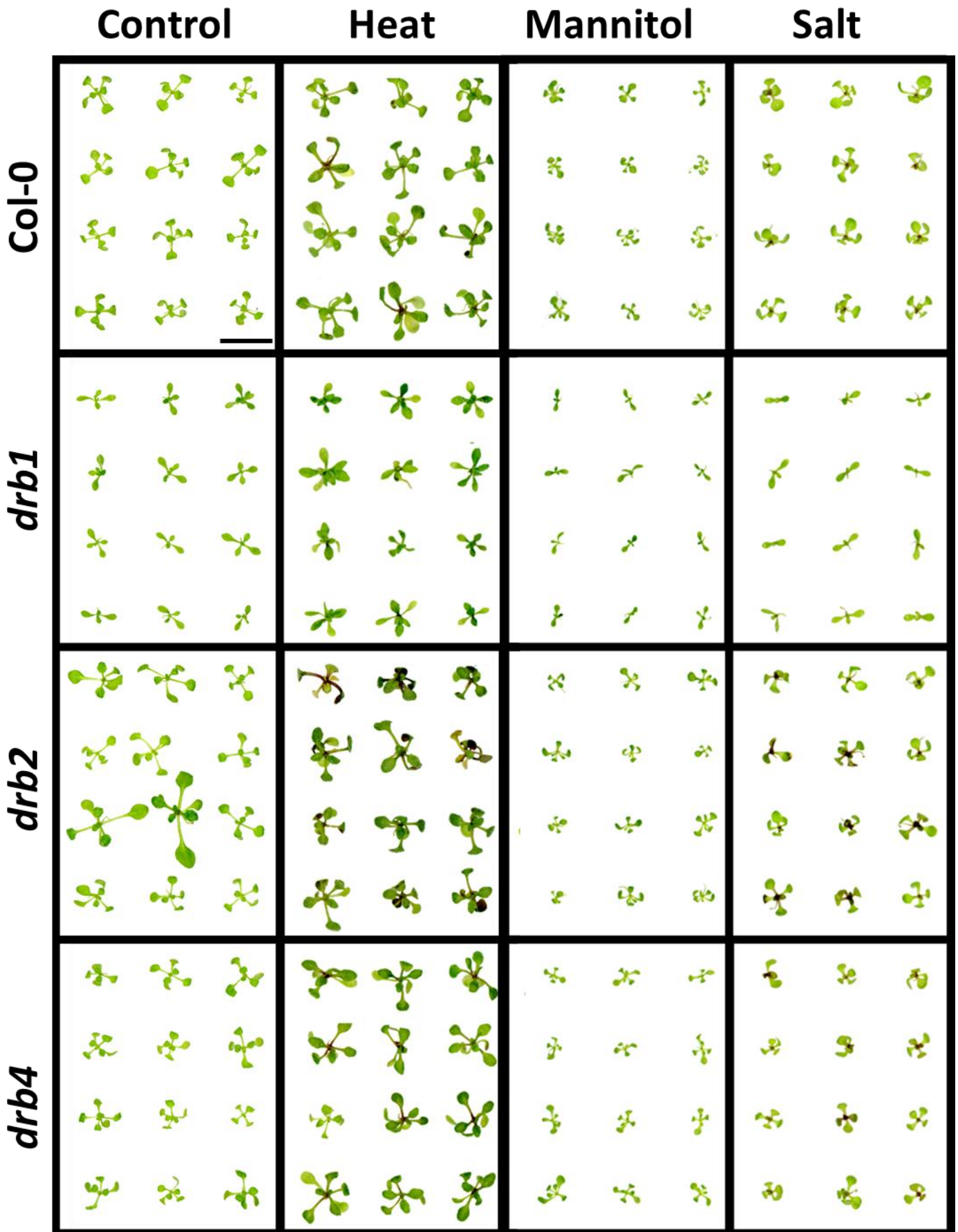


Figure 2.2 Phenotypic and physiological consequence of a heat, mannitol or salt stress treatment on 15 d old wild-type *Arabidopsis* (Col-0) and DRB-knockout mutant lines *drb1*, *drb2* and *drb4*. Phenotypes displayed by 15 d old *Arabidopsis* whole seedlings post a 7 d treatment with heat, mannitol or salt stress, compared to non-stressed seedlings of the same age (left panel). Scale bar = 1.0 centimeter (cm).

2.4.1.1 *Fresh Weight*

One of the most visually striking phenotypic responses displayed by each *Arabidopsis* line under assessment post exposure to the 7 d treatment period of heat, mannitol or salt stress, was modification to the overall shoot architecture (**Figure 2.2**). To quantify this response, the fresh weight of each plant line was determined. Post exposure to heat stress, the fresh weight of all plant lines was significantly increased by 75.3% ($\pm 12.9\%$), 208.2% ($\pm 35.7\%$), 309.1% ($\pm 72.1\%$) and 288.8% ($\pm 99.1\%$), for Col-0, *drb1*, *drb2* and *drb4* plants, respectively (**Figure 2.3**). The observed promotion of fresh weight of 15 d old heat stressed Col-0, *drb1*, *drb2* and *drb4* plants was in direct contrast to the response of each plant line to the 7 d mannitol stress treatment. Specifically, the fresh weight of Col-0, *drb1*, *drb2* and *drb4* plants was significantly decreased by 68.4% ($\pm 0.6\%$), 64.5% ($\pm 0.6\%$), 54.9% ($\pm 0.9\%$) and 57.6% ($\pm 1.3\%$), respectively, in response to the imposed mannitol stress (**Figure 2.3**). Interestingly, unlike the heat and mannitol stress treatments which respectively induced uniform promotion and reduction to the fresh weight of each plant line assessed, the four plant lines under assessment responded differently to the salt stress treatment. Specifically, the 7 d salt stress treatment caused the fresh weight of Col-0 and *drb1* plants to decrease by 23.7% ($\pm 2.2\%$) and 25.1% ($\pm 1.5\%$), respectively. However, the fresh weight of *drb2* and *drb4* plants was determined to be increased by 30.93% ($\pm 5.8\%$) and 27.24% ($\pm 7.5\%$), respectively (**Figure 2.3**). It is important to note here that the response displayed by each plant was determined to be statistically significant, regardless of whether the fresh weight of the plant line was promoted or reduced by the 7 d salt stress treatment period (**Figure 2.3**).

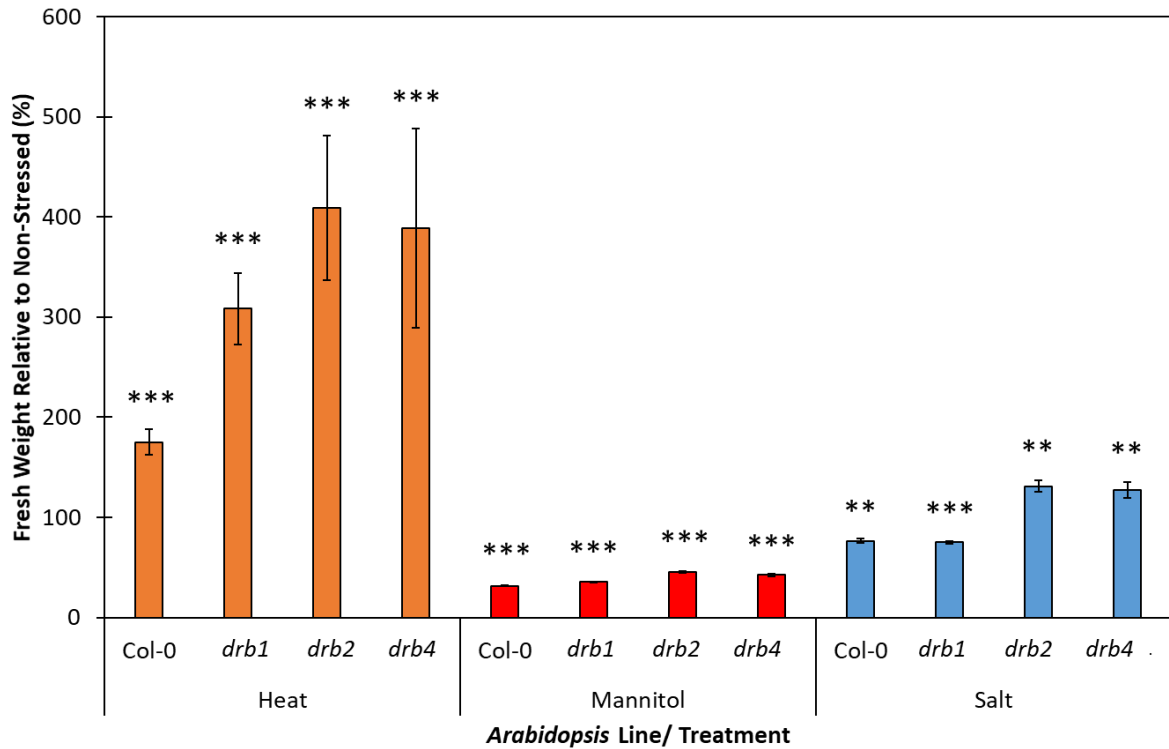


Figure 2.3 Whole seedling fresh weight of heat, mannitol and salt stressed *Arabidopsis* Col-0 and DRB-knockout mutant lines, *drb1*, *drb2* and *drb4*, compared to their non-stressed counterparts of the same age. Error bars represent the \pm SD of 4 biological replicates and each biological replicate consisted of a pool of six individual plants. The presence of an asterisk above a column represents a statistically significant difference between the stress treated sample and the non-stressed control sample (P-value: * < 0.05; ** < 0.005; *** < 0.001).

2.4.1.2 Rosette Area

Alteration of rosette development has been shown to be one of the key phenotypic responses of *Arabidopsis* to a changed growth environment (Claeys *et al.*, 2014). Considering the documented promotion of fresh weight of Col-0, *drb1*, *drb2* and *drb4* plants post their exposure to the 7 d heat stress treatment period (**Figure 2.3**), it was unsurprising to also observe an increase in the rosette area of the four assessed plant lines. Compared to the non-stress control of each plant line under assessment, the 7 d heat stress treatment increased the rosette area of 15 d old Col-0, *drb1*, *drb2* and *drb4* plants by 127.1% ($\pm 5.4\%$), 91.8% ($\pm 26.5\%$), 22.2% ($\pm 6.3\%$) and 109.9% ($\pm 17.0\%$), respectively (**Figure 2.4**). The 7 d mannitol treatment on the other hand, reduced the rosette area of 15 d old Col-0, *drb1*, *drb2* and *drb4* seedlings by 61.7% ($\pm 0.5\%$), 59.4% ($\pm 0.7\%$), 74.7% ($\pm 0.6\%$) and 59.6% ($\pm 1.0\%$), respectively (**Figure 2.4**). The 7 d salt stress treatment was determined to have a similar impact on Col-0, *drb1*, *drb2* and *drb4* development as documented for the mannitol stress. That is, compared to the respective control plants, the rosette area of Col-0, *drb1*, *drb2* and *drb4* plants was reduced by 20.5% ($\pm 2.9\%$), 39.9% ($\pm 1.8\%$), 51.2% ($\pm 0.7\%$) and 27.3% ($\pm 2.2\%$), respectively (**Figure 2.4**). A reduced rosette area for salt-stressed *drb2* and *drb4* plants was unexpected considering that this stress increased fresh weight of these two plant lines by ~31 and 27%, respectively (**Figure 2.3**).

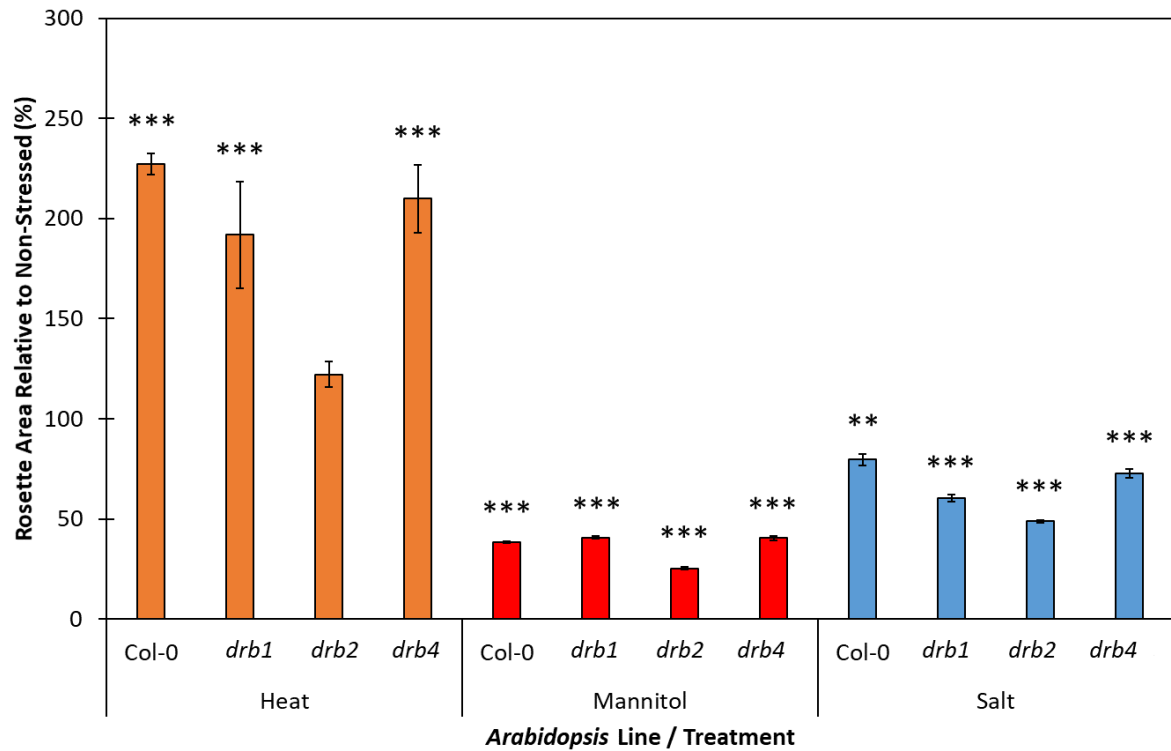


Figure 2.4 Rosette area of heat, mannitol and salt stressed *Arabidopsis* Col-0 and DRB-knockout mutant lines, *drb1*, *drb2* and *drb4*, compared to their non-stressed counterparts of the same age. Error bars represent the \pm SD of 4 biological replicates and each biological replicate consisted of a pool of six individual plants. The presence of an asterisk above a column represents a statistically significant difference between the stress treated sample and the non-stressed control sample (P-value: * < 0.05; ** < 0.005; *** < 0.001).

2.4.1.3 Primary Root Length

A universal phenotypic response of plants to a changed environment, including (but not limited to) variations in water availability (reduced or depleted water supplies), solute toxicity, or the reduced abundance of essential nutrients, is modification to root architecture and function (Acora *et al.*, 2011; Gao *et al.*, 2007; Pasternak *et al.*, 2005). In *Arabidopsis* for example, the elongation rate of the primary root is perturbed in response to elevated salt. Moreover, as the concentration of salt in the growth environment increases, so does the degree of the severity of the phenotypic response (Sun *et al.*, 2008; West *et al.*, 2004). In addition, when a plant organ, such as the root system experiences localised stress, the entire organism responds in an attempt to ensure a degree of 'tolerance' or 'adaption' to the imposed stress. Such a response can only be achieved via complex and interrelated molecular signalling pathways which ensure effective communication between root and shoot tissues (Choi *et al.*, 2014).

Compared to their non-stressed counterparts, primary root length was only reduced by 10.6% ($\pm 3.2\%$) and 7.2% ($\pm 5.5\%$) by the imposed heat stress treatment in Col-0 and *drb1* plants, respectively (**Figure 2.5**). In *drb2* and *drb4* plants however, cultivation for a 7 d period under elevated day and night temperatures, reduced primary root length by 30.9% ($\pm 1.0\%$) and 38.3% ($\pm 5.3\%$), respectively. The mannitol stress treatment failed to influence the primary root length of Col-0 plants (**Figure 2.5**). Furthermore, this stress regime was also determined to only have a mild effect on *drb4* primary root development with the primary root length of mannitol stressed *drb4* plants reduced by 7.3% ($\pm 3.1\%$). Cultivation for a 7 d period on growth media supplemented with mannitol did however significantly impact primary root development in the *drb1* and *drb2* mutant backgrounds with the primary root length of mannitol-stressed *drb1* and *drb2* plants reduced by 29.0% ($\pm 5.2\%$) and 17.3% ($\pm 3.1\%$), respectively (**Figure 2.5**). **Figure 2.5** also clearly shows that for all four plant lines assessed in this study, the imposed salt stress had the greatest impact on primary root development. Specifically, compared to the respective control plants, the primary root length of 15 d old salt-stressed Col-0, *drb1*, *drb2* and *drb4* plants was reduced considerably by 60.0% ($\pm 0.4\%$), 44.3% ($\pm 2.4\%$), 50.4% ($\pm 1.4\%$) and 39.8% ($\pm 1.8\%$), respectively.

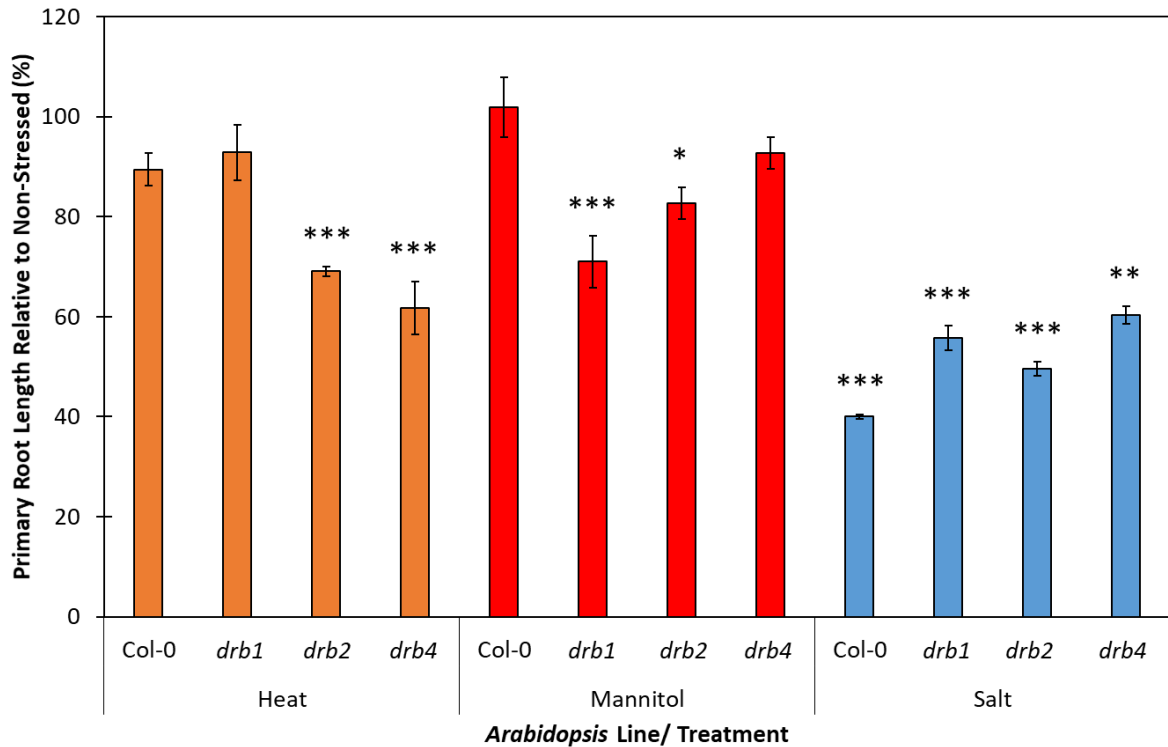


Figure 2.5 Primary root length of heat, mannitol and salt stressed *Arabidopsis* Col-0 and DRB-knockout mutant lines, *drb1*, *drb2* and *drb4*, compared to their non-stressed counterparts of the same age. Error bars represent the \pm SD of 4 biological replicates and each biological replicate consisted of a pool of six individual plants. The presence of an asterisk above a column represents a statistically significant difference between the stress treated sample and the non-stressed control sample (P-value: * < 0.05; ** < 0.005; *** < 0.001).

2.4.1.4 Anthocyanin Accumulation

Figure 2.2 clearly shows that both the imposed heat and salt stress treatments altered the rosette pigmentation of the Col-0, *drb2* and *drb4* plants, and it has been well documented that a common plant defence mechanism to attempt to provide a degree of tolerance to abiotic stresses such as those imposed here, is accumulation of the flavonoid pigment, anthocyanin (Akula and Ravishankar, 2011; Chalker-Scott, 1999; Kovicich *et al.*, 2015). In numerous plant species, anthocyanins accumulate in response to stress due to the ability of anthocyanin to scavenge reactive oxygen species (ROS), toxic biomolecules that would otherwise cause cellular damage if not negated (Chalker-Scott, 1999; Howitz and Sinclair, 2008; Kovicich *et al.*, 2015; Manetas, 2006; Marko *et al.*, 2004; Sperdouli and Moustakas, 2012; Wang *et al.*, 1997).

Quantification of anthocyanin accumulation for heat stressed plants revealed that Col-0, *drb2* and *drb4* seedlings, had significantly increased anthocyanin accumulation of 177.6% ($\pm 52.6\%$), 213.4% ($\pm 14.1\%$) and 134.4% ($\pm 22.0\%$), respectively (**Figure 2.6**). The salt stress treatment induced a similar response in these three plant lines with anthocyanin content increased by 59.3% ($\pm 7.4\%$), 123.3% ($\pm 16.1\%$) and 93.7% ($\pm 25.4\%$) in Col-0, *drb2* and *drb4* plants, respectively (**Figure 2.6**). However, in the *drb1* mutant background, the heat and salt stress treatments failed to result in a statistically significant alteration to anthocyanin abundance compared to its levels in *drb1* control plants (heat = 53.4% ($\pm 26.2\%$), and; salt = 9.2% ($\pm 9.9\%$)). In response to a 7 d cultivation period on mannitol supplemented growth media, the alteration to the abundance of anthocyanin was determined to not be statistically significant for all four assessed *Arabidopsis* plant lines. For example, anthocyanin accumulation remained unchanged between the non-stress controls and mannitol-stressed Col-0 and *drb2* plants, and was only mildly elevated by 23.6% ($\pm 16.9\%$) and 8.6% ($\pm 14.7\%$) in the *drb1* and *drb4* mutant backgrounds, respectively.

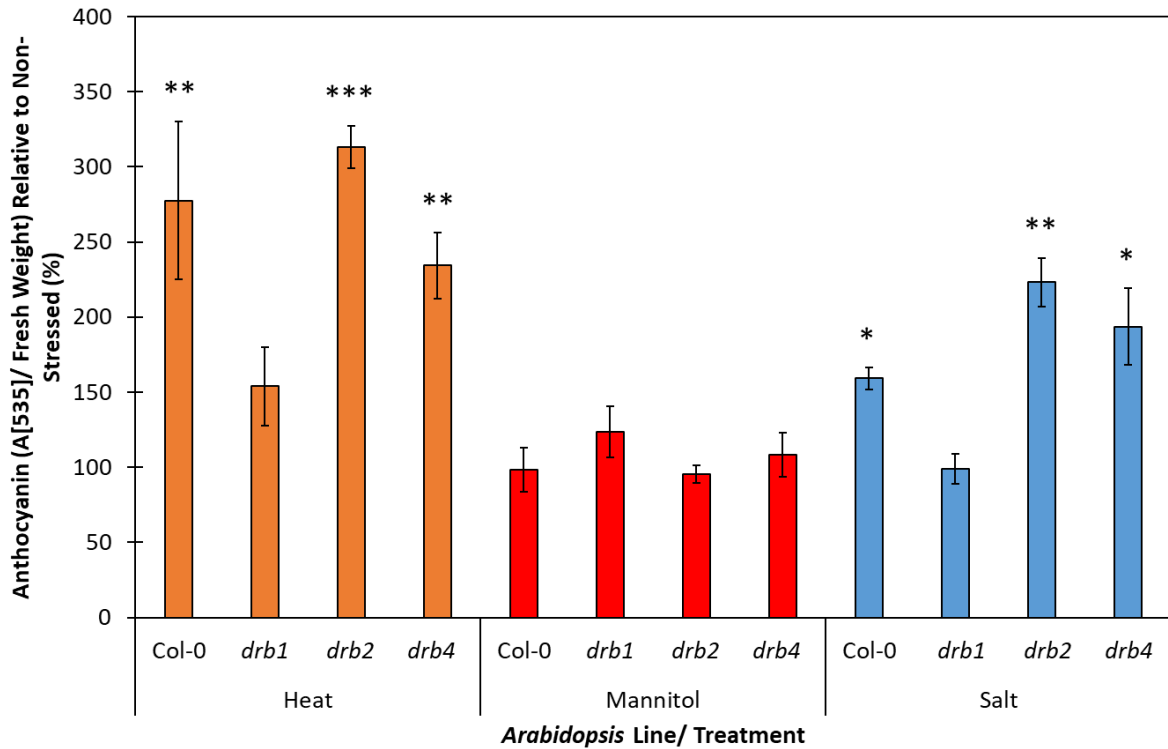


Figure 2.6 Anthocyanin accumulation of heat, mannitol and salt stressed *Arabidopsis* Col-0 and DRB-knockout mutant lines, *drb1*, *drb2* and *drb4*, compared to their non-stressed counterparts of the same age. Error bars represent the \pm SD of 4 biological replicates and each biological replicate consisted of a pool of six individual plants. The presence of an asterisk above a column represents a statistically significantly difference between the stress treated sample and the non-stressed control sample (P-value: * < 0.05; ** < 0.005; *** < 0.001).

2.4.1.5 Chlorophyll *a* and *b* Content

As photosynthesis is the key pathway to fix carbon and to provide energy for plant growth and development, spectrophotometry was used to quantify the abundance of the two central photosynthetic pigments, chlorophyll *a* and *b*. Specifically, the primary photosynthetic pigment, chlorophyll *a* is responsible for converting photons to chemical energy via the light-dependent reactions of photosynthesis (Björn *et al.*, 2009). While chlorophyll *b* is not essential for photosynthesis to occur, it acts as an auxiliary pigment, increasing the absorption spectrum to allow for photosynthesis to continue under a broader range of light regimes (Björn *et al.*, 2009). Due to the essential role that these two energy absorbing pigments play in the photosynthetic pathway, the reduced abundance of either pigment is a strong indicator of the sensitivity of a plant to the imposed abiotic stress (Pasternak *et al.*, 2005; Yamaguchi *et al.*, 2006; Zawoznik *et al.*, 2007). In 15 d old heat stressed Col-0, *drb1*, *drb2* and *drb4* seedlings, spectrophotometric analysis revealed that chlorophyll *a* abundance was significantly elevated by 56.2% ($\pm 0.4\%$), 99.8% ($\pm 20.2\%$), 45.8% ($\pm 6.3\%$) and 58.4% ($\pm 18.1\%$), respectively (**Figure 2.7A**). Conversely, when the same four plant lines were exposed to the 7 d mannitol stress treatment, chlorophyll *a* content was reduced by 23.8% ($\pm 1.7\%$), 34.9% ($\pm 7.2\%$), 57.7% ($\pm 1.4\%$) and 32.0% ($\pm 5.6\%$) in Col-0, *drb1*, *drb2* and *drb4* plants, respectively (**Figure 2.7A**). The 7 d salt stress treatment was also determined to cause significant reductions to the chlorophyll *a* content of Col-0 ($18.3 \pm 1.9\%$), *drb1* ($13.3 \pm 3.6\%$), *drb2* ($25.1 \pm 7.1\%$) and *drb4* seedlings ($29.2 \pm 3.6\%$) (**Figure 2.7A**).

The observed trends for the chlorophyll *a* abundance of each assessed plant line, and abiotic stress treatment, were mirrored by the chlorophyll *b* content data (**Figure 2.7B**). More specifically, exposure to heat stress increased the chlorophyll *b* content of Col-0, *drb1*, *drb2* and *drb4* seedlings by 68.9% ($\pm 3.9\%$), 64.3% ($\pm 25.5\%$), 114.7% ($\pm 23.2\%$) and 82.2% ($\pm 23.1\%$), respectively. In response to the imposed mannitol stress, the chlorophyll *b* content of Col-0, *drb1*, *drb2* and *drb4* seedlings was significantly reduced by 23.4% ($\pm 1.6\%$), 24.5% ($\pm 12.9\%$), 58.1% ($\pm 1.4\%$), and 31.1% ($\pm 6.5\%$), respectively. Similarly, the chlorophyll *b* content of Col-0, *drb1*, *drb2* and *drb4* seedlings was again determined to be significantly reduced by 36.7% ($\pm 8.9\%$), 34.4% ($\pm 1.8\%$), 20.2% ($\pm 7.4\%$), and 27.7% ($\pm 7.8\%$) respectively, in response to the 7 d salt stress treatment.

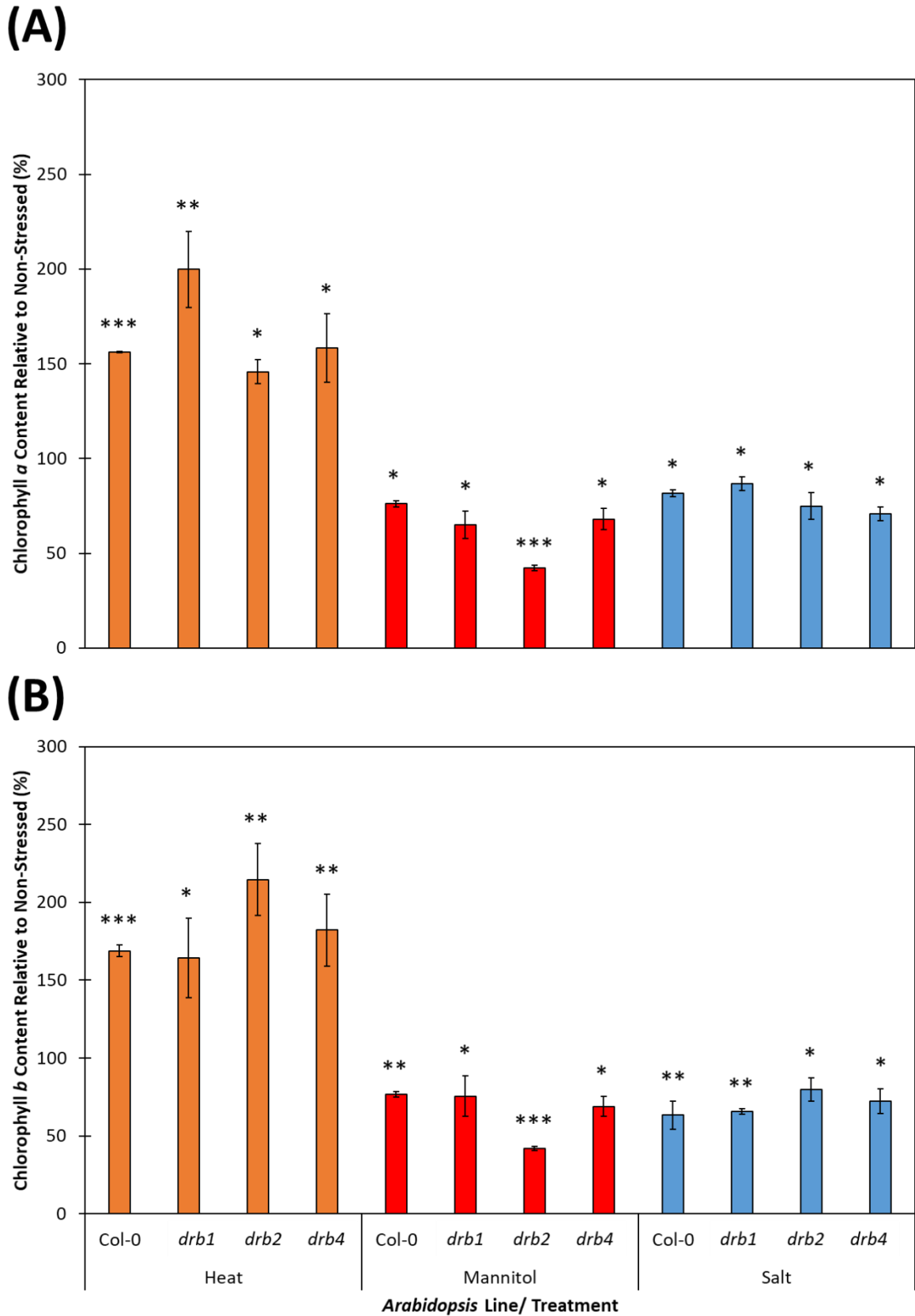


Figure 2.7 Chlorophyll *a* (A) and *b* (B) content of heat, mannitol and salt stressed *Arabidopsis* Col-0 and DRB-knockout mutant lines, *drb1*, *drb2* and *drb4*, compared to their non-stressed counterparts of the same age. Error bars represent the \pm SD of 4 biological replicates and each biological replicate consisted of a pool of six individual plants. The presence of an asterisk above a column represents a statistically significantly difference between the stress treated sample and the non-stressed control sample (P-value: * < 0.05; ** < 0.005; *** < 0.001).

2.4.2 **The Molecular Response of Wild-Type *Arabidopsis* Plants and the *drb* Knockout Mutant Lines to Heat, Mannitol and Salt Stress**

2.4.2.1 **Quantification of the Expression of Δ 1-PYRROLINE 5-CARBOXYLATE SYNTHETASE1 (*P5CS1*)**

The well characterised *Arabidopsis* stress responsive gene, *P5CS1* (*AT2G39800*), encodes for the protein, Δ 1-PYRROLINE-5-CARBOXYLATE SYNTHETASE (*P5CS*); the rate limiting-enzyme of the proline biosynthesis pathway (Székely *et al.*, 2008; Yoshiba *et al.*, 1999). Proline is a crucial amino acid, accumulating in plants in response to a range of abiotic stress stimuli due to its central role in scavenging free radicals and replenishing Nicotinamide Adenine Dinucleotide Phosphate (NADP⁺) levels (Ashraf and Foolad, 2007; Szabados and Savoure, 2010). It is therefore unsurprising that the expression of the *P5CS1* locus is induced in *Arabidopsis* in response to its exposure to the abiotic stresses, dehydration stress, drought stress and salt stress (Strizhov *et al.*, 1997; Urano *et al.*, 2009; Yoshiba *et al.*, 1999).

In order to determine if Col-0, *drb1*, *drb2* and *drb4* plants were responding at the molecular level to the three imposed stresses, *P5CS1* expression was quantified via RT-qPCR. Compared to *P5CS1* expression in Col-0, *drb1*, *drb2* and *drb4* control plants, RT-qPCR revealed *P5CS1* transcript abundance to be significantly elevated by 3.0-, 4.7-, 2.3- and 3.0-fold in heat-stressed Col-0, *drb1*, *drb2* and *drb4* plants, respectively (**Figure 2.8**). Similarly, the mannitol stress treatment was also demonstrated by RT-qPCR to induce *P5CS1* expression in Col-0, *drb1*, *drb2* and *drb4* plants by 1.7-, 8.0-, 2.5- and 2.6-fold, respectively (**Figure 2.8**). **Figure 2.8** further clearly shows that the 7 d salt stress treatment also induced the expression of *P5CS1* in all four plant lines under assessment. Specifically, *P5CS1* levels were determined to be elevated by 45.2-, 15.5-, 6.5- and 4.2-fold respectively, in salt-stressed Col-0, *drb1*, *drb2* and *drb4* plants.

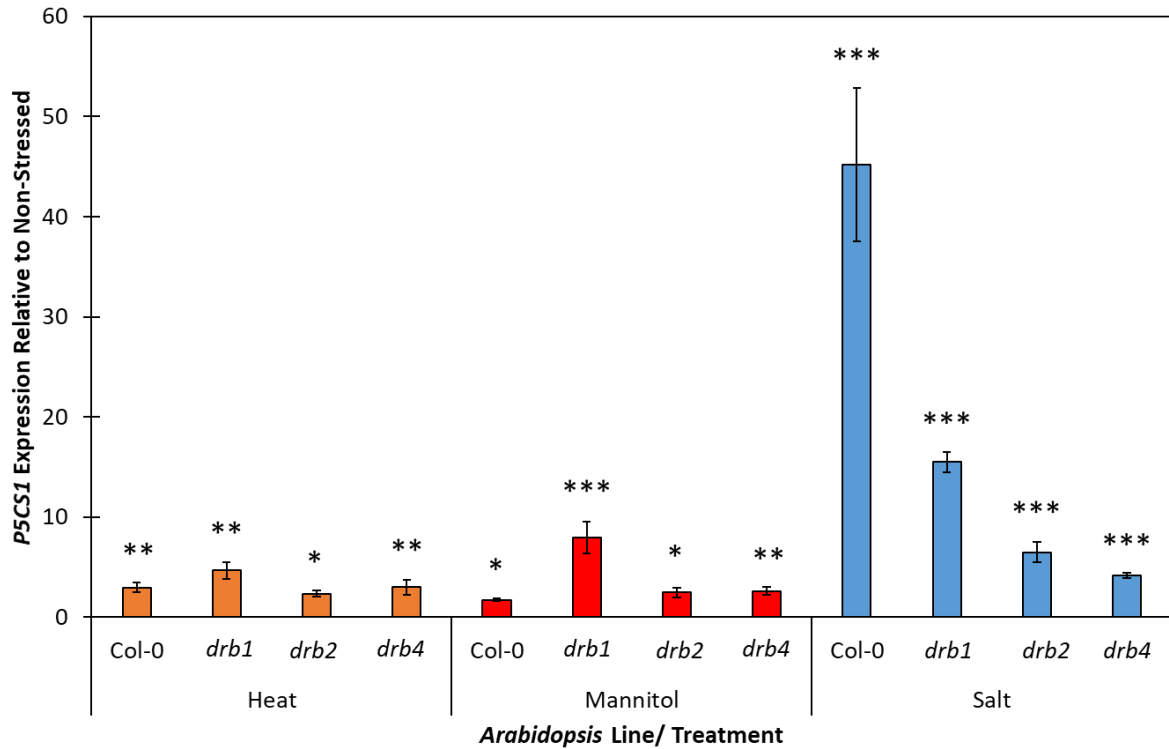


Figure 2.8 RT-qPCR analysis of *P5CS1* expression in heat, mannitol and salt stressed *Arabidopsis* Col-0 and DRB-knockout mutant lines, *drb1*, *drb2* and *drb4*, compared to their non-stressed counterparts of the same age. Error bars represent the \pm SD of 4 biological replicates with each biological replicate consisting of 6 individual plants. The presence of an asterisk above a column represents a statistically significant difference between the stress treated sample and the non-stressed control sample (P-value: * < 0.05; ** < 0.005; *** < 0.001).

2.4.2.2 *The Use of High Throughput Sequencing to Determine the Contribution of DRB1, DRB2 and DRB4 to the MicroRNA Landscape of Arabidopsis thaliana*

It is well established that the three nuclear DRB proteins, DRB1, DRB2 and DRB4, are core pieces of protein machinery required for sRNA production, including miRNA production, across a range of *Arabidopsis* tissues (Eamens *et al.*, 2011; Eamens *et al.*, 2012a; Hiraguri *et al.*, 2005; Pélissier *et al.*, 2011; Pouch- Pélissier *et al.*, 2008). In an attempt to further define the contribution of DRB1, DRB2 and DRB4 to the production stage of the *Arabidopsis* miRNA pathway, a high throughput sequencing approach was employed to profile the sRNA fraction of Col-0, *drb1*, *drb2* and *drb4* whole seedlings cultivated under standard growth conditions and post their exposure to the abiotic stress of heat, mannitol and salt stress.

The sRNA-seq approach revealed that compared to 15 d old Col-0 control seedlings, the abundance of 73, 1 and 31 miRNA sRNAs was significantly (>2.0-fold) downregulated in 15 d old *drb1*, *drb2* and *drb4* control seedlings, respectively (**Figure 2.9**). Additionally, and again compared to 15 d old Col-0 controls, 5, 14 and 11 miRNAs were determined to have significantly upregulated abundance in the *drb1*, *drb2*, and *drb4* controls (**Figure 2.9**). Three additional miRNA cohorts were also identified via this profiling approach, namely; (1) 19 miRNAs had significantly elevated abundance in 2 or 3 of the assessed *drb* mutant backgrounds; (2) the abundance of 10 miRNAs was reduced by more than 2.0-fold in 2 of the 3 *drb* mutants assessed, and; (3) 34 miRNAs had reciprocal abundance trends (significantly elevated or reduced abundance in the different *drb* mutants) in either one or both of the other two *drb* mutants assessed (**Figure 2.9**).

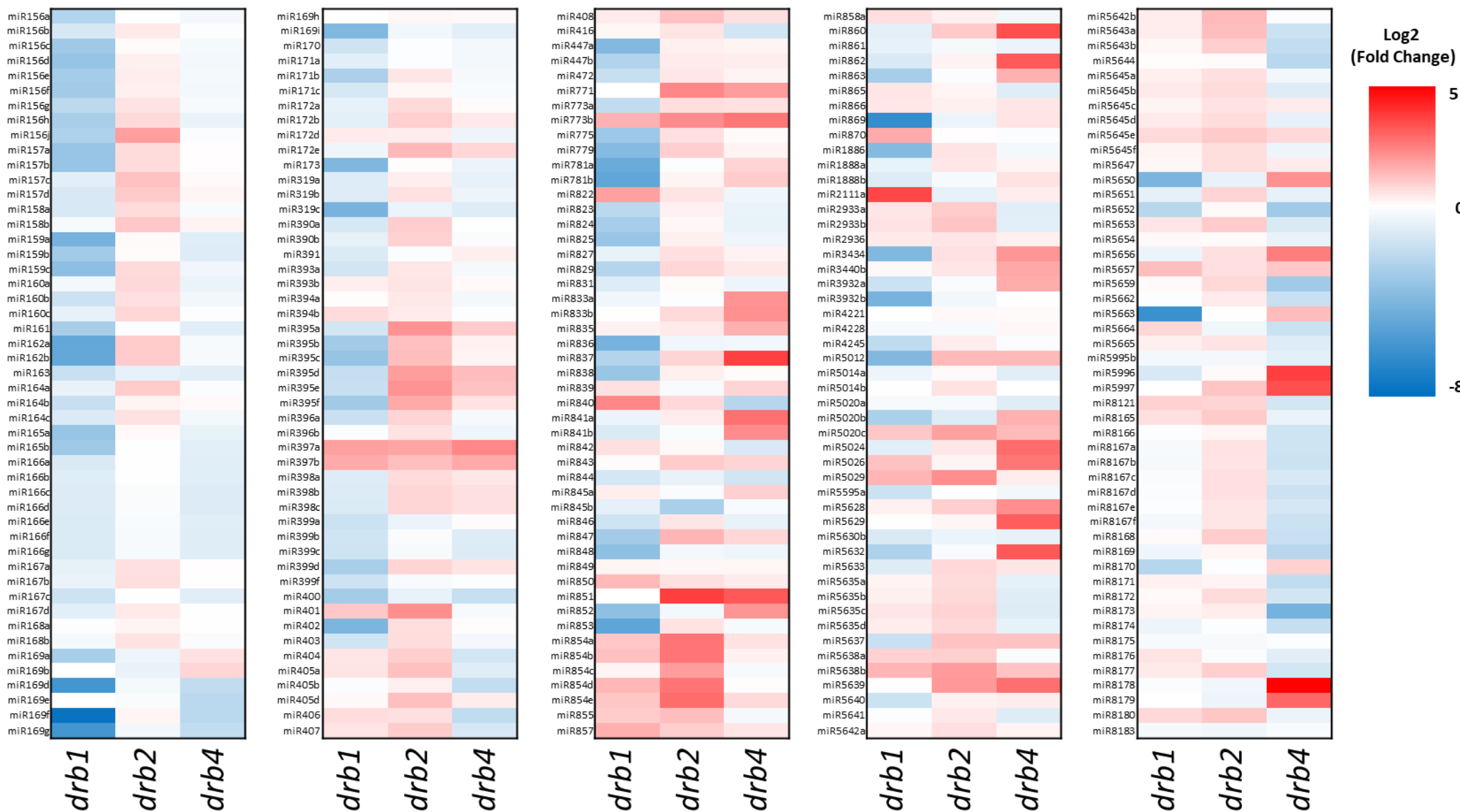


Figure 2.9 Heat map of miRNA accumulation in the *Arabidopsis* DRB mutants, *drb1*, *drb2* and *drb4*. Red and blue tiles indicate a Log2 fold-change up or down, respectively, in the abundance of each miRNA comparative to *Arabidopsis* Col-0 seedlings.

2.4.2.3 *The Use of High Throughput Sequencing to Profile the MicroRNA Landscape of Heat, Mannitol and Salt Stressed Col-0, drb1, drb2 and drb4 Plants*

Post characterisation of the phenotypic and physiological consequences of exposing 15 d old *Arabidopsis* Col-0, *drb1*, *drb2* and *drb4* seedlings to a 7 d heat, mannitol or salt stress growth regime (see **Sections 2.4.1- 2.4.1.5**), sRNA-seq was further utilised to profile the miRNA landscape of each *Arabidopsis* line. This approach revealed that compared to the control of each plant line, large miRNA cohorts were either significantly (>2.0-fold) up- or downregulated in abundance post stress exposure (**Figure 2.10**). More specifically, compared to wild-type control seedlings, the abundance of 121, 123 and 118 miRNAs was significantly altered in heat, mannitol and salt stressed Col-0 seedlings, respectively. In *drb1* whole seedlings exposed to heat, mannitol or salt stress, 100, 101 and 82 miRNAs were determined to have significantly altered abundance. A total of 108, 58 and 83 miRNAs were significantly altered in their abundance in *drb2* seedlings post the exposure of this plant line to heat, mannitol and salt stress, respectively. In heat, mannitol and salt stressed *drb4* seedlings, sRNA-seq revealed that 184, 95 and 108 miRNAs were significantly altered in abundance, respectively.

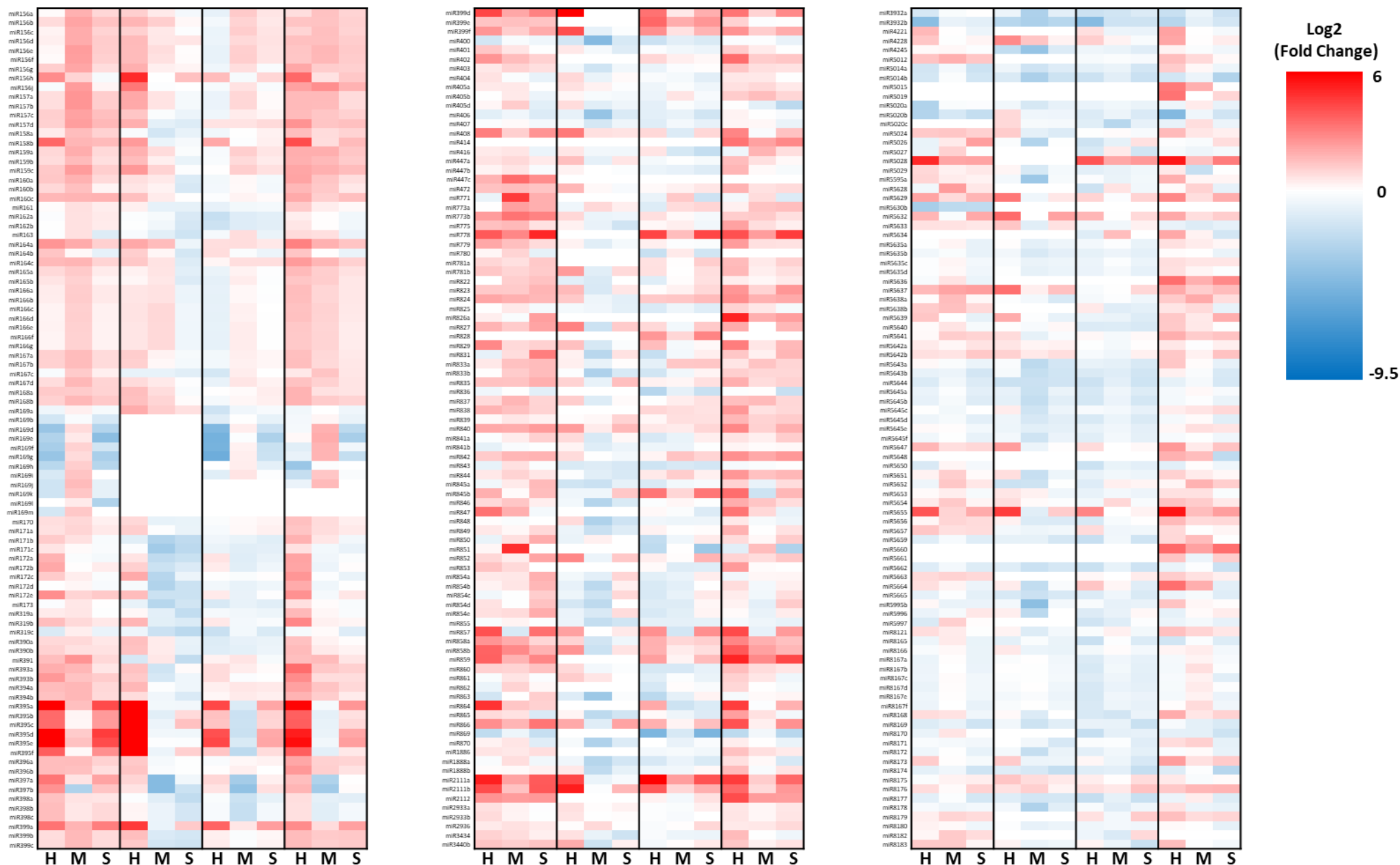


Figure 2.10 Small-RNA sequencing analysis of the miRNA accumulation profiles of 15 d old *Arabidopsis* Col-0 seedlings and DRB-Knockout mutants, *drb1*, *drb2* and *drb4* seedlings exposed to heat (H), mannitol (M) or salt stress (S), relative to non-stressed control counterparts. Red and blue tiles indicate a Log₂ fold-change up or down, respectively, in the abundance of each miRNA.

2.4.2.4 *RT-qPCR Analysis of DCL1, DRB1, DRB2 and DRB4 Expression in Heat, Mannitol and Salt Stressed Col-0, drb1, drb2 and drb4 Plants*

In an attempt to generate a more detailed understanding of what was occurring at a molecular level in heat, mannitol and salt stressed *Arabidopsis* seedlings, RT-qPCR was employed to assess variations in the gene expression of key miRNA pathway protein machinery (**Figure 2.11**). This analysis was utilised to identify changes in *DCL1*, *DRB1*, *DRB2* and *DRB4* transcript levels in heat, mannitol and salt stressed *Arabidopsis* seedlings relative to the control grown Col-0 counterparts. Specifically, all the RT-qPCR data on the expression *DCL1*, *DRB1*, *DRB2* and *DRB4* in each of the *Arabidopsis* seedlings in **Figure 2.11** is presented relative to non-stressed Col-0 seedlings to further allow for the documentation of any redundant, competitive or hierarchical relationships of *DRB1*, *DRB2* and *DRB4* under standard growth conditions, in addition to further documenting the role of *DCL1*, and the three nuclear *DRBs* in the response of *Arabidopsis* plants to heat, mannitol or salt stress.

In comparison to control grown Col-0 seedlings, RT-qPCR analysis revealed that exposure to heat stress failed to significantly alter the expression of *DCL1* (-1.1-fold) and *DRB4* (1.5-fold), while the expression of *DRB1* and *DRB2* were significantly elevated by 1.8- and 2.7-fold, respectively. When Col-0 seedlings were grown on media supplemented with 200 mM mannitol, significant reductions of 1.7-fold were observed for both *DCL1* and *DRB1* expression, in contrast to the mild increases in expression observed for *DRB2* (1.3-fold) and *DRB4* (1.1-fold). Similarly, salt stress treatment of Col-0 seedlings resulted in a significant 1.5-fold reduction in *DCL1* expression. However, the expression of *DRB1*, *DRB2* and *DRB4* were all determined to be significantly elevated in comparison to the control grown counterparts (1.4-, 3.6- and 1.6-fold, respectively).

As previous research has demonstrated that in specific *Arabidopsis* tissues where there is overlap of *DRB* expression / *DRB* localisation, *DRB2* is antagonistic to the expression of *DRB1* and *DRB4* (Eamens *et al.*, 2012a; Pélissier *et al.*, 2011; Reis *et al.*, 2015), confirmation of the expression profiles of *DCL1*, *DRB1*, *DRB2* and *DRB4* in non-stressed *drb1*, *drb2* and *drb4* seedlings was next sort. This assessment revealed that the expression of *DCL1* in non-stressed *drb1* seedlings was significantly upregulated 1.7-fold. As expected, *DRB1* expression was not detected in *drb1* seedlings. In the absence of *DRB1* expression in the *drb1* mutant, *DRB2* expression was elevated by 2.6-fold, while the expression of *DRB4* was reduced by 1.4-fold. Comparable to the change in *DCL1* expression in control grown *drb1* seedlings, when *drb1* seedlings were exposed to heat stress, *DCL1* expression was significantly upregulated 1.6-fold, while the expression levels of *DRB2* and *DRB4* were determined to be greatly upregulated 7.4- and 5.9-fold, respectively. Comparative to the

observed expression changes for *DRB2* and *DRB4* in heat stressed Col-0 seedlings, the much larger increases observed for heat stressed *drb1* seedlings readily highlights the dramatic impact the absence of a DRB has on the expression of the other DRBs. Post exposure to a 7 d mannitol stress treatment, again *drb1* seedlings presented a significant 1.7-fold upregulation of *DCL1* expression levels. In contrast, *DRB2* expression was mildly reduced 1.1-fold while, *DRB4* expression was upregulated 2.9-fold. Identical to the response of *drb1* seedling exposed to each of the other growth regimes of this study, when treated with 150 mM salt stress for 7 d, *DCL1* expression was significantly upregulated 1.6-fold. Further, in the same *drb1* seedlings exposed to a salt stress growth regime, *DRB2* was significantly upregulated 1.7-fold and *DRB4* was only mildly upregulated 1.2-fold.

When *drb2* seedlings were grown under standard growth conditions it was determined that the expression levels of *DCL1* remained unchanged from non-stressed Col-0 counterparts (1.1- fold) while *DRB1* expression was elevated 2.1-fold. As expected, *DRB2* expression was not detected in control grown *drb2* seedlings, nor in *drb2* seedlings exposed to each stress regime. Analysis of *DRB4* expression revealed a significant reduction of 2.8-fold in control grown *drb2* seedlings when compared to identically grown Col-0 seedlings. Alike non-stressed *drb2* seedlings, when grown under elevated temperatures, *drb2* seedlings presented no significant alteration to *DCL1* expression levels (1.2-fold). However, RT-qPCR analysis revealed the expression levels of *DRB1* and *DRB4* were significantly increased, 1.9- and -2.5-fold, respectively. Similarly to the response of control grown *drb2* seedlings, when *drb2* seedlings were grown in the presence of 200 mM mannitol for 7 d, both *DCL1* and *DRB1* expression levels remained insignificantly altered (-1.3-fold and unchanged, respectively), while again, *DRB4* expression was found to be greatly reduced (2.4-fold). As with the *drb2* seedlings exposed to each of the other growth regimes, the expression level of *DCL1* in salt stressed *drb2* seedlings remained insignificantly changed (1.1-fold) and *DRB4* expression levels were significantly decreased 2.1-fold. Following the elevated expression trend in *drb2* seedlings exposed to heat stress, *DRB1* was elevated 1.5-fold in *drb2* seedlings exposed to a 7 d salt stress, however this alteration was not determined to be statistically significant.

When grown under standard growth conditions, *drb4* seedlings presented no significant alteration to *DCL1* or *DRB2* expression levels (reduced 1.1-, 1.2-fold, respectively) in comparison to non-stressed wild-type expression levels. Interestingly, the expression level of *DRB1* was determined to be greatly upregulated 3.2-fold. Alike, *drb1* and *drb2* seedlings, RT-qPCR further confirmed that *drb4* seedlings are defective in the production of the respective *DRB*, *DRB4*. As such, *DRB4* expression levels were not detected in any *drb4* seedlings regardless of the growth conditions they were cultivated on. When *drb4* seedlings were exposed to a heat stress growth regime, both *DCL1* and *DRB1* were significantly

elevated (2.9- and 10.6-fold, respectively). Contrastingly, the expression of *DRB2* was found to be mildly reduced 1.3-fold in the same heat stressed *Arabidopsis* seedlings. Almost identically to the response of *drb4* seedlings cultivated under a standard control growth regime, *drb4* seedlings exposed to a mannitol stress treatment displayed both unaffected *DCL1* expression levels (-1.3-fold) and a significant 2.8-fold increase in *DRB1* expression levels. It was therefore not surprising that in the same mannitol stressed *drb4* seedlings, *DRB2* expression was significantly reduced 2.6-fold. The exposure of *drb4* seedlings to a 7 d salt stress growth regime resulted in very similar expression trends observed for *drb4* seedlings cultivated under each of the growth regimes of this study. Specifically, *DCL1* expression levels were mildly elevated 1.3-fold, while *DRB1* expression was significantly elevated 6.0-fold. Inversely, the expression of *DRB2* in the same *drb4* seedlings was found to be significantly reduced 1.7-fold.

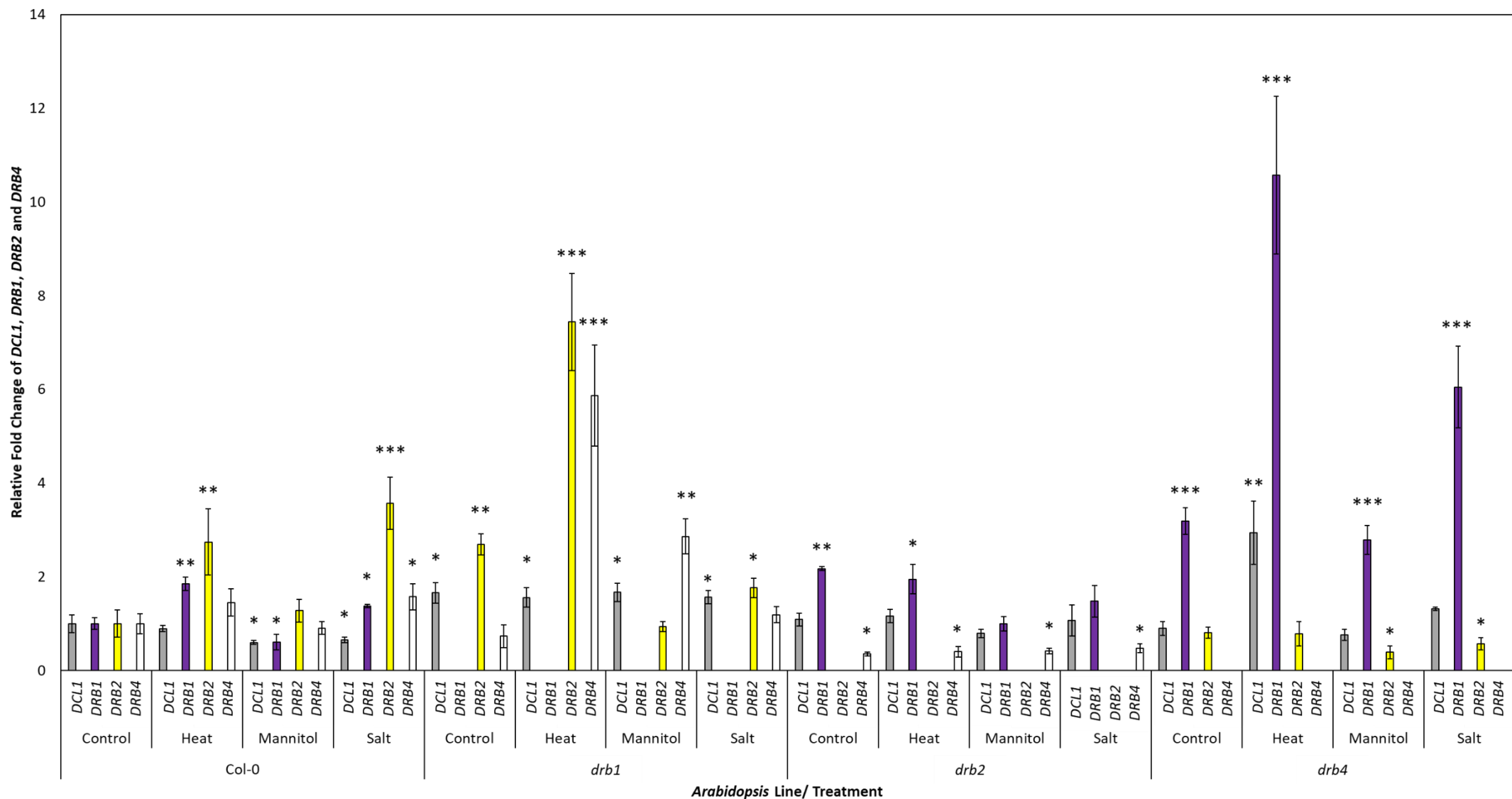


Figure 2.11 RT-qPCR assessment of *DCL1*, *DRB1*, *DRB2* and *DRB4* in non-stressed and stress treated *Arabidopsis* plant lines. The RT-qPCR determined expression of *DCL1* (grey), *DRB1* (purple), *DRB2* (yellow) and *DRB4* (white) in *Arabidopsis* Col-0 seedlings and DRB-knockout mutants, *drb1*, *drb2* and *drb4* exposed to each abiotic stress is presented relative to control grown Col-0 seedlings. Error bars represent the \pm SD of 4 biological replicates with each biological replicate consisting of 6 individual plants. The presence of an asterisk indicates a statistically significant difference between the expression of each gene determined for control Col-0 seedling (p-value: < 0.05, *; P < 0.005, **; P < 0.001, ***).

2.4.2.5 *Experimental Validation of Altered MicroRNA Abundance in Control and Abiotically Stressed Wild-Type Arabidopsis Whole Seedlings*

To experimentally validate the miRNA abundance changes documented via high throughput sequencing of the sRNA fraction of non-stressed and heat, mannitol and salt stressed wild-type *Arabidopsis* whole seedlings, a modified RT-qPCR approach was applied. This analysis can be found in the publication:

Pegler, J. L., Oultram, J. M., Grof, C. P., and Eamens, A. L. (2019). Profiling the Abiotic Stress Responsive microRNA Landscape of *Arabidopsis thaliana*. *Plants*, 8(3), 58.

<https://www.mdpi.com/2223-7747/8/3/58>

A copy of this publication can be found in **Appendix 1 (A.1.3)** of this thesis (pages 193-210), with the respective RT-qPCR validation of sRNA-seq determined miRNA accumulation trends located on page 199.

Subsequent to RT-qPCR validation of altered miRNA abundance in non-stressed and heat, mannitol and salt stressed Col-0 seedlings, three highly conserved plant miRNAs, namely miR396, miR399 and miR408, were selected for further molecular characterisation. The selection of miR396, miR399 and miR408 for further molecular characterisation was based on; (1) the significant alteration in the abundance of each miRNA in response to exposing 15 d old Col-0 seedlings to heat, mannitol and salt stress (**Figure 2.10**), and; (2) the known role(s) of the respective target genes of these three miRNAs in standard *Arabidopsis* development and/or post exposure of *Arabidopsis* to abiotic stress (Bari *et al.*, 2006; Hewezi and Baum, 2012; Pilon, 2017; Van der Knaap *et al.*, 2000).

2.4.2.6 *Molecular Profiling of the miR396 Regulatory Module in Heat, Mannitol and Salt Stressed Col-0, drb1, drb2 and drb4 Whole Seedlings*

In several plant species, the miR396 sRNA has been demonstrated to be a key transcriptional regulator of several members of the GROWTH REGULATING FACTOR (GRF) family of plant-specific transcription factors (Hewezi and Baum, 2012; Liu *et al.*, 2009; Omidbakhshfard *et al.*, 2015). In *Arabidopsis*, the known miR396 target gene, *GRF7* (*AT5G53660*) and its encoded protein, GRF7, has been proposed to play a central role in mounting an adaptive response to the abiotic stresses of heat, mannitol and salt stress (Kim *et al.* 2012). Therefore, *GRF7* was selected as the target gene to molecularly profile in parallel to its targeting miRNA, miR396. A RT-qPCR approach was first employed to confirm the accuracy of the miR396 abundance trends determined for heat, mannitol and salt stressed seedlings, compared to the non-stressed counterpart of each respective *Arabidopsis* line, as determined by sRNA sequencing.

This approach confirmed the miR396 abundance trends determined by sequencing, except for heat stressed *drb1* seedlings (**Figure 2.12A**). More specifically, sRNA-seq indicated that compared to non-stressed Col-0, miR396 abundance was elevated by 3.0-, 2.9- and 1.9-fold in heat, mannitol and salt stressed Col-0 seedlings, respectively (**Figure 2.12A**). RT-qPCR confirmed elevated trends in abundance for heat, mannitol and salt stressed Col-0 seedlings with the quantified level of the miR396 sRNA determined to be elevated by 2.9-, 3.1- and 2.8-fold, respectively (**Figure 2.12A**). In the *drb1* background, sRNA-seq indicated that in response to heat, mannitol and salt stress exposure, the abundance of the miR396 sRNA was elevated by 2.6-fold, mildly reduced by 0.2-fold, and remained unchanged, respectively (**Figure 2.12A**). Interestingly, RT-qPCR quantification of miR396 abundance revealed a different accumulation trend, a 2.6-fold reduction, for heat stressed *drb1* seedlings, and not an elevated level of the miR396 sRNA as determined by sequencing. In mannitol-stressed *drb1* seedlings, RT-qPCR determined that the level of the miR396 sRNA was significantly reduced by 4.2-fold compared to its levels in non-stressed *drb1* whole seedlings: a more severe reduction than the mild 0.2-fold reduction to miR396 levels as indicated by sRNA-seq. RT-qPCR again revealed miR396 abundance to be reduced, albeit a mild 0.4-fold reduction, post exposure of *drb1* plants to the salt stress treatment. However, this trend again differed to that identified via sRNA-seq which indicated that miR396 abundance remained unchanged in salt-stressed *drb1* whole seedlings.

In comparison to non-stressed *drb2* whole seedlings, sRNA-seq revealed miR396 abundance remained unchanged by the heat stress treatment and only mildly elevated by the mannitol (0.2-fold) and salt stress (0.1-fold) treatments (**Figure 2.12A**). The RT-qPCR

approach revealed largely similar trends in abundance post heat, mannitol and salt stress treatment of *drb2* seedlings, that is; miR396 abundance was mildly reduced by 0.1-fold by both the heat and salt stress treatments and was elevated by 0.5-fold in response to mannitol stress treatment (**Figure 2.12A**). In heat, mannitol and salt stressed *drb4* whole seedlings, sRNA-seq revealed miR396 abundance to be elevated by 4.8-, 2.2- and 0.8-fold, respectively. Elevated miR396 abundance was confirmed by RT-qPCR which documented 2.7-, 2.5- and 2.0-fold increases in miR396 levels in heat, mannitol and salt stressed *drb4* whole seedlings, respectively (**Figure 2.12A**).

The expression of *GRF7*, the selected target gene of miR396, was next assessed via RT-qPCR (**Figure 2.12B**). Compared to non-stressed Col-0 whole seedlings, *GRF7* expression was significantly reduced by 2.2-, 2.7- and 2.7-fold in heat, mannitol and salt stressed Col-0 seedlings, respectively. Reduced *GRF7* expression in heat, mannitol and salt stressed Col-0 whole seedlings was expected considering that the abundance of the targeting miRNA, miR396, was elevated by these three stress regimes in wild-type seedlings (**Figure 2.12A**). In heat stressed *drb1* whole seedlings, *GRF7* expression was elevated by 2.2-fold. Elevated *GRF7* expression in heat stressed *drb1* plants was expected considering that miR396 abundance was demonstrated to be reduced by 2.6-fold by RT-qPCR (**Figure 2.12A**). *GRF7* expression was also determined to be reduced by 1.8- and 2.6-fold respectively, in mannitol and salt stressed *drb1* plants (**Figure 2.12B**). This expression trend formed an interesting result with the abundance of the *GRF7* transcript scaling with the reduced accumulation of its targeting miRNA, miR396, in mannitol and salt stressed *drb1* whole seedlings (**Figure 2.12A**). Compared to the expression in non-stressed *drb2* whole seedlings, *GRF7* transcript abundance was reduced by 2.4-, 2.0- and 2.2-fold in heat, mannitol and salt stressed *drb2* plants. This again formed an unexpected result considering that miR396 levels were determined to remain largely unchanged in heat and salt stressed *drb2* plants, and only mildly elevated (0.5-fold) in the *drb2* mutant background post the mannitol stress treatment (**Figure 2.12A**). In mannitol and salt stressed *drb4* whole seedlings, RT-qPCR revealed *GRF7* expression to be reduced by 1.7 and 2.5-fold, respectively. Curiously, RT-qPCR repeatedly failed to detect the *GRF7* transcript in *drb4* whole seedlings post their exposure to the heat stress regime (**Figure 2.12B**). In mannitol and salt stressed *drb4* plants however, miR396 abundance was determined to be elevated by 2.5- and 2.0-fold, respectively (**Figure 2.12A**). Therefore, reduced *GRF7* expression in this mutant background post its exposure to mannitol and salt stress was expected.

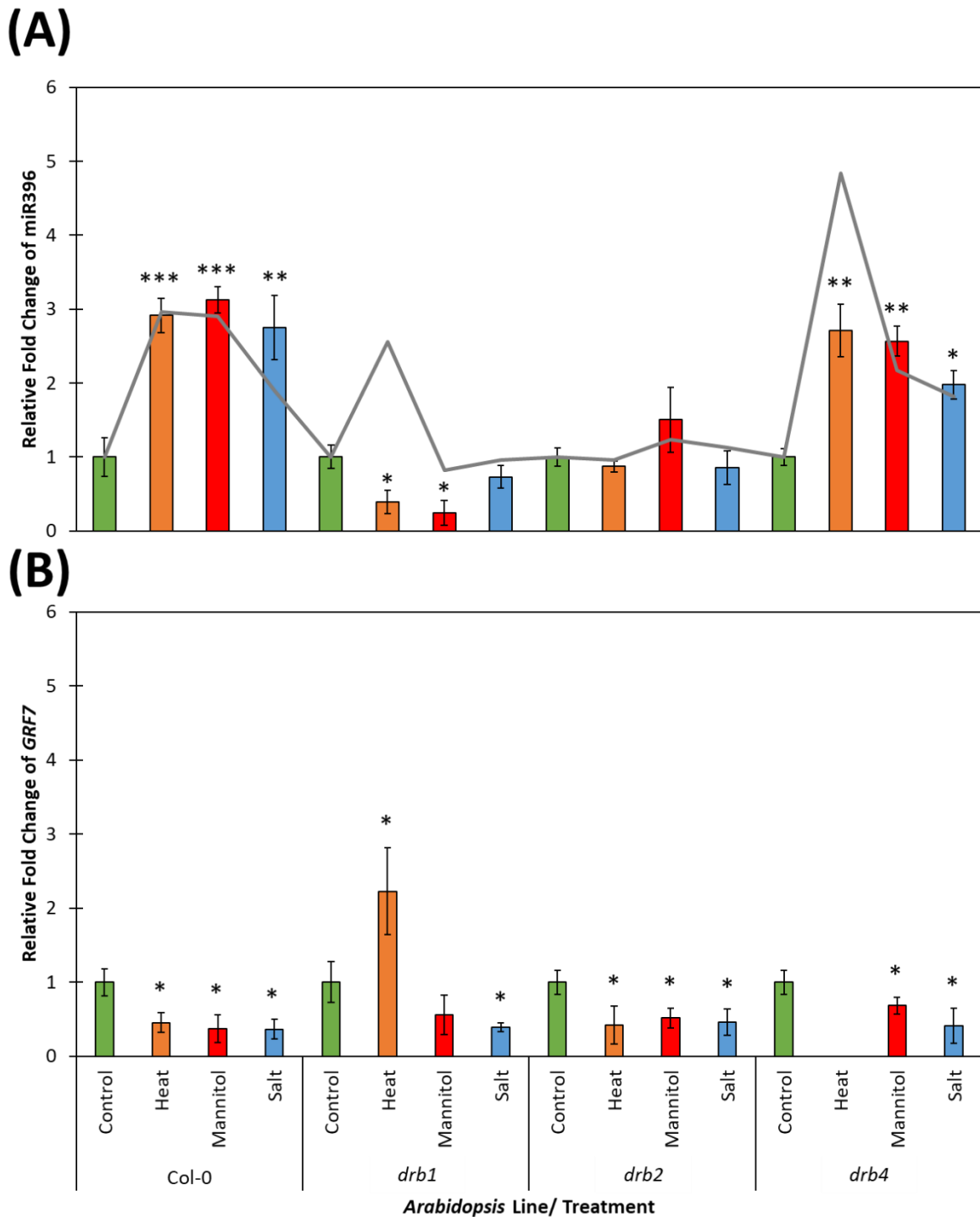


Figure 2.12 Molecular analysis of the miR396/GRF7 regulatory module in 15 d old *Arabidopsis* Col-0 seedlings and DRB-knockout mutants, *drb1*, *drb2* and *drb4* exposed to heat, mannitol or salt stress, relative to untreated (control) seedlings. (A) The SL-RT-qPCR determined abundance of miR396 in *Arabidopsis* Col-0 seedlings and DRB-knockout mutants, *drb1*, *drb2* and *drb4* exposed to each abiotic stress is presented as fold-change relative to control grown seedlings for each *Arabidopsis* line (coloured bars). The grey line indicates the respective fold-change in miR396 accumulation for each *Arabidopsis* line as assessed with sRNA-seq. (B) RT-qPCR analyses of miR396 target gene, *GRF7*, expression changes of *Arabidopsis* lines, Col-0, *drb1*, *drb2* and *drb4* in response to heat, mannitol or salt stress, compared to non-stress growth conditions. Error bars represent the \pm SD of 4 biological replicates with each biological replicate consisting of 6 individual plants. The presence of an asterisk indicates a statistically significant difference between the control and stress treated seedlings for miR396 and *GRF7* (p-value: < 0.05, *; P < 0.005, **; P < 0.001, *).**

2.4.2.7 *Molecular Profiling of the miR399 Regulatory Module in Heat, Mannitol and Salt Stressed Col-0, drb1, drb2 and drb4 Whole Seedlings*

The regulation of *PHOSPHATE2* (*PHO2*; *AT2G33770*) by miR399 is required for *Arabidopsis* to mount an adaptive response to conditions of low inorganic phosphorous (Pi) (Fujii *et al.*, 2005; Hsieh *et al.*, 2009; Liu *et al.*, 2014). This well documented miR399/*PHO2* regulatory module in response to Pi deficiency, in conjunction with the sRNA-seq data (**Figure 2.10**), which indicated that the miR399 sRNA is also responsive to heat, mannitol and salt stress, presented the miR399 regulatory module as an ideal candidate for further investigation.

Initially, an RT-qPCR based approach was employed to experimentally validate the miR399 abundance trends identified by sequencing. As demonstrated for the miR396 sRNA, RT-qPCR quantification of the abundance of miR399 supported the sequencing results (**Figure 2.13A**). Specifically, sRNA-seq revealed that compared to non-stressed Col-0 whole seedlings, the abundance of the miR399 sRNA was elevated by 7.0-, 3.2- and 4.4-fold in heat, mannitol and salt stressed Col-0 seedlings, respectively (**Figure 2.13A**). This trend of upregulated levels of the miR399 sRNA in Col-0 whole seedlings exposed to the three assessed stresses was confirmed by RT-qPCR which showed that miR399 abundance was elevated by 2.2-, 2.7- and 2.9-fold for heat, mannitol and salt stressed Col-0 plants, respectively (**Figure 2.13A**). In the *drb1* mutant background, sRNA-seq indicated that compared to non-stressed *drb1* whole seedlings, miR399 abundance was greatly elevated by 28.0-fold post the application of the 7 d heat stress growth regime. However, RT-qPCR quantification in heat stressed *drb1* plants revealed a very different accumulation trend for miR399, that is; miR399 abundance was reduced by 0.6-fold (**Figure 2.13A**). Similar abundance trends were however documented for mannitol and salt stressed *drb1* plants by the sRNA-seq and RT-qPCR analyses. Specifically, sRNA-seq revealed miR399 abundance to be reduced by 2.7- and 0.3-fold in mannitol and salt stressed *drb1* whole seedlings respectively, and similarly, RT-qPCR showed that mannitol and salt stress treatment of *drb1* whole seedlings reduced miR399 levels by 0.3- and 0.1-fold, respectively (**Figure 2.13A**).

The sRNA-seq approach indicated that miR399 abundance was elevated by 7.3-, 0.7- and 3.4-fold in *drb2* whole seedlings in response to the 7 d exposure to the heat, mannitol and salt stress growth regimes, respectively. Elevated miR399 abundance in the *drb2* mutant background post its exposure to the three assessed stresses was confirmed by RT-qPCR which showed miR399 levels to be increased by 2.1-, 0.6- and 2.0-fold in heat, mannitol and salt stressed *drb2* plants (**Figure 2.13A**). Compared to non-stressed *drb4* whole seedlings, miR399 abundance was determined to be up-regulated by 5.1-, 1.9- and 3.5-fold by sRNA-seq of heat, mannitol and salt stressed *drb4* plants, respectively (**Figure 2.13A**).

Similarly, RT-qPCR documented 2.1-, 1.7- and 1.6-fold increases in miR399 abundance in heat, mannitol and salt stressed *drb4* whole seedlings, respectively (**Figure 2.13A**); a finding that confirmed the sRNA-seq identified abundance trends for the miR399 sRNA.

Well documented as the sole target gene of miR399-directed expression regulation in *Arabidopsis*, *PHO2* transcript abundance was next quantified by RT-qPCR. Compared to non-stressed Col-0 plants, *PHO2* expression was significantly repressed by 5.5-, 4.5- and 2.8-fold in Col-0 whole seedlings post their exposure to heat, mannitol and salt stress treatment, respectively (**Figure 2.13B**). Reduced *PHO2* expression in heat, mannitol and salt stressed Col-0 whole seedlings was expected considering that RT-qPCR revealed miR399 sRNA abundance to be elevated by each of the three assessed stresses (**Figure 2.13A**). An opposing expression trend for *PHO2* was revealed by RT-qPCR in the *drb1* mutant background, that is; *PHO2* transcript abundance was elevated by 57.2-, 4.3- and 2.8-fold in heat, mannitol and salt stressed *drb1* plants (**Figure 2.13B**). Increased *PHO2* expression in the *drb1* mutant background post its exposure to the three assessed stresses was expected considering that RT-qPCR had previously revealed that miR399 abundance was reduced in response to all three stresses (**Figure 2.13A**). However, the highly dramatic elevation to *PHO2* expression (57.2-fold) in response to the mild 0.6-fold reduction in miR399 abundance in heat stressed *drb1* whole seedlings, remained a highly curious result. Potentially, this curious finding indicates that in the *drb1* mutant background where DRB1 functional activity is absent, and therefore, the production stage of the miRNA is defective, any degree of miR399-directed expression regulation of the *PHO2* transcript is completely abolished, thereby accounting for the dramatically altered expression of the *PHO2* target transcript in response to the mild reduction to miR399 abundance.

In response to heat, mannitol and salt stress treatment, *PHO2* expression was only mildly altered by -1.3-, 1.5- and 1.5-fold respectively, in *drb2* whole seedlings (**Figure 2.13B**). Reduced *PHO2* expression in heat stressed *drb2* plants was expected considering that RT-qPCR revealed miR399 abundance to be elevated by 2.1-fold (**Figure 2.13A**). However, elevated *PHO2* expression in response to increased miR399 levels in mannitol and salt stressed *drb2* whole seedlings formed an unexpected miRNA/target gene regulation trend. *PHO2* transcript abundance was determined to be significantly down-regulated by 7.1-, 6.7- and 3.2-fold post exposure of *drb4* whole seedlings to heat, mannitol and salt stress (**Figure 2.13B**). Reduced *PHO2* expression in the *drb4* mutant background was expected considering that miR399 abundance was determined to be elevated in response to each of the three assessed stresses (**Figure 2.13A**).

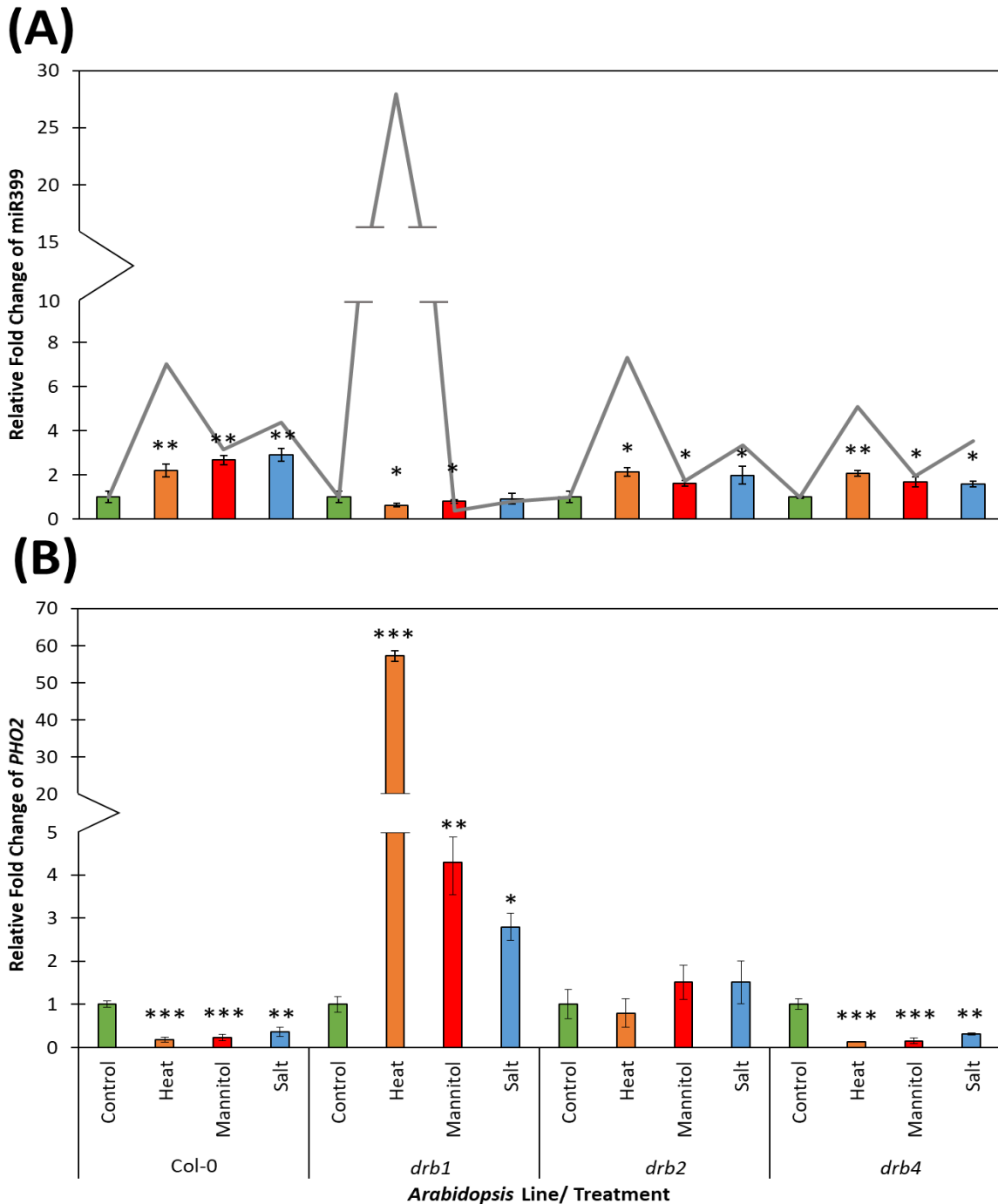


Figure 2.13 Molecular analysis of the miR399/*PHO2* regulatory module in 15 d old *Arabidopsis* Col-0 seedlings and DRB-knockout mutants, *drb1*, *drb2* and *drb4* exposed to heat, mannitol or salt stress, relative to untreated (control) seedlings. **(A)** The SL-RT-qPCR determined abundance of miR399 in *Arabidopsis* Col-0 seedlings and DRB-knockout mutants, *drb1*, *drb2* and *drb4* exposed to each abiotic stress is presented as fold-change relative to control grown seedlings for each *Arabidopsis* line (coloured bars). The grey line indicates the respective fold-change in miR399 accumulation for each *Arabidopsis* line as assessed with sRNA-seq. **(B)** RT-qPCR analyses of miR399 target gene, *PHO2*, expression changes of *Arabidopsis* lines, Col-0, *drb1*, *drb2* and *drb4* in response to heat, mannitol or salt stress, compared to non-stress growth conditions. Due to the large difference in expression change of *PHO2*, the relative mean expression value is provided. Error bars represent the \pm SD of 4 biological replicates with each biological replicate consisting of 6 individual plants. The presence of an asterisk indicates a statistically significant difference between the control and stress treated seedlings for miR399 and *PHO2* (p-value: < 0.05, *; P < 0.005, **; P < 0.001, ***).

2.4.2.8 *Molecular Profiling of the miR408 Regulatory Module in Heat, Mannitol and Salt Stressed Col-0, drb1, drb2 and drb4 Whole Seedlings*

Like miR399, the miR408 sRNA has been demonstrated to be a stress responsive miR408 in *Arabidopsis*. More specifically, in *Arabidopsis*, miR408 abundance is altered in response to copper (Cu) deficiency, and this alteration to miR408 abundance is believed to be required to regulate the expression of key Cu responsive genes (Abdel-Ghany and Pilon, 2008; Zhang *et al.*, 2014). Therefore, altered miR408 abundance post exposure of *Arabidopsis* Col-0 whole seedlings to the abiotic stresses of heat, mannitol and salt stress, identified miR408 as the third miRNA of interest for further investigation.

Compared to control Col-0 seedlings, miR408 abundance was determined by sRNA-seq to be elevated by 8.2-, 2.2- and 5.8-fold in heat, mannitol and salt stressed Col-0 seedlings, respectively (**Figure 2.14A**). Elevated miR408 abundance in Col-0 plants in response to heat, mannitol and salt stress, was confirmed via RT-qPCR which revealed 5.9-, 3.0- and 3.5-fold elevated miR408 abundance, respectively (**Figure 2.14A**). The applied sRNA-seq approach indicated that exposure of the *drb1* mutant to heat stress, induced a 9.0-fold increase in the abundance of the miR408 sRNA (**Figure 2.14A**). However, RT-qPCR suggested that heat stress had an opposing influence on miR408 abundance, a 1.5-fold reduction. The sRNA-seq and RT-qPCR approaches did however return matching miR408 abundance trends for mannitol and salt stressed *drb1* plants. Specifically, sRNA-seq showed that the level of the miR408 sRNA in mannitol stressed *drb1* plants was elevated 1.7-fold, with RT-qPCR indicating a 1.9-fold elevation. Similarly, in salt stressed *drb1* plants, miR408 abundance was determined to be elevated by 1.6- and 1.2-fold by sRNA-seq and RT-qPCR, respectively (**Figure 2.14A**).

In heat and salt stressed *drb2* seedlings, miR408 abundance was determined by sequencing to be increased by 1.9-fold, compared to its levels in non-stressed *drb2* plants. RT-qPCR confirmed the sequencing identified miR408 abundance trends for heat (2.0-fold) and salt (1.6-fold) stressed *drb2* whole seedlings. In comparison, the sRNA-seq approach revealed that miR408 abundance was reduced by 2.5-fold in the *drb2* mutant post its exposure to mannitol stress (**Figure 2.14A**). However, RT-qPCR indicated that miR408 abundance remained largely unchanged (reduced by 1.1-fold) by the mannitol stress treatment. Compared to non-stressed *drb4* seedlings, sRNA-seq suggested that the level of the miR408 sRNA was elevated by 7.4- and 2.7-fold in heat and salt stressed *drb4* plants, respectively. Both abundance trends were confirmed by RT-qPCR which revealed that the level of the miR408 sRNA was elevated 1.6- and 1.9- fold in heat and salt stressed *drb4* plants, respectively (**Figure 2.14A**). Sequencing further indicated that the mannitol stress treatment

mildly reduced miR408 abundance by 1.2-fold in the *drb4* mutant background. Again, the sequencing-identified abundance trend was confirmed by RT-qPCR which also revealed that the miR408 sRNA was only mildly reduced in its abundance (1.4-fold) in mannitol stressed *drb4* plants.

The miR408 sRNA is known to regulate the expression of a number of Cu-containing proteins at the transcriptional level, including PLANTACYANIN (AT2G02850), LACCASE3 (AT2G30210), LACCASE12 (AT5G05390), LACCASE13 (AT5G07130), UCLACYANIN2 (AT2G44790), and CUPREDOXIN (AT1G72230; Abdel-Ghany *et al.*, 2008; Ma *et al.*, 2015; Pilon, 2018). The *LAC3* transcript was selected for further investigation via RT-qPCR with this approach revealing that compared to non-stressed Col-0 plants, *LAC3* expression was increased 12.2, 13.5- and 12.8-fold in heat, mannitol or salt stress Col-0 plants, respectively (**Figure 2.14B**). High levels of up-regulated *LAC3* expression in heat, mannitol and salt stressed Col-0 plants formed a surprise finding considering that RT-qPCR also revealed miR408 abundance to be elevated by 5.9-, 3.0- and 3.5-fold by the imposed stress regimes (**Figure 2.14A**). In the *drb1* mutant background, the heat and mannitol stress treatments elevated *LAC3* expression by 5.0- and 2.5-fold, respectively. Salt stress treatment of the *drb1* mutant however failed to significantly alter the expression of the miR408 target gene. Specifically, compared to non-stressed *drb1* plants, *LAC3* expression was only increased by 1.2-fold in salt-stressed *drb1* whole seedlings (**Figure 2.14B**). Taking into consideration the scaling of miR408 abundance and *LAC3* expression trends observed for Col-0 seedlings, this trend was again observed in the *drb1* mutant background post its exposure to mannitol and salt stress. More specifically, the 1.9-fold and unchanged abundance of the miR408 sRNA was correlated with the 2.5- and 1.2-fold elevations documented for *LAC3* expression. Although the 5.0-fold upregulation in the expression of *LAC3* in heat stressed *drb1* seedlings would be expected given the RT-qPCR determined 1.5-fold reduction in miR408 abundance, this abundance relationship did however form a somewhat unexpected finding when the miR408/*LAC3* scaling observed in the Col-0 and *drb1* backgrounds is considered.

Post the exposure of *drb2* seedlings to the heat, mannitol and salt stress regimes, RT-qPCR determined *LAC3* expression to only be mildly altered by -1.3-, 1.4- and 1.7-fold, respectively. Based on the unchanged abundance of the miR408 sRNA in mannitol and salt stressed *drb2* seedlings, the mild alteration to *LAC3* expression was expected. However, as miR408 abundance was elevated by 2.0-fold in heat stress *drb2* seedlings, the statistically insignificant change in *LAC3* expression in the same *Arabidopsis* seedlings was curious. Similar to the molecular response of Col-0 seedlings, significant increases of 1.9- and 2.1-fold in *LAC3* expression was observed for *drb4* seedlings exposed to heat and salt stress, respectively, while a mild and statistically insignificant increase in *LAC3* expression (1.1 ± 0.3 -

fold) was determined for *drb4* seedlings grown under a mannitol stress growth regime. Similar to each of the other *Arabidopsis* seedlings (excluding heat treated *drb1*) seedlings, no *drb4* seedlings presented *LAC3* expression profile reciprocal to the miR408 abundance changes, as anticipated with increases in both miR408 and *LAC3* observed under heat and salt stress while the inverse accumulation trends were observed in response to mannitol stress.

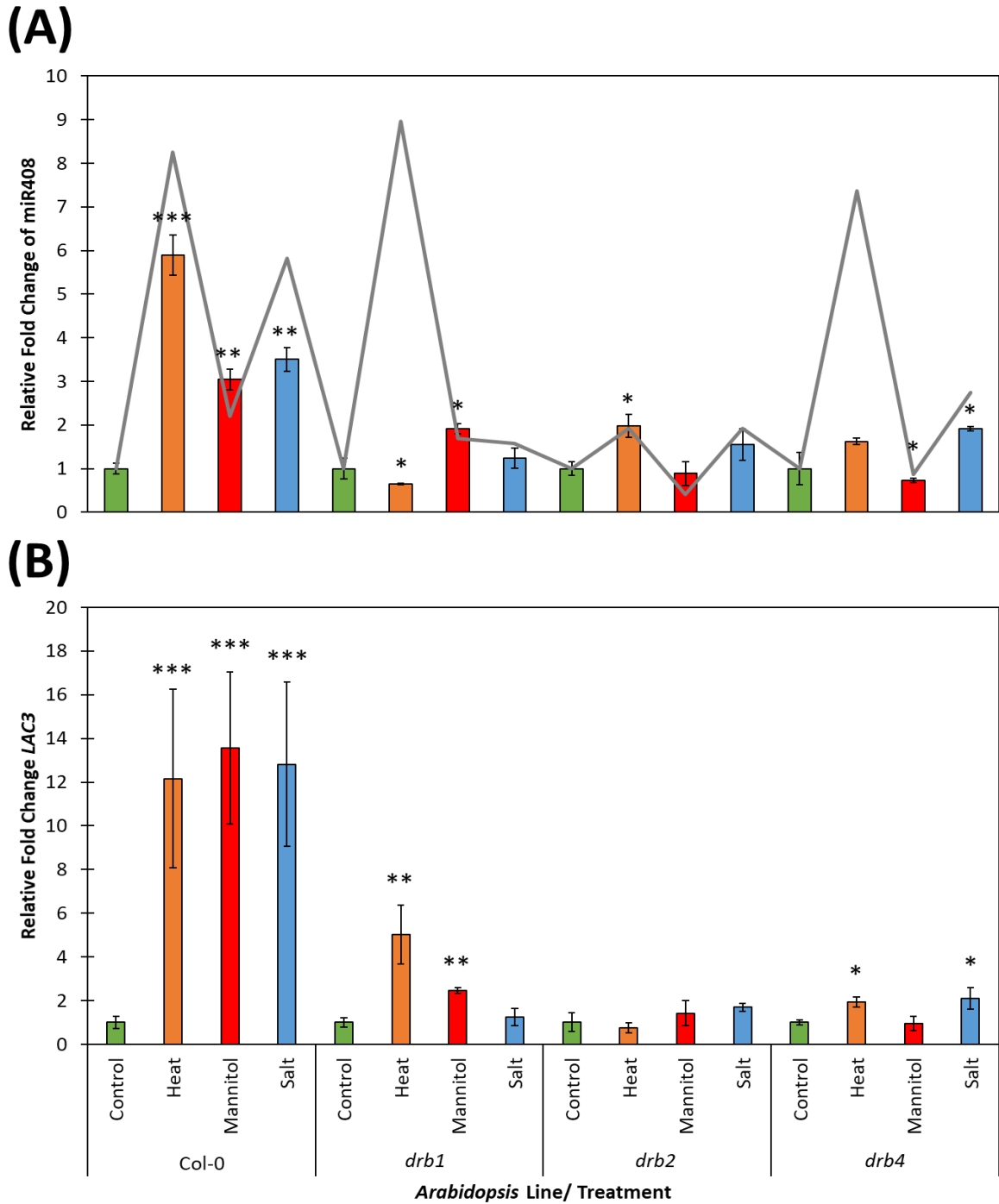


Figure 2.14 Molecular analysis of the miR408/LAC3 regulatory module in 15 d old *Arabidopsis* Col-0 seedlings and DRB-knockout mutants, *drb1*, *drb2* and *drb4* exposed to heat, mannitol or salt stress, relative to untreated (control) seedlings. (A) The SL-RT-qPCR determined abundance of miR408 in *Arabidopsis* Col-0 seedlings and DRB-knockout mutants, *drb1*, *drb2* and *drb4* exposed to each abiotic stress is presented as fold-change relative to control grown seedlings for each *Arabidopsis* line (coloured bars). The grey line indicates the respective fold-change in miR408 accumulation for each *Arabidopsis* line as assessed with sRNA-seq. (B) RT-qPCR analyses of miR408 target gene, *LAC3*, expression changes of *Arabidopsis* lines, Col-0, *drb1*, *drb2* and *drb4* in response to heat, mannitol or salt stress, compared to non-stress growth conditions. Error bars represent the \pm SD of 4 biological replicates with each biological replicate consisting of 6 individual plants. The presence of an asterisk indicates a statistically significant difference between the control and stress treated seedlings for miR408 and *LAC3* (p-value: < 0.05, *, P < 0.005, **, P < 0.001, *).**

2.5 Discussion

Post the 7 d heat, mannitol and salt stress exposure, 15 d old Col-0, *drb1*, *drb2* and *drb4* plants were visually compared to their respective non-stressed counterparts (**Figure 2.2**). The heat stress treatment resulted in an increase in rosette area, downward curling of the rosette leaves, and induced a notable darkening to the colouration (due to anthocyanin over accumulation) of the tissues surrounding the shoot apical meristem (SAM) region and extending into the petioles of rosette leaves of Col-0, *drb2* and *drb4* plants. The rosette leaves of mannitol- or salt-stressed Col-0, *drb1*, *drb2* and *drb4* plants also curled in a downwards direction toward the growth media, however, in direct contrast to heat-stressed plants, the mannitol and salt stress treatments reduced the size of the rosette of each assessed plant line (**Figure 2.2**). In addition, a dark colouration was again observed to develop in the region surrounding the SAM and rosette leaf petioles of salt-stressed Col-0, *drb2* and *drb4* plants. The prominent, yet varied degree of severity that each of these phenotypic indicators of stress was displayed by each plant line under assessment (**Figure 2.2**), led to the subsequent quantitative analyses of whole plant fresh weight (**Figure 2.3**), rosette area (**Figure 2.4**), primary root length (**Figure 2.5**), anthocyanin accumulation (**Figure 2.6**), and chlorophyll *a* and *b* content (**Figure 2.7A-B**). To ensure the quantified phenotypic and physiological changes observed for each *Arabidopsis* plant line was a result of abiotic stress directed molecular changes, an RT-qPCR approach assessed the expression change of the plant stress gene *P5SC1* in response to each abiotic stress growth regime (**Figure 2.8**).

In addition to the phenotypic and physiological analyses, the sRNA-seq and RT-qPCR approaches were additionally applied in an attempt to correlate the molecular responses of the stressed plant lines to the observed phenotypic and physiological responses of Col-0, *drb1*, *drb2* and *drb4* seedlings to each of the imposed stresses. Specifically, sRNA-seq was used to not only highlight the necessity of the contribution of DRB1, DRB2 and DRB4 function to the global miRNA landscape of *Arabidopsis* (**Figure 2.9**), but to determine how the miRNA accumulation profiles of each *Arabidopsis* seedling is altered in response to each of the three imposed stresses (**Figure 2.10**). To provide a clearer understanding of the contribution of each nuclear DRB protein on miRNA production during non-stress and abiotic stress conditions, RT-qPCR analysis was used to document the expression of *DCL1*, *DRB1*, *DRB2*, and *DRB4* in each *Arabidopsis* plant line, in attempt to correlate miRNA abundance changes with any changes in the expression of these four genes which encode for key miRNA production machinery proteins (**Figure 2.11**). Having used RT-qPCR to validate the miRNA abundance trends (see **Publication Three, A.1.3**, pages 193-210) determined by sRNA-seq (**Figure 2.10**), three miRNAs, including miR396, miR399 and miR408, were selected for further

experimental assessments. RT-qPCR was again used to determine the abundance of miR396 (**Figure 2.12A**), miR399 (**Figure 2.13A**) and miR408 (**Figure 2.14A**), and the accumulation of a single gene targeted by each of the assessed miRNAs, specifically *GRF7* (**Figure 2.12B**), *PHO2* (**Figure 2.13B**) and *LAC3* (**Figure 2.14B**), respectively.

2.5.1 **The Phenotypic and Physiological Consequences of a Heat Stress Growth Regime**

Investigation of shoot biomass and architecture in response to abiotic stress has been presented as an effective and sensitive avenue for the determination of the degree of stress tolerance displayed by an individual plant genotype (Claeys *et al.*, 2014). Although supported by the phenotypes presented in **Figure 2.2**, it was a curious finding that in response to the 7 d heat stress treatment, the growth of each assessed *Arabidopsis* plant line was promoted (**Figure 2.3** and **Figure 2.4**, respectively). Although elevated whole seedling fresh weight and rosette area suggested a 'positive' response to this form of abiotic stress, other phenotypic stress markers, including, considerable downward leaf curling (**Figure 2.2**), anthocyanin over-accumulation (**Figure 2.6**) and the significant induction of *P5CS1* expression (**Figure 2.8**), all indicated that the four assessed *Arabidopsis* lines were in actual fact stressed by the 7 d cultivation period at an elevated temperature. It has been previously established that photosynthesis can function without irreversible damage to the plant between the temperature range of 10 to 35°C, depending on whether a particular plant species has adapted to growth in either a 'cold' or 'hot' climate. In addition, other growth parameters, such as light intensity and CO₂ concentration, have been shown to also play a primary role in determining the thermal optimum of each plant species (Berry and Bjorkman, 1980; Sage and Kubien, 2007; Vasseur *et al.*, 2011). The significant increase in plant shoot growth exhibited by the four *Arabidopsis* plant lines assessed here, could have resulted from the elevated growth temperature increasing the rate limiting capacity of key photosynthetic components, such as the enzyme, Ribulose-1,5-bisphosphate carboxylase/oxygenase (RuBisCO), or from alterations to the rate of electron transport, the efficiency of the Calvin cycle, or *P_i* regeneration rates, all of which would in turn potentially result in an elevated net CO₂ assimilation rate ($\mu\text{mol m}^{-2} \text{s}^{-1}$) (Sage and Kubien, 2007). In addition, the study conducted by Gray and colleagues (1998) showed that when *Arabidopsis* was cultivated at an elevated temperature of 29°C (a 9°C increase in temperature compared to the control grown seedlings of their study), seedlings displayed a dramatic increase in auxin-mediated hypocotyl elongation, a phenotypic response similarly observed for heat treated *Arabidopsis* in the Koini *et al.*, (2009) study. Together, the findings detailed in these previously published studies, may in part, account, for the promotion of growth observed here for 15 d old *Arabidopsis* plants post the 7 d heat stress treatment period, growth promotion that potentially stemmed from a modified photosynthetic capacity and/or altered plant hormone pathways (Gray *et al.*, 1998; Sage and Kubien, 2007). Adding further weight to the suggestion that the elevated temperature accompanying the heat stress growth regime may be impacting the photosynthetic pathway of each plant line is **Figure 2.7** which

shows that heat stressed Col-0, *drb1*, *drb2* and *drb4* *Arabidopsis* seedlings all had significant increases in chlorophyll *a* and *b* content, compared to those of their respective controls.

In addition to modification of the photosynthetic pigment chlorophyll, it is well established that plants employ the pigment anthocyanin to assist in mounting a molecular defense against elevated ROS levels induced by abiotic stress such as extreme temperature, drought or salinity (Akula and Ravishankar, 2011; Chalker-Scott, 1999; Howitz and Sinclair, 2008; Kovich *et al.*, 2015; Manetas, 2006; Marko *et al.*, 2004; Sperdoui and Moustakas, 2012; Wang *et al.*, 1997). As such, it was therefore surprising to observe that unlike heat stressed Col-0, *drb2* and *drb4* seedlings that all displayed significant increases in anthocyanin content (**Figure 2.6**), the anthocyanin content of heat stressed *drb1* seedlings remained unchanged from the levels documented for control *drb1* seedlings (*discussed further in Section 2.5.3*, page 57).

In conjunction with phenotypic and physiological characteristics of the plant shoot, root architecture, and specifically, the length of the primary root was also assessed, as reduced primary root length is a known phenotypic marker of abiotic stress (**Figure 2.5**; Claeys *et al.*, 2014). In response to a heat stress growth regime, significant reduction to the length of the primary roots of *drb2* and *drb4* seedlings was observed. A similar trend of reduced primary root length in response to elevated temperature was also observed for heat stressed Col-0 and *drb1* seedlings. However, the degree of reduction in primary root length of heat stressed Col-0 *drb1* plants was deemed to be statistically insignificant. Previous studies by Li *et al.*, (2009) and Rizhsky *et al.*, (2004) have also observed the ability of heat stress to reduce primary root length of *Arabidopsis*.

2.5.2 Mannitol and Salt Stress Growth Conditions Elicit Similar Phenotypic and Physiological Consequences

As conducted for the heat stress analyses, the fresh weight and rosette area of each *Arabidopsis* line was assessed in response to a mannitol or salt stress growth regime due to the sensitivity of these phenotypic measurements to abiotic stress (Claeys *et al.*, 2014). These analyses revealed both phenotypic measurements to be significantly reduced in response to a 7 d cultivation period on plant growth medium supplemented with either mannitol or salt. Although both stress regimes reduced both of the assessed parameters, the most severe reductions in shoot architecture for each *Arabidopsis* line occurred in response to the mannitol stress treatment (**Figure 2.3- 2.4**). This forms an unsurprising result that supports the phenotypes presented in **Figure 2.2**. Further, this finding is supported by the literature, with the *in vitro* stress assays conducted by Claeys *et al.* (2014), demonstrating that shoot growth is highly sensitive to either stress, and further, the degree of growth inhibition was determined to be dose-dependent.

Inhibition of primary root growth is another sensitive indicator of abiotic stress severity (Claeys *et al.*, 2014; Qi *et al.*, 2007; Valenzuela *et al.*, 2016). Unsurprisingly, when exposed to a 7 d salt stress growth regime, each of the *Arabidopsis* plant lines exhibited significant reductions to primary root length (**Figure 2.5**). This finding is in agreement with previous studies by Duan *et al.*, (2013), Liu *et al.*, (2015), Valenzuela *et al.*, (2016) and Wang *et al.*, (2009), who all reported that *Arabidopsis* primary root length is reduced in response to a salt stress growth regime. Furthermore, the Liu *et al.*, (2015), Valenzuela *et al.*, (2016) and Wang *et al.*, (2009) went on to demonstrate that reduced primary root length is the result of salt stress induced suppression of the root meristem and/or cell elongation (Liu *et al.*, 2015; Valenzuela *et al.*, 2016; Wang *et al.*, 2009). Curiously, in response to a mannitol stress growth regime, while *drb1* and *drb2* seedlings displayed a significant reduction to the length of their primary roots, there was no significant impact on the length of the primary roots of Col-0 and *drb4* seedlings exposed to the same stress regime. It should be noted here that previous studies using a similar mannitol stress regime similarly reported minimal variation to primary root length post stress exposure (Pandey *et al.*, 2013; Seo *et al.*, 2009).

Measured as a physiological marker of stress, anthocyanin accumulation was readily observed in **Figure 2.2**, particularly for Col-0, *drb2* and *drb4* seedlings exposed to heat and salt stress. Similar to the impact of a heat stress growth regime (see **Section 2.5.1**), salt stress resulted in statistically significant increases to the anthocyanin content of Col-0, *drb2* and *drb4* seedlings (**Figure 2.6**). While a marked increase in anthocyanin was expected in all *Arabidopsis* plant lines, a pigmentation alteration that assists *Arabidopsis* to negate the impact

of abiotic stress associated ROS increases, it was curious that anthocyanin levels remained unchanged in the *drb1* seedlings (*discussed further in Section 2.5.3*).

The inability of a mannitol stress growth regime to significantly alter anthocyanin accumulation in each of the *Arabidopsis* plant lines studied is a result of the ability of mannitol to inhibit key genes involved in the regulation of the *Arabidopsis* flavonoid and anthocyanin biosynthetic pathway (Solfanelli *et al.*, 2006). Several key genes involved in the synthesis of the enzymes of the flavonoid and anthocyanin pathway, namely, *PRODUCTION OF ANTHOCYANIN PIGMENT 1 (PAP1, AT1G56650)*, *PHE AMMONIA-LYASE (PAL1; AT2G37040)*, *CHALCONE SYNTHASE (CHS; AT5G13930)*, *DIHYDROFLAVONOL 4-REDUCTASE (DFR; AT5G42800)* and *UDP-GLUCOSE:FLAVONOID 3-O-GLUCOSYLTRANSFERASE (UF3GT; AT5G54060)* have previously been shown to be heavily downregulated in their abundance, and/or their activity fails to be induced by sucrose when *Arabidopsis* seedlings are treated with mannitol (Solfanelli *et al.*, 2006).

Comparable to the significant impact mannitol and salt stress had on reducing the fresh weight (**Figure 2.3**) and rosette area (**Figure 2.4**) of each of the *Arabidopsis* plant lines, both chlorophyll *a* and *b* were spectrophotometrically determined to be significantly reduced in all *Arabidopsis* lines grown under a mannitol or salt stress growth regime (**Figure 2.7A-B**). As reduced chlorophyll content has been shown to be a morphogenic response to abiotic stress conditions such as mannitol (Qin *et al.*, 2014) and salt stress (Yamaguchi *et al.*, 2006), this formed an expected finding.

2.5.3 ***Anthocyanin Production is Defective in drb1 Seedlings***

As previously stated, anthocyanin assists in mounting a molecular defense against the elevated levels of ROS associated with abiotic stress growth regimes (Akula and Ravishankar, 2011; Chalker-Scott, 1999; Howitz and Sinclair, 2008; Kovicich *et al.*, 2015; Manetas, 2006; Marko *et al.*, 2004; Speredouli and Moustakas, 2012; Wang *et al.*, 1997). It was therefore a surprise finding to identify that unlike the *Arabidopsis* lines, Col-0, *drb2* and *drb4* which as expected over accumulated anthocyanin in response to heat and salt stress conditions, *drb1* failed to display an altered anthocyanin content from that of non-stressed, control *drb1* plants, when exposed to either stress (**Figure 2.6**). Although the absence of anthocyanin induction in *drb1* plants is somewhat indicative that it is not stressed to the same degree as the other assessed *Arabidopsis* lines in response to each abiotic stress, this finding could also suggest that the anthocyanin biosynthesis pathway in the *drb1* mutant background is impacted as a result of loss of the activity of this key miRNA pathway machinery protein. More specifically, key genes involved in the *Arabidopsis* anthocyanin biosynthesis pathway, specifically *PAP1*, *PAP2* (*PAP2*; *AT1G66390*) and *MYB113* (*AT1G66370*), have been shown to be regulated by *TAS4* derived tasiRNAs (Luo *et al.*, 2012). The production of *TAS4* derived tasiRNAs result from the cleavage of the *TAS4* precursor transcript by the targeting miRNA, miR828 (Felippes and Weigel, 2009; Luo *et al.*, 2012; Montgomery *et al.*, 2008). Additionally, a study by Gou *et al.*, (2011) found that SQUAMOSA PROMOTER BINDING PROTEIN-LIKE 9 (*SPL9*; *AT2G42200*) negatively regulates anthocyanin accumulation in *Arabidopsis* stems, with *SPL9* being under miR156 directed expression regulation: a miRNA that requires *DRB1* for its production (**Figure 2.9**). It can therefore be hypothesised that the loss of *DRB1* activity in the *drb1* mutant has disrupted the anthocyanin biosynthesis pathway either via the disruption of the *TAS4* tasiRNA pathway, and/or the miR156/*SPL9* regulatory module (Guo *et al.*, 2011; Luo *et al.*, 2012).

2.5.4 Molecular Confirmation of Abiotic Stress

To confirm that the phenotypic characteristics displayed by each *Arabidopsis* plant line in response to heat, mannitol and salt, were a result of the induction of abiotic stress at a molecular level, the expression level of the well characterised *Arabidopsis* stress gene, *P5CS1* was analysed (**Figure 2.8**). RT-qPCR analyses confirmed that in response to heat, mannitol and salt stress, all *Arabidopsis* plant lines had statistically significant increases in *P5CS1* expression. This was an unsurprising finding as long-standing literature has thoroughly established the role of *P5CS1* in the accumulation of proline (Yoshida *et al.*, 1999; Székely *et al.*, 2008). In an attempt to adapt to, or to tolerate abiotic stress, proline accumulation, in addition to increases in anthocyanin and soluble sugars, has been shown to assist a plant to acclimatise to mild or moderate abiotic stress (Sperdouli and Moustakas, 2012). As a result of the RT-qPCR confirmation that Col-0, *drb1*, *drb2* and *drb4* plants were responding to the imposed abiotic stresses at the molecular level (**Figure 2.8**), investigation of the impact that the three imposed abiotic stresses had on the miRNA landscape of each plant line under investigation presented itself as a promising avenue for the identification of miRNAs responsive to each imposed stress.

2.5.5 ***DRB1, DRB2 and DRB4 are Required for MicroRNA Production***

Previous research has shown that DRB1, DRB2 and DRB4 are required for the production of miRNA subsets, miRNA subsets that are processed from structurally distinct precursor transcripts, that upon maturation, are required to regulate the expression of a diverse array of functionally distinct genes, genes that are required for all aspects of plant development and for the plant to mount a defensive response against invading pathogens or to adapt to abiotic stress (Eamens *et al.*, 2012a; Fukudome *et al.*, 2011; Hiraguri *et al.*, 2005; Pélissier *et al.*, 2011; Pouch-Pélissier *et al.*, 2008). In the specific tissues where *DRB1* and *DRB2* expression overlaps, DRB2 is thought to compete with DRB1 for functional interaction with DCL1 in order to mediate its involvement in DCL1-catalysed processing of conserved miRNAs from their imperfectly structured, dsRNA hairpin precursors (Eamens *et al.*, 2012a). In addition, DRB2 has also been shown to be antagonistic to the function of DRB4 in the DRB4/DCL4-catalysed processing of non-conserved, or newly-evolved miRNA sRNAs from their '*more perfectly*' structured dsRNA precursors (Eamens *et al.*, 2012a; Hiraguri *et al.*, 2005; Pélissier *et al.*, 2011; Pouch-Pélissier *et al.*, 2008).

The contribution of DRB1, DRB2 and DRB4 to the generation of a '*truly*' global miRNA population was again demonstrated here via the use of a sRNA-seq approach to profile the miRNA landscape of the *drb1*, *drb2* and *drb4* mutants (**Figure 2.9**). In agreement with the previous reports by Vazquez *et al.*, (2004) and Eamens *et al.*, (2009), the significant reduction in the abundance of 111 miRNAs, of which 73 miRNAs were solely reduced in their abundance in *drb1* seedlings, cemented DRB1 as the primary DRB family member required for the production of both the conserved and non-conserved classes of miRNA in *Arabidopsis*. Further, RT-qPCR analysis of *DCL1*, *DRB2* and *DRB4* expression in the *drb1* plants added additional weight to this with significantly elevated *DCL1* and wild-type equivalent levels of both *DRB2* and *DRB4* failing to maintain an appropriate miRNA landscape (**Figure 2.11**). This finding is unsurprising given the widespread expression of *DRB1* throughout *Arabidopsis* development (Eamens *et al.*, 2012a), in combination with the severely impaired developmental phenotype expressed by the *drb1* mutant (Eamens *et al.*, 2012a; see **Figure 2.2**). It should be noted here that in this study, the accuracy of miRNA categorisation as either a conserved land plant miRNA, or as a non-conserved miRNA was ensured via the application of the parameters proposed by Axtell and Meyers in their 2018 publication (Axtell and Meyers, 2018). Specifically, to classify a miRNA as a conserved land plant miRNA; (1) the *MIR* gene family must be annotated in miRBase 21 (<http://www.mirbase.org/>) in at least two of the eight major plant taxonomic divisions, including the eudicot-rosid, eudicot-asterid, eudicot-ranunculid, monocot, Amborella, gymnosperm, lycophyte and bryophyte taxonomic divisions, and; (2) the

designated miRBase 21 annotations must be of '*high-confidence*'; a stringent criteria that only classifies 36 of the 2026 *MIR* gene families reported for land plants as being '*truly*' conserved miRNAs (Axtell and Meyers, 2018).

In non-stressed *drb4* whole seedlings, the abundance of 48 miRNAs was reduced (**Figure 2.9**). Furthermore, of these 48 miRNAs, 31 were (1) only reduced in abundance in the *drb4* mutant, and (2) all 31 of these miRNAs were classified as non-conserved miRNAs using the criteria of Axtell and Meyers (2018). In addition, 9 conserved miRNAs from five *MIR* gene families, including the *MIR159*, *MIR166*, *MIR169*, *MIR319* and *MIR399* gene families, were reduced in their abundance in both the *drb1* and *drb4* mutant backgrounds. This result suggests that in addition to being the primary DRB responsible for the production of tasiRNAs and p4-siRNAs (Pélissier *et al.*, 2011), DRB4 is the primary DRB protein responsible for the production of non-conserved miRNAs in *Arabidopsis*, a finding that both agrees with, and greatly expands on the original finding of Bartell and colleagues, whom demonstrated a small number of miRNAs, specifically miR822, miR839 and miR840, required the DRB4/DCL4 partnership for their maturation from their precursor transcripts (Rajagopalan *et al.*, 2006).

While DRB2 is also required for the production of a number of non-conserved miRNAs, primarily in the vegetative tissues where *DRB2* is expressed in wild-type plants (namely, the region surrounding the SAM) (Eamens *et al.*, 2012a; Reis *et al.*, 2015), the miRNA profiling presented here indicated that DRB2 cannot adequately compensate for the loss of DRB4 function across all of the vegetative tissues of 15 d old *Arabidopsis* whole seedlings. Conversely, the wide expression domain of *DRB4* in *Arabidopsis* vegetative development (Curtin *et al.*, 2008), appears to allow for DRB4 to compensate for the loss of DRB2 activity in 15 d old *Arabidopsis* seedlings with only one miRNA, miR845b, determined to be significantly downregulated in abundance in *drb2* whole seedlings.

Taken together, the significant alteration to the miRNA accumulation profile of non-stressed, 15 d old *drb1*, *drb2* and *drb4* whole seedlings, when compared to the global miRNA landscape of Col-0 plants of the same age, readily highlights (1) the high degree of synergistic and/or antagonistic functional interplay between DRB1, DRB2 and DRB4 in the production stage of the *Arabidopsis* miRNA pathway, and (2) the necessity of this hierarchical order of DRB function for the generation of the miRNA landscape of wild-type *Arabidopsis* seedlings.

2.5.6 Small RNA Sequencing Identified MicroRNAs Central to the Adaptive Response of *Arabidopsis* to Heat, Mannitol and Salt Stress

Arabidopsis is the long-standing experimental model for C₃ dicotyledonous plant species, a model that has allowed plant biologists to uncover a wealth of molecular knowledge surrounding plant growth and development, and the ability of a plant to mount an adaptive response to either abiotic or biotic stress. In the years that have followed the initial discovery of miRNAs, and the subsequent demonstration that this class of sRNA is a central regulator of plant gene expression (Reinhart *et al.*, 2002), a number of studies have attempted to uncover the role that miRNAs mediate in the adaptive response of a plant to the unfavourable growth conditions that stem from abiotic or biotic stress (Barciszewska-Pacak *et al.*, 2015; Denver and Ullah, 2019; Fujii *et al.*, 2005; Guan *et al.*, 2013; Khraiwesh *et al.*, 2012; Liu *et al.*, 2008; Ma *et al.*, 2015). While most of these studies have focused their attention on the molecular characterisation of a single miRNA, it is curious that following the advent and widespread application of high-throughput sequencing, there remains a lack of studies (with the exception of the Barciszewska-Pacak *et al.*, (2015) study) that have employed a sequencing approach to profile the miRNA landscape of abiotically stressed *Arabidopsis*.

Here, large miRNA cohorts were determined to differently accumulate across the four plant lines, and three stress regimes assessed. More specifically, 18 to 56% of the 326 *Arabidopsis* miRNAs currently annotated on miRBase22, (released October 2018) were determined to have altered abundance in either control, or heat, mannitol and salt stressed Col-0, *drb1*, *drb2* and *drb4* whole seedlings. Interestingly, members of highly conserved plant miRNA gene families (such as the *MIR156*, *MIR159*, *MIR160*, *MIR162*, *MIR164*, *MIR166*, *MIR167*, *MIR168*, *MIR169*, *MIR171*, *MIR172*, *MIR319*, *MIR390*, *MIR393*, *MIR394*, *MIR396*, *MIR397*, *MIR398*, *MIR399*, *MIR403*, *MIR408* and *MIR2111*) were determined to have altered accumulation post exposure of 15 d old Col-0 plants post a 7 d exposure to either heat, mannitol or salt stress, a finding that clearly highlights that conserved miRNAs are not only important regulators of developmental gene expression in *Arabidopsis*, but also play a central regulatory role in modulating the expression of genes that are required by *Arabidopsis* to mount an adaptive response to abiotic stress.

Interestingly, in addition to the highly conserved plant miRNAs identified by this sRNA-seq analysis, this approach further revealed that the accumulation of a large number of 'newly evolved' and/or 'non-conserved' miRNAs was also differentially altered in response to each imposed abiotic stress. This finding indicates that a degree of caution must be used when selecting a model species for explorative studies to identify abiotic stress responsive miRNAs crucial to the adaptive response of a plant to the imposed stress, as the identified miRNAs

could potentially be specific to the studied species, and therefore, not conserved across plant species, nor reflective of the miRNA-mediated adaptive response to abiotic stress of other plant species, including even closely related plant species. Further, this may mean that a plant biology researcher may have to perform their miRNA analyses in their specific plant species of interest which likely lacks the experimentally favourable characteristics of a 'true' model plant species such as *Arabidopsis*.

2.5.7 **The Nuclear-Localised DRB Hierarchy and DCL1 Expression Profile in Response to Heat, Mannitol and Salt Stress**

In an attempt to generate a more detailed understanding of what was occurring at a molecular level in heat, mannitol and salt stressed *Arabidopsis* seedlings, RT-qPCR was employed to assess variations in the expression of the encoding locus of the DCL protein repeatedly demonstrated as the absolutely essential *Arabidopsis* DCL endonuclease required for miRNA precursor transcript processing, *DCL1*, and of the expression of the three nuclear-localised DRBs, specifically DRB1, DRB2 and DRB4, known to be required for miRNA production (Eamens *et al.*, 2011; Eamens *et al.*, 2012a; Fukudome *et al.*, 2011; Hiraguri *et al.*, 2005; Pélissier *et al.*, 2011; Pouch- Pélissier *et al.*, 2008; **Figure 2.11**). While this analysis was primarily conducted to identify any correlation in altered expression of *DCL1*, with any change in the expression profiles of *DRB1*, *DRB2* and *DRB4*, or to the miRNA abundance profiles documented by sRNA-seq (**Figure 2.10**), RT-qPCR further revealed the nuclear-localised *DRB* hierarchal relationship under control and/or conditions of abiotic stress. It should be noted here that the expression of each gene, presented in **Figure 2.11**, is discussed relative to the expression of the assessed gene in control grown, 15 d old Col-0 seedlings.

When examining the RT-qPCR data obtained for *DCL1*, it was noted that in the *drb1* mutant background, the expression of *DCL1* was significantly elevated in all four growth conditions assessed (**Figure 2.9**). This formed an interesting result, especially considering that *DCL1* transcript abundance remained unchanged from its wild-type levels in both the *drb2* and *drb4* mutant backgrounds (excluding heat stressed *drb2* and *drb4* plants). This finding suggests that either; (1) the overaccumulation of miRNA precursor transcripts in the absence of DRB1 activity (Dong *et al.*, 2008; Vazquez *et al.*, 2004) forms a feedback loop that results in enhanced expression of the *DCL1* locus in an attempt to translate more DCL1 protein to process the now overly abundant miRNA precursor transcripts, or; (2) *DCL1* transcript abundance is elevated due to a highly reduced rate of miR162-directed DCL1 transcript cleavage (Xie *et al.*, 2003).

As previous research has demonstrated antagonism and synergism between DRB2 and DRB1 and DRB4 (Eamens *et al.*, 2012a; Pélissier *et al.*, 2011), together with the demonstration that each of these three nucleus-localised DRBs are required for miRNA production (Eamens *et al.*, 2011; Eamens *et al.*, 2012a; Fukudome *et al.*, 2011; Hiraguri *et al.*, 2005; Pélissier *et al.*, 2011; Pouch- Pélissier *et al.*, 2008), it was important to document the expression profiles of *DRB1*, *DRB2* and *DRB4* in the *drb1*, *drb2* and *drb4* mutant backgrounds. Due to the previously demonstrated antagonism of DRB1 function by DRB2 (Eamens *et al.*, 2012a), non-stressed *drb1* seedlings presented a significant upregulation in *DRB2* expression,

while *DRB4* expression remained largely unchanged. While this was also the case for *drb1* seedlings exposed to salt stress, both the *DRB2* and *DRB4* expression levels were significantly elevated in response to heat stress, and in mannitol stressed *drb1* seedlings, only *DRB4* expression was significantly increased. When liberated from the competitive inhibition of DRB1 interaction with DCL1 for miRNA precursor transcript processing, the expression changes in *DRB2* and/or *DRB4* transcript abundance in response to each growth regime indicated that the expression of at least one of the two other nuclear *DRB* genes was upregulated in order to attempt to compensate for the loss of DRB1 activity.

The antagonistic relationship between DRB2, and both *DRB1* and *DRB4*, has been demonstrated by Pélissier *et al.*, (2011) and Reis *et al.*, (2015) who showed that DRB2 represses the expression of either *DRB1* or *DRB4* to increase its ability to interact with either DCL1 and DCL4 for the production of either miRNAs or miRNAs and/or siRNAs, respectively. Therefore, it was anticipated in the absence of DRB2, the expression of *DRB1* and *DRB4* would be elevated, and this was indeed observed for *DRB1* expression in all *drb2* seedlings excluding those exposed to mannitol stress, where *DRB1* expression was determined to remain unchanged. Interestingly, the expression of *DRB4* was found to be significantly reduced in *drb2* seedlings, regardless of the growth condition, a finding which strongly indicated that in the absence of DRB2, the elevated *DRB1* expression in addition to the already extensive spatial overlap between the *DRB1* and *DRB4* expression domains (Curtin *et al.*, 2008), results in the significant repression of *DRB4* expression.

Similarly to the expression profiles observed in the *drb2* mutant background, in the absence of DRB4 activity, *DRB1* expression was significantly upregulated under both the non-stress and stress growth regimes. Interestingly, the 3.2-, 10.6-, 2.8- and 6.0-fold elevation in *DRB1* expression in *drb4* control, heat, mannitol and salt stress seedlings, respectively, was accompanied by reduced *DRB2* expression levels, of -1.2-, -1.3-, -2.6- and -1.7-fold. The expression changes observed for *drb4* seedling, in conjunction with those observed for *drb2* seedlings, strongly suggested that elevated *DRB1* expression may competitively inhibit the expression of the two other nucleus-localised *DRBs* in order to ensure its access to DCL1 for miRNA production during either standard growth conditions or when *Arabidopsis* experiences abiotic stress.

2.5.8 **The miR396 Regulatory Module in Response to Heat, Mannitol and Salt Stress**

Selected on the basis of its altered abundance in heat, mannitol and salt stressed Col-0, *drb1*, *drb2* and *drb4* plants (**Figure 2.10**), miR396 was selected for further molecular assessment. In addition to experimentally validating the sequencing-identified alterations to miR396 abundance, RT-qPCR was also used to quantify *GRF7* expression, one of the target genes of miR396 in *Arabidopsis*. A target gene of miR396, in addition to the sRNA itself, was also assessed in this study via RT-qPCR to determine if; (1) the entire miR396 regulatory module was responsive to each applied stress, or; (2) if only the miR396 sRNA itself was responding to each applied stress.

In heat, mannitol and salt stressed Col-0 whole seedlings, RT-qPCR revealed that enhanced miR396 abundance resulted in the repression of *GRF7* expression (**Figure 2.12A and Figure 2.12B**). Identification of reciprocal abundance profiles for miR396 and *GRF7* in the Col-0 background indicated that; (1) miR396 abundance increased in order to repress the expression of its target gene(s), and; (2) the mode of miR396-directed repression of *GRF7* expression was via the canonical mechanism of miRNA-directed RNA silencing in plants, target transcript cleavage. Elevated miR396 abundance and reduced *GRF7* expression in heat, mannitol and salt stressed Col-0 whole seedlings formed an expected molecular profile with previous research showing that *GRF7* inhibits the transcription of the known *Arabidopsis* stress gene, *DEHYDRATION-RESPONSE ELEMENT BINDING2A* (*DREB2A*; Kim *et al.*, 2012). Elevated *DREB2A* abundance upon exposure of *Arabidopsis* to abiotic stress, is correlated with heightened stress tolerance as a direct result of the ability of *DREB2A* to bind with a *cis*-acting dehydration-responsive element harboured in the regulatory regions of genes essential for *Arabidopsis* to respond to abiotic stress. Conversely, excess *DREB2A* in *Arabidopsis* plants cultivated under standard growth conditions, has been shown to inhibit the growth of *Arabidopsis* (Kim *et al.*, 2012; Sakuma *et al.*, 2006; Yamaguchi-Shinozaki and Shinozaki, 2006). Therefore, in heat, mannitol and salt stressed Col-0 whole seedlings, reduced *GRF7* expression as a result of enhanced miR396-directed RNA silencing, would in turn release the repressive influence of *GRF7* on *DREB2A* gene expression (Kim *et al.*, 2012) leading to elevated *DREB2A* protein abundance.

A similar mode of miR396-directed repression of *GRF7* expression was observed for heat stressed *drb1* whole seedlings, that is; enhanced miR396 abundance lead to reduced *GRF7* expression (**Figure 2.12A and Figure 2.12B**). However, this form of *GRF7* expression regulation by the miR396 sRNA was not observed for either mannitol or salt stressed *drb1* plants. More specifically, the abundance of both miR396 and *GRF7* was reduced in the *drb1* background post its exposure to mannitol and salt stress. This result indicates that either; (1)

both of the applied stresses repress the expression of the loci that encode for both the miR396 sRNA and for *GRF7*, or; (2) the mode of miR396-directed expression regulation of *GRF7* changes from a mRNA cleavage-based mechanism of RNA silencing to a translational repression based mode of miR396-directed expression regulation (Schwab *et al.*, 2005).

In the *drb2* mutant background, heat, mannitol and salt stress failed to significantly alter miR396 abundance (-1.05-, 1.2- and 1.1-fold, respectively) (**Figure 2.12A**). However, *GRF7* expression was reduced by 2.4-, 1.9- and 2.2-fold in heat, mannitol and salt stressed *drb2* whole seedlings, respectively (**Figure 2.12B**). Although it was surprising to observe that miR396 abundance was insignificantly impacted in response to each of the applied abiotic stresses, the significant reduction in *GRF7* expression indicated that the *drb2* seedlings were attempting to mount a wild-type equivalent adaptive response to the imposed abiotic stress growth regimes (Kim *et al.*, 2012). Altered *GRF7* expression in the absence of a significant change to the abundance of its known regulatory sRNA, miR396, in each of the assessed stress treatments, suggests that in the *drb2* mutant background, a miR396-independent mechanism of *GRF7* expression regulation was initiated. Along these lines, in addition to forming a central functional component for miRNA production in *Arabidopsis*, DRB2 has been demonstrated to also be required for the production of a class of siRNA, termed polymerase IV-dependent (p4)-siRNAs that are believed to be required for the maintenance of chromatin structure (Pélissier *et al.*, 2011). Therefore, altered *GRF7* expression under all three stress conditions assessed in this study putatively suggests that in the absence of DRB2 activity, the structure of the chromatin surrounding the *GRF7* locus is altered allowing for the continued access to the regulatory sequence of the gene by the transcriptional machinery (potentially a repressive transcription factor) regardless of the cellular conditions.

Similar to the profile constructed for the miR396/*GRF7* regulatory module in Col-0 whole seedlings, exposure of the *drb4* mutant to heat, mannitol and salt stress, significantly enhanced the accumulation of the miR396 sRNA by 2.7-, 2.6- and 2.0-fold, respectively (**Figure 2.12A**), and further, that enhanced miR396 accumulation led to the repressed expression of *GRF7* by 'undetectable', 1.5- and 2.4-fold, respectively (**Figure 2.12B**). This expected finding of upregulated miR396 abundance in conjunction with reduced *GRF7* expression was anticipated, with the reduction of *GRF7* in heat stressed *drb4* seedlings to 'undetectable' levels forming a very interesting result. As heat stress resulted in a 2.7-fold elevation in miR396 abundance in *drb4*, an increase that was slightly higher than the 2.6-fold elevation observed for mannitol treated *drb4* seedling, yet, unlike *drb4* seedlings exposed to a heat stress growth regime, *GRF7* was still detected in mannitol stressed counterparts, a finding that strongly suggested that the heat stress may be directly repressing the expression of the *GRF7* loci, in addition to enhanced miR396-directed *GRF7* expression repression in

drb4 seedlings. Nonetheless, the obtainment of reciprocal abundance profiles for the miR396 sRNA and for one of its target genes, *GRF7*, in heat, mannitol and salt stressed *drb4* whole seedlings, strongly indicated that miR396 directs the canonical mode of mRNA cleavage based silencing to regulate *GRF7* expression in this mutant background post its exposure to the three abiotic stresses assessed in this study.

2.5.9 The miR399 Regulatory Module in Response to Heat, Mannitol and Salt Stress

Given the documented role of miR399-directed expression regulation of *PHO2/PHO2* in aiding *Arabidopsis* to mount a molecular based adaptive response to conditions of limited Pi, a highly interesting finding uncovered in this study was that the abundance of the miR399 sRNA was also altered by heat, mannitol and salt stress (**Figure 2.10**). While to date, the miR399/*PHO2* regulatory module has not been profiled in *Arabidopsis* under the abiotic stress conditions of heat, mannitol or salt stress, this regulatory module has been thoroughly studied with regard to Pi starvation (Aung *et al.*, 2006; Bari *et al.*, 2006). Specifically, *MIR399* gene expression, and therefore miR399 accumulation, is significantly elevated in response to Pi starvation, a molecular response that in turn leads to enhanced miR399-directed expression repression of *PHO2*, and ultimately, reduced PHO2 protein abundance (Aung *et al.*, 2006; Bari *et al.*, 2006). Reduced PHO2 abundance removes the ubiquitin-mediated degradation of the P transporters, PHOSPHATE TRANSPORTER1;4 (PHT1;4), PHT1;8 and PHT1;9, resulting in enhanced root-to-shoot translocation of Pi (Aung *et al.*, 2006; Bari *et al.*, 2006). Given the essential role of Pi in plant growth and development (Schachtman *et al.*, 1998), in conjunction with the well documented and extensive cross-talk between the nutrient and hormone pathways in both standard *Arabidopsis* development and in the response of *Arabidopsis* to growth conditions of abiotic stress (Kohli *et al.*, 2013; Peleg and Blumwald, 2011; Yu *et al.*, 2015), the molecular behaviour of the miR399/*PHO2* regulatory module was profiled under the abiotic stress conditions of heat, mannitol and salt stress, to determine if the miR399/*PHO2* regulatory module would mimic, or differ to, the behaviour of the regulatory module in Pi deficient conditions.

The reciprocal miR399 abundance and *PHO2* expression trends observed by heat, mannitol and salt stressed Col-0 whole seedlings strongly suggested that miR399 regulates the expression of *PHO2* via an mRNA cleavage based mechanism of RNA silencing. More specifically, elevated miR399 abundance (**Figure 2.13A**) was repeatedly demonstrated in conjunction with reduced *PHO2* expression (**Figure 2.13B**) by RT-qPCR in heat, mannitol and salt stressed Col-0 seedlings. A similar molecular profile of elevated miR399 abundance and reduced *PHO2* expression was also obtained by RT-qPCR analyses of heat, mannitol and salt stressed *drb4* whole seedlings (**Figure 2.13A-B**). This finding again indicated that the abundance of the *PHO2* transcript is regulated via a miR399-directed transcript cleavage mechanism of RNA silencing in this mutant background post their exposure to heat, mannitol and salt stress, and further, that the DRB4 protein was not required for this miRNA/target gene regulatory module.

As P serves as an essential plant macronutrient, required as a fundamental element in phospholipids, nucleic acids, enzyme regulation, energy metabolism and signal transduction cascades, it is not unreasonable to suggest in an attempt to maintain development during a period of abiotic stress, *Arabidopsis* is increasing P translocation to the shoot tissue by repressing *PHO2* expression and therefore suppressing the functional activity of the *Arabidopsis* PHT family members (Poirier and Bucher, 2002). However, unlike Col-0 and *drb4* seedlings, this molecular response appears to be largely impacted in the absence of DRB1. More specifically, the loss of DRB1 results in the inability of the *drb1* mutant to upregulate miR399 abundance during heat, mannitol or salt stress. As a direct result of defective miR399-directed expression regulation of *PHO2* expression in the *drb1* mutant, *PHO2* expression is highly upregulated in *drb1* seedlings exposed to each of the abiotic stress growth regimes imposed in this study. This is not unsurprising as DRB1 is well established as the primary DRB required for the production of a large proportion of the *Arabidopsis* miRNA landscape, and further, the sRNA-seq data shown in **Figure 2.9** confirms DRB1 as the primary DRB required for miR399 production.

Curiously, loss of the other crucial nucleus localised DRB, DRB2, also impacted the appropriate regulation of the miR399/*PHO2* module in response to heat mannitol and salt stress. More specifically, while miR399 abundance was significantly increased in response to each of the abiotic stresses applied, elevation in miR399 sRNA accumulation failed to have a significant impact on the expression of *PHO2* (**Figure 2.13A-B**). Taken together, this unexpected result suggested that miR399-directed expression regulation of *PHO2* expression via a mRNA cleavage-based mechanism of RNA silencing is completely defective in the absence of DRB2 activity, and that the observed mild alterations to *PHO2* transcript abundance is the result of the miR399 sRNA alternatively regulating the expression of *PHO2/PHO2* via a translational repression mode of miRNA-directed RNA silencing. However, this proposed explanation of the molecular behaviour of the miR399/*PHO2* regulatory module documented here in the *drb2* mutant background requires further experimental validation at the protein level. Specifically, documentation of altered miR399 and *PHO2* abundance, in parallel with relatively unchanged levels of the *PHO2* transcript, would confirm that the miR399 sRNA regulates the levels of *PHO2/PHO2* via a translational repression mode of RNA silencing in the *drb2* mutant background.

2.5.10 The miR408 Regulatory Module in Response to Heat, Mannitol and Salt Stress

Previous research (Hajyzadeh *et al.*, 2015; Jovanović *et al.*, 2014; Ma *et al.*, 2015; Mutum *et al.*, 2013; Wu and Jinn, 2012) has repeatedly demonstrated the responsiveness of the Cu responsive miRNA, miR408, to a range of abiotic stress treatments (including drought, heat, salinity, osmotic and oxidative stress) across a range of evolutionary unrelated plant species, including, *Arabidopsis*, *Cicer arietinum* (chickpea), *Pisum sativum* (pea) and *Oryza sativa* (rice). Based on the findings outlined in these previous reports (Hajyzadeh *et al.*, 2015; Jovanović *et al.*, 2014; Ma *et al.*, 2015; Mutum *et al.*, 2013; Wu and Jinn, 2012), it was expected that RT-qPCR would reveal miR408 abundance to be increased in *Arabidopsis* whole seedlings exposed to heat, mannitol and salt stress. RT-qPCR confirmed that miR408 abundance was indeed elevated post the exposure of Col-0 seedlings to heat, mannitol and salt stress (**Figure 2.14A**). However, it was a surprise to observe a similar increase in *LAC3* expression, a target gene of miR408-directed expression regulation, in heat, mannitol and salt stressed Col-0 plants (**Figure 2.14B**). Scaling of *LAC3* transcript levels in proportion to the abundance of the miR408 sRNA in Col-0 plants was highly suggestive that miR408 regulates *LAC3/LAC3* levels via translational repression mechanism of RNA silencing in *Arabidopsis*. The upregulation of *LAC3* in Col-0 seedlings exposed to heat, mannitol or salt stress was a curious finding as it was initially suspected each of the Cu containing proteins targeted by miR408 would be downregulated in response to an abiotic stress insult. More specifically, as *LAC3* houses Cu, it was expected that in an attempt to mount an effective adaptive response to conditions of heat, mannitol or salt stress, elevated miR408 abundance would repress the abundance of the *LAC3* transcript, in turn liberating additional Cu to undertake its role in oxidative stress assistance, photosynthesis and electron transport, all cellular responses shown to alleviate the negative impacts of these abiotic stresses (Ding and Zhu, 2009). However, as *LAC3* is also believed to play a key role in the lignin biosynthesis pathway (Boudet, 2000; Turlapati *et al.*, 2011), elevated *LAC3* expression, and therefore *LAC3* protein abundance, could be essential during conditions of heat, mannitol or salt stress, as lignin biosynthesis and deposition to the cell wall have been shown to be altered by both biotic and abiotic stress (Moura *et al.*, 2010). As there are five miR408 target genes in *Arabidopsis*, including *CUPREDOXIN*, *PLANTACYANIN*, *UCLACYANIN2*, *LAC12* and *LAC13*, it is not unreasonable to suspect that potentially one of these other Cu containing proteins are responsible for establishing the Cu pool when *Arabidopsis* is mounting a molecular defence to conditions of heat, mannitol or salt stress. Further, Ma and colleagues (2015) revealed the variety of expression changes observed for miR408, and each of its target genes, under each of the abiotic stress growth regimes of their study, including Cu starvation, cold, salinity,

oxidative, PEG and drought stress, further highlights the complexity of the miR408/target gene regulation module depending on the abiotic stress under investigation. Specifically, depending on the stress elicited, and the particular miR408 target gene selected, the expression change in miR408 target genes were sometimes significantly altered in the same direction as miR408 accumulation changes, while other times, the same target gene would present a reciprocal expression change to that observed for miR408 abundance. An additional study found during *Arabidopsis* senescence, the expression of *LAC3* (and *CUPREDOXIN*) were reduced in proportion with an increase in miR408, a finding typically indicative of miRNA-directed mRNA cleavage repression (Thatcher *et al.*, 2015), this finding (in conjunction with the findings of Ma *et al.*, 2015 and the miR408/*LAC3* expression changes observed in **Figure 2.14A-B**) raises the possibility that depending on the molecular pathway (i.e. growth and development or the specific abiotic stress adaptation pathways), miR408 can regulate each of its target genes by either mRNA cleavage or a translational repression mechanism of RNA silencing, dependent of the gene expression outcome of the molecular response.

The complexity of the molecular mechanism by which miR408 regulates *LAC3* becomes readily apparent when assessing the accumulation levels of both miR408 and *LAC3* in each of the *drb* mutant lines post their exposure to heat, mannitol and salt stress. The exposure of *drb1* seedlings to heat stress resulted in miR408 abundance being reduced, and *LAC3* expression being upregulated; reciprocal abundance trends that were highly indicative of a miR408-directed mRNA cleavage mode of gene expression regulation. However, when *drb1* is exposed to mannitol stress, the levels of both the miR408 sRNA and the *LAC3* target gene were upregulated. Scaling of the abundance of the miRNA and its targeted gene could potentially indicate that under this specific stress condition, miR408 is regulating *LAC3* expression via the alternate mode of miRNA-directed expression regulation, translational repression. However, considering that a similar enhanced abundance for miR408 and *LAC3* was observed in mannitol stressed Col-0 plants, the obtained profile could simply indicate that the expression of both encoding loci (*MIR408* and *LAC3*) is enhanced by mannitol stress in *Arabidopsis* irrespective of the genetic background. In response to a 7 d salt stress growth regime, the accumulation of miR408 and the expression of *LAC3* failed to be significantly altered in *drb1* seedlings, compared to control *drb1* seedlings, a finding that suggested that the expression of the encoding loci, *MIR408* and *LAC3* is not influenced by this form of abiotic stress. This variety of miR408/*LAC3* profile responses observed in the *drb1* mutant background, were somewhat expected as previous data presented by Ma *et al.*, (2015) highlighted the variety of miR408/target gene profile trends observed in response to varied growth conditions. In addition to this, the *drb1* seedlings have a severe developmental phenotype (**Figure 2.2**), a phenotype which may be impacting on the appropriate regulation

of the *LAC3* transcript due to its speculated role in lignin biosynthesis (Boudet, 2000; Turlapati *et al.*, 2011).

Similarly to Col-0 *Arabidopsis* seedlings, when *drb2* seedlings were exposed to heat stress, the accumulation of miR408 was significantly upregulated compared to non-stressed *drb2* seedlings. However, *LAC3* expression was not significantly altered, but the mild reduction in the expression of *LAC3* in heat stressed *drb2* seedlings suggested that the miR408 sRNA was regulating *LAC3* transcript abundance via the canonical mRNA cleavage mode of RNA silencing. In contrast to this finding, when *drb2* seedlings were exposed to either mannitol or salt stress, there is no statistically significant alteration to either miR408 abundance or *LAC3* expression from that of non-stressed *drb2* seedlings. Again, the apparent loss in ability of *drb2* seedlings to appropriately regulate miR408 abundance and *LAC3* expression to wild-type equivalence could stem from; (1) *LAC3* regulation being altered due to the variation in developmental phenotype between Col-0 and *drb2* seedlings, and/or; (2) the previously documented variation in miR408/miR408 target gene accumulation patterns depending on the growth regime that *Arabidopsis* seedlings are exposed to (Ma *et al.*, 2015).

Similar to the miR408/*LAC3* abundance profiles observed for Col-0 counterparts, *drb4* seedlings exposed to a heat, mannitol and salt stress growth regime displayed miR408 and *LAC3* expression changes that were indicative of miRNA-directed translation repression. Specifically, when exposed to heat, mannitol or salt stress growth regimes, in comparison to non-stressed counterparts, the abundance of miR408, and the expression level of *LAC3*, were both increased by the heat and salt stress treatment, yet both were decreased by the mannitol stress treatment. Again, the varying miR408/*LAC3* accumulation profiles observed for *drb4* seedlings in response to each of the three abiotic stresses assessed in this study, highlights the complexity of the miR408/*LAC3* regulatory module in response to abiotic stress conditions.

Chapter III

The Phenotypic and Molecular
Consequence of Manipulating the
miR396 Regulatory Module in
Arabidopsis

3.1 Chapter Overview/ Rationale

The sRNA-seq approach and the subsequent experimental validation via miRNA-specific RT-qPCR, identified multiple miRNAs with altered abundance in response to each imposed stress. As documented in **Chapter II**, for wild-type *Arabidopsis* seedlings, the abundance of miRNAs, miR396 and miR399, was significantly upregulated in response to the three assessed abiotic stresses (see **Figure 2.10** and **Figures 2.12- 2.14**). In addition to these findings, both miRNAs are highly conserved across a diverse range of plant species, and have been demonstrated to regulate the expression of target genes involved in crucial aspects of plant growth and development, and/or to regulate the expression of key genes involved in the abiotic stress response of a plant (Axtell and Meyers, 2018; Bari *et al.*, 2006; Ma *et al.*, 2015; Omidbakhshfard *et al.*, 2015). It was also interesting to note that the well documented P responsive miR399/*PHO2* expression module, was significantly responsive to the imposed conditions of heat, mannitol and salt stress. As it is not uncommon to identify molecular pathways involved in multiple stress responses (see **Figure 2.10**; Khraiwesh *et al.*, 2012), this finding raised the possibility that other miRNAs identified as responsive to the abiotic stress conditions of heat, mannitol and salt stress may also be central to the phenotypic response of *Arabidopsis* attempting to adapt to growth in a P deficient (P⁻) environment. Therefore, in addition to characterising the miRNA-directed responses to salt stress in this results chapter, and in the subsequent results chapter of this thesis (**Chapter IV**), miRNA-directed responses in *Arabidopsis* to growth in a P deficient environment was also characterised. While it would have been ideal to further investigate the miRNA-directed response of heat and mannitol stress, four stress growth regimes (in addition to control grown seedlings) was not feasible within the available growth facilities. Therefore, salt stress was preferentially selected over heat stress and mannitol stress as information determined here on the miRNA-directed salt stress response is of high interest to other projects currently being undertaken.

To characterise the role that the miR396/*GRF* expression module was potentially playing in the ability of *Arabidopsis* plants to mount an adaptive response to the abiotic stresses of P deficiency and salinity, the miR396 expression module was manipulated in the Col-0 background. Specifically, two molecular approaches were employed in this study, and included;

- (1) Knockdown of mature miR396 abundance via the use of miRNA target mimicry technology (Franco-Zorrilla *et al.*, 2007) to generate an *Arabidopsis* plant line (*MIM396* plants) with reduced miR396 abundance, and;
- (2) The overexpression (OE) of the *MIR396* precursor transcript to generate an *Arabidopsis* plant line (*MIR396* plants) with elevated miR396 sRNA abundance.

Post generation of *MIM396* and *MIR396* plants, the plant lines Col-0, *MIM396* and *MIR396* were cultivated under standard (non-stress) growth conditions, and in P deficient and elevated salt growth regimes. This parallel cultivation approach was applied here to determine if, compared to wild-type Col-0 plants, the *MIM396* or *MIR396* plant lines expressed any phenotypic and/or physiological sensitivity, or tolerance, to either P deficiency or salt stress. In order to further attempt to identify any miR396-directed responses to the two applied stresses, RT-qPCR was used to document the molecular profiles of the newly generated *MIM396* and *MIR396 Arabidopsis* plant lines. Specifically, miR396 abundance and the expression of the miR396 target genes, *GRF1*, *GRF2*, *GRF3*, *GRF7*, *GRF8* and *GRF9*, was assessed in wild-type *Arabidopsis*, and in *MIM396* and *MIR396* plants post their cultivation in non-stress, P deficient, and salt stress growth conditions.

3.2 Introduction

3.2.1 ***Improved Phosphate Use Efficiency Equates to Improved Crop Production***

Phosphorous (P) is an essential plant macronutrient, acting as a central cellular building block required for the production of nucleic acids, phospholipids, a multitude of coenzymes, and the synthesis of chemical energy in the form of ATP; all of which are essential for all of the molecular and metabolic processes of a plant cell (Marschner, 2011; Raghothama, 2000). The vital requirement for adequate P supplies in plant cells is evidenced by the extensive P sensing, signalling, and transport networks of plants (Rouached *et al.*, 2010; Wang *et al.*, 2018), and by the detrimental phenotypic markers of P deficiency, specifically, altered root morphology, inhibited shoot growth, and anthocyanin over-accumulation (Raghothama, 1999). Further, when considering the productivity of economically significant crops, up to 40% of the global crop yield is limited by P, a deficiency that is currently addressed with fertilisers due to the extremely low availability of P in most cultivated soils (Vance *et al.*, 2003). This presents a serious issue as the P fertilisers used to maintain grain crop productivity, are themselves sourced from the finite and rapidly diminishing depositions of phosphorite, with global phosphorite sources predicted to be completely depleted within the next 50 to 100 years. The seriousness of this alarming trend is evidenced by the prediction that demand will outweigh supply by 2035 (Cordell *et al.*, 2009; Elser and Bennett, 2011; Smil, 2000). Further, while only 15-30% of the applied P is acquired by crops within 12 months of its application (Syer *et al.*, 2008), excessive fertiliser application has also been shown to have a direct negative impact on aquatic and terrestrial ecosystems, driving eutrophication of the habitats proximal to cropping areas (Bennett *et al.*, 2001; Huang *et al.*, 2017; Khan and Mohammad, 2014). Compounding this issue, is that the global population is continuing to rapidly increase, meaning that current crop production outputs must approximately double by 2050 to meet the consumer demand on agriculture (Ray *et al.*, 2013). One avenue to attempt to achieve this demand is to improve P use efficiency and/or the rate of P acquisition of plants to maximise productivity, growth and/or survival during growth conditions of minimal P: essential steps to reduce fertiliser use, and therefore, the reliance on P supply, a rapidly depleting resource. Focusing on only P use efficiency, Veneklaas and colleagues (2012) suggested that in order to improve P use efficiency in plants, key targets for modification would be; (i) reducing the excess of ribosomal RNAs; (ii) substitution of phospholipids for alternatives (i.e. sulfolipids); (iii) increased P remobilisation, and; (iv) efficient partitioning of P throughout the phenologically distinct phases of plant development (Veneklaas *et al.*, 2012).

3.2.2 The MicroRNA396 Regulatory Module

Initially discovered in rice (*Oryza sativa*) in 2000, GROWTH REGULATING FACTORS (GRFs) form a highly conserved plant specific family of transcription factors (van der Knaap *et al.*, 2000). At the protein level, each GRF is characterised by the presence of two conserved amino-terminal domains, including; (1) the eukaryotic glutamine, leucine, glutamine (QLQ) domain, and; (2) the plant-specific tryptophan, arginine, cysteine (WRC) domain (**Figure 3.1**; Ahmadi *et al.*, 2014; van der Knaap *et al.*, 2000). Proximal to the GRF 5' terminus, the QLQ domain was so termed based on the highly conserved QX₃LX₂Q amino acid peptide arrangement (Treich *et al.*, 1995; van der Knaap *et al.*, 2000). A study conducted on the SWITCH2/SUCROSE NONFERMENTING2 (SWI2/SNF2) complex of *Saccharomyces cerevisiae*, suggested that the QLQ domain played an important role in mediating the protein-protein interactions required for the formation of this chromatin-remodelling complex (Treich *et al.*, 1995). The WRC domain is characterised by the highly conserved amino acid sequence, CX₉CX₁₀CX₂H. This C₃H-type zinc finger motif is central to both the DNA binding and nucleus trafficking capabilities of each GRF transcription factor and for the other unrelated proteins that also harbour this domain (Raventós *et al.*, 1998; van der Knaap *et al.*, 2000).

At the transcriptional level, it is well established that the expression of most *GRFs* is regulated by the miRNA, miR396 (Hewezi and Baum, 2012; Liu *et al.*, 2009; Omidbakhshfard *et al.*, 2015). Studies across multiple monocotyledonous and dicotyledonous plant species have associated the miR396/*GRF* regulatory module with an array of plant processes, including; (1) grain development and yield in rice (Che *et al.*, 2015; Gao *et al.*, 2015); (2) stem elongation in rice (van der Knaap *et al.*, 2000); (3) leaf development in *Arabidopsis* (Horiguchi *et al.*, 2005; Kim *et al.*, 2003); (4) cell proliferation and cell aging in *Arabidopsis* (Horiguchi *et al.*, 2005; Kim *et al.*, 2003); (5) root growth and development in *Arabidopsis* (Bao *et al.*, 2014; Hewezi and Baum, 2012); (6) floral organ development in *Arabidopsis* (Liang *et al.*, 2014; Pajoro *et al.*, 2014); (7) kernel and ear development in maize (Zhang *et al.*, 2008), and; (8) responses to the abiotic stresses of salt, osmotic, ABA, UV, cold and drought stress in rice, wheat, maize and *Arabidopsis* (Casati, 2013; Kantar *et al.*, 2011; Kim *et al.*, 2012; Liu *et al.*, 2008; Shen *et al.*, 2010).

Although the miR396/*GRF* regulatory module has been associated with an extensive array of developmental processes across a range of plant species, a limited number of studies have characterised the GRF-coordinated response to abiotic stress in *Arabidopsis* (Kim *et al.*, 2012; Liu *et al.*, 2014). In drought stress response studies in *Arabidopsis*, it has been established that elevated levels of the DEHYDRATION-RESPONSE ELEMENT BINDING2A (DREB2A) protein correspond with plant growth inhibition (i.e., cell elongation), but a

heightened tolerance to the abiotic stimuli, heat, drought and salt stress (Kim *et al.*, 2012; Sakuma *et al.*, 2006; Yamaguchi-Shinozaki and Shinozaki, 2006). Moreover, research conducted by Kim and colleagues (2012) showed that in order to avoid growth inhibition of *Arabidopsis* wild-type seedlings during non-stressed conditions, GRF7 binds to a *cis*-element in the promoter of the *DREB2A* gene, to repress the expression of the gene. Furthermore, in the *Arabidopsis* *grf7* mutant background, a plant line that harbours a knockout insertion mutation in *GRF7* encoding locus, the expression of numerous abiotic stress responsive genes was demonstrated to be elevated, and further, the enhanced expression of this gene cohort resulted in the *grf7* mutant displaying a heightened tolerance to osmotic stress (Kim *et al.*, 2012; Liu *et al.*, 1998).

Assessment of miRNA levels via either a microarray, sRNA-seq or RT-qPCR based approach in drought stressed *Medicago truncatula*, *Sorghum bicolor*, *Triticum dicoccoides* (Emmer wheat) and rice, repeatedly identified miR396 as a drought responsive miRNA, that is; miR396 abundance is reduced in drought stressed plants (Hamza *et al.*, 2016; Kantar *et al.*, 2011; Wang *et al.*, 2011; Zhou *et al.*, 2010). For example, in the studies conducted by Hamza *et al.* (2016), Kantar *et al.*, (2011), Wang *et al.*, (2011) and Zhou *et al.*, (2010), miR396 abundance was demonstrated to be reduced by up to 2.0-fold in drought stressed *Sorghum bicolor*, Emmer wheat, *Medicago truncatula* and rice, respectively.

In addition to having been repeatedly associated with responses to abiotic stress stimuli, alterations to the miR396/*GRF* regulatory module has also been associated with altered plant development. Specifically, the Che *et al.*, (2015), Duan *et al.*, (2015) and Gao *et al.*, (2015) studies, co-published in the same issue of the peer-reviewed journal, *Nature Plants*, demonstrated that in rice, miR396 limits rice yield via repressing the expression of *OsaGRF4* and/or *OsaGRF6*. Via a molecular approach, these studies went on to show that when these two miR396 target gene transcripts are liberated from miR396 regulation, elevated *OsaGRF4* and *OsaGRF6* transcript abundance resulted in increased grain size and inflorescence (panicle) branching, respectively, with both of these phenotypic alterations ultimately resulting in increased yield. However, it was noted that both positive traits were not displayed in rice plants where miR396 abundance had been reduced via a target mimicry approach (Gao *et al.*, 2015). This is not a surprise finding and further provides an excellent example of the biological complexity of the pathways, intermediates, and protein machinery required for all aspects of growth and development in crop species. Moreover, the findings outlined by Gao *et al.*, (2015), Che *et al.*, (2015) and Duan *et al.*, (2015) reveal an attractive avenue of investigation for the development of superior crops via a molecular approach to enhance agricultural food output.

3.3 Material and Methods

3.3.1 Preparation and Storage of Bacterial Competent Cells

3.3.1.1 Escherichia coli (DH5 α)

A single colony of *Escherichia coli* (*E.coli*) DH5 α was inoculated in 10 (millilitres) mL of (Luria-Bertani) LB liquid medium (**Appendix 2 (A.2.2.2)**, page 240) at 37°C for 16 h. One mL of this culture was added to 100 mL of fresh LB liquid medium and incubated at 37°C until the culture reached an OD₅₅₀ of 0.6. The 100 mL culture was divided into four individual 25 mL aliquots and stored on ice for 10 min prior to a 5 min, 1,000·g centrifugation at 4°C. The supernatant was discarded, and the pelleted bacteria resuspended in 10 mL of chilled 0.1M CaCl₂ (**Appendix 2 (A.2.1.7)**, page 239), and incubated on ice for 1 h. The above centrifugation step was repeated, the supernatant discarded, and the pelleted cells were resuspended in 5.0 mL of chilled 0.1M CaCl₂ and 15% glycerol for distribution of 100 μ L aliquots in 1.5 mL microfuge tubes for subsequent storage at -80°C.

3.3.1.2 Agrobacterium tumefaciens (AGL1)

A single colony of *Agrobacterium tumefaciens* (*Agrobacterium*) AGL1 was inoculated in 10 mL of Yeast Extract Peptone (YEP) liquid medium (**Appendix 2 (A.2.2.3)**, page 240) supplemented with Rifampicin (**Appendix 5 (A.5.4)**, page 252) and cultured at 28°C for 48 h. Five hundred microlitres (μ L) of culture was added to 100 mL of fresh YEP liquid medium containing Rifampicin and incubated at 28°C until an OD₆₀₀ of 0.6 was reached. The 100 mL culture of *Agrobacterium* competent cells was processed and stored identically to the DH5 α competent cells (see the steps outlined in **Section 3.3.1.1**).

3.3.2 Cloning

3.3.2.1 Transgene Sequence Amplification or Synthesis

The DNA sequences for miR396-specific constructs were ordered from Integrated DNA Technologies (IDT, Australia) as gBlock[®] gene fragments or amplified from wild-type *Arabidopsis* (Col-0) genomic DNA (**Appendix 5 (A.5.1)**, page 251). Amplification of DNA sequences for subsequent transgenesis work was done using a standard PCR approach (**Appendix 3 (A.3.1.6)**, page 244) and the GoTaq[®] Long PCR Master Mix (Promega, Australia) according to the manufacturers' protocol.

3.3.2.2 *A-tailing of Transgene Insertion Fragments*

The gBlock[®] fragments were resuspended in TE buffer (**Appendix 2, A.2.1.8**, page 239) to a final concentration of 20 nanograms (ng)/ μ L. Prior to rapid (T/A) cloning into the pGEM-T Easy vector (**Appendix 5, A.5.3**, page 251), each gene block had an adenosine (A) overhang added to its blunt ends. A standard A-tailing reaction was prepared with the following components; gBlock[®] fragment (50 ng), Taq DNA polymerase (1-3 units (U)), 10X Taq DNA polymerase buffer (to 1X), dATP (to 0.05 mM), MgCl₂ (to 1.5 mM) and MQ-H₂O to a final reaction volume of 15 μ L. The reaction was incubated at 70°C for 20 min and used in subsequent ligation reactions (**Section 3.3.2.5**).

3.3.2.3 *Bacterial Plasmid DNA Purification*

All plasmid DNA purifications from *E.coli* DH5 α cells were conducted using a QIAprep Spin Miniprep kit (QIAGEN, Australia) according to the manufacturers' instructions.

3.3.2.4 *Restriction Digestion and Fragment Purification*

All restriction endonucleases used for DNA digestion were obtained from New England Biolabs (NEB), Australia. All restriction digests were set-up according to the manufacturers' protocol, however, an overnight (16 h) incubation at 37°C was used for all digestion reactions to ensure that the DNA digest was complete. Digested DNA fragments used in subsequent ligation reactions (**Section 3.3.2.5**) were isolated from an Ethidium bromide-stained 1.5% (w/v) agarose gel and purified with a QIAquick Gel Extraction kit (QIAGEN, Australia), following the manufacturers' protocol.

3.3.2.5 *DNA Ligation*

Ligation reactions contained a 3:1 molar ratio of insertion fragment to destination vector. In some instances, when non-directional cloning was necessary, a calf alkaline phosphatase (NEB, Australia) dephosphorylating reaction was conducted according to the manufacturers' protocol to prevent self-ligation of the digested plasmid DNA backbone. The 3:1 (insert:vector) ligation mixture was mixed thoroughly by vortexing prior to a 5 min, 65°C incubation. The ligation mixture was immediately transferred to ice and incubated for 5 min and subsequently made up to 10 μ L with 200 U of T4 DNA ligase (NEB, Australia), 10X ligation buffer and MQ-H₂O. The final ligation reaction was mixed by manual pipetting and incubated overnight at 22°C to allow the reaction to proceed.

3.3.2.6 *Heat Shock Transformation of DH5 α Competent Cells and the Identification of Insert Positive Bacterial Clones via PCR*

Stored 100 μ L aliquots of *DH5 α* competent cells (see **Section 3.3.1.1**) were thawed on ice for 10 min. Ten microlitres of DNA ligation mixture (see **Section 3.3.2.5**) was carefully pipetted with the competent cell mixture and incubated on ice for 30 min. The cells were 'heat-shocked' via incubation at 42°C for 35 s and immediately returned to incubate on ice for 5 min. Nine hundred microlitres of liquid LB media was added to the cells and incubated at 37°C on a rotating platform with gentle agitation for 1 h. Typically, 100-200 μ L of this suspension was plated on solid LB medium in petri dishes which had been supplemented with the appropriate antibiotic(s) (**Appendix 5, (A.5.3 and A.5.4)**, page 252) and incubated at 37°C overnight to identify putatively transformed colonies. To confirm the uptake of the inserted DNA fragment into the plasmid DNA backbone, a standard colony PCR was performed according to **Table A.3.5 (Appendix 3 (A.3.1.5)**, page 244) and with the appropriate primer pairs (**Appendix 4 (A.4.1.2)**, page 246)

3.3.2.7 *DNA Sequencing for Insert Confirmation*

The Australian Genome Research Facility (AGRF), Queensland node (Brisbane, Australia), performed sequencing reactions on 12 μ L samples containing 800 ng of plasmid DNA and 1 picomolar (pmol/ μ L) of forward primer. The returned sequences were analysed using the freely available geneious R9 software (Kearse *et al.*, 2012).

3.3.2.8 *Electroporation*

On ice, 200 ng of plasmid DNA was gently yet thoroughly mixed with a 40 μ L aliquot of electro-competent AGL1 cells (see **Section 3.3.1.2**). The entire mixture volume was transferred to an electroporation cuvette and electroporated on an Electroporator (Gene Pulser[®] II, Bio-Rad Laboratories, Australia). The electroporation cuvette was immediately placed on ice and 500 μ L of **Super Optimal** broth with **Catabolite** repression (SOC) liquid media (**Appendix 2 (A.2.2.4)**, page 241) was added prior to incubation at 28°C for 1 h. Cultures were spread on solid LB medium supplemented with Ampicillin, Spectinomycin and Rifampicin (**Appendix 5 (A.5.4)**, page 252) for 48 h at 28°C. Recovered putative transformant colonies were inoculated in 10 mL of LB liquid medium for 48 h at 28°C in the dark prior to 500 μ L of this culture being added to a 50% glycerol solution for storage at -80°C.

3.3.2.9 *Floral Dip Transformation and Screening for Putative Transformant Lines.*

Agrobacterium harbouring the desired plant expression vectors (described in **Section 3.3.2.8**) were streaked on to petri dishes containing solid LB medium supplemented with Ampicillin, Spectinomycin and Rifampicin (**Appendix 5 (A.5.4)**, page 252). Each plate was covered in aluminum foil, to keep in the dark, and grown at 28°C for 48 h. A single resulting *Agrobacterium* colony was isolated and further cultured in the dark for 48 h at 28°C in 40 mL of liquid LB medium supplemented with Ampicillin, Spectinomycin and Rifampicin (**Appendix 5 (A.5.4)**, page 252). *Agrobacterium* cultures were pelleted by centrifugation at 1,000·g for 15 min at 4°C. Each *Agrobacterium* pellet was resuspended a 5.0% (w/v) sucrose solution supplemented with 0.05% (v/v) of the Silwet-L77 wetting agent (Lehle Seeds, USA).

Soil cultivated *Arabidopsis* Col-0 seedlings were grown under standard growth conditions (see **Section 2.3.1.1**), watered with 500 mL per tray of plants (n=15) every 48 h and pruned to retain only the main inflorescence and unopened terminal floral buds. Each plant was then dipped into the *Agrobacterium* solution for 30 seconds between 10:30 to 11:30 am (to encourage T-DNA uptake due to the 'openness' and/or 'receptiveness' of *Arabidopsis* flowers at this time of the day). Post dipping, plants were enclosed in clear plastic film and incubated at 22°C in the dark for 24 h. After this incubation period, the plastic film was removed and plants were then grown under normal growth conditions until the dipped plants set seed. Subsequently, seeds were harvested from each dipped plant and then stored at RT for a minimum of 8 weeks to ensure hardening of the seed coat. An aliquot of each collection of seeds was surfaced sterilised with chloride gas (see **Section 2.3.1.1**), and then sown on standard MS medium supplemented with glufosinate ammonium (PPT) and Timentin (**Appendix 5 (A.5.4)**, page 252). Plants resistant to PPT (T₁ plants) were transferred to soil for self-pollination to allow for the collection of T₂ seeds. The T₂ seeds were sterilised with chloride gas and sown on standard MS media supplemented with PPT. Seedlings resistant to the PPT selective agent were transferred to soil for self-pollination to allow for the obtainment of T₃ seeds: the T₃ plants which germinated from the seed collected from the T₂ plants was the transformant generation used for experimental analysis reported in this study. Putative T₃ transformants were confirmed to be genuine transformants with a standard PCR reaction (**Appendix 3 (A.3.1.1)**, page 243) using primers specific to the pBART plant expression vector which housed each of the desired transgene inserts (**Appendix 5 (A.5.2)**, page 252) prior to their use for experimental analyses.

3.3.3 **Plant Growth Conditions**

The materials and methods used to induce plant growth in a P deficient environment and a salt stress environment in this Chapter can be found in the following publications:

Pegler, J. L., Oultram, J. M., Grof, C. P., and Eamens, A. L. (2019). DRB1, DRB2 and DRB4 Are Required for Appropriate Regulation of the microRNA399/PHOSPHATE2 Expression Module in *Arabidopsis thaliana*. *Plants*, 8(5), 124.

<https://www.mdpi.com/2223-7747/8/5/124>

Pegler, J. L., Oultram, J. M., Grof, C. P., and Eamens, A. L. (2019). Profiling the Abiotic Stress Responsive microRNA Landscape of *Arabidopsis thaliana*. *Plants*, 8(3), 58.

<https://www.mdpi.com/2223-7747/8/3/58>

A copy of these publication can be found in **Appendix 1 (A.1.4)** and **Appendix 1 (A.1.3)** of this thesis, pages 211-236 and pages 193-210, respectively. The relevant experimental methodologies are detailed in sections; '*Plant Material and Phosphate Stress Treatment*', page 231 and '*4.1 Plant Material*', page 205, respectively

3.3.4 **Phenotypic and Physiological Analyses of Transformed Col-0 Seedlings**

The phenotypic and physiological analyses were conducted on 15 d old seedlings that had been cultivated under either a standard non-stress growth regime for the entire 15 d period, or which had been exposed to a 7 d period of P deficiency or salt stress. Specifically, assessments of the; (i) fresh weight; (ii) rosette area; (iii) primary root length; (iv) anthocyanin accumulation, and; (v) chlorophyll *a* and *b* content, have previously been described in **Chapter II, Section 2.3.2.1- 2.3.2.5** (pages 15-16), respectively.

3.3.5 Molecular Analyses of Transformed Col-0 Seedlings

For all molecular analyses conducted in this chapter, specifically, those materials and methods pertaining to the preparation and analysis of *Arabidopsis* samples for sRNA-seq and RT-qPCR analyses, please refer to the following publication:

Pegler, J. L., Oultram, J. M., Grof, C. P., and Eamens, A. L. (2019). Profiling the Abiotic Stress Responsive microRNA Landscape of *Arabidopsis thaliana*. *Plants*, 8(3), 58.
<https://www.mdpi.com/2223-7747/8/3/58>

A copy of this publication can be found in **Appendix 1 (A.1.3)** of this thesis, pages 193-210. The relevant experimental methodologies are detailed in sections; '*Total RNA extraction and high throughput sequencing of the small RNA fraction*', page 206, '*Bioinformatic assessment of the microRNA landscape of Arabidopsis whole seedlings*', page 206, and '*Quantitative reverse transcriptase polymerase chain reaction analyses*', page 207.

3.4 Results

3.4.1 **The Requirement of DRB1, DRB2 and DRB4 in Appropriate Regulation of the Phosphate Responsive, miR396/GRF7 Regulatory Module in Arabidopsis**

Due to the surprising finding that miR399, a known P deficient responsive miRNA, was highly responsive to each of the abiotic stresses assessed in this study (**Figure 2.10**), the response of miR396, a miRNA shown to be responsive to heat, mannitol and salt stress treatments (**Figure 2.10**), was reciprocally exposed to P deficient conditions. Additionally, identifying the role of DRB1, DRB2 and DRB4 in the appropriate regulation of the miR396/*GRF7* regulatory module under a P⁻ growth regime was central to the phenotypic and molecular analyses reported here.

All the phenotypic results pertaining to **Section 3.4.1** can be found in the publication:

Pegler, J. L., Oultram, J. M., Grof, C. P., and Eamens, A. L. (2019). DRB1, DRB2 and DRB4 Are Required for Appropriate Regulation of the microRNA399/PHOSPHATE2 Expression Module in *Arabidopsis thaliana*. *Plants*, 8(5), 124.

<https://www.mdpi.com/2223-7747/8/5/124>

A copy of this publication can be found in **Appendix 1 (A.1.4)** of this thesis, pages 211-236.

When exposed to a 7 d cultivation period in the absence of P, surprisingly each of the *Arabidopsis* lines, Col-0, *drb1*, *drb2*, and *drb4*, all had reduced miR396 abundance, specifically; miR396 abundance was reduced by 9.1-, 1.8-, 3.8- and 7.6-fold respectively in Col-0, *drb1*, *drb2* and *drb4* P stressed plants, compared to their control grown counterparts (**Figure 3.2A**). Similarly, when the expression of *GRF7* was investigated in the seedlings of each *Arabidopsis* plant line, Col-0 and *drb1* seedlings had significant reductions of 2.7- and 3.6-fold, while curiously, in both the *drb2* and *drb4* seedlings, RT-qPCR failed to detect the *GRF7* transcript (**Figure 3.2B**).

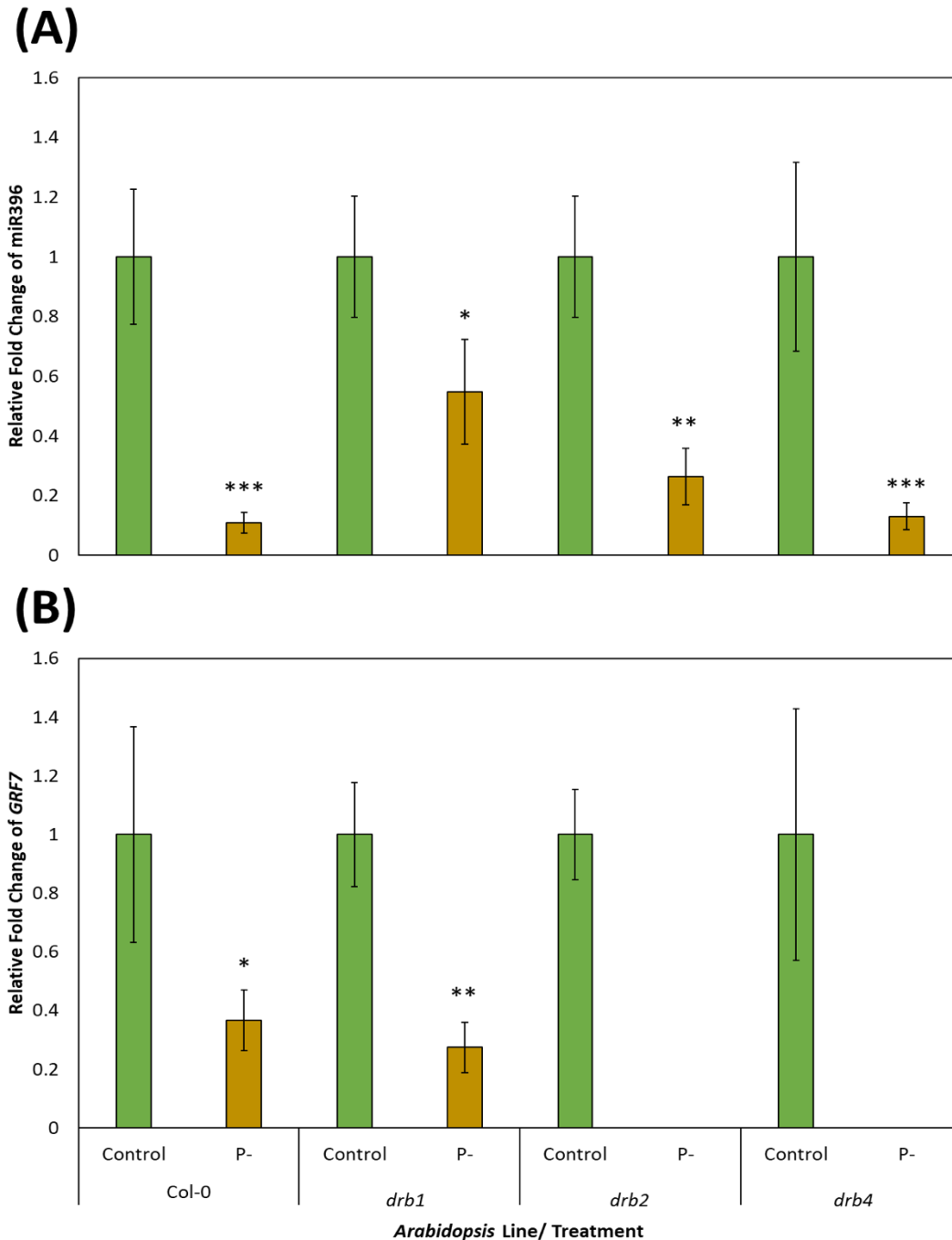


Figure 3.2 Molecular analysis of the miR396/GRF7 regulatory module in the shoot tissue of 15 d old *Arabidopsis* Col-0 seedlings and DRB-knockout mutants, *drb1*, *drb2* and *drb4* exposed to P deficiency, relative to untreated (control) seedlings. (A) The SL-RT-qPCR determined abundance of miR396 in *Arabidopsis* Col-0 seedlings and DRB-knockout mutants, *drb1*, *drb2* and *drb4* exposed to conditions of phosphate stress (B) RT-qPCR analyses of miR396 target gene, *GRF7*, expression changes of *Arabidopsis* lines, Col-0, *drb1*, *drb2* and *drb4* in response P stress, compared to non-stress growth conditions. Error bars represent the \pm SD of 4 biological replicates with each biological replicate consisting of the shoot tissue of 6 individual plants. The presence of an asterisk indicates a statistically significant difference between the control and stress treated seedlings for miR396 and *GRF7* (p-value: < 0.05, *; P < 0.005, **; P < 0.001, *).**

3.4.2 The Phenotypic Response of *Arabidopsis* miR396 Molecularly Modified Plant Lines to Phosphate Deficiency and Salt Stress

Having confirmed the miR396/*GRF* regulatory module was indeed responsive to P deficiency, the molecularly modified plant lines were investigated for their physiological and molecular responses to P⁻ and salt stress conditions. Maintaining the same cultivation conditions as described in Chapter II (**Section 2.4.1**), and post germination, 8 d old Col-0, *MIM396* and *MIR396* seedlings were exposed to a 7 d treatment period of either P⁻ or salt stress. Presented in **Figure 3.3**, is the phenotypic response displayed by each of the assessed *Arabidopsis* lines to control (non-stress), P deficiency (P⁻) or salt stress growth conditions. Compared to control Col-0 seedlings, a variable level of sensitivity to the P⁻ deficiency and/or salt stress growth regimes was displayed. Similarly to **Chapter II (Sections 2.4.1.1- 2.4.1.5)**, the visually striking variation of the degree of sensitivity to the abiotic stress conditions observed between the *Arabidopsis* lines was quantified via assessments of; (1) fresh weight (**Figure 3.4**), (2) rosette area (**Figure 3.5**), (3) primary root length (**Figure 3.6**), (4) anthocyanin accumulation (**Figure 3.7**) and, (5) chlorophyll *a* and *b* content (**Figure 3.8A-B**). Additionally, as the *MIM396* and *MIR396* plant lines are newly generated *Arabidopsis* lines, all phenotypic (and molecular) analyses found in this chapter are presented comparative to non-stressed Col-0 seedlings as any phenotypic (or molecular) differences between control grown Col-0 seedlings and the novel *Arabidopsis* plants that harbour molecular modifications of the miR396 regulatory module were of high interest.

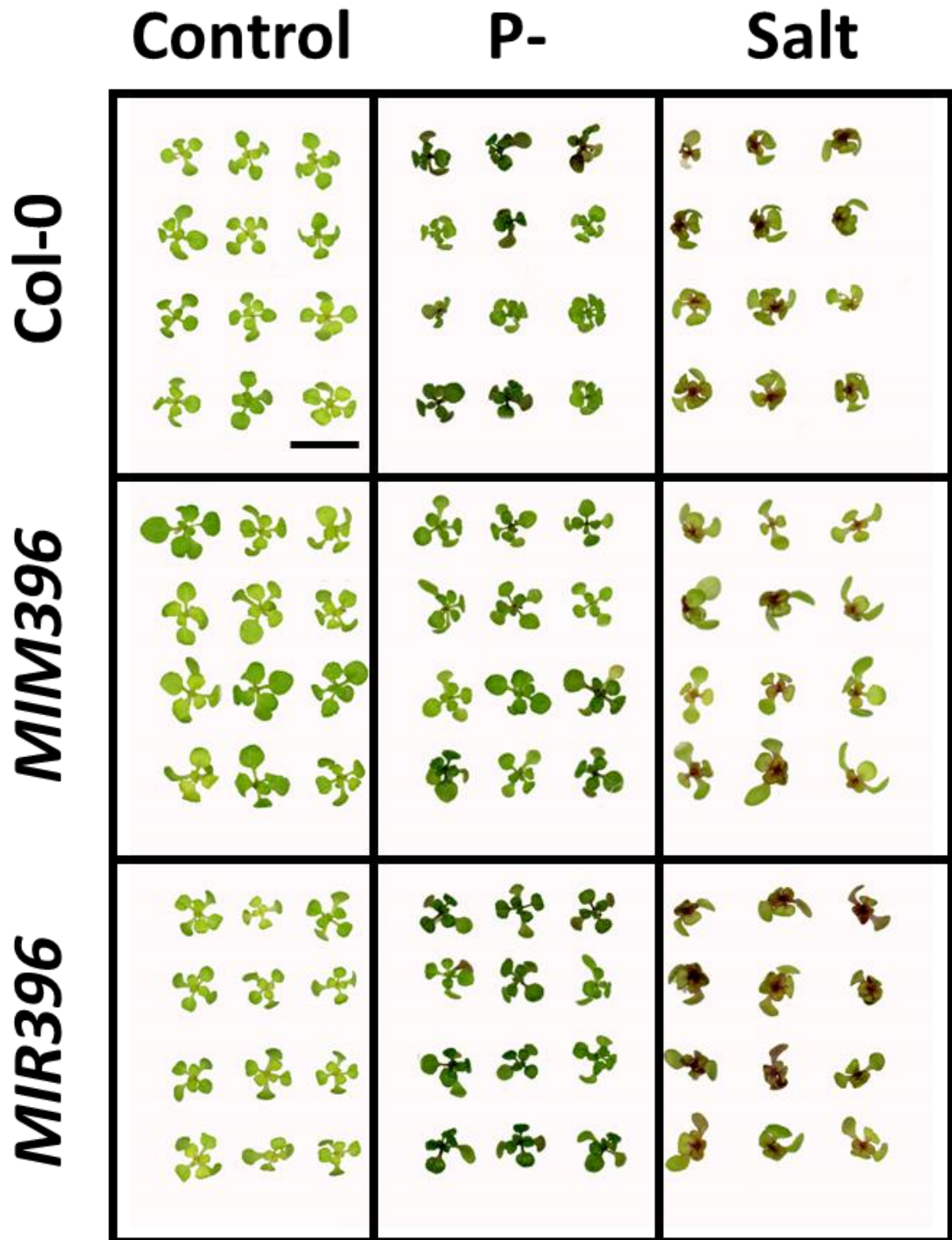


Figure 3.3 Phenotypic and physiological consequence of a P deficiency (P⁻) or salt stress treatment on 15 d old wild-type *Arabidopsis* (Col-0), *MIM396* and *MIR396*. Phenotypes displayed by 15 d old *Arabidopsis* whole seedlings post a 7 d treatment with P⁻ or salt stress, compared to non-stressed seedlings of the same age (left panel). Scale bar = 1.0 centimeter (cm).

3.4.2.1 *Fresh Weight*

When visualising the phenotypic response of the Col-0, *MIM396* and *MIR396* seedlings to the conditions of P deficiency or salt stress, it was readily apparent that in comparison to their non-stressed counterparts, overall shoot architecture was altered. To determine significant variations in overall plant morphology when Col-0 seedlings and the miR396 molecularly modified *Arabidopsis* plant lines were exposed to P⁻ or salt stress, fresh weight was measured (**Figure 3.4**). Comparable to previously obtained fresh weight data on Col-0 whole seedlings exposed to P⁻ or salt stress (**Appendix A.1.3**, pages 193-210; **Appendix A.1.4**, pages 211-236), it was unsurprising to observe significant 32.1% ($\pm 1.8\%$) and 26.1% (± 3.8) reductions to this phenotypic parameter when compared to control Col-0 seedlings. To determine if manipulation of the miR396 regulatory module resulted in phenotypic alterations under control conditions, the fresh weight of non-stressed *MIM396* seedlings was compared to non-stressed Col-0 seedlings, an initial analysis which revealed that the *MIM396* seedlings were significantly heavier with a 20.2% ($\pm 3.1\%$) increase in their fresh weight compared to non-stress Col-0 seedlings of the same age. When the same *MIM396 Arabidopsis* seedlings were exposed to P deficiency, the fresh weight of these seedlings was reduced by 21.9% ($\pm 2.3\%$), in comparison to control *MIM396* plants, a much milder reduction than what was observed for P stressed Col-0 seedlings. Further, while the fresh weight of *MIM396* seedlings was significantly reduced by 41.2% ($\pm 3.4\%$) in response to the salt stress growth regime, a much larger reduction than what was observed for salt stressed Col-0 seedlings ($32.1 \pm 1.8\%$), *MIM396* plants remained the heaviest of the three salt stressed plant lines. The reciprocally modified miR396 plant line, *MIR396*, was determined to have the same fresh weight ($95.1 \pm 4.6\%$) as Col-0 seedlings when both plant lines were cultivated under standard growth conditions. When exposed to P deficiency, the fresh weight of *MIR396* seedlings was significantly reduced by $25.0 \pm 4.1\%$. This negative growth trend was also observed for salt stressed *MIR396* plants with a 42.2% ($\pm 2.4\%$) reduction to fresh weight documented: the largest reduction to fresh weight observed for the three assessed plant lines post salt stress. The exposure of Col-0, *MIM396* and *MIR396* seedlings to P⁻ stress revealed that the imposed stress had the greatest impact on the fresh weight of Col-0 seedlings, compared to both *MIM396* and *MIR396* seedlings. Alternatively, the fresh weight of Col-0 was observed to be the least sensitive of the three assessed *Arabidopsis* lines post their exposure to salt stress. It should be noted here however, that when compared to their respective non-stress counterparts, although the fresh weight of *MIM396* seedlings was impacted to the greatest degree by each of the two imposed stresses, this plant line still remained the heaviest of the three plant lines assessed, regardless of the growth conditions.

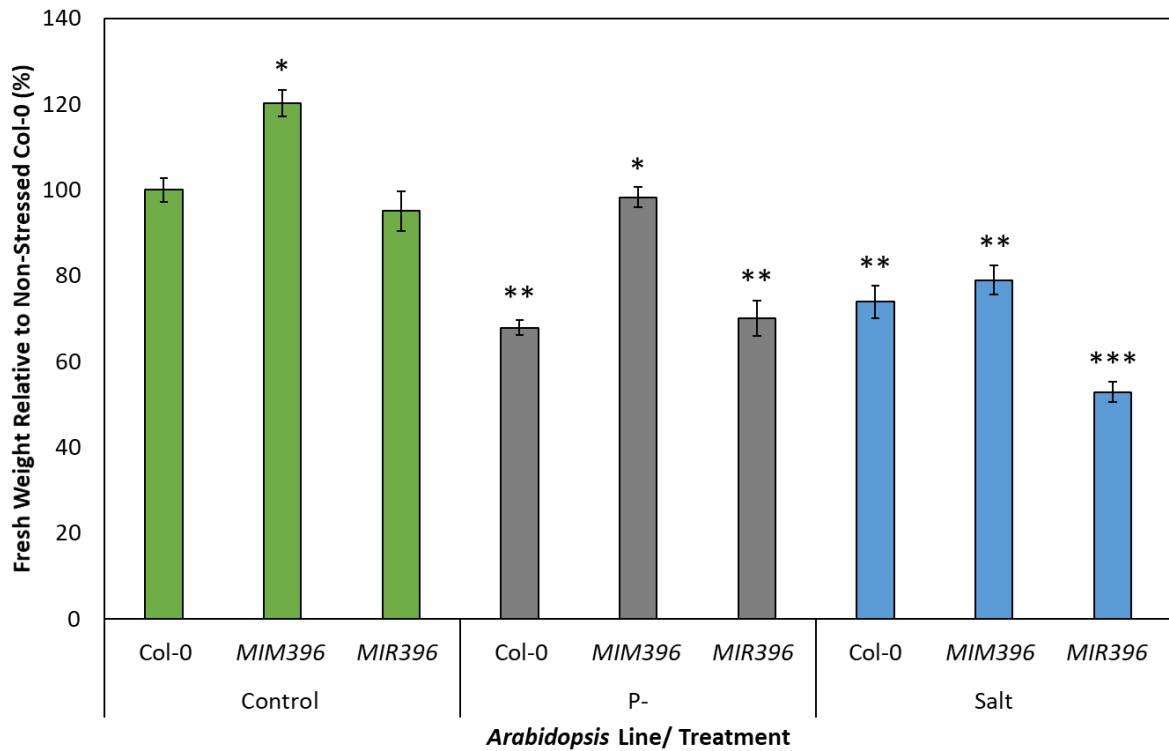


Figure 3.4 Whole seedling fresh weight of P⁻ and salt stressed *Arabidopsis* Col-0 and miR396 altered lines, *MIM396* and *MIR396*, relative to non-stressed Col-0 seedlings. Error bars represent the \pm SD of 4 biological replicates and each biological replicate consisted of a pool of six individual plants. The presence of an asterisk above a control grown *MIM396* or *MIR396* column represents a statistically significant difference comparative to control grown Col-0. Additionally an asterisk above a P⁻ or salt treated *Arabidopsis* plant line represents a statistically significantly difference between the stress treated sample and the respective non-stressed control sample (P-value: * < 0.05; ** < 0.005; *** < 0.001).

3.4.2.2 Rosette Area

To complement the whole seedling fresh weight analysis, rosette area measurements were again selected as an accurate indicator of the tolerance or sensitivity of each plant line to each imposed stress. Similar to the fresh weight observations, when exposed to P⁻ or salt stress conditions, the rosette area of Col-0 seedlings was significantly reduced by 41.6% (\pm 3.7%) and 39.9% (\pm 3.5%), respectively (**Figure 3.5**). Compared to the rosette area of Col-0 control seedlings, it was determined that the rosette area of *MIM396* control seedlings was significantly increased by 21.3% (\pm 2.9%). Exposure of the *MIM396* seedlings to P⁻ and salt stress resulted in rosette area reductions of 39.9% (\pm 2.9%) and 44.8% (\pm 2.2%) respectively, compared to control *MIM396* seedlings (**Figure 3.5**). While these reductions were significant, the rosette area of *MIM396* seedlings remained the largest of the three plant lines assessed. When compared to control grown Col-0 seedlings, the rosette area of control *MIR396* was determined to only be reduced by 6.5% (\pm 4.1%) (**Figure 3.5**). Compared to the rosette area reductions observed for P⁻ and salt stressed Col-0 and *MIM396* plants, the rosette area reductions of 18.8% (\pm 2.9%) and 33.5% (\pm 1.4%) for P⁻ and salt stressed *MIR396* plants respectively, were mild. While this comparatively mild reduction to *MIR396* seedling fresh weight tentatively indicates that the *MIR396* plant line is less sensitive to abiotic stress conditions of P⁻ and salt stress, than is the *MIM396* plant line, it should still be noted here that the overall rosette area of *MIR396* seedlings was smaller than that of *MIM396* seedlings under all growth regimes. Largely following the same trends observed for the fresh plant weight, the rosette area of Col-0 seedlings was determined to be impacted to a greater degree by the P deficient growth conditions than were either of the molecularly modified plant lines. This was not the case however in response to the imposed salt stress. Specifically, in comparison to the respective control of each plant line, the rosette area of the *MIM396* plant line was impacted to the greatest degree, while the *MIR396* plant line was impacted least by the imposed stress.

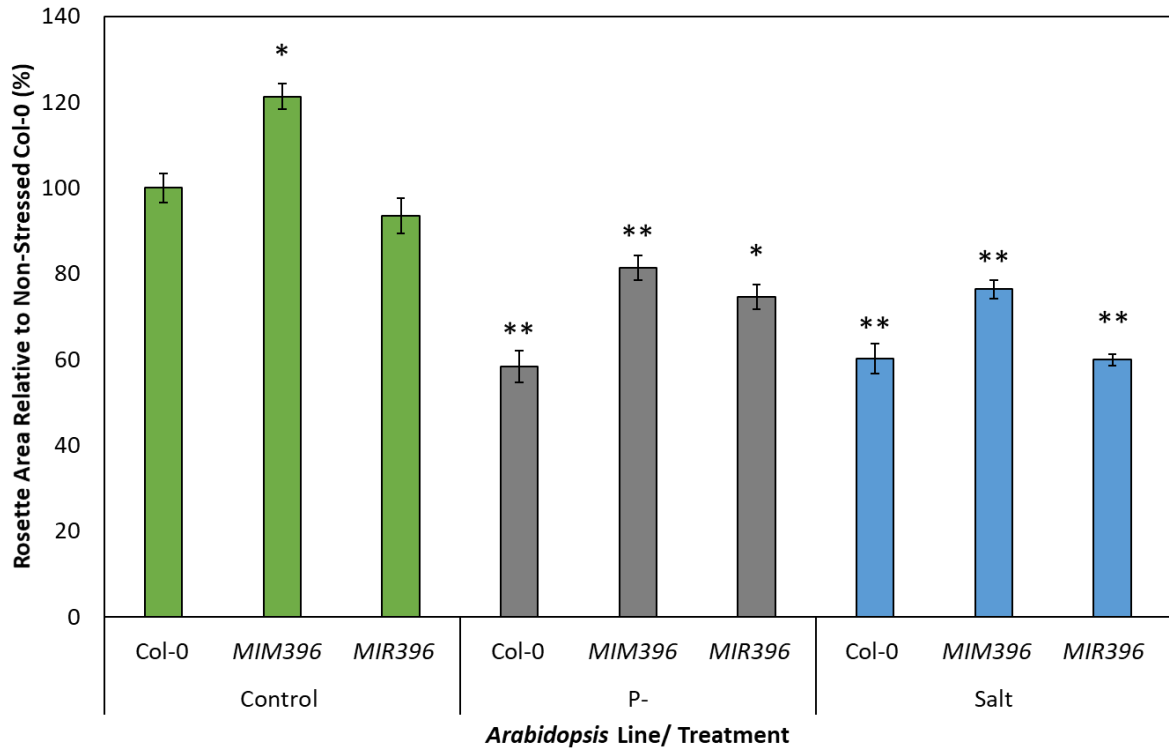


Figure 3.5 Rosette area of P⁻ and salt stressed *Arabidopsis* Col-0 and miR396 altered lines, *MIM396* and *MIR396*, compared to non-stressed Col-0 seedlings. Error bars represent the \pm SD of 4 biological replicates and each biological replicate consisted of a pool of six individual plants. The presence of an asterisk above a control grown *MIM396* or *MIR396* column represents a statistically significant difference comparative to control grown Col-0. Additionally an asterisk above a P⁻ or salt treated *Arabidopsis* plant line represents a statistically significantly difference between the stress treated sample and the respective non-stressed control sample (P-value: * < 0.05; ** < 0.005; *** < 0.001).

3.4.2.3 Primary Root Length

Given the significant alterations to plant shoot development of the three assessed plant lines, together with the well documented sensitivity of plant root architecture to P deficient conditions or salt stress (Acora *et al.*, 2011; Fujii *et al.*, 2005; Gao *et al.*, 2007; Pasternak *et al.*, 2005), primary root length was next quantified. Post exposure to P deficient conditions or salt stress, the primary root length of Col-0 seedlings was reduced by 47.5% ($\pm 1.8\%$) and 54.4% ($\pm 1.8\%$), respectively, compared to that of Col-0 control seedlings. When the primary root length of control grown *MIM396 Arabidopsis* seedlings was compared to that of Col-0 control seedlings, a mild and statistically insignificant increase of 9.3% ($\pm 2.7\%$) was documented (**Figure 3.6**). Interestingly, when *MIM396* plants were exposed to the P⁻ growth regime, no significant reduction (-12.7% $\pm 1.7\%$) to primary root length was observed compared to that of non-stressed *MIM396* plants. In direct contrast to this finding however was the significant 50.2% ($\pm 0.8\%$) reduction to primary root length of salt stressed *MIM396* seedlings. Similar to the reported shoot tissue observations for *MIR396* seedlings cultivated under control growth conditions, the primary root length of this plant line was found to remain unchanged (98.1% $\pm 3.9\%$) compared to Col-0 control primary root length. However, when *MIR396* seedlings were exposed to either the P deficient or salt stress growth regimes, primary root length was dramatically reduced by 47.4% ($\pm 1.9\%$) and 54.1% ($\pm 1.4\%$) respectively, compared to that of *MIR396* control seedlings. Although the primary root development of *MIM396* seedlings was largely unhindered by the absence of P, the primary root length of Col-0 and *MIR396* plants were both significantly reduced to near identical degrees relative to their respective control plants. The significant negative impact a 7 d salt stress treatment had on *Arabidopsis* root development was readily apparent with each plant line displaying a greater than 50% reduction to the length of their primary root compared to their respective non-stressed controls.

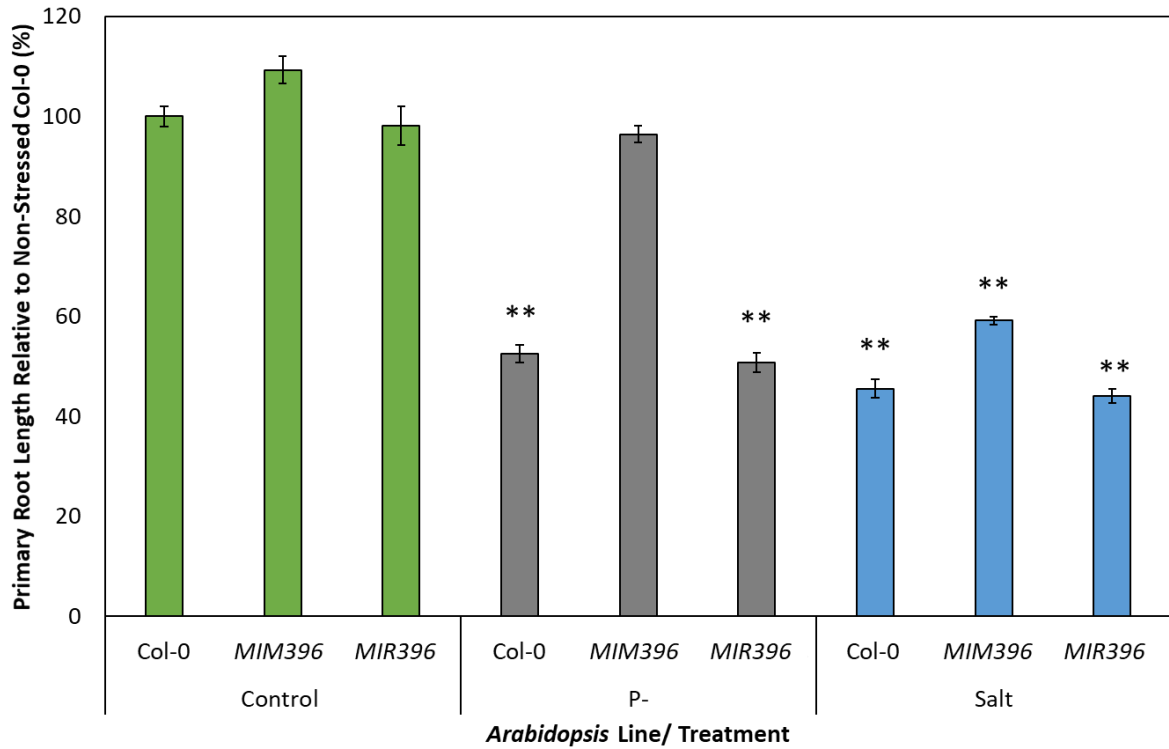


Figure 3.6 Primary root length of P⁻ and salt stressed *Arabidopsis* Col-0 and miR396 altered lines, *MIM396* and *MIR396*, compared to non-stressed Col-0 seedlings. Error bars represent the \pm SD of 4 biological replicates and each biological replicate consisted of a pool of six individual plants. The presence of an asterisk above a control grown *MIM396* or *MIR396* column represents a statistically significant difference comparative to control grown Col-0. Additionally an asterisk above a P⁻ or salt treated *Arabidopsis* plant line represents a statistically significantly difference between the stress treated sample and the respective non-stressed control sample (P-value: * < 0.05; ** < 0.005; *** < 0.001).

3.4.2.4 Anthocyanin Accumulation

When viewing the phenotypes displayed in **Figure 3.3**, striking variation in the shoot pigmentation was readily evident between control grown *Arabidopsis* seedlings and those cultivated for a 7 d period in either the absence of P, or in the presence of 150 mM NaCl. Again, this prominent darkening in pigmentation, particularly in the region surrounding the shoot apex, including newly emerging rosette leaves and the petioles of emerged leaves, was suspected to be the result of the accumulation of the well documented, abiotic stress associated pigment, anthocyanin (Akula and Ravishankar, 2011; Chalker-Scott, 1999; Kovinich *et al.*, 2015). Therefore, the abundance of anthocyanin was determined for control grown and stressed Col-0, *MIM396* and *MIR396* seedlings. Consistent with previous results (**Appendix A.1.3**, pages 193-210; **Appendix A.1.4**, pages 211-236), Col-0 seedlings grown on MS medium which either lacked P, or that was supplemented with 150 mM NaCl, accumulated 60.3% ($\pm 5.0\%$) and 80.8% ($\pm 2.8\%$) more anthocyanin respectively, than did control grown Col-0 seedlings (**Figure 3.7**). When *MIM396* seedlings were cultivated to 15 d of age under standard growth conditions, there was no significant variation in anthocyanin content compared to that of non-stressed Col-0 seedlings (98.2% $\pm 6.9\%$). Further, and as reported for Col-0 plants exposed to stress, anthocyanin accumulation was elevated by 57.6% ($\pm 6.4\%$) and 76.9% ($\pm 5.4\%$) in P⁻ and salt stressed *MIM396* seedlings respectively, compared to *MIM396* control seedlings. When comparing the anthocyanin accumulation profile of control grown *MIR396* seedlings to that of control Col-0 seedlings, anthocyanin levels were determined to remain largely unchanged (95.6% $\pm 7.1\%$). Interestingly, *MIR396* seedlings again displayed the greatest sensitivity to both of the assessed stresses with the largest increases in anthocyanin accumulation post P⁻ and salt stress exposure observed. Specifically, when compared to *MIR396* control seedlings, anthocyanin levels were elevated by 94.8% ($\pm 1.1\%$) and 135.9% ($\pm 3.2\%$) in P⁻ and salt stressed *MIR396* seedlings, respectively. Taken together, this analysis revealed that the extent of anthocyanin accumulation in response to a P⁻ stress was nearly identical in Col-0 and *MIM396* seedlings, while the anthocyanin content of *MIR396* plants was elevated to a much greater degree. This was also determined to be the case in Col-0, *MIM396* and *MIR396* salt stressed seedlings. Specifically, anthocyanin was determined to accumulate to a much greater degree in salt stressed *MIR396* seedlings than in either salt stressed Col-0 or *MIM396* seedlings.

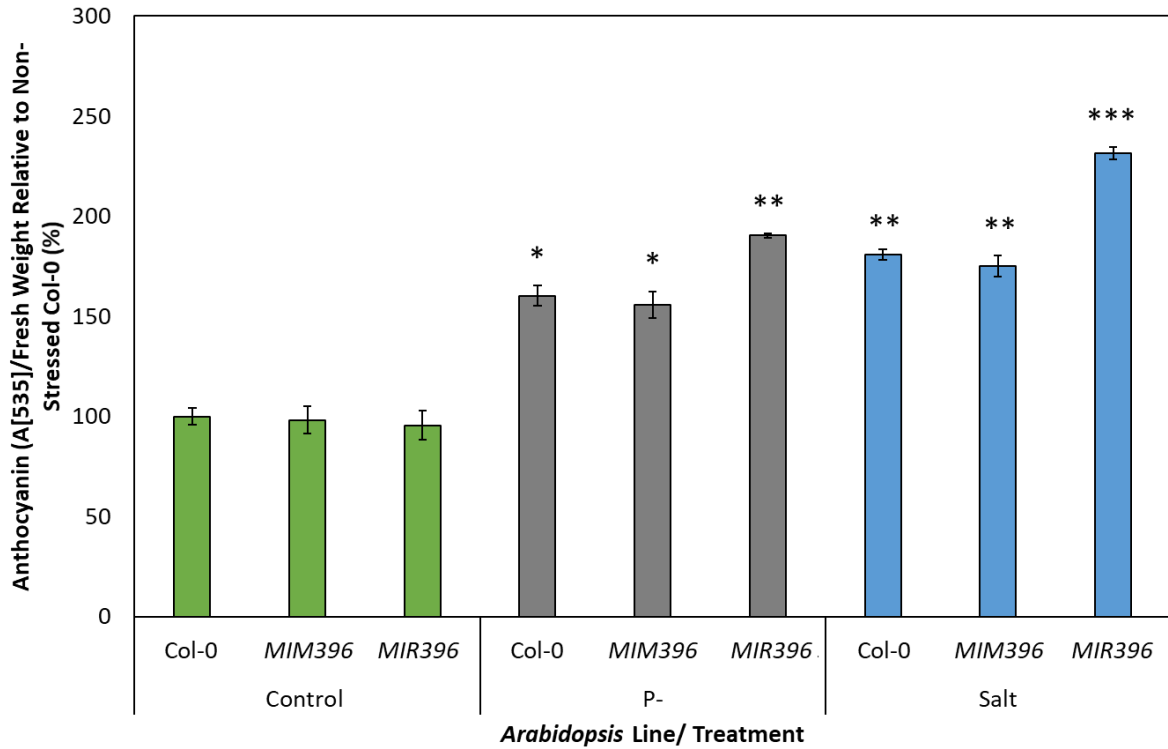


Figure 3.7 Anthocyanin accumulation of P⁻ and salt stressed *Arabidopsis* Col-0 and miR396 altered lines, *MIM396* and *MIR396*, compared to non-stressed Col-0 seedlings. Error bars represent the \pm SD of 4 biological replicates and each biological replicate consisted of a pool of six individual plants. The presence of an asterisk above a control grown *MIM396* or *MIR396* column represents a statistically significant difference comparative to control grown Col-0. Additionally an asterisk above a P⁻ or salt treated *Arabidopsis* plant line represents a statistically significantly difference between the stress treated sample and the respective non-stressed control sample (P-value: * < 0.05; ** < 0.005; *** < 0.001).

3.4.2.5 Chlorophyll *a* and *b* Content

Consistent with the physiological assessments conducted in **Chapter II**, chlorophyll *a* and *b* content were assessed (**Figure 3.8A-B**) to determine if the photosynthetic competency of the newly generated *Arabidopsis* plant lines was altered by the introduced molecular modifications to the miR396/*GRF* regulatory module. When exposed to P⁻ conditions, chlorophyll *a* content of Col-0 seedlings remained equivalent (95.6% ± 5.2%) to that of its non-stressed counterpart (**Figure 3.8A**). Salt stress exposure was again determined to have a significant negative impact on the chlorophyll *a* content of Col-0 seedlings, a 20.8% (± 5.0%) reduction. Analysis of the chlorophyll *a* content of control grown *MIM396* seedlings revealed that reduced miR396 abundance in this plant line did not result in a statistically significant difference to chlorophyll *a* content (110.0% ± 3.5%) compared to that of non-stressed Col-0 seedling. This also proved to be the case for P stressed *MIM396* seedlings. Namely, the chlorophyll *a* content of P stressed *MIM396* seedlings was only slightly increased by 3.3% (± 1.0%) compared to that of control *MIM396* seedlings. In direct contrast, when *MIM396* seedlings were grown on salt supplemented growth media, chlorophyll *a* content was determined to be significantly decreased by 18.0% (± 1.2%) compared to control grown *MIM396* plants. Maintaining a near identical response to the *MIM396* line, *MIR396* seedlings had near approximate wild-type levels of chlorophyll *a* under the control (95.6% ± 2.1%) and P deficient (92.1% ± 6.9%) growth regimes, while the salt stress growth regime resulted in a significant 19.8% (±3.3%) reduction in chlorophyll *a* content compared to that of control grown *MIR396* plants.

It was unsurprising that the chlorophyll *b* content (**Figure 3.8B**) of each plant line closely mirrored the trends observed for chlorophyll *a* content (**Figure 3.8A**). Specifically, in comparison to control grown Col-0 seedlings, the chlorophyll *b* content of P⁻ Col-0 seedlings remained largely unchanged (5.1% ± 6.8%), while the chlorophyll *b* content of salt stressed Col-0 seedlings was reduced by 40.0% (± 3.9%). Similarly, the chlorophyll *b* content of *MIM396* control (112.8% ± 5.0%) and P⁻ (111.5% ± 5.6%) seedlings largely remained at levels approximate to those of control grown Col-0 seedlings. The salt stress growth regime again caused the greatest impact to chlorophyll *b* content, with chlorophyll *b* abundance significantly reduced by 36.8% (± 5.6%) in salt stressed *MIM396* plants (compared to control grown *MIM396* plants). A similar chlorophyll *b* profile was constructed for the *MIR396* plant line, that is; control and P⁻ *MIR396* seedlings maintained wild-type equivalent levels of chlorophyll *b* at 92.4% ± 3.4% and 99.1% ± 6.1% respectively, while the chlorophyll *b* content of salt stressed *MIR396* seedlings was significantly reduced by 37.5% (± 1.0%). Interestingly, when taken together, the **Figure 3.8** analyses indicate that the cultivation of Col-0, *MIM396* and *MIR396* seedlings in the absence of P for a 7 d period, had no significant impact on the abundance of

the two primary photosynthetic pigments, chlorophyll *a* and *b*. In direct contrast to this finding however, were the salt stressed Col-0, *MIM396* and *MIR396* plants with all three plant lines displaying almost identical, and significant reductions to their chlorophyll *a* and *b* contents.

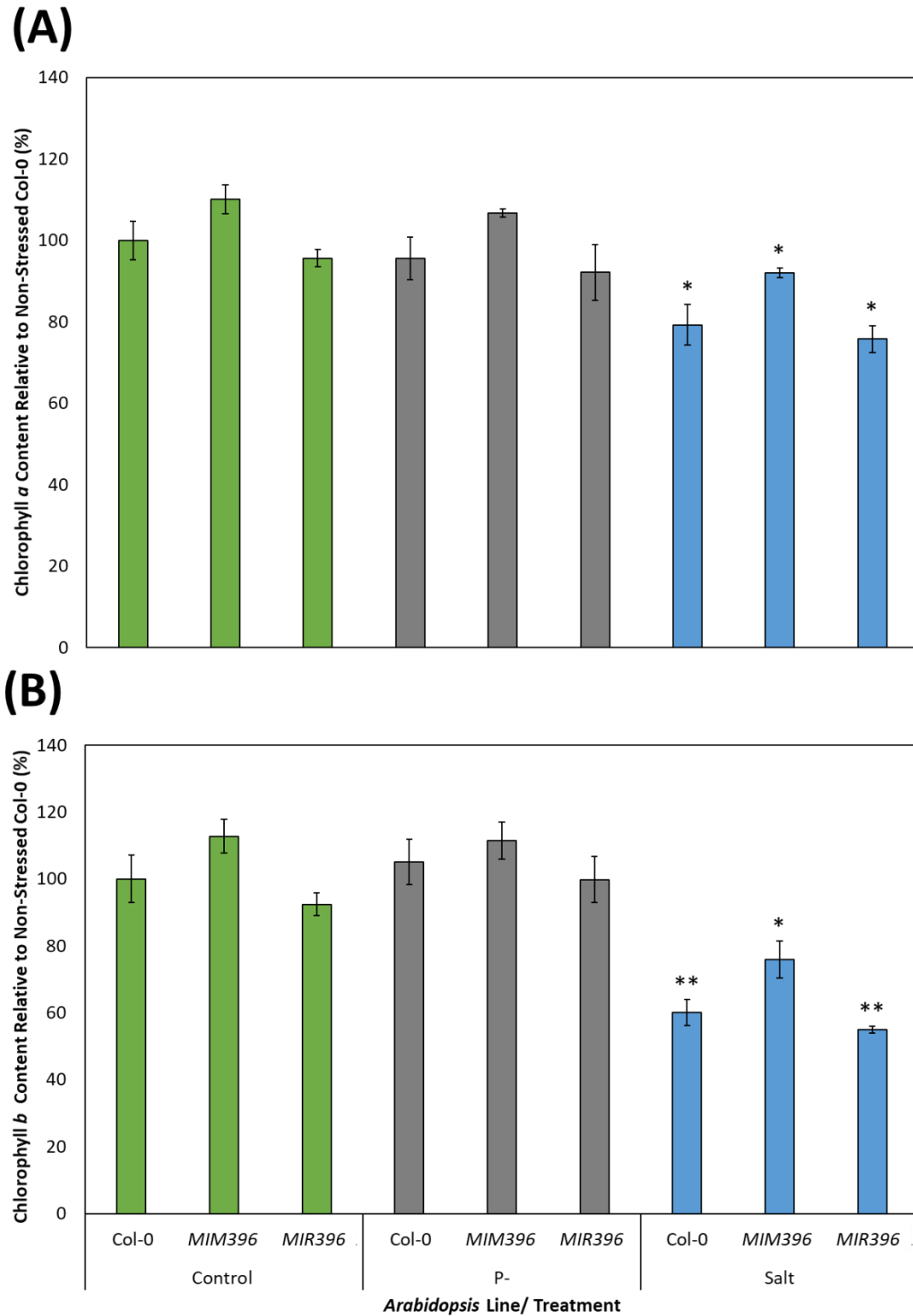


Figure 3.8 Chlorophyll a (A) and b (B) content of P⁻ and salt stressed *Arabidopsis* Col-0 and miR396 altered lines, *MIM396* and *MIR396*, compared to non-stressed Col-0 seedlings. Error bars represent the \pm SD of 4 biological replicates and each biological replicate consisted of a pool of six individual plants. The presence of an asterisk above a control grown *MIM396* or *MIR396* column represents a statistically significant difference comparative to control grown Col-0. Additionally an asterisk above a P⁻ or salt treated *Arabidopsis* plant line represents a statistically significantly difference between the stress treated sample and the respective non-stressed control sample (P-value: * < 0.05; ** < 0.005; *** < 0.001).

3.4.3 **The Molecular Response of Arabidopsis Plant Lines With Molecularly Altered miR396 Abundance to Phosphate Deficiency and Salt Stress**

It is well established in *Arabidopsis* that the highly conserved miRNA sRNA, miR396, is responsible for the transcriptional regulation of six of the nine members of the GRF transcription factor family, including *GRF1*, *GRF2*, *GRF3*, *GRF7*, *GRF8* and *GRF9* (Jones-Rhoades and Bartel, 2004). Each of these plant-specific transcription factors have been documented in a diverse number of plant species to play numerous roles in all aspects of plant vegetative and reproductive development, as well as the defence against abiotic and biotic stress (Bao *et al.*, 2014; Beltramino *et al.*, 2018; Che *et al.*, 2015; Gao *et al.*, 2015; Hewezi and Baum, 2012; Kim and Kende, 2004; Kim *et al.*, 2003; Kim *et al.*, 2012; Liang *et al.*, 2014; Omidbakhshfard *et al.*, 2018; Pajoro *et al.*, 2014; van der Knaap *et al.*, 2000). It was therefore of high interest to determine how the expression of each of these *GRF* family members was regulated in response to; (1) altered miR396 abundance, and; (2) the abiotic stress growth regimes of P deficiency and salt stress (**Figure 3.9**). It was hypothesised that RT-qPCR assessments of the regulation of these transcription factors would in part, account for the varying phenotypic and physiological responses observed between wild-type *Arabidopsis* and the two molecularly modified plant lines generated in this study, *MIM396* and *MIR396* plants. While it is noted that in *Arabidopsis* miR396 has also been speculated to regulate the expression of three ceramidase-like genes (*CERAMIDASE-LIKE1-3*; Liu and Yu, 2009), miR396-directed expression regulation of these three *CERAMIDASE-LIKE* transcripts requires further investigation which is outside the scope of this study.

Similar to previously obtained results (**Figure 3.2**), when Col-0 seedlings were cultivated in the absence of P, miR396 was found to be reduced in abundance by 2.6-fold (**Figure 3.9**). It was therefore surprising to observe that each of the miR396 target genes, *GRF1*, *GRF2*, *GRF3*, *GRF7*, *GRF8* and *GRF9* were also reduced in abundance by 2.0-, 2.3-, 2.6-, 2.7-, 4.5- and 2.4- fold, respectively (**Figure 3.9**). In contrast to the reduced miR396 accumulation documented for P stressed Col-0 seedlings, miR396 abundance was elevated by 2.1-fold in salt stressed Col-0 seedlings. Curiously, the expression of *GRF1*, *GRF2* and *GRF3* was only mildly reduced by the elevated level of the miR396 sRNA in salt stressed Col-0 plants. For the three additional miR396 target genes assessed via RT-qPCR, *GRF7* and *GRF8* expression was reduced by 2.4- and 2.1-fold respectively, while *GRF9* was found to be slightly increased in its expression level (1.3-fold).

In the *MIM396* plant line, and when cultivated under growth conditions, miR396 accumulation was reduced by 3.3-fold compared to its abundance in Col-0 control plants (**Figure 3.9**). Given the reduced abundance of the mature miR396 sRNA, it was not a surprise

to observe that *GRF1*, *GRF2*, *GRF3*, *GRF8* and *GRF9* expression was significantly elevated by 4.5-, 2.6-, 4.1-, 7.5- and 2.2-fold respectively, in *MIM396* control plants, compared to their respective expression levels in Col-0 control plants. The expression of *GRF7* followed an opposite trend, being mildly reduced by 1.3-fold. Exposure of *MIM396* plants to a P deficient growth environment further reduced miR396 abundance, compared to non-stressed Col-0 seedlings, by 3.8-fold. As demonstrated for *MIM396* control plants, this resulted in *GRF* expression to be elevated by 4.2-, 1.9-, 2.2- and 1.7-fold *GRF1*, *GRF2*, *GRF3*, and *GRF8*, respectively. Interestingly, *GRF9* expression only mildly followed this trend to be elevated by 1.3-fold. In contrast to the expression trend documented for the other assessed GRFs, *GRF7* expression was again revealed to be reduced by 2.2-fold in P⁻ stressed *MIM396* plants.

In response to the salt stress growth regime, miR396 abundance in *MIM396* seedlings remained largely unchanged compared to miR396 levels in non-stressed Col-0 plants. Considering that in non-stressed *MIM396* plants, miR396 abundance was reduced by 3.3-fold, yet returned to Col-0 control levels in salt stressed *MIM396* plants, this finding strongly suggests that miR396 is indeed responsive to salt stress. Although miR396 levels were returned to approximate wild-type levels in salt stressed *MIM396* plants, the expression of *GRF1*, *GRF2*, *GRF3* and *GRF9* was elevated by 3.2-, 2.7- 3.4- and 3.0-fold, respectively: a result that suggested in addition to miR396, *GRF1*, *GRF2*, *GRF3* and *GRF9* are also responsive to salt stress. In addition, *GRF8* expression was determined to remain at its Col-0 control levels in salt stressed *MIM396* seedlings, however, *GRF7* transcript abundance was reduced by 3.8-fold (**Figure 3.9**).

Compared to non-stressed Col-0 plants, use of the CaMV 35S promoter to direct the *PRI-MIR396* transcript expression in *MIR396* plants, resulted in a 1.9-fold elevation in mature miR396 sRNA abundance (**Figure 3.9**). As target gene expression alteration reciprocal to the abundance of the targeting miRNA is strongly indicative of a miRNA-directed target mRNA cleavage mode of expression repression in *Arabidopsis*, it was expected that the expression of the miR396-targeted *GRFs* in control grown *MIR396* seedlings would be reduced compared to their expression level in control grown Col-0 seedlings. This was determined to be the case for *GRF1* and *GRF8*, with the expression of both transcription factors downregulated by 1.6-fold. Similarly, the expression of *GRF2*, *GRF3* and *GRF7* was mildly reduced in non-stressed *MIR396* plants, however the degree of reduction in the expression of each of these three *GRFs* was not considered to be statistically significant compared to control grown Col-0 plants. Curiously, in non-stressed *MIR396* plants, *GRF9* expression was determined to be mildly elevated, and not reduced as expected for a miRNA target gene with expression regulation directed by a mRNA cleavage mode of RNA silencing.

When the *MIR396* plant line was cultivated in a P deficient environment, no significant variation in the accumulation of the miR396 sRNA (1.2-fold), nor in the expression of each of the assessed *GRFs* was detected when compared to control grown Col-0 seedlings. However, when exposed to salt stress, miR396 abundance was found to be increased by 2.9-fold in *MIR396* seedlings. With the exception of *GRF8* whose expression was reduced by 2.4-fold, it was a surprise observation that no significant alternations in the expression of the other five *GRF* target genes assessed was detected in this plant line post its exposure to salt stress.

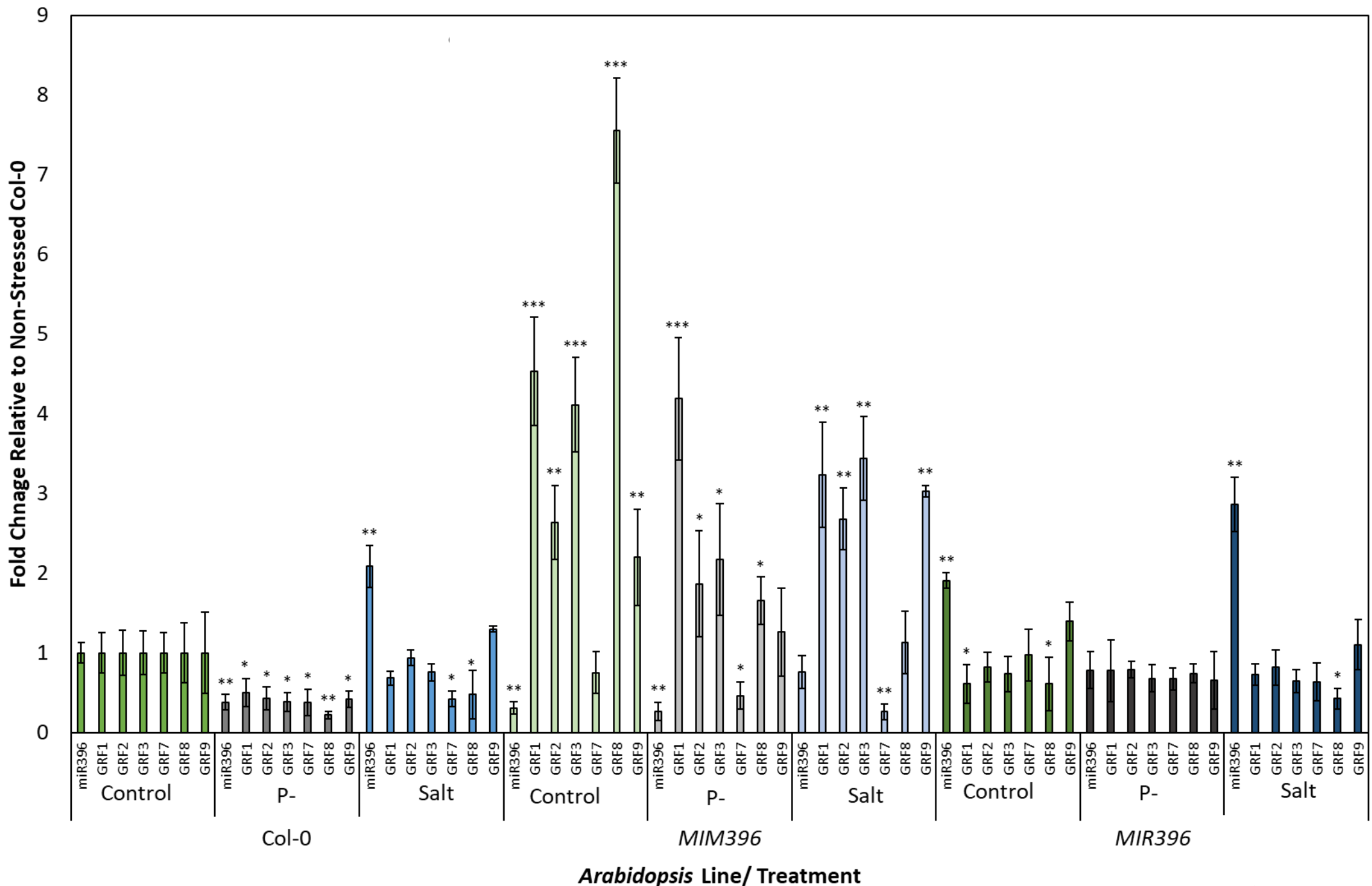


Figure 3.9 RT-qPCR assessment of miR396 and miR396 targeted GRFs, GRF1-3; 7-9 in non-stressed and stress treated Arabidopsis plant lines. The RT-qPCR determined accumulation of miR396 and GRF1-3; 7-9 in Arabidopsis Col-0, MIM396 and MIR396 Arabidopsis seedlings exposed to each abiotic stress is presented relative to control grown Col-0 seedlings. Error bars represent the \pm SD of 4 biological replicates with each biological replicate consisting of 6 individual plants. The presence of an asterisk indicates a statistically significant difference between the expression of each gene determined for control Col-0 seedling (p-value: < 0.05, *, P < 0.005, **, P < 0.001, ***).

3.5 Discussion

3.5.1 *The Impact of Phosphate Deficiency on the miR396 Regulatory Module*

While the appropriate regulation of the miR399/*PHO2* regulatory module is necessary for *Arabidopsis* to mount an adaptive response to conditions of P deficiency (Bari *et al.*, 2006), no study, to date (to the best of my knowledge) has identified miR396 as a P stress responsive miRNA. Interestingly, RT-qPCR analyses revealed that when Col-0, *drb1*, *drb2* and *drb4* seedlings were exposed to P deficient growth conditions, the abundance of the miR396 sRNA was significantly reduced in each assessed *Arabidopsis* line (**Figure 3.2A**). Further, this large reduction in miR396 abundance correlated with significant reductions to *GRF7* in Col-0 and *drb1* seedlings exposed to P stress growth conditions and failure of RT-qPCR to detect *GRF7* expression in *drb2* and *drb4* seedlings exposed to the same stress regime (**Figure 3.2B**). This data suggests that in each of the *Arabidopsis* plant lines investigated, and in response to growth in a P deficient environment, reduced *GRF7* accumulation, and therefore *GRF7* abundance, is required for *Arabidopsis* to mount an adaptive response to limited P. The heavily reduced expression of *GRF7* in each of the *Arabidopsis* plant lines after exposure to conditions absent of P was somewhat expected as Kim *et al.*, (2012) has previously shown *Arabidopsis* lines deficient in *GRF7* have elevated osmotic stress tolerance as a result of reduced *GRF7*-directed repression of the expression of the abiotic stress responsive gene *DREB2A*. The identification of the miR396/*GRF7* regulatory module as responsive to growth in a P deficient environment, resulted in the selection of phosphate deficient growth conditions for further investigation of *Arabidopsis* plant lines modified to harbour altered miR396/*GRF* profiles.

3.5.2 Manipulation of the miR396/GRF Regulatory Module Results in Altered Growth and Development and the Response of Arabidopsis to Abiotic Stress

As this study has confirmed the highly conserved plant miRNA, miR396, as a key miRNA responsive to abiotic stress conditions of heat, mannitol, P⁻ and salt stress, molecularly manipulating the accumulation of the miR396 sRNA in *Arabidopsis* was of high interest. Post cultivation of 8 d old seedlings for a 7 d period in conditions of controlled growth or the abiotic stress conditions of P deficiency or salinity, *MIM396* and *MIR396* seedlings were visually compared to non-stressed Col-0 seedlings to; (1) determine any impact that altered miR396 accumulation had on the growth and development of 15 d old *Arabidopsis* seedlings under control growth conditions, and; (2) determine if altered miR396 abundance changed the phenotypic and/or physiological sensitivity of *Arabidopsis* to conditions of P deficiency or salt stress. As the phenotypic and physiological response of Col-0 seedlings exposed to P⁻ or salt stress conditions has previously been discussed (**Appendices A.1.3 and A.1.4**, pages 193-210; 211-236, respectively), this discussion will primarily focus on the phenotypic and physiological characteristics of the newly generated molecularly modified plant lines, *MIM396* and *MIR396*, in comparison to control grown, non-stressed Col-0 seedlings. Specifically, when visualising the phenotypic response of each of the *Arabidopsis* seedlings, under each growth condition, there was striking variation in the growth and development of each *Arabidopsis* plant line (**Figure 3.3**). Therefore, the same quantitative measurements utilised in **Chapter II**, including; fresh weight (**Figure 3.4**), rosette area (**Figure 3.5**), primary root length (**Figure 3.6**), anthocyanin accumulation (**Figure 3.7**) and chlorophyll *a* and *b* content (**Figure 3.8A-B**), were selected to quantify the varying degree of stress response displayed by each of the three assessed plant lines. In addition to these phenotypic and physiological analyses, RT-qPCR was employed to quantify the abundance of the miR396 sRNA and the expression of each of its targeted genes in *Arabidopsis*, including *GRF1*, *GRF2*, *GRF3*, *GRF7*, *GRF8* and *GRF9* (**Figure 3.9**). This analysis was conducted to provide a more detailed understanding of the abundance profiles of miR396 and each of its targeted *GRFs* required to equip *Arabidopsis* with the phenotypic and/or physiological ability to adapt to, and/or to tolerate the abiotic stress conditions of P deficiency and salinity. While the developmental phenotype of *MIM396* and *MIR396* plants at 15 d old (under control and abiotic stress conditions) was the focus of this study, the vegetative and reproductive development for of *MIM396* and *MIR396* is presented in **Figure A.6.2** (page 269).

3.5.2.1 *Molecularly Modified miR396 Abundance Provides Arabidopsis Seedlings with Superior Phenotypic Traits Under Non-Stress Growth Conditions*

In order to document any influence that the miR396/*GRF* regulatory module was having on the growth and development of 15 d old *Arabidopsis* seedlings, the phenotypic traits and molecular profiles quantified for control grown *MIM396* and *MIR396* plants were compared to that of non-stressed Col-0 seedlings. It was highly promising to observe that control grown *MIM396* seedlings had elevated fresh weight (**Figure 3.4**) and rosette area (**Figure 3.5**) metrics in comparison to control grown Col-0 seedlings. However, the remaining phenotypic assessments of primary root length (**Figure 3.6**), anthocyanin accumulation (**Figure 3.7**) and chlorophyll *a* and *b* content (**Figure 3.8A-B**) remained largely unchanged compared to those of control grown Col-0 plants. When considering the molecular data presented in **Figure 3.9**, that is, in comparison to Col-0 seedlings, miR396 abundance was significantly reduced, while the expression of each of the targeted *GRFs* (excluding *GRF7*) was significantly elevated, the documented increase in the fitness of the shoot architecture of *MIM396* plants is unsurprising. More specifically, the miR396 targeted *GRFs*, *GRF1*, *GRF2*, *GRF3* and *GRF9*, have each been shown to play a role in leaf growth and development, specifically leaf morphology (Beltramino *et al.*, 2018; Kim and Kende, 2004; Kim *et al.*, 2003; Omidbakhshfard *et al.*, 2018), potentially accounting for the documented increase in fresh weight and rosette area for control grown *MIM396* plants. Previous studies by Kim and Kende (2004), Kim *et al.*, (2003) and Beltramino *et al.*, (2018), each demonstrated that elevated *GRF1*, *GRF2* or *GRF3* expression correlated with shoot growth promotion in *Arabidopsis*. Conversely, heightened *GRF9* accumulation has been previously considered a negative regulator of leaf development (Omidbakhshfard *et al.*, 2018). Therefore, the documented 2.2-fold increase in the expression of *GRF9* in *MIM396* seedlings could be considered insubstantial compared to the cumulative 4.5-, 2.6-, 4.1-fold increases in the expression of the positive growth regulators, *GRF1*, *GRF2* and *GRF3*, respectively. As *GRF7* has primarily been associated with abiotic stress responses in *Arabidopsis*, it was not surprising to observe that its expression was not altered across control grown Col-0 and *MIM396* plants (Kim *et al.*, 2012). While it was interesting to note that *GRF8* expression was 7.5-fold higher in control grown *MIM396* seedlings compared to its expression in the Col-0 controls, no research has been conducted to date that has reported a role for *GRF8* in *Arabidopsis* development, with this lack of *GRF8* characterisation presenting an interesting avenue for further investigation in the future.

Via the comparison of the phenotypic characteristics displayed by control grown *MIR396* seedlings to those of Col-0 control seedlings of the same age, mild reductions were observed for all phenotypic and physiological assessments conducted on the miR396

overexpression line. However, none of the observed reductions were considered to be statistically significant compared to the corresponding metric expressed by control grown Col-0 seedlings (**Figure 3.4-3.8A-B**). When considering the miR396 accumulation and *GRF* expression profiles of *MIR396* seedlings to those of Col-0 plants (**Figure 3.9**), miR396 accumulation was modestly elevated 1.9-fold. Although this elevated level was determined to be statistically significant, this alteration to miR396 abundance resulted in mild alterations to the expression profiles of its targeted *GRFs*, particularly those involved in *Arabidopsis* growth and development. More specifically, while *GRF1* expression was significantly reduced by 1.6-fold, *GRF2*, *GRF3* and *GRF9* expression was altered by -1.2-, -1.3- and 1.4-fold, respectively. As *GRF1*, *GRF2* and *GRF3*, have been previously identified as positive regulators of leaf development and morphology, and *GRF9* a negative regulator of these traits; the mild alterations in the expression of each of these *GRFs* may account for the mild and statistically insignificant alterations in the phenotypic and physiological characteristics displayed by the *MIR396* plant line (**Figure 3.4-3.8A-B**; Beltramino *et al.*, 2018; Kim and Kende, 2004; Kim *et al.*, 2003; Omidbakhshfard *et al.*, 2018). Similar to *MIM396* seedlings, it was unsurprising to note that under control growth conditions, *GRF7*, a known stress responsive *GRF*, was unchanged from its Col-0 expression level. It was also of interest to observe that the expression of the *GRF8* transcript was significantly reduced. However, again, the potential role of *GRF8* in *Arabidopsis* growth and development (if any) remains to be experimentally characterised.

3.5.2.2 *Molecularly Modified miR396 Abundance Alter the Tolerance of Arabidopsis Seedlings to P Deficiency and Salt stress*

Prior to assessing how *Arabidopsis* seedlings with molecularly modified miR396 abundance responded to the P⁻ and salt stress growth regimes, Col-0 seedlings were phenotypically and molecularly analysed to determine the response of 15 d old wild-type *Arabidopsis* to these two abiotic stresses. Consistent with previously obtained phenotypic and physiological data (**Appendices A.1.3 and A.1.4**, pages 193-210; 211-236, respectively), exposure to P deficiency or salt stress resulted in significant reductions to the fresh weight (**Figure 3.4**), rosette area (**Figure 3.5**) and primary root length (**Figure 3.6**) of Col-0 plants. Further, P⁻ and salt stressed Col-0 seedlings were determined to have significantly elevated anthocyanin abundance (**Figure 3.7**). Interestingly, while P⁻ stress was determined to have no impact on the chlorophyll *a* and *b* content of Col-0 seedlings, salt stress induced significant reductions to the abundance of both photosynthetic pigments (**Figure 3.8A-B**). To attempt to account for this sensitivity to each of the imposed 7 d abiotic stress growth regimes, RT-qPCR was used to assess the accumulation level of miR396 and the expression of each of its targeted *GRFs*, including *GRF1*, *GRF2*, *GRF3*, *GRF7*, *GRF8* and *GRF9* (**Figure 3.9**). As previously shown (**Figure 3.2**), miR396 accumulation and *GRF7* abundance were again determined to be significantly reduced in response to P deficiency. Given the documented role of *GRF7* in the repression of the well characterised *Arabidopsis* stress responsive gene, *DREB2A*, this reduction in *GRF7* expression, and therefore *GRF7* protein abundance, would be necessary for Col-0 seedlings to mount a molecular response to P⁻ stress (Kim *et al.*, 2012). Interestingly, the expression of each of the other *GRFs* assessed, namely *GRF1*, *GRF2*, *GRF3*, *GRF8* and *GRF9*, were also significantly downregulated by 2.0-, 2.3- and 2.6-, 4.5- and 2.4-fold, respectively. As the predominate mode of target gene regulation directed by a plant miRNA is mRNA cleavage, it was surprising to observe miR396 accumulation and miR396-targeted *GRF* expression were both reduced in response to P⁻ stress. While this finding is suggestive of the less favoured miRNA-directed translational repression mode of target gene expression regulation, the reduction in *GRF* abundance may partially account for the phenotypic sensitivity observed in Col-0 seedlings exposed to P⁻ stress. Specifically, *GRF1*, *GRF2* and *GRF3* have each been identified as positive regulators of the size and morphology of *Arabidopsis* leaves (Beltramino *et al.*, 2018; Kim and Kende, 2004; Kim *et al.*, 2003). Therefore, it is reasonable to suggest that the significant reduction in whole plant fresh weight and rosette area observed in Col-0 seedlings exposed to a 7 d P⁻ growth regime may in part stem from the significant reduction in *GRF1*, *GRF2* and *GRF3* expression. Alternatively, *GRF9* has been identified as a negative regulator of leaf development, and while it would be expected

that the documented 2.4-fold reduction to *GRF9* expression would be accompanied by the promotion of cell proliferation in leaf primordia, this is perhaps negated by the large reductions observed in the expression level of *GRF1*, *GRF2* and *GRF3* (Omidbakhshfard *et al.*, 2018). Interestingly, while the expression of *GRF8* was found to be reduced 4.5-fold in Col-0 seedlings grown under P deficient conditions, in *Arabidopsis*, a role (if any) for *GRF8* in response to abiotic stress has not yet been identified. However, in rice, *OsGRF8* has been shown to play a role in mediating the flavonoid biosynthetic pathway and plant resistance to brown planthopper infestation (Dai *et al.*, 2019).

To account for the severe phenotypic and physiological impact a 7 d 150 mM NaCl treatment had on Col-0 plants, RT-qPCR again was employed to assess miR396 accumulation and the expression of its targeted transcripts. Near identical to the previously obtained data (**Figure 2.12**) for Col-0 seedlings post their exposure to salt stress, miR396 abundance was determined to be significantly upregulated by 2.1-fold while the expression of *GRF7* was revealed to be accordingly reduced by 2.4-fold (**Figure 3.9**). Again, given that *GRF7* has been documented to be a negative regulator of the *Arabidopsis* stress responsive gene, *DREB2A*, this reduction in *GRF7* expression, and therefore *GRF7* protein abundance, in salt stressed Col-0 seedlings formed an unsurprising result (Kim *et al.*, 2012). As the salt stress growth regime significantly impaired Col-0 shoot architecture development, it was a surprise observation that the expression of *GRF1*, *GRF2*, *GRF3* and *GRF9*, known regulators of *Arabidopsis* leaf morphology, was only mildly altered. However, it should be noted that while the expression of *GRF1*, *GRF2*, *GRF3* and *GRF9* was only mildly altered by -1.5-, -1.1-, -1.3- and 1.3-fold, respectively, these expression changes are consistent with the reduced fresh weight and rosette area observed for salt stressed Col-0 seedlings (**Figure 3.4-3.5**; Beltramino *et al.*, 2018; Kim and Kende, 2004; Kim *et al.*, 2003; Omidbakhshfard *et al.*, 2018). Similar to the observed impact that P⁻ stress had on Col-0 seedlings in response to salt stress, *GRF8* expression was again observed to be significantly altered by -2.1-fold. This expression change again suggested that reduced *GRF8* expression, and therefore *GRF8* protein abundance, forms a necessary molecular change in order for Col-0 seedlings to respond to conditions of abiotic stress.

To determine if either of the molecularly modified plant lines provided *Arabidopsis* with an altered tolerance to either P⁻ or salt stress, each of the phenotypic and physiological assessment were compared to that of control grown Col-0 seedlings (**Figure 3.4-3.7**). Again, *MIM396* seedlings produced the most interesting finding, appearing to be the most tolerant of the three *Arabidopsis* lines assessed to both P⁻ and salt stress, based on each of the characterised phenotypic and physiological markers of stress. Specifically, in comparison to the *MIM396* controls, when *MIM396* plants were cultivated under P⁻ growth conditions, *they*

were determined to have a milder reduction in fresh weight (**Figure 3.4**), rosette area (**Figure 3.5**), primary root length (**Figure 3.6**) and chlorophyll *a* and *b* content (**Figure 3.8A-B**), while also displaying the mildest increase in anthocyanin accumulation (**Figure 3.7**). Together, the assessed parameters repeatedly indicated that the *MIM396* plant line had an elevated tolerance to the imposed stress. Similarly, in response to salt stress, the *MIM396* plant line again presented a milder degree of reduction to its primary root length (**Figure 3.6**) and chlorophyll *a* and *b* content (**Figure 3.8A-B**), while also displaying the mildest increase in anthocyanin accumulation (**Figure 3.7**). To account for the elevated phenotypic and physiological tolerance that the *MIM396* plant line displayed compared to Col-0 seedlings post their exposure to the two assessed stresses, the miR396 accumulation and GRF expression profiles were next assessed (**Figure 3.9**). This analysis revealed that P⁻ stressed *MIM396* seedlings accumulated 3.8-fold less mature miR396 sRNA than control grown Col-0 seedlings. It was therefore unsurprising to observe the expression of *GRF1*, *GRF2* and *GRF3* was significantly elevated by 4.2-, 1.9-, 2.2- fold respectively, in P⁻ stressed *MIM396* seedlings. The elevated accumulation of these three positive regulators of *Arabidopsis* leaf development may partially account for the milder reductions observed in shoot architecture (Beltramino *et al.*, 2018; Kim and Kende, 2004; Kim *et al.*, 2003; Omidbakhshfard *et al.*, 2018). Further to this point, the negative regulator of *Arabidopsis* leaf development, *GRF9*, presented an insignificantly altered expression change (Omidbakhshfard *et al.*, 2018). Consistent with observations made of P⁻ stressed Col-0 seedlings, *GRF7* expression was reduced by 2.2-fold in P⁻ stressed *MIM396* plants. As Kim *et al.*, (2012) has shown *Arabidopsis* seedlings with reduced GRF7 are more tolerant to osmotic stress, it can be speculated that the 2.2-fold reduction in *GRF7* expression could potentially be assisting the *MIM396* seedlings to mount an adaptive response to growth in a phosphate deficient environment.

Similar miR396 accumulation and *GRF* expression trends were determined for salt stressed *MIM396* seedlings. That is, the expression of the positive regulators of *Arabidopsis* leaf morphology, *GRF1*, *GRF2* and *GRF3*, was significantly elevated by 3.2-, 2.7-, 3.4- fold, respectively. Further, the expression of *GRF7* was again demonstrated to be significantly reduced by 3.8-fold in salt stressed *MIM396* seedlings: an expected result based on the previous findings that revealed that reduced GRF7 protein abundance is critical for the subsequent upregulation of *DREB2A* gene expression, with the subsequent enhanced abundance of the *DREB2A* protein necessary for *Arabidopsis* to mount an abiotic stress response (Kim *et al.*, 2012). It was very interesting to note that when *MIM396* seedlings were exposed to salt stress, *GRF9* abundance was elevated 3.0-fold in comparison to non-stressed Col-0 seedlings. As a previous study by He and colleagues (2015) demonstrated that an *Arabidopsis* GRF9-overexpression line maintained 'better whole-plant growth and root growth'

in response to PEG treatment, this elevation in *GRF9* expression (and therefore elevated *GRF9* protein abundance) may in part account for the milder reduction in primary root development observed in salt stressed *MIM396* seedlings.

In comparison to non-stressed *MIR396* seedlings, when exposed to P⁻ and salt stress growth regimes, *MIR396* seedlings had large reductions in primary root length (**Figure 3.6**) and chlorophyll *a* and *b* content (**Figure 3.8A-B**), while also displaying the largest increase in anthocyanin accumulation (**Figure 3.7**). Additionally, in response to a P⁻ stress growth regime, *MIR396* seedlings presented large reductions in fresh weight and rosette area in comparison to non-stressed *MIR396* seedlings, but these phenotypic parameters were not as sensitive as Col-0 seedlings and *MIM396*, largely due to the reduced non-stressed fresh weight and rosette area of these seedlings. Further in response to a salt stress growth regime, while *MIR396* seedlings did not present the greatest reduction to either fresh weight (**Figure 3.4**) or rosette area (**Figure 3.5**), largely due to the smaller sized shoot architecture displayed by non-stressed *MIR396* seedlings, they were certainly the smallest of all three *Arabidopsis* lines after exposure to a 7 d 150mM salt stress growth regime. This positioned *MIR396* seedlings as more susceptible to P⁻ and salt stress in comparison to *MIM396* seedlings and more susceptible to salt stress than Col-0 plants. When RT-qPCR was utilised to determine what was occurring at a molecular level in *MIR396* seedlings exposed to P⁻ stress, it was determined that the abundance of miR396 and each of the *GRFs* all remained at approximate non-stressed Col-0 levels (**Figure 3.9**). Although miR396 abundance in P⁻ *MIM396* plants was reduced in comparison to non-stressed *MIR396* seedlings, failure to modify the miR396 targeted *GRF* profile readily highlights the regulatory module has been disrupted in *MIR396* plants.

Similarly in response to salt stress and despite miR396 accumulation levels being upregulated 2.9-fold, the accumulation levels of each of the miR396-targeted *GRFs* were determined to be at approximate non-stressed wild-type levels, excluding *GRF8* which was reduced 2.4-fold. While this result was surprising, this failure to largely modify *GRF* accumulation levels in response to a P⁻ or salt stress growth regime may account for the phenotypic and physiological sensitivity of *MIR396* seedlings. Specifically, as elevated *GRF3* and *GRF9*, in addition to reduced *GRF7* are associated with improved abiotic stress tolerance, the unchanged accumulation levels of *GRF3*, *GRF7* and *GRF9* comparative to non-stressed Col-0 seedlings may partially account for the poor phenotypic performance of these seedlings when exposed to conditions of P⁻ or salt stress (Beltramino *et al.*, 2018; He *et al.*, 2015; Kim *et al.*, 2012).

Chapter IV

The Phenotypic and Molecular
Consequence of Manipulating the
miR399 Regulatory Module in
Arabidopsis

4.1 Chapter Overview/ Rationale

Stemming from the molecular data presented in **Chapter II**, the miR399/*PHO2* regulatory module was selected for further investigation. Specifically, RT-qPCR analysis indicated that the miR399/*PHO2* regulatory module was highly responsive to each of the applied abiotic stress growth regimes, including heat, mannitol and salt stress. In addition, DRB1, DRB2 and DRB4 were also demonstrated to play central roles to ensure the appropriate regulation of miR399 abundance and/or *PHO2* expression (**Figure 2.11 and Figure 2.13**).

As the miR399/*PHO2* regulatory module is well demonstrated to be crucial to the ability of a plant to attempt to adapt to growth in a P deficient environment (Bari *et al.*, 2006; Fujii *et al.*, 2005; Hsieh *et al.*, 2009; Lin *et al.*, 2008), Col-0, *drb1*, *drb2* and *drb4* were exposed to P deficient growth conditions to attempt to further define the roles that DRB1, DRB2 and DRB4 mediate for the appropriate balance of the miR399 and *PHO2* RNA molecules under an abiotic stress previously shown to directly impact this regulatory module. Moreover, as the miR399/*PHO2* regulatory module was shown to be highly responsive to salt stress (**Figure 2.10**), this chapter utilised the same two molecular approaches presented in **Chapter III** to create *Arabidopsis* plant lines with reduced and elevated mature miR399 sRNA abundance, termed '*MIM399*' and '*MIR399*' plants, respectively. As outlined in thesis **Chapter III** for the miR396/*GRF* regulatory module, *MIM399* and *MIR399* seedlings were cultivated along with Col-0 seedlings under control, P deficient and salt stress growth regimes to identify any phenotypic and/or physiological sensitivity or tolerance to either P deficiency and/or salt stress. Further, RT-qPCR was used to determine the molecular profiles of the newly generated *MIM399* and *MIR399* plant lines. Specifically, miR399 abundance and the expression of *PHO2* was compared between wild-type *Arabidopsis* (Col-0) plants, and the *MIM399* and *MIR399* lines under control, P deficient and salt stress conditions.

4.2 Introduction

4.2.1 *The microRNA399/PHOSPHATE2 Regulatory Module in the Plant Development and Abiotic Stress Response*

The miR399/*PHO2* regulatory module has been well documented to direct a central role in modulating phosphate (P) uptake and to maintain phosphorous (P) homeostasis, both essential processes needed to ensure a plant can tolerate P deficient growth conditions (Bari *et al.*, 2006; Fujii *et al.*, 2005; Hsieh *et al.*, 2009; Lin *et al.*, 2008). A detailed literature review on the role of the *Arabidopsis* miR399/*PHO2* molecular module in maintaining P homeostasis, can be found in the '1. Introduction' section of the following publication:

Pegler, J. L., Oultram, J. M., Grof, C. P., and Eamens, A. L. (2019). DRB1, DRB2 and DRB4 are required for appropriate regulation of the microRNA399/ *PHOSPHATE2* expression module in *Arabidopsis thaliana*. *Plants*, 8(5), 124.

A copy of this publication can be found in **Appendix 1 (A.1.4)** of this thesis (pages 211-236), with '1. Introduction' presented on pages 211-213.

Further, **Figure 4.1** provides a simplified, schematic overview of the role of miR399-directed expression regulation of *PHO2* in root to shoot translocation of Pi under P deficient conditions. In addition to the well characterised role the miR399/*PHO2* regulatory module plays in the ability of *Arabidopsis* to maintain P homeostasis when cultivated in the absence of P, this miRNA/target gene regulatory module has been implicated in other aspects of plant growth and development. Specifically, in *Arabidopsis*, the miR399/*PHO2* regulatory module has been associated with the early flowering phenotype expressed by *Arabidopsis* seedlings exposed to reduced ambient temperatures (Kim *et al.*, 2011). More recently, the study published by Zhu and colleagues (2020), revealed that miR399-directed regulation of *PHO2* expression is required for proper stomatal development in *Arabidopsis*. Specifically, molecularly modified *Arabidopsis* seedlings overexpressing the *MIR399B* precursor transcript not only had highly reduced levels of *PHO2* expression, but also developed increased stomatal numbers due to an elevated stomatal density (Zhu *et al.*, 2020). From this demonstration, it can be suggested that this phenotypic alteration could modulate the ability of a *MIR399B* overexpressing plant line to respond to various abiotic stresses that demand reduced transpiration for plant survival.

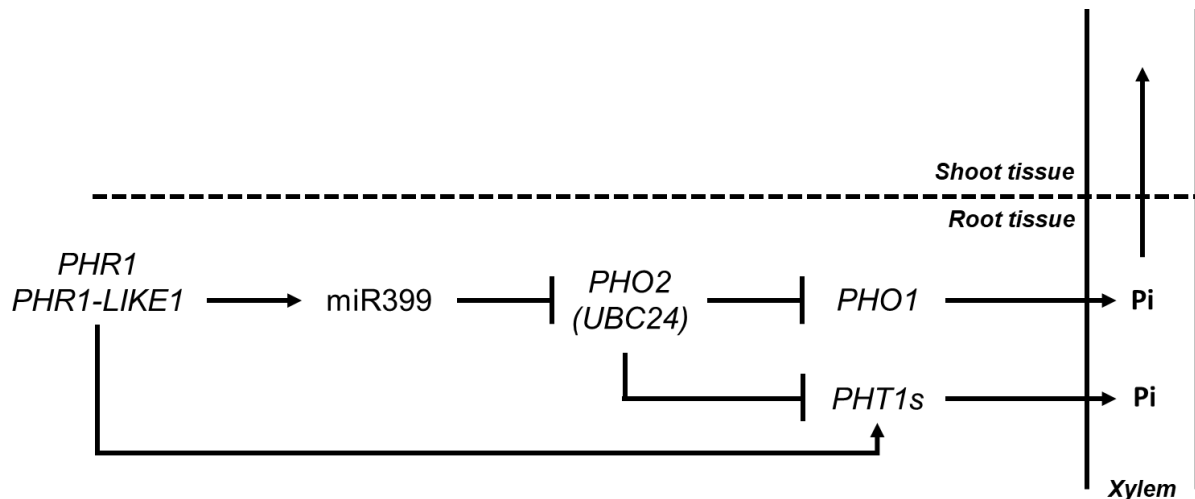


Figure 4.1 The *Arabidopsis* miR399/PHO2 pathway under phosphate (Pi) deficient growth conditions. When the soil proximal to the root system of *Arabidopsis* is deficient in phosphate, PHOSPHATE STARVATION RESPONSE REGULATOR1 (PHR1) and PHR1-LIKE1 transcriptionally activate both *MIR399* and *PHOSPHATE TRANSPORTER1* (*PHT1*) family members. The mature miR399 sRNA directly targets and represses the expression of *PHOSPHATE2* (*PHO2/UBC24*). Therefore, elevated miR399 abundance results in reduced *PHO2* expression and the alleviation of PHO2-directed repression of PHOSPHATE1 (*PHO1*) and *PHT1* family members. This, in turn, allows for enhanced loading of Pi into the xylem for transport to plant source tissues such as actively photosynthesising leaves.

While a large proportion of fundamental studies characterising the miR399/*PHO2* regulatory module have been conducted in the longstanding genetic model plant species, *Arabidopsis* (Bari *et al.*, 2006; Fujii *et al.*, 2005; Hsieh *et al.*, 2009; Lin *et al.*, 2008), the miR399/*PHO2* module is highly functionally conserved across the plant kingdom (Axtell and Meyers, 2018). For example, studies in *Hordeum vulgare* L. (barley), maize, rice and wheat, have all identified the miR399/*PHO2* regulatory module to be central to the ability of these cropping species to respond to phosphate deficient growth conditions (Du *et al.*, 2018; Hackenberg *et al.*, 2013; Hu *et al.*, 2015; Ouyang *et al.*, 2016). While the miR399/*PHO2* regulatory module has been shown to play an additional role in flowering time and stomatal development in *Arabidopsis*, no study (to the best of my knowledge) has been published to date reporting on the characterisation of additional roles for this molecular module in the growth and development of plant species other than *Arabidopsis*. Further, only a very limited number of studies have identified and/or characterised the role of the miR399/*PHO2* regulatory module in assisting plants to adapt to forms of abiotic stress other than growth in a P deficient environment (Jian *et al.*, 2016; Wang *et al.*, 2011).

4.3 Material and Methods

All material and methods used in **Chapter IV**, pertaining to the; (1) Preparation and storage of bacterial competent cells, (2) Molecular cloning, (3) Phenotypic analyses of transformed *Arabidopsis* lines, and; (4) Molecular analyses of transformed Col-0 seedlings, have been previously described in **Chapter III, Section 3.3** (Pages 81-86). In addition, the materials and methods used to induce plant growth in a P deficient environment and under conditions of salt stress in this Chapter can be found in the following publications:

Pegler, J. L., Oultram, J. M., Grof, C. P., and Eamens, A. L. (2019). DRB1, DRB2 and DRB4 Are Required for Appropriate Regulation of the microRNA399/*PHOSPHATE2* Expression Module in *Arabidopsis thaliana*. *Plants*, 8(5), 124.

<https://www.mdpi.com/2223-7747/8/5/124>

Pegler, J. L., Oultram, J. M., Grof, C. P., and Eamens, A. L. (2019). Profiling the Abiotic Stress Responsive microRNA Landscape of *Arabidopsis thaliana*. *Plants*, 8(3), 58.

<https://www.mdpi.com/2223-7747/8/3/58>

A copy of these publications can be found in **Appendix 1 (A.1.4)** and **Appendix 1 (A.1.3)** of this thesis, pages 211-236 and pages 193-210, respectively. The relevant experimental methodologies are detailed in sections; '*Plant Material and Phosphate Stress Treatment*', page 231 and '*4.1 Plant Material*', page 205, respectively

4.4 Results

4.4.1 **The Requirement of DRB1, DRB2 and DRB4 for Appropriate Regulation of the Phosphate Responsive, miR399/PHO2 Regulatory module in Arabidopsis**

Given the established role of the miR399/*PHO2* regulatory module to P deficient growth conditions, the crucial role that each of the nuclear localised DRB proteins plays in the regulation of this module during P deficient growth conditions was investigated prior to investigation of the miR399/*PHO2* responsiveness to other abiotic stress conditions of heat, mannitol and salt stress: growth conditions to which the miR399/*PHO2* module has not been investigated for previously. All the phenotypic results in Section 4.4.1 of this chapter, in addition to the molecular data pertaining to the characterisation of the miR399/*PHO2* regulatory module, can be found in the publication:

Pegler, J. L., Oultram, J. M., Grof, C. P., and Eamens, A. L. (2019). DRB1, DRB2 and DRB4 Are Required for Appropriate Regulation of the microRNA399/*PHOSPHATE2* Expression Module in *Arabidopsis thaliana*. *Plants*, 8(5), 124.

<https://www.mdpi.com/2223-7747/8/5/124>

A copy of this publication can be found in **Appendix 1 (A.1.4)** of this thesis, pages 211-236.

The key finding of the above publication reveals the necessity of each of the nuclear localised DRBs in the appropriate regulation of either the abundance of the miR399 sRNA, or the regulation of *PHO2* expression during periods of P stress, an encouraging finding that further presents the miR399/*PHO2* regulatory module as a miRNA-target gene regulatory network of interest for additional molecular profiling during periods of heat, mannitol and salt stress. While the miR399/*PHO2* regulatory module has been extensively characterised for the key role it plays in P homeostasis (Aung *et al.*, 2006; Bari *et al.*, 2006; Fujii *et al.*, 2005), very few studies have investigated the role of this regulatory module in response to other abiotic stresses (with the exception of the Jian *et al.*, (2016) and Wang *et al.*, (2011) publications, studies that respectively identified the miR399/*PHO2* module as abiotic stress responsive in *Brassica napus* (rapeseed) and *Medicago truncatula*). Given the (1) high conservation of miR399 among land plants (Axtell and Meyers, 2018), (2) diverse protein machinery required for appropriate regulation of miR399 abundance and/or *PHO2* target gene expression, (3) degree of cross talk between nutrient regulation, plant hormones, and the plant abiotic stress response (Kohli *et al.*, 2013; Peleg and Blumwald, 2011; Yu *et al.*, 2015), and (4) sRNA-Seq analyses revealing the highly responsive nature of the miR399/*PHO2* regulatory module to

heat, mannitol and salt stress (**Figure 3.4A-B**), the miR399/*PHO2* regulatory module was selected for molecular modification in *Arabidopsis* with the overarching aim of providing additional molecular insights into the interplay between this miRNA and its target gene in *Arabidopsis* development and in the response of *Arabidopsis* to exposure to either a P deficient or saline environment.

4.4.2 The Phenotypic Response of Arabidopsis miR399 Molecularly Modified Plant Lines to Phosphate deficiency and Salt Stress

Having confirmed the miR399/*PHO2* regulatory module is responsive to P deficiency and salt stress, a miR399 knockdown (*MIM399*) and a miR399 overexpression (*MIR399*) line was generated in the Col-0 background of *Arabidopsis* to determine if plants harbouring a manipulated miR399/*PHO2* regulatory module displayed improved phenotypic and/or physiological tolerance to either of the imposed stresses. Consistent with the growth regimes used in **Chapter II** and **Chapter III**, post germination, 8 d old Col-0, *MIM399* and *MIR399* seedlings were exposed to a 7 d treatment period of either P deficient (P⁻) or salt stress prior to phenotypic and physiological assessments being performed. When each plant line was visualised at 15 d of age, it was readily evident that the phenotypic response of *MIM399* and *MIR399* seedlings was distinct to Col-0 plants of the same age under each assessed growth regime (**Figure 4.2**). To quantify this variation in phenotypic response, assessments of; (1) fresh weight (**Figure 4.3**), (2) rosette area (**Figure 4.4**), (3) primary root length (**Figure 4.5**), (4) anthocyanin accumulation (**Figure 4.6**) and, (5) chlorophyll *a* and *b* content (**Figure 4.7A-B**) were performed to determine the degree of response of each *Arabidopsis* line to P⁻ and salt stress conditions. As the Col-0 seedlings used for comparative analysis in this chapter are identical to those used in **Chapter III**, the results presented here (**Section 4.4.2.1- 4.4.2.5**) will be primarily focused on the phenotype of the *MIM399* and *MIR399* seedlings cultivated under control, P⁻ or salt stress growth regimes. Similar to **Chapter III**, as the *MIM399* and *MIR399* *Arabidopsis* plants are newly created mutant *Arabidopsis* lines, all phenotypic (and molecular) analyses found in this chapter are presented comparative to non-stressed Col-0 seedlings as detailing of any phenotypic (and molecular) differences between control grown Col-0 seedlings and the novel *Arabidopsis* plants harbouring molecular modifications to the miR399/*PHO2* regulatory module was of high interest.

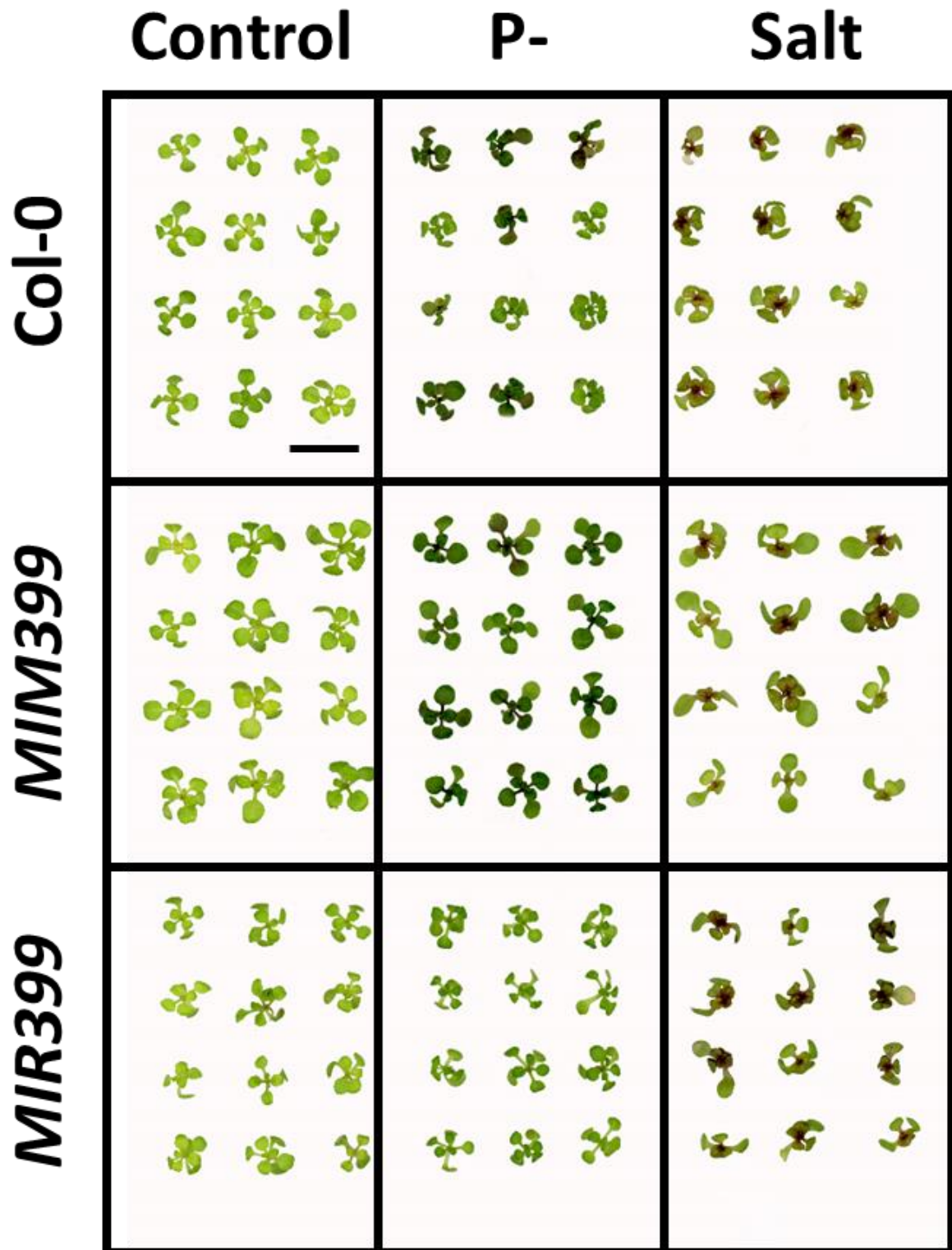


Figure 4.2 Phenotypic and physiological consequence of a P deficiency (P⁻) or salt stress treatment on 15 d old wild-type *Arabidopsis* (Col-0), *MIM399* and *MIR399*. Phenotypes displayed by 15 d old *Arabidopsis* whole seedlings post a 7 d treatment with P⁻ or salt stress, compared to non-stressed seedlings of the same age (left panel). Scale bar = 1.0 centimeter (cm).

4.4.2.1 *Fresh Weight*

Whole plant fresh weight was employed to document the readily apparent variation in plant size observed for Col-0, *MIM399* and *MIR399* seedlings post a 7 d cultivation period on control, P⁻ and salt stress media (**Figure 4.2**). As previously shown (**Figure 3.4**), when compared to 15 d old control Col-0 seedlings, Col-0 plants of the same age exposed to P⁻ and salt stress presented 32.1% ($\pm 1.8\%$) and 26.1% ($\pm 3.8\%$) reductions of plant fresh weight (**Figure 3.4 and Figure 4.3**). Analysis of the whole seedling fresh weight of control *MIM399* plants for comparison to control 15 d old control Col-0 seedlings revealed the overall fresh weight of miR399 knockdown line remained largely unchanged ($106.6\% \pm 5.1\%$) (**Figure 4.3**). Interestingly, exposure of *MIM399* seedlings to the P⁻ stress growth regime failed to cause a significant reduction (reduced by $11.6\% \pm 3.4\%$) in the fresh weight of *MIM399* plants compared to their non-stressed counterparts. However, this mild reduction to fresh weight was not observed in *MIM399* seedlings grown in the presence of 150 mM NaCl. Rather, these seedlings presented a severe 35.9% ($\pm 3.2\%$) reduction in fresh weight compared to *MIM399* control seedlings (**Figure 4.3**). When assessing if the *Arabidopsis* plant line generated to over accumulate the miR399 sRNA had an altered phenotype compared to unmodified Col-0 seedlings, it was interesting to observe that control grown *MIR399* seedlings had a mildly reduced fresh weight (down by $14.2\% \pm 4.1\%$). Post exposure of *MIR399* plants to a 7 d growth period in either the absence of P, or in the presence of 150 mM NaCl, the fresh weight of *MIR399* seedlings was reduced by 15.4% ($\pm 3.1\%$) and 35.6% ($\pm 1.9\%$) respectively, compared to 15 d old *MIR399* control plants (**Figure 4.3**). It was interesting to note that with respect to overall fresh weight, both miR399 altered lines, *MIM399* and *MIR399* plants, appeared to be more tolerant, at least at the phenotypic level, to cultivation in a P deficient environment than were unmodified Col-0 plants. However, the opposite phenotypic trend was observed for these two molecularly modified plant lines in response to a 7 d cultivation period on plant growth media supplemented with 150 mM NaCl, that is; *MIM399* and *MIR399* plants were more sensitive than unmodified Col-0 plants were to salt stress.

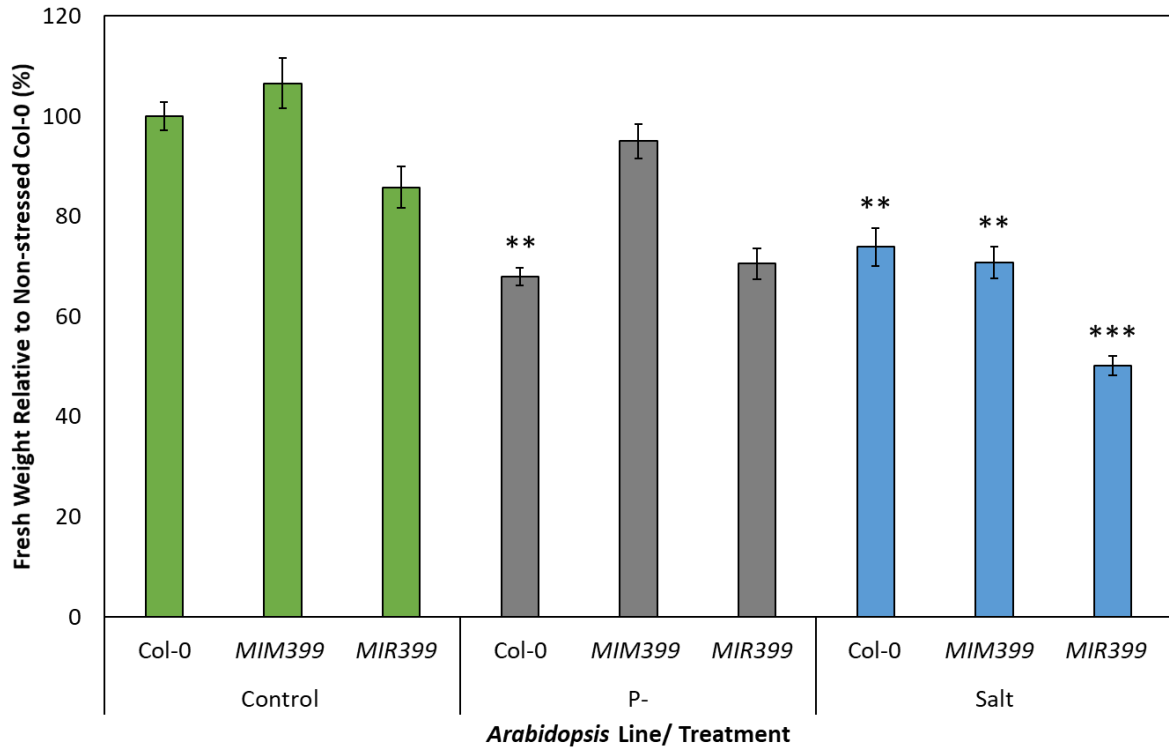


Figure 4.3 Whole seedling fresh weight of P⁻ and salt stressed *Arabidopsis* Col-0 and miR399 altered lines, *MIM399* and *MIR399*, compared to non-stressed Col-0 seedlings. Error bars represent the \pm SD of 4 biological replicates and each biological replicate consisted of a pool of six individual plants. The presence of an asterisk above a control grown *MIM399* or *MIR399* column represents a statistically significant difference comparative to control grown Col-0. Additionally an asterisk above a P⁻ or salt treated *Arabidopsis* plant line represents a statistically significantly difference between the stress treated sample and the respective non-stressed control sample (P-value: * < 0.05; ** < 0.005; *** < 0.001).

4.4.2.2 Rosette Area

The visually striking variation in shoot architecture displayed by Col-0, *MIM399* and *MIR399* plants across the three assessed growth regimes (**Figure 4.2**), further presented rosette area analysis as an appropriate assessment metric of varied plant line responses to the imposed stresses. Closely paralleling the fresh weight trends observed for Col-0 seedlings exposed to P⁻ and salt stress (**Figure 4.3**), the rosette area of P⁻ and salt stressed Col-0 seedlings was significantly reduced by 39.9% ($\pm 3.5\%$) and 46.6% ($\pm 3.5\%$) respectively, compared to 15 d old control Col-0 plants (**Figure 3.5 and Figure 4.4**). When the rosette area was quantified for control grown *MIM399* seedlings, a mild increase of 12.6% ($\pm 3.4\%$) was determined post comparison to that of control Col-0 seedlings of the same age (**Figure 4.4**). It was interesting to note that exposure of *MIM399* plants to the P⁻ growth regime, failed to direct any real alteration to the rosette area of *MIM399* plants. Specifically, when compared to the rosette area of control *MIM399* plants, only a mild 4.2% ($\pm 3.2\%$) reduction to rosette area was documented for P⁻ *MIM399* plants. The presence of 150 mM NaCl again caused the most significant phenotypic response, resulting in a large reduction (down by 45.5% $\pm 3.2\%$) to the rosette area of salt stressed *MIM399* plants, compared to that of *MIM399* control plants (**Figure 4.4**). Potentially underpinning the significant reduction in seedling fresh weight observed in control grown *MIR399* seedlings (**Figure 4.3**), the rosette area of *MIR399* control seedlings was determined to be reduced by 20.4% ($\pm 3.8\%$) compared to 15 d old control grown *Arabidopsis* plants. This decline in rosette area became more pronounced when *MIR399* seedlings were exposed to P⁻ and salt stress growth conditions. Namely, compared to *MIR399* control seedlings, P⁻ and salt stressed *MIR399* seedlings had rosette areas that were reduced by 17.4% ($\pm 2.5\%$) and 27.4% ($\pm 1.1\%$), respectively (**Figure 4.4**). Largely following the same trends observed for plant fresh weight, when compared to the non-stressed counterparts, the shoot architecture of Col-0 seedlings appeared to be more sensitive to growth in a P deficient environment than either of the molecularly modified plant lines. Curiously, the rosette area of salt stressed seedlings did not follow the same trends as observed for plant fresh weight. Specifically, when compared to their non-stressed counterparts, the *MIR399* plant line appeared to be least sensitive to the application of a 7 d cultivation period on plant growth medium supplemented with 150 mM NaCl.

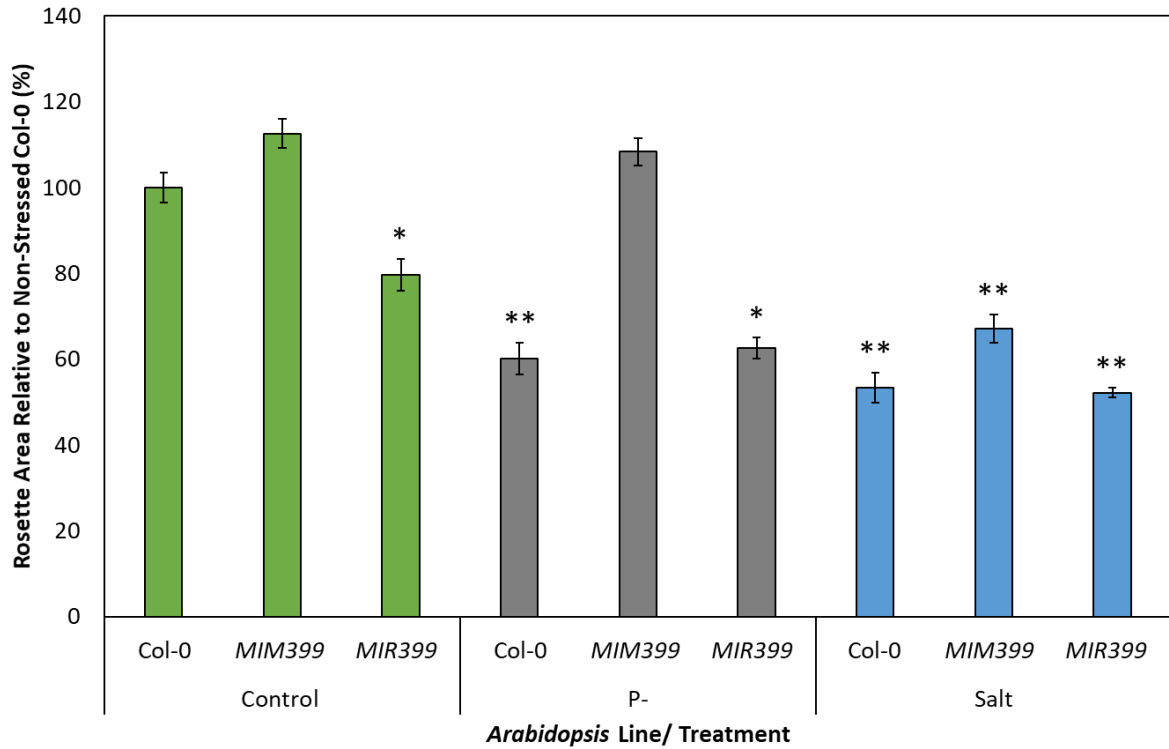


Figure 4.4 Rosette area of P⁻ and salt stressed *Arabidopsis* Col-0 and miR399 altered lines, *MIM399* and *MIR399*, compared to non-stressed Col-0 seedlings. Error bars represent the \pm SD of 4 biological replicates and each biological replicate consisted of a pool of six individual plants. The presence of an asterisk above a control grown *MIM399* or *MIR399* column represents a statistically significant difference comparative to control grown Col-0. Additionally an asterisk above a P⁻ or salt treated *Arabidopsis* plant line represents a statistically significantly difference between the stress treated sample and the respective non-stressed control sample (P-value: * < 0.05; ** < 0.005; *** < 0.001).

4.4.2.3 Primary Root Length

As altered root architecture is a well-documented response to P⁻ and salt stress (Acora *et al.*, 2011; Fujii *et al.*, 2005; Gao *et al.*, 2007; Pasternak *et al.*, 2005), the primary root length was quantified for Col-0, *MIM399* and *MIR399* plants in response to all three growth regimes. Compared to the primary root length of 15 d old control grown Col-0 plants, when 8 d old Col-0 seedlings were cultivated for a 7 d period on plant growth media devoid of P or supplemented with 150 mM NaCl, primary root length was reduced by 47.5% (\pm 1.8%) and 54.4% (\pm 1.8%), respectively (**Figure 3.6 and Figure 4.5**). Closely paralleling the aerial tissue observations, and when compared to non-stressed Col-0 seedlings of the same age, control grown *MIM399* plants developed primary roots of near identical length (100.4% \pm 2.8%). Interestingly, the primary root length of *MIM399* plants was largely unaffected by the absence of P with only a mild reduction of 2.5% (\pm 2.7%) in primary root length observed. On the other hand, exposure to salt stress had a significant impact on the *MIM399* primary root development, resulting in a 31.0% (\pm 1.2%) reduction to primary root length (**Figure 4.5**). While elevated miR399 abundance had significant implications for shoot development of control grown *MIR399* plants (**Figure 4.3**), the primary root length of these seedlings was impacted to a lesser degree. Namely, compared to control grown Col-0 plants, *MIR399* seedlings displayed a mild 12.4% (\pm 2.9%) reduction in primary root length. Similar to the shoot tissue observations, P⁻ and salt stress resulted in 13.5% (\pm 4.9%) and 39.2% (\pm 1.3%) reductions to *MIR399* primary root length, respectively, when compared to *MIR399* control plants (**Figure 4.5**). Contrary to the large impact that the P deficient growth regime had on the primary root length of Col-0 seedlings, this form of abiotic stress failed to have a significant impact on the primary root length of 15 d old *MIM399* or *MIR399* plants. In direct contrast to this observation, the 7 d salt stress growth regime significantly inhibited the development of the primary roots of all three *Arabidopsis* plant line assessed. However, the analysis presented in **Figure 4.5** did indicate that Col-0 plants were most sensitive to cultivation in a saline environment, and *MIM399* seedlings the least sensitive.

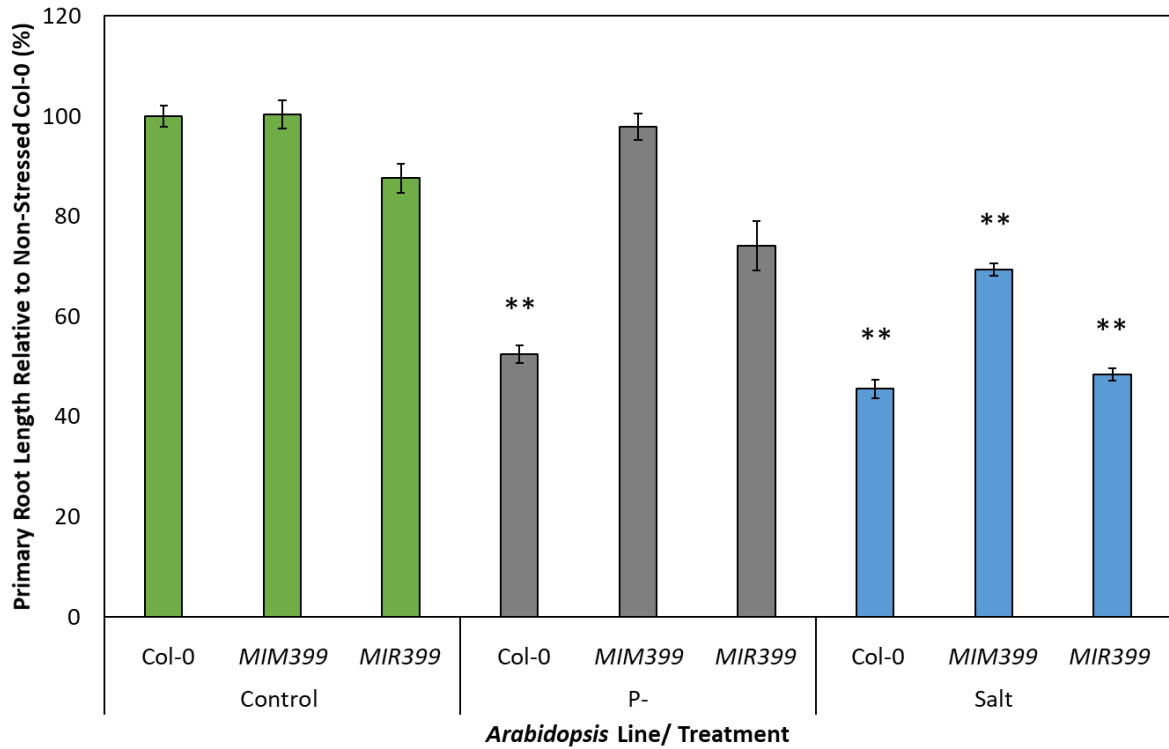


Figure 4.5 Primary root length of P- and salt stressed *Arabidopsis* Col-0 and miR399 altered lines, *MIM399* and *MIR399*, compared to non-stressed Col-0 seedlings. Error bars represent the \pm SD of 4 biological replicates and each biological replicate consisted of a pool of six individual plants. The presence of an asterisk above a control grown *MIM399* or *MIR399* column represents a statistically significant difference comparative to control grown Col-0. Additionally an asterisk above a P- or salt treated *Arabidopsis* plant line represents a statistically significantly difference between the stress treated sample and the respective non-stressed control sample (P-value: * < 0.05; ** < 0.005; *** < 0.001).

4.4.2.4 Anthocyanin Accumulation

It is readily apparent in **Figure 4.2** that Col-0, *MIM399* and *MIR399* plants displayed a range of pigmentation in the aerial tissues surrounding the shoot apical meristem (SAM) region and extending into the petioles of rosette leaves. This varied pigmentation was suspected to be the result of the well documented abiotic stress associated pigment, anthocyanin, and therefore, anthocyanin accumulation in each *Arabidopsis* plant line, and assessed growth condition, was determined (Akula and Ravishankar, 2011; Chalker-Scott, 1999; Kovicich *et al.*, 2015). As presented in **Chapter III (Figure 3.7)**, cultivation of Col-0 seedlings on plant growth medium either lacking P or supplemented with 150 mM NaCl caused a significant 60.3% ($\pm 5.0\%$) and 80.8% ($\pm 2.8\%$) rise in anthocyanin accumulation when compared to control grown plants, respectively (**Figure 3.7 and Figure 4.6**). Manipulation of the miR399 abundance profile had no impact on anthocyanin accumulation in the shoot tissues of control grown *Arabidopsis* plants. Specifically, the anthocyanin content of control *MIM399* seedlings remained largely unchanged at 94.0% ($\pm 5.1\%$) of control Col-0 seedling levels (**Figure 4.6**). However, when exposed to P⁻ growth conditions, the anthocyanin accumulation of *MIM399* was drastically increased by 126.2% ($\pm 6.3\%$), compared to control *MIM399* anthocyanin levels. Similarly, when *MIM399* seedlings were cultivated under a salt stress growth regime, a dramatic increase in anthocyanin accumulation (76.8% $\pm 7.7\%$) was observed compared to control grown *MIM399* seedlings (**Figure 4.6**).

Analysis of anthocyanin accumulation in non-stressed *MIR399* seedlings revealed that this physiological parameter remained largely unchanged (96.2% $\pm 2.1\%$) from that of control grown Col-0 seedlings. When *MIR399* seedling were cultivated on plant growth media deficient in P for a 7 d period, the anthocyanin accumulation of these seedlings was only mildly increased by 33.7% ($\pm 8.2\%$) in comparison to non-stressed *MIR399* plants. This however was determined to not be the case when *MIR399* seedlings were cultivated under salt stress conditions with a significant 163.2% ($\pm 5.0\%$) increase in anthocyanin documented (**Figure 4.6**). With respect to the accumulation of anthocyanin, it was a surprise observation that exposure to a P deficient growth environment resulted in the *MIM399* plant line presenting a larger degree of sensitivity to this environment than did Col-0 plants. It was also unexpected to observe that with respect to anthocyanin accumulation, seedlings of the *MIR399* plant line appeared to be the least impacted by this stress regime. This trend was not maintained in response to salt stress with *MIR399* seedlings accumulating anthocyanin to a much higher degree than both the Col-0 and *MIM399* plant lines.

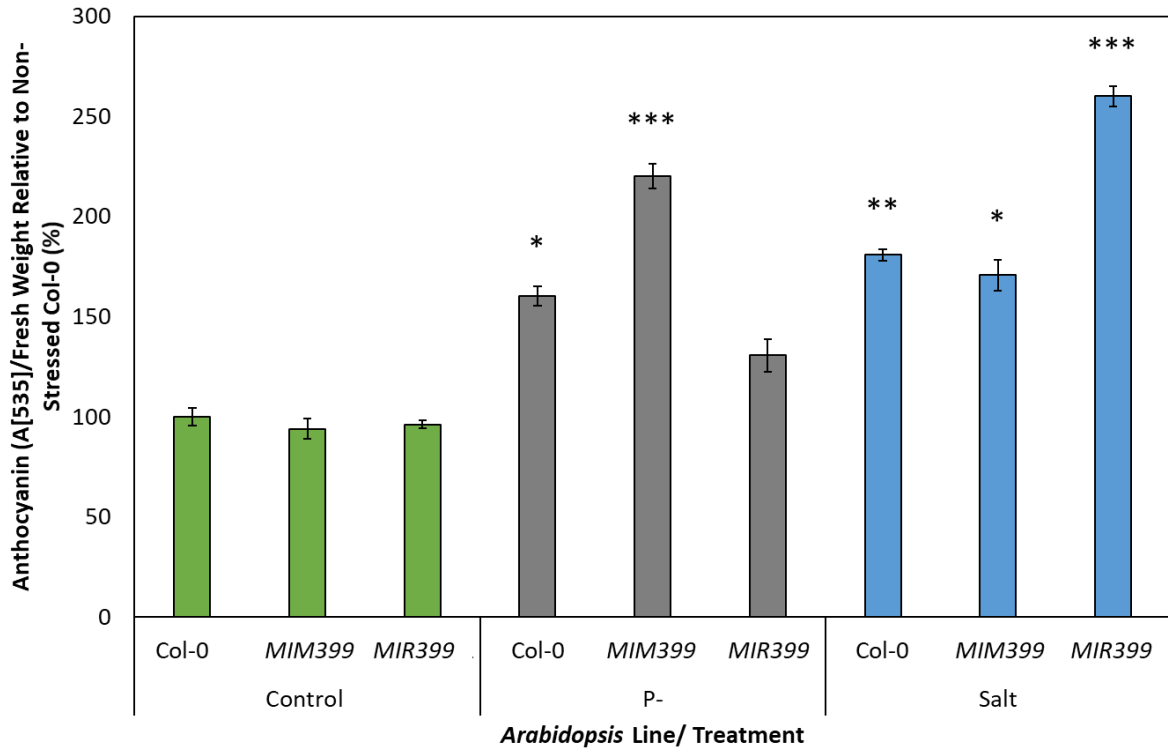


Figure 4.6 Anthocyanin accumulation of P⁻ and salt stressed *Arabidopsis* Col-0 and miR399 altered lines, *MIM399* and *MIR399*, compared to non-stressed Col-0 seedlings. Error bars represent the \pm SD of 4 biological replicates and each biological replicate consisted of a pool of six individual plants. The presence of an asterisk above a control grown *MIM399* or *MIR399* column represents a statistically significant difference comparative to control grown Col-0. Additionally an asterisk above a P⁻ or salt treated *Arabidopsis* plant line represents a statistically significantly difference between the stress treated sample and the respective non-stressed control sample (P-value: * < 0.05; ** < 0.005; *** < 0.001).

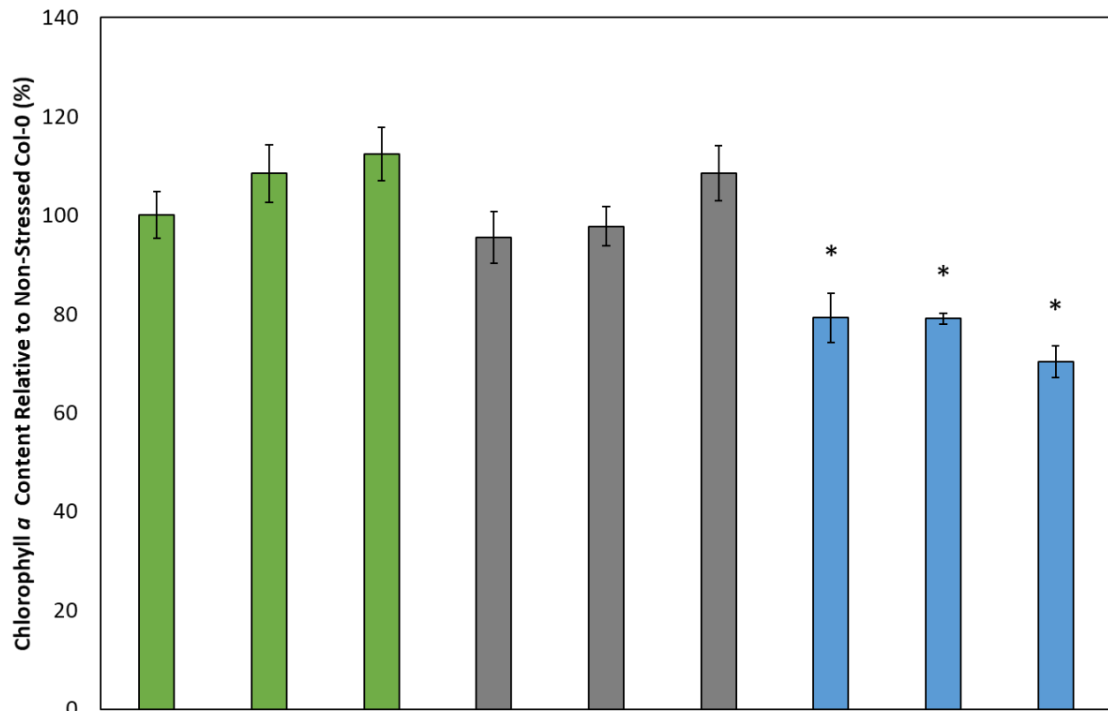
4.4.2.5 Chlorophyll *a* and *b* Content

As the photosynthetic capability of a plant is inhibited by exposure to abiotic stress (Sudhir and Murthy, 2004), chlorophyll *a* and *b* content was next assessed to determine any variation in the physiological sensitivity of Col-0, *MIM399* and *MIR399* plants across the three growth regimes. As detailed previously (**Figure 3.8A**), cultivation of Col-0 seedlings in P deficient growth conditions had no significant impact on the chlorophyll *a* content ($95.6\% \pm 5.2\%$) (**Figure 3.8A and Figure 4.7A**). This was observed to not be the case when Col-0 seedlings were exposed to salt stress conditions with chlorophyll *a* levels reduced by 20.8% ($\pm 5.0\%$) (**Figure 3.8A and Figure 4.7A**). As determined for the anthocyanin assessment, the determination of the chlorophyll *a* content of non-stressed *MIM399* plants revealed that this photosynthetic pigment remained at approximate wild-type levels ($108.5\% \pm 5.8\%$). Similarly, when *MIM399* seedlings were cultivated under P⁻ stress, only a mild change in chlorophyll *a* content (reduced by $10.7 \pm 3.9\%$) was detected when compared to *MIM399* control seedlings. The deleterious impact of salt stress on *Arabidopsis* growth and development was again evident from this analysis with chlorophyll *a* content reduced by 29.4% ($\pm 1.1\%$) in salt stressed *MIM399* plants, compared to *MIM399* control seedlings (**Figure 4.7A**). The chlorophyll *a* content of *MIR399* seedlings followed very similar trends to those observed of *MIM399* seedlings. Specifically, under the control growth regime, the chlorophyll *a* content of *MIR399* plants was only mildly elevated by 12.4% ($\pm 5.4\%$) compared to that of non-stressed wild-type seedlings. Further, this level of chlorophyll *a* content was maintained when *MIR399* seedlings were exposed to the P deficient growth regime with no significant alteration to chlorophyll *a* levels observed (reduced by $3.9\% \pm 5.6\%$). In contrast to this result, salt stress caused a dramatic reduction in the chlorophyll *a* level of *MIR399* plants, reduced by 42.0% ($\pm 3.2\%$) compared to the chlorophyll *a* content of *MIR399* control seedlings (**Figure 4.7A**).

As expected, the chlorophyll *b* content of Col-0 seedlings closely mirrored the chlorophyll *a* trends. More specifically, P stress was determined to have no significant impact on chlorophyll *b* content ($5.1\% \pm 6.8\%$), whereas the exposure of Col-0 seedlings to salt stress significantly reduced the chlorophyll *b* content by 40.0% ($\pm 3.9\%$), compared to that of Col-0 control plants of the same age (**Figure 3.8A and Figure 4.7B**). The chlorophyll *b* content trends observed for *MIM399* and *MIR399* seedlings also closely mirrored those determined for chlorophyll *a* content. Namely, for control grown *MIM399* seedlings, and when compared to Col-0 control seedlings, chlorophyll *b* content was only mildly elevated by 13.8% ($\pm 7.1\%$). Similarly, a 7 d exposure of *MIM399* plants to P⁻ stress failed to significantly alter their chlorophyll *b* content (reduced by $9.4\% \pm 3.3\%$) compared to that of control grown *MIR399* plants. In response to the imposed salt stress growth regime, it was unsurprising to observe that the chlorophyll *b* content of *MIM399* seedlings was reduced by 48.5% ($\pm 2.3\%$) compared

to its level in *MIM399* control plants (**Figure 4.7B**). As identified for chlorophyll *a* content of *MIR399* seedlings, a standard growth regime resulted in mild increase of 16.0% (\pm 6.4%) in the chlorophyll *b* content of this *Arabidopsis* line when compared to Col-0 control seedlings. Further, exposure of *MIR399* plants to a 7 d growth period in the absence of P, resulted in a very mild 5.8% (\pm 4.1%) reduction to the chlorophyll *b* content compared to its level in control grown *MIR399* seedlings. However, exposure to the 7 d salt stress growth regime dramatically impacted the chlorophyll *b* content of *MIR399* seedlings with a significant 57.9% (\pm 5.9%) reduction determined. When taken together, the data presented in **Figure 4.7** clearly shows that the cultivation of Col-0, *MIM399* and *MIR399* plants for a 7 d period in the absence of P had no significant impact on the chlorophyll *a* and *b* content of these three *Arabidopsis* lines. However, in direct contrast, the 7 d cultivation period in the presence of 150 mM NaCl reduced the content of both chlorophyll *a* and *b* in the three assessed plant lines, with the largest reduction to the level of both of these photosynthetic pigments observed in the *MIR399* plant line, and the lowest degree of reduction observed in Col-0 seedlings.

(A)



(B)

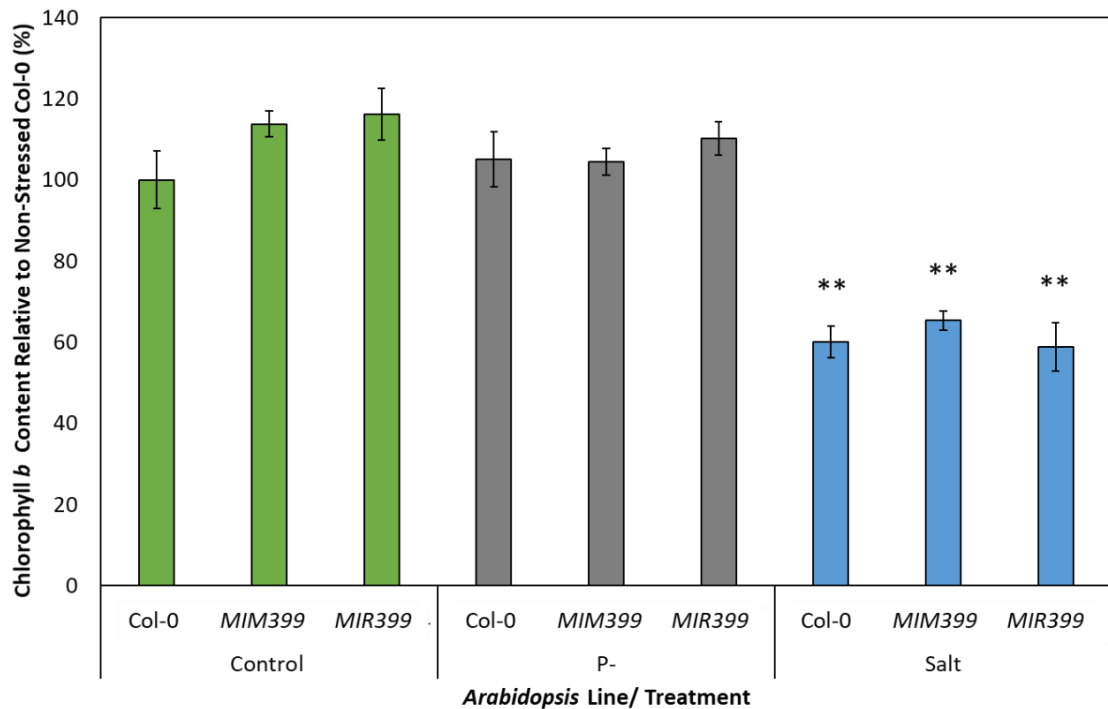


Figure 4.7 Chlorophyll a (A) and b (B) content of P⁻ and salt stressed *Arabidopsis* Col-0 and miR399 altered lines, *MIM399* and *MIR399*, compared to non-stressed Col-0 seedlings. Error bars represent the \pm SD of 4 biological replicates and each biological replicate consisted of a pool of six individual plants. The presence of an asterisk above a control grown *MIM399* or *MIR399* column represents a statistically significant difference comparative to control grown Col-0. Additionally an asterisk above a P⁻ or salt treated *Arabidopsis* plant line represents a statistically significantly difference between the stress treated sample and the respective non-stressed control sample (P-value: * < 0.05; ** < 0.005; *** < 0.001).

4.4.3 The Molecular Response of Arabidopsis Plant Lines With Molecularly Altered miR399 Abundance to Phosphate Deficiency and Salt Stress

The highly conserved plant miRNA, miR399, is a well-documented P responsive miRNA that modulates the expression of *PHO2* in response to the level of P in the growth environment (Bari *et al.*, 2006). Previous studies have shown that this regulatory module is responsible for P uptake, and the maintenance of P homeostasis; both essential processes of a plant in an attempt to tolerate growth in a P deficient environment (Bari *et al.*, 2006; Fujii *et al.*, 2005; Hsieh *et al.*, 2009; Lin *et al.*, 2008). RT-qPCR was next utilised to document the molecular variations in the miR399/*PHO2* regulatory module across each of the *Arabidopsis* lines grown under the control, P⁻ and salt stress growth regimes. This analysis was conducted to account, at least in part, for the varied phenotypic and physiological responses displayed by 15 d old Col-0, *MIM399* and *MIR399* to the three growth regimes assessed. As previously demonstrated via RT-qPCR (**Figure 2.13A** and **Section 4.4.1**), and when compared to non-stressed Col-0 seedlings, miR399 accumulation is elevated by 1.9- and 2.4-fold respectively, in P⁻ and salt stressed Col-0 seedlings (**Figure 4.8**). It was therefore unsurprising to observe that in P⁻ and salt stressed Col-0 seedlings, *PHO2* expression was reduced by 5.0-fold and 4.2-fold, respectively.

Determination of the efficacy of the miR399 targeting, miRNA target mimicry construct in 15 d old control *MIM399* seedlings, revealed that the abundance of the targeted miRNA was reduced by 1.9-fold. It was therefore unexpected that the applied RT-qPCR approach also revealed that *PHO2* expression was also reduced (by ~2.0-fold) in *MIM399* control seedlings (**Figure 4.8**). Interestingly, exposure of *MIM399* seedlings to a P deficient growth regime resulted in the wild-type equivalent accumulation of the miR399 sRNA. Considering this, it was highly surprisingly that RT-qPCR revealed that *PHO2* expression was dramatically reduced by 19.5-fold. When the *MIM399* plant line was exposed to salt stress, RT-qPCR revealed miR399 abundance to be elevated by 1.9-fold, and the expression of *PHO2* to be reduced by 1.7-fold (**Figure 4.8**).

In non-stressed *MIR399* seedlings, the abundance of the miR399 sRNA was elevated by 3.2-fold. However, in this plant line, *PHO2* expression was only mildly reduced by 1.1-fold. Further elevations to the abundance of the miR399 sRNA was observed in P⁻ stressed *MIR399* seedlings when exposed to a P⁻ growth regime with miR399 accumulation 4.5-fold higher in *MIR399* when compared to non-stressed Col-0 seedlings. Unsurprisingly, the reciprocal trend was observed for *PHO2* expression in the same P⁻ stressed *MIR399* seedlings, specifically, *PHO2* had accumulated to a level 2.7-fold less than control grown Col-0 seedlings. A 7 d growth regime in the presence of 150 mM salt resulted in a large 6.0-fold elevation in the

miR399 accumulation while appropriately, *PHO2* was determined by RT-qPCR to be reduced by 4.5-fold.

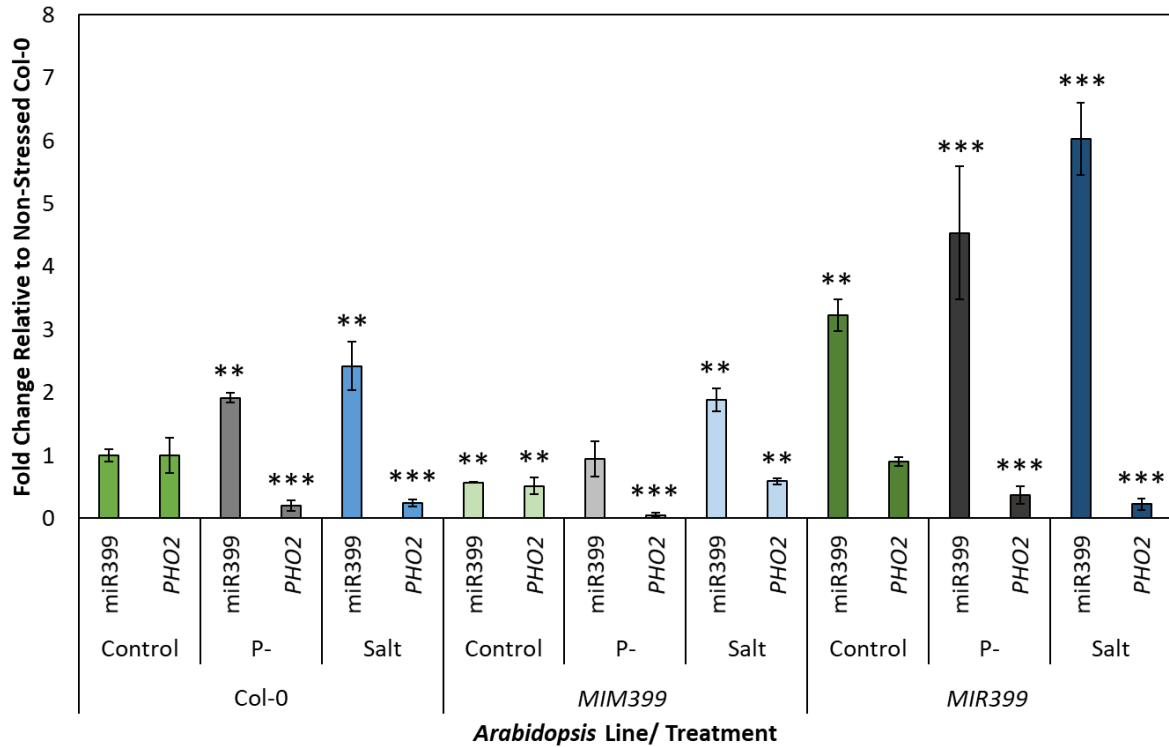


Figure 4.8 RT-qPCR assessment of miR399 and miR399 target gene, *PHO2*, in non-stressed and stress treated *Arabidopsis* plant lines. The RT-qPCR determined accumulation of miR399 and *PHO2* in *Arabidopsis* Col-0, *MIM399* and *MIR399* *Arabidopsis* seedlings exposed to each abiotic stress is presented relative to control grown Col-0 seedlings. Error bars represent the \pm SD of 4 biological replicates with each biological replicate consisting of 6 individual plants. The presence of an asterisk indicates a statistically significant difference between the expression of each gene determined for control Col-0 seedling (p-value: < 0.05, *; P < 0.005, **; P < 0.001, ***).

4.5 Discussion

4.5.1 *The Requirement of DRB1, DRB2 and DRB4 for Appropriate Regulation of the miR399/PHO2 Regulatory Module in Arabidopsis*

As P homeostasis is crucial to both plant development and the adaptive response of a plant to abiotic stress, confirming the molecular machinery required for *Arabidopsis* to maintain the appropriate accumulation of the miR399/*PHO2* regulatory module was of high interest. The requirement of each of the nuclear localised DRBs, namely the requirement of DRB1, DRB2 and DRB4 in the production of miR399, the regulation of the expression of the miR399 target gene, *PHO2*, and/or the maintenance of P homeostasis, are all discussed in the following publication:

Pegler, J. L., Oultram, J. M., Grof, C. P., and Eamens, A. L. (2019). DRB1, DRB2 and DRB4 Are Required for Appropriate Regulation of the microRNA399/*PHOSPHATE2* Expression Module in *Arabidopsis thaliana*. *Plants*, 8(5), 124.

<https://www.mdpi.com/2223-7747/8/5/124>

A copy of this publication can be found in **Appendix 1 (A.1.4)** of this thesis, pages 211-236.

4.5.2 *Manipulation of the miR399/PHO2 Regulatory Module Results in Altered Growth and Development and the Response of Arabidopsis to Abiotic Stress*

Having confirmed the; (1) necessity of each of the nuclear localised DRBs, including DRB1, DRB2 and DRB4, in the appropriate regulation of the miR399/*PHO2* regulatory module in *Arabidopsis*, and; (2) altered regulation of the miR399/*PHO2* regulatory module in *Arabidopsis* plant lines defective in the activity of each of the three nuclear DRBs resulted in varied phenotypic and/or physiological responses to P⁻ growth conditions being expressed by each plant line, the exposure of the newly generated *MIM399* and *MIR399* plant lines to conditions of P⁻ and salt stress was conducted to determine what impact the direct molecular manipulation of the miR399/*PHO2* regulatory module would have on the ability of *Arabidopsis* to respond to the two imposed abiotic stresses.

Post cultivation under control, P deficient, and saline growth conditions, *MIM399* and *MIR399* seedlings were visually compared to their Col-0 counterparts to determine what impact modulation of miR399 abundance had on (1) the growth and development of 15 d old *Arabidopsis* seedlings under control growth conditions, and/or (2) the adaptive response of

these plant lines to exposure to P⁻ and salt stress. As the phenotypic and physiological response of Col-0 seedlings exposed to conditions of P⁻ or salt stress has been previously discussed (**Appendices A.1.3 and A.1.4, pages 193-210; 211-236, respectively**), this discussion will primarily focus on the phenotypic and physiological characteristics of the newly generated molecularly modified *Arabidopsis* lines via their comparison to Col-0 seedlings of the same age. Specifically, when visualising the phenotypic response of each of the *Arabidopsis* seedlings, under each growth condition, there was striking variation in the growth and development of each *Arabidopsis* plant line (**Figure 4.2**). For that reason and maintaining the same quantitative measurements utilised in **Chapter II** and **Chapter III**, fresh weight (**Figure 4.3**), rosette area (**Figure 4.4**), primary root length (**Figure 4.5**), anthocyanin accumulation (**Figure 4.6**) and chlorophyll *a* and *b* content (**Figure 4.7A-B**), were once again applied here to document the varying degree of abiotic stress indicators displayed by each assessed plant line. In addition to these phenotypic and physiological analyses, RT-qPCR was also employed to quantify the abundance of both the miR399 sRNA, and of its targeted gene, *PHO2* (**Figure 4.8**). This analysis was conducted in an attempt to obtain a more detailed understanding of the appropriate molecular profile of miR399/*PHO2* regulatory module required to equip *Arabidopsis* with the phenotypic and/or physiological ability to adapt to, or to tolerate exposure to P⁻ and/or salt stress. While the developmental phenotype of *MIM399* and *MIR399* plants at 15 d old (under control and abiotic stress conditions) was the focus of this study, the vegetative and reproductive development for of *MIM399* and *MIR399* is presented in **Figure A.6.2** (page 269).

4.5.2.1 *Molecularly Modified miR399 Abundance Provides Arabidopsis Seedlings with Superior Phenotypic Traits Under Non-stress Growth Conditions*

In order to uncover what influence the miR399/*PHO2* regulatory module has on the growth and development of 15 d old *Arabidopsis* seedlings, the phenotypic traits and molecular profiles of control grown *MIM399* and *MIR399* plants were compared to those of Col-0. When initially assessing the phenotypic and physiological parameters of the *MIM399* plant line, it was noted that the fresh weight (**Figure 4.3**), rosette area (**Figure 4.4**), primary root length (**Figure 4.5**), anthocyanin accumulation (**Figure 4.6**) and chlorophyll *a* and *b* content (**Figure 4.7A-B**) were only mildly altered compared to each of these respective metrics determined for Col-0 control seedlings. To ensure that the *MIM399* seedlings harboured a molecular alteration to the miR399/*PHO2* regulatory module, RT-qPCR was employed (**Figure 4.8**). This analysis revealed that miR399 abundance was reduced by 1.9-fold in

MIM399 control seedlings, compared to Col-0 control seedlings of the same age. It was therefore an unexpected finding that the expression of the miR399-regulated transcript, *PHO2*, was also reduced to a similar degree (reduced by 2.0-fold) in 15 d old *MIM399* control seedlings. Given the well documented role of miR399 in regulating *PHO2* transcript abundance (Aung *et al.*, 2006; Bari *et al.*, 2006), it was expected that reduced miR399 abundance would have resulted in elevated *PHO2* expression in *MIM399* control seedlings. The observed reduction to both the level of the miR399 sRNA and that of its targeted transcript, *PHO2*, suggested that either; (1) in addition to predominately regulating *PHO2* via mRNA cleavage mode of expression regulation, miR399 can additionally modulate *PHO2* transcript abundance by a translational repression mode of sRNA-directed expression regulation (Aung *et al.*, 2006), or (2) *PHO2* expression in *MIM399* plants was being modulated by a gene expression regulatory mechanism other than that directed by the miR399 sRNA.

Assessment of the phenotypic and physiological parameters of 15 d old control grown *MIR399* seedlings revealed clear mild reductions to the fresh weight (**Figure 4.3**) and rosette area (**Figure 4.4**) of this newly generated plant line, compared to those of Col-0 control seedlings of the same age. However, this analysis series also showed that primary root length (**Figure 4.5**), anthocyanin content (**Figure 4.6**) and chlorophyll *a* and *b* content (**Figure 4.7A-B**) remained largely unchanged in *MIR399* control seedlings, from those of Col-0 control plants. In control grown *MIR399* seedlings, the molecular analysis revealed that the abundance of the miR399 sRNA was elevated by 3.2-fold. However, in spite of this enhancement to sRNA abundance, the expression of the *PHO2* target gene remained relatively constant, compared to its expression in Col-0 control seedlings of the same age (**Figure 4.8**). While it was surprising to observe that *PHO2* expression in *MIR399* plants remained similar to that of wild-type *Arabidopsis*, it was somewhat expected that this miRNA overexpression line would be phenotypically distinct to Col-0 plants due to a deregulated Pi root to shoot translocation pathway. For example, Aung *et al.*, (2006) have previously demonstrated that *Arabidopsis* plants overexpressing the miR399 sRNA, or defective in the activity of *PHO2* (i.e., the *Arabidopsis pho2* mutant line), excessive Pi accumulation in the shoot tissue led to reduced rosette area and the development of areas of both chlorosis and necrosis in mature leaves (see **Figure A.6.2E**, page 269).

4.5.2.2 *Molecularly Modified miR399 Abundance Alters the Tolerance of Arabidopsis Seedlings to P Deficiency and Salt stress*

Prior to the assessment of how the two newly generated *Arabidopsis* plant lines that harbour a molecularly modified miR399/*PHO2* regulatory module responded to P⁻ and salt stress, this regulatory module was molecularly profiled in the Col-0 background to determine the wild-type response of this module to the two applied stresses. As previously stated in **Chapter III (Section 3.5.2.2)**, exposure of 15 d old Col-0 seedlings to P⁻ or salt stress for a 7 d period, resulted in significant reductions to Col-0 seedling fresh weight (**Figure 4.3**), rosette area (**Figure 4.4**) and primary root length (**Figure 4.5**). Further, both P⁻ and salt stressed Col-0 seedlings also displayed a significantly elevated anthocyanin content (**Figure 4.6**). Interestingly, while P⁻ stress has no impact on the chlorophyll *a* and *b* content of Col-0 seedlings, salt stress resulted in significant reductions to the abundance of both photosynthetic pigments (**Figure 4.7A-B**). To account for this sensitivity to each stress, RT-qPCR was used to assess the accumulation of the miR399 sRNA and to profile the expression of *PHO2* (**Figure 4.8**). RT-qPCR revealed that miR399 abundance was elevated by 1.9- and 2.4-fold in response to P⁻ and salt stress respectively, while accordingly, *PHO2* expression was reduced by 5.0- and 4.2-fold in response to the upregulated abundance of the miR399 sRNA in P⁻ and salt stressed Col-0 seedlings. The altered molecular profile of the miR399/*PHO2* regulatory model in Col-0 seedlings post their exposure to P⁻ stress was unsurprising with previous research having demonstrated that in the absence of Pi, the transcriptional activators, PHR1 and PHR1-LIKE, promote expression of members of both the *MIR399* and *PHT1* gene families (see **Figure 4.1**; Rubio *et al.*, 2001). This, in turn, results in elevated miR399 sRNA abundance and reduced *PHO2* expression, with reduced *PHO2* protein activity relieving the ubiquitin-mediated repression of *PHO1* and the *PHT1* proteins, proteins that play central roles in Pi acquisition and the translocation of the acquired Pi from root to shoot tissue, via the xylem (Hamburger *et al.*, 2002; Huang *et al.*, 2013; Poirier *et al.*, 1991). Further, once Pi is unloaded from the xylem into photosynthetically active leaves, it is either utilised by the source tissue, or it is alternately loaded into the phloem for distribution to other aerial tissues such as the reproductive organs or juvenile leaves (Liu *et al.*, 2014). It therefore stands to reason that the same behaviour of the miR399/*PHO2* regulatory module in response to a salt stress growth regime (i.e., elevated miR399 levels and reduced *PHO2* expression) is to provide additional cellular resources to the aerial tissues of *Arabidopsis* to assist in responding to this form of abiotic stress. Specifically, as salt stress is well documented to have a major impact on primary plant functions, such as photosynthesis and cell growth in the shoot tissues of an exposed plant (Feng *et al.*, 2014; Meloni *et al.*, 2003; Sudhir and Murthy, 2004), the increased allocation of Pi, a key building block of cellular energy and components of photosynthesis, to these

tissues may be an attempt to negate the negative impacts resulting from reduced photosynthetic capacity and other plant growth parameters with high chemical energy demands.

The assessment of 15 d old seedling fresh weight (**Figure 4.3**), rosette area (**Figure 4.4**), primary root length (**Figure 4.5**), anthocyanin content (**Figure 4.6**), and chlorophyll *a* and *b* content (**Figure 4.7A-B**) were next conducted on P⁻ and salt stressed *MIM399* seedlings to identify any sensitivity or tolerance to either of the assessed stresses displayed by this molecularly modified plant line. Interestingly, when *MIM399* seedlings were cultivated in a P deficient environment for a period of 7 d, the phenotypic and physiological parameters of fresh weight, rosette area, primary root length, and chlorophyll *a* and *b* content were unchanged from those determined for control grown *MIM399* seedlings. However, considering the readily observable darkened pigmentation displayed by P⁻ stressed *MIM399* seedlings, it was not a surprise to determine that the anthocyanin content of this plant line had been significantly elevated. To assess the extent of which the miR399/*PHO2* regulatory module was underpinning the maintenance of the 'non-stressed' or 'control' phenotype displayed by P⁻ stressed *MIM399* seedlings, RT-qPCR was utilised (**Figure 4.8**). Unexpectedly, RT-qPCR revealed miR399 accumulation to remain largely unchanged from that observed in control grown wild-type seedlings, yet *PHO2* expression was determined to be reduced by 19.5-fold in P⁻ stressed *MIM399* seedlings. However, this greatly reduced expression of *PHO2* may, in part, account for both the (1) maintenance of most of the growth and development metrics assessed in this study, and (2) significant increase in the stress induced accumulation of anthocyanin. Specifically, given that the greatly reduced expression of *PHO2* in P⁻ stressed *MIM399* seedlings, and therefore, great reduced *PHO2* protein abundance in this plant line, is likely resulting in the uninhibited *PHO1*/*PHT1*s (namely; *PHT1;4*, *PHT1;8* and *PHT1;9*) directed Pi translocation to the shoot tissue of these seedlings (Hamburger *et al.*, 2002; Huang *et al.*, 2013; Poirier *et al.*, 1991), excess Pi, one of the central molecular building blocks for cellular process such as photosynthesis and cellular growth, would allow these processes to continue in P⁻ stressed *MIM399* seedlings. Further support of this suggestion is the recent study by Shukla and colleagues (2017) which showed that mild doses of Pi (1.25-10 mM) lead to *Arabidopsis* seedlings developing significantly larger rosettes. Accounting for the elevated anthocyanin accumulation that was additionally displayed by P⁻ stressed *MIM399* seedlings, are the results reported in a previous study that showed that when *Arabidopsis* is cultivated under phosphate starvation conditions, the activity of the anthocyanin biosynthesis pathway is strongly induced by the Gibberellin-DELLA signalling pathway, a pathway which can be induced by Pi starvation of *Arabidopsis* roots (Jiang *et al.*, 2007).

When 8 d old *MIM399* seedlings were cultivated on plant growth medium supplemented 150 mM NaCl, significant reductions to fresh weight (**Figure 4.3**), rosette area (**Figure 4.4**), primary root length (**Figure 4.5**) and chlorophyll *a* and *b* content (**Figure 4.7A-B**) were observed. In addition, salt stressed *MIM399* seedlings further presented a significant increase in anthocyanin accumulation (**Figure 4.6**). Given that *MIM399* plants displayed a Col-0-like response to salt stress, it was not surprising to observe *MIM399* seedlings had a 1.9-fold elevation in miR399 abundance, and a 1.7-fold reduction to *PHO2* expression, molecular profile alterations comparable to those documented for salt stressed Col-0 seedlings (**Figure 4.8**). Again, it stands to reason that in order for *Arabidopsis* seedlings to mount an adaptive response to salt stress, it is necessary for miR399 abundance to be elevated, and for *PHO2* expression to be reduced, as this molecular profile is consistent with the need to provide additional Pi to the shoot tissue of *Arabidopsis* to maintain processes such as photosynthesis and cellular growth, processes that are heavily impacted by salinity (Liu *et al.*, 2014; Sudhir and Murthy, 2004).

An identical set of phenotypic and physiological assessments were conducted on *MIR399* seedlings cultivated under P deficient and salt stress conditions to determine any quantifiable sensitivity or tolerance of this plant line to each assessed stress (**Figure 4.3- 4.7A-B**). When grown in the absence of P, significant reductions were observed in the fresh weight (**Figure 4.3**) and rosette area of P⁻ stressed *MIR399* plants (**Figure 4.4**), compared to *MIR399* control seedlings of the same age. Interestingly, each of the other phenotypic and physiological assessments, including, primary root length (**Figure 4.5**), anthocyanin accumulation (**Figure 4.6**) and chlorophyll *a* and *b* content (**Figure 4.7A-B**), remained reasonably similar to those documented for control grown *MIR399* seedlings. Molecular profiling of the miR399/*PHO2* regulatory module in P⁻ stressed *MIR399* seedlings revealed miR399 abundance to be increased by 4.5-fold, and accordingly, the expression of the *PHO2* target gene to be reduced by 2.7-fold (**Figure 4.8**). As the phenotypic and physiological response of *MIR399* seedlings was comparable to that of P⁻ stressed Col-0 seedlings, the documented accumulation profiles for miR399 and *PHO2* were anticipated and likely stem from the need of *Arabidopsis* to mobilise any available Pi stored in the root system for translocation and utilisation in the aerial tissues of the plant (Hamburger *et al.*, 2002; Huang *et al.*, 2013; Poirier *et al.*, 1991)

Of the three *Arabidopsis* lines assessed in this study, *MIR399* seedlings appeared to be the most phenotypically and physiologically sensitive to a 7 d cultivation period on plant growth medium supplemented with 150 mM NaCl. Specifically, compared to *MIR399* control seedlings, salt stressed *MIR399* seedlings presented the largest increase in anthocyanin content and large reductions in fresh weight, rosette area, primary root length and chlorophyll

a and *b* content. Interestingly, salt stressed *MIR399* plants were determined to have the largest increase in miR399 accumulation level, a 6.0-fold elevation to miR399 abundance, when compared to Col-0 control seedlings. It was therefore unsurprising that RT-qPCR revealed *PHO2* expression to be reduced by 4.5-fold in response to this significant elevation in miR399 levels in salt stressed *MIR399* plants. The sensitivity of 8 d old *MIR399* seedlings to a 7 d cultivation period in a saline environment may result from the additive impact of multiple stresses, specifically; (1) the toxic overaccumulation of Pi which has been shown to occur in *Arabidopsis* seedlings that overexpress the miR399 sRNA, or which lack the functional activity of PHO2 (Aung *et al.*, 2006), and; (2) the toxic overaccumulation of Na⁺ and Cl⁻ ions shown to cause the detrimental phenotypic effects associated with plant growth in a salty environment (Munns, 2002; Tester and Davenport, 2003).

Chapter V

Summary and Future Directions

5.1 Summary of Key Results

5.1.1 **Generation of a Heat, Mannitol and Salt Stress Responsive MicroRNA Dataset**

The overarching aim of this research thesis was to molecularly dissect the miRNA regulatory modules that potentially contribute to the ability of *Arabidopsis* plants to tolerate exposure to the abiotic stresses of heat, mannitol and salt stress. Post molecular confirmation that wild-type *Arabidopsis* seedlings were indeed stressed by a 7 d growth regime in the presence of heat, mannitol or salt stress (see **Chapter II**), a sRNA-seq approach was employed and revealed that the abundance of 121, 123 and 118 miRNAs was significantly altered (>2.0-fold) in response to heat, mannitol and salt stress, respectively (**Figure 2.10**). Not only did this analysis lay the foundation for the selection of the miRNAs, miR396 and miR399, for molecular manipulation for the further experimental characterisation of their respectively regulatory modules (**Chapter III** and **Chapter IV**, respectively), but the dataset generated via the applied sRNA-seq approach, post its annotation, also provides an outstanding source of reference for the future selection of miRNA regulatory modules for their molecular manipulation to also further their experimental characterisation (see **Section 5.2.1**). This research was published in the peer-review journal, *Plants*, in 2019 to allow for fellow plant biology researchers to select key abiotic stress responsive miRNAs for their own specific research endeavours (see Publication 3, **Appendix A.1.3**, pages 193-210).

5.1.2 **The Contribution of the Nuclear-Localised DRB Proteins to the Arabidopsis MicroRNA Landscape**

Previous studies have established that the nuclear-localised DRB proteins, DRB1, DRB2 and DRB4, each play an essential role in the production stage of the *Arabidopsis* miRNA pathway (Eamens *et al.*, 2011; Eamens *et al.*, 2012a; Fukudome *et al.*, 2011; Hiraguri *et al.*, 2005; Pélissier *et al.*, 2011; Pouch-Pélissier *et al.*, 2008). The data presented in Chapter II of this research thesis provides further extensive evidence of the essential regulatory role that DRB1, DRB2 and DRB4 play in miRNA production, both in non-stressed *Arabidopsis* plants, and in *Arabidopsis* post its exposure to heat, mannitol and salt stress, or when *Arabidopsis* is cultivated in a P deficient environment. Specifically, in the absence of DRB1 activity (control grown *drb1* seedlings), 111 miRNAs were significantly reduced in their abundance, with 73 of these miRNA sRNAs demonstrated to be solely down in the *drb1* mutant background (**Figure 2.9**). Reduced abundance in the *drb1* mutant background only, provides strong evidence that these 73 miRNA sRNAs are 'DRB1-dependent' with respect to their production. This finding also further cemented DRB1, from the five DRB proteins encoded by the *Arabidopsis* genome,

as the primary DRB protein required for the production of both the conserved and non-conserved miRNA species in *Arabidopsis*. In addition, this large alteration to the appropriate miRNA landscape of *Arabidopsis* in the *drb1* mutant may have potentially underpinned the highly interesting observation that anthocyanin accumulation was lost in this mutant background (**Figure 2.6**; discussed in **Section 2.5.3**). Loss of DRB4 function also had a significant impact on the global *Arabidopsis* miRNA landscape. Specifically, the accumulation of 48 miRNAs was reduced in the *drb4* mutant background, with 31 of these miRNAs only reduced in the absence of DRB4 activity. In addition, all 31 of these ‘DRB4-dependent’ miRNAs are classed as non-conserved *Arabidopsis* miRNAs (classified according to Axtell and Meyers, 2018). Therefore, this finding identified DRB4 as the primary DRB protein family member responsible for the production of non-conserved miRNAs in 15 d old *Arabidopsis* seedlings. In addition to the identification of the requirement of DRB1 and DRB4 for the production of conserved and non-conserved miRNAs respectively, the requirement of all three nucleus localised DRB proteins for the appropriate regulation of miRNA regulatory modules was demonstrated via the RT-qPCR-based analyses presented in **Section 3.4.1** and **Publication 4 (Appendix A.1.4)**. Specifically, the loss of DRB1, DRB2 or DRB4 activity resulted in altered miR396 and miR399 regulatory module behaviour when these *Arabidopsis* lines were cultivated in the absence of phosphate. Taken together, the data stemming from this research thesis readily highlights; (1) the high degree of synergistic and/or antagonistic functional interplay between DRB1, DRB2 and DRB4 in the production stage of the *Arabidopsis* miRNA pathway, and; (2) the necessity of this hierarchical order of DRB protein function for the generation of the miRNA landscape of wild-type *Arabidopsis* seedlings under both normal growth conditions and when *Arabidopsis* is exposed to the abiotic stresses of elevated temperature, mannitol, P deficiency and salinity.

5.1.3 Characterisation of the *Arabidopsis* miR396 Regulatory Module

Previous studies have identified miR396 and its targeted genes, members of the GRF family of plant specific transcription factors, to play a key role in the growth and development of *Arabidopsis*, in addition to modulating the response of *Arabidopsis* to heat, osmotic and salt stress (Hewezi and Baum, 2012; Kim *et al.*, 2012; Liu *et al.*, 2009; Omidbakhshfard *et al.*, 2015 Sakuma *et al.*, 2006; Yamaguchi-Shinozaki and Shinozaki, 2006). The data presented here in this research thesis further revealed that when miR396 is molecularly reduced in the Col-0 background via a miRNA target mimicry approach, the growth of this plant line, *MIM396* plants, was promoted when cultivated in control conditions (**Figure 3.4-3.5**). Further, post a 7 d period of exposure to either a P deficient or salt stress environment, *MIM396* plants were determined

to be less sensitive to these two altered growth environments than non-modified Col-0 seedlings of the same age for the majority of the phenotypic and physiological assessments conducted (**Figure 3.3-3.8**). To date, and to the best of my knowledge, no study has previously identified the *Arabidopsis* miR396 regulatory module as responsive to phosphate deficiency. Molecular characterisation of miR396 abundance, and the expression its targeted genes, including *GRF1*, *GRF2*, *GRF3*, *GRF7*, *GRF8* and *GRF9*, in *MIM396* plants tentatively suggested that, elevation of the positive regulators of *Arabidopsis* growth, namely *GRF1*, *GRF2* and *GRF3*, in conjunction with reduced expression of the negative abiotic stress response regulator, *GRF7*, was potentially responsible for the elevated tolerance displayed by *MIM396* plants to growth in either a P deficient or saline environment (**Figure 3.9**). Due to the varied expression responses of the miR396 target genes, *GRF8* and *GRF9*, to P⁻ and salt stress respectively, this study also revealed that further characterisation of the role that these two plant specific transcription factors mediate in the response of *Arabidopsis* to abiotic stress is required in the near future to further advance our currently understanding of the global role that this miRNA regulatory modules plays both in *Arabidopsis* growth and development, and in the response of *Arabidopsis* to abiotic stress.

5.1.4 Characterisation of the *Arabidopsis* miR399 Regulatory Module

While it is well established that the miR399 regulatory module is central to the response of plants to P deficiency, the results presented here (**Figure 2.10**) revealed that the *Arabidopsis* miR399 regulatory module is also responsive to conditions of heat, mannitol and salt stress. To further characterise the role of the miR399 regulatory module in the adaptative response of *Arabidopsis* to P⁻ and salt stress conditions, miR399 knockdown (*MIM399*) and overexpression (*MIR399*) plant expression vectors were introduced into the Col-0 background via *Agrobacterium*-mediated transformation. This approach revealed that under non-stressed conditions, shoot architecture of *MIM399* plants was mildly promoted compared to their wild-type counterparts. In *MIR399* plants however, shoot architecture was clearly compromised (**Figure 4.2-4.4**). Further, when collectively considering the phenotypic and physiological assessments of plant lines with molecularly altered miR399 abundance, in response to both P⁻ and salt stress growth regimes, *MIM399* plants were determined to display a higher degree of tolerance to both stress treatments than did either wild-type *Arabidopsis* plants or the *MIR399* line (**Figure 4.2- 4.7**). It is speculated that the observed reduction in *PHO2* abundance in *MIM399* plants was likely resulting in unregulated *PHO1* and/or *PHT1* mediated Pi translocation to the shoot tissue of this plant line (Hamburger *et al.*, 2002; Huang *et al.*, 2013; Poirier *et al.*, 1991). Pi is one of the central molecular building blocks for cellular processes

such as photosynthesis and cell growth, therefore; an abundance of Pi in *MIM399* plants would allow for such processes to continue during period of stress. While the molecular manipulation of the miR399 regulatory module in *MIM399* plants appeared to have a positive impact on *Arabidopsis* growth and development, it was readily apparent that the manipulation of the same miRNA regulatory module in *MIR399* plants, had a negative impact on plant development. This finding is largely attributed to; (1) toxic Pi accumulation which has been shown to occur in *Arabidopsis* plants molecularly modified to overexpress the miR399 sRNA, or which lack the functional activity of PHO2 (Aung *et al.*, 2006), and; (2) toxic accumulation of Na⁺ and Cl⁻ ions shown to cause the detrimental phenotypic effects associated with plant growth in a saline environment (Munns, 2002; Tester and Davenport, 2003).

5.2 Future Directions

5.2.1 ***Selection of Heat, Mannitol and Salt Responsive MicroRNAs for Further Characterisation***

This study used a transformation approach to further characterise two *Arabidopsis* miRNAs via their *in planta* molecular manipulation. The miRNAs, miR396 and miR399, were selected out of a total of 179 miRNAs identified to be responsive to the abiotic stresses of heat, mannitol and/or salt stress (**Chapter II-IV**). The miRNA dataset generated in this study provides an extensive source of reference for the selection of additional candidate abiotic stress responsive miRNAs for their future functional characterisation studies via a similar molecular manipulation approach. Further to this point, during the duration of this research thesis, miR408 knockdown and overexpression plant expression vectors were generated and transformed into the Col-0 background. While T₃ transformant lines were obtained, the phenotypic, physiological and molecular characterisation of these molecularly altered miR408 plant lines under non-stressed and abiotic stress conditions remains an avenue of high interest for future research with project time constraints unfortunately prohibiting the completion of these analyses as part of this study.

5.2.2 ***Western Blot Analysis to Demonstrate Translational Repression as a Mechanism of Regulation of miRNA Target Gene Expression***

While the predominant mode of miRNA-directed target gene expression regulation in plants is via a mRNA cleavage mode of RNA silencing, current research is continuing to indicate that translational repression also forms an important mode of miRNA target gene

expression regulation (Eamens *et al.*, 2012a; Eamens *et al.*, 2012b; Li *et al.*, 2013; Reis *et al.*, 2015). When RT-qPCR analysis is used to profile a miRNA regulatory module where the mRNA cleavage mechanism of RNA silencing forms the predominant mode of target gene expression regulation, miRNA and target gene abundance will show an opposing trend to one another. More specifically, if miRNA abundance is elevated in response to an abiotic stress, target gene expression will be expected to be reduced due to enhanced target transcript cleavage by miRISC. However, when RT-qPCR assessment reveals that the abundance of both assessed transcripts trends in the same direction, translational repression is suspected to form the predominant mode of miRNA target gene expression regulation. Such a profile is presented in thesis figures, **Figure 2.12-2.14, 3.9 and 4.8**, a finding that suggests that a translational repression mode of target gene expression regulation was being directed by the miRNA(s) driving the observed expression changes in these regulatory modules. To provide more comprehensive evidence that miRNA-directed translational repression is playing a role in target gene expression regulation in the assessed regulatory module(s), a western blot hybridisation approach using target gene specific antibodies is required to further advance the molecular characterisation of the module. Further, comparison of the western blotting results to those obtained by RT-qPCR for a given miRNA regulatory module would also allowed for the distinction of miRNA-directed translational repression from both the miRNA encoding gene (the *MIR gene*) and the miRNA target gene, responding similarly to the imposed stress.

Appendix 1

Publications

A.1 Publications

A.1.1 *Publication One*



Chapter 2

The Plant microRNA Pathway: The Production and Action Stages

Joseph L. Pegler, Christopher P. L. Grof, and Andrew L. Eamens

Abstract

Plant microRNAs are an endogenous class of small regulatory RNA central to the posttranscriptional regulation of gene expression in plant development and environmental stress adaptation or in response to pathogen challenge. The plant microRNA pathway is readily separated into two distinct stages: (1) the *production stage*, which is localized to the plant cell nucleus and where the microRNA small RNA is processed from a double-stranded RNA precursor transcript, and (2) the *action stage*, which is localized to the plant cell cytoplasm and where the mature microRNA small RNA is loaded into an effector complex and is used by the complex as a sequence specificity guide to direct expression repression of target genes harboring highly complementary microRNA target sequences. Historical research indicated that the plant microRNA pathway was a highly structured, almost linear pathway requiring a small set of core machinery proteins. However, contemporary research has demonstrated that the plant microRNA pathway is highly dynamic, and to allow for this flexibility, a large and highly functionally diverse set of machinery proteins is now known to be required. For example, recent research has shown that plant microRNAs can regulate target gene expression via a translational repression mechanism of RNA silencing in addition to the standard messenger RNA cleavage-based mechanism of RNA silencing: a mode of RNA silencing originally assigned to all plant microRNAs. Using *Arabidopsis thaliana* as our model system, here we report on both the *core* and *auxiliary* sets of machinery proteins now known to be required for both microRNA production and microRNA action in plants.

Key words *Arabidopsis thaliana*, microRNA, microRNA pathway, microRNA production, microRNA action, RNA silencing, Gene expression regulation, Core machinery protein, Auxiliary machinery protein

1 Introduction

microRNAs (miRNAs), small regulatory RNAs 21 to 24 nucleotides (21–24 nts) in length, were first reported in the genetic model plant species *Arabidopsis thaliana* by David Bartel's group in 2002 [1]. Since this initial report, and especially in recent years with the advent and widespread application of high-throughput sequencing technology, miRNAs have now been documented across the plant kingdom, including the agronomically important species, rice

(*Oryza sativa* [2]), wheat (*Triticum aestivum* [3]), maize (*Zea mays* [4]), potato (*Solanum tuberosum* [5]), and sugarcane (*Saccharum officinarum* [6]). In the Bartel group's initial report on plant miRNAs, the authors went on to further reveal that 8 of the 16 miRNAs originally cloned from *Arabidopsis thaliana* were perfectly conserved across the length of the mature miRNA small RNA (sRNA) sequence in rice [1]. Absolute conservation at the miRNA sRNA level, and across the dicotyledonous/monocotyledonous evolutionary divide, immediately identified miRNAs as directing highly important roles within plants, roles likely essential for plant survival. Indeed, miRNA-directed gene expression regulation has now been demonstrated central to all aspects of vegetative and reproductive development in plants [7–10]. The essential requirement for miRNA-directed gene expression regulation in plant development is most effectively demonstrated by the severe to embryo-lethal phenotypes, displayed by the *Arabidopsis thaliana* plant lines defective in the activity of the core machinery proteins of the miRNA pathway, including the *se*, *dcl1*, *hyl1* (*drb1*), *hen1*, *hst*, and *ago1* knockout mutants [11–14]. Recent research has further demonstrated that in addition to directing central roles in plant development, miRNA-directed gene expression regulation is also essential for a plant to effectively mount either a defense response against invading bacterial, viral, or fungal pathogens [15–17] or an adaptive response to environmental challenges, including adaptation to the abiotic stresses, salt, extreme temperature (chilling or heat), and drought or the maintenance of viable growth in a nutrient-deficient environment [18–21].

Plant *MICRORNA* (*MIR*) genes have evolved, with many still actively evolving, in parallel to the protein-coding gene(s) that is under expression regulation by the mature miRNA [22, 23]. Plant *MIR* genes can therefore be grouped into one of the two classes: (1) *conserved miRNAs*, miRNAs isolated from unrelated species across the plant kingdom, and (2) *non-conserved miRNAs*, miRNAs only found in a smaller and usually more closely related group of plant species (*note*: this *grouping* of plant species can be at the genus, family, order, or even class taxonomy level). Due to the non-conserved class of miRNA being limited to a smaller population of plant species, or from a plant species that is actively evolving (which most are), this class of miRNA has also been referred to as *young*, *newly evolved* or *species-specific*. Further, the widespread application of high-throughput sequencing technology to the field of plant miRNA research has resulted in the identification of new members that putatively belong to the non-conserved class of miRNA, with this exercise now being the most frequently reported finding in the field. However, the historical mechanistic discoveries made on the plant miRNA pathway were limited to the conserved class of miRNA and to *Arabidopsis thaliana* [11–14]. Today (February, 2018), entering the search term *Ath* into the search

engine of miRBase, the miRNA database (<http://www.mirbase.org>), limits the database search parameters to *Arabidopsis thaliana* miRNAs only and retrieves 760 unique results. Of these, 325 database entries return a precursor transcript sequence in addition to the mature miRNA sRNA sequence; 427 database entries only match to a mature miRNA sRNA sequence, and the remaining 8 entries are now classed as *dead* entries (*note*: all 8 dead *Ath* entries remain in the database but have been assigned new naming nomenclature). The identification of a precursor transcript sequence from which the miRNA sRNA is potentially liberated from by the core machinery proteins of the miRNA pathway is a strong indication that a *real* or *bona fide* miRNA has been bioinformatically discovered and entered into the miRBase database. However, all new entries deposited into miRBase require experimental validation to confirm their: (1) genomic origin (including identification of the precursor transcript sequence of the miRNA and the *MIR* gene from which the precursor transcript is transcribed) and (2) the mechanism of RNA silencing directed by the newly identified miRNA to regulate target gene expression.

Using *Arabidopsis thaliana* as our model, the plant miRNA pathway can be divided into two distinct stages, stages that can be readily separated from one another as each stage of the pathway occurs in a different compartment of the cell. The first stage of the miRNA pathway, the *production stage* (Fig. 1), occurs in specialized processing bodies in the plant cell nucleus, and it is in these nuclear Dicing bodies (D-bodies) where miRNA precursor transcripts are sequentially processed to produce the mature miRNA sRNA. Upon maturation, the miRNA sRNA is exported from the nucleus to the cytoplasm of the plant cell. In the cytoplasm, the miRNA enters the second stage of the miRNA pathway, the *action stage* (Fig. 2), and is loaded into the miRNA-induced silencing complex (miRISC). miRISC uses the loaded miRNA as a sequence specificity guide to direct expression regulation almost exclusively at the posttranscriptional level of miRNA target genes, protein-coding transcripts that harbor a highly complementary target sequence to each miRNA [11–14]. Here, we detail our current knowledge on the *production* and *action* stages of the plant miRNA pathway based on the research findings stemming from the genetic model plant species, *Arabidopsis thaliana* (*Arabidopsis*).

2 The Production Stage of the Plant microRNA Pathway

2.1 The Role of Core Protein Machinery

Most plant miRNAs originate from a *MIR* gene, and the DNA sequence-based features of the *MIR* gene body are identical to those of the body of a protein-coding gene, namely, a promoter and terminator region, separated by a stretch of DNA sequence that encodes for a transcription product. For *MIR* genes, the

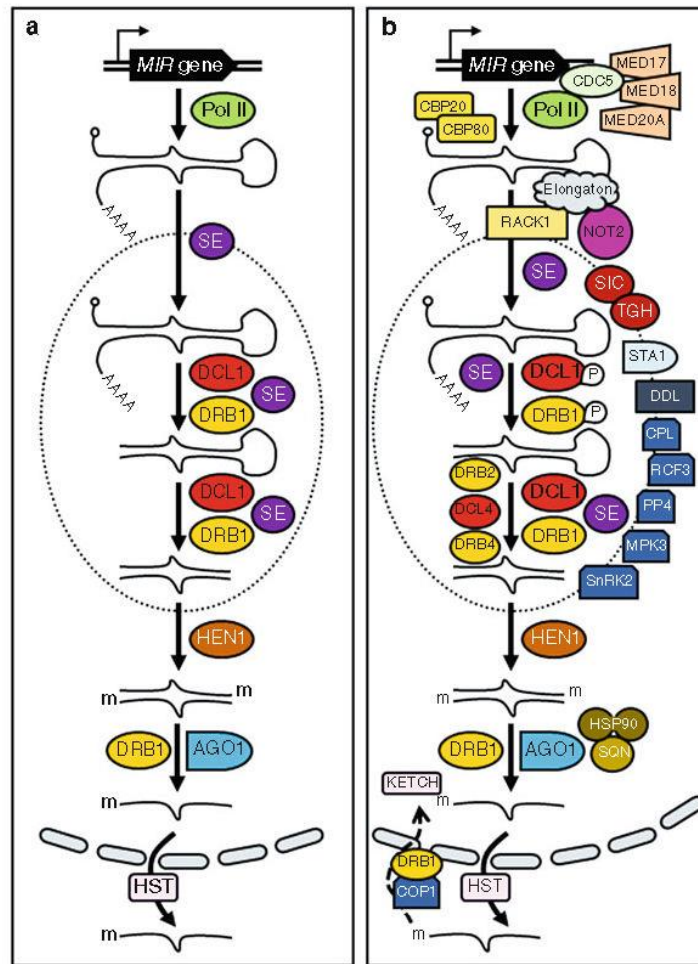


Fig. 1 The core and auxiliary machinery proteins of the production stage of the plant microRNA pathway. **(a)** *MIR* genes are used as transcription templates by Pol II to transcribe a nonprotein-coding RNA transcript that folds back onto itself to form the pri-miRNA. The pri-miRNA is bound by SE and transported to nuclear D-bodies (black dashed oval), and the pri-miRNA is processed by the DCL1/DRB1 functional partnership to generate the pre-miRNA and subsequently the miRNA/miRNA* duplex, via a two-step cleavage mechanism. HEN1 methylates the 3' terminus of each duplex strand, and DRB1 orientates the duplex for miRNA* passenger strand removal by AGO1. The mature miRNA sRNA is then exported out of the nucleus to cytoplasm by HST. **(b)** MED17, MED18, MED20A, Elongator, NOT2, and CDC5 are required by Pol II for efficient transcription initiation and elongation of pri-miRNA transcripts from *MIR* gene loci. The cap-binding proteins, CBP20 and CBP80, interact with SE and NOT2, and the scaffolding protein, RACK1, also interacts with Dicing complex component, SE. These interactions potentially link *MIR* gene transcription with pri-miRNA processing in D-bodies. CPL, RCF3, MPK3, SnRK2, and PP4 are all involved in the phosphoregulation of DRB1 activity in the plant cell nucleus. DRB1 is under

transcribed product is a non-protein-coding RNA transcript: such transcripts do not harbor start or stop codons for subsequent use as translation templates. However, the presence of a promoter region upstream of the DNA sequence used as the transcription template results in plant *MIR* genes being transcribed by DNA-dependent RNA polymerase II (Pol II), the same RNA polymerase responsible for transcription of protein-coding genes in plants [24, 25]. Transcription of the initial non-protein-coding RNA from a *MIR* gene, termed the primary miRNA (pri-miRNA) transcript, by Pol II identifies the nascent transcript for modification. Pri-miRNA modification includes the addition of a 7-methylguanosine capping structure at the 5' terminus (5' cap) and a polyadenylated tail (poly(A) tail) at the 3' terminus of the transcript. Further, some pri-miRNA transcripts harbor introns in addition to the 5' cap and 3' poly(A) tail, identifying these precursors for additional modification via intron splicing [26–29].

All pri-miRNAs contain a region of sequence partial self-complementarity, and it is this region that allows the transcript to fold back onto itself to form a stem-loop structured, imperfectly double-stranded RNA (dsRNA). Post pri-miRNA folding, serrate (SE), a zinc-finger protein with RNA-binding activity, binds the folded pri-miRNA and transports the precursor to D-bodies in the plant cell nucleus [13, 30]. Dicing bodies contain the miRNA precursor transcript Dicing complex, a protein complex containing DICER-LIKE1 (DCL1) and DOUBLE-STRANDED BINDING1 (DRB1) in addition to SE at its functional core [31, 32]. *Arabidopsis* encodes four DCLs, DCL1 to DCL4, with DCL1 almost the exclusive DCL required for miRNA precursor transcript processing [33, 34]. The *Dicing* domains of DCL1, RNaseIIIa and RNaseIIIb, sit exactly 21 nts away from each other on DCL1 dsRNA substrates, and accordingly, almost all *Arabidopsis* miRNA sRNAs are 21 nts in length upon maturity. The DCL1 protein also encodes tandem dsRNA-binding domains that enable DCL1 to bind and

Fig. 1 (continued) additional phosphoregulation in the plant cell cytoplasm by COP1, and the DRB1 protein is stabilized via its importation into the nucleus, a process that requires KETCH. SIC and TGH are also involved in the regulation of DRB1 activity at the posttranslational level in the plant cell nucleus. Like DRB1, DCL1 activity is regulated posttranslationally by auxiliary machinery proteins, STA1 and DDL. Interaction with HSP90 and SQN is required by AGO1 to mediate the role of AGO1 in miRNA guide strand maturation via cleavage-mediated removal of the corresponding duplex strand, the miRNA* passenger strand. In specific tissues, a smaller cohort of conserved *Arabidopsis* miRNAs require DRB2 (presumably functioning together with DCL1) for their production, and not the canonical DRB1/DCL1 functional partnership. The DRB4/DCL4 functional partnership is required for the processing of the structurally distinct precursor transcripts of non-conserved miRNAs

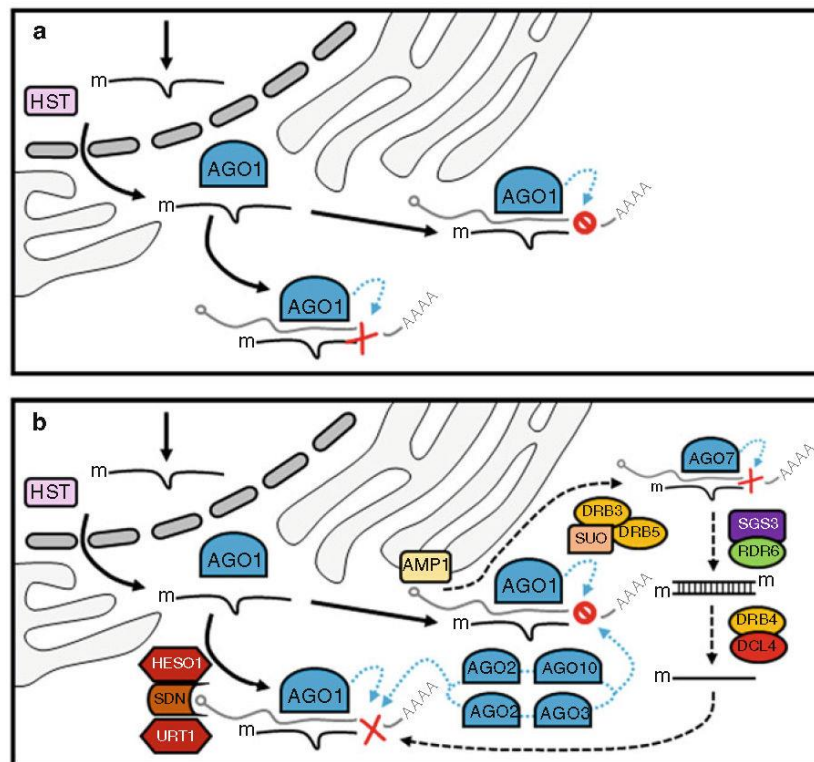


Fig. 2 The core and auxiliary machinery proteins of the action stage of the plant microRNA pathway. **(a)** Post maturation in the plant cell nucleus and exported to the cytoplasm, the mature miRNA sRNA is loaded by AGO1 to form miRISC. miRISC uses the loaded miRNA as a sequence specificity determinant to guide microRNA-directed RNA silencing of target gene expression via either a mRNA cleavage mode of RNA silencing (red-colored cross symbol) or a translational repression mechanism of RNA silencing (red color no symbol). **(b)** AMP1, SUO, DRB3, and DRB5 have all been assigned roles associated with AGO1-mediated translational repression. AGO proteins, AGO2, AGO3, AGO5, and AGO10, have also been identified as putative effectors of miRNA-directed RNA silencing via either a target gene mRNA cleavage or translational repression mode of RNA silencing (light blue-colored and dashed arrows). AGO7 selectively loads miR390 to target the *TAS3* transcript, and miR390-directed, AGO7-mediated cleavage of *TAS3* triggers dsRNA synthesis by RDR6/SGS3. The resulting dsRNA is processed by DCL4/DRB4, and the resulting *TAS3*-derived siRNAs are loaded by AGO1 to direct target gene expression repression in *trans*. The activity of each miRNA sRNA is further regulated by uridylation by the nucleotidyl transferases, HESO1 and URT1, or via degradation by SDNs, SDN1 to SDN3

process miRNA precursors. However, the accuracy (*cleavage position*) and efficiency (*rate of cleavage*) of DCL1-catalyzed processing of miRNA precursors is greatly enhanced in the presence of the Dicing complex core machinery proteins, SE and DRB1 [31, 35].

The processing of miRNA precursor transcripts by DCL1/DRB1/SE to generate a mature miRNA sRNA is a two-step process. The first cleavage event removes the unpaired (non-dsRNA) regions of the pri-miRNA to produce the smaller-sized processing intermediate, the precursor miRNA (pre-miRNA). The pre-

miRNA is further processed by DCLI/DRB1/SE to remove the majority of the dsRNA arms of the stem and the loop region of the pre-miRNA stem-loop, and this second cleavage event liberates the much smaller-sized dsRNA molecule, the miRNA/miRNA* duplex [36, 37]. Alternate and detailed models outlining the exact position of DCLI-catalyzed cleavage, as well as the order of precursor transcript processing events, have been reported [38–40]; however, these alternate processing models have the same outcome: liberation of the miRNA/miRNA* duplex from the pri-miRNA and pre-miRNA precursor transcripts. Due to the action of DCLI-catalyzed cleavage, a 2 nt overhang remains at the 3' terminus of both the guide (miRNA) and passenger (miRNA*) strand of the miRNA duplex, and it is this feature that is modified by the sRNA-specific methyltransferase, HUA ENHANCER1 (HEN1) [11, 41]. Specifically, HEN1 modifies the 3' terminal nucleotide of each duplex strand via 2'-O-methylation. Modification of the 3' terminal nucleotide of all sRNA species that accumulate in a plant cell is exceptionally important. Once the duplex strands are separated from one another, the now single-stranded sRNA must be readily distinguishable from other RNA species of a similar size, such as mRNA degradation products. Therefore, HEN1-directed methylation of plant sRNAs ensures that the mature sRNA is *not* cleared from the plant cell prior to being loaded by a RNA silencing effector complex [11, 16]. Further, *in vitro* studies have also indicated putative protein-protein interactions between HEN1 and Dicing complex proteins, DCLI and DRB1 [42]. Such interactions would facilitate close linkage between pri-miRNA and pre-miRNA processing and miRNA duplex strand modification prior to the two strands of the duplex being separated from one another.

The mechanism responsible for the separation of the two strands of the miRNA duplex post strand modification by HEN1 is a long-standing question of the *Arabidopsis* miRNA pathway. However, the localization of ARGONAUTE1 (AGO1), the catalytic core of miRISC, to the nucleus and cytoplasm of *Arabidopsis* cells [27, 43] strongly implicated the involvement of AGO1 in this process. We favor the model put forward to the *Arabidopsis* miRNA research community by Iki and colleagues (2010), a model based on their elegant *in vitro* characterization of miRISC assembly [44]. Specifically, the molecular chaperone, HEAT SHOCK PROTEIN90 (HSP90), forms a dimer and next complexes with AGO1. Once the AGO1/HSP90 complex forms, chemical energy in the form of adenosine triphosphate (ATP) is bound by HSP90 to promote a conformational change to AGO1, and this in turn facilitates the incorporation of the miRNA/miRNA* duplex into AGO1. HSP90 hydrolyses ATP, and this reaction drives the dissociation of AGO1 from the molecular chaperone and to undergo a second conformational change. It is the dissociation of AGO1 from

HSP90 and the associated conformational change to the AGO1 protein that induces the *slicer* activity of AGO1 to act upon the miRNA* passenger strand of the loaded duplex. Removal of the miRNA* strand from the miRNA guide strand, and from miRNA-loaded AGO1, results in the formation of a mature and functional miRISC [44]. Adding further weight to this nucleus-localized model is the demonstration that in addition to ensuring DCL1-catalyzed cleavage accuracy and efficiency, DRBI also directs the preferential selection and loading of the miRNA guide strand over the miRNA* passenger strand into miRISC [45]. This is achieved via orientating the miRNA duplex loading into AGO1 (miRISC) based on the thermodynamic stability at the 5' terminus of each duplex strand [45]. Furthermore, most plant miRNA guide strands harbor a uracil (U) residue at their 5' terminus, whereas the corresponding miRNA* strands of these miRNAs commonly have either an adenosine (A) or cytosine (C) residue at this position. *Arabidopsis* AGO1 has been shown to preferentially load sRNAs with a 5' U, and *Arabidopsis* AGO2 and AGO5 also show preferential loading of sRNAs based on the 5' terminal nucleotide. AGO2 loads sRNAs with a 5' A residue, and AGO5 preferentially interacts with sRNA sequences that harbor a C residue at the 5' terminal position. Based on these sRNA loading preferences, it was not surprising that AGO pull-down experiments, and the subsequent profiling of the AGO-loaded sRNAs, revealed preferential loading of miRNA guide strands by AGO1 and miRNA* strands with 5' terminal A and C residues among the sRNAs loaded by AGO2 and AGO5, respectively [46, 47].

Export of the mature miRNA, either *naked* or complexed with a protein(s), from the nucleus to the cytoplasm is an essential requirement for the second stage of the *Arabidopsis* miRNA pathway, the *action stage*. HASTY (HST) is the *Arabidopsis* orthologue of the animal RanGTP-dependent dsRNA-binding protein, Exportin-5, and in *Arabidopsis hst* mutants, the accumulation of individual miRNAs is affected to different degrees [11, 48]. The authors also elegantly demonstrated that in the nucleus of *Arabidopsis* cells, miRNAs accumulate in their mature single-stranded form, a finding that adds further weight to the model that all steps in the production stage of the *Arabidopsis* miRNA pathway occur in the nucleus. The Park et al. (2005) report also revealed that the abundance of each assessed miRNA was higher in the cytoplasm than in the nucleus of wild-type plants, a trend also observed in the *hst* background, that is, although miRNA levels were reduced in *hst* plants, the miRNA abundance ratio remained unchanged in the analyzed nuclear/cytoplasmic fractions [11]. It does remain curious though as to why AGO1 would release its miRNA guide strand cargo in the nucleus only to reload the same miRNA cargo in the cytoplasm once the mature miRNA sRNAs are exported out of the nucleus via a HST-mediated mechanism of transport. However, HSP90 has

also been shown to be required for miRISC loading in the *Arabidopsis* cell cytoplasm in addition to the characterized role for HSP90-mediated loading of miRNA/miRNA* duplexes and subsequent miRNA guide strand selection by AGO1 in the nucleus [44]. A similar role has also been documented for SQUINT (SQN), the *Arabidopsis* orthologue of the animal cyclophilin 40 (Cyp40) protein. *Arabidopsis* SQN has been shown to interact with HSP90 and to influence AGO1 activity during miRNA guide strand selection and loading into miRISC as part of miRISC formation [49, 50]. Taken together, (1) the nucleus-localized, HSP90/AGO1 mature miRNA guide strand selection model proposed by Iki et al. (2010); (2) the identification of single-stranded mature miRNAs in the *Arabidopsis* nucleus and the differential effect that loss of HST function has on the abundance of individual miRNAs [11]; and (3) the involvement of cytoplasmic HSP90 (and SQN) in miRISC loading in the cytoplasm [49, 50] strongly indicate that detailed functional knowledge on the exact role that HST plays in the *Arabidopsis* miRNA pathway is still lacking. Further experimental characterization of the nucleus export step of the *Arabidopsis* miRNA pathway should be a high priority item considering that this step is the transition point in the pathway, with the now mature miRNA exiting the *production stage* (localized to the nucleus) and entering the *action stage* (almost exclusive to the cytoplasm of the cell) of the miRNA pathway.

2.2 The Role of Auxiliary Protein Machinery

Since the initial report on *Arabidopsis* miRNAs [1] and the functional characterization of the specific roles played by core machinery proteins of the miRNA pathway, including SE, DCLI, DRB1, HEN1, AGO1, and HST, research into the pathway has continued to identify additional machinery proteins required for the production of all, or only a specific cohort of miRNAs. The general transcription activators, MEDIATOR17 (MED17), MED18, and MED20A, are required by Pol II to initiate *MIR* gene transcription via recruiting Pol II to *MIR* gene loci [51]. In addition to the MED proteins, the Elongator complex, NEGATIVE ON TATA LESS2 (NOT2), and the DNA-binding protein, CELL DIVISION CYCLE5 (CDC5), are also required for efficient transcription initiation and elongation of the non-protein-coding RNAs transcribed from *MIR* gene loci [27, 52, 53]. Further to interacting with Pol II and specific components of the Elongator complex, the NOT2 and CDC5 proteins have been shown to also interact with components of the pri-miRNA Dicing complex, such as DCLI, an interaction that likely couples *MIR* gene transcription to pri-miRNA transcript processing in the nucleus [27, 52, 53]. The nuclear cap-binding complex (CBC) interacts with the 5' capping structure post cap addition to all de novo transcripts transcribed by Pol II, and the CBC components, CAP BINDING PROTEIN20 (CBP20) and CBP80, have also been shown to interact with Dicing

complex component, SE, and with NOT2 [26, 52]. The exact mechanism of how CBP20 and CBP80 interact with SE and NOT2 remains unclear. However, one can confidently assume that these interactions promote (1) miRNA precursor transcript stability and (2) the coupling of *MIR* gene transcription to pri-miRNA transcript processing. RACK1 (RECEPTOR FOR ACTIVATED C KINASE1) has also been shown to interact with miRNA Dicing complex components, specifically interaction with SE [54, 55]. In animals and nematodes, RACK1 acts as a scaffolding protein by promoting interaction between each of the proteins that need to come together to form a functional complex [54, 55]. *Arabidopsis* RACK1 can conceivably mediate a similar scaffolding role in the formation or positioning of Dicing complex components via promoting interaction between complex components, including SE, DCL1, and DRB1.

A wealth of work has further uncovered a diverse array of transcription factors involved in regulating the expression of specific *MIR* genes. Interestingly, many of the transcription factors associated with regulating *MIR* gene transcription are themselves known miRNA target genes [56–58]. For example, the *Arabidopsis* *SQUAMOSA PROMOTER BINDING PROTEIN-LIKE9* (*SPL9*) transcript harbors a miR156 target site and is therefore one member of a small clade of *SPL* transcription factor genes targeted by the miR156 sRNA for expression regulation. As *Arabidopsis* transitions from the juvenile to adult phase of vegetative development, miR156 abundance decreases, and therefore, miR156-directed repression of *SPL9* gene expression is released. Elevated *SPL9* abundance, together with *SPL10*, promotes pri-miRNA transcription from the *MIR172B* locus, and post processing of the *PRI-MIR172B* and *PRE-MIR172B* precursor transcripts, the now abundant miR172 sRNA reduces the level of the floral repressor, *APETALA2* (*AP2*). A reduction in *AP2* abundance allows *Arabidopsis* to make the transition from vegetative to reproductive development [56–58]. This is just one of the many elegant examples of the complexity of miRNA-directed gene expression cascades and/or regulatory modules central to *Arabidopsis* development.

The core machinery proteins, SE, DCL1, and AGO1, are all under additional regulation at the posttranscriptional level with the *SE*, *DCL1*, and *AGO1* transcripts harboring target sites for the miR863, miR162, and miR168 sRNAs, respectively. To date, no *Arabidopsis* miRNA, or another sRNA species, has been identified that could potentially regulate *DRB1* transcript abundance. However, the *DRB1* protein is under considerable regulation at the posttranslational level. *DRB1* requires dephosphorylation for activation, and C-TERMINAL DOMAIN PHOSPHATASE-LIKE (CPL)-mediated dephosphorylation of *DRB1* enhances both (1) the cleavage accuracy of DCL1-catalyzed processing of pri-miRNA and pre-miRNA precursors and (2) the efficiency of miRNA guide

strand selection and loading into AGO1 [59]. REGULATOR OF CBF GENE EXPRESSION3 (RCF3) also promotes DRB1 dephosphorylation; however, the action of RCF3 on DRB1 is indirect via RCF3 interacting with CPL [60]. MITOGEN-ACTIVATED PROTEIN KINASE3 (MPK3) and the protein, SNF1-related protein kinase subfamily2 (SnRK2), further influence DRB1 functionality via antagonizing the dephosphorylation activity of PROTEIN PHOSPHATASE4 (PP4) on DRB1 [61–63]. The stability of the DRB1 protein is also influenced by diurnal rhythm. Specifically, during the day, CONSTITUTIVE PHOTOMORPHOGENIC1 (COPI) localizes to the cytoplasm of the cell and inhibits the cleavage-based degradation of DRB1 by an unknown protease. At night however, COPI is imported into the nucleus, allowing protease-mediated cleavage of DRB1 to again occur [64]. The stability of the DRB1 protein is further enhanced via the nuclear importation of DRB1 following its translation in the cytoplasm by the β class importin protein, KARYOPHERIN ENABLING THE TRANSPORT OF THE CYTOPLASMIC HYL1 (KETCH1) [65]. The proline-rich protein, SICKLE (SIC), and the RNA-binding protein TOUGH (TGH), further regulate the involvement of DRB1 in the miRNA pathway. In the nucleus, SIC co-localizes with DRB1, and in *Arabidopsis* sic mutants, mature miRNA accumulation is reduced, and abnormal splice variants of many pri-miRNA and pre-mRNA transcripts are observed [66]. Via interaction with the DCLI/DRB1/SE complex, TGH promotes the interaction between DRB1 and its pri-miRNA substrates, thus indirectly influencing the accuracy and efficiency of DCLI-catalyzed processing of miRNA precursor transcripts [67].

In addition to miR162-directed regulation of the *DCLI* transcript, DCLI appears further regulated at the posttranslational level, potentially by the action of the pre-messenger RNA (pre-mRNA) processing factor, STABILIZED1 (STAI) [68]. A subpopulation of *Arabidopsis* pri-miRNAs transcripts house introns; therefore, a direct role for STAI in processing this cohort of miRNA precursor transcripts is readily apparent. However, the involvement of STAI in the miRNA pathway may not be limited to miRNAs that originate from pri-miRNA precursors harboring introns. In the *Arabidopsis* *sta1* mutant, *DCLI* transcript abundance is reduced (while interestingly, *DRB1*, *SE*, *HEN1*, and *HST1* transcript abundance remains at approximate wild-type levels), and this reduction in *DCLI* levels (and presumably DCLI protein abundance) results in the reduced accumulation of many miRNA sRNAs [68]. This finding infers that STAI may play a much broader role in the *production stage* of the miRNA pathway than it was initially assigned due to the influence the STAI protein has on the abundance (and/or stability) of the *DCLI* transcript. In addition to STAI, the forkhead-associated (FHA) domain protein, DWADLE (DDL) interacts with DCLI via its FHA domain, and this DCLI-

DDL interaction is thought to be mediated by DCLI phosphorylation. Namely, the loss of DCLI phosphorylation is demonstrated to abolish the DCLI-DDL interaction [69]. Curiously, both pri-miRNA abundance and miRNA accumulation are reduced in *Arabidopsis ddl* mutants, and this reduction is observed in the absence of any notable alteration to *MIR* gene promoter activity (i.e., the rate of *MIR* gene expression remains unchanged) [69]. Together, these observations indicate additional detailed experimental analyses are required to confidently state the exact mechanism(s) by which DDL influences DCLI activity and therefore the miRNA pathway in general.

A small number of *Arabidopsis* miRNAs, including miR822, miR839, miR840, and miR869, are processed from structurally distinct precursor transcripts [45, 70]. Such precursors have high levels of complementarity between the nucleotides of the 5' and 3' arms of the stem region of the stem-loop. Therefore, post precursor transcript folding, extensive base pairing between the two stem-loop arms occurs. This class of precursor also tends to have small-sized loops, composed of a small number of unpaired nucleotides, separating the two highly complementary arms of the stem-loop. Due to their unique structure, this group of *Arabidopsis young* or *newly evolved* miRNA precursors are bound by DRB4, and not by DRB1, thus leading to their processing by the functional partner of DRB4, DCL4 [45, 70, 71]. It is likely however, that apart from the involvement of the DRB4/DCL4 functional partnership for the processing of these uniquely structured precursor stem-loops, the remaining core machinery proteins of the miRNA pathway, including SE, HEN1, AGO1, and HST, are required for all of the other remaining aspects of the production of this class of miRNA sRNA. In addition to DRB4, DRB2 also appears required for the production of this small group of non-conserved *Arabidopsis* miRNAs [70]. However, whether DRB2 functions with either DCL4 or with DCLI for the production of this class of miRNA remains to be determined. DRB2 is also required for the production of a subset of conserved *Arabidopsis* miRNAs [72]. The involvement of DRB2 in the production of conserved miRNAs is however restricted to the developmentally important tissues of wild-type *Arabidopsis* plants where *DRB2* is expressed, including the shoot and root apical meristems (SAM and RAM, respectively) and in immature pollen housed in anther pollen sacs [72, 73]. Of particular interest is the finding that the abundance of individual miRNAs was either elevated or reduced in the *drv2* mutant. This curious observation suggests that DRB2 acts both antagonistically or synergistically to the established DRB1/DCLI functional partnership for the production of miRNAs with altered abundance in *drv2* plants. Like DRB1, the involvement of DRB2 in the miRNA pathway most likely occurs at the initial precursor transcript processing steps in the nucleus. This is supported by the finding that the

precursor transcripts of miRNAs with reduced abundance in the *drb2* background are elevated, a finding that indicates less efficient processing of these precursor transcripts by DCL1 in the absence of DRB2 activity. Conversely, the precursor transcripts of miRNAs with elevated levels in *drb2* plants were demonstrated to be reduced in their abundance. This finding suggests that this group of precursor transcripts is more readily accessible to DRB1 for DCL1-catalyzed processing in the absence of DRB2. An early in vitro study by Hiraguri and colleagues (2005) revealed DRB1 to have a 50-fold stronger interaction with DCL1, compared to the interaction of DRB1 with either DCL2, DCL3, or DCL4 [74]. Intriguingly, *DRB1* gene expression is elevated 2-fold, and DRB1 protein abundance is elevated to an even greater degree in *drb2* plants [75]. This finding indicates that in the tissues of wild-type *Arabidopsis* where *DRB2* is expressed, and therefore where DRB2 is most likely functionally active, DRB2-mediated repression of *DRB1*/DRB1 abundance would potentially allow DRB2 to gain some degree of interaction with DCL1 to facilitate its involvement in the *production stage* of the miRNA pathway.

3 The Action Stage of the Plant microRNA Pathway

3.1 The Role of the Core Machinery Protein ARGONAUTE1

Post maturation in the nucleus, and export to the cytoplasm, the first step of the second stage of the plant miRNA pathway, the *action stage*, is loading of the mature miRNA into an effector complex, namely, miRNA loading into RISC, forming an activated miRISC. The protein encoded by the founding member of the ten-member ARGONAUTE (AGO) protein family, AGO1, forms the catalytic core of miRISC for almost all experimentally analyzed *Arabidopsis* miRNAs [76]. AGO1 is also essential for directing the action of RISC complexes loaded with small-interfering RNAs (siRNAs) of the 21 nt size class. However, most *Arabidopsis* miRNAs are loaded to AGO1 due to this sRNA species being almost exclusively 21 nts in length upon maturity, combined with most mature *Arabidopsis* miRNA sRNAs harboring a uracil residue at their 5' terminal nucleotide, the demonstrated size and 5' terminal nucleotide preference of AGO1 [46, 76]. Further, plant lines either partially or fully defective in AGO1 activity, *ago1* mutants, express severe developmental phenotypes due to greatly reduced mature miRNA abundance and therefore deregulated miRNA target gene expression [77, 78]. The localization of the AGO1 protein within the plant cell is dynamic, with labeled AGO1 protein visualized in both the nucleus and cytoplasm of *Arabidopsis* cells [31, 43]. As outlined above, nuclear AGO1 is thought to function in miRNA guide strand selection and subsequent separation from the miRNA* passenger strand during the *production stage* of the miRNA pathway [44, 45]. Cytoplasmic AGO1 however, is believed

to form the catalytic core of miRISC, directing target gene expression repression for most *Arabidopsis* miRNAs [43, 76]. The importance of regulating AGO1 homeostasis for the maintenance of miRNA pathway functionality throughout *Arabidopsis* development is evidenced by the elegant demonstrations that: (1) *AGO1* transcript expression is controlled by miR168-directed, AGO1-catalyzed Slicing of *AGO1* (i.e., cleavage of its own mRNA) (2) *AGO1* protein abundance is regulated via miR168-directed, AGO10-mediated translational repression of *AGO1*, and (3) the natural (pathogen attack) or artificial (transgene directed) alteration of *AGO1*/*AGO1* levels is rapidly modulated in *Arabidopsis* via a corresponding alteration to the abundance of miR168 [79, 80].

3.2 The Role of Auxiliary Machinery Proteins

ARGONAUTE proteins are widely conserved throughout eukaryotes, and once loaded with a preferred species of sRNA, the AGO becomes primed to form the catalytic core of RISC [77]. Across the eukaryotes, AGOs are very large proteins of 100 to 140 kDa molecular mass and that harbor three functional domains in their C-terminus, the PAZ (PIWI/Argonaute/Zwille), MID (middle), and PIWI (P-element-induced Wimpy Testes) domains [81, 82]. The PAZ and MID domain of each AGO recognizes and anchors the 5' and 3' ends of the loaded sRNA to the targeted nucleic acid [81, 83]. The PIWI domain serves as the catalytic domain of each AGO. It has a similar structure to that of RNaseH enzymes and provides the endonuclease or Slicer activity of cleavage component AGOs [81]. The ten AGO proteins encoded by the *Arabidopsis* genome can be divided into three distinct clades based on the composition of the amino acid sequence of each AGO. Clade I AGOs include *AGO1*, *AGO5*, and *AGO10*. *AGO2*, *AGO3*, and *AGO7* form Clade II, and Clade III members include *AGO4*, *AGO6*, *AGO8*, and *AGO9*. Clade III AGOs are associated with transcriptional gene silencing via a RNA-directed DNA methylation (RdDM) mechanism of RNA silencing [84, 85]. Of the Clade I and Clade II AGOs, and in addition to *AGO1*, AGOs *AGO2*, *AGO3*, *AGO5*, *AGO7*, and *AGO10* also appear to potentially mediate minor roles in the *action stage* of the miRNA pathway, functioning as effectors post loading of a specific miRNA subset or even the loading of only a single miRNA sRNA.

Like *AGO1*, the Clade I AGO, *AGO5*, has a dynamic subcellular localization, localizing to both the nucleus and cytoplasm of *Arabidopsis* cells [86]. However, unlike *AGO1*: (1) *AGO5* primarily loads siRNAs that are 24 nts in length and that express a 5' terminal C residue, and (2) *AGO5* gene expression is tissue-specific with the *AGO5* transcript highly abundant in the sperm cell cytoplasm of mature pollen grains and in growing pollen tubes [86]. Irrespective of the 24 nt sRNA size preference of *AGO5*, *AGO5* has been shown to additionally load a small subset of conserved

miRNAs, with miR156, miR158, and miR169 among those loaded by AGO5, in addition to a collection of pollen-enriched miRNAs. Given its high level of sequence similarity to AGO1 and AGO10, two documented effectors of miRNA-directed RNA silencing in *Arabidopsis*, it is highly likely that AGO5 also functions as an effector for these sperm-specific miRNAs, miRNAs possibly important for male germline development and/or beyond (i.e., pre- or postfertilization of the oocyte) [86–88]. Like AGO5, the expression domain of fellow Clade I member, AGO10, is restricted to developmentally important tissues, namely the shoot apical and floral meristems [89]. AGO10 is the closest paralogue of AGO1, and this has led to the suggestion of functional redundancy between AGO1 and AGO10 in tissues where their activity overlaps [85, 90]. Adding considerable weight to this suggestion is the demonstration that the *ago1 ago10* double mutant is embryo lethal, a finding that strongly infers AGO1/AGO10 functional redundancy post embryonic development [91]. Moreover, AGO10 has been shown to function with AGO1 as an effector of miR165/166- and miR172-directed RNA silencing in floral meristems to drive the termination of floral stem cells during reproductive development [89]. In the SAM, AGO10 exhibits a higher affinity than AGO1 for the loading of members of the miR165/166 family. Both miR165 and miR166 regulate the expression of members of the HD-ZIP III transcription factor family, transcription factors demonstrated essential in determining the developmental fate of the SAM [92, 93]. The higher affinity for miR165/166 loading by AGO10 in the SAM sequesters these sRNAs away from AGO1. This in turn prevents AGO1-mediated, miR165/166-directed expression regulation of HD-ZIP III activity in the SAM, thereby indirectly influencing the fate of the SAM [94].

The Clade II AGO, AGO2, loads sRNAs that are 21 nts in length upon maturity and that harbor a 5' terminal A residue. Consistent with this sRNA size and terminal nucleotide loading preference, AGO2 has been demonstrated to function redundantly with AGO1 as an effector for miR408-directed expression regulation [95]. The miR408 sRNA is one of a few miRNAs that begins with a 5' A residue [46, 47]. As documented for AGO1/AGO1 and miR168, AGO2/AGO2 abundance is tightly regulated at the post-transcriptional level by AGO1-catalyzed, miR403-directed RNA silencing [96]. Tight control of the abundance of AGO2/AGO2 by miR403 infers that AGO2 may potentially play a much broader role in plant development and/or physiology than currently known. However, AGO2 also binds numerous 21 nt siRNAs from endogenous and exogenous substrates (namely, specific plant viruses); therefore, the primarily role of AGO2-mediated gene expression regulation may not be miRNA pathway specific [96, 97]. Further, the loading of siRNAs from invading viruses in addition to a select subset of miRNAs, and miRNA* sequences,

suggests that the role of AGO2 in the *Arabidopsis* miRNA pathway may be stress induced. The *AGO3* locus is immediately adjacent to the *AGO2* gene on *Arabidopsis* chromosome 1 and is thought to be the result of *AGO2* gene duplication. Like *AGO2*, the *AGO3* transcript harbors a putative target site for miR403-directed expression regulation. However, due to the position of the miR403 target site in the 3' UTR of *AGO3*, it remains to be determined whether the *AGO3* transcript, in addition to the *AGO2* mRNA, is regulated by miR403. Further, establishment of functional redundancy between these two adjacent *AGO* loci is almost impossible to assess via a traditional T-DNA insertion knockout mutant approach, that is, genetic crossing of the T-DNA insertion mutant plant lines, *ago2* and *ago3*, to generate an *ago2 ago3* double mutant. The expression of *AGO3* is highly upregulated in *se* plants [30, 85], and elevated *AGO3* abundance in a mutant background where miR403 levels are likely reduced strongly suggests that the *AGO3* transcript is indeed under miR403-directed expression regulation. Confirmation that *AGO3/AGO3* is a *bona fide* target of miR403 and further establishing the degree of functional redundancy between AGO2 and AGO3 should be of high priority for future miRNA pathway research in *Arabidopsis*.

A reverse genetics screen for *Arabidopsis* lines displaying accelerated transition from juvenile to adult vegetative development identified mutations in the *AGO7* gene, along with those loci encoding DCL4, RNA-DEPENDENT RNA POLYMERASE6 (RDR6) and SUPPRESSOR OF GENE SILENCING3 (SGS3) [98, 99]. Subsequent studies have revealed central requirements for AGO7, DCL4, RDR6, and SGS3 (along with DRB4) in the miR390-triggered, *trans*-acting siRNA (tasiRNA) pathway [57, 98]. To date, four distinct tasiRNA pathways have been characterized in *Arabidopsis*, namely, the *TASI* to *TAS4* pathways [98, 99]. Interestingly, DCL4, DRB4, RDR6, and SGS3 are demonstrated to be required for the *TASI* (triggered by miR173), *TAS2* (triggered by miR173), and *TAS4* (triggered by miR828) pathways in *Arabidopsis*; however, the miR390/AGO7 interaction is specific to the *TAS3* pathway [100]. The miR390/AGO7-triggered *TAS3* pathway is further distinct to the *TASI/2/4* pathways via the demonstration that of the two miR390 target sites harbored by the *TAS3* non-protein-coding RNA, miR390 only directs AGO7-catalyzed cleavage of the 3' target site while remaining bound to the 5' target site [99, 100]. Cleavage at the 3' miR390 target site of the *TAS3* transcript by AGO7 results in the recruitment of RDR6 and SGS3 for dsRNA synthesis using the cleaved *TAS3* transcript as template. The resulting perfectly dsRNA molecule is subsequently processed by the DCL4/DRB4 functional partnership [57, 98]. Interestingly, AGO7 almost exclusively loads miR390 over the loading of a subset of miRNAs based on the composition of the 5' terminal nucleotide of each miRNA within the loaded subset

[100]. The specificity of miR390 loading into AGO7 was experimentally confirmed by Takeda and colleagues (2008) via their elegant demonstration that conversion of the wild-type 5' terminal A residue with a C residue failed to influence the preferential loading of the miR390 sRNA by AGO7 [47].

Many *Arabidopsis* miRNAs are now known to regulate target gene expression via a translational repression mode of miRNA-directed RNA silencing, and not exclusively via the originally documented mRNA cleavage-based mechanism of miRNA-directed RNA silencing. This is evidenced by numerous plant miRNAs having been associated with polysomes (the site where miRNA target gene transcripts are being used as translation templates), and further, miRNA/polysome association is AGO1-dependent [101, 102]. In addition, translational repression appears to exclusively occur on polysomes associated with the rough endoplasmic reticulum (rER) and has been shown to additionally require the rER transmembrane protein, ALTERED MERISTEMS PROGRAM1 (AMPI) [103]. AGO1 also co-localizes to the rER, and here, AMPI appears to block the entry of miRISC (AGO1)-loaded miRNA target transcripts to rER-bound polysomes [103]. However, exactly how AMPI directs miRNA target transcripts away from membrane bound polysomes, thereby blocking their use as a translation template, requires additional experimental investigation. In addition to AMPI, the glycine and tryptophan (GW) protein, SUO ("shuttle" in Chinese), has also been associated with the translational repression mode of miRNA-directed RNA silencing in *Arabidopsis* [104]. *Arabidopsis suo* mutants display a developmental phenotype characteristic of those expressed by plant lines with defective AGO1 activity, including reduced overall size, serration of rosette leaf margins, and an altered time to transition from juvenile to adult vegetative development [104]. At the molecular level, miRNA and target transcript abundance remain relatively unchanged in *suo* mutants compared to their respective levels in wild-type *Arabidopsis*. However, the abundance of miR398 targets, COPPER/ZINC SUPEROXIDE DISMUTASE1 (CSD1) and CSD2, and of reporter gene fusions with the miR156 target proteins, SPL3 and SPL9, was elevated in the *suo* background. Further, the authors [104] went on to show that miRNA precursor transcript abundance was also elevated in *suo* plants for a number of miRNA-encoding loci, a finding that indicates (1) feedback from the target gene protein level (i.e., elevated target protein promotes *MIR* gene expression to elevate the levels of the targeting miRNA) and (2) translational repression that is a widespread mechanism of target gene expression regulation directed by *Arabidopsis* miRNAs.

Three of the five members of the *Arabidopsis* DRB protein family, including DRB1, DRB2, and DRB4, play functional roles (to differing degrees; DRB1 > DRB2 > DRB4) in the *production stage* of the *Arabidopsis* miRNA pathway. The two remaining

members of the DRB protein family, DRB3 and DRB5, also appear involved in the miRNA pathway in *Arabidopsis*. However, unlike DRB1, DRB2, and DRB4, DRB3 and DRB5 likely function in the *action stage* of the *Arabidopsis* miRNA pathway, post miRNA production and export from the plant cell nucleus. Via the use of the transient leaf infiltration experiments in *Nicotiana benthamiana*, fluorescent reporter-tagged versions of *Arabidopsis* DRB3 and DRB5 were demonstrated to localize to the cytoplasm [105]. Artificial miRNA (amiRNA) technology was additionally used to show that amiRNA-directed RNA silencing was defective in the *drb3* and *drb5* mutant backgrounds, but only in the vegetative tissues where *DRB3* and *DRB5* are expressed in wild-type *Arabidopsis* (i.e., the shoot apex and rosette leaf petioles) [73, 105]. In addition, assessment of the molecular phenotypes of amiRNA expressing *drb3* and *drb5* plants curiously revealed that although amiRNA-directed RNA silencing was defective in specific vegetative tissues, no change in pri-amiRNA abundance, amiRNA accumulation, or target transcript expression was observed in the *drb3* and *drb5* backgrounds compared to the corresponding tissues of wild-type *Arabidopsis* plants expressing the same amiRNA. Adding further weight to the assignment of functional roles for DRB3 and DRB5 in the *action stage* of the *Arabidopsis* miRNA pathway was the demonstration that amiRNA-directed RNA silencing was completely defective in the *drb235* triple mutant background when the amiRNA sRNA was delivered via a miRNA precursor transcript known to require DRB2 (together with DCL1) for processing, and not the well-characterized DRB1/DCL1 functional partnership [105]. However, further experimentation is required to definitively assign functional roles for these two DRB protein family members. This is especially the case for accurate assignment of function to DRB3, as DRB3 has also been demonstrated to be involved in directing DNA methylation of viral genomes in the plant cell nucleus of geminivirus-infected plant cells [106].

The two nucleotidyl transferases, HEN1 SUPPRESSOR1 (HESO1) and UTP:RNA URIDYLYLTRANSFERASE1 (URT1), uridylylate miRNA sRNAs that have not been methylated at their 3' terminal nucleotide by HEN1 [107–109]. In the *hen1* mutant, for example, both HESO1 and URT1 uridylylate unmethylated miRNAs which leads to their subsequent degradation and therefore loss of their activity in the *action stage* of the miRNA pathway. The specificity of HESO1 and URT1 for unmethylated miRNAs has been confirmed in vitro with both nucleotidyl transferases uridylylating unmethylated RNA oligonucleotides, while neither transferase used RNA oligonucleotides of the same sequence composition that were methylated at their 3' terminal nucleotide as substrate [107–109]. Via profiling of the terminal nucleotide composition of miRNA sRNAs in the *hen1 heso1* double mutant,

substantial elevation in the accumulation of monouridylated miRNAs was documented, a finding that suggests that in vivo, URT1 adds a single uridine to the 3' terminus of unmethylated miRNAs and subsequently this now *marked* pool of sRNA may in turn be used as a substrate by HESO1 to add additional U residues to form longer U tails (and therefore entry of the now *marked* miRNA into the sRNA degradation pathway) [107–109]. In addition to identifying unmethylated miRNAs for subsequent degradation, uridylation at the 3' terminus of a miRNA may potentially be a mechanism used by the plant cell to modulate miRNA activity. For example, monouridylation of miR171a by URT1 in *hen1* mutants redirected this sRNA into the pathway that triggers phased siRNA (phasiRNA) production post target gene mRNA cleavage [110]. Further, in vitro experiments demonstrated that the uridylation of miR165/miR166 by URT1 repressed the ability of AGO1-loaded miR165/miR166 to direct AGO1-catalyzed cleavage of miR165/miR166 target transcripts [109]. It has also been shown that artificially synthesized miRNAs engineered to harbor 3' A-tails were degraded at a much slower rate than the RNA oligonucleotides that lacked this feature, a finding that suggests that adenylation of miRNA sRNAs in vivo may contribute to the overall stability, and therefore longevity, of the activity of the modified miRNA [111]. The three SMALL RNA DEGRADING NUCLEASE (SDN) proteins, SDN1 to SDN3, are sRNA-specific 3' to 5' exonucleases that are crucial in controlling the steady-state levels of *Arabidopsis* miRNAs [112]. SDN1 has been shown in vitro to act upon AGO1-loaded miRNAs to produce a pool of miRNA species of varying length [113]. Unlike HESO1 and URT1, SDN1 acts upon methylated miRNAs, a finding that indicates that SDN1 may potentially modify AGO1-loaded miRNAs to remove the 3' terminal nucleotide (or to just remove the attached methyl group) to mark these miRNAs for uridylation by HESO1 and/or URT1 leading to their subsequent degradation and ultimately loss of the ability of the miRNA to remain active to continue to direct miRISC-catalyzed repression of target gene expression [113].

4 Tools for the Functional Characterization of the Plant miRNA Pathway

In recent years, the development of high-throughput sequencing technology to further characterize the plant miRNA pathway has resulted in the vast majority of published literature detailing either the: (1) bioinformatic-based identification of new and novel miRNA sRNAs, as well as the putative target genes of these newly identified miRNAs, or (2) cataloguing of abundance changes to the accumulation of individual miRNA sRNAs in model or non-model plant species cultivated under standard growth conditions or under differing stress (biotic or abiotic) regimes. This widespread

application of sequencing and bioinformatic technologies has resulted in a significant reduction in the frequency of research publications reporting findings on either the experimental validation of novel or known miRNAs, and their targeted genes, as well as the functional characterization of known or new machinery proteins required for either the *production* or *action* stage of the plant miRNA pathway. However, as plant miRNA pathway researchers, we now have an extensive and highly impressive toolkit available to advance our current knowledge on the central role the miRNA pathway plays in plant development, environmental stress adaptation, or in response to pathogen challenge. For example, miRNA abundance can be either elevated or repressed via the *in planta* expression of *MIR* gene overexpression constructs or molecular sponge encoding transgenes, respectively. A transgene-based approach can also be used in parallel to modulate the levels of miRNA target gene abundance for further functional characterization of individual miRNA/target gene expression modules. This can be achieved via the *in planta* expression of a transgene that encodes a miRNA resistance version of a miRNA target gene. Plant molecular biologists can now also add the site-specific nuclease (SSN) genome editing tools, zinc-finger nucleases (ZFNs), transcription activator-like effector nucleases (TALENs), and clustered regularly interspaced short palindromic repeat (CRISPR/*Cas9*) to their ever-increasing arsenal of molecular modification approaches. The new SSN approach provides an alternate avenue for the generation of knockout mutations in loci encoding for miRNA pathway machinery proteins for which the traditional approach of characterizing a T-DNA insertion knockout mutant is not feasible. Together, the wealth of tools now available for either miRNA identification, miRNA abundance profiling, or the subsequent experimental validation of new or known miRNAs, as well as maintaining momentum in the biological assessment of the functional roles of machinery proteins in either the *production* or *action* stages of the plant miRNA pathway, marks the current day as an exciting time to perform plant miRNA pathway research.

References

1. Reinhart BJ, Weinstein EG, Rhoades MW, Bartel B, Bartel DP (2002) MicroRNAs in plants. *Genes Dev* 16:1616–1626
2. Wang JF, Zhou H, Chen YQ, Luo QJ, Qu LH (2004) Identification of 20 microRNA from *Oryza sativa*. *Nucl Acids Res* 32:1688–1695
3. Yao Y, Guo G, Ni Z, Sunkar R, Du J, Zhu JK, Sun Q (2007) Cloning and characterization of microRNAs from wheat (*Triticum aestivum* L.). *Genome Biol* 8:R96
4. Juarez MT, Kuri JS, Thomas J, Heller BA, Timmermans MC (2004) microRNA-mediated repression of rolled leaf1 specifies maize leaf polarity. *Nature* 428:84–88
5. Zhang W, Luo Y, Gong X, Zeng W, Li S (2009) Computational identification of 48 potato microRNAs and their targets. *Comput Biol Chem* 33:84–93
6. Zanca AS, Vicentini R, Ortiz-Morea FA, Del Bem LE, da Silva MJ, Vincentz M, Nogueira FT (2010) Identification and expression

- analysis of microRNAs and targets in the bio-fuel crop sugarcane. *BMC Plant Biol* 10:260
7. Mallory AC, Dugas DV, Bartel DP, Bartel B (2004) MicroRNA regulation of NAC-domain targets is required for proper formation and separation of adjacent embryonic, vegetative, and floral organs. *Curr Biol* 14:1035–1046
 8. Achard P, Herr A, Baulcombe DC, Harberd NP (2004) Modulation of floral development by a gibberellin-regulated microRNA. *Development* 131:3357–3365
 9. Gandikota M, Birkenbihl RP, Höhmann S, Cardon GH, Saedler H, Huijser P (2007) The miRNA156/157 recognition element in the 3' UTR of the Arabidopsis SBP box gene SPL3 prevents early flowering by translational inhibition in seedlings. *Plant J* 49:683–693
 10. Aukerman MJ, Sakai H (2003) Regulation of flowering time and floral organ identity by a MicroRNA and its APETALA2-like target genes. *Plant Cell* 15:2730–2741
 11. Park W, Li J, Song R, Messing J, Chen X (2002) CARPEL FACTORY, a Dicer homolog, and HEN1, a novel protein, act in microRNA metabolism in *Arabidopsis thaliana*. *Curr Biol* 12:1484–1495
 12. Han MH, Goud S, Song L, Fedoroff N (2004) The Arabidopsis double-stranded RNA-binding protein HYL1 plays a role in microRNA-mediated gene regulation. *PNAS* 101:1093–1098
 13. Yang L, Liu Z, Lu F, Dong A, Huang H (2006) SERRATE is a novel nuclear regulator in primary microRNA processing in Arabidopsis. *Plant J* 47:841–850
 14. Bohmert K, Camus I, Bellini C, Bouchez D, Caboche M, Benning C (1998) AGO1 defines a novel locus of Arabidopsis controlling leaf development. *EMBO J* 17:170–180
 15. Jagadeeswaran G, Zheng Y, Sumathipala N, Jiang H, Arrese EL, Soulages JL, Zhang W, Sunkar R (2010) Deep sequencing of small RNA libraries reveals dynamic regulation of conserved and novel microRNAs and microRNA-stars during silkworm development. *BMC Genomics* 11:52
 16. Boutet S, Vazquez F, Liu J, Béclin C, Fagard M, Gratias A, Morel JB, Créte P, Chen X, Vaucheret H (2003) Arabidopsis HEN1: a genetic link between endogenous miRNA controlling development and siRNA controlling transgene silencing and virus resistance. *Curr Biol* 13:843–848
 17. Radwan O, Liu Y, Clough SJ (2011) Transcriptional analysis of soybean root response to *Fusarium virguliforme*, the causal agent of sudden death syndrome. *Mol Plant-Microbe Interact* 24:958–972
 18. Sunkar R, Zhou X, Zheng Y, Zhang W, Zhu JK (2008) Identification of novel and candidate miRNAs in rice by high throughput sequencing. *BMC Plant Biol* 8:25
 19. Yan K, Liu P, Wu CA, Yang GD, Xu R, Guo QH, Huang JG, Zheng CC (2012) Stress-induced alternative splicing provides a mechanism for the regulation of microRNA processing in *Arabidopsis thaliana*. *Mol Cell* 48:521–531
 20. Fujii H, Chiou TJ, Lin SI, Aung K, Zhu JK (2005) A miRNA involved in phosphate-starvation response in Arabidopsis. *Curr Biol* 15:2038–2043
 21. Matthewman CA, Kawashima CG, Húska D, Csorba T, Dalmay T, Kopriva S (2012) miR395 is a general component of the sulfate assimilation regulatory network in Arabidopsis. *FEBS Lett* 586:3242–3248
 22. Vazquez F, Blevins T, Ailias J, Boller T, Meins F Jr (2008) Evolution of Arabidopsis *MIR* genes generates novel microRNA classes. *Nucleic Acids Res* 36:6429–6438
 23. Gazzani S, Li M, Maistri S, Scarponi E, Graziola M, Barbaro E, Wunder J, Furini A, Saedler H, Varotto C (2009) Evolution of MIR168 paralogs in Brassicaceae. *BMC Evol Biol* 9:62
 24. Meyers BC, Green PJ, Lu C (2008) miRNAs in the plant genome: all things great and small. *Genome Dyn* 4:108–118
 25. Xie Z, Khanna K, Ruan S (2010) Expression of microRNAs and its regulation in plants. *Semin Cell Dev Biol* 21:790–797
 26. Kim S, Yang JY, Xu J, Jang IC, Prigge MJ, Chua NH (2008) Two cap-binding proteins CBP20 and CBP80 are involved in processing primary MicroRNAs. *Plant Cell Physiol* 49:1634–1644
 27. Fang X, Cui Y, Li Y, Qi Y (2015) Transcription and processing of primary microRNAs are coupled by Elongator complex in Arabidopsis. *Nat Plants* 1:15075
 28. Bielewicz D, Kalak M, Kalyna M, Windels D, Barta A, Vazquez F, Szweykowska-Kulinska Z, Jarmolowski A (2013) Introns of plant pri-miRNAs enhance miRNA biogenesis. *EMBO Rep* 14:622–628
 29. Knop K, Stepien A, Barciszewska-Pacak M, Taube M, Bielewicz D, Michalak M, Borst JW, Jarmolowski A, Szweykowska-Kulinska Z (2016) Active 5' splice sites regulate the biogenesis efficiency of Arabidopsis

- microRNAs derived from intron-containing genes. *Nucleic Acids Res* 45:2757–2775
30. Lobbes D, Rallapalli G, Schmidt DD, Martin C, Clarke J (2006) SERRATE: a new player on the plant microRNA scene. *EMBO Rep* 7:1052–1058
 31. Fang Y, Spector DL (2007) Identification of nuclear dicing bodies containing proteins for microRNA biogenesis in living Arabidopsis plants. *Curr Biol* 17:818–823
 32. Fujioka Y, Utsumi M, Ohba Y, Watanabe Y (2007) Location of a possible miRNA processing site in Smd3/SmB nuclear bodies in Arabidopsis. *Plant Cell Physiol* 48:1243–1453
 33. Gascioli V, Mallory AC, Bartel DP, Vaucheret H (2005) Partially redundant functions of Arabidopsis DICER-like enzymes and a role for DCL4 in producing *trans*-acting siRNAs. *Curr Biol* 15:1494–1500
 34. Bouché N, Laressergues D, Gascioli V, Vaucheret H (2006) An antagonistic function for Arabidopsis DCL2 in development and a new function for DCL4 in generating viral siRNAs. *EMBO J* 25:3347–3356
 35. Dong Z, Han MH, Fedoroff N (2008) The RNA-binding proteins HYL1 and SE promote accurate *in vitro* processing of pri-miRNA by DCL1. *PNAS* 105:9970–9975
 36. Vazquez F, Gascioli V, Crété P, Vaucheret H (2004) The nuclear dsRNA binding protein HYL1 is required for microRNA accumulation and plant development, but not posttranscriptional transgene silencing. *Curr Biol* 14:346–351
 37. Kurihara Y, Takashi Y, Watanabe Y (2006) The interaction between DCL1 and HYL1 is important for efficient and precise processing of pri-miRNA in plant microRNA biogenesis. *RNA* 12:206–212
 38. Song L, Axtell MJ, Fedoroff NV (2010) RNA secondary structural determinants of miRNA precursor processing in Arabidopsis. *Curr Biol* 20:37–41
 39. Werner S, Wollmann H, Schneeberger K, Weigel D (2010) Structure determinants for accurate processing of miR172a in *Arabidopsis thaliana*. *Curr Biol* 20:42–48
 40. Bologna NG, Schapire AL, Zhai J, Chorostecky U, Boisbouvier J, Meyers BC, Palatnik JF (2013) Multiple RNA recognition patterns during microRNA biogenesis in plants. *Genome Res* 23:1675–1689
 41. Chen X, Liu J, Cheng Y, Jia D (2002) HEN1 functions pleiotropically in Arabidopsis development and acts in C function in the flower. *Development* 129:1085–1094
 42. Baranauskė S, Mickutė M, Plotnikova A, Finke A, Venclovas Č, Klimišauskas S, Vilkaitis G (2015) Functional mapping of the plant small RNA methyltransferase: HEN1 physically interacts with HYL1 and DICER-LIKE 1 proteins. *Nucleic Acids Res* 43:2802–2812
 43. Lanet E, Delannoy E, Sormani R, Floris M, Brodersen P, Crété P, Voinnet O, Robaglia C (2009) Biochemical evidence for translational repression by Arabidopsis microRNAs. *Plant Cell* 21:1762–1768
 44. Iki T, Yoshikawa M, Meshi T, Ishikawa M (2012) Cyclophilin 40 facilitates HSP90-mediated RISC assembly in plants. *EMBO J* 31:267–278
 45. Eamens AL, Smith NA, Curtin SJ, Wang MB, Waterhouse PM (2009) The *Arabidopsis thaliana* double-stranded RNA binding protein DRB1 directs guide strand selection from microRNA duplexes. *RNA* 15:2219–2235
 46. Mi S, Cai T, Hu Y, Chen Y, Hodges E, Ni F, Wu L, Li S, Zhou H, Long C, Chen S, Hannon GJ, Qi Y (2008) Sorting of small RNAs into Arabidopsis argonaute complexes is directed by the 5' terminal nucleotide. *Cell* 133:116–127
 47. Takeda A, Iwasaki S, Watanabe T, Utsumi M, Watanabe Y (2008) The mechanism selecting the guide strand from small RNA duplexes is different among argonaute proteins. *Plant Cell Physiol* 49:493–500
 48. Bollman KM, Aukerman MJ, Park MY, Hunter C, Berardini TZ, Poethig RS (2003) HASTY, the Arabidopsis ortholog of exportin 5/MSN5, regulates phase change and morphogenesis. *Development* 130:1493–1504
 49. Smith MR, Willmann MR, Wu G, Berardini TZ, Möller B, Weijers D, Poethig RS (2009) Cyclophilin 40 is required for microRNA activity in Arabidopsis. *PNAS* 106:5424–5429
 50. Earley KW, Poethig RS (2011) Binding of the cyclophilin 40 ortholog SQUINT to Hsp90 protein is required for SQUINT function in Arabidopsis. *J Biol Chem* 286:38184–38189
 51. Kim YJ, Zheng B, Yu Y, Won SY, Mo B, Chen X (2011) The role of mediator in small and long noncoding RNA production in *Arabidopsis thaliana*. *EMBO J* 30:814–822
 52. Wang L, Song X, Gu L, Li X, Cao S, Chu C, Cui X, Chen X, Cao X (2013) NOT2 proteins promote polymerase II-dependent transcription and interact with multiple MicroRNA biogenesis factors in Arabidopsis. *Plant Cell* 25:715–727

53. Zhang S, Xie M, Ren G, Yu B (2013) CDC5, a DNA binding protein, positively regulates posttranscriptional processing and/or transcription of primary microRNA transcripts. *PNAS* 110:17555–17593
54. Speth C, Willing EM, Rausch S, Schneeberger K, Laubinger S (2013) RACK1 scaffold proteins influence miRNA abundance in Arabidopsis. *Plant J* 76:433–445
55. Speth C, Laubinger S (2014) RACK1 and the microRNA pathway: is it déjà-vu all over again? *Plant Signal Behav* 9:e27909
56. Wang JW, Czech B, Weigel D (2009) miR156-regulated SPL transcription factors define an endogenous flowering pathway in *Arabidopsis thaliana*. *Cell* 138:738–749
57. Wu G, Park MY, Conway SR, Wang JW, Weigel D, Poethig RS (2009) The sequential action of miR156 and miR172 regulates developmental timing in Arabidopsis. *Cell* 138:750–759
58. Zhao L, Kim Y, Dinh TT, Chen X (2007) miR172 regulates stem cell fate and defines the inner boundary of APETALA3 and PISTILLATA expression domain in Arabidopsis floral meristems. *Plant J* 51:840–849
59. Manavella PA, Hagmann J, Ott F, Laubinger S, Franz M, Macek B, Weigel D (2012) Fast-forward genetics identifies plant CPL phosphatases as regulators of miRNA processing factor HYL1. *Cell* 151:859–870
60. Karlsson P, Christie MD, Seymour DK, Wang H, Wang X, Hagmann J, Kulcheski F, Manavella PA (2015) KH domain protein RCF3 is a tissue-biased regulator of the plant miRNA biogenesis cofactor HYL1. *PNAS* 112:14096–14101
61. Raghuram B, Sheikh AH, Rustagi Y, Sinha AK (2015) MicroRNA biogenesis factor DRB1 is a phosphorylation target of mitogen activated protein kinase MPK3 in both rice and Arabidopsis. *FEBS J* 282:521–536
62. Su C, Li Z, Cheng J, Li L, Zhong S, Liu L, Zheng Y, Zheng B (2017) The protein Phosphatase 4 and SMEK1 complex dephosphorylates HYL1 to promote miRNA biogenesis by antagonizing the MAPK Cascade in Arabidopsis. *Dev Cell* 41:527–539
63. Yan J, Wang P, Wang B, Hsu CC, Tang K, Zhang H, Hou YJ, Zhao Y, Wang Q, Zhao C, Zhu X, Tao WA, Li J, Zhu JK (2017) The SnRK2 kinases modulate miRNA accumulation in Arabidopsis. *PLoS Genet* 13:e1006753
64. Cho SK, Ben Chaabane S, Shah P, Poulsen CP, Yang SW (2014) COP1 E3 ligase protects HYL1 to retain microRNA biogenesis. *Nat Commun* 5:5867
65. Zhang Z, Guo X, Ge C, Ma Z, Jiang M, Li T, Koiwa H, Yang SW, Zhang X (2017) KETCH1 imports HYL1 to nucleus for miRNA biogenesis in Arabidopsis. *PNAS* 114:4011–4016
66. Zhan X, Wang B, Li H, Liu R, Kalia RK, Zhu JK, Chinnusamy V (2012) Arabidopsis proline-rich protein important for development and abiotic stress tolerance is involved in microRNA biogenesis. *PNAS* 109:18198–18203
67. Ren G, Xie M, Dou Y, Zhang S, Zhang C, Yu B (2012) Regulation of miRNA abundance by RNA binding protein TOUGH in Arabidopsis. *PNAS* 109:12817–12821
68. Ben Chaabane S, Liu R, Chinnusamy V, Kwon Y, Park JH, Kim SY, Zhu JK, Yang SW, Lee BH (2013) STA1, an Arabidopsis pre-mRNA processing factor 6 homolog, is a new player involved in miRNA biogenesis. *Nucleic Acids Res* 41:1984–1997
69. Yu B, Bi L, Zheng B, Ji L, Chevalier D, Agarwal M, Ramachandran V, Li W, Lagrange T, Walker JC, Chen X (2008) The FHA domain proteins DAWDLE in Arabidopsis and SNIP1 in humans act in small RNA biogenesis. *PNAS* 105:10073–10078
70. Pélissier T, Clavel M, Chaparro C, Pouch-Pélissier MN, Vaucheret H, Deragon JM (2011) Double-stranded RNA binding proteins DRB2 and DRB4 have an antagonistic impact on polymerase IV-dependent siRNA levels in Arabidopsis. *RNA* 17:1502–1510
71. Nakazawa Y, Hiraguri A, Moriyama H, Fukuhara T (2007) The dsRNA-binding protein DRB4 interacts with the Dicer-like protein DCL4 *in vivo* and functions in the *trans*-acting siRNA pathway. *Plant Mol Biol* 63:777–785
72. Eamens AL, Kim KW, Curtin SJ, Waterhouse PM (2012) DRB2 is required for microRNA biogenesis in *Arabidopsis thaliana*. *PLoS One* 7:e35933
73. Curtin SJ, Watson JM, Smith NA, Eamens AL, Blanchard CL, Waterhouse PM (2008) The roles of plant dsRNA-binding proteins in RNAi-like pathways. *FEBS Lett* 582:2753–2760
74. Hiraguri A, Itoh R, Kondo N, Nomura Y, Aizawa D, Murai Y, Koiwa H, Seki M, Shinozaki K, Fukuhara T (2005) Specific interactions between Dicer-like proteins and HYL1/DRB-family dsRNA-binding proteins in *Arabidopsis thaliana*. *Plant Mol Biol* 57:173–188

75. Reis RS, Hart-Smith G, Eamens AL, Wilkins MR, Waterhouse PM (2015) Gene regulation by translational inhibition is determined by Dicer partnering proteins. *Nat Plants* 1:14027
76. Baumberger N, Baulcombe DC (2005) *Arabidopsis* ARGONAUTE1 is an RNA slicer that selectively recruits microRNAs and short interfering RNAs. *PNAS* 102:11928–11933
77. Fagard M, Boutet S, Morel JB, Bellini C, Vaucheret H (2002) AGO1, QDE-2, and RDE-1 are related proteins required for post-transcriptional gene silencing in plants, quelling in fungi, and RNA interference in animals. *PNAS* 97:11650–11654
78. Vaucheret H, Vazquez F, Cr  t   P, Bartel DP (2004) The action of ARGONAUTE1 in the miRNA pathway and its regulation by the miRNA pathway are crucial for plant development. *Genes Dev* 18:1187–1197
79. Mallory A, Vaucheret H (2009) ARGONAUTE 1 homeostasis invokes the coordinate action of the microRNA and siRNA pathways. *EMBO Rep* 10:521–526
80. Mallory A, Vaucheret H (2010) Form, function, and regulation of ARGONAUTE proteins. *Plant Cell* 22:3879–3889
81. Song JJ, Smith SK, Hannon GJ, Joshua-Tor L (2004) Crystal structure of Argonaute and its implications for RISC slicer activity. *Science* 305:1434–1437
82. Cerutti L, Mian N, Bateman A (2000) Domains in gene silencing and cell differentiation proteins: the novel PAZ domain and redefinition of the Piwi domain. *Trends Biochem Sci* 25:481–482
83. Boland A, Huntzinger E, Schmidt S, Izauralde E, Weichenrieder O (2011) Crystal structure of the MID-PIWI lobe of a eukaryotic Argonaute protein. *PNAS* 108:10466–10471
84. Kim KW, Eamens AL, Waterhouse PM (2011) RNA processing activities of the *Arabidopsis* Argonaute protein family. In: Grabowski P (ed) *RNA processing*. InTech, Rijeka
85. Vaucheret H (2008) Plant ARGONAUTES. *Trends Plant Sci* 13:350–358
86. Borges F, Pereira PA, Slotkin RK, Martienssen RA, Becker JD (2011) MicroRNA activity in the *Arabidopsis* male germline. *J Exp Botany* 62:1611–1620
87. Chambers C, Shuai B (2009) Profiling microRNA expression in *Arabidopsis* pollen using microRNA array and real-time PCR. *BMC Plant Biol* 9:87
88. Li XM, Sang YL, Zhao XY, Zhang XS (2013) High-throughput sequencing of small RNAs from pollen and silk and characterization of miRNAs as candidate factors involved in pollen-silk interactions in maize. *PLoS One* 8:e72852
89. Ji L, Liu X, Yan J, Wang W, Yumul RE, Kim YJ, Dinh TT, Liu J, Cui X, Zheng B, Agarwal M, Liu C, Cao X, Tang G, Chen X (2011) ARGONAUTE10 and ARGONAUTE1 regulate the termination of floral stem cells through two microRNAs in *Arabidopsis*. *PLoS Genet* 7:e1001358
90. Mallory AC, Hinze A, Tucker MR, Bouch   N, Gascioli V, Elmayan T, Laussergues D, Jauvion V, Vaucheret H, Laux T (2009) Redundant and specific roles of the ARGONAUTE proteins AGO1 and ZLL in development and small RNA-directed gene silencing. *PLoS Genet* 5:e1000646
91. Lynn K, Fernandez A, Aida M, Sedbrook J, Tasaka M, Masson P, Barton MK (1999) The PINHEAD/ZWILLE gene acts pleiotropically in *Arabidopsis* development and has overlapping functions with the ARGONAUTE1 gene. *Development* 126:469–481
92. Jung JH, Park CM (2007) *MIR166/165* genes exhibit dynamic expression patterns in regulating shoot apical meristem and floral development in *Arabidopsis*. *Planta* 225:1327–1338
93. Zhou GK, Kubo M, Zhong R, Demura T, Ye ZH (2007) Overexpression of miR165 affects apical meristem formation, organ polarity establishment and vascular development in *Arabidopsis*. *Plant Cell Physiol* 48:391–404
94. Zhu H, Hu F, Wang R, Zhou X, Sze SH, Liou LW, Barefoot A, Dickman M, Zhang X (2011) *Arabidopsis* Argonaute10 specifically sequesters miR166/165 to regulate shoot apical meristem development. *Cell* 145:242–256
95. Maunoury N, Vaucheret H (2011) AGO1 and AGO2 act redundantly in miR408-mediated Plantacyanin regulation. *PLoS One* 6:e28729
96. Harvey JJ, Lewsey MG, Patel K, Westwood J, Heimst  dt S, Carr JP, Baulcombe DC (2011) An antiviral defense role of AGO2 in plants. *PLoS One* 6:e14639
97. Wang XB, Jovel J, Udomborn P, Wang Y, Wu Q, Li WX, Gascioli V, Vaucheret H, Ding SW (2011) The 21-nucleotide, but not 22-nucleotide, viral secondary small interfering RNAs direct potent antiviral defense by two cooperative argonautes in *Arabidopsis thaliana*. *Plant Cell* 23:1625–1638

98. Peragine A, Yoshikawa M, Wu G, Albrecht HL, Poethig RS (2004) SGS3 and SGS2/SDE1/RDR6 are required for juvenile development and the production of *trans*-acting siRNAs in Arabidopsis. *Genes Dev* 18:2368–2379
99. Yoshikawa M, Peragine A, Park MY, Poethig RS (2005) A pathway for the biogenesis of *trans*-acting siRNAs in Arabidopsis. *Genes Dev* 19:2164–2175
100. Montgomery TA, Howell MD, Cuperus JT, Li D, Hansen JE, Alexander AL, Chapman EJ, Fahlgren N, Allen E, Carrington JC (2008) Specificity of ARGONAUTE7-miR390 interaction and dual functionality in TAS3 *trans*-acting siRNA formation. *Cell* 133:128–141
101. Brodersen P, Sakvarelidze-Achard L, Bruun-Rasmussen M, Dunoyer P, Yamamoto YY, Sieburth L, Voinnet O (2008) Widespread translational inhibition by plant miRNAs and siRNAs. *Science* 320:1185–1190
102. Brodersen P, Sakvarelidze-Achard L, Schaller H, Khafif M, Schott G, Bendahmane A, Voinnet O (2012) Isoprenoid biosynthesis is required for miRNA function and affects membrane association of ARGONAUTE 1 in Arabidopsis. *PNAS* 109:1778–1783
103. Li S, Liu L, Zhuang X, Yu Y, Liu X, Cui X, Ji L, Pan Z, Cao X, Mo B, Zhang F, Raikhel N, Jiang L, Chen X (2013) MicroRNAs inhibit the translation of target mRNAs on the endoplasmic reticulum in Arabidopsis. *Cell* 153:562–574
104. Yang L, Wu G, Poethig RS (2012) Mutations in the GW-repeat protein SUO reveal a developmental function for microRNA-mediated translational repression in Arabidopsis. *PNAS* 109:315–320
105. Eamens AL, Kim KW, Waterhouse PM (2012) DRB2, DRB3 and DRB5 function in a non-canonical microRNA pathway in *Arabidopsis thaliana*. *Plant Signal Behav* 7:1224–1229
106. Raja P, Jackel JN, Li S, Heard IM, Bisaro DM (2014) Arabidopsis double-stranded RNA binding protein DRB3 participates in methylation-mediated defense against geminiviruses. *J Virol* 88:2611–2622
107. Zhao Y, Yu Y, Zhai J, Ramachandran V, Dinh TT, Meyers BC, Mo B, Chen X (2012) The Arabidopsis nucleotidyl transferase HESO1 uridylates unmethylated small RNAs to trigger their degradation. *Curr Biol* 22:689–694
108. Ren G, Chen X, Yu B (2012) Uridylation of miRNAs by *hen1 suppressor1* in Arabidopsis. *Curr Biol* 22:695–700
109. Tu B, Liu L, Xu C, Zhai J, Li S, Lopez MA, Zhao Y, Yu Y, Ramachandran V, Ren G, Yu B, Li S, Meyers BC, Mo B, Chen X (2015) Distinct and cooperative activities of HESO1 and URT1 nucleotidyl transferases in microRNA turnover in Arabidopsis. *PLoS Genet* 11:e1005119
110. Zhai J, Zhao Y, Simon SA, Huang S, Petsch K, Arikat S, Pillay M, Ji L, Xie M, Cao X, Yu B, Timmermans M, Yang B, Chen X, Meyers BC (2013) Plant microRNAs display differential 3' truncation and tailing modifications that are ARGONAUTE1 dependent and conserved across species. *Plant Cell* 25:2417–2428
111. Lu S, Sun YH, Chiang VL (2009) Adenylation of plant miRNAs. *Nucleic Acids Res* 37:1878–1885
112. Ramachandran V, Chen X (2008) Degradation of microRNAs by a family of exoribonucleases in Arabidopsis. *Science* 321:1490–1492
113. Yu Y, Ji L, Le BH, Zhai J, Chen J, Luscher E, Gao L, Liu C, Cao X, Mo B, Ma J, Meyers BC, Chen X (2017) ARGONAUTE10 promotes the degradation of miR165/6 through the SDN1 and SDN2 exonucleases in Arabidopsis. *PLoS Biol* 15:e2001272

A.1.2 Publication Two



agronomy



Profiling of the Differential Abundance of Drought and Salt Stress-Responsive MicroRNAs Across Grass Crop and Genetic Model Plant Species

Joseph L. Pegler*, Christopher P. L. Grof and Andrew L. Eamens

Centre for Plant Science, School of Environmental and Life Sciences, Faculty of Science, University of Newcastle, Callaghan, NSW 2308, Australia; chris.grof@newcastle.edu.au (C.P.L.G.); andy.eamens@newcastle.edu.au (A.L.E.)

* Correspondence: Joseph.Pegler@uon.edu.au; Tel.: +61-413-922-093

Received: 21 May 2018; Accepted: 10 July 2018; Published: 13 July 2018

Abstract: In recent years, it has become readily accepted among interdisciplinary agriculturalists that the current global crop yield to land capability ratio is significantly insufficient to achieve food security for the predicted population of 9.5 billion individuals by the year 2050. This issue is further compounded by the: (1) food versus biofuel debate; (2) decreasing availability of arable land; (3) required reductions to the extensive and ongoing environmental damage caused by either poor agricultural practices or agriculture expansion, and; (4) increasingly unfavorable (duration and severity) crop cultivation conditions that accompany man-made climate change, driven by ever-expanding urbanization and its associated industrial practices. Mounting studies are repeatedly highlighting the critical importance of linking genotypes to agronomically beneficial phenotypes and/or using a molecular approach to help address this global crisis, as “simply” clearing the remaining natural ecosystems of the globe for the cultivation of additional, non-modified crops is not efficient, nor is this practice sustainable. The majority of global food crop production is sourced from a small number of members of the *Poaceae* family of grasses, namely; maize (*Zea mays* L.), wheat (*Triticum aestivum* L.) and rice (*Oryza sativa* L.). It is, therefore, of significant concern that all three of these *Poaceae* grass species are susceptible to a range of abiotic stresses, including drought and salt stress. Highly conserved among monocotyledonous and dicotyledonous plant species, microRNAs (miRNAs) are now well-established master regulators of gene expression, influencing all aspects of plant development, mediating defense responses against pathogens and adaptation to environmental stress. Here we investigate the variation in the abundance profiles of six known abiotic stress-responsive miRNAs, following exposure to salt and drought stress across these three key *Poaceae* grass crop species as well as to compare these profiles to those obtained from the well-established genetic model plant species, *Arabidopsis thaliana* (L.) Heynh. Additionally, we outline the variables that are the most likely primary contributors to instances of differential miRNA abundance across the assessed species following drought or salt stress exposure, specifically; (1) identifying variations in the experimental conditions and/or methodology used to assess miRNA abundance, and; (2) the distribution of regulatory transcription factor binding sites within the putative promoter region of a *MICRORNA* (*MIR*) gene that encodes the highly conserved, stress-responsive miRNA. We also discuss the emerging role that non-conserved, species-specific miRNAs play in mediating a plant’s response to drought or salt stress.

Keywords: drought stress; salt stress; *MICRORNA* gene expression; microRNAs; microRNA-directed gene expression regulation; differential microRNA accumulation; *Poaceae* grass species; *Arabidopsis thaliana*

1. Introduction

The global human population relies heavily on the major *Poaceae* cereal grasses, maize (*Zea mays* L.), wheat (*Triticum aestivum* L.), and rice (*Oryza sativa* L.), for their daily calorie intake [1,2]. Covering a large proportion of the global terrestrial land space, *Poaceae* grasses not only act as a primary sustenance source for humans (in the form of calories) but also contribute to agricultural pastures (e.g., rye (*Secale cereal* L.)) used to feed livestock [1,3]. Two other *Poaceae* grass species, Sorghum (*Sorghum bicolor* (L.) Moench) and sugarcane (*Saccharum officinarum* L.), form the primary basis of the plant material source for biofuel production, further highlighting the central importance of *Poaceae* grasses [4,5]. It is no longer debatable that modern society is challenged with the task of trying to address the consequences of climate change, with interdisciplinary research now aiming to provide food crop security for an exponentially growing population during times of increasingly unfavorable conditions, and in unsuitable crop cultivation environments [6]. Alarming, numerous studies have demonstrated that drought and/or salinity reduce the yield potential of the major cereal crops maize, wheat and rice, every growing season [7–14]. Moreover, use of regression modeling based on historical data and the predictions based on extrapolated trends of crop yield and climatic trends have highlighted the negative impact climate change associated factors (e.g., reduced precipitation) have had, and are continuing to have, on global *Poaceae* crop yield [15,16]. Having greatly modified the global land cover over the last fifty years, there has been a shift from the historical clearing of depleted grasslands and savannas, to the alarming and current practice of clearing land rich in biodiversity, such as tropical forests, for additional grass crop production [17,18]. As one of the largest contributing factors to greenhouse gas emissions and biodiversity reduction, this practice reinforces the urgent need for an alternate, molecular-based approach that targets crop yield maximization.

In addition to their central role in regulating developmental gene expression, plant microRNAs (miRNAs), and more specifically, miRNA-directed gene expression regulation, have more recently been identified as key regulators of plant metabolism, pathogen defense and for a plant to mount an effective adaptive response to abiotic stress [19–21]. Alterations to; (1) miRNA accumulation, and/or; (2) miRNA-directed target gene expression regulation have been extensively described in a wide range of plant species following exposure of the plant under study to abiotic stimuli such as drought stress, salt stress, extreme temperature (both elevated and reduced temperatures) and nutrient deficiency [19–26]. Such research has aimed to construct a more detailed molecular understanding of the fundamental, abiotic stress induced, miRNA-directed gene expression networks in plants. For example, the goal of many groups now actively researching in this space is use of knowledge gained to develop future plant varieties that have been modified to harbor genetic improvements that will aid in the modified plant's ability to cope with, or adapt to, an altered growth environment. Additional studies have further emphasized the critical importance of using a molecular approach to help address this global crisis, as “simply” clearing even more natural ecosystems for the cultivation of additional, non-modified crop species is not efficient, nor is this practice sustainable [1,27,28].

Considering the high level of conservation of many *MICRORNA* (*MIR*) gene families across the monocotyledonous and dicotyledonous evolutionary divide, in conjunction with the phylogenetic proximity of agronomically significant *Poaceae* crop species [29], investigating and manipulating abiotic stress-responsive miRNA/miRNA target gene expression modules presents a promising new and relatively unexplored avenue for the future development of phenotypically superior cropping species. However, a high level of caution is still required when a traditional genetic model plant species, such as *Arabidopsis thaliana* (L.) Heynh (*Arabidopsis*), is used as the basis of the research platform for knowledge advancement in an unrelated and agronomically important species. Furthermore, even the use of a closely related plant species can be problematic when researching a multilayered molecular mechanism such as miRNA-directed gene expression regulation. Here, we will highlight examples of the degree of variation in the profile of six highly conserved miRNAs across several plant species in response to each species being challenged with either the insult of drought or salt stress. Moreover, the degree of variation in the response of stress-responsive miRNAs to abiotic stress, becomes an even

more pronounced challenge when attempting to translate findings made in the traditional genetic model plant species, *Arabidopsis*, to agronomically important *Poaceae* grass crop species.

1. The Impact of Drought and Salt Stress on American and Australian Agriculture

Plant agricultural yield is heavily dictated by climatic conditions [30–32], and although crops are equipped to cope with year-to-year weather variability, recent research has shown that the increasingly unfavorable conditions that accompany man-made climate change are continuing to have a negative impact on global agricultural yield [19,30,33]. The Food and Agriculture Organization (FAO) defines the four key dimensions of food security as; (1) availability; (2) stability; (3) access, and; (4) use, with each of these key dimensions hindered to differing degrees by climate change events, such as prolonged periods of drought [34–36]. This growing and alarming trend is ultimately reducing the global capability to produce the “viable” crop volume required to provide food security, and to additionally provide the required volume of material to offer an alternate and sustainable biofuel source for an exponentially growing world population [27,37,38]. In recent years, it has become widely accepted among plant biologists that the current yield to land capability ratio is significantly insufficient to meet the needs of the predicted world population of 9.5 billion individuals by the year 2050; a population that will require an additional global agricultural output of 60% to 110% [38–40]. To highlight the negative impacts accompanying the abiotic stresses, drought and salt stress, abiotic stresses that significantly reduce global agricultural output annually, this review focuses on key agricultural crop producing regions of the United States of America (US) and Australia, specifically, the crop producing areas of the west coast of the US that rely on irrigation sourced from the Colorado River, and the Murray-Darling Basin of Australia, respectively.

In the US, during the 2015–2016 financial year, 345 million (M) tons of maize were produced, equating to a projected total dollar value of approximately 49 billion (B) US dollars (\$USD; \$USD49B) [41]. The total tonnage and dollar value of the 2015/2016 US maize crop is not surprising considering that from 2013 onwards, 70% of the total human calories consumed globally were derived from grasses, and of this 70%, maize comprised 91.7% of the C₄ grass fraction [42]. However, the possibility of drought to devastate crop yield potential is readily apparent with Daryanto and colleagues (2016) demonstrating that a 40% reduction in water availability results in a 39.3% reduction to total maize yield [43]. Furthermore, this alarming finding is in addition to the study published in the journal, *Nature Climate Change* in 2013. Using historical weather records in combination with modern prediction software, Dai (2013) confidently modeled that the US will suffer from severe and widespread incidents of drought throughout the next century as a direct result of reduced precipitation and/or elevated evaporation [15].

Domestically, the terrestrial surface of the Australian mainland consists of approximately 70% (5.5 million km²) rangeland of mostly arid to semi-arid climate [44,45]. This environment is characterized by; (1) low rainfall; (2) long periods of extreme dryness; (3) infertile soils, and; (4) largely being an inappropriate environment to sustain standard agricultural practices [33,44,45]. The lack of suitability of this environment within the Australian mainland for agricultural use is further shown by the current (March 2018) trend maps obtained from The Australian Government, Bureau of Meteorology (retrieved from <http://www.bom.gov.au/>). These trend maps clearly display an increase in annual mean temperature from 1970–2015, a decline in total annual rainfall over the same period (1970–2015), and a decline in the Normalized Difference Vegetation Index (NDVI), as of August 2015. This publicly available data clearly emphasizes the alarming trends of a rising mean temperature, a reduction in total rainfall, and the almost complete absence of vegetation across the majority of inland Australia (as shown by the lack of “green” vegetation observed by satellite generated NDVI imagery). Australian agriculture therefore remains heavily reliant on the farming practices of the Murray-Darling Basin, an agricultural region that currently contributes approximately 40% of the nation’s agricultural output, equating to \$15B Australian dollars (\$AUD; \$AUD15B) annually [46,47]. This is an impressive production figure considering that the Murray-Darling Basin only represents

approximately 14% of Australia's total land surface area [46,47]. Of considerable concern however, are the reports indicating that by 2030, surface water availability in this region will be drastically reduced, with the utilized data suggesting that this "climatological disaster" has the potential to greatly impede Australia's agricultural commodity production capabilities by up to, and in excess of 27% [48–50]. Furthermore, Australia is the world's sixth largest exporter of agricultural commodities, including: (1) dairy products (\$AUD2.5B); (2) wheat (\$AUD2.0B); (3) other cereal-derived flours (\$AUD1.5B), and; (4) wine (\$AUD3B). Together, these commodities contribute significantly to the global food supply and to the national revenue of Australia [47]. It is, therefore, in the nation's best interest to enhance and refine current farming practices to ensure their future stability, efficiency and production capabilities [47].

On a global scale, over 800 million hectares of soil is impacted by salinity, including groundwater-associated salinity, transient salinity, and irrigation-related salinity [51]. Excluding contributing climatic and topographic factors, the severity and prevalence of salinity affected soil is enhanced by the destructive impact of human activities, be it agricultural or industrial practices [52,53]. Similar to the impact of drought stress, increasing salinity is reducing the global capability to meet the ever-increasing demands for ensuring food security while providing an alternate and sustainable source for biofuel production [37,39]. Therefore, the rapidly growing demands for additional cultivatable soil poses a significant issue that also requires urgent attention to achieve sustainable food and energy production [30–32].

In the US, one of the most salt affected rivers, the Colorado River, is also one of the nation's longest rivers, spanning 2330 km across seven US states, and two additional states in neighboring Mexico. The Colorado River is also the main source of agricultural irrigation and domestic water supply for the Southwest coast of North America. Over three decades ago, Holburt (1984) highlighted that up until 1982, salinity was causing \$USD113M in damage annually in this region, and further predicted that this dollar figure would at least double in future decades [54]. This prediction has proved accurate with a 2004 study [55] revealing that salinity associated issues within the Colorado basin, were causing \$USD150M of annual damage to the entire US agriculture industry, and a total of \$USD300M damage to the US economy [55]. Moreover, the United States Department of Agriculture (USDA) estimated that the state of California (one of the seven US states that the Colorado River and its associated tributaries flow through), contributed a total agricultural market value of \$USD42.6B in 2012 to the US economy: a figure that represents 10.8% of the total US dollar value for that year (<https://www.agcensus.usda.gov/>). Further, when the USDA further breaks this dollar value down into individual contributions made by the crops, maize, wheat and rice, the 2012 Californian crop market value of each species in 2012 was \$USD419M, \$USD341M and \$USD782M, respectively (or, equating to 0.62%, 2.17% and 27% of the total US value of each cropping species, respectively) (<https://www.agcensus.usda.gov/>). Therefore, considering the dollar value that these three *Poaceae* grass crop species contribute to the US economy, in combination with the demonstrated susceptibility of the yield of maize [56], wheat [57,58] and rice [14,59] to salt stress, the immediate requirement for adoption of a molecular approach to generate future phenotypically superior varieties of each of these species, becomes clear.

The Murray-Darling Basin again provides an excellent example of the negative impact salinity has on Australian agriculture, with approximately 71% of the nation's irrigated agricultural production occurring in this region [46]. The process of large-scale commodity production is rapidly exhausting the Murray-Darling Basin's ecological capabilities because of exploitation, drought (see above), and the ever-increasing levels of salinity due to relentless irrigation practices [60,61]. As outlined above, this environmental damage has a direct and negative impact on total crop yield and therefore, Australia's annual agricultural revenue [46,62]. In 2004, the Wilson Report estimated that dryland salinity was costing the Murray-Darling Basin an approximate \$AUD305M loss in profit per annum [63]. Further, this dollar value estimate did not include the cost of damage to indigenous heritage sites, nor the natural environment of the Murray-Darling basin as a whole [63]. Moreover, given that the agricultural practices on which the Wilson Report data was generated, have continued largely unchanged since

the release of the Report in 2004, it is reasonable to suggest that this extensive level of damage, and the monetary costs associated with this ongoing damage, have only increased in each of the fourteen years since the Report's findings were released. It is also reasonable to state that if measures are not implemented in the very near future to enhance current crop capabilities, while in parallel adjusting traditional and unfavorable farming practices under the constantly changing environment, rising salinity will continue to have a widespread and negative impact for; (1) landholders; (2) rural communities; (3) countries that import Australian agriculture products, and obviously; (4) the Australian nation and its economy as a whole [46,47,62,64].

2. The Role of Plant microRNAs in Response to Drought and Salt Stress

Abiotic stress, including drought and salt stress, is one of the major contributors to global crop destruction and yield loss. Although plants are evolutionary equipped to employ physiological and phenotypical mechanisms to adapt to, or to at least tolerate abiotic stress, it is becoming increasingly evident that molecular-based approaches offer a new, alternate, and attractive avenue to generate plant lines with enhanced tolerance to this form of stress [65]. Abiotic stress tolerance can be engineered into new plant lines via the molecular modification of hormone signaling or perception pathways, root and/or shoot architecture, osmotic potential, or metabolic pathways [66]. Such a molecular approach primarily requires switching on, or switching off, the expression of a specific gene(s) that encodes for a specific protein product that is functional at a specific stage of plant development. However, a molecular approach may also be used to modulate, or to "fine tune", the expression of a gene to ensure that a key metabolic enzyme or other biologically relevant protein product is; (1) at the correct level; (2) localized to the appropriate cell or tissue type, or cellular compartment, and; (3) functional as a rate limiting step in a complex biochemical pathway [25,67,68].

In the genetic model species *Arabidopsis*, and once processed from the precursor transcript, the mature miRNA is loaded by the endonuclease, ARGONAUTE1 (AGO1), to form the catalytic core of the miRNA-directed, RNA Induced Silencing Complex (RISC), termed miRISC [69]. The activated miRISC uses the loaded miRNA small RNA (sRNA) as a sequence specificity determinant to target highly complementary messenger RNA (mRNA) transcripts for expression repression via either a mRNA cleavage or translational repression mechanism of miRNA-directed RNA silencing [69]. miRNAs are well known regulators of developmental gene expression [70] and have more recently been identified to also act as central regulators of gene expression in plants to effectively mount; (1) a defense response against invading pathogens (including viruses, bacteria, and fungi), or; (2) an adaptive response to environmental challenge, namely to respond to abiotic stress stimuli [20,71]. Taken together, these findings identify the miRNA class of sRNA, an ideal target for molecular modification as part of the future development of plant lines with engineered resistance (or enhanced resistance) to abiotic or biotic stress. The first step in the development of such plant lines is the molecular manipulation of individual miRNA/miRNA target gene expression modules. The most direct route to achieve this goal is the generation of plant lines with altered miRNA abundance. miRNA overexpression is a very straightforward procedure and is achieved via fusion of the DNA sequence encoding the miRNA precursor transcript to a constitutively, and frequently ubiquitously expressed, promoter such as the 35S promoter from the *Cauliflower mosaic virus* (CaMV), a widely used promoter in *Arabidopsis* transformation approaches [72-75]. Such an approach essentially generates a knockout mutation for each gene transcript that harbors a target site sequence complementary to the miRNA sRNA being over-expressed (see studies; [76-78], respectively for *Arabidopsis*, rice, and wheat-specific examples). miRNA knockdowns, or complete knockouts, have been generated *in planta* via the use of a range of molecular technologies, including the miRNA mimicry [79,80], MIR gene promoter methylation [81], artificial miRNA [82], short tandem target mimicry [83], and miRNA sponge [84] technologies. Each approach differs in the degree of efficacy it offers for the suppression of miRNA abundance (which also differs for each targeted miRNA, per technology). However, each technology allows for the generation of a plant line with elevated miRNA target gene expression, and therefore,

enabling use of the generated plant line to study the biological consequence of miRNA target gene overexpression. The parallel generation of both a miRNA overexpression (a miRNA target gene knockdown plant line) and knockdown (a miRNA target gene overexpression plant line) plant line is highly recommended for the accurate assignment of biological function to the miRNA target gene whose expression is altered in the resulting engineered plant lines: modified plant lines that would be expected to display reciprocal phenotypes when applying the miRNA overexpression and knockdown approaches in parallel.

Numerous studies across the key grass crop species, maize, wheat, and rice, have identified both conserved (found across numerous plant species within the plant kingdom) and non-conserved (found only in a single species, or a group of closely related species within the plant kingdom) miRNAs responsive to either drought or salt stress [85–90]. For example, the studies of [85–88], identified 34, 13, 30 and 5 miRNAs, respectively in maize, wheat, rice, and *Arabidopsis*, responsive to drought stress. Drought-responsive miRNAs were identified in all four of these studies via the application of miRNA microarray hybridization technology. This approach enables direct comparison of the miRNA abundance profiles of “stressed” versus “non-stressed” plants [85–88]. Similarly, 98, 44 and 10 miRNAs were determined responsive to salt stress in the microarray hybridization assays performed in maize [89], wheat [90] and *Arabidopsis* [88], respectively. Additionally, Shen and colleagues (2010) used a modified high throughput assessment, a one-tube, stem-loop primer-based, reverse transcriptase approach to quantify miRNA abundance via subsequent RT-qPCR assessment [91]. This approach identified 18 salt responsive miRNAs in rice [91]. More recent miRNA detection studies, primarily rely on the use of next-generation RNA sequencing (of the sRNA fraction) to identify known and novel miRNAs responsive to either drought or salt stress [23,92,93]. Next-generation sequencing is a high throughput approach that allows for the identification and quantification of transcriptome-wide stress-responsive miRNAs (or other RNA transcripts), compared to a more traditional technology, such as miRNA microarrays. For example, a next-generation sequencing approach was used in rice [93] and wheat [23], to identify 18 and 66 drought-responsive miRNAs, respectively.

3. The Varying Responses of Six Highly Conserved microRNAs to Drought and Salt Stress

Curiously, despite instances of high conservation of miRNA sequence, and miRNA target gene function, across diverse plant species, in combination with the close phylogenetic proximity of key agronomical *Poaceae* family members, numerous examples of differential miRNA accumulation responses to either drought or salt stress have been reported. This is a major issue that requires consideration when comparing the profile of *Arabidopsis* abiotic stress-responsive miRNAs, to those obtained from agronomically important crop species. For example, Zhou and colleagues (2010) revealed that nine miRNAs (including miRNAs, miR156, miR168, miR170, miR171, miR172, miR319, miR396, miR397, and miR408) in drought-stressed rice, returned an opposing accumulation profile comparative to the miRNA profile of drought-stressed *Arabidopsis* [87,88]. Such differences in the response of individual miRNAs to the same abiotic stress treatment (as determined by sRNA abundance fold changes) across *Arabidopsis*, maize, wheat, and rice, are highlighted in Figure 1. Figure 1 clearly shows that the accumulation trend of six highly conserved miRNAs, including miR159, miR164, miR167, miR168, miR396 and miR397, can differ following either drought or salt stress treatment of these four plant species. The selection of the six miRNAs listed in Figure 1 was based on each miRNA being: (1) firmly classified as a highly conserved miRNA; (2) reported in each of the four plant species discussed here, and; (3) demonstrated to direct a regulatory role in a plant’s response to abiotic stress in at least one of the four plant species focused on in this study. We, the authors, readily acknowledge that several recent review articles have detailed the abundance trends of much larger cohorts of miRNAs, and across additional plant species to those reported on here (see the following recent reviews [68,94–97]). However, the primary focus of this article is to identify the experimental and molecular variables that when taken together, potentially account for the reported accumulation differences in the same miRNA

sRNA following exposure to abiotic stresses, drought, and salt stress, across the four plant species under analysis.

Treatment	Species	miR159	miR164	miR167	miR168	miR396	miR397
Target genes		MYB	NAC	ARF	AGO	GRF	LAC
Drought	<i>Arabidopsis</i>	Green	Black	Green	Green	Green	Green
	Rice	Blue	Blue	Blue	Blue	Blue	Red
	Wheat	Blue	Blue	Blue	Blue	Blue	Red
	Maize	Green	Green	Green	Blue	Blue	Black
Salt	<i>Arabidopsis</i>	Green	Green	Green	Green	Green	Green
	Rice	Red	Red	Red	Red	Red	Black
	Wheat	Blue	Blue	Blue	Blue	Blue	Blue
	Maize	Green	Blue	Blue	Blue	Blue	Black

Figure 1. MicroRNA accumulation trends in *Arabidopsis*, rice, wheat, and maize in response to drought and salt stress. The accumulation of miRNAs, miR159, miR164, miR167, miR168, miR396 and miR397, in response to drought and salt stress in *Arabidopsis*, rice, wheat and maize. Green shaded boxes indicate elevated miRNA abundance in response to the applied stress. Red shaded boxes indicate reduced miRNA abundance in response to the applied stress. Blue shaded boxes indicate that miRNA abundance has been reported by different studies to have an opposing abundance trend post exposure to the same stress. Black shaded boxes identify miRNAs for which data is currently lacking in the assessed species. The gene family to which the target gene(s) of each of the 6 selected miRNAs belongs is indicated in the line immediately below the name of the targeting miRNA at the top of each column, more specifically MYB (*MYELOBLASTOSIS*), NAC (*NAM/ATAF/CUC2*), ARF (*AUXIN RESPONSE FACTOR*), AGO (*ARGONAUTE*), GRF (*GROWTH REGULATING FACTOR*) and LAC (*LACCASE*). The data used to construct Figure 1 was sourced from studies [23,68,85–103].

Taking a single example, miR396, from the six presented in Figure 1, differential accumulation trends have been reported for this miRNA in drought-stressed *Arabidopsis* and maize. Namely, in *Arabidopsis*, miR396 abundance was elevated 2.6-fold by drought stress treatment (200 mM mannitol) however, miR396 levels were only mildly upregulated by 0.7-fold in drought-stressed maize (16% *w/v* polyethylene glycol (PEG)-6000) [88,101]. Furthermore, this “positive” drought-induced accumulation profile for the miR396 sRNA is not universal across plant species. For example, microarray assays of “drought-shocked” Emmer wheat (*Triticum dicoccoides* (Körn.) Thell), demonstrated a negative response for miR396 to this stress with miR396 abundance reduced 3.0-fold [86]. Differential abundance trends are also observed for miR396 to salt stress across individual plant species. For example, Liu and colleagues (2008) showed that in *Arabidopsis*, miR396 abundance was upregulated 3.0-fold in response to a 300 mM salt (sodium chloride (NaCl)) stress growth regime, while an opposing and negative accumulation profile was reported for the miR396 sRNA in maize post exposure to salt stress [88,89]. It is important to note here however, that the accumulation profile for miR396 was determined via microarray analysis in *Arabidopsis* [88], whereas a PCR-based approach was used to quantify miR396 abundance in the salt-stressed maize samples [89]. The variation in miRNA abundance profiles across the four assessed plant species in response to drought and salt stress exposure extends beyond miR396, as readily demonstrated for the other five miRNAs also profiled in Figure 1. Figure 1 also clearly

highlights the degree of caution that needs to be exercised by a researcher when assessing miRNA accumulation profiles in response to abiotic stress across individual plant species.

4. Investigation of the Transcription Factor Binding Site Landscapes of *MICRORNA* Gene Promoters

To attempt to account, at least partially, for the reported variability in miRNA accumulation profiles across plant species exposed to the same abiotic stress, the promoter regions of the *MIR* gene loci of maize, rice and *Arabidopsis* that encode miRNAs, miR159, miR164, miR167, miR168, miR396 and miR397, were assessed for the presence of known plant-specific *cis*-regulatory elements (*CREs*). Utilizing PlantCARE (<http://bioinformatics.psb.ugent.be/webtools/plantcare/html/>), an online database that houses 435 known, plant-specific *CREs*, the three kilobase (kb; 3000 base-pairs) region immediately upstream of the *MIR* gene sequence encoding the precursor-miRNA (*pre*-miRNA) transcript (*pre*-miRNA; the region of the larger sized non-protein-coding transcript, the primary miRNA (*pri*-miRNA) that folds back onto itself to form the stem-loop structure of miRNA precursor transcript) of each assessed miRNA was retrieved from the NCBI (<https://www.ncbi.nlm.nih.gov/>) database for this analysis [104]. To reduce the number of *CREs* returned for this analysis, search parameters within the PlantCARE database were limited to only *CREs* previously associated with responses to plant hormones, circadian rhythm, or abiotic stress (see Table 1).

Table 1. The number of transcriptional *cis*-regulatory sites in *MICRORNA* gene promoter regions. The presence of known plant-specific *cis*-regulatory elements (*CREs*) were identified within the 3 kb region immediately upstream of the *pre*-miRNA encoding sequence (the putative promoter region of each assessed *MIR* gene). Only plant hormone, circadian rhythm, and abiotic stress-related *CREs*, were reported for the putative promoter regions of the 70 *MIR* genes that encode the mature miRNAs, miR159, miR164, miR167, miR168, miR396 and miR397, of maize, rice, and *Arabidopsis*, were included in this analysis.

Mature miRNA	Number of Pre-miRNAs	Number of <i>cis</i> -Regulatory Elements in Promoter Region of <i>PRE-MIRNA</i> Encoding Sequence			Total
		Hormone Related	Circadian Rhythm-Related	Abiotic Stress Related	
		<i>Ath</i> -miR159	3 (A-C)	20	
<i>Osa</i> -miR159	6 (A-F)	40	8	47	95
<i>Zma</i> -miR159	8 (A-H)	66	15	56	137
<i>Ath</i> -miR164	3 (A-C)	25	4	25	54
<i>Osa</i> -miR164	6 (A-F)	54	5	65	124
<i>Zma</i> -miR164	8 (A-H)	88	11	76	175
<i>Ath</i> -miR167	4 (A-D)	20	4	31	55
<i>Osa</i> -miR167	10 (A-J)	95	28	82	205
<i>Zma</i> -miR167	4 (A-D)	33	6	31	43
<i>Ath</i> -miR168	2 (A-B)	11	2	10	23
<i>Osa</i> -miR168	1 (A)	6	1	14	21
<i>Zma</i> -miR168	2 (A-B)	16	6	11	33
<i>Ath</i> -miR396	2 (A-B)	18	2	25	45
<i>Osa</i> -miR396	3 (A-C)	26	5	16	47
<i>Zma</i> -miR396	2 (A-B)	12	2	20	34
<i>Ath</i> -miR397	2 (A-B)	10	3	17	30
<i>Osa</i> -miR397	2 (A-B)	22	4	9	35
<i>Zma</i> -miR397	2 (A-B)	17	0	9	26

The online miRNA Repository, the miRBase database (<http://www.mirbase.org>), was initially used to identify the *pre*-miRNA transcript sequences from which the six mature miRNA sRNAs under analysis are liberated. This approach identified 70 unique *pre*-miRNA transcripts from maize, rice and *Arabidopsis*, and subsequent use of these 70 *pre*-miRNA transcript sequences in NCBI, further revealed

that each is derived from a distinct chromosomal position (a unique *MIR* gene locus) within the three searched plant genomes. Upon screening the 3 kb putative “promoter region” upstream of each of the 70 *MIR* genes, a total of 1209 *CREs* relating to plant hormones ($n = 579$ *CREs*), circadian rhythm ($n = 110$ *CREs*) and abiotic stress ($n = 560$ *CREs*) were identified using PlantCARE (Table 1). The abiotic stress-related *CREs* included in this analysis have been demonstrated responsive to, extreme temperature (heat or chilling), drought, anoxic response, aerobic response, and abscisic acid (ABA) signaling. Although abiotic stresses such as extreme temperatures or flooding (driving an anaerobic response) are not the focus of this review, *CREs* responsive to such stimuli were included nonetheless. Their inclusion was to attempt to document the considerable overlap in complex gene networks that the protein products encoded by these genes function in, in a plant that is mounting an adaptive response to an array of abiotic stresses [105,106]. Similarly, given the high degree of documented crosstalk between the plant hormone directed gene expression pathways throughout development, and/or in response to either abiotic and biotic stress [106–109], all plant hormone related *CREs* responsive to, ethylene, salicylic acid, auxin, ABA, gibberellin, and methyl jasmonate, were also included in the PlantCARE analyses (Table 1). Table 1 clearly shows that there is a distinct occurrence of *CREs* harbored within the putative promoter region of each *MIR* gene family assessed (the *MIR159*, *MIR164*, *MIR167*, *MIR168*, *MIR396* and *MIR397* gene families), and further, that the number, and class of *CRE*, differs widely per *MIR* gene family, and per plant species (*Arabidopsis*, rice, and maize). This wide variability in *CREs* presence/absence, and frequency per *MIR* gene locus/gene family, could explain in part, the documented differences in response of *MIR* gene expression (and subsequent mature miRNA accumulation) to either drought or salt stress across *Arabidopsis*, rice, and maize. Table 1 also clearly indicates that when studying miRNA-directed responses to either drought or salt stress, all experimental analyses should be performed in the specific species of interest, in parallel to the functional characterization of the miRNA/miRNA target gene expression module in *Arabidopsis* (if such functional studies cannot also be performed in the specific plant species of interest).

5. Timing, Treatment, Tissue and “Tolerance” to Drought and Salt Stress

To further account for the variability in miRNA accumulation profiles in response to drought or salt stress stimuli, the experimental methodology of the stress treatment must also be considered. It is readily apparent from investigation of the large body of work stemming from either drought or salt stress treatment of plants, that although the “same” abiotic stress is under investigation, there are distinct differences arising from variations in the treatment or preparation of tissues being sampled for subsequent molecular analyses. Specifically; (1) the time of day the tissue is sampled (morning sampling versus sampling in either the afternoon, evening, or night); (2) the developmental phase of the plant (e.g. is the plant being stressed during, vegetative phase, reproductive phase or grain/seed development?); (3) the tissue type selected for analysis (whole plant or seedling versus sampling of only the root tissue, shoot tissue, or reproductive tissue); (4) the form of stress treatment applied (withholding water from soil cultivated plants versus the use of various osmotica in growth media for tissue culture cultivated plants); (5) the severity, timing and length of stress application (mild stress application over an extended treatment period versus a short and intense burst of stress application), and; (6) the degree of stress tolerance across cultivars of an investigated species, across subspecies, or even across closely related plant species. Each of these listed parameters will add to the overall degree of observed variance in miRNA accumulation, and therefore, miRNA-directed target gene expression regulation, in response to either drought or salt stress.

Assessment of the *CRE* landscape of the promoter regions of the six assessed *MIR* gene families, including the *MIR159*, *MIR164*, *MIR167*, *MIR168*, *MIR396* and *MIR397* gene families, across maize, rice and *Arabidopsis*, identified 110 *CREs* related to circadian rhythm harbored within these putative promoter sequences (Table 1). The frequency at which circadian rhythm-related *CREs* were identified, suggests that the transcription of these *MIR* genes is likely already influenced by environmental cues, even in the absence of abiotic stress stimuli. Similar findings have already been reported for *Arabidopsis*

miRNAs, miR167, miR168, miR171 and miR398, with the abundance of each sRNA demonstrated to oscillate between night and day [110]. Further, a tiling array of 114 *Arabidopsis* miRNAs [111] identified multiple circadian rhythm-related miRNAs. These two *Arabidopsis* focused studies, together with the CRE data presented here in Table 1, clearly identify the importance of considering temporal dynamics when a researcher is deciding on the appropriate time of day to harvest their tissue(s) of interest for subsequent molecular assessment of miRNA accumulation and miRNA-regulated gene expression responses to drought or salt stress treatment. The diurnal cycle has also been shown to influence the stability of the key machinery protein, DOUBLE-STRANDED RNA BINDING1 (DRB1). In the plant cell nucleus, DRB1 together with functional partners, DICER-LIKE1 (DCL1; an endonuclease), and SERRATE (SE; a zinc-finger protein with binding affinity for double-stranded RNA (dsRNA)), are an absolute requirement for the accurate and efficient processing of miRNA precursor transcripts as part of the production of the mature miRNA sRNA [112–115]. Cho and colleagues (2014) demonstrated that in the cytoplasm of *Arabidopsis* cells, the E3 ubiquitin ligase, CONSTITUTIVE PHOTOMORPHOGENIC1 (COP1), functions to prevent the protease-mediated degradation of DRB1 [116]. At night however, COP1 is imported into the nucleus and this relocation allows for protease-mediated cleavage of DRB1 (in the absence of COP1 in the cytoplasm) [116]. Given the vital role DRB1 plays in accurate and efficient DCL1-catalyzed miRNA production, this elegant study further identifies the importance of considering the time of day that samples are to be harvested post drought or salt stress treatment of *Arabidopsis*.

Another concern in relation to “timing” is selection of the developmental stage for the application of drought or salt stress to the plant. As a plant transitions between developmental stages, such as the transition from vegetative to reproductive development (floral transition), or the subsequent transition from reproductive to grain and/or seed development, there are pronounced variations to both the physiological and phenotypic characteristics of the plant, both of which are underpinned by intricate, yet distinct genetic networks [117,118]. Moreover, the gene networks controlling these transitions in development, have been shown to be themselves, regulated by miRNAs [119–121]. It is, therefore, highly probable that if an abiotic stress such as drought is encountered by a cropping species such as rice during vegetative development, that the molecular responses underpinning the physiological and phenotypic alterations at this stage of development, would vary greatly compared to those of a rice plant during the reproductive phase of development if an identical stress was encountered. For example, He and colleagues (2012) showed that drought stress during reproductive development in rice resulted in reduced fertility and therefore, overall yield [122]. However, if rice (as well as most other plant species) encounters drought stress during vegetative development, the stressed plant will induce ABA regulatory pathways to ensure that its developmental processes are maintained [123–125]. Therefore, these two vastly distinct physiological responses to the same stress, when encountered at different stages of plant development, would be directed by highly distinct molecular pathways, including unique miRNA-directed gene expression regulation profiles [123,124].

Stress severity is a very important consideration when designing an experiment. A plant will employ specific molecular and physiological networks depending upon the severity, and the duration, of the encountered stress (i.e. is the stress application mild, over an extended treatment period requiring the plant to adapt with adjustments in photosynthetic rates and stomatal conductance or is the stress application intense, for a brief treatment period, requiring the plant to circumvent irreversible damage with heavily reduced transpiration rates and water retention?). In addition to the severity of the applied stress, one must consider the known limitations that exist when using non-ionic stress osmotica, such as mannitol (a penetrating osmotica), or PEG (a semi-penetrating osmotica), as a substitute for drought stress. Osmotica are frequently used to simulate “drought stress” in the genetic model plant *Arabidopsis*, as a desired concentration (and therefore stress severity) is easily included into standard plant cultivation media, allowing for straightforward monitoring and maintenance of environmental variables. With these points taken into consideration, not only is there variation in the severity of the stress based on the selected osmotica, unlike “real” drought stress, molecular

data has the potential to be skewed when osmotica are used: the molecular and/or physiological response of the plant may be accounting for the reduced water status proximal to the root structure, and/or to the *in planta* accumulation of absorbed mannitol or PEG. When investigating miRNA accumulation studies across key grasses and *Arabidopsis*, differences in the treatment used to stimulate drought stress exposure are readily apparent. Of the five papers that investigated miRNA responses to drought stress in either maize, wheat, rice, or *Arabidopsis*; one study used mannitol [88], a second study used PEG [101], 2 studies withheld water to soil cultivated plants (but to differing degrees) [85,87], and Kantar and colleagues (2011) placed plants on paper toweling to induce “drought-shock” [86]. Obviously, each of these different approaches to stimulate drought stress would yield different miRNA responses, even if each approach was being applied to the same species, and at the same stage of development. Furthermore, such a degree of caution should be extended when considering the tissue type to be sampled for subsequent molecular profiling. The division of higher plant organs into source and sink tissues is well documented. More specifically, source tissues include those organs that are photosynthetically active, primarily mature leaves, while sink tissues broadly encompass the photosynthetically inert tissues such as immature leaves, seeds, and roots [126,127]. Given the vastly different roles played by these tissues types, in conjunction with the known crosstalk between the activity of these tissues and plant hormones during periods of abiotic stress, it can be assumed that there would be variance (potentially considerable variance) in miRNA levels between these tissue/organ types communicating each tissue’s changed physiological requirements during abiotic stress [128,129]. Again, when considering the same five papers as above, Liu and colleagues (2008) used whole *Arabidopsis* seedlings 14 days post germination [88], while studies [85–87,101] sampled a variety of young, mature, or whole leaf tissue samples for each plant species under investigation. Such sampling differences will also add further variance in the results generated, namely the abundance of individual miRNA sRNAs under investigation.

It is also important to note that, given the demonstrated regulation of the abundance of the key miRNA pathway machinery protein, DRB1, to external cues such as circadian rhythm (see above), we next determined whether the encoding genes of other key miRNA pathway machinery proteins, including the *DCL1*, *SE*, *DRB1*, *DRB2* and *AGO1* loci, are responsive to drought or salt stress. To address this, the online tool “Expression Angler” was utilized on The Bio-Analytic Resource for Plant Biology (<http://bar.utoronto.ca/ExpressionAngler/>) [130]. The gene identification numbers for *DCL1*, *SE*, *DRB1*, *DRB2* and *AGO1* (*AT1G01040*, *AT2G27100*, *AT1G09700*, *AT2G28380* and *AT1G01040*, respectively) were retrieved from The *Arabidopsis* Information Resource (TAIR, <https://www.arabidopsis.org/>). This analysis revealed that there were no significant expression changes for the *DCL1*, *SE*, *DRB1*, *DRB2* or *AGO1* genes when *Arabidopsis* was exposed to a salt or drought stress growth regime. This finding was unsurprising given that in response to exposure to either stress, the abundance of some *Arabidopsis* miRNAs is elevated while that abundance of a different set of *Arabidopsis* miRNAs is reduced.

It is important to note that all plant species, cultivars, or genotypes of a specific species, respond differently to either drought or salt stress due to the respective baseline tolerance of each to either stress stimulus. Within the *Poaceae* family of grasses for example, maize, wheat, and rice, are all deemed sensitive to reduced water availability or salinity, with each displaying severe yield reductions in response to either stress. However, barley (*Hordeum vulgare* L.), a closely related member within the *Poaceae* family, appears largely unaffected when exposed to either stress [131]. Moreover, it is common within abiotic responsive miRNA studies to profile the miRNA landscape of a “tolerant” versus a “sensitive” cultivar. Frequently, such studies elegantly demonstrate considerable differences in miRNA accumulation profiles for these almost genetically identical plant lines. For example, studies comparing maize [89], or wheat [90] cultivars, identified reciprocal miRNA abundance profiles for 8 (an additional ten miRNAs were only detected in one cultivar and not the other) and nine miRNAs, respectively in response to salt stress. Similarly, a contrast in stress-responsive miRNA, or transcriptome profiles, is noted for genotypes of the same crop species [23,132,133]. Many contemporary research groups

are utilizing genotype-specific molecular stress responses to compare transcriptomes and/or miRNA profiles between genotypes classed as “stress-sensitive” or “stress-tolerant” for the development of superior phenotypes for incorporation into future cereal crop breeding programs [23,132,133]. More specifically, [23] revealed that the significant difference in stress (water-deficiency) tolerance between four closely related genotypes of durum wheat was underpinned by notable differences in their respective miRNA profiles. Most notably, 5 novel, and 16 conserved miRNAs, were demonstrated to have reciprocal abundance profiles in the two “stress-sensitive” and “stress-tolerant” genotypes. Each of the above outlined variables, including the; (1) timing of stress application; (2) specific form of stress treatment applied; (3) tissue sampled for subsequent miRNA profiling, and; (4) degree of stress “tolerance” of the assessed species, all require careful consideration when designing a study to identify either drought or salt stress-responsive miRNAs in the plant species under investigation, or when a researcher is considering translating miRNA findings made in one species, to a second species, regardless of the degree of relatedness of these two species.

6. Non-Conserved microRNAs Responsive to Drought or Salt Stress

A further significant limitation to the use of *Arabidopsis* as a model species for stress-responsive miRNA studies is that many of the miRNAs determined “stress responsive” in the species under investigation, are not present in *Arabidopsis*. The advent of high throughput sequencing technologies has repeatedly highlighted that each plant species produces a population of miRNA sRNAs specific to that species (or across a small clade of closely related species). Such miRNAs are termed, “non-conserved” or “species-specific” miRNAs, a discovery that further questions the use of *Arabidopsis* as an appropriate model for researchers interested in functionally characterizing miRNA-directed stress responses in species such as maize, wheat and rice. For example, Sunkar and colleagues (2008) conducted RNA sequencing to produce control, drought-stressed and salt-stressed sRNA libraries. This approach resulted in the identification of 23 lowly abundant, previously unidentified miRNAs, and an additional, 40 candidate novel miRNAs. Furthermore, each of these newly identified miRNAs were also shown to have differing abundance across the three generated libraries [102]. Similarly, studies by Jiao et al. (2011) and Wei et al. (2009) identified 66 and 23 novel miRNAs in maize and wheat, respectively [85,134]. Although these two studies did not investigate the responsiveness of the identified species-specific miRNAs to drought or salt stress, these two studies in conjunction with the findings of Sunkar et al. (2008), readily highlight the shortcomings of using *Arabidopsis* as a model to study miRNA-directed responses to drought or salt stress application in agronomically important cropping species [85,102,134]. Further, given the high prevalence of contemporary research to employ high throughput sequencing technologies, one can safely hypothesize that the continued identification of species-specific miRNAs, also demonstrated responsive to abiotic stress stimuli, will only further highlight this class of miRNA as potential central players in the future development of modified plant lines with resistance, or enhanced tolerance, to either drought or salt stress. This is evidenced with several recent next-generation sequencing studies identifying novel miRNAs that differentially accumulate in response to abiotic stress, such as drought, in the key cereal crops, rice and wheat [23,92,93]. Interestingly, of the three novel miRNAs (*Osa-cand027*, *Osa-cand052* and *Osa-cand056*) identified as drought responsive by Berrera and colleagues (2012), published degradome analysis failed to identify a putative target gene(s), for any of these three novel miRNAs [93]. Given that target genes, such as phosphate transporters, amino acid transporters, and ATP-dependent RNA helicases, were identified as target genes for other novel rice miRNAs also identified by Berrera et al. (2012), future studies where target genes of these novel species-specific miRNAs are identified, would form an additional and interesting avenue of further research.

7. Conclusions and Future Perspectives

While not always the case, the accumulation profile of an abiotic stress-responsive miRNA can vary considerably across different plant species following exposure to drought or salt stress. This

variation is particularly prevalent when attempting to translate research findings made in the classic genetic model plant species, *Arabidopsis*, to agronomically significant crops, such as maize, wheat or rice. Although *Arabidopsis* has long served as an exceptional model to functionally characterize the plant miRNA pathway, including the characterization of miRNA-directed gene expression regulatory responses to abiotic stress, findings made in *Arabidopsis* may have little, to no, biological relevance in an agronomically important crop species. Therefore, miRNA-directed responses to drought or salt stress need to be experimentally validated in the crop species under assessment prior to the researcher undertaking molecular modification of a specific miRNA/miRNA target gene expression module. Such an approach will ensure that a similar biological response is elicited in the modified species, while also ensuring that other agronomically important parameters, such as yield, are not adversely affected by this modification.

Many researchers now regard plant phenotyping as the bottleneck when attempting to link genotype to phenotype for crop improvement [135,136]. Implementation of a high throughput phenotyping platform is therefore ideal to overcome this bottleneck as such an approach allows for a highly controlled environment, including; watering capabilities in combination with non-destructive imagery techniques that can monitor a plants response to stress at regular intervals across the course of plant development. Further, the parallel application of high throughput sRNA sequencing technologies to complement the high throughput phenotyping platform will allow researchers to identify abiotic stress-responsive, and potentially species-specific miRNAs, that underpin a specific crop plant's ability to mount an effective response against the imposed stress; miRNAs that would otherwise remain elusive if the same miRNA sRNA exploration study was conducted in the long-standing genetic model species, *Arabidopsis*.

Author Contributions: J.L.P., C.P.L.G and A.L.E. conceived and designed the study. J.L.P. performed the reported analyzes and analyzed the data. J.L.P., C.P.L.G and A.L.E. authored the manuscript.

Funding: This research received no external funding.

Conflicts of Interest: The authors declare no conflict of interest.

References

1. Foley, J.A.; Ramankutty, N.; Brauman, K.A.; Cassidy, E.S.; Gerber, J.S.; Johnston, M.; Mueller, N.D.; O'Connell, C.; Ray, D.K.; West, P.C.; et al. Solutions for a cultivated planet. *Nature* **2011**, *478*, 337–342. [[CrossRef](#)] [[PubMed](#)]
2. Glover, J.D.; Reganold, J.P.; Bell, L.W.; Borevitz, J.; Brummer, E.C.; Buckler, E.S.; Cox, C.M.; Cox, T.S.; Crews, T.E.; Culman, S.W.; et al. Increased food and ecosystem security via perennial grains. *Science* **2010**, *328*, 1638–1639. [[CrossRef](#)] [[PubMed](#)]
3. Sarwar, M.H.; Sarwar, M.F.; Sarwar, M.; Qadri, N.A.; Moghal, S. The importance of cereals (Poaceae: Gramineae) nutrition in human health: A review. *J. Cereals Oilseeds* **2013**, *4*, 32–35. [[CrossRef](#)]
4. Mullet, J.; Morishige, D.; McCormick, R.; Truong, S.; Hilley, J.; McKinley, B.; Anderson, R.; Olson, S.N.; Rooney, W. Energy Sorghum – A genetic model for the design of C4 grass bioenergy crops. *J. Exp. Bot.* **2014**, *65*, 3479–3489. [[CrossRef](#)] [[PubMed](#)]
5. Hoang, N.V.; Furtado, A.; Botha, F.C.; Simmons, B.A.; Henry, R.J. Potential for genetic improvement of sugarcane as a source of biomass for biofuels. *Front. Bioeng. Biotechnol.* **2015**, *3*, 182. [[CrossRef](#)] [[PubMed](#)]
6. Baulcombe, D.; Crute, I.; Davies, B.; Dunwell, J.; Gale, M.; Jones, J.; Pretty, J.; Sutherland, W.; Toulmin, C. *Reaping the Benefits: Science and the Sustainable Intensification of Global Agriculture*; The Royal Society: London, UK, 2009; p. 72.
7. Liu, H.; Searle, I.R.; Mather, D.E.; Able, A.J.; Able, J.A. Morphological, physiological and yield responses of durum wheat to pre-anthesis water-deficit stress are genotype-dependent. *Crop Pasture Sci.* **2015**, *66*, 1024–1038. [[CrossRef](#)]
8. Earl, H.J.; Davis, R.F. Effect of drought stress on leaf and whole canopy radiation use efficiency and yield of maize. *Agron. J.* **2003**, *95*, 688–696. [[CrossRef](#)]

9. Giunta, F.; Motzo, R.; Deidda, M. Effect of drought on yield and yield components of durum wheat and triticale in a Mediterranean environment. *Field Crops Res.* **1993**, *33*, 399–409. [[CrossRef](#)]
10. Katerji, N.; Van Hoorn, J.W.; Hamdy, A.; Karam, F.; Mastrorilli, M. Effect of salinity on water stress, growth, and yield of maize and sunflower. *Agric. Water Manag.* **1996**, *30*, 237–249. [[CrossRef](#)]
11. Pessaraki, M.; Tucker, T.C.; Nakabayashi, K. Growth response of barley and wheat to salt stress. *J. Plant Nutr.* **1991**, *14*, 331–340. [[CrossRef](#)]
12. Samarah, N.H. Effects of drought stress on growth and yield of barley. *Agron. Sustain. Dev.* **2005**, *25*, 145–149. [[CrossRef](#)]
13. Venuprasad, R.; Lafitte, H.R.; Atlin, G.N. Response to direct selection for grain yield under drought stress in rice. *J. Trop. Crop Sci.* **2007**, *47*, 285–293. [[CrossRef](#)]
14. Zeng, L.; Shannon, M.C.; Lesch, S.M. Timing of salinity stress affects rice growth and yield components. *Agric. Water Manag.* **2001**, *48*, 191–206. [[CrossRef](#)]
15. Dai, A. Increasing drought under global warming in observations and models. *Nat. Clim. Chang.* **2013**, *3*, 52–58. [[CrossRef](#)]
16. Lobell, D.B.; Field, C.B. Global scale climate–crop yield relationships and the impacts of recent warming. *Environ. Res. Lett.* **2007**, *2*, 014002. [[CrossRef](#)]
17. Foley, J.A.; Asner, G.P.; Costa, M.H.; Coe, M.T.; DeFries, R.; Gibbs, H.K.; Howard, E.A.; Olson, S.; Patz, J.; Ramankutty, N.; et al. Amazonia revealed: Forest degradation and loss of ecosystem goods and services in the Amazon Basin. *Front. Ecol. Environ.* **2007**, *5*, 25–32. [[CrossRef](#)]
18. Monfreda, C.; Ramankutty, N.; Foley, J.A. Farming the planet: 2. Geographic distribution of crop areas, yields, physiological types, and net primary production in the year 2000. *Glob. Biogeochem. Cycles* **2008**, *22*. [[CrossRef](#)]
19. Ding, Y.; Tao, Y.; Zhu, C. Emerging roles of microRNAs in the mediation of drought stress response in plants. *J. Exp. Bot.* **2013**, *64*, 3077–3086. [[CrossRef](#)] [[PubMed](#)]
20. Khraiweh, B.; Zhu, J.K.; Zhu, J. Role of miRNAs and siRNAs in biotic and abiotic stress responses of plants. *BBA Gene Regul. Mech.* **2012**, *1819*, 137–148. [[CrossRef](#)] [[PubMed](#)]
21. Kruszka, K.; Pieczynski, M.; Windels, D.; Bielewicz, D.; Jarmolowski, A.; Szweykowska-Kulinska, Z.; Vazquez, F. Role of microRNAs and other sRNAs of plants in their changing environments. *J. Plant Physiol.* **2012**, *169*, 1664–1672. [[CrossRef](#)] [[PubMed](#)]
22. Budak, H.; Zhang, B. MicroRNAs in model and complex organisms. *Funct. Integr. Genom.* **2017**, *17*, 121–124. [[CrossRef](#)] [[PubMed](#)]
23. Liu, H.; Searle, I.R.; Watson-Haigh, N.S.; Baumann, U.; Mather, D.E.; Able, A.J.; Able, J.A. Genome-wide identification of microRNAs in leaves and the developing head of four durum genotypes during water deficit stress. *PLoS ONE* **2015**, *10*, e0142799. [[CrossRef](#)] [[PubMed](#)]
24. Seki, M.; Narusaka, M.; Ishida, J.; Nanjo, T.; Fujita, M.; Oono, Y.; Shinozaki, K. Monitoring the expression profiles of 7000 *Arabidopsis* genes under drought, cold and high-salinity stresses using a full-length cDNA microarray. *Plant J.* **2002**, *31*, 279–292. [[CrossRef](#)] [[PubMed](#)]
25. Sunkar, R. MicroRNAs with macro-effects on plant stress responses. *Semin. Cell Dev. Biol.* **2010**, *21*, 805–811. [[CrossRef](#)] [[PubMed](#)]
26. Sunkar, R.; Chinnusamy, V.; Zhu, J.; Zhu, J.K. Small RNAs as big players in plant abiotic stress responses and nutrient deprivation. *Trends Plant Sci.* **2007**, *12*, 301–309. [[CrossRef](#)] [[PubMed](#)]
27. Godfray, H.C.J.; Beddington, J.R.; Crute, I.R.; Haddad, L.; Lawrence, D.; Muir, J.F.; Toulmin, C. Food security: The challenge of feeding 9 billion people. *Science* **2010**, *327*, 812–818. [[CrossRef](#)] [[PubMed](#)]
28. Tester, M.; Langridge, P. Breeding technologies to increase crop production in a changing world. *Science* **2010**, *327*, 818–822. [[CrossRef](#)] [[PubMed](#)]
29. Soreng, R.J.; Peterson, P.M.; Romaschenko, K.; Davidse, G.; Zuloaga, F.O.; Judziewicz, E.J.; Filgueiras, T.S.; Davis, J.I.; Morrone, O. A worldwide phylogenetic classification of the Poaceae (Gramineae). *J. Syst. Evol.* **2015**, *53*, 117–137. [[CrossRef](#)]
30. Mittler, R.; Blumwald, E. Genetic engineering for modern agriculture: Challenges and perspectives. *Annu. Rev. Plant Biol.* **2010**, *61*, 443–462. [[CrossRef](#)] [[PubMed](#)]
31. Schlenker, W.; Lobell, D.B. Robust negative impacts of climate change on African agriculture.

- Environ. Res. Lett.* **2010**, *5*, 014010. [CrossRef]
32. Schlenker, W.; Roberts, M.J. Nonlinear temperature effects indicate severe damages to US crop yields under climate change. *Proc. Natl. Acad. Sci. USA* **2009**, *106*, 15594–15598. [CrossRef] [PubMed]
 33. McAlpine, C.A.; Syktus, J.; Ryan, J.G.; Deo, R.C.; McKeon, G.M.; McGowan, H.A.; Phinn, S.R. A continent under stress: Interactions, feedbacks and risks associated with impact of modified land cover on Australia's climate. *Glob. Chang. Biol.* **2009**, *15*, 2206–2223. [CrossRef]
 34. World Food Programme. *The State of Food Insecurity in the World 2013 – The Multiple Dimensions of Food Security*; FAO: Rome, Italy, 2013.
 35. Pinstrup-Andersen, P. Food security: Definition and measurement. *Food Secur.* **2009**, *1*, 5–7. [CrossRef]
 36. Schmidhuber, J.; Tubiello, F.N. Global food security under climate change. *Proc. Natl. Acad. Sci. USA* **2007**, *104*, 19703–19708. [CrossRef] [PubMed]
 37. Lal, R. Soils and food sufficiency. A review. *Agron. Sustain. Dev.* **2009**, *29*, 113–133. [CrossRef]
 38. Long, S.P.; Marshall-Colon, A.; Zhu, X.G. Meeting the global food demand of the future by engineering crop photosynthesis and yield potential. *Cell* **2015**, *161*, 56–66. [CrossRef] [PubMed]
 39. Ray, D.K.; Mueller, N.D.; West, P.C.; Foley, J.A. Yield trends are insufficient to double global crop production by 2050. *PLoS ONE* **2013**, *8*, e66428. [CrossRef] [PubMed]
 40. Tilman, D.; Balzer, C.; Hill, J.; Befort, B.L. Global food demand and the sustainable intensification of agriculture. *Proc. Natl. Acad. Sci. USA* **2011**, *108*, 20260–20264. [CrossRef] [PubMed]
 41. National Corn Growers Association. The World of Corn. Available online: <http://www.worldofcorn.com/> (accessed on 12 December 2017).
 42. FAOSTAT. *Food and Agriculture Organization of the United Nations Statistic Division*; FAO: Rome, Italy, 2015.
 43. Daryanto, S.; Wang, L.; Jacinthe, P.A. Global synthesis of drought effects on maize and wheat production. *PLoS ONE* **2016**, *11*, e0156362. [CrossRef] [PubMed]
 44. Brown, D.; Taylor, J.; Bell, M. The demography of desert Australia. *Rangel. J.* **2008**, *30*, 29–43. [CrossRef]
 45. Turner, D.; Ostendorf, B.; Lewis, M. An introduction to patterns of fire in arid and semi-arid Australia, 1998–2004. *Rangel. J.* **2008**, *30*, 95–107. [CrossRef]
 46. Connor, J.; Schwabe, K.; King, D.; Kaczan, D.; Kirby, M. Impacts of climate change on lower Murray irrigation. *Aust. J. Agric. Resour. Econ.* **2009**, *53*, 437–456. [CrossRef]
 47. Qureshi, M.E.; Hanjra, M.A.; Ward, J. Impact of water scarcity in Australia on global food security in an era of climate change. *Food Policy* **2013**, *38*, 136–145. [CrossRef]
 48. Cline, W.R. *Global Warming and Agriculture: Impact Estimates by Country*; Peterson Institute: Washington, DC, USA, 2007.
 49. Gunasekera, D.; Kim, Y.; Tulloh, C.; Ford, M. Climate change-impacts on Australian agriculture. *Aust. Commod. Forecasts Issues* **2007**, *14*, 657–676.
 50. McJannet, D.L.; Webster, I.T.; Stenson, M.P.; Sherman, B.S. *Estimating Open Water Evaporation for the Murray-Darling Basin: A Report to the Australian Government from the CSIRO Murray-Darling Basin Sustainable Yields Project*; CSIRO: Canberra, Australia, 2008.
 51. Rengasamy, P. Soil processes affecting crop production in salt-affected soils. *Funct. Plant Biol.* **2010**, *37*, 613–620. [CrossRef]
 52. Rengasamy, P. World salinization with emphasis on Australia. *J. Exp. Bot.* **2006**, *57*, 1017–1023. [CrossRef] [PubMed]
 53. Scanlon, B.R.; Jolly, I.; Sophocleous, M.; Zhang, L. Global impacts of conversions from natural to agricultural ecosystems on water resources: Quantity versus quality. *Water Resour. Res.* **2007**, *43*. [CrossRef]
 54. Holburt, M. The lower Colorado – A salty river. *Calif. Agric.* **1984**, *38*, 6–8.
 55. Borda, C. *Economic Impacts from Salinity in the Lower Colorado River Basin*; Technical Memorandum Number EC-04-02; US Department of the Interior, Bureau of Reclamation: Washington, DC, USA, 2004.
 56. Hütsch, B.W.; Jung, S.; Schubert, S. Comparison of Salt and Drought-Stress Effects on Maize Growth and Yield Formation with Regard to Acid Invertase Activity in the Kernels. *J. Agron. Crop Sci.* **2015**, *201*, 353–367. [CrossRef]
 57. Maas, E.V.; Grieve, C.M. Spike and leaf development of salt-stressed wheat. *Crop Sci.* **1990**, *30*, 1309–1313. [CrossRef]
 58. Maas, E.V.; Lesch, S.M.; Francois, L.E.; Grieve, C.M. Tiller development in salt-stressed wheat. *Crop Sci.* **1994**,

- 34, 1594–1603. [[CrossRef](#)]
59. Khatun, S.; Flowers, T.J. Effects of salinity on seed set in rice. *Plant Cell Environ.* **1995**, *18*, 61–67. [[CrossRef](#)]
 60. Axelrod, J. Water Crisis in the Murray-Darling Basin: Australia Attempts to Balance Agricultural Need with Environmental Reality. *Sustain. Dev. Law Policy* **2012**, *12*, 13.
 61. Goss, K.F. Environmental flows, river salinity and biodiversity conservation: Managing trade-offs in the Murray–Darling basin. *Aust. J. Bot.* **2003**, *51*, 619–625. [[CrossRef](#)]
 62. Mullen, J.D.; Crean, J. *Productivity Growth in Australian Agriculture: Trends, Sources, Performance*; This Report Was Prepared for the Australian Farm Institute, the Rural Industries Research and Development Corporation, the Grains Research and Development Corporation, and Meat and Livestock Australia; Australian Farm Institute: Surry Hills, Australia, 2007.
 63. Wilson, S.M. *Dryland and Urban Salinity Costs across the Murray-Darling Basin. An Overview and Guidelines for Identifying and Valuing the Impacts*; Murray-Darling Basin Commission: Canberra, Australia, 2004.
 64. Connor, J.D.; Schwabe, K.; King, D.; Knapp, K. Irrigated agriculture and climate change: The influence of water supply variability and salinity on adaptation. *Ecol. Econ.* **2012**, *77*, 149–157. [[CrossRef](#)]
 65. Mickelbart, M.V.; Hasegawa, P.M.; Bailey-Serres, J. Genetic mechanisms of abiotic stress tolerance that translate to crop yield stability. *Nat. Rev. Genet.* **2015**, *16*, 237–251. [[CrossRef](#)] [[PubMed](#)]
 66. Pierik, R.; Testerink, C. The art of being flexible: How to escape from shade, salt, and drought. *Plant Physiol.* **2014**, *166*, 5–22. [[CrossRef](#)] [[PubMed](#)]
 67. Liu, Q.; Chen, Y.Q. A new mechanism in plant engineering: The potential roles of microRNAs in molecular breeding for crop improvement. *Biotechnol. Adv.* **2010**, *28*, 301–307. [[CrossRef](#)] [[PubMed](#)]
 68. Zhang, B. MicroRNA: A new target for improving plant tolerance to abiotic stress. *J. Exp. Bot.* **2015**, *66*, 1749–1761. [[CrossRef](#)] [[PubMed](#)]
 69. Baumberger, N.; Baulcombe, D.C. *Arabidopsis* ARGONAUTE1 is an RNA Slicer that selectively recruits microRNAs and short interfering RNAs. *Proc. Natl. Acad. Sci. USA* **2005**, *102*, 11928–11933. [[CrossRef](#)] [[PubMed](#)]
 70. Jones-Rhoades, M.W.; Bartel, D.P.; Bartel, B. MicroRNAs and their regulatory roles in plants. *Annu. Rev. Plant Biol.* **2006**, *57*, 19–53. [[CrossRef](#)] [[PubMed](#)]
 71. Kumar, R. Role of microRNAs in biotic and abiotic stress responses in crop plants. *Appl. Biochem. Biotechnol.* **2014**, *174*, 93–115. [[CrossRef](#)] [[PubMed](#)]
 72. Franck, A.; Guilley, H.; Jonard, G.; Richards, K.; Hirth, L. Nucleotide sequence of cauliflower mosaic virus DNA. *Cell* **1980**, *21*, 285–294. [[CrossRef](#)]
 73. Baker, C.C.; Sieber, P.; Wellmer, F.; Meyerowitz, E.M. The early extra petals1 mutant uncovers a role for microRNA miR164c in regulating petal number in *Arabidopsis*. *Curr. Biol.* **2005**, *15*, 303–315. [[CrossRef](#)] [[PubMed](#)]
 74. Fujii, H.; Chiou, T.J.; Lin, S.I.; Aung, K.; Zhu, J.K. A miRNA involved in phosphate-starvation response in *Arabidopsis*. *Curr. Biol.* **2005**, *15*, 2038–2043. [[CrossRef](#)] [[PubMed](#)]
 75. Guo, H.S.; Xie, Q.; Fei, J.F.; Chua, N.H. MicroRNA directs mRNA cleavage of the transcription factor NAC1 to downregulate auxin signals for *Arabidopsis* lateral root development. *Plant Cell* **2005**, *17*, 1376–1386. [[CrossRef](#)] [[PubMed](#)]
 76. Wu, M.F.; Tian, Q.; Reed, J.W. *Arabidopsis* microRNA167 controls patterns of ARF6 and ARF8 expression, and regulates both female and male reproduction. *Development* **2006**, *133*, 4211–4218. [[CrossRef](#)] [[PubMed](#)]
 77. Zhang, Y.C.; Yu, Y.; Wang, C.Y.; Li, Z.Y.; Liu, Q.; Xu, J.; Liao, J.Y.; Wang, X.J.; Qu, L.H.; Chen, F.; et al. Overexpression of microRNA OsmiR397 improves rice yield by increasing grain size and promoting panicle branching. *Nat. Biotechnol.* **2013**, *31*, 848–852. [[CrossRef](#)] [[PubMed](#)]
 78. Jian, C.; Han, R.; Chi, Q.; Wang, S.; Ma, M.; Liu, X.; Zhao, H. Virus-Based MicroRNA Silencing and Overexpressing in Common Wheat (*Triticum aestivum* L.). *Front. Plant Sci.* **2017**, *8*, 500. [[CrossRef](#)] [[PubMed](#)]
 79. Franco-Zorrilla, J.M.; Valli, A.; Todesco, M.; Mateos, I.; Puga, M.I.; Rubio-Somoza, I.; Leyva, A.; Weigel, D.; García, J.A.; Paz-Ares, J. Target mimicry provides a new mechanism for regulation of microRNA activity. *Nat. Genet.* **2007**, *39*, 1033–1037. [[CrossRef](#)] [[PubMed](#)]
 80. Todesco, M.; Rubio-Somoza, I.; Paz-Ares, J.; Weigel, D. A collection of target mimics for comprehensive analysis of microRNA function in *Arabidopsis thaliana*. *PLoS Genet.* **2010**, *6*, e1001031. [[CrossRef](#)] [[PubMed](#)]
 81. Vaistij, F.E.; Elias, L.; George, G.L.; Jones, L. Suppression of microRNA accumulation via RNA interference

- in *Arabidopsis thaliana*. *Plant Mol. Biol.* **2010**, *73*, 391–397. [[CrossRef](#)] [[PubMed](#)]
82. Eamens, A.L.; Agius, C.; Smith, N.A.; Waterhouse, P.M.; Wang, M.B. Efficient silencing of endogenous microRNAs using artificial microRNAs in *Arabidopsis thaliana*. *Mol. Plant* **2011**, *4*, 157–170. [[CrossRef](#)] [[PubMed](#)]
 83. Yan, J.; Gu, Y.; Jia, X.; Kang, W.; Pan, S.; Tang, X.; Chen, X.; Tang, G. Effective small RNA destruction by the expression of a short tandem target mimic in *Arabidopsis*. *Plant Cell* **2012**, *24*, 415–427. [[CrossRef](#)] [[PubMed](#)]
 84. Reichel, M.; Li, Y.; Li, J.; Millar, A.A. Inhibiting plant microRNA activity: Molecular SPONGEs, target MIMICs and STTMs all display variable efficacies against target microRNAs. *Plant Biotechnol. J.* **2015**, *13*, 915–926. [[CrossRef](#)] [[PubMed](#)]
 85. Wei, L.; Zhang, D.; Xiang, F.; Zhang, Z. Differentially expressed miRNAs potentially involved in the regulation of defense mechanism to drought stress in maize seedlings. *Int. J. Plant Sci.* **2009**, *170*, 979–989. [[CrossRef](#)]
 86. Kantar, M.; Lucas, S.J.; Budak, H. miRNA expression patterns of *Triticum dicoccoides* in response to shock drought stress. *Planta* **2011**, *233*, 471–484. [[CrossRef](#)] [[PubMed](#)]
 87. Zhou, L.; Liu, Y.; Liu, Z.; Kong, D.; Duan, M.; Luo, L. Genome-wide identification and analysis of drought-responsive microRNAs in *Oryza sativa*. *J. Exp. Bot.* **2010**, *61*, 4157–4168. [[CrossRef](#)] [[PubMed](#)]
 88. Liu, H.H.; Tian, X.; Li, Y.J.; Wu, C.A.; Zheng, C.C. Microarray-based analysis of stress-regulated microRNAs in *Arabidopsis thaliana*. *RNA* **2008**, *14*, 836–843. [[CrossRef](#)] [[PubMed](#)]
 89. Ding, D.; Zhang, L.; Wang, H.; Liu, Z.; Zhang, Z.; Zheng, Y. Differential expression of miRNAs in response to salt stress in maize roots. *Ann. Bot.* **2009**, *103*, 29–38. [[CrossRef](#)] [[PubMed](#)]
 90. Eren, H.; Pekmezci, M.Y.; Okay, S.; Turktas, M.; Inal, B.; Ilhan, E.; Atak, M.; Erayman, M.; Unver, T. Hexaploid wheat (*Triticum aestivum*) root miRNome analysis in response to salt stress. *Ann. Appl. Biol.* **2015**, *167*, 208–216. [[CrossRef](#)]
 91. Shen, J.; Xie, K.; Xiong, L. Global expression profiling of rice microRNAs by one-tube stem-loop reverse transcription quantitative PCR revealed important roles of microRNAs in abiotic stress responses. *Mol. Genet. Genom.* **2010**, *284*, 477–488. [[CrossRef](#)] [[PubMed](#)]
 92. Bakhshi, B.; Fard, E.M.; Gharechahi, J.; Safarzadeh, M.; Nikpay, N.; Fotovat, R.; Azimi, M.R.; Salekdeh, G.H. The contrasting microRNA content of a drought tolerant and a drought susceptible wheat cultivar. *Plant Physiol.* **2017**, *216*, 35–43. [[CrossRef](#)] [[PubMed](#)]
 93. Barrera-Figueroa, B.E.; Gao, L.; Wu, Z.; Zhou, X.; Zhu, J.; Jin, H.; Liu, R.; Zhu, J.K. High throughput sequencing reveals novel and abiotic stress-regulated microRNAs in the inflorescences of rice. *BMC Plant Biol.* **2012**, *12*, 132. [[CrossRef](#)] [[PubMed](#)]
 94. Noman, A.; Fahad, S.; Aqeel, M.; Ali, U.; Anwar, S.; Baloch, S.K.; Zainab, M. miRNAs: Major modulators for crop growth and development under abiotic stresses. *Biotechnol. Lett.* **2017**, *39*, 685–700. [[CrossRef](#)] [[PubMed](#)]
 95. Shriram, V.; Kumar, V.; Devarumath, R.M.; Khare, T.S.; Wani, S.H. MicroRNAs as potential targets for abiotic stress tolerance in plants. *Front. Plant Sci.* **2016**, *7*, 817. [[CrossRef](#)] [[PubMed](#)]
 96. Liu, H.; Able, A.J.; Able, J.A. SMARTER de-stressed cereal breeding. *Trends Plant Sci.* **2016**, *21*, 909–925. [[CrossRef](#)] [[PubMed](#)]
 97. Alptekin, B.; Langridge, P.; Budak, H. Abiotic stress miRNomes in the *Triticeae*. *Funct. Integr. Genom.* **2017**, *17*, 145–170. [[CrossRef](#)] [[PubMed](#)]
 98. Aravind, J.; Rinku, S.; Pooja, B.; Shikha, M.; Kaliyugam, S.; Mallikarjuna, M.G.; Kumar, A.; Rao, A.R.; Nepolean, T. Identification, characterization, and functional validation of drought-responsive microRNAs in subtropical maize inbreds. *Front. Plant Sci.* **2017**, *8*, 941. [[CrossRef](#)] [[PubMed](#)]
 99. Bakhshi, B.; Fard, E.M.; Nikpay, N.; Ebrahimi, M.A.; Bihamta, M.R.; Mardi, M.; Salekdeh, G.H. MicroRNA signatures of drought signaling in rice root. *PLoS ONE* **2016**, *11*, e0156814. [[CrossRef](#)] [[PubMed](#)]
 100. Mittal, D.; Sharma, N.; Sharma, V.; Sopory, S.K.; Sanan-Mishra, N. Role of microRNAs in rice plant under salt stress. *Ann. Appl. Biol.* **2016**, *168*, 2–18. [[CrossRef](#)]
 101. Li, J.S.; Fu, F.L.; Ming, A.N.; Zhou, S.F.; She, Y.H.; Li, W.C. Differential expression of microRNAs in response to drought stress in maize. *J. Integr. Agric.* **2013**, *12*, 1414–1422. [[CrossRef](#)]
 102. Sunkar, R.; Zhou, X.; Zheng, Y.; Zhang, W.; Zhu, J.K. Identification of novel and candidate miRNAs in rice by high throughput sequencing. *BMC Plant Biol.* **2008**, *8*, 25. [[CrossRef](#)] [[PubMed](#)]

103. Wang, B.; Sun, Y.F.; Song, N.; Wei, J.P.; Wang, X.J.; Feng, H.; Yin, Z.Y.; Kang, Z.S. MicroRNAs involving in cold, wounding and salt stresses in *Triticum aestivum* L. *Plant Physiol. Biochem.* **2014**, *80*, 90–96. [[CrossRef](#)] [[PubMed](#)]
104. Lescot, M.; Déhais, P.; Moreau, Y.; De Moor, B.; Rouzé, P.; Rombauts, S. PlantCARE: A database of plant cis-acting regulatory elements and a portal to tools for in silico analysis of promoter sequences. *Nucleic Acids Res.* **2002**, *30*, 325–327. [[CrossRef](#)] [[PubMed](#)]
105. Dolferus, R.; Klok, E.J.; Ismond, K.; Delessert, C.; Wilson, S.; Good, A.; Peacock, J.; Dennis, L. Molecular basis of the anaerobic response in plants. *IUBMB Life* **2001**, *51*, 79–82. [[CrossRef](#)] [[PubMed](#)]
106. Knight, H.; Knight, M.R. Abiotic stress signalling pathways: Specificity and cross-talk. *Trends Plant Sci.* **2001**, *6*, 262–267. [[CrossRef](#)]
107. Robert-Seilaniantz, A.; Grant, M.; Jones, J.D. Hormone crosstalk in plant disease and defense: More than just jasmonate-salicylate antagonism. *Annu. Rev. Phytopathol.* **2011**, *49*, 317–343. [[CrossRef](#)] [[PubMed](#)]
108. Peleg, Z.; Blumwald, E. Hormone balance and abiotic stress tolerance in crop plants. *Curr. Opin. Plant Biol.* **2011**, *14*, 290–295. [[CrossRef](#)] [[PubMed](#)]
109. Verma, V.; Ravindran, P.; Kumar, P.P. Plant hormone-mediated regulation of stress responses. *BMC Plant Biol.* **2016**, *16*, 86. [[CrossRef](#)] [[PubMed](#)]
110. Siré, C.; Moreno, A.B.; Garcia-Chapa, M.; López-Moya, J.J.; Segundo, B.S. Diurnal oscillation in the accumulation of *Arabidopsis* microRNAs, miR167, miR168, miR171 and miR398. *FEBS Lett.* **2009**, *583*, 1039–1044. [[CrossRef](#)] [[PubMed](#)]
111. Hazen, S.P.; Naef, F.; Quisel, T.; Gendron, J.M.; Chen, H.; Ecker, J.R.; Borevitz, J.O.; Kay, S.A. Exploring the transcriptional landscape of plant circadian rhythms using genome tiling arrays. *Genome Biol.* **2009**, *10*, 17. [[CrossRef](#)] [[PubMed](#)]
112. Dong, Z.; Han, M.H.; Fedoroff, N. The RNA-binding proteins HYL1 and SE promote accurate in vitro processing of pri-miRNA by DCL1. *Proc. Natl. Acad. Sci. USA* **2008**, *105*, 9970–9975. [[CrossRef](#)] [[PubMed](#)]
113. Han, M.H.; Goud, S.; Song, L.; Fedoroff, N. The *Arabidopsis* double-stranded RNA-binding protein HYL1 plays a role in microRNA-mediated gene regulation. *Proc. Natl. Acad. Sci. USA* **2004**, *101*, 1093–1098. [[CrossRef](#)] [[PubMed](#)]
114. Park, W.; Li, J.; Song, R.; Messing, J.; Chen, X. CARPEL FACTORY, a Dicer homolog, and HEN1, a novel protein, act in microRNA metabolism in *Arabidopsis thaliana*. *Curr. Biol.* **2002**, *12*, 1484–1495. [[CrossRef](#)]
115. Yang, L.; Liu, Z.; Lu, F.; Dong, A.; Huang, H. SERRATE is a novel nuclear regulator in primary microRNA processing in *Arabidopsis*. *Plant J.* **2006**, *47*, 841–850. [[CrossRef](#)] [[PubMed](#)]
116. Cho, S.K.; Chaabane, S.B.; Shah, P.; Poulsen, C.P.; Yang, S.W. COPI E3 ligase protects HYL1 to retain microRNA biogenesis. *Nat. Commun.* **2014**, *5*, 5867. [[CrossRef](#)] [[PubMed](#)]
117. Koornneef, M.; Alonso-Blanco, C.; Peeters, A.J.; Soppe, W. Genetic control of flowering time in *Arabidopsis*. *Annu. Rev. Plant Biol.* **1998**, *49*, 345–370. [[CrossRef](#)] [[PubMed](#)]
118. Araki, T. Transition from vegetative to reproductive phase. *Curr. Opin. Plant Biol.* **2001**, *4*, 63–68. [[CrossRef](#)]
119. Wang, J.W. The Multifaceted Roles of miR156-targeted SPL Transcription Factors in Plant Developmental Transitions. *Plant Transcr. Factors* **2015**, 281–293.
120. Fan, T.; Li, X.; Yang, W.; Xia, K.; Ouyang, J.; Zhang, M. Rice osa-miR171c mediates phase change from vegetative to reproductive development and shoot apical meristem maintenance by repressing four OsHAM transcription factors. *PLoS ONE* **2015**, *10*, e0125833. [[CrossRef](#)] [[PubMed](#)]
121. Jung, C.; Pillen, K.; Staiger, D.; Coupland, G.; von Korff, M. Recent Advances in Flowering Time Control. *Front. Plant Sci.* **2017**, *7*, 2011. [[CrossRef](#)] [[PubMed](#)]
122. He, H.; Serraj, R. Involvement of peduncle elongation, anther dehiscence and spikelet sterility in upland rice response to reproductive-stage drought stress. *Environ. Exp. Bot.* **2012**, *75*, 120–127. [[CrossRef](#)]
123. Fujita, Y.; Fujita, M.; Shinozaki, K.; Yamaguchi-Shinozaki, K. ABA-mediated transcriptional regulation in response to osmotic stress in plants. *J. Plant Res.* **2011**, *124*, 509–525. [[CrossRef](#)] [[PubMed](#)]
124. Harb, A.; Krishnan, A.; Ambavaram, M.M.; Pereira, A. Molecular and physiological analysis of drought stress in *Arabidopsis* reveals early responses leading to acclimation in plant growth. *Plant Physiol.* **2010**, *154*, 1254–1271. [[CrossRef](#)] [[PubMed](#)]
125. Yamaguchi-Shinozaki, K.; Shinozaki, K. Transcriptional regulatory networks in cellular responses and tolerance to dehydration and cold stresses. *Annu. Rev. Plant Biol.* **2006**, *57*, 781–803. [[CrossRef](#)] [[PubMed](#)]
126. Roitsch, T. Source-sink regulation by sugar and stress. *Curr. Opin. Plant Biol.* **1999**, *2*, 198–206. [[CrossRef](#)]

127. White, A.C.; Rogers, A.; Rees, M.; Osborne, C.P. How can we make plants grow faster? A source–sink perspective on growth rate. *J. Exp. Bot.* **2015**, *67*, 31–45. [[CrossRef](#)] [[PubMed](#)]
128. Yu, S.M.; Lo, S.F.; Ho, T.H.D. Source–sink communication: Regulated by hormone, nutrient, and stress cross-signalling. *Trends Plant Sci.* **2015**, *20*, 844–857. [[CrossRef](#)] [[PubMed](#)]
129. Kong, L.; Guo, H.; Sun, M. Signal transduction during wheat grain development. *Planta* **2015**, *241*, 789–801. [[CrossRef](#)] [[PubMed](#)]
130. Austin, R.S.; Hiu, S.; Waese, J.; Ierullo, M.; Pasha, A.; Wang, T.T.; Fan, J.; Foong, C.; Breit, R.; Desveaux, D.; et al. New BAR tools for mining expression data and exploring *Cis*-elements in *Arabidopsis thaliana*. *Plant J.* **2016**, *88*, 490–504. [[CrossRef](#)] [[PubMed](#)]
131. Landi, S.; Hausman, J.F.; Guerriero, G.; Esposito, S. Poaceae vs. Abiotic Stress: Focus on Drought and Salt Stress, Recent Insights and Perspectives. *Front. Plant Sci.* **2017**, *8*, 1214. [[CrossRef](#)] [[PubMed](#)]
132. Lenka, S.K.; Katiyar, A.; Chinnusamy, V.; Bansal, K.C. Comparative analysis of drought-responsive transcriptome in Indica rice genotypes with contrasting drought tolerance. *Plant Biotechnol. J.* **2011**, *9*, 315–327. [[CrossRef](#)] [[PubMed](#)]
133. Liu, H.; Able, A.J.; Able, J.A. Genotypic water-deficit stress responses in durum wheat: Association between physiological traits, microRNA regulatory modules and yield components. *Funct. Plant Biol.* **2017**, *44*, 538–551. [[CrossRef](#)]
134. Jiao, Y.; Song, W.; Zhang, M.; Lai, J. Identification of novel maize miRNAs by measuring the precision of precursor processing. *BMC Plant Biol.* **2011**, *11*, 141. [[CrossRef](#)] [[PubMed](#)]
135. Fahlgren, N.; Feldman, M.; Gehan, M.A.; Wilson, M.S.; Shyu, C.; Bryant, D.W.; Hill, S.T.; McEntee, C.J.; Warnasooriya, S.N.; Kumar, I.; et al. A versatile phenotyping system and analytics platform reveals diverse temporal responses to water availability in *Setaria*. *Mol. Plant* **2015**, *8*, 1520–1535. [[CrossRef](#)] [[PubMed](#)]
136. Furbank, R.T.; Tester, M. Phenomics–technologies to relieve the phenotyping bottleneck. *Trends Plant Sci.* **2011**, *16*, 635–644. [[CrossRef](#)] [[PubMed](#)]



© 2018 by the authors. Licensee MDPI, Basel, Switzerland. This article is an open access article distributed under the terms and conditions of the Creative Commons Attribution (CC BY) license (<http://creativecommons.org/licenses/by/4.0/>).

A.1.3 Publication Three



Profiling the Abiotic Stress Responsive microRNA Landscape of *Arabidopsis thaliana*

Joseph L. Pegler, Jackson M. J. Oultram, Christopher P.L. Grof and Andrew L. Eamens *

Centre for Plant Science, School of Environmental and Life Sciences, Faculty of Science, University of Newcastle, Callaghan 2308, Australia; Joseph.Pegler@uon.edu.au (J.L.P.); Jackson.Oultram@uon.edu.au (J.M.J.O.); chris.grof@newcastle.edu.au (C.P.L.G.)

* Correspondence: andy.eamens@newcastle.edu.au; Tel.: +61-249-217-784

Received: 5 February 2019; Accepted: 6 March 2019; Published: 10 March 2019

Abstract: It is well established among interdisciplinary researchers that there is an urgent need to address the negative impacts that accompany climate change. One such negative impact is the increased prevalence of unfavorable environmental conditions that significantly contribute to reduced agricultural yield. Plant microRNAs (miRNAs) are key gene expression regulators that control development, defense against invading pathogens and adaptation to abiotic stress. *Arabidopsis thaliana* (*Arabidopsis*) can be readily molecularly manipulated, therefore offering an excellent experimental system to alter the profile of abiotic stress responsive miRNA/target gene expression modules to determine whether such modification enables *Arabidopsis* to express an altered abiotic stress response phenotype. Towards this goal, high throughput sequencing was used to profile the miRNA landscape of *Arabidopsis* whole seedlings exposed to heat, drought and salt stress, and identified 121, 123 and 118 miRNAs with a greater than 2-fold altered abundance, respectively. Quantitative reverse transcriptase polymerase chain reaction (RT-qPCR) was next employed to experimentally validate miRNA abundance fold changes, and to document reciprocal expression trends for the target genes of miRNAs determined abiotic stress responsive. RT-qPCR also demonstrated that each miRNA/target gene expression module determined to be abiotic stress responsive in *Arabidopsis* whole seedlings was reflective of altered miRNA/target gene abundance in *Arabidopsis* root and shoot tissues post salt stress exposure. Taken together, the data presented here offers an excellent starting platform to identify the miRNA/target gene expression modules for future molecular manipulation to generate plant lines that display an altered response phenotype to abiotic stress.

Keywords: *Arabidopsis thaliana*; abiotic stress; heat stress; drought stress; salt stress; microRNAs (miRNAs); miRNA target gene expression; RT-qPCR

Introduction

Anthropogenically driven climate change is a rapidly growing concern globally, forcing interdisciplinary research collaborations to provide solutions that address and/or negate the numerous negative consequences of a changing climate, with the provision of sustainable food security the overarching goal of contemporary agricultural research [1–3]. Throughout the last half-century, agriculture has attempted to continue to achieve the food demands of an ever-growing global population via the unsustainable practice of clearing biodiverse terrestrial ecosystems for additional cultivation of traditional cropping species, an alarming practice that further contributes to the global carbon footprint and climate change [4,5]. Considering the capability limitation of the current maximum annual global crop yield to land area ratio, it is obvious that alternate strategies are now required if cropping agriculture is to continue to ensure food security, whilst terminating unsustainable farming practices, and while achieving these goals in an ever increasingly unfavorable environment [4].

Lacking the mobility of metazoa, the sessile nature of a plant requires intricate and interrelated gene expression networks to mediate the plant's ability to physiologically and phenotypically respond to its surrounding environment. Such multilayered molecular networks are especially important to a plant's adaptive and/or defensive response when either abiotic or biotic stress is encountered [6,7]. Elucidating the gene expression cascades that underpin the ability of a plant to adapt to, or mitigate, the negative impact of abiotic stress is the first key step in the development of new plant lines harboring molecular modifications which allow the plant to display an altered response phenotype when exposed to abiotic stress. The genetic model plant, *Arabidopsis thaliana* (*Arabidopsis*), is readily amenable to molecular modification, thereby offering plant biology researchers an excellent experimental system to validate which introduced molecular modifications mediate the expression of abiotic stress tolerance phenotypes.

Since their initial identification in *Arabidopsis* in 2002 [8], plant microRNAs (miRNAs), small non-protein-coding regulatory RNAs, have been repeatedly demonstrated to be key regulators of gene expression across all phases of plant development [9,10], in mediating a defense response against invading viral, bacterial or fungal pathogens [11,12], or to direct a plant's adaptive response to exposure to abiotic stress, including the stresses of heat, drought and salt stress [13,14]. Each *Arabidopsis* miRNA is processed from a stem-loop structured precursor transcript, a non-protein-coding RNA that has folded back upon itself to form this structure, post RNA polymerase II (Pol II)-catalyzed transcription from a unique *MICRORNA* (*MIR*) gene [15–17]. Like protein coding loci, the promoter regions of many *MIR* genes harbor *cis*-elements that contribute to the control of *MIR* gene expression in response to numerous signals external to the cell, including the signals that stem from abiotic stress [18–20]. Altered *MIR* gene expression, and therefore altered mature miRNA abundance, in turn leads to changes in miRNA target gene expression, with each miRNA loaded by the miRNA-induced silencing complex (miRISC) to be used as a sequence specificity guide to modulate target gene expression via either a messenger RNA (mRNA) cleavage or translational repression mechanism of RNA silencing [9,21–23]. To date, in *Arabidopsis*, numerous miRNA/target gene expression modules have been demonstrated to be responsive to abiotic stress, with alteration to the molecular profile of some expression modules further shown to assist the plant to adapt to abiotic stress due to molecular-driven changes to key pathways, such as the photosynthesis, sugar signaling, stomatal control and hormone signaling pathways [6,7]. Of particular interest is the demonstration that considerable numbers of *MIR* gene families identified as abiotic stress responsive in *Arabidopsis*, play a conserved functional role across phylogenetically diverse dicotyledonous and monocotyledonous species, including many of the major monocot grasses (such as *Zea mays*, *Oryza sativa* and *Triticum aestivum*) cultivated to provide much of the daily calorific intake of the world's population [24–28]. This demonstration identifies the use of *Arabidopsis* as an ideal experimental system to molecularly modify the profile of such conserved abiotic stress responsive miRNA expression modules to determine if the introduced modifications enable *Arabidopsis* to display an altered response phenotype to abiotic stress.

High throughput sequencing was therefore employed here to profile the miRNA landscape of wild-type *Arabidopsis* plants exposed to heat, drought and salt stress. Sequencing identified large miRNA cohorts responsive to each applied stress, with 121, 123 and 118 miRNA sRNAs determined to have a greater than 2.0-fold abundance change post heat, drought and salt stress treatment of *Arabidopsis* whole seedlings, respectively. For each assessed stress, a quantitative reverse transcriptase polymerase chain reaction (RT-qPCR)-based approach was used to experimentally confirm the abundance of five miRNA sRNAs. For each miRNA experimentally validated to have altered abundance post stress exposure, RT-qPCR was additionally used to document reciprocal target gene expression profiles to further confirm each miRNA/target gene expression module as abiotic stress responsive. Sequencing, and the initial RT-qPCR profiling of miRNA abundance and miRNA target gene expression was performed on whole seedling samples, therefore RT-qPCR was next employed to confirm the documented whole seedling expression trends in *Arabidopsis* root and shoot tissues post salt stress exposure. This analysis showed that the initial abiotic stress responsive miRNA expression profiles

identified in whole plant samples were an accurate representation of the tissue-specific profile of each assessed expression module. Taken together, the data presented here identifies numerous miRNA/target gene expression modules that could be targeted for future molecular modification to determine if such modification allows *Arabidopsis* to display an altered response to abiotic stress. Furthermore, the information gathered in *Arabidopsis* using such a molecular approach could be potentially translated to an agronomically important cropping species for the future generation of plant lines that display an adaptive phenotypic response to abiotic stress.

1. Results

1.1. Response of Wild-type *Arabidopsis* Seedlings to Heat, Drought and Salt Stress

Post germination and cultivation on standard growth media, 8 day old wild-type *Arabidopsis* seedlings (ecotype Columbia-0 (Col-0)) were exposed to a 7-day period of either heat, drought or salt stress. Figure 1A displays the phenotypes expressed by heat, drought and salt stressed Col-0 plants, compared to that of 15 day old, non-stressed wild-type *Arabidopsis*. The growth of drought (mannitol supplemented media) and salt stressed plants was significantly repressed, to differing degrees, after 7 days of exposure to both stress treatments, as readily demonstrated by a reduction to rosette tissue fresh weight (Figure 1B), and rosette diameter (Figure 1C). Furthermore, salt stress treatment induced the accumulation of anthocyanin (Figure 1D), an antioxidant produced by plants to combat the cellular stress caused by reactive oxygen species [29,30], specifically in the shoot apex of salt stressed *Arabidopsis* whole seedlings (Figure 1A). Unlike the reductions observed to rosette tissue fresh weight and the diameter of the rosette of drought and salt stressed Col-0 plants, the 7-day heat stress treatment resulted in the promotion of both of these phenotypic parameters. Specifically, compared to non-stressed control plants, the rosette leaf fresh weight (Figure 1B), and rosette diameter (Figure 1C), were increased by 75% and 127% respectively, in heat stressed Col-0 plants. Promotion of specific aerial tissue growth parameters, namely hypocotyl and rosette leaf petiole elongation, has been reported previously for *Arabidopsis* plants cultivated under conditions of elevated temperature [31,32]. Although promotion of aerial tissue growth suggested that the 7-day heat stress treatment had a positive influence on *Arabidopsis* development, the 177% increase in anthocyanin accumulation observed in parallel (Figure 1D), alternatively suggested that this treatment actually induced high levels of stress in *Arabidopsis* cells, specifically the cells of the shoot apex and rosette leaf petioles (Figure 1A). Therefore, to additionally demonstrate that each applied stress was influencing *Arabidopsis* at the molecular level, the expression of the well characterized stress-induced gene, $\Delta 1$ -PYRROLINE-5-CARBOXYLATE SYNTHETASE1 (*P5CS1*; AT2G39800) [33–35] was quantified by RT-qPCR. This analysis revealed that *P5CS1* transcript abundance was upregulated 3.0-, 1.7- and 45-fold in heat, drought and salt stressed *Arabidopsis* whole seedlings, respectively (Figure 1E).

1.2. Profiling of the microRNA Landscape of Heat, Drought and Salt Stressed *Arabidopsis* Whole Seedlings

Demonstrated induction of *P5CS1* expression (Figure 1E), a well characterized [33–35] stress-induced gene in *Arabidopsis*, post exposure to heat, drought and salt stress, suggested that all three applied stresses were inducing molecular responses in *Arabidopsis*. Therefore, total RNA was extracted from non-stressed plants, and from heat, drought and salt stressed *Arabidopsis* whole seedlings, and the sRNA fraction of each analyzed via high throughput sequencing to profile the respective miRNA landscapes (Figure 2A). In total, 333 miRNA sRNAs were identified by sequencing across the control and stress treatments (see Supplemental Table S1). Sequencing further revealed a greater than 2-fold abundance change for 121, 123 and 118 mature miRNA sRNAs for heat, drought and salt stressed *Arabidopsis* whole seedlings, respectively (Figure 2B). More specifically, heat stress promoted the accumulation of 90 miRNAs (miR395a abundance was increased to the greatest degree at 89.4-fold) and repressed the abundance of 17 miRNAs (miR3932b levels showed the greatest degree of reduction at -19.6-fold). Exposure of wild-type *Arabidopsis* whole seedlings to drought stress enhanced

the abundance of 111 miRNAs and reduced the levels of 2 miRNAs, with the accumulation of miRNAs, miR851 (31.1-fold) and miR397b (-7.8-fold), determined to be influenced to the greatest degree by drought stress treatment. Post salt stress exposure, 86 miRNAs were determined to have a greater than 2-fold elevated abundance (miR778 was upregulated to the greatest degree at 34.0-fold), and further, 22 miRNAs were determined to be reduced in their abundance (miR169g showed the greatest degree of reduction at -8.7-fold). It was also of interest to document reciprocal abundance trends for an additional 5, 5 and 1 miRNA sRNAs upon comparison of each of the applied stresses, namely the heat/drought, heat/salt and drought/salt stress comparisons, respectively. In addition, a further 4 miRNA sRNAs, including miR169f, miR169h, miR397b and miR857, were determined to have an opposing change in abundance upon exposure to each of the three abiotic stresses assessed (Figure 2B). These findings indicate that the promoter regions of the encoding loci of these miRNAs harbor multiple *cis*-elements that direct the changes in *MIR* gene expression which would be required to result in the observed changes in the abundance of this miRNA cohort post exposure to different abiotic stresses [18–20].

A modified RT-qPCR approach [36] was next employed to experimentally validate the sequencing determined abundance of five miRNAs for each stress treatment. For heat stressed *Arabidopsis* whole seedlings, sequencing determined that the abundance of miRNAs, miR169, miR395 and miR396, was altered -7.4, 37.8 and 2.9-fold, respectively, compared to their abundance in non-stressed plants. The altered abundance trend of all three miRNAs was confirmed by RT-qPCR with quantified fold changes of -3.2-, 2.2- and 2.9-fold for the miR169, miR395 and miR396 sRNAs, respectively (Figure 3A–C). Although the abundance changes determined by RT-qPCR were not as dramatic as those determined via sequencing for miRNAs miR169 and miR395 (especially for miR395), the obtainment of a matching abundance trend for each quantified miRNA post heat stress exposure was highly encouraging. Therefore, RT-qPCR was again applied to confirm the sequencing identified abundance fold changes of -2.7-, 4.0- and 2.7-fold for miRNAs, miR857, miR156 and miR399, respectively (Figure 3D–F). Fold changes of -4.3-, 3.0- and 3.2-fold were determined for the miR857, miR156 and miR399 sRNAs respectively, post the 7-day drought stress treatment of *Arabidopsis* whole seedlings by RT-qPCR. RT-qPCR also confirmed the sequencing identified miRNA abundance trends for salt stressed *Arabidopsis* whole seedlings. Fold changes of -2.5-, 2.9- and 3.9-fold were determined by RT-qPCR for miRNAs, miR169, miR399 and miR778 respectively (Figure 3G–I), compared to the abundance fold changes of -4.8-, 4.0- and 34.0-fold determined via sequencing for these three miRNAs in response to salt stress treatment. In addition, miR839 and miR855 abundance in heat, drought and salt stressed plants was also quantified via RT-qPCR due to sequencing indicating that the level of both of these miRNAs did not vary significantly post application of each stress (Figure 3J,K). RT-qPCR confirmed that the levels of these two miRNAs varied less than 0.5-fold post stress exposure, a finding that suggests that neither miRNA is abiotic stress responsive. Taken together, the data presented in Figure 3 demonstrated that the high throughput sequencing employed here (Figure 2) was a reliable tool for profiling miRNA abundance changes in abiotic stressed *Arabidopsis* whole seedlings, and that once identified, RT-qPCR quantification provides a more biologically accurate reflection of the changes in sRNA abundance post exposure to each stress treatment.

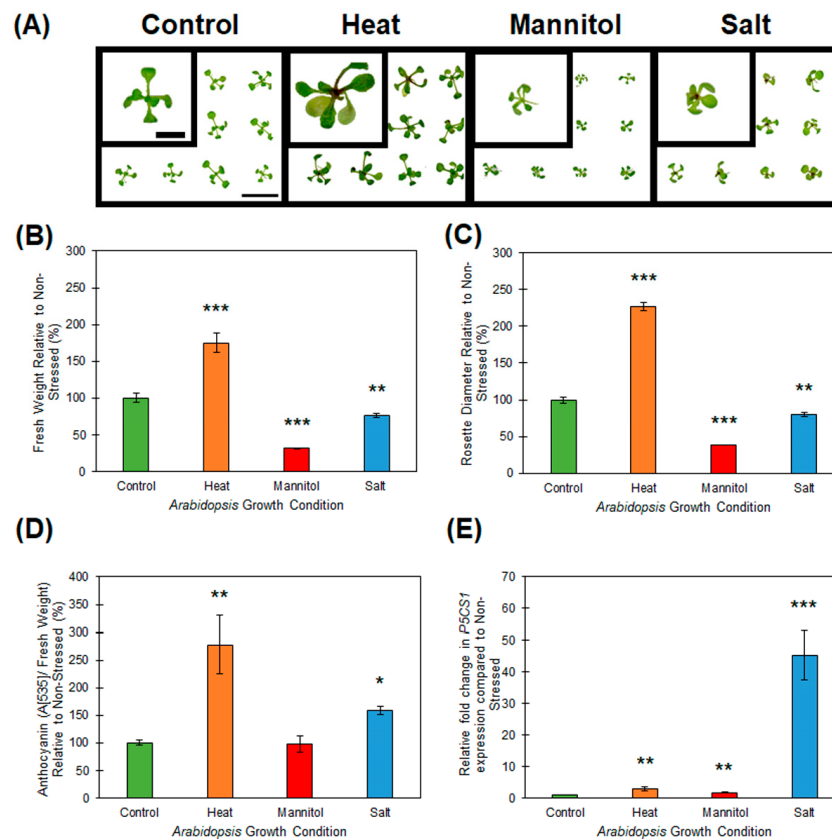


Figure 1. Phenotypic and physiological consequence of heat, drought and salt stress treatment of 15-day-old wild-type *Arabidopsis* whole seedlings. **(A)** Phenotypes displayed by 15-day old wild-type *Arabidopsis* whole seedlings post a 7-day treatment regime with heat, drought or salt stress, compared to non-stressed seedlings of the same age (left panel). Scale bar = 1.0 centimeter (cm) on larger sized panels and 0.5 cm on the superimposed images of a single representative seedling. **(B)** Whole seedling fresh weight of heat, drought (mannitol) and salt stressed *Arabidopsis* compared to their non-stressed counterparts of the same age. **(C)** Rosette diameter of 15-day-old *Arabidopsis* whole seedlings post 7-day exposure to heat, drought (mannitol) and salt stress compared to the non-stressed control. **(D)** Anthocyanin accumulation in heat, drought (mannitol) and salt stressed *Arabidopsis* whole seedlings compared to non-stressed whole seedlings of the same age (15 days). **(E)** RT-qPCR assessment of the expression of the stress induced gene, $\Delta 1$ -PYRROLINE-5-CARBOXYLATE SYNTHETASE1 (*P5CS1*; *AT2G39800*) expression in 15-day-old *Arabidopsis* whole seedlings post a 7-day heat, drought (mannitol) and salt stress treatment regime compared to the abundance of the *P5CS1* transcript in non-stressed *Arabidopsis* whole seedlings of the same age. **(B–E)** Error bars represent the standard deviation of four biological replicates and each biological replicate consisted of a pool of six individual plants. The presence of an asterisk above a column represents a statistically significantly difference between the stress treated sample and the non-stressed control sample (p -value: * < 0.05; ** < 0.005; *** < 0.001).

1.3. Assessment of microRNA Target Gene Expression in Heat, Drought and Salt Stressed *Arabidopsis* Whole Seedlings

It has been extensively documented in *Arabidopsis* that miRNA sRNAs direct expression regulation of their targeted gene(s) via either a mRNA cleavage or translational repression mode of miRNA-directed RNA silencing [9,21–23]. Therefore, to identify the mode of target gene expression regulation directed by the miRNAs experimentally validated here to be responsive to heat, drought or salt stress, RT-qPCR was next employed to reveal the changes in miRNA target gene transcript abundance post exposure of *Arabidopsis* whole seedlings to these three abiotic stresses. For miRNAs, miR169, miR395 and miR396, the three miRNAs determined to be responsive to heat stress treatment via their RT-qPCR-determined, -3.2-, 2.2- and 2.9-fold change in abundance, the transcript level of a

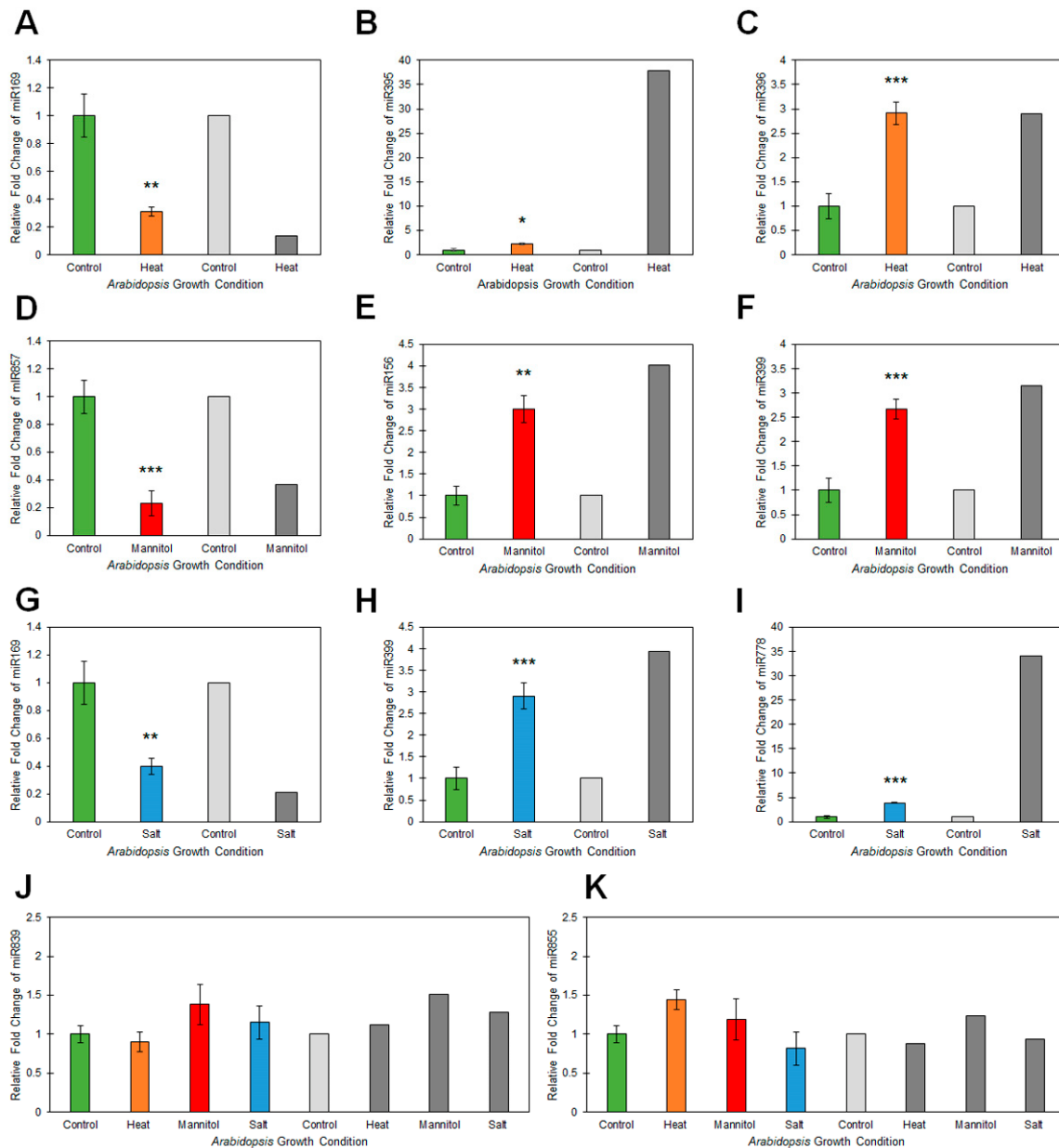


Figure 3. Quantification of miRNA abundance via RT-qPCR analysis of 15-day-old wild-type *Arabidopsis* whole seedlings post exposure to heat, drought and salt stress treatment. (A–C) RT-qPCR assessment of miR169 (A), miR395 (B) and miR396 (C) abundance in heat stressed *Arabidopsis* whole seedlings. (D–F) RT-qPCR assessment of miR857 (D), miR156 (E) and miR399 (F) abundance in drought (mannitol) stressed *Arabidopsis* whole seedlings. (G–I) RT-qPCR assessment of miR169 (G), miR399 (H) and miR778 (I) abundance in salt stressed *Arabidopsis* whole seedlings. (J,K) RT-qPCR assessment of miR839 (J) and miR855 (K) abundance across heat, drought (mannitol) and salt stressed *Arabidopsis* whole seedlings. (A–K) Colored columns (green = non-stressed control; orange = heat stress; red = drought stress, and; blue = salt stress) represent RT-qPCR determined abundance of each quantified miRNA sRNA and the light (control) and dark grey (stress) shaded columns present the fold changes in miRNA abundance as determined via high throughput sequencing. Error bars represent the standard deviation of four biological replicates and each biological replicate consisted of a pool of six individual plants. The presence of an asterisk above a column represents a statistically significantly difference between the stress treated sample and the non-stressed control sample (p -value: * < 0.05; ** < 0.005; *** < 0.001).

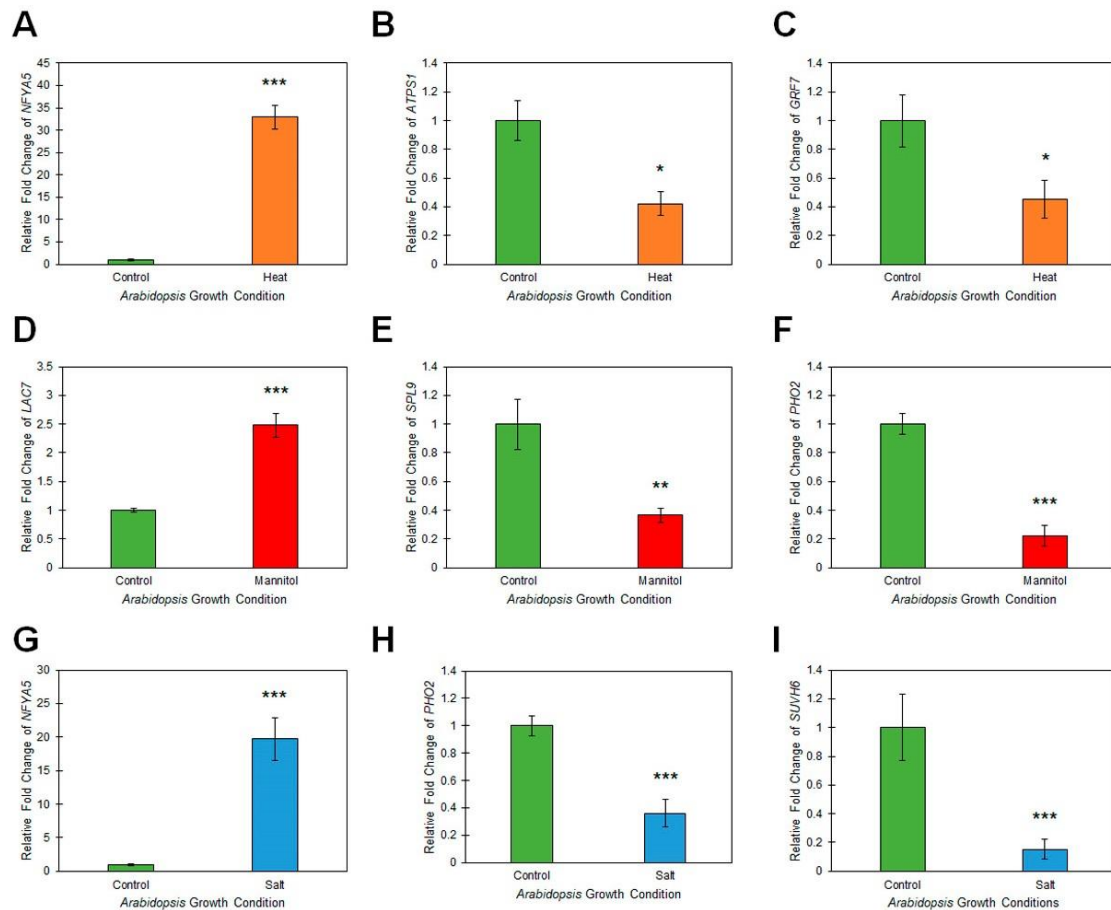


Figure 4. Determination of miRNA target gene expression via RT-qPCR analysis of 15-day-old wild-type *Arabidopsis* whole seedlings post exposure to heat, drought and salt stress treatment. (A–C) RT-qPCR assessment of *NFYA5* (A), *ATPS1* (B) and *GRF7* (C) miRNA target gene expression in heat stressed *Arabidopsis* whole seedlings. (D–F) RT-qPCR assessment of *LAC7* (D), *SPL9* (E) and *PHO2* (F) miRNA target gene expression in drought (mannitol) stressed *Arabidopsis* whole seedlings. (G–I) RT-qPCR assessment of *NFYA5* (G), *PHO2* (H) and *SUVH6* (I) miRNA target gene expression in salt stressed *Arabidopsis* whole seedlings. (A–I) Colored columns (green = non-stressed control; orange = heat stress; red = drought stress, and; blue = salt stress) represent RT-qPCR quantified expression of a single target gene for each miRNA assessed via RT-qPCR analysis in Figure 3. Error bars represent the standard deviation of four biological replicates and each biological replicate consisted of a pool of six individual plants. The presence of an asterisk above a column represents a statistically significantly difference between the stress treated sample and the non-stressed control sample (p -value: * < 0.05; ** < 0.005; *** < 0.001).

Reciprocal expression trends were again observed post RT-qPCR assessment of target gene expression in salt stressed samples. Namely, *NFYA5* transcript abundance was significantly elevated 19.7-fold (Figure 4G) in response to the RT-qPCR documented 2.5-fold reduction in miR169 levels (Figure 3G). Further, the transcript abundance of *PHO2* and *SU(VAR)3-9 HOMOLOG6* (*SUVH6*; *AT2G22740*) was reduced by -2.8- (Figure 4H) and -6.6-fold (Figure 4I), respectively. Reduced *PHO2* and *SUVH6* expression in salt stressed *Arabidopsis* whole seedlings was not a surprising observation considering that the abundance of their targeting miRNAs, miR399 and miR778, was determined to be elevated by 2.9- and 3.9-fold (Figure 3H,I), respectively. Taken together, the target gene expression data presented in Figure 4 indeed suggested that altered miRNA abundance in response to each assessed stress was in turn leading to changes in miRNA target gene transcript abundance. In addition, demonstration of reciprocal trends in abundance for the miRNAs determined to be abiotic stress responsive in Figure 3 compared to the miRNA target gene expression profiles presented in Figure 4,

strongly suggested that each abiotic stress responsive miRNA was regulating the expression of its assessed target gene via a mRNA cleavage mode of miRNA-directed RNA silencing.

1.4. Profiling of Salt Responsive microRNA Expression Modules in *Arabidopsis* Root and Shoot Tissues

To determine whether the documented alterations to abiotic stress responsive miRNA expression modules identified in *Arabidopsis* whole seedlings was an accurate indication of the changes occurring in specific and developmentally distinct *Arabidopsis* tissues, the three miRNA expression modules determined to be salt responsive in *Arabidopsis* whole seedlings (the miR169/*NFYA5*, miR399/*PHO2* and miR778/*SUVH6* expression modules), were profiled in *Arabidopsis* root and shoot tissue by RT-qPCR post exposure to salt stress. Prior to performing this molecular analysis however, the root architecture of wild-type *Arabidopsis* plants cultivated on vertically orientated control and salt stress growth media was assessed. It has been demonstrated previously that the major phenotypic response of the *Arabidopsis* root system to exposure to salt stress is reduced expansion of the primary root [37]. Figure 5A clearly shows that compared to non-stressed wild-type *Arabidopsis* seedlings, the primary phenotypic response of the root system of Col-0 plants exposed to the 7-day salt stress regime was inhibition of primary root elongation, with primary root length reduced by ~60% in salt stressed plants compared to the primary root length of non-stressed control plants (Figure 5A,B).

Inhibition of primary root elongation, coupled with the vertically cultivated salt stressed plants again displaying reductions to the overall size of aerial tissue (i.e., rosette size; Figure 5A), as demonstrated in Figure 1A for *Arabidopsis* plants cultivated on horizontally orientated growth media, led us to next assess *P5CS1* expression in the vertically cultivated salt stressed *Arabidopsis* root and shoot tissue (Figure 5C). Compared to its levels in non-stressed roots and shoots, RT-qPCR revealed *P5CS1* expression to be significantly induced with transcript abundance elevated by 9.1- and 44.0-fold respectively, in salt stressed *Arabidopsis* roots and shoots (Figure 5C). This finding strongly suggested that both tissues types were indeed 'stressed' by the 7 days of vertical cultivation on plant growth media supplemented with 150 mM sodium chloride. RT-qPCR was therefore next employed to profile the miR169/*NFYA5*, miR399/*PHO2* and miR778/*SUVH6* expression modules in salt stressed root and shoot samples and revealed an opposing trend in abundance for each profiled expression module across both assessed tissues. For example, miR169 abundance was determined to be reduced by 1.6- and 2.2-fold in salt stressed roots and shoots respectively (Figure 5D), while *NFYA5* expression was elevated 4.6- and 16.5-fold in these two tissues (Figure 5E). Similar altered trends in abundance for the miR399 sRNA and its targeted transcript, the *PHO2* mRNA, were also revealed by RT-qPCR, namely; miR399 abundance was elevated by 3.7- and 3.0-fold in salt stressed roots and shoots (Figure 5F), and *PHO2* target gene expression was repressed accordingly in the corresponding tissues by 3.6- and 2.3-fold (Figure 5G), respectively. In addition, RT-qPCR revealed that the abundance of the *SUVH6*-targeting miRNA, miR778, was elevated in both salt stressed root and shoot tissue (Figure 5H). The 3.9- and 2.1-fold elevated abundance of the miR778 sRNA in *Arabidopsis* roots and shoots following the salt stress treatment was determined to result in repressed target gene expression, with the abundance of the *SUVH6* transcript reduced by ~2.0-fold in both assessed tissues (Figure 5I). Taken together, the data presented in Figure 5 confirmed that for the three miRNAs determined to be responsive to salt stress, via their profiling in *Arabidopsis* whole seedlings using a high throughput sequencing approach, provided an accurate reflection of the altered abundance of these three miRNAs in developmentally distinct tissues.

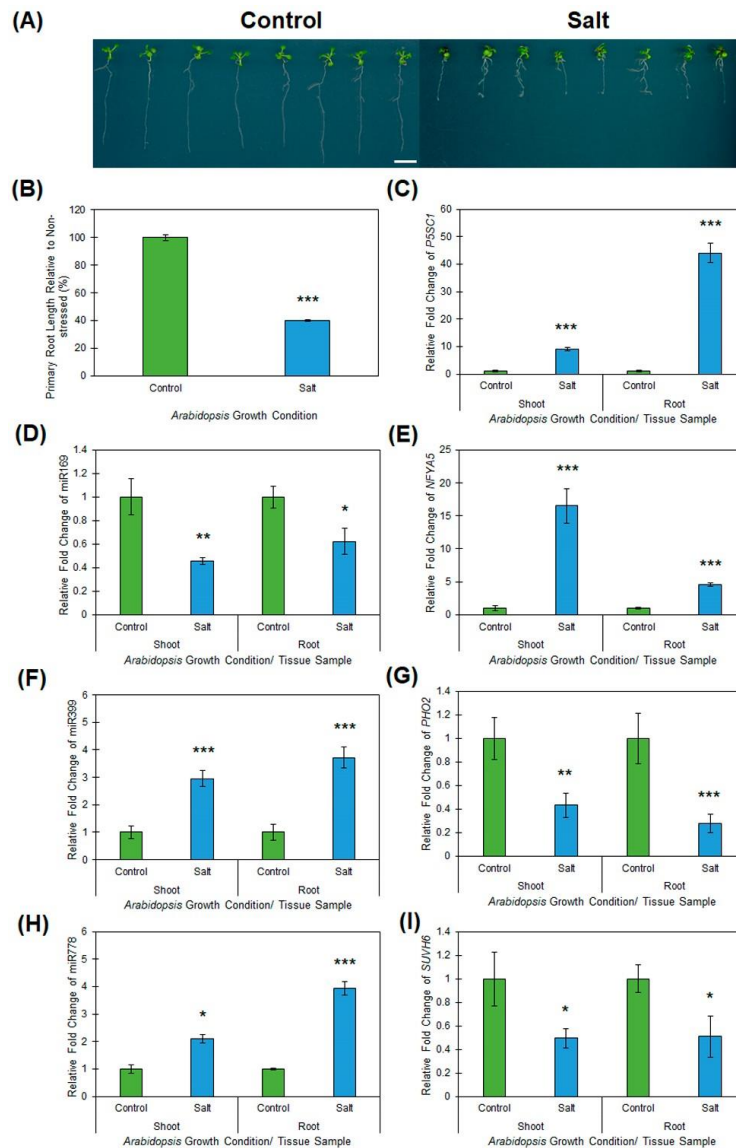


Figure 5. Phenotypic and molecular assessment of the root and shoot tissues of 15-day-old wild-type *Arabidopsis* plants post the 7-day salt stress treatment regime. **(A)** Root and shoot architecture of 15-day-old wild-type *Arabidopsis* seedlings post a 7-day salt stress treatment (right panel) during which the growth media plates were orientated for vertical growth. Scale bar = 1.0 cm. **(B)** Primary root length of 15-day-old *Arabidopsis* whole seedlings cultivated on vertically oriented media growth plates that contained either standard *Arabidopsis* growth media (non-stressed control) or growth media that had been supplemented with 150 mM sodium chloride (stress treatment). **(C)** RT-qPCR assessment of the expression of the stress induced gene, *P5CS1*, expression in 15-day-old *Arabidopsis* root and shoot material post 7-day salt stress treatment compared to the abundance of the *P5CS1* transcript in non-stress control plants of the same age. **(D,E)** RT-qPCR quantification of miR169 abundance **(D)** and *NFYA5* target gene expression **(E)** in salt stressed *Arabidopsis* root and shoot tissues. **(F,G)** RT-qPCR quantification of miR399 abundance **(F)** and *PHO2* target gene expression **(G)** in salt stressed *Arabidopsis* root and shoot tissues. **(H,I)** RT-qPCR quantification of miR778 abundance **(H)** and *SUVH6* target gene expression **(I)** in salt stressed *Arabidopsis* root and shoot tissues. **(B–I)** Colored columns represent the values obtained for non-stressed control plants (green colored columns) and the salt stressed samples (blue colored columns). Error bars represent the standard deviation of four biological replicates and each biological replicate consisted of a pool of six individual plants. The presence of an asterisk above a column represents a statistically significantly difference between the salt stress sample and the non-stressed controls (p -value: * < 0.05; ** < 0.005; *** < 0.001).

2. Discussion

In an attempt to provide sustainable food security into the future, it is essential that the complex, fundamental molecular networks that underpin the ability of a plant to maintain yield, particularly during extended periods of abiotic stress, are elucidated. This would provide the foundation for plant biology researchers to use a molecular approach to develop new plant lines that are readily able to adapt to, or mitigate the negative impacts that result from exposure to abiotic stress. With the miRNA class of sRNA demonstrated to be a key regulator of all aspects of plant development, as well as playing a central role in the ability of a plant to mount a defensive response against invading pathogens, or to mediate an adaptive response to abiotic stress, there currently remains a significant lack of resource datasets available for *Arabidopsis* to allow researchers to identify candidate miRNA expression modules for molecular modification as part of the future development of new plant lines that display adaptive phenotypes to abiotic stress. Towards this goal, here the genetic model plant species, *Arabidopsis thaliana*, was used to profile the miRNA landscape that potentially underpins, in part, the physiological and phenotypic responses of *Arabidopsis* to exposure to the abiotic stresses, heat, drought and salt stress. Most notably, sRNA sequencing revealed that the abundance of 121, 123 and 118 mature miRNA sRNAs was significantly (>2.0-fold) up- or down-regulated in response to heat, drought and salt stress treatment of *Arabidopsis* whole seedlings, respectively. The subsequent experimental validation of the miRNA abundance changes identified via high throughput sequencing by RT-qPCR, in combination with the additional use of RT-qPCR to document reciprocal trends in transcript abundance for each assessed miRNA target gene, was essential to confidently identify the miRNA expression modules responsive to each assessed stress.

In response to heat stress, a significant reduction to miR169 abundance (-3.2-fold) was observed in *Arabidopsis* whole seedlings (Figure 3A). Reduced miR169 levels have been reported previously for *Arabidopsis* post exposure to either drought stress or nitrogen starvation [38,39]. Further, [39] went on to demonstrate that reduced miR169 abundance in drought stressed *Arabidopsis* resulted in deregulated *NFYA5* expression, a target gene expression trend also observed here for heat stressed *Arabidopsis* (Figure 4A). The authors also revealed that overexpression of *NFYA5* in *Arabidopsis* resulted in these molecularly modified plant lines displaying reduced leaf water loss, due to reduced stomatal aperture, and drought stress tolerance [39]. Documentation of similar alterations to the miR169/*NFYA5* expression module in this study post heat stress treatment of *Arabidopsis* whole seedlings (Figure 3A, Figure 4A), to those previously reported for drought stressed *Arabidopsis* [39], suggests that these molecular changes are potentially in part driving the physical adaptation of *Arabidopsis* to both stresses, namely, alteration of stomatal aperture to promote water retention during exposure to such stress. It is also important to note here that the expression of several of the *MIR169* gene loci from which the miR169 precursor transcripts are transcribed were demonstrated to be induced in *Arabidopsis* by heat stress [40]. Induction of *MIR169* gene expression would be expected to result in elevated mature miR169 sRNA accumulation, and not reduced miR169 abundance, as observed here (Figure 3A). Curiously however, [40] did not report on whether *MIR169* gene expression induction actually resulted in elevated miR169 abundance in heat stressed *Arabidopsis* plants. The noted reduction to miR169 abundance reported here for heat stressed *Arabidopsis* plants, suggests that in *Arabidopsis*, heat stress represses *MIR169* gene expression, rather than promote transcription from these loci as reported by [40]. The opposing effect of heat stress exposure on miR169 accumulation in *Arabidopsis* reported here in Figure 3A, to that previously reported [40], could potentially be the result of differences in the application of the stress. Specifically, in [40], two-week-old *Arabidopsis* plants were transferred to moistened filter paper and exposed to the 40 °C heat stress treatment for a duration of either 3 or 6 h, whereas here, 8-day-old *Arabidopsis* seedlings were exposed to a prolonged 7-day heat stress treatment of elevated day/night (16/8 h) temperatures of 32 °C/28 °C. Nonetheless, the detection of elevated target gene (*NFYA5*) expression (Figure 4A), in accordance with the documented reduction in the abundance of the miR169 sRNA (Figure 3A), indicates that the alterations to the miR169/*NFYA5* expression module observed here in heat stressed *Arabidopsis*, are biologically relevant.

Elevated abundance has previously been reported for miRNAs, miR395 and miR396, post exposure of *Arabidopsis* to heat stress [41,42]. Similar abundance changes for the miR395 (Figure 3B) and miR396 (Figure 3C) sRNAs were observed here for heat stressed wild-type *Arabidopsis* whole seedlings. In addition, elevated miRNA abundance was further demonstrated to direct enhanced miRNA-directed target gene expression repression, with both the miR395 and miR396 target genes, *ATPS1* (Figure 4B) and *GRF7* (Figure 4C) respectively, determined to have reduced transcript abundance in heat stressed *Arabidopsis*. Taken together, comparison of the findings reported here, to those reported previously for miR395 and miR396 [41,42], strongly suggest that these two miRNAs are indeed heat stress responsive miRNAs, and further, that enhanced miR395- and miR396-directed expression repression of *ATPS1* and *GRF7*, respectively, potentially forms part of the adaptive response of *Arabidopsis* to elevated temperature.

Here, mannitol was used as an osmoticum to stimulate osmotic stress in *Arabidopsis* whole seedlings in an attempt to replicate drought stress conditions in a tightly controlled growth environment (i.e., sealed plant tissue culture plates). Post stress treatment, miR857 abundance was revealed to be reduced in *Arabidopsis* whole seedlings via both high throughput sequencing and RT-qPCR (Figure 2A, Figure 3D). The miR857 sRNA has previously been demonstrated to post-transcriptionally regulate the expression of *LAC7*, a laccase enzyme involved in mediating lignin deposition in the secondary xylem [43]. In addition to revealing reduced miR857 abundance, RT-qPCR showed that *LAC7* expression was elevated in drought stressed *Arabidopsis* whole seedlings (Figure 4D). Considering its documented role in secondary xylem development, the observed alterations to the miR857/*LAC7* expression module may potentially mediate an adaptive response to osmotic stress in *Arabidopsis*, potentially directing a change to tissue architecture in response to drought stress. Unlike miR857, miR156 and miR399 abundance was elevated by the mannitol-induced drought stress treatment (Figure 3E,F). In accordance, RT-qPCR showed that the transcript abundance of *SPL9* (Figure 4E) and *PHO2* (Figure 4F), the target genes of miR156 and miR399, respectively, was reduced in response to the elevated abundance of their targeting miRNA sRNAs. Interestingly, the miR156/*SPL9* expression module, together with the downstream gene, *DIHYDROFLAVONOL-4-REDUCTASE* (*DFR*; *AT5G42800*) have been demonstrated previously to play a role in anthocyanin metabolism [44], and Figure 1D shows that anthocyanin accumulation remained at its non-stressed levels in *Arabidopsis* plants cultivated on standard growth media supplemented with 200 mM mannitol, in spite of these plants displaying reductions to their fresh weight and rosette diameter, in addition to elevated expression of the stress induced gene, *P5CS1* (Figure 1E). Furthermore, in *Arabidopsis*, both of these miRNAs (miR156 and miR399) have been previously demonstrated to be responsive to mannitol-induced drought stress [41,44], findings that when taken together with those presented here in Figures 3 and 4, strongly suggest that the miR156/*SPL9* and miR399/*PHO2* expression modules are indeed responsive to mannitol-induced drought stress.

High throughput sRNA sequencing and RT-qPCR revealed miR169 abundance to be reduced by -4.8 and -2.5-fold respectively, post exposure to salt stress. This abundance change opposes that reported previously for the miR169 sRNA in rice and cotton [45,46], where miR169 accumulation was demonstrated to be induced by salt stress. However, the observed differences in miR169 abundance post salt stress exposure in rice [45], cotton [46] and *Arabidopsis* (Figure 3G), is most likely the result of unique *cis*-element landscapes of the promoter regions of *MIR169* loci across these three species [19]. In *Arabidopsis*, miR169 abundance has been previously demonstrated to be reduced by drought stress [40], conditions of limited phosphate [47], and nitrogen starvation [38]. The findings of these reports [38,40,47], together with those presented here, namely deregulated *NFYA5* target gene expression in *Arabidopsis* whole seedlings (Figure 4G), roots and shoots (Figure 5E), due to loss of miR169-directed *NFYA5* expression repression in these tissues, indicates that the miR169/*NFYA5* expression module potentially plays a central role in mediating the response of *Arabidopsis* to a range of abiotic stresses, potentially even forming a 'crosstalk junction' to link the highly complicated molecular

networks that are required to direct the physiological and phenotypic responses of *Arabidopsis* to abiotic stress.

Salt stress treatment was shown to enhance miR399 sRNA abundance in *Arabidopsis* whole seedlings (Figure 3H) as well as in root and shoot tissue (Figure 5F), a previously reported finding [41]. Furthermore, and using a molecular approach in *Arabidopsis*, [48] revealed *MIR399F* gene expression to be induced by salt stress and that *Arabidopsis* plants modified to constitutively overexpress the *MIR399F* gene were more tolerant to salt stress than unmodified wild-type plants. Given *PHO2* targeting by miR399, and the previously documented role for phosphate in modulating root system architecture alterations under salt stress conditions in *Arabidopsis*, the elevated abundance of miR399 shown here, in conjunction with the demonstrated reductions to the level of the *PHO2* target transcript (Figure 4H, Figure 5G), are consistent with the proposed role of the miR399/*PHO2* expression module in the complex phosphate-salt regulatory network in *Arabidopsis* tissues [49,50]. Like miR399, miR778 has previously been classed as a phosphate responsive miRNA in *Arabidopsis* [47,51,52]. Here we demonstrate that miR778 abundance is also elevated in response to salt stress in *Arabidopsis* whole seedlings (Figure 3I), roots and shoots (Figure 5H). Accordingly, via a RT-qPCR approach, we further revealed that elevated miR778 abundance resulted in enhanced expression repression of the miR778 target gene, *SUVH6*, in salt stressed *Arabidopsis* tissues (Figure 4I, Figure 5I). Interestingly, the miR778 target, *SUVH6*, is involved in directing methylation of the lysine 9 residue of histone H3 (H3K9 methylation), and further, *SUVH6* expression repression via the constitutive overexpression of the *MIR778* precursor transcript resulted in the modified *Arabidopsis* plants displaying moderately enhanced primary and lateral root growth, and elevated levels of free phosphate and anthocyanin accumulation in the aerial tissues of these plants when cultivated in a phosphate deficient growth environment [52]. These findings, together with the alterations to both the miR399/*PHO2* and miR778/*SUVH6* expression module reported here for salt stressed *Arabidopsis* (Figures 3 and 5), add further weight to the importance of phosphate-mediated responses in *Arabidopsis* tissues as part of the adaptive response of *Arabidopsis* to salt stress.

Altered miRNA abundance, and miRNA target gene expression, have been identified as key molecular responses to an array of abiotic stresses across an evolutionary diverse range of plant species [6,14,24,41,48,49]. Here we have specifically assessed alterations to the miRNA landscapes of heat, drought and salt stressed wild-type *Arabidopsis* whole seedlings and identified large miRNA cohorts responsive to each stress. Alteration to a select number of miRNA/target gene expression modules for the heat, drought and salt stress treatments were experimentally validated via an RT-qPCR approach. Considering that many abiotic responsive miRNAs have been demonstrated to play a conserved functional role across phylogenetically diverse plant species [14,24,25], it is envisaged that the dataset generated in this study forms a valuable resource for the wider plant biology research community; a resource that can be used as the starting point to identify the specific miRNA expression modules to be molecularly manipulated in plant species amenable to genetic modification as part of the future development of plant lines with an altered miRNA and/or miRNA target gene abundance that display a tolerance phenotype to either heat, drought or salt stress. Alternatively, for plant species that are not readily amenable to genetic modification, this dataset can additionally be used to identify the specific miRNA expression modules to be targeted for rapid high throughput screening (via RT-qPCR) across diverse germplasm of a specific species to select those genotypes that harbor natural alterations to the molecular profile of the miRNA expression module of interest.

3. Materials and Methods

3.1. Plant Material

The seeds of wild-type *Arabidopsis thaliana* (*Arabidopsis*), ecotype Columbia-0 (Col-0), were surface sterilized using chlorine gas and post sterilization, seeds were plated out onto standard *Arabidopsis* plant growth media (half strength Murashige and Skoog (MS) salts) and stratified in the dark at 4°C

for 48 h. Post stratification, sealed plates containing the surface sterilized seeds were transferred to a temperature-controlled growth cabinet (A1000 Growth Chamber, Conviron® Australia) and cultivated for 8 days under a standard growth regime of 16 h light/8 h dark and a 22 °C/18 °C day/night temperature. Following this 8-day cultivation period, equal numbers of Col-0 seedlings were transferred under sterile conditions to either fresh standard *Arabidopsis* plant growth media (control treatment), or to plant growth media that had been supplemented with 200 millimolar (mM) mannitol (drought stress treatment) or 150 mM of sodium chloride (salt stress treatment). Post seedling transfer, the non-stressed control and the drought and salt stress treatment plates were returned to the growth cabinet and cultivated for an additional 7-day period under standard growth conditions. For the heat stress treatment, 8-day-old seedlings were also transferred under sterile conditions to standard growth media, however the 16/8 h day/night temperature was elevated to 32 °C/28 °C for the duration of the 7-day stress treatment period. At the end of the 7-day treatment period, all of the phenotypic and molecular assessments reported here were conducted on 15 day old *Arabidopsis* whole seedlings. For the tissue specific analyses reported in Figure 5, plants were treated exactly as outlined above, except for the 7-day treatment period, when 8 day old seedlings were transferred and cultivated on control and salt stress media plates that were orientated for vertical growth.

3.2. Phenotypic and Physiological Assessments

All phenotypic assessments reported here were conducted on 15 day old *Arabidopsis* seedlings. The performance of wild-type *Arabidopsis* plants exposed to each assessed stress is therefore presented relative to non-stressed control plants. More specifically, each phenotypic measurement collected for *Arabidopsis* seedlings exposed to each assessed abiotic stress regime is presented as a percentage of the corresponding measurement determined for non-stressed control seedlings cultivated under standard growth conditions for the duration of the 7-day stress treatment period. Rosette diameter and primary root length analysis was determined via assessment of photographic images using the ImageJ software. A standard 99:1 (v/v) methanol:HCl extraction protocol was used to extract anthocyanin from control and stress treated Col-0 plants. Post extraction, anthocyanin content was determined using a spectrophotometer (Thermo Scientific, Australia) at an absorbance wavelength of 535 nanometers (A_{535}) and using the 99:1 (v/v) methanol:HCl solution as the blank.

3.3. Total RNA Extraction and High Throughput Sequencing of the small RNA Fraction

Total RNA was isolated from four biological replicates (each biological replicate contained 6 individual plants) of 15 day old Col-0 whole seedlings cultivated under normal growth conditions for the duration of the experimental period, or post 7-days of heat, drought or salt stress treatment, using TRIzol™ Reagent (Invitrogen™) according to the manufacturer's instructions. The quality and quantity of the isolated total RNA was assessed using a Nanodrop spectrophotometer (NanoDrop® ND-1000, Thermo Scientific, Australia) and via standard electrophoresis on a 1.2% (w/v) ethidium bromide-stained agarose gel to allow for RNA visualization. Next, 5.0 micrograms (µg) of each of the four biological replicates for each treatment, were pooled together and diluted in RNase-free water to obtain a final preparation of 25 microliters (µL) of total RNA at a concentration of 800 nanograms (ng) per µL. Samples were shipped to the Australian Genome Research Facility (AGRF; Melbourne node, Australia) with the AGRF performing all subsequent preparatory steps prior to sequencing the small RNA fraction of each sample on an Illumina HiSeq 2500 platform.

3.4. Bioinformatic Assessment of the microRNA Landscape of Arabidopsis Whole Seedlings

Using the Qiagen CLC Genomics Workbench (11) software, next-generation sequencing adapter sequences were removed prior to performing sequence quality trimming to remove any sRNA reads that were either shorter than 15 nucleotides (nts), or longer than 35 nts in length. Additionally, parameters within the CLC Genomic Workbench were applied to remove any ambiguous nucleotides at either the 5' or 3' terminus of each sequencing read (i.e., the removal of any 'N' nucleotides on

sequence ends), or to ‘trim’ low quality sequences using a modified ‘*Mott trimming*’ algorithm. The remaining sequences that aligned perfectly (i.e., zero mismatches) to known *Arabidopsis* miRNAs listed in miRBase 22 were then annotated. The values determined for the; (1) raw read count of each detected miRNA sRNA across the four treatments (control, heat, drought and salt); (2) Log₂ fold change in abundance for each miRNA sRNA per stress treatment, compared to the non-stressed control values; (3) total number of high quality raw reads per library; (4) total number of miRNA sRNA raw reads per library, and; (5) percentage of the total library size that the miRNA class of sRNA represents, is presented in Supplemental Table S1.

3.5. Quantitative Reverse Transcriptase Polymerase Chain Reaction Analyses

Quantitative reverse transcriptase polymerase chain reaction (RT-qPCR) assessment of miRNA sRNA and miRNA target gene transcript abundance was conducted on 4 biological replicates: the same four biological replicates that were pooled together to perform the high throughput sequencing analysis of the sRNA fraction of each sample. The synthesis of miRNA-specific complementary DNA (cDNA) was conducted using 200 ng of DNase I treated (New England BioLabs, Australia) total RNA as template and 1.0 unit (U) of ProtoScript[®] II Reverse Transcriptase (New England BioLabs, Australia) according to manufacturer’s instructions. The cycling conditions for miRNA-specific cDNA synthesis were: 1 cycle at 16°C for 30 min; 60 cycles of 30°C for 30 s, 42°C for 30 s 50°C for 2 s, and; 1 cycle of 85°C for 5 min. To generate a global high molecular weight cDNA library for the quantification of miRNA target gene expression, 5.0 µg of total RNA was treated with 5.0 U of DNase I (New England BioLabs, Australia) according to manufacturer’s instructions. Post DNase I treatment, the total RNA was purified using an RNeasy Mini Kit according to the manufacturer’s instructions (Qiagen, Australia), and then 1.0 µg of this preparation was used as template for cDNA synthesis with 1.0 U of ProtoScript[®] II Reverse Transcriptase according to the manufacturer’s instructions (New England Biolabs, Australia) along with 2.5 µM of oligo dT₍₁₈₎. All single stranded cDNA preparations were next diluted to 50 ng/µL in RNase-free water prior to RT-qPCR quantification of miRNA sRNA abundance or miRNA target gene expression. The GoTaq[®] qPCR Master Mix (Promega, Australia) was used as the fluorescent reagent for all performed RT-qPCRs, and all RT-qPCRs had the same cycling conditions of: 1 cycle of 95°C for 10 min, followed by 45 cycles of 95°C for 10 s and 60°C for 15 s. The abundance of each assessed miRNA sRNA and the expression of each examined miRNA target gene was determined using the 2^{-ΔΔCT} method with the small nucleolar RNA, *snoR101*, and *UBIQUITIN10* (*UBI10*; *AT4G05320*) used as the respective internal controls to normalize the relative abundance of each assessed transcript. All DNA oligonucleotides used for either miRNA-specific cDNA synthesis or the quantification of miRNA target gene expression are provided in Supplemental Table S2. For the synthesis of miRNA-specific cDNA of a miRNA sRNA that belongs to a multimember family, and where multiple family members were detected via the high throughput sequencing approach, a miRNA family consensus sequence was determined and the primer designed to hybridize will all detected family members.

Supplementary Materials: The following are available online at <http://www.mdpi.com/2223-7747/8/3/58/s1>, Table S1: Raw miRNA reads and the Log₂ fold change in abundance of each *Arabidopsis thaliana* miRNA sRNA detected via high throughput sRNA sequencing, Table S2: Sequences of the DNA oligonucleotides used in this study for the synthesis of miRNA-specific cDNAs and the RT-qPCR based quantification of miRNA abundance or miRNA target gene expression.

Author Contributions: C.P.L.G. and A.L.E. conceived and designed the research. J.L.P. and J.M.J.O. performed the experiments and analyzed the data. J.L.P., C.P.L.G., J.M.J.O. and A.L.E. authored the manuscript and, J.L.P., C.P.L.G., J.M.J.O. and A.L.E. have read and approved the final version of the manuscript.

Funding: This research received no external funding.

Acknowledgments: The authors would like to thank fellow members of the Centre for Plant Science for their guidance with plant growth care and RT-qPCR experiments.

Conflicts of Interest: The authors declare no conflict of interest.

References

1. Erb, K.H.; Haberl, H.; Plutzer, C. Dependency of global primary bioenergy crop potentials in 2050 on food systems, yields, biodiversity conservation and political stability. *Energy Policy* **2012**, *47*, 260–269. [[CrossRef](#)] [[PubMed](#)]
2. Godfray, H.C.J.; Beddington, J.R.; Crute, I.R.; Haddad, L.; Lawrence, D.; Muir, J.F.; Pretty, J.; Robinson, S.; Thomas, S.M.; Toulmin, C. Food security: The challenge of feeding 9 billion people. *Science* **2010**, *327*, 812–818. [[CrossRef](#)] [[PubMed](#)]
3. Tilman, D.; Balzar, C.; Hill, J.; Befort, B.L. Global food demand and the sustainable intensification of agriculture. *Proc. Natl. Acad. Sci. USA* **2011**, *108*, 20260–20264. [[CrossRef](#)] [[PubMed](#)]
4. Foley, J.A.; Ramankutty, N.; Brauman, K.A.; Cassidy, E.S.; Gerber, J.S.; Johnston, M.; Mueller, N.D.; O'Connell, C.; Ray, D.K.; West, P.C.; et al. Solutions for a cultivated planet. *Nature* **2011**, *478*, 337–342. [[CrossRef](#)] [[PubMed](#)]
5. Ramankutty, N.; Evan, A.T.; Monfreda, C.; Foley, J.A. Farming the planet: 1. Geographic distribution of global agricultural lands in the year 2000. *Glob. Biogeochem. Cycles* **2008**, *22*. [[CrossRef](#)]
6. Khraiwesh, B.; Zhu, J.K.; Zhu, J. Role of miRNAs and siRNAs in biotic and abiotic stress responses of plants. *Biochim. Biophys. Acta* **2012**, *1819*, 137–148. [[CrossRef](#)] [[PubMed](#)]
7. Sunkar, R.; Chinnusamy, V.; Zhu, J.; Zhu, J.K. Small RNAs as big players in plant abiotic stress responses and nutrient deprivation. *Trends Plant Sci.* **2007**, *12*, 301–309. [[CrossRef](#)] [[PubMed](#)]
8. Reinhart, B.J.; Weinstein, E.G.; Rhoades, M.W.; Bartel, B.; Bartel, D.P. MicroRNAs in plants. *Genes Dev.* **2002**, *16*, 1616–1626. [[CrossRef](#)] [[PubMed](#)]
9. Chen, X. A microRNA as a translational repressor of *APETALA2* in *Arabidopsis* flower development. *Science* **2004**, *303*, 2022–2025. [[CrossRef](#)] [[PubMed](#)]
10. Palatnik, J.F.; Allen, E.; Wu, X.; Schommer, C.; Schwab, R.; Carrington, J.C.; Weigel, D. Control of leaf morphogenesis by microRNAs. *Nature* **2003**, *425*, 257–263. [[CrossRef](#)] [[PubMed](#)]
11. Kasschau, K.D.; Xie, Z.; Allen, E.; Llave, C.; Chapman, E.J.; Krizan, K.A.; Carrington, J.C. P1/HC-Pro, a viral suppressor of RNA silencing, interferes with *Arabidopsis* development and miRNA function. *Dev. Cell* **2003**, *4*, 205–217. [[CrossRef](#)]
12. Li, Y.; Zhang, Q.; Zhang, J.; Wu, L.; Qi, Y.; Zhou, J.M. Identification of microRNAs involved in pathogen-associated molecular pattern-triggered plant innate immunity. *Plant Physiol.* **2010**, *152*, 2222–2231. [[CrossRef](#)] [[PubMed](#)]
13. Liu, H.H.; Tian, X.; Li, Y.J.; Wu, C.A.; Zheng, C.C. Microarray-based analysis of stress-regulated microRNAs in *Arabidopsis thaliana*. *RNA* **2008**, *14*, 836–843. [[CrossRef](#)] [[PubMed](#)]
14. Sunkar, R.; Zhu, J.K. Novel and stress-regulated microRNAs and other small RNAs from *Arabidopsis*. *Plant Cell* **2004**, *16*, 2001–2019. [[CrossRef](#)] [[PubMed](#)]
15. Bartel, D.P. MicroRNAs: Genomics, biogenesis, mechanism, and function. *Cell* **2004**, *116*, 281–297. [[CrossRef](#)]
16. Kurihara, Y.; Takashi, Y.; Watanabe, Y. The interaction between DCL1 and HYL1 is important for efficient and precise processing of pri-miRNA in plant microRNA biogenesis. *RNA* **2006**, *12*, 206–212. [[CrossRef](#)] [[PubMed](#)]
17. Vazquez, F.; Gascioli, V.; Cr  t  , P.; Vaucheret, H. The nuclear dsRNA binding protein HYL1 is required for microRNA accumulation and plant development, but not posttranscriptional transgene silencing. *Curr. Biol.* **2004**, *14*, 346–351. [[CrossRef](#)] [[PubMed](#)]
18. Megraw, M.; Baev, V.; Rusinov, V.; Jensen, S.T.; Kalantidis, K.; Hatzigeorgiou, A.G. MicroRNA promoter element discovery in *Arabidopsis*. *RNA* **2006**, *21*, 1612–1619. [[CrossRef](#)] [[PubMed](#)]
19. Pegler, J.L.; Grof, C.P.L.; Eamens, A.L. Profiling of the differential abundance of drought and salt stress-responsive microRNAs across grass crop and genetic model plant species. *Agronomy* **2018**, *8*, 118. [[CrossRef](#)]
20. Zhao, X.; Li, L. Comparative analysis of microRNA promoters in *Arabidopsis* and rice. *Genom. Proteom. Bioinform.* **2013**, *11*, 56–60. [[CrossRef](#)] [[PubMed](#)]
21. Baulcombe, D.C. RNA silencing in plants. *Nature* **2004**, *431*, 356–363. [[CrossRef](#)] [[PubMed](#)]
22. Baumberger, N.; Baulcombe, D.C. *Arabidopsis* ARGONAUTE1 is an RNA Slicer that selectively recruits microRNAs and short interfering RNAs. *Proc. Natl. Acad. Sci. USA* **2005**, *102*, 11928–11933. [[CrossRef](#)] [[PubMed](#)]

23. Reis, R.S.; Hart-Smith, G.; Eamens, A.L.; Wilkins, M.R.; Waterhouse, P.M. Gene regulation by translational inhibition is determined by Dicer partnering proteins. *Nat. Plants* **2015**, *1*, 14027. [[CrossRef](#)] [[PubMed](#)]
24. Noman, A.; Fahad, S.; Aqeel, M.; Ali, U.; Amanullah; Anwar, S.; Baloch, S.K.; Zainab, M. miRNAs: Major modulators for crop growth and development under abiotic stresses. *Biotechnol. Lett.* **2017**, *39*, 685–700. [[CrossRef](#)] [[PubMed](#)]
25. Shriram, V.; Kumar, V.; Devarumath, R.M.; Khare, T.S.; Wani, S.H. MicroRNAs as potential targets for abiotic stress tolerance in plants. *Front. Plant Sci.* **2016**, *14*, 817. [[CrossRef](#)] [[PubMed](#)]
26. Zhang, B. MicroRNA: A new target for improving plant tolerance to abiotic stress. *J. Exp. Bot.* **2015**, *66*, 1749–1761. [[CrossRef](#)] [[PubMed](#)]
27. Zhang, B.; Unver, T. A critical and speculative review on microRNA technology in crop improvement: Current challenges and future directions. *Plant Sci.* **2018**, *274*, 193–200. [[CrossRef](#)] [[PubMed](#)]
28. Liu, H.; Able, A.J.; Able, J.A. SMARTER De-Stressed Cereal Breeding. *Trends Plant Sci.* **2016**, *21*, 909–925. [[CrossRef](#)] [[PubMed](#)]
29. Chalker-Scott, L. Environmental significance of anthocyanins in plant stress responses. *Photochem. Photobiol.* **1999**, *70*, 1–9. [[CrossRef](#)]
30. Lotkowska, M.E.; Tohge, T.; Fernie, A.R.; Xue, G.P.; Balazadeh, S.; Mueller-Roeber, B. The *Arabidopsis* transcription factor MYB112 promotes anthocyanin formation during salinity and under high light stress. *Plant Physiol.* **2015**, *169*, 1862–1880. [[CrossRef](#)] [[PubMed](#)]
31. Gray, W.M.; Östin, A.; Sandberg, G.; Romano, C.P.; Estelle, M. High temperature promotes auxin-mediated hypocotyl elongation in *Arabidopsis*. *Proc. Natl. Acad. Sci. USA* **1998**, *95*, 7197–7202. [[CrossRef](#)] [[PubMed](#)]
32. Koini, M.A.; Alvey, L.; Allen, T.; Tilley, C.A.; Harberd, N.P.; Whitlam, G.C.; Franklin, K.A. High temperature-mediated adaptations in plant architecture require the bHLH transcription factor PIF4. *Curr. Biol.* **2009**, *19*, 408–413. [[CrossRef](#)] [[PubMed](#)]
33. Lv, W.T.; Lin, B.; Zhang, M.; Hua, X.J. Proline accumulation is inhibitory to *Arabidopsis* seedlings during heat stress. *Plant Physiol.* **2011**, *156*, 1921–1933. [[CrossRef](#)] [[PubMed](#)]
34. Urano, K.; Maruyama, K.; Ogata, Y.; Morishita, Y.; Takeda, M.; Sakurai, N.; Suzuki, H.; Saito, K.; Shibata, D.; Kobayashi, M.; et al. Characterization of the ABA-regulated global responses to dehydration in *Arabidopsis* by metabolomics. *Plant J.* **2009**, *56*, 106–1078. [[CrossRef](#)] [[PubMed](#)]
35. Strizhov, N.; Abrahám, E.; Okrész, L.; Blickling, S.; Zilberstein, A.; Schell, J.; Koncz, C.; Szabados, L. Differential expression of two P5CS genes controlling proline accumulation during salt-stress requires ABA and is regulated by ABA1, ABI1 and AXR2 in *Arabidopsis*. *Plant J.* **1997**, *12*, 557–569. [[CrossRef](#)] [[PubMed](#)]
36. Mestdagh, P.; Feys, T.; Bernard, N.; Guenther, S.; Chen, C.; Speleman, F.; Vandesompele, J. High-throughput stem-loop RT-qPCR miRNA expression profiling using minute amounts of input RNA. *Nucleic Acids Res.* **2008**, *36*, e143. [[CrossRef](#)] [[PubMed](#)]
37. Potters, G.; Pasternak, T.P.; Guisez, Y.; Palme, K.J.; Jansen, M.A.K. Stress-induced morphogenic responses: Growing out of trouble? *Trends Plant Sci.* **2007**, *12*, 98–105. [[CrossRef](#)] [[PubMed](#)]
38. Zhao, M.; Ding, H.; Zhu, J.K.; Zhang, F.; Li, W.X. Involvement of miR169 in the nitrogen-starvation responses in *Arabidopsis*. *New Phytol.* **2011**, *190*, 906–915. [[CrossRef](#)] [[PubMed](#)]
39. Li, W.X.; Oono, Y.; Zhu, J.; He, X.J.; Wu, J.M.; Iida, K.; Lu, X.Y.; Cui, X.; Jin, H.; Zhu, J.K. The *Arabidopsis* NFYA5 transcription factor is regulated transcriptionally and posttranscriptionally to promote drought resistance. *Plant Cell* **2008**, *20*, 2238–2251. [[CrossRef](#)] [[PubMed](#)]
40. Li, Y.; Fu, Y.; Ji, L.; Wu, C.; Zheng, C. Characterization and expression analysis of the *Arabidopsis* miR169 family. *Plant Sci.* **2010**, *178*, 271–280. [[CrossRef](#)]
41. Barciszewska-Pacak, M.; Milanowska, K.; Knop, K.; Bielewicz, D.; Nuc, P.; Plewka, P.; Pacak, A.M.; Vazquez, F.; Karlowski, W.; Jarmolowski, A.; et al. *Arabidopsis* microRNA expression regulation in a wide range of abiotic stress responses. *Front. Plant Sci.* **2015**, *6*, 410. [[CrossRef](#)] [[PubMed](#)]
42. Zhong, S.H.; Liu, J.Z.; Jin, H.; Lin, L.; Li, Q.; Chen, Y.; Yuan, Y.X.; Wang, Z.Y.; Huang, H.; Qi, Y.J.; et al. Warm temperatures induce transgenerational epigenetic release of RNA silencing by inhibiting siRNA biogenesis in *Arabidopsis*. *Proc. Natl. Acad. Sci. USA* **2013**, *110*, 9171–9176. [[CrossRef](#)] [[PubMed](#)]
43. Zhao, Y.; Lin, S.; Qiu, Z.; Cao, D.; Wen, J.; Deng, X.; Wang, X.; Lin, J.; Li, X. MicroRNA857 is involved in the regulation of secondary growth of vascular tissues in *Arabidopsis*. *Plant Physiol.* **2015**, *169*, 2539–2552. [[CrossRef](#)] [[PubMed](#)]

44. Cui, L.G.; Shan, J.X.; Shi, M.; Gao, J.P.; Lin, H.X. The *miR156-SPL9-DFR* pathway coordinates the relationship between development and abiotic stress tolerance in plants. *Plant J.* **2014**, *80*, 1108–1117. [[CrossRef](#)] [[PubMed](#)]
45. Zhao, B.; Ge, L.; Liang, R.; Li, W.; Ruan, K.; Lin, H.; Jin, Y. Members of the miR-169 family are induced by high salinity and transiently inhibit the NF-YA transcription factor. *BMC Mol. Biol.* **2009**, *10*, 29. [[CrossRef](#)] [[PubMed](#)]
46. Yin, Z.; Li, Y.; Yu, J.; Liu, Y.; Li, C.; Han, X.; Shen, F. Difference in miRNA expression profiles between two cotton cultivars with distinct salt sensitivity. *Mol. Biol. Rep.* **2012**, *39*, 4961–4970. [[CrossRef](#)] [[PubMed](#)]
47. Hsieh, L.C.; Lin, S.I.; Shih, A.C.; Chen, J.W.; Lin, W.Y.; Tseng, C.Y.; Li, W.H.; Chiou, T.J. Uncovering small RNA-mediated responses to phosphate deficiency in *Arabidopsis* by deep sequencing. *Plant Physiol.* **2009**, *151*, 2120–2132. [[CrossRef](#)] [[PubMed](#)]
48. Baek, D.; Chun, H.J.; Kang, S.; Shin, G.; Park, S.J.; Hong, H.; Kim, C.; Kim, D.H.; Lee, S.Y.; Kim, M.C.; et al. A role for *Arabidopsis miR399f* in salt, drought, and ABA signaling. *Mol. Cell* **2015**, *39*, 111–118.
49. Bari, R.; Pant, B.D.; Stitt, M.; Scheible, W.-R. PHO₂, microRNA399, and PHR1 define a phosphate-signaling pathway in plants. *Plant Physiol.* **2006**, *141*, 988–999. [[CrossRef](#)] [[PubMed](#)]
50. Kawa, D.; Julkowska, M.M.; Sommerfield, H.M.; Ter Horst, A.; Haring, M.A.; Testerink, C. Phosphate-dependent root system architecture responses to salt stress. *Plant Physiol.* **2016**, *172*, 690–706. [[CrossRef](#)] [[PubMed](#)]
51. Pant, B.D.; Musialak-Lange, M.; Nuc, P.; May, P.; Buhtz, A.; Kehr, J.; Walther, D.; Scheible, W.R. Identification of nutrient-responsive *Arabidopsis* and rapeseed microRNAs by comprehensive real-time polymerase chain reaction profiling and small RNA sequencing. *Plant Physiol.* **2009**, *150*, 1541–1555. [[CrossRef](#)] [[PubMed](#)]
52. Wang, L.; Zeng, J.H.Q.; Song, J.; Feng, S.J.; Yang, Z.M. miRNA778 and *SUVH6* are involved in phosphate homeostasis in *Arabidopsis*. *Plant Sci.* **2015**, *238*, 273–285. [[CrossRef](#)] [[PubMed](#)]



© 2019 by the authors. Licensee MDPI, Basel, Switzerland. This article is an open access article distributed under the terms and conditions of the Creative Commons Attribution (CC BY) license (<http://creativecommons.org/licenses/by/4.0/>).

A.1.4 Publication Four



DRB1, DRB2 and DRB4 Are Required for Appropriate Regulation of the microRNA399/*PHOSPHATE2* Expression Module in *Arabidopsis thaliana*

Joseph L. Pegler, Jackson M. J. Oultram, Christopher P. L. Grof and Andrew L. Eamens *

Centre for Plant Science, School of Environmental and Life Sciences, Faculty of Science, University of Newcastle, Callaghan 2308, New South Wales, Australia; Joseph.Pegler@uon.edu.au (J.L.P.); Jackson.Oultram@uon.edu.au (J.M.J.O.); chris.grof@newcastle.edu.au (C.P.L.G.)

* **Correspondence:** andy.eamens@newcastle.edu.au; Tel.: +61-249-217-784

Received: 15 April 2019; Accepted: 9 May 2019; Published: 13 May 2019

Abstract: Adequate phosphorous (P) is essential to plant cells to ensure normal plant growth and development. Therefore, plants employ elegant mechanisms to regulate P abundance across their developmentally distinct tissues. One such mechanism is *PHOSPHATE2* (*PHO2*)-directed ubiquitin-mediated degradation of a cohort of phosphate (PO_4) transporters. *PHO2* is itself under tight regulation by the PO_4 responsive microRNA (miRNA), miR399. The DOUBLE-STRANDED RNA BINDING (DRB) proteins, DRB1, DRB2 and DRB4, have each been assigned a specific functional role in the *Arabidopsis thaliana* (*Arabidopsis*) miRNA pathway. Here, we assessed the requirement of DRB1, DRB2 and DRB4 to regulate the miR399/*PHO2* expression module under PO_4 starvation conditions. Via the phenotypic and molecular assessment of the knockout mutant plant lines, *drb1*, *drb2* and *drb4*, we show here that; (1) DRB1 and DRB2 are required to maintain P homeostasis in *Arabidopsis* shoot and root tissues; (2) DRB1 is the primary DRB required for miR399 production; (3) DRB2 and DRB4 play secondary roles in regulating miR399 production, and; (4) miR399 appears to direct expression regulation of the *PHO2* transcript via both an mRNA cleavage and translational repression mode of RNA silencing. Together, the hierarchical contribution of DRB1, DRB2 and DRB4 demonstrated here to be required for the appropriate regulation of the miR399/*PHO2* expression module identifies the extreme importance of P homeostasis maintenance in *Arabidopsis* to ensure that numerous vital cellular processes are maintained across *Arabidopsis* tissues under a changing cellular environment.

Keywords: *Arabidopsis thaliana*; phosphorous (P); phosphate (PO_4) stress; microRNA (miRNA); miR399; *PHOSPHATE2* (*PHO2*); DOUBLE-STRANDED RNA BINDING (DRB) proteins DRB1; DRB2; DRB4; miR399-directed *PHO2* expression regulation; RT-qPCR

1. Introduction

Phosphorous (P) is one of the most limiting factors for plant growth worldwide [1–3], with large quantities of P an essential requirement for numerous processes vital to the plant cell, including energy trafficking, signaling cascades, enzymatic reactions and nucleic acid and phospholipid synthesis [3,4]. Inorganic phosphate (Pi), in the form of PO_4 , is the predominant form of P taken up by a plant from the soil, however, soil PO_4 primarily exists in organic or insoluble forms that are largely inaccessible to plant root uptake mechanisms [1]. Therefore, due to limited soil PO_4 availability, combined with the importance of an adequate concentration of P in plant cells to ensure normal growth and development, plants employ elegant mechanisms to spatially regulate P abundance across their developmentally distinct tissues [5,6]. Phosphorous homeostasis is therefore tightly controlled and involves both the

remobilization of internal P stores and the increased acquisition of external PO₄ [5,7]. For example, P limitation triggers the release of organic acids from the plant root system into the soil rhizosphere to chelate with metal ions to promote soluble PO₄ uptake to maintain or increase intracellular P concentration [1,8]. In addition, the P stored in the older leaves of a plant when the plant experiences P stress is remobilized; this allows for (1) continued growth of actively expanding tissues, and (2) the promotion of new growth. Enhanced P trafficking is achieved via promoting the expression of genes encoding PO₄ transporter proteins, and in turn, elevated PO₄ transporter protein abundance generally ensures that the cellular P concentration is maintained irrespective of external PO₄ levels [1,7]. In *Arabidopsis thaliana* (*Arabidopsis*), the first protein identified to be required for the maintenance of P homeostasis under PO₄ limiting conditions was PHOSPHATE1 (PHO1) [9]. The gene encoding PHO1 (*PHO1*; *AT1G14040*) was identified by [9] via their characterization of *pho1* plants, an *Arabidopsis* mutant line demonstrated to over-accumulate P in root tissues due to defective P translocation to the shoot. Although the *Arabidopsis* PHO1 protein, and the PHO1 proteins of other plant species characterized to date, do not closely resemble other PO₄ transporter proteins, PHO1 is indeed central to P movement in plants. The PHO1 protein is essential for PO₄ efflux into the root vascular cylinder; the first step in P transportation to the upper aerial tissues [10,11]. PHOSPHATE2 (PHO2) was the second protein demonstrated essential for the maintenance of P homeostasis with the *pho2* mutant shown to accumulate P to toxic levels in shoot tissues [12,13]. The *PHO2* gene (*AT2G33770*) has since been shown to encode a ubiquitin conjugating enzyme24 (UBC24), with the PHO2 UBC24 proposed to direct ubiquitin-mediated degradation of PO₄ transporters, PHOSPHATE TRANSPORTER1;4 (PHT1;4), PHT1;8 and PHT1;9 [14]. Further, *PHO2* is almost ubiquitously expressed in *Arabidopsis* shoot and root tissues [15], with the loss of PHO2-directed suppression of PHT1;4, PHT1;8 and PHT1;9 abundance in *pho2* plants leading to the enhanced translocation of P from the roots to the shoot tissue [14]. In addition to PHO1 and PHO2, traditional mutagenesis-based approaches have further identified other proteins essential to P homeostasis maintenance, including PHOSPHATE STARVATION RESPONSE1 (PHR1), a MYB domain transcription factor that regulates the expression of numerous P responsive genes [16,17].

More contemporary research, however, has concentrated on documenting the regulatory role directed at the posttranscriptional level by small regulatory RNAs (sRNA), specifically the microRNA (miRNA) class of sRNA, in order to maintain P homeostasis [18,19]. The advent of high throughput sequencing technologies has made sRNA profiling across plant species, and under different growth regimes, including exposure of a plant to abiotic and biotic stress, a routine experimental procedure in modern research [14,20,21]. Such profiling has identified a common suite of conserved miRNAs (miRNAs identified across multiple, evolutionary unrelated plant species) that accumulate differentially when mineral nutrients are lacking, including P, nitrogen (N), copper and sulphur [20,21]. Responsiveness of a single miRNA to multiple mineral nutrient stresses is not surprising considering the considerable overlap in the complex regulation of metal ion transport and/or uptake in plants [14,22,23]. In *Arabidopsis* for example, P and N uptake mechanisms are reciprocally linked to one another, therefore; a miRNA with enhanced accumulation during periods of P stress will usually be reduced in abundance during N starvation [19,24,25].

The miRNA, miR399, has been conclusively linked with the maintenance of P homeostasis and the regulation of PO₄ uptake in *Arabidopsis* [18,19]. In *Arabidopsis*, the miR399 sRNA is processed from six precursor transcripts, namely *PRE-MIR399A* to *PRE-MIR399F*, transcribed from five genomic loci (*MIR399A-MIR399D* and *MIR399EIF*). The miR399 sRNA is unique amongst *Arabidopsis* miRNAs in that it acts as a mobile systemic signal upon PO₄ stress [21,26]. More specifically, when P becomes limited in *Arabidopsis* shoots, *MIR399* gene expression is stimulated by PHR1 [27], and following processing of the now abundant miR399 precursor transcripts by the protein machinery of the *Arabidopsis* miRNA pathway, the mature miR399 sRNA is transported to the roots. Here, miR399 is actively loaded by the miRNA-induced silencing complex (miRISC) to direct miRISC-mediated cleavage of *PHO2*, the target transcript of miR399 [7,21,27]. Reduced PHO2 protein abundance, due to elevated miRISC-mediated cleavage of the *PHO2* transcript, in turn removes the PHO2-mediated suppression

of PO₄ transporters, PHT1;4, PHT1;8 and PHT1;9, to ultimately promote root-to-shoot P transport in an attempt to maintain shoot P homeostasis in P limited conditions [28–31]. Additional regulatory complexity to the miR399/*PHO2* expression module is offered by the non-protein-coding RNA, *INDUCED BY PHOSPHATE STARVATION1* (*IPS1*) [32]. Once transcribed, *IPS1* acts as an endogenous target mimic (eTM) of miR399 activity [33]. Specifically, the miR399 target site harbored by *IPS1* contains a three nucleotide mismatch bulge across miR399 nucleotide positions 10 and 11: the position at which the catalytic core of miRISC, ARGONAUTE1 (AGO1), catalyzes the cleavage of miRNA target transcripts [34]. The bulge that forms at this position once miR399-directed AGO1 binds *IPS1*, renders *IPS1* resistant to AGO1-catalyzed cleavage, thereby effectively sequestering away miR399 activity [33]. Three of the five members of the *Arabidopsis* DOUBLE-STRANDED RNA BINDING (DRB) protein family, including DRB1, DRB2 and DRB4, have been assigned functional roles in the *Arabidopsis* miRNA pathway [35–39]. Both DRB1 and DRB4 form functional partnerships with DICER-LIKE (DCL) proteins, RNase III-like endonucleases that cleave molecules of double-stranded RNA (dsRNA). More specifically, the DRB1/DCL1 partnership processes stem-loop structured molecules of imperfectly dsRNA that form post miRNA precursor transcript folding [35–37], and the DRB4/DCL4 partnership is central for the processing of a small subset of miRNA precursor transcripts that fold to form stem-loop structures with high levels of base-pairing due to the almost perfect complementarity of the nucleotide sequences of the stem-loop arms [39]. More recently, DRB2 has also been assigned a functional role in the *Arabidopsis* miRNA pathway due to its demonstrated antagonism and/or synergism with the roles of both DRB1 and DRB4 in sRNA production [37,40]. Here, we therefore assessed the requirement of DRB1, DRB2 and DRB4 in the regulation of the miR399/*PHO2* expression module, both under non-stressed growth conditions and when wild-type *Arabidopsis* plants (ecotype Columbia-0 (Col-0)) and the *drb1*, *drb2* and *drb4* mutant lines are exposed to PO₄ starvation. More specifically, we aimed to determine; (1) the contribution of DRB1, DRB2 and/or DRB4 to miR399 production; (2) the mode of silencing directed by miR399 to regulate *PHO2* expression, and; (3) whether either DRB1, DRB2 or DRB4 are required for P homeostasis maintenance. Phenotypic and molecular assessment of Col-0, *drb1*, *drb2* and *drb4* plants post exposure to a 7-day period of PO₄ starvation, revealed that DRB1 and DRB2 are required for P homeostasis maintenance. Further, DRB1 was established as the primary DRB protein required to regulate miR399 production. However, DRB2 and DRB4 were demonstrated to play a secondary role in miR399 production regulation. Furthermore, miR399 appears to regulate the expression of its targeted transcript, *PHO2*, via both the canonical mechanism of plant miRNA-directed target gene expression repression, target mRNA cleavage, and via the alternative mode of target gene expression regulation, translational repression. Taken together, the hierarchical contribution of DRB1, DRB2 and DRB4 to the regulation of the miR399/*PHO2* expression module in *Arabidopsis* shoots and roots identifies the extreme importance of maintaining P homeostasis to ensure that numerous vital cellular processes are maintained across *Arabidopsis* tissue types and under a changing cellular environment.

2. Results

2.1. The Phenotypic and Physiological Response to PO₄ Stress in the Shoot Tissues of *Arabidopsis* Plant Lines Defective in DRB Protein Activity

To determine the consequence of loss of DRB activity on P homeostasis maintenance in 15-day old *Arabidopsis* plants post a 7-day period of PO₄ starvation, a series of phenotypic and physiological parameters were assessed in Col-0, *drb1*, *drb2* and *drb4* shoots. The severe developmental phenotype of the *drb1* mutant has been reported previously [36,41,42]. Figure 1A clearly reveals the reduced size of the *drb1* mutant at 15 days of age, compared to Col-0 plants, when both *Arabidopsis* lines are cultivated on standard growth media (P⁺ media). The retarded development of the *drb1* mutant is further evidenced in Figure 1B where the fresh weight of 8-day old Col-0 and *drb1* seedlings is presented. Specifically, prior to seedling transfer to either P⁺ or P⁻ media, the fresh weight of an 8-day old *drb1* seedling (13.5 ± 1.0 mg) is 53.4% less than that a Col-0 seedling (29.0 ± 3.5 mg). Compared to *drb1*, the *drb2* and *drb4* mutants display mild developmental phenotypes [37,42] as evidenced by those

displayed by 15-day old *drb2* and *drb4* plants cultivated on P⁺ growth media (Figure 1A), and by the fresh weights of 8-day old *drb2* (26.8 ± 4.2 mg) and *drb4* (22.9 ± 1.4 mg) seedlings. Although the *drb1* mutant displayed the most severe phenotype, *drb1* development appeared to be the least affected by the 7-day PO₄ stress treatment. The fresh weight of P⁻ *drb1* plants (35.5 ± 1.0 mg) was only reduced by 21.6% compared to P⁺ *drb1* plants (45.3 mg \pm 1.5 mg) (Figure 1C). The development of Col-0, *drb2* and *drb4* plants was negatively impacted to a similar degree by the 7-day PO₄ stress treatment, with their fresh weights reduced by 36.6%, 39.1% and 36.3%, respectively (Figure 1C). Determination of rosette area revealed largely similar trends across the *drb* mutant lines analyzed, that is, *drb1* rosette area was reduced by 29.3%, while the rosette development of P⁻ *drb2* and P⁻ *drb4* plants was reduced by 48.0% and 38.7%, respectively (Figure 1D). Interestingly, the observed reductions to the rosette area of P⁻ *drb1*, P⁻ *drb2* and P⁻ *drb4* plants was considerably less than the 60.1% reduction to the rosette area of P⁻ Col-0 plants (11.2 ± 1.7 mm²) compared to P⁺ Col-0 plants (28.1 ± 5.5 mm²) (Figure 1D).

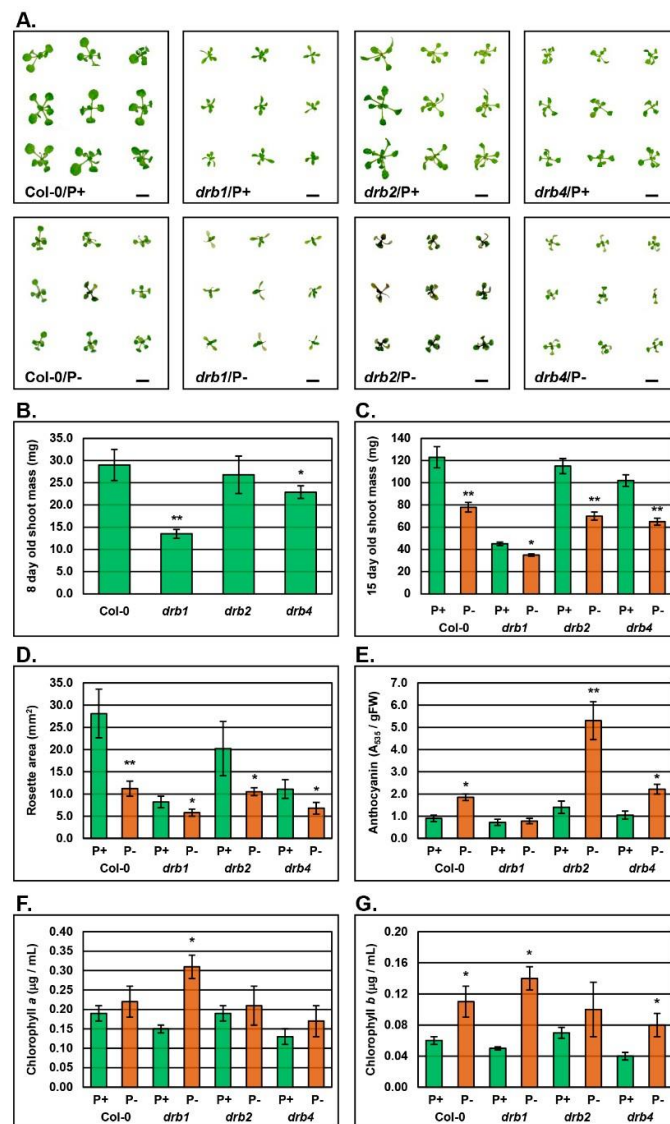


Figure 1. The aerial tissue phenotypes displayed by 15-day old *Arabidopsis* plant lines Col-0, *drb1*, *drb2* and *drb4* post exposure to a 7-day period of PO₄ starvation. (A) The aerial tissue phenotypes expressed by non-stressed (top row of panels) and PO₄-stressed (bottom row of panels) 15-day old Col-0, *drb1*, *drb2* and *drb4* plants. Scale bar = 1cm. (B) Quantification of the shoot mass of 8-day old Col-0, *drb1*, *drb2* and *drb4* seedlings germinated and cultivated under standard growth conditions. (C) The shoot mass of non-stressed and PO₄-stressed 15-day old Col-0, *drb1*, *drb2* and *drb4* plants. (D) The rosette area of

non-stressed and PO₄-stressed 15-day old *Arabidopsis* lines, Col-0, *drb1*, *drb2* and *drb4*. (E) Anthocyanin accumulation in the shoot tissues of 15-day old Col-0, *drb1*, *drb2* and *drb4* plants cultivated under standard growth conditions, or for 7-days under PO₄ starvation. (F and G) Chlorophyll *a* (F) and chlorophyll *b* (G) abundance in the aerial tissues of non-stressed and PO₄-stressed Col-0, *drb1*, *drb2* and *drb4* plants. (B-G) Error bars represent the standard deviation of four biological replicates and each biological replicate consisted of a pool of twelve individual plants. The presence of an asterisk above a column represents a statistically significant difference either between non-stressed Col-0 plants and each assessed *drb* mutant post cultivation under either a non-stressed or stressed growth regime (B) or between the non-stressed and PO₄-stressed sample of each plant line (C-G) (p -value: * < 0.05; ** < 0.005; *** < 0.001).

Anthocyanin, chlorophyll *a* and chlorophyll *b* content of Col-0, *drb1*, *drb2* and *drb4* shoots was also determined. Phosphate starvation has been previously shown to elevate the levels of PRODUCTION OF ANTHOCYANIN PIGMENT1 (PAP1/MYB75), PAP2 (MYB90) and MYB113, three MYB domain transcription factors that in turn stimulate the expression of a cohort of genes required for anthocyanin production in vegetative tissues [19,43]. These reports, in combination with the readily observable pigmentation that accumulated in the rosette leaves of P⁻ Col-0, P⁻ *drb2* and P⁻ *drb4* plants (Figure 1A), identified anthocyanin as an ideal metric to further assess the response of each *drb* mutant to PO₄ starvation. The anthocyanin content of non-stressed Col-0, *drb1*, *drb2* and *drb4* shoots was similar (Figure 1E). However, when PO₄ is limited, an approximate 2.0-fold increase in anthocyanin accumulation was detected for P⁻ Col-0 shoots. Further promotion of anthocyanin accumulation was determined for PO₄-stressed *drb2* and *drb4* plants, with anthocyanin content elevated 3.7- and 2.8-fold in P⁻ *drb2* and P⁻ *drb4* plants, respectively (Figure 1E). As readily observable in Figure 1A, anthocyanin accumulation was not promoted in the shoot tissue of P⁻ *drb1* plants. However, spectrophotometry revealed abundance changes for both chlorophyll *a* and chlorophyll *b* in the shoot tissue of P⁻ *drb1* plants. Specifically, chlorophyll *a* (Figure 1F) and chlorophyll *b* (Figure 1G) abundance was elevated by 2.1- and 2.8-fold in P⁻ *drb1* shoots, compared to P⁺ *drb1* shoots. In PO₄-stressed Col-0, *drb2* and *drb4* shoots, the chlorophyll *a* level remained largely unchanged compared to the non-stressed counterpart of each plant line (Figure 1F). Chlorophyll *b* accumulation however, was determined to be promoted in Col-0 and *drb4* shoots, by 1.8- and 2.0-fold, by the 7-day PO₄ starvation period (Figure 1G).

2.2. Molecular Profiling of the miR399/PHO2 Expression Module in the Shoot Tissues of *Arabidopsis* Plant Lines Defective in DRB Protein Activity

The results presented in Figure 1 strongly indicated that each *drb* mutant was responding differently to the applied stress and when this finding is considered together with the documented roles of DRB1, DRB2 and DRB4 in the *Arabidopsis* miRNA pathway [35–39], including the demonstrated antagonism between DRB1 and DRB2 [37] and between DRB2 and DRB4 [40] in miRNA production, the miR399/PHO2 expression module was next profiled via a RT-qPCR-based approach. RT-qPCR profiling was conducted in an attempt to determine if the observed differences in the response of each *drb* mutant line to PO₄ stress was a result of dysfunction of the miR399/PHO2 expression module.

In *Arabidopsis* shoots, *PHR1* promotes *MIR399* gene expression when PO₄ supplies become limited, resulting in elevated miR399 abundance [27]. Therefore, RT-qPCR was first used to assess *PHR1* expression in control and PO₄-stressed Col-0, *drb1*, *drb2* and *drb4* shoots (Figure 2A). *PHR1* expression was only mildly elevated by 1.5-, 1.6- and 1.7-fold in P⁺ *drb1*, P⁺ *drb2* and P⁺ *drb4* shoots respectively, compared to its levels in non-stressed Col-0 shoots (Figure 2A). RT-qPCR further revealed that PO₄ stress only induced mild elevations to *PHR1* expression in P⁻ Col-0 (1.00 to 1.22 relative expression) and P⁻ *drb2* shoots (1.62 to 1.74 relative expression) (Figure 2A). This result was not unexpected in view of the previous report of only mild *PHR1* expression induction in PO₄-stressed *Arabidopsis* [17]. Interestingly, *PHR1* expression was reduced by 19.6% and 31.2% in P⁻ *drb1* and P⁻ *drb4* shoots, respectively (Figure 2A), and not mildly elevated as expected.

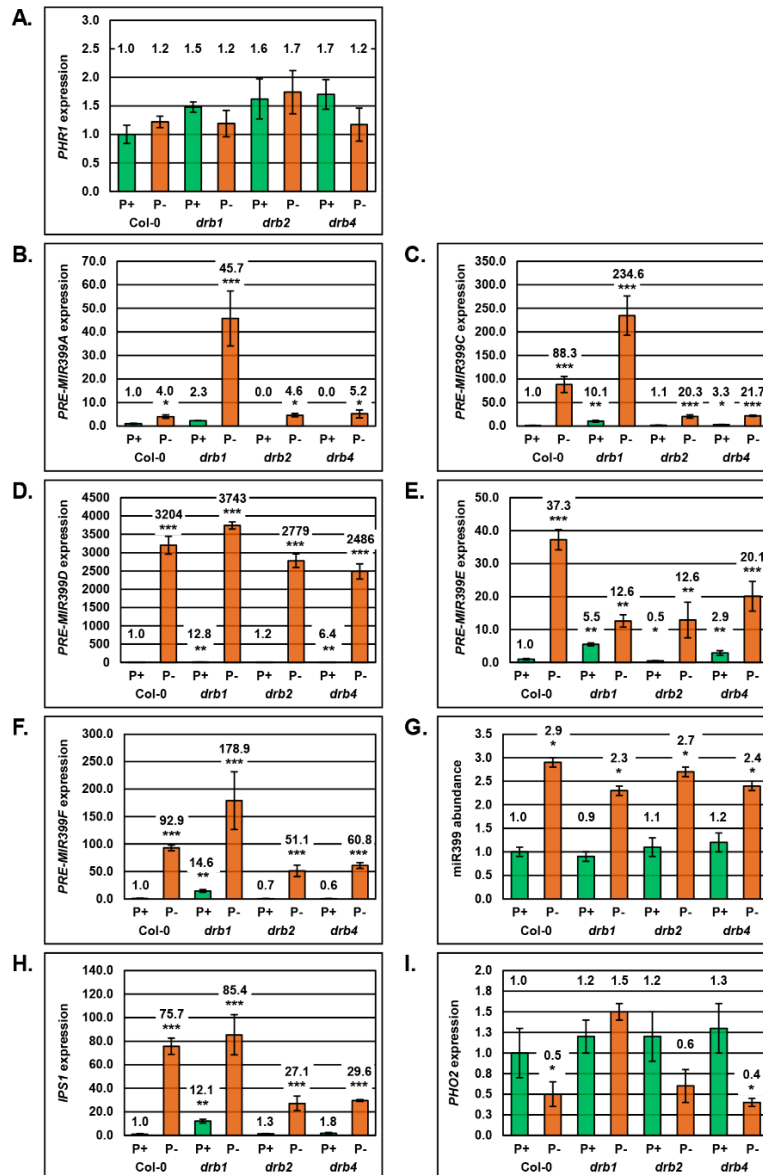


Figure 2. Molecular profiling of the miR399/*PHO2* expression module in the aerial tissues of non-stressed and PO_4 -stressed Col-0, *drb1*, *drb2* and *drb4* plants. (A) RT-qPCR assessment of the expression of the PO_4 responsive transcription factor PHR1 in the aerial tissues of non-stressed and PO_4 -stressed Col-0, *drb1*, *drb2* and *drb4* plants. (B to F) RT-qPCR profiling of miR399 precursor transcript abundance in the aerial tissues of non-stressed and PO_4 -stressed Col-0, *drb1*, *drb2* and *drb4* plants, including precursors *PRE-MIR399A* (B), *PRE-MIR399C* (C), *PRE-MIR399D* (D), *PRE-MIR399E* (E) and *PRE-MIR399F* (F). (G) Quantification of miR399 abundance in the aerial tissues of non-stressed and PO_4 -stressed Col-0, *drb1*, *drb2* and *drb4* plants. (H) Assessment of the expression of the non-cleavable decoy of miR399 activity, *IPS1*, via RT-qPCR in the aerial tissues of non-stressed and PO_4 -stressed *Arabidopsis* lines, Col-0, *drb1*, *drb2* and *drb4*. (I) RT-qPCR analysis of the expression of the miR399 target gene, *PHO2*, in the aerial tissues of non-stressed and PO_4 -stressed *Arabidopsis* lines, Col-0, *drb1*, *drb2* and *drb4*. (A–I) Error bars represent the standard deviation of four biological replicates and each biological replicate consisted of a pool of twelve individual plants. Due to the vastly different levels of each assessed transcript, the relative expression value for each plant line/growth regime is provided above the corresponding column. The presence of an asterisk above a column represents a statistically significant difference between non-stressed Col-0 plants and each of the assessed *drb* mutant lines, post cultivation under either a standard or stressed growth regime (p -value: * < 0.05; ** < 0.005; *** < 0.001).

The miR399 sRNA is processed from six structurally distinct precursor transcripts (*PRE-MIR399A* to *PRE-MIR399F*), transcribed from five genomic loci (*MIR399A* to *MIR399D* and *MIR399EIF*) in *Arabidopsis*. RT-qPCR only failed to detect *PRE-MIR399B* expression in Col-0 shoots. RT-qPCR did however clearly reveal that PO₄ stress induced the expression of the five detectable miR399 precursor transcripts by 4.0-, 88.3-, 3204-, 37.3- and 92.9-fold in the shoots of P⁻ Col-0 plants (Figure 2B-F). Of the three members of the *Arabidopsis* DRB protein family analyzed here, Figure 2B-F clearly show that DRB1 is the primary DRB protein required to regulate miR399 production in *Arabidopsis* shoots with the abundance of *PRE-MIR399A*, *PRE-MIR399C*, *PRE-MIR399D*, *PRE-MIR399E* and *PRE-MIR399F* elevated by 2.3-, 10.1-, 12.8-, 5.5- and 14.6-fold, respectively, in P⁺ *drb1* shoots. The primary role of DRB1 in regulating miR399 production in *Arabidopsis* shoots was further highlighted for *PRE-MIR399A*, *PRE-MIR399C*, *PRE-MIR399D* and *PRE-MIR399F* via additional elevations to their respective expression levels, specifically 45.7-, 234.6- 3743- and 178.9-fold increases to transcript abundance in P- *drb1* shoots (Figure 2B-D,F).

Failure to detect the *PRE-MIR399A* precursor by RT-qPCR in P⁺ *drb2* shoots, and a similar degree of over-accumulation of this precursor in P⁻ Col-0 (4.0-fold) and P⁻ *drb2* shoots (4.6-fold), indicated that DRB2 is not required to regulate miR399 production from this precursor (Figure 2B). Wild-type-like accumulation of *PRE-MIR399C* (1.1-fold) and *PRE-MIR399D* (1.2-fold) in P⁺ *drb2* shoots, and a lower degree of over-accumulation of these two precursors in P⁻ *drb2* shoots, compared to P⁻ Col-0 shoots, indicated that DRB2 plays a secondary role in regulating miR399 production from these two precursors (Figure 2C,D). A similar level of expression of *PRE-MIR399E* in PO₄-stressed *drb1* and *drb2* shoots suggested that both DRB1 and DRB2 are required for miR399 production from this precursor (Figure 2E). However, lower transcript abundance (0.5 relative expression) in P⁺ *drb2* shoots, compared to relative expression levels of 1.0 and 5.5 in P⁺ Col-0 and P⁺ *drb1* shoots, respectively (Figure 2E), again indicated that under standard growth conditions, DRB2 plays a secondary role in regulating miR399 production from the *PRE-MIR399E* precursor. The abundance of the *PRE-MIR399F* transcript is also reduced in P⁺ *drb2* shoots compared to its levels in P⁺ Col-0 shoots, and further, the degree of over-accumulation of *PRE-MIR399F* is less in P⁻ *drb2* shoots compared to its levels in P⁻ Col-0 shoots (Figure 2F). When these expression trends are considered together with those documented for P⁺ and P⁻ *drb1* shoots, they again indicate a secondary role for DRB2 in regulating miR399 production from this precursor.

As demonstrated for P⁺ *drb2* shoots, the *PRE-MIR399A* transcript remained below the detection sensitivity of RT-qPCR in P⁺ *drb4* shoots (Figure 2B). RT-qPCR did however, reveal *PRE-MIR399A* expression to be elevated by 5.2-fold in P⁻ *drb4* shoots, a similar degree of transcript elevation to that observed in P⁻ Col-0 shoots (4.0-fold increase) (Figure 2B). This indicates that DRB4 is not involved in regulating miR399 production from this precursor. Comparison of the RT-qPCR generated expression trends for *PRE-MIR399C*, *PRE-MIR399D* and *PRE-MIR399E* in P⁺ and P⁻ *drb4* shoots, to those of P⁺ Col-0, P⁻ Col-0, P⁺ *drb1* and P⁻ *drb1* shoots, revealed a secondary role for DRB4 in regulating miR399 production from these three precursor transcripts (Figure 2C-E). DRB4 also appears to play a role in regulating miR399 production from the *PRE-MIR399F* transcript, with *PRE-MIR399F* abundance reduced by 40% in P⁺ *drb4* shoots (Figure 2F). RT-qPCR also revealed that the expression of this precursor transcript was elevated to a relative expression level of 60.8 in PO₄-stressed *drb4* shoots; a lower degree of relative expression than observed in either P⁻ Col-0 (92.9 relative expression) or P⁻ *drb1* (178.9 relative expression) shoots (Figure 2F). This finding suggests that in the absence of DRB4 activity, miR399 is more efficiently processed from the *PRE-MIR399F* precursor transcript.

RT-qPCR was next applied to quantify miR399 abundance in the shoot material of non-stressed or PO₄-stressed Col-0, *drb1*, *drb2* and *drb4* plants. This analysis revealed that in spite of the considerable variation in precursor transcript abundance in the shoot tissues of P⁺ Col-0, P⁺ *drb1*, P⁺ *drb2* and P⁺ *drb4* plants, miR399 levels remained largely unchanged (Figure 2G). This was an especially surprising finding for control *drb1* plants, with the *PRE-MIR399A*, *PRE-MIR399C*, *PRE-MIR399D*, *PRE-MIR399E* and *PRE-MIR399F* transcripts demonstrated to over-accumulate by 4.0-, 10.1-, 12.8-, 5.5- and 14.6-fold in P⁺ *drb1* shoots, compared to their respective levels in P⁺ Col-0 shoots. However, miR399 abundance

was only reduced by 10% in P⁺ *drb1* shoots. Similarly, although the expression level of the five miR399 precursors varied considerably in P⁺ *drb2* and P⁺ *drb4* shoots, miR399 abundance was only elevated by 10% and 20%, respectively (Figure 2G). Enhanced miR399 accumulation in P⁺ *drb2* and P⁺ *drb4* shoots did however further identify that both of these DRB proteins are required to correctly regulate miR399 abundance in *Arabidopsis* shoots. The degree of alteration to miR399 abundance was demonstrated to be higher in the shoot tissues of the four assessed plant lines when these lines were cultivated on PO₄ deplete media. Specifically, RT-qPCR revealed 2.9-, 2.6-, 2.5- and 2.0-fold enhancement to miR399 abundance in PO₄-stressed Col-0, *drb1*, *drb2* and *drb4* shoots, respectively (Figure 2G).

The mild alteration to miR399 abundance quantified by RT-qPCR in non-stressed and PO₄-stressed shoots (Figure 2G) led us to next assess the expression of *IPS1*, the eTM of miR399 [32–34]. Due to *IPS1* being a PO₄ stress-induced gene, it was unsurprising to only observe mild (P⁺ *drb2* and P⁺ *drb4* shoots) to moderate differences (P⁺ *drb1* shoots) in *IPS1* transcript abundance in the shoot tissue of non-stressed Col-0, *drb1*, *drb2* and *drb4* plants (Figure 2H). Further, and as expected, RT-qPCR showed that PO₄ stress induced the expression of *IPS1*, with *IPS1* transcript abundance elevated by 75.7-, 7.1-, 20.8- and 16.4-fold in the shoot tissues of PO₄ stressed Col-0, *drb1*, *drb2* and *drb4* plants, respectively (compared to the non-stressed counterpart of each plant line).

Next, the expression of the target gene of miR399, *PHO2*, was determined by RT-qPCR to largely remain at wild-type levels (P⁺ Col-0 shoots) in the shoot tissues of P⁺ *drb1*, P⁺ *drb2* and P⁺ *drb4* plants (Figure 2I). This was an unsurprising result considering that RT-qPCR also revealed only mild changes to miR399 abundance across the three *drb* mutant lines assessed when each plant line was cultivated on standard *Arabidopsis* culture media (Figure 2G). RT-qPCR also revealed that elevated miR399 abundance in P⁻ Col-0, P⁻ *drb2* and P⁻ *drb4* plants, promoted miR399-directed expression repression of *PHO2*, with the abundance of the *PHO2* transcript reduced by 50%, 40% and 60% in the shoot tissues of these three plant lines, respectively (Figure 2I). In P⁻ *drb1* shoots however, the level of the *PHO2* transcript was increased by 50% (Figure 2I). Elevated *PHO2* expression in P⁻ *drb1* shoots, a tissue where miR399 abundance was also demonstrated to be elevated, indicated that in the absence of DRB1 activity, miR399-directed mRNA cleavage-mediated regulation of *PHO2* expression is lost.

2.3. The Phenotypic and Physiological Response to PO₄ Stress of the Root System of *Arabidopsis* Plant Lines Defective in DRB Protein Activity

The unique phenotypic (Figure 1) and molecular (Figure 2) response displayed by *drb1*, *drb2* and *drb4* shoots to PO₄ starvation led us to next repeat these assessments on the root system of each mutant background. As reported for the aerial tissue phenotypes expressed by the *drb1*, *drb2* and *drb4* mutants (Figure 1), Figure 3A again clearly displays the severe developmental phenotype expressed by the *drb1* mutant as well as the comparatively mild phenotypes that result from the loss of either DRB2 or DRB4 activity in *drb2* and *drb4* plants, respectively. The severity of the developmental phenotypes expressed by the three *drb* mutants assessed in this study is further evidenced when the fresh weight of the root system of 8-day old seedlings cultivated on standard growth media was determined. Specifically, the fresh weight of the root system of 8-day old *drb2* and *drb4* seedlings, 7.95 ± 0.20 mg and 8.00 ± 0.15 mg respectively, was equivalent to the fresh weight of the root system of Col-0 plants, 8.25 ± 0.45 mg (Figure 3B). However, the fresh weight of the root system of 8-day old *drb1* plants, 4.25 ± 0.15 mg, was approximately 50% less than that of an 8-day old Col-0 seedling (Figure 3B).

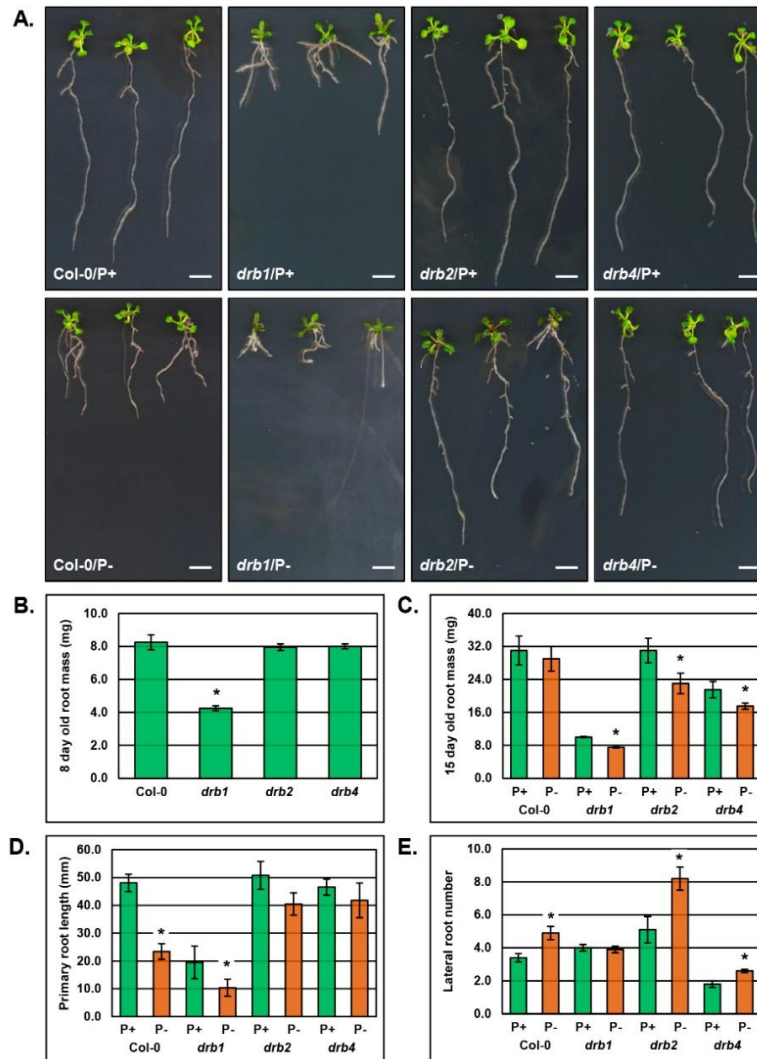


Figure 3. The root system phenotypes displayed by 15-day old *Arabidopsis* plant lines Col-0, *drb1*, *drb2* and *drb4* post exposure to a 7-day period of PO₄ starvation. **(A)** The root system phenotypes expressed by non-stressed (top row of panels) and PO₄-stressed (bottom row of panels) 15-day old Col-0, *drb1*, *drb2* and *drb4* plants. Scale bar = 1cm. **(B)** Quantification of the root mass of 8-day old Col-0, *drb1*, *drb2* and *drb4* seedlings cultivated under standard growth conditions. **(C)** The root mass of non-stressed and PO₄-stressed 15-day old Col-0, *drb1*, *drb2* and *drb4* plants. **(D)** The primary root length of non-stressed and PO₄-stressed 15-day old *Arabidopsis* lines, Col-0, *drb1*, *drb2* and *drb4*. **(E)** The number of lateral roots formed from the primary root of 15-day old Col-0, *drb1*, *drb2* and *drb4* plants cultivated under standard growth conditions, or post the 7-day PO₄ starvation period. **(B–E)** Error bars represent the standard deviation of four biological replicates and each biological replicate consisted of a pool of twelve individual plants. The presence of an asterisk above a column represents a statistically significant difference either between non-stressed Col-0 plants and each assessed *drb* mutant post cultivation under either a non-stressed or stressed growth regime **(B)** or between the non-stressed and PO₄-stressed sample of each plant line **(C–E)** (p -value: * < 0.05; ** < 0.005; *** < 0.001).

Figure 3C shows that at the completion of the 7-day PO₄ starvation period, the fresh weight of 15-day old P⁻ Col-0 roots (29.0 ± 3.0 mg) was only reduced by 2.0 mg compared to P⁺ Col-0 roots (31.0 ± 3.5 mg), a mild 6.5% reduction. The fresh weight of the root system of PO₄ stressed *drb1*, *drb2* and *drb4* plants all showed a much greater reduction when compared to their non-stressed counterparts (Figure 3C). That is, the fresh weight of the root system of 15-day old P⁻ *drb1* (7.5 ± 0.15 mg), P⁻ *drb2* (23.0 ± 2.5 mg) and P⁻ *drb4* plants (17.5 ± 0.75 mg) was reduced by 25.0%, 25.8% and 18.6%, respectively (Figure 3C).

Inhibition of primary root length is one of the main phenotypic responses of *Arabidopsis* to PO₄ stress [2,44], and accordingly, Figure 3A,D clearly show that the primary root length of 15-day old P⁻ Col-0 plants (23.4 ± 2.8 mm) was significantly reduced by 51.2% compared to non-stressed P⁺ Col-0 plants (48.1 ± 3.1 mm) (Figure 3D). Although primary root length is already severely inhibited due to detrimental consequences of the loss of DRB1 activity on *Arabidopsis* development, the 7-day stress treatment caused a 46.7% reduction to the primary root length of P⁻ *drb1* plants (10.4 ± 3.1 mm) compared to P⁺ *drb1* plants (19.5 ± 5.9 mm) (Figure 3D). Interestingly, PO₄ stress impacted primary root development to a much lower degree in both the *drb2* and *drb4* mutant backgrounds. Namely, primary root length was reduced by 20.3% and 10.3% in P⁻ *drb2* (40.5 ± 4.0 mm) and P⁻ *drb4* (41.8 ± 6.2 mm) plants respectively, compared to the primary root length of P⁺ *drb2* (50.8 ± 5.0 mm) and P⁺ *drb4* (46.6 ± 2.9 mm) plants (Figure 3D).

In parallel with inhibition to primary root length, promotion of lateral root development is a commonly reported phenotypic response of *Arabidopsis* plants exposed to PO₄ stress [2,44]. It was therefore unsurprising to document a 44% increase in the number of lateral roots that formed on 15-day old P⁻ Col-0 plants (4.9 ± 0.4) compared to P⁺ Col-0 plants (3.4 ± 0.3) (Figure 3E). Interestingly, this phenotypic response to PO₄ stress appeared completely defective in the *drb1* mutant background with both P⁺ *drb1* (4.0 ± 0.2) and P⁻ *drb1* (3.9 ± 0.2) plants forming approximately the same number of lateral roots. Unlike the *drb1* mutant, lateral root development was promoted by ~61% in the *drb2* mutant background with P⁻ *drb2* plants forming 8.2 ± 0.7 lateral roots compared to P⁺ *drb2* plants which formed 5.1 ± 0.8 lateral roots. Lateral root formation was also induced by PO₄ stress in the *drb4* mutant with the number of lateral roots increased by 44% in P⁻ *drb4* plants (2.6 ± 0.1) compared to their number in P⁺ *drb4* plants (1.8 ± 0.2).

2.4. Molecular Profiling of the miR399/PHO2 Expression Module in the Root System of *Arabidopsis* Plant Lines Defective in DRB Protein Activity

Due to its demonstrated role in inducing *MIR399* gene expression in PO₄ depleted conditions [27], RT-qPCR was initially used to profile *PHR1* expression in PO₄-stressed Col-0, *drb1*, *drb2* and *drb4* roots (Figure 4A). This analysis revealed that compared to the root system of each plant line's non-stressed counterpart, *PHR1* expression remained remarkably constant in P⁻ Col-0, P⁻ *drb1*, P⁻ *drb2* and P⁻ *drb4* roots (Figure 4A). Although RT-qPCR revealed that *PHR1* expression remained constant in the roots of control and PO₄-stressed plants, RT-qPCR was next applied to profile the expression of the six *MIR399* precursor transcripts in the roots of P⁺ and P⁻ plants. Of the six miR399 precursors, RT-qPCR only allowed for expression quantification of three miR399 precursors, namely *PRE-MIR399A*, *PRE-MIR399C* and *PRE-MIR399D* in *Arabidopsis* roots (Figure 4B-D). In P⁻ Col-0 roots, RT-qPCR clearly revealed that PO₄ stress induced the expression of the miR399 precursors, *PRE-MIR399A*, *PRE-MIR399C* and *PRE-MIR399D*, by 4.0-, 40.6- and 1546-fold, respectively (Figure 4B-D). When compared to P⁺ Col-0 roots, the moderate 2.3- and 3.6-fold elevation in the abundance of *PRE-MIR399A* and *PRE-MIR399C* in P⁺ *drb1* roots, identified DRB1 as the primary DRB required for miR399 production regulation from these two precursor transcripts in the roots of wild-type *Arabidopsis* plants (Figure 4B,C). The primary role of DRB1 in *PRE-MIR399A* and *PRE-MIR399C* processing in non-stressed Col-0 roots is further evidenced by the wild-type equivalent accumulation of these two precursors in P⁺ *drb2* and P⁺ *drb4* roots, and by the highest degree of *PRE-MIR399A* and *PRE-MIR399C* precursor transcript over-accumulation in P⁻ *drb1* roots (Figure 4B,C). Considering this result, it was therefore of considerable interest to observe the greatest degree of *PRE-MIR399D* over-accumulation, an 8.2-fold increase, in P⁺ *drb4* roots and not in P⁺ *drb1* roots (4.3-fold increase) (Figure 4D). This finding suggests that in non-stressed wild-type *Arabidopsis* roots, DRB4 is the primary DRB responsible for regulating miR399 production from this precursor transcript. In addition, and under PO₄ stress conditions, the *PRE-MIR399D* transcript increased in its abundance to relative expression values of 829, 849 and 1271 in *drb1*, *drb2* and *drb4* roots, respectively (Figure 4D). Although these determined increases in precursor transcript abundance are all highly significant, they are not as significant as the 1546 relative expression value obtained for the

PRE-MIR399D transcript in P^- Col-0 roots. A lower degree of precursor transcript over-accumulation in each assessed *drb* mutant background, compared to the expression induction observed in wild-type roots, indicated that all three DRB proteins potentially play a role in fine-tuning the regulation of miR399 production from the *PRE-MIR399D* precursor in PO_4 -stressed *Arabidopsis* roots (Figure 4D).

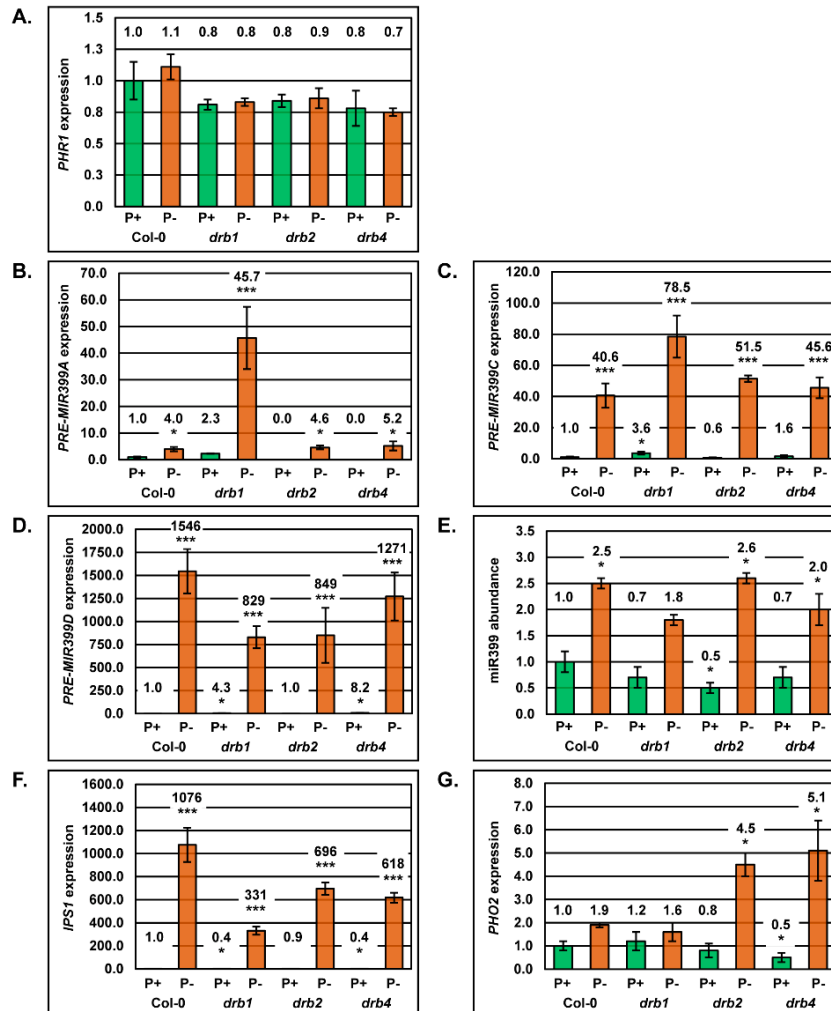


Figure 4. Molecular profiling of the miR399/*PHO2* expression module in the root system of non-stressed and PO_4 -stressed Col-0, *drb1*, *drb2* and *drb4* plants. (A) RT-qPCR assessment of the expression of the PO_4 responsive transcription factor *PHR1* in the roots of non-stressed and PO_4 -stressed Col-0, *drb1*, *drb2* and *drb4* plants. (B–D) RT-qPCR profiling of miR399 precursor transcript abundance in the root system of non-stressed and PO_4 -stressed Col-0, *drb1*, *drb2* and *drb4* plants, including precursors *PRE-MIR399A* (B), *PRE-MIR399C* (C) and *PRE-MIR399D* (D). (E) Quantification of miR399 abundance in the roots of non-stressed and PO_4 -stressed Col-0, *drb1*, *drb2* and *drb4* plants. (F) Assessment of *IPS1* transcript abundance in the roots of non-stressed and PO_4 -stressed *Arabidopsis* lines, Col-0, *drb1*, *drb2* and *drb4*. (G) RT-qPCR analysis of *PHO2* expression, the target gene of miR399, in the root system of non-stressed and PO_4 -stressed *Arabidopsis* lines, Col-0, *drb1*, *drb2* and *drb4*. (A–G) Error bars represent the standard deviation of four biological replicates and each biological replicate consisted of a pool of twelve individual plants. Due to the vastly different level of each assessed transcript, the relative expression value for each plant line/growth regime is provided above the corresponding column. The presence of an asterisk above a column represents a statistically significant difference between non-stressed Col-0 plants and each of the assessed *drb* mutant lines, post cultivation under either a standard or stressed growth regime (p -value: * < 0.05; ** < 0.005; *** < 0.001).

Post-establishment of highly variable expression profiles for *PRE-MIR399A*, *PRE-MIR399C* and *PRE-MIR399D* in non-stressed *drb1*, *drb2* and *drb4* roots (Figure 4B–D), miR399 abundance reductions of 30%, 50% and 30% in P⁺ *drb1*, P⁺ *drb2* and P⁺ *drb4* roots, respectively, was expected (Figure 4E). Quantification of miR399 abundance, 2.5-, 1.8-, 2.6- and 2.0-fold elevations, respectively, in the root tissues of PO₄-stressed Col-0, *drb1*, *drb2* and *drb4* plants, revealed that the considerable induction to *PRE-MIR399A*, *PRE-MIR399C* and *PRE-MIR399D* expression (Figure 4B–D), did not however, result in an overly altered miR399 accumulation profile (Figure 4E).

Failure to establish a strong correlation between precursor transcript expression and miR399 abundance in either control or PO₄-stressed Col-0, *drb1*, *drb2* and *drb4* roots, led us to next assess *IPS1* expression in this tissue (Figure 4F). *IPS1* transcript abundance remained relatively unchanged in the root tissues of non-stressed Col-0 and *drb2* plants (Figure 4F). Interestingly, *IPS1* expression was reduced by 60% in P⁺ *drb1* and P⁺ *drb4* roots (Figure 4F). Significant induction of *IPS1* expression was observed in PO₄-stressed *drb1*, *drb2* and *drb4* roots, 331-, 696- and 618-fold elevations, respectively. Interestingly, RT-qPCR demonstrated that *IPS1* expression was promoted to its greatest degree, 1076-fold, in PO₄-stressed Col-0 roots (Figure 4F).

The expression of the miR399 target gene, *PHO2*, was next quantified by RT-qPCR in non-stressed and PO₄-stressed Col-0, *drb1*, *drb2* and *drb4* roots (Figure 4G). In P⁺ *drb1* and P⁺ *drb2* roots, RT-qPCR revealed *PHO2* expression to be elevated and reduced by 20%, respectively, and in P⁺ *drb4* roots, *PHO2* expression was reduced by 30%. Elevated *PHO2* expression in P⁺ *drb1* roots was expected considering the slight reduction to miR399 abundance observed in this tissue (Figure 4E). However, the reduced *PHO2* transcript levels in P⁺ *drb2* and P⁺ *drb4* roots was a surprise finding considering that miR399 abundance was also reduced in these two mutant lines by 50% and 30%, respectively (Figure 4E). *PHO2* expression was demonstrated by RT-qPCR to be elevated by 1.9-, 1.6-, 4.5- and 5.1-fold in PO₄-stressed Col-0, *drb1*, *drb2* and *drb4* roots, respectively (Figure 4G). This finding also formed an unexpected result considering that PO₄ starvation induced the accumulation of the miR399 sRNA in all four assessed plant lines (Figure 4E).

2.5. Correct Inorganic Phosphate Partitioning Between the Shoot and Root Tissue of *Arabidopsis* Requires *DRB1* and *DRB2*

The molecular profiling of alterations to the miR399/*PHO2* expression module in the shoot and root tissue of *Arabidopsis* Col-0, *drb1*, *drb2* and *drb4* plants under PO₄ stress, in combination with each plant line displaying a unique phenotypic response to this stress, led us to next assess Pi partitioning in the aerial tissue and root system of P⁺ and P⁻ Col-0, *drb1*, *drb2* and *drb4* plants. In the shoot tissues of 15-day old plants cultivated in PO₄ replete conditions, Pi content was only altered in the *drb2* mutant background, with the Pi content of P⁺ *drb2* shoots (13.8 μmol/gFW) reduced by 27.4% compared to the Pi content of P⁺ Col-0 shoots (19.0 μmol/gFW) (Figure 5A). When cultivated in PO₄-stress conditions however, only the Pi content of P⁻ *drb1* shoots (1.15 μmol/gFW) differed to that of P⁻ Col-0 shoots (1.75 μmol/gFW); a 34.3% reduction (Figure 5A). In non-stressed roots, the Pi content of P⁺ *drb1* (11.4 μmol/gFW) and P⁺ *drb2* (9.8 ± 0.8 μmol/gFW) roots was determined to be elevated by 58.3% and 37.5% respectively, compared to P⁺ Col-0 roots (7.2 μmol/gFW) (Figure 5B). As demonstrated for non-stressed *drb1* and *drb2* roots, the Pi content of P⁻ *drb1* (1.84 μmol/gFW) and P⁻ *drb2* (0.65 μmol/gFW) roots also differed to that of PO₄-stressed Col-0 roots (1.25 μmol/gFW), elevated and reduced by 47.2% and 48%, respectively (Figure 5B).

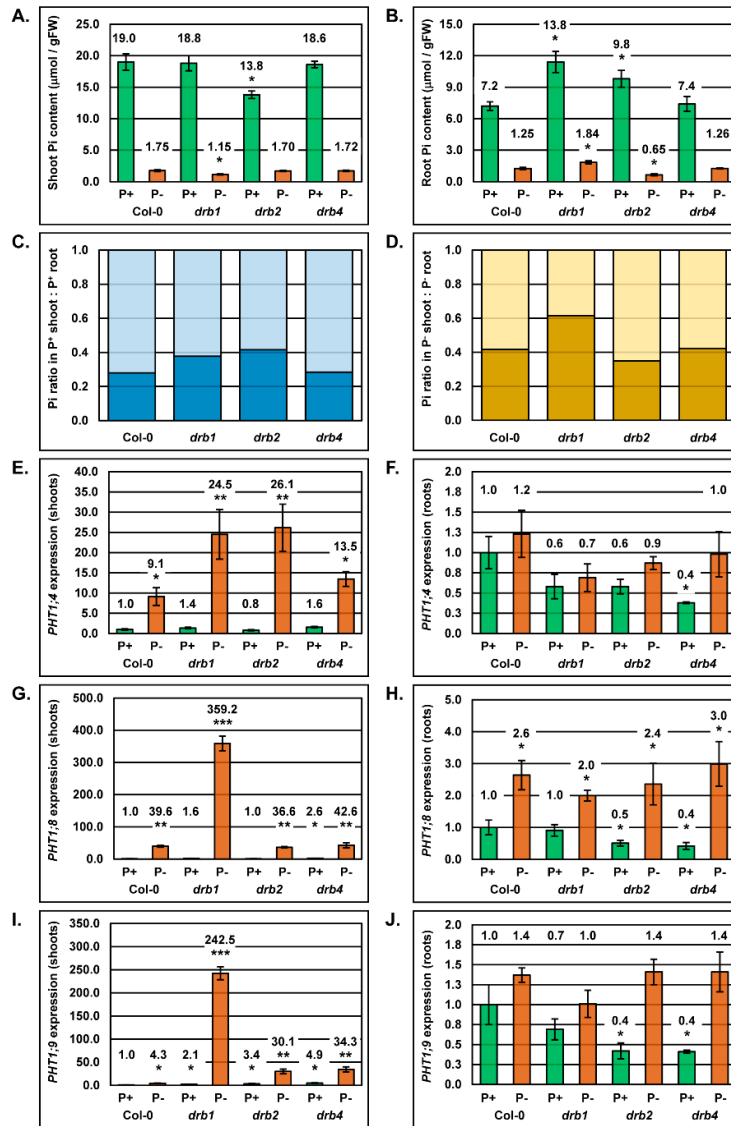


Figure 5. Pi content and PO_4 transporter gene expression in the shoot and root tissue of 15-day old *Arabidopsis* plant lines Col-0, *drb1*, *drb2* and *drb4* cultivated under either a standard growth regime or post-exposure to a 7-day period of PO_4 starvation. (A,B) Comparison of the Pi content of the shoots and roots (B) of 15-day old non-stressed and PO_4 -stressed Col-0, *drb1*, *drb2* and *drb4* plants. (C) Pi content shoot (light blue) to root (dark blue) ratio of 15-day old Col-0, *drb1*, *drb2* and *drb4* plants cultivated under standard growth conditions. (D) Pi content shoot (light gold) to root (dark gold) ratio of 15-day old Col-0, *drb1*, *drb2* and *drb4* plants post 7-days of PO_4 starvation. (E,F) Quantification of *PHT1;4* expression in the shoot (E) and root (F) tissues of 15-day old Col-0, *drb1*, *drb2* and *drb4* plants cultivated under standard growth conditions or post a 7-day period of PO_4 starvation. (G,H) RT-qPCR assessment of *PHT1;8* transcript abundance in the shoots (G) and roots (H) of 15-day old Col-0, *drb1*, *drb2* and *drb4* plants cultivated under either standard or PO_4 stress conditions. (I,J) *PHT1;9* expression in the shoot (I) and root (J) material of non-stressed or PO_4 -stressed Col-0, *drb1*, *drb2* and *drb4* plants at 15 days of age. (A,B,E–J) Error bars represent the standard deviation of four biological replicates and each biological replicate consisted of a pool of twelve individual plants. Due to the vastly different levels of each assessed transcript, the relative expression value for each plant line/growth regime is provided above the corresponding column. The presence of an asterisk above a column represents a statistically significant difference between the non-stressed and PO_4 -stressed sample of each plant line (A,B) or between non-stressed Col-0 plants and each *drb* mutant line, post cultivation under either a standard or stressed growth regime (E–J) (p -value: * < 0.05; ** < 0.005; *** < 0.001).

The reduced Pi content of P⁺ *drb2* shoots (Figure 5A), together with the elevated Pi contents of P⁺ *drb1* and P⁺ *drb2* roots (Figure 5B), suggested that Pi partitioning was potentially defective in these two mutant backgrounds. We therefore next determined the Pi content ratio of the shoot and root of non-stressed and PO₄-stressed Col-0, *drb1*, *drb2* and *drb4* plants. Figure 5C clearly shows that Pi partitioning between the shoot and root tissue of P⁺ *drb1* and P⁺ *drb2* plants is defective, even when these two mutant lines are cultivated on standard *Arabidopsis* growth media. Under PO₄ stress conditions, defective Pi partitioning is even more readily evident in the *drb1* mutant background which showed a 0.38:0.62 shoot to root Pi content ratio, compared to the shoot to root Pi content ratio of 0.58:0.42 for P⁻ Col-0 plants. Although not as striking as determined for P⁺ *drb2* plants, the altered shoot to root Pi content ratio (0.65:0.35) of PO₄-stressed *drb2* plants again indicated that Pi partitioning is defective in this mutant background (Figure 5D).

Altered shoot to root Pi content ratios in *drb1* and *drb2* plants strongly suggested that Pi partitioning is defective in these two mutant backgrounds. Considering that PO₄ transporters, PHT1;4, PHT1;8 and PHT1;9, are known targets of PHO2-mediated ubiquitination [7,14], together with our demonstration in Figures 2 and 4 that the miR399/PHO2 expression module is altered to differing degrees in the shoot and root tissues of each of the three assessed *drb* mutants, RT-qPCR was next applied to profile PHT1;4, PHT1;8 and PHT1;9 expression in non-stressed and PO₄-stressed Col-0, *drb1*, *drb2* and *drb4* plants. RT-qPCR revealed that PO₄ starvation promoted PHT1;4, PHT1;8 and PHT1;9 expression by 9.1-, 39.6- and 4.3-fold in Col-0 shoots (Figure 5E,G,I), and by 1.2-, 2.6- and 1.4-fold in Col-0 roots, respectively (Figure 5F,H,J). In non-stressed *drb1* shoots, the abundance of the PHT1;4, PHT1;8 and PHT1;9 transcripts were only mildly altered compared to their respective expression levels in P⁺ Col-0 shoots, returning 1.4-, 1.6- and 2.1-fold changes in expression. A similar mild degree of expression alteration was observed for P⁺ *drb1* roots. Specifically, compared to P⁺ Col-0 roots, the PHT1;4, PHT1;8 and PHT1;9 transcripts returned fold changes in abundance of 0.6, 1.0 and 0.7, respectively. The expression of these three PO₄ transporters was significantly induced by the 7-day stress period, returning abundance fold changes of 24.5 (PHT1;4), 359.2 (PHT1;8) and 242.5 (PHT1;9), respectively (Figure 5E,G,I), in P⁻ *drb1* shoots. In spite of the significant induction of PHT1 gene expression in P⁻ *drb1* shoots, PHT1;4, PHT1;8 and PHT1;9 levels were reduced (0.7-fold), elevated (2.0-fold) and unchanged (1.0-fold), respectively (Figure 5F,H,J) in the root system of PO₄-stressed *drb1* roots. As demonstrated for P⁺ *drb1* shoots, RT-qPCR again revealed that PHT1;4, PHT1;8 and PHT1;9 expression was mildly altered in P⁺ *drb2* shoots by 0.8-, 1.0- and 3.4-fold, respectively. In non-stressed *drb2* roots however, the expression of all three PO₄ transporters was reduced by 40%, 50% and 60%, respectively, compared to their expression levels in non-stressed Col-0 roots. Furthermore, Figure 5E-J clearly show that the 7-day PO₄ starvation period induced the expression of these three PO₄ transporter encoding genes in both the P⁻ *drb2* shoot and root samples, compared to their expression levels in non-stressed *drb2* shoot and roots. Considering that Pi content of non-stressed and PO₄-stressed *drb4* shoots and roots was determined to be the same as that of the corresponding tissues in P⁺ and P⁻ Col-0 plants, it was unexpected to observe such varied differences in PO₄ transporter expression across both assessed tissues/growth conditions. For example, in P⁺ *drb4* roots, PHT1;4, PHT1;8 and PHT1;9 levels were each reduced by 60%, compared to P⁺ Col-0 roots (Figure 5F,H,J), yet the Pi content of non-stressed Col-0 and *drb4* roots was identical (Figure 5B).

3. Discussion

A lack of available P in the soil is a key limitation for plant growth globally [3,45] and as a consequence of P limitation, land plants have evolved highly complex regulatory mechanisms to control both the uptake of external P from the soil, primarily in the form of PO₄ (Pi), as well as the remobilization of internal stores of P during periods of low external PO₄ availability [46]. These elaborate P responsive mechanisms allow a plant to attempt to (1) maintain growth and development and (2) regulate cellular P content, regardless of external P concentration [1,2,7]. More contemporary research has focused on the regulatory role played by a suite of PO₄ responsive miRNA sRNAs that

either initiate or maintain PO₄ signaling pathways across the plant kingdom [4,20]. Central to this PO₄ responsive miRNA cohort, is miR399, with the miR399 sRNA required to regulate the abundance of the *PHO2* transcript, to in turn regulate the level of the PHO2 protein, an E2 ubiquitin conjugase that mediates the ubiquitin-directed turnover of a group of PO₄ transporter proteins [7,14,47]. The DRB family members, DRB1, DRB2 and DRB4, have each been ascribed a specific functional role in the *Arabidopsis* miRNA pathway [35–40,48,49]. Therefore, we sought to document the involvement of these three DRBs in the production of the PO₄ responsive miRNA, miR399, and to determine the mode of action directed by the miR399 sRNA during PO₄ starvation to regulate *PHO2* abundance in the *drb1*, *drb2* and *drb4* mutant backgrounds. Specifically, we attempted to determine what effect an altered miR399/*PHO2* expression module profile would have on the response of *drb1*, *drb2* or *drb4* mutant plants to the imposed stress in order to establish the contribution of either DRB1, DRB2 and/or DRB4 to the maintenance of P homeostasis in *Arabidopsis*.

3.1. DRB1 is Required to Maintain Phosphorous Homeostasis in *Arabidopsis*

Here, it was discovered that the maintenance of P homeostasis is impaired in the *drb1* loss-of-function mutant. The most compelling evidence for this was the documented alteration of the shoot to root Pi content ratio in both non-stressed (Figure 5C) and PO₄-stressed *drb1* plants (Figure 5D), relative to wild-type *Arabidopsis* (P⁺ or P⁻ Col-0 plants). Specifically, the shoot Pi content was reduced to a much greater degree in PO₄-stressed *drb1* plants than the observed reduction to Pi content in P⁻ Col-0 shoots. Furthermore, Pi was demonstrated to over-accumulate in the roots of both P⁺ and P⁻ *drb1* plants (Figure 5A,B), compared to the Pi content of the corresponding tissue, and growth regime, of Col-0 plants. The maintenance of appropriate P content in plant tissues is essential for the production of macromolecules, energy trafficking and for numerous signaling pathways [1,2,46]. Therefore, alterations to the P content of the shoot and root tissues of *drb1* plants indicated that in the absence of functional DRB1, P partitioning is impaired. Assessment of the expression of PO₄ transporters, *PHT1;4*, *PHT1;8* and *PHT1;9*, revealed that the abundance of each transporter was highly elevated by 24.5- 359.2- and 242.5-fold respectively, in the shoot tissue of P⁻ *drb1* plants. Phosphate transporter expression was also demonstrated to be altered in both P⁺ (*PHT1;4* reduced by 1.7-fold and *PHT1;9* reduced by 1.5-fold) and P⁻ (*PHT1;4* reduced by 1.5-fold and *PHT1;8* elevated by 2.0-fold) *drb1* roots, expression alterations that when taken together indicated that incorrect Pi partitioning in *drb1* plants potentially results from defective PO₄ transport from the root system to the aerial tissue in this mutant background.

Defective root to shoot PO₄ transport in the *drb1* mutant was further evidenced by the unique phenotypic response displayed by the *drb1* shoot to PO₄ stress. Specifically, the fresh weight of the shoot of 15-day old P⁻ *drb1* plants was only reduced by 21.6% compared to its non-stressed counterpart (Figure 1C). The rosette area of P⁻ *drb1* plants was also demonstrated to only be reduced by 29.3% post the 7-day PO₄ stress treatment (Figure 1D). Both responses were comparatively mild compared to the 36.6% and 60.1% reductions to fresh weight and rosette area respectively, documented for Col-0 shoots post the application of PO₄ stress. In addition, anthocyanin failed to change in abundance in the shoot tissues of P⁻ *drb1* plants compared to the shoots of non-stressed P⁺ *drb1* plants (Figure 1E). Anthocyanin production is a general response to a range of abiotic stresses, including PO₄ starvation [19,50]. The impaired ability of *drb1* shoots to produce anthocyanin in response to PO₄ stress may implicate DRB1, and the functional partnership DRB1 forms with DCL1, in the induction of PO₄ responsive gene expression pathways. Considering these mild responses displayed by *drb1* shoots, it was therefore surprising to observe that chlorophyll *a* and *b* overaccumulation was promoted to the greatest extent in the aerial tissues of *drb1* plants starved of PO₄. Altered chlorophyll content in P⁺ *drb1* shoots indicated that (1) *drb1* shoots are indeed negatively impacted by the imposed PO₄ stress, and (2) that DRB1 may potentially mediate a PO₄-directed role in regulating photosynthesis in *Arabidopsis* chloroplasts.

Considering the well-established role of the DRB1/DCL1 functional partnership in the production of the majority of miRNAs that accumulate in *Arabidopsis* tissues, it was unsurprising to observe that the miR399 precursors, *PRE-MIR399A*, *PRE-MIR399C*, *PRE-MIR399D*, *PRE-MIR399E* and *PRE-MIR399F*, over-accumulated to the greatest extent in P^+ *drb1* shoots (Figure 2A–E). In addition, precursors *PRE-MIR399A*, *PRE-MIR399C*, *PRE-MIR399D* and *PRE-MIR399F* were further demonstrated to be most highly abundant in the shoot tissues of PO_4 -stressed *drb1* plants. The enhanced abundance of miRNA precursor transcripts in the *drb1* mutant background is most likely the result of inefficient precursor transcript processing by DCL1 in the absence of DRB1 functional assistance, with DRB1 accurately positioning DCL1 on each miRNA precursor to direct accurate processing [48,49]. In spite of the readily observable evidence of inefficient miR399 precursor transcript processing in P^+ *drb1* shoots, miR399 levels were only reduced by 10% (Figure 5G). Similarly, although miR399 precursor transcript abundance was elevated to a much greater degree in P^- *drb1* shoots due to a combination of (1) *MIR399* gene expression induction in response to PO_4 starvation, and (2) inefficient precursor transcript processing in the absence of DRB1 activity, miR399 abundance was again demonstrated to be only mildly elevated by 2.3-fold in the shoots of PO_4 -stressed *drb1* plants (Figure 5G). Further, the abundance of the miR399 target transcript, *PHO2*, was only mildly elevated by 1.2-fold in response to the 10% reduction in miR399 levels in P^+ *drb1* shoots (Figure 2I). Surprisingly, *PHO2* transcript abundance was elevated by 1.5-fold in response to the 2.3-fold elevation in miR399 accumulation in P^- *drb1* shoots, and not reduced as expected. However, in P^+ Col-0 shoots, and as expected, the 2.9-fold enhancement to miR399 abundance led to a 50% reduction in *PHO2* expression (Figure 5G,I). Therefore, elevated *PHO2* abundance in response to enhanced miR399 levels in P^- *drb1* shoots, readily demonstrates that miR399-directed *PHO2* transcript cleavage, to regulate *PHO2* expression, is defective in the absence of DRB1 activity.

Altered PO_4 transporter expression in *drb1* roots indicated that the response of the root system of the *drb1* mutant to PO_4 stress would differ to that of the root system of wild-type *Arabidopsis*. Accordingly, the fresh weight of PO_4 -stressed *drb1* roots was reduced by 25.0% compared to the mild 6.5% reduction to the fresh weight of P^- Col-0 roots, a 3.8-fold enhancement to the severity of this phenotypic response (Figure 3C). It was therefore curious to observe a similar degree of reduction to primary root length in P^- *drb1* (46.7%) and P^- Col-0 (51.2%) plants (Figure 3D). A greater degree of reduction to the fresh weight of P^- *drb1* roots, compared to P^- Col-0 roots, could be partially explained by the observation that the induction of lateral root formation by PO_4 stress was completely defective in P^- *drb1* roots, compared to a 44.0% increase in lateral root number in P^- Col-0 roots (Figure 3D). Considering that the measurement of fresh weight is largely assessing the moisture content of a plant, the observed reduction to fresh weight of P^- *drb1* roots could potentially be indicating that under PO_4 stress conditions, DRB1 is somehow involved in regulating the moisture content of the root system of *Arabidopsis*. However, this was not assessed in this study with the mechanism driving the enhancement of fresh weight reductions requiring further investigation in the future.

Similar to its establishment as the primary DRB protein required to regulate miR399 production from the *PRE-MIR399A*, *PRE-MIR399C*, *PRE-MIR399D*, *PRE-MIR399E* and *PRE-MIR399F* precursors in the aerial tissues of non-stressed *Arabidopsis* plants, DRB1 was again demonstrated to be the primary DRB protein required to regulate miR399 production from the *PRE-MIR399A* and *PRE-MIR399C* precursor transcripts in the *Arabidopsis* root system with both precursors demonstrated to accumulate to the greatest degree in P^+ and P^- *drb1* roots (Figure 4B,C). Reduced *PRE-MIR399A* and *PRE-MIR399C* processing efficiency in the absence of DRB1 activity, reduced miR399 abundance by 30% in P^+ *drb1* roots (Figure 4E), and in turn, this moderate reduction to miR399 levels led to a mild elevation (1.2-fold) in the expression of the miR399 target gene, *PHO2* (Figure 4G). As documented in P^- *drb1* shoots, the 1.8-fold elevation to miR399 levels in P^- *drb1* roots, resulted in a moderate elevation to *PHO2* transcript abundance (1.6-fold), and not a reduction in target gene expression as would be expected for a miRNA that regulates the expression of its targeted genes solely via a mRNA cleavage mode of RNA silencing. However, considering that a similar miRNA/target gene expression profile of elevated miR399 abundance (2.5-fold), together with enhanced *PHO2* expression (1.9-fold)

was also observed in PO₄-stressed Col-0 roots, this curious finding indicates that miR399-directed *PHO2* transcript cleavage may not be the predominant mechanism of target gene expression regulation directed by the miR399 sRNA in the *Arabidopsis* root system. Alternatively, elevated *PHO2* expression in P⁺ Col-0 and P⁺ *drb1* roots when miR399 abundance is also elevated may result from the enhanced expression of the eTM of miR399 activity, *IPS1*. In P⁻ Col-0 shoots for example, where elevated miR399 abundance was demonstrated to direct enhanced expression repression of the *PHO2* transcript (Figure 2G,I), *IPS1* abundance was elevated by 75.7-fold, compared to its abundance in P⁺ Col-0 shoots (Figure 2H). In PO₄-stressed roots, however, *IPS1* expression was elevated to a much greater degree, by 1076-fold (Figure 4F). This 14.2-fold greater promotion to *IPS1* expression in P⁻ Col-0 roots, than that observed in P⁻ Col-0 shoots, would be expected to sequester a higher amount of miR399, which in turn, could have led to the observed elevation in *PHO2* expression in P⁻ Col-0 roots in the presence of 2.5-fold greater abundance of the *PHO2* targeting miRNA, miR399.

3.2. DRB2 is Required to Maintain Phosphate Homeostasis in *Arabidopsis*

As documented for the *drb1* mutant, P homeostasis was determined to be defective in the *drb2* mutant. Specific to *drb2* plants however, was the 27.8% reduction to the Pi content of non-stressed *drb2* shoots (Figure 5A). Of the four *Arabidopsis* plant lines assessed in this study, *drb2* was the only line determined to have a reduced aerial tissue Pi content when cultivated under standard growth conditions. Furthermore, in P⁺ *drb2* shoots, *PHT1;4* (Figure 5E) and *PHT1;8* (Figure 5G) expression was determined to be reduced and elevated by 1.2- and 3.4-fold respectively, compared to the expression of these two PO₄ transporters in P⁺ Col-0 shoots. In addition, Pi was determined to over-accumulate by 36.1% in P⁺ *drb2* roots. In P⁺ *drb2* roots, *PHT1;4*, *PHT1;8* and *PHT1;9* expression was reduced by 1.7-, 2.0- and 2.4-fold respectively, compared to their expression levels in P⁺ Col-0 roots. Together, (1) reduced Pi content of P⁺ *drb2* shoots, (2) elevated Pi content in P⁺ *drb2* roots, and (3) reduced PO₄ transporter gene expression in P⁺ *drb2* roots, indicated that PO₄ root to shoot transport is defective in non-stressed *drb2* plants. Based on this finding, it was curious to observe a similar Pi content in P⁻ *drb2* shoots and P⁻ Col-0 shoots (Figure 5A), especially considering the document enhancement to *PHT1;4* and *PHT1;9* expression in P⁻ *drb2* shoots, with the expression of these two PO₄ transporters elevated by 2.8- and 7.0-fold respectively, compared to the degree of expression induction observed in P⁻ Col-0 roots (Figure 5E,I). However, and as demonstrated for P⁺ *drb2* shoots and roots, the Pi content of the root system of PO₄-stressed *drb2* plants was altered, reduced by 48% compared to the Pi content of P⁻ Col-0 roots. Interestingly, RT-qPCR revealed similar degrees of elevated *PHT1;8* (Figure 5H) and *PHT1;9* (Figure 5J) expression in PO₄-stressed Col-0 and *drb2* roots with only the *PHT1;4* transcript returning a slight difference in its expression in P⁻ Col-0 roots (elevated by 1.2-fold compared to P⁺ Col-0 roots) and P⁻ *drb2* roots (reduced by 1.1-fold compared to P⁺ Col-0 roots). The PO₄ transporters, *PHT1;1* and *PHT1;4*, have been demonstrated to be responsible for the import of more than half of the Pi that is taken up from the soil [51]. It therefore seems unlikely that the mild 10% reduction to *PHT1;4* transcript abundance documented in PO₄-stressed *drb2* roots, is the sole cause of the considerable reduction to the Pi content of the root system in the *drb2* mutant background.

Considering that the Pi content of PO₄-stressed Col-0 and *drb2* shoots was determined to be similar, it was unsurprising to document a similar degree of reduction to fresh weight of the shoot tissues of P⁻ Col-0 (36.6%) and P⁻ *drb2* (39.1%) plants (Figure 1C). Rosette area was also decreased by a similar degree in P⁻ Col-0 (60.1%) and P⁻ *drb2* (48.0%) plants (Figure 1D). However, compared to PO₄-stressed Col-0 shoots, anthocyanin accumulated to considerably higher levels in the aerial tissues of *drb2* plants when exposed to PO₄ stress (Figure 1E). The induction of anthocyanin production is a well-characterized response to PO₄ starvation [19,50]. Therefore, the considerable enhancement of anthocyanin accumulation in P⁻ *drb2* shoots, compared to the shoot tissues of PO₄-stressed Col-0 plants, suggests that this P-responsive pathway is hyperactivated in the absence of DRB2 activity,

as well as potentially implicating DRB2 in mediating a regulatory role in a range of other P-responsive pathways in *Arabidopsis* aerial tissues that were not assessed in this study.

We have previously demonstrated a role for DRB2 in the production stage of the *Arabidopsis* miRNA pathway with the abundance of specific miRNA cohorts altered in the *drb2* mutant background [37]. More specifically, DRB2 can either be antagonistic or synergistic to DRB1 function in the DRB1/DCL1 partnership for the production of specific miRNAs, resulting in miRNA abundance either being enhanced (antagonistic) or reduced (synergistic) in *drb2* plants [37,38]. Reduced precursor transcript abundance in non-stressed *drb2* shoots, indicated that DRB2 plays a secondary role in regulating miR399 production from the *PRE-MIR399A*, *PRE-MIR399E* and *PRE-MIR399F* precursors, potentially via antagonism of DRB1 function (Figure 2B,E,F). The antagonism of DRB2 on the DRB1/DCL1 partnership becomes more readily apparent via the profiling of miR399 precursor transcript expression in P⁻ *drb2* shoots, with lower degrees of expression induction observed for the *PRE-MIR399C*, *PRE-MIR399D*, *PRE-MIR399E* and *PRE-MIR399F* precursors (Figure 2C–F). Reduced precursor transcript abundance in P⁻ *drb2* shoots, compared to the respective abundance of each precursor in either P⁻ Col-0 or P⁻ *drb1* shoots, indicates that in the absence of DRB2 activity, precursor transcript processing efficiency is enhanced due to more precursor transcript being freely available to enter the canonical DRB1/DCL1 production pathway.

As demonstrated in P⁺ *drb1* shoots, significantly altered precursor transcript abundance in P⁺ *drb2* shoots, failed to have a strong influence on the accumulation of miR399, with miR399 levels only mildly elevated by 10% in P⁺ *drb2* shoots, compared to P⁺ Col-0 shoots (Figure 5G). However, DRB2 antagonism was still evidenced by this mild increase to miR399 abundance compared to the 10% reduction in miR399 levels observed in P⁺ *drb1* shoots. The antagonism of DRB2 on miR399 production was further evidenced by the enhanced expression repression of *PHO2* in P⁻ *drb2* shoots (Figure 2I). The abundance of miR399 was elevated by 2.7-fold in P⁻ *drb2* shoots, and therefore, a further degree of reduced *PHO2* expression in P⁻ *drb2* shoots, compared to P⁻ *drb1* shoots where miR399 levels were elevated by 2.3-fold and *PHO2* expression was enhanced by 1.5-fold, clearly demonstrated enhanced DRB1-mediated, miR399-directed, *PHO2* transcript cleavage in the absence of DRB2 antagonism. Similarly, it is important to note here that *IPS1* transcript abundance was enhanced to a much lower degree in P⁻ *drb2* shoots (27.1-fold) compared to *IPS1* abundance induction in either PO₄-stressed Col-0 (75.7-fold) or *drb1* (85.4-fold) shoots. This unexpected observation again indicated that in the absence of DRB2 activity, miR399-directed target transcript cleavage was enhanced. Although *IPS1* has been identified as a non-cleavable eTM of miR399 activity, the *IPS1* expression trends presented in Figure 5H suggest that miR399 may well be capable of directing miRISC-catalyzed cleavage of the *IPS1* transcript in addition to solely being sequestered by *IPS1*.

Compared to the mild 6.5% reduction to the fresh weight of P⁻ Col-0 roots, the negative response of the root system of the *drb2* mutant to PO₄ stress was considerably more pronounced at 25.8% (Figure 3C). Considering that the correct regulation of Pi content is dysfunctional in both control and PO₄-stressed *drb2* roots, differing responses to PO₄ stress in *drb2* roots, compared to P⁻ Col-0 roots, was not surprising. Similarly, inhibition of the primary root length of P⁻ *drb2* plants at 20.3% was comparatively mild compared to the severe 51.2% inhibition to the primary root length observed for P⁻ Col-0 plants (Figure 5D). The degree of lateral root induction also differed between PO₄-stressed Col-0 and *drb2* roots (Figure 5E), specifically; lateral root formation was enhanced by ~44% in P⁻ Col-0 plants, and in PO₄-stressed *drb2* plants, lateral root formation was further promoted by 17% with P⁻ *drb2* plants developing ~61% more lateral roots than their non-stressed counterparts. When these phenotypic responses of the root system of PO₄-stressed *drb2* plants are considered together, including a lower degree of primary root length inhibition (2.5-fold less than P⁻ Col-0 plants), and a more pronounced enhancement to lateral root formation (1.4-fold more than P⁻ Col-0 plants), it was highly surprising that the fresh weight of P⁻ *drb2* roots was reduced by a 4.0-fold greater degree than documented for P⁻ Col-0 roots. Similar levels of expression of *PRE-MIR399A* in both non-stressed

and PO₄-stressed Col-0 and *drb2* roots revealed that DRB2 does not play a role in regulating miR399 processing from this precursor transcript (Figure 4B). Reduced expression of *PRE-MIR399C* in P⁺ *drb2* roots (compared to P⁻ Col-0 and P⁻ *drb1* roots) and a lower level of precursor over-accumulation in P⁻ *drb2* roots (compared to P⁻ *drb1* roots), identified DRB2 as playing a secondary role in regulating miR399 production from this precursor transcript in the *Arabidopsis* root system (Figure 4C) via antagonism of DRB1 function. The expression trend of *PRE-MIR399D* in P⁻ *drb2* roots additionally identified a secondary role for DRB2 in regulating miR399 production from the third miR399 precursor transcript detected in the root system of the four *Arabidopsis* plant lines assessed in this study. However, for the *PRE-MIR399D* precursor, DRB2 appears to be antagonistic to the DRB4/DCL4 partnership, and not to the canonical DRB1/DCL1 partnership demonstrated to be required for the production of the majority of *Arabidopsis* miRNAs. DRB2 has been demonstrated previously to be antagonistic to DRB4 function in the DRB4/DCL4 partnership for the production of a small subset of newly evolved *Arabidopsis* miRNAs processed from precursor transcripts that fold to form highly complementary stem-loop structures [39,40]. Considering that in P⁺ *drb2* roots, *PRE-MIR399A* and *PRE-MIR399D* remained at their approximate wild-type levels, and that the *PRE-MIR399C* precursor was reduced in its abundance by 1.7-fold, a finding that initially indicated that this precursor is more efficiently processed by DRB1/DCL1 in the absence of DRB2 activity, the 2.0-fold reduction to miR399 abundance alternatively indicated that *MIR399C* gene expression may in fact be reduced in PO₄-stressed *drb2* roots. It was therefore curious to observe *PHO2* expression to be reduced by 1.3-fold in P⁺ *drb2* roots, and not elevated in response to reduced miR399 abundance as expected. However, this observation is potentially demonstrating that in spite of being reduced in abundance, this lower level of miR399 directs more efficient cleavage of the *PHO2* transcript in the absence of DRB2 activity. In P⁻ *drb2* roots, miR399 abundance was determined to be elevated by 2.6-fold compared to its abundance in P⁻ Col-0 roots (Figure 4E). As observed in P⁺ *drb2* roots, *PHO2* expression scaled in accordance with elevated miR399 abundance, with *PHO2* expression increased by 4.5-fold in PO₄-stressed *drb2* roots. It is interesting to note here that *PHO2* expression scaled with miR399 abundance in six out of the eight root tissue samples molecularly assessed by RT-qPCR in this study. We have previously demonstrated that DRB2-dependent miRNAs direct a translational repression mode of miRNA-directed target gene expression repression [52], and scaling of miRNA target transcripts together with their targeting miRNA, has been previously reported for miRNA sRNAs that direct a translational repression mode of target gene expression regulation [52–54].

3.3. DRB4 is Required For miR399 Production in *Arabidopsis* Roots

Profiling of PO₄ transporter expression in the shoots and roots of P⁺ and P⁻ *drb4* plants revealed considerable alteration to *PHT1;4*, *PHT1;8* and *PHT1;9* transcript abundance across both assessed tissues and growth regimes (Figure 5E–J). However, in spite of these documented differences in PO₄ transporter gene expression in *drb4* shoots and roots, the Pi content of non-stressed and PO₄-stressed *drb4* tissues remained at levels comparable to P⁺ and P⁻ Col-0 shoots and roots (Figure 5A,B). Considering this finding, it was unsurprising that the developmental progression of Col-0 and *drb4* plants was impeded to the same extent when cultivated in the absence of PO₄ for a 7-day period. Specifically, the fresh weight of both P⁻ Col-0 and P⁻ *drb4* shoots was reduced by ~36% compared to their non-stressed counterparts of the same age (Figure 1C). In addition, anthocyanin, chlorophyll *a* and chlorophyll *b* were all elevated to the same degree in PO₄-stressed Col-0 and *drb4* shoots, compared to their respective non-stressed counterparts. It was therefore surprising that the rosette area of P⁻ *drb4* plants was only reduced by 38.7% compared to the more severe 60.1% reduction observed for P⁻ Col-0 plants. Although an unexpected finding, this result clearly indicated that some of the responses of the *drb4* mutant to PO₄ starvation differ to those of wild-type *Arabidopsis*.

Considering the well-established role of the DRB4/DCL4 partnership in *trans*-acting siRNA (tasiRNA) [55,56] and p4-siRNA [40] production, and for the processing of a small number of newly evolved miRNAs from their highly complementary precursor transcripts [39], it was highly surprising

to additionally establish the widespread involvement of DRB4 in regulating the production of the highly conserved miRNA, miR399, in *Arabidopsis* shoots (Figure 2). Specifically, DRB4 was determined to play a secondary role to DRB1 in regulating the efficiency of miR399 production from all five precursors detectable by RT-qPCR in non-stressed *Arabidopsis* shoots. As demonstrated for DRB2, the involvement of DRB4 in miR399 production in *Arabidopsis* shoots is most likely via antagonism of the canonical DRB1/DCL1 partnership. Antagonism of the DRB1/DCL1 partnership by DRB4 was again demonstrated by the accumulation profiles of precursors, *PRE-MIR399C*, *PRE-MIR399D*, *PRE-MIR399E* and *PRE-MIR399F*, in the shoot tissues of PO₄-stressed *drb4* plants (Figure 2C–F). Although precursor transcript abundance was highly variable in *drb4* shoots, miR399 levels were only mildly elevated by 1.2- and 2.4-fold in P⁺ *drb4* and P⁻ *drb4* shoots, respectively (Figure 2G). Surprisingly, in spite of the 20% elevation to miR399 levels in P⁺ *drb4* shoots, *PHO2* expression was elevated to a similar degree (30% increase), and not reduced as expected (Figure 5I). In P⁻ *drb4* shoots, however, the 2.4-fold elevated abundance of the miR399 sRNA was determined, as expected, to reduce the expression of *PHO2* by 2.5-fold. This result clearly indicated that in the absence of DRB4 activity in *Arabidopsis* shoots, the efficiency of DRB1-mediated, miR399-directed cleavage of the *PHO2* transcript is enhanced. The fresh weight of P⁻ *drb4* roots was reduced by 18.6% compared to the fresh weight of P⁺ *drb4* roots, a 2.9-fold further enhancement of this phenotypic response to PO₄ stress, compared to the mild response of P⁻ Col-0 roots (6.5% fresh weight reduction compared to P⁺ Col-0 roots). The response of the primary root of the *drb4* mutant to PO₄ stress also differed to that of wild-type roots. Namely, the length of P⁻ *drb4* primary root was only reduced by 10.3% compared to the significant 51.2% reduction to the length of the primary root of P⁻ Col-0 plants (Figure 3D). Although lateral root development was induced to the same degree (44%) in the root system of PO₄-stressed Col-0 and *drb4* plants, the considerable differences observed for the fresh weight of the *drb4* root system, and the lack of inhibition to primary root length in P⁻ *drb4* plants, clearly revealed that the *drb4* mutant background is defective in some of its responses to PO₄ starvation, compared to the responses of the Col-0 root system to this stress.

At the molecular level, the wild-type-like expression of the *PRE-MIR399A* precursor in the roots of non-stressed and PO₄-stressed *drb4* plants indicated that DRB4 does not play a role in regulating miR399 production from this precursor in *Arabidopsis* roots. Expression analysis of *PRE-MIR399C* did however identify a secondary role for DRB4 in regulating miR399 production from this precursor, potentially via antagonism of DRB1 function (Figure 4C). Of particular interest stemming from miR399 precursor transcript profiling in non-stressed and PO₄-stressed *Arabidopsis* roots is the unexpected finding that DRB4 appears to be the primary DRB required to regulate miR399 production from the *PRE-MIR399D* precursor (Figure 4D), with the abundance of the *PRE-MIR399D* precursor over-accumulating to its highest levels in both P⁺ and P⁻ *drb4* roots. Curiously, assessment of the stem-loop folding structures of the six precursors from which the miR399 sRNA is liberated does not readily distinguish the *PRE-MIR399D* structure from the folding structures of the other five miR399 precursor transcripts. Therefore, the establishment of a role for DRB4 in regulating miR399 processing efficiency from its precursor transcripts was a highly unexpected finding, a finding that requires additional experimentation in the future to identify the precursor transcript-based sequence and/or structural features that recruits the involvement of DRB4 to the miR399/*PHO2* expression module.

The elevated abundance of the *PRE-MIR399C* and *PRE-MIR399D* precursors in P⁺ *drb4* roots indicated reduced precursor transcript processing efficiency in the absence of DRB4. Accordingly, a 30% reduction to miR399 accumulation was observed in P⁺ *drb4* roots (Figure 4E). Surprisingly, this 1.4-fold reduction to miR399 levels in P⁺ *drb4* roots led to a 2.0-fold reduction to *PHO2* expression (Figure 4G). This result suggested that although miR399 levels were reduced in non-stressed *drb4* roots, the reduced amount of the miR399 sRNA was actually directing enhanced *PHO2* expression repression via unimpeded DRB1-mediated, miR399-directed, *PHO2* cleavage. However, enhanced miR399-directed *PHO2* cleavage appeared to be lost in PO₄-stressed *drb4* roots with both miR399 and *PHO2* levels elevated by 2.0- and 5.1-fold, respectively (Figure 4E,G). Therefore, when taken together,

although miR399-directed *PHO2* cleavage appeared to be enhanced in P⁺ *drb4* roots, the scaling of *PHO2* expression together with miR399 abundance in PO₄-stressed *drb4* roots, potentially suggests that in a cell type with altered physiology, and where DRB4 function is defective, the miR399 sRNA changed from directing an mRNA cleavage mode of RNA silencing, to directing a translational repression mode of RNA silencing.

3.4. DRB1, DRB2 and DRB4 Are Required to Regulate the miR399/PHO2 Expression Module in Arabidopsis Shoots and Roots

Here we demonstrate that the phenotypic and molecular response to PO₄ starvation were unique to each *drb* mutant background assessed due to the hierarchical contribution of DRB1, DRB2 and DRB4 to the regulation of the miR399/*PHO2* expression module. Specifically, the molecular profiling of miR399 precursor transcript expression identified DRB1 as the primary DRB required for efficient miR399 production from each precursor in non-stressed and PO₄-stressed shoots and roots. Deregulated miR399 precursor transcript processing efficiency in the absence of DRB1 activity was demonstrated to result in defective P homeostasis maintenance, altering the shoot to root ratio of Pi content in the *drb1* mutant background. The maintenance of P homeostasis was also defective in *drb2* plants, with the Pi content shoot to root ratio altered in this mutant background, both under standard growth conditions and in conditions of PO₄ starvation. An altered Pi content in *drb2* tissues appeared to result from defective PO₄ transport between the root system and aerial tissues in the absence of DRB2 function. Further, DRB2 was determined to play a secondary role to DRB1 in regulating miR399 production from the profiled *PRE-MIR399* precursor transcripts. The secondary role of DRB2 in regulating miR399 production from the assessed *PRE-MIR399* precursor transcripts was revealed to most likely be via antagonism of DRB1 function. DRB4 was also determined to play a secondary role in regulating the miR399/*PHO2* expression module in *Arabidopsis* shoots and roots, and as demonstrated for the secondary role of DRB2 in providing additional regulatory complexity to this expression module, DRB4 also appeared to be antagonistic to the primary functional role of DRB1 in regulating miR399 precursor transcript processing efficiency. Furthermore, DRB4 also appeared to be the primary DRB required for miR399 production from the *PRE-MIR399D* precursor in non-stressed and PO₄-stressed *Arabidopsis* roots. When taken together, the hierarchical contribution of DRB1, DRB2 and DRB4 to the regulation of the miR399/*PHO2* expression module documented here, readily demonstrates the crucial importance of maintaining P homeostasis in *Arabidopsis* tissues to ensure the maintenance of a wide range of cellular processes to which P is essential.

4. Materials and Methods

4.1. Plant Material and Phosphate Stress Treatment

The T-DNA insertion knockout mutant lines used in this study, including the *drb1* (*drb1-1*; SALK_064863), *drb2* (*drb2-1*; GABI_348A09) and *drb4* (*drb4-1*; SALK_000736) mutants, have been described previously [42]. The seeds of these three *drb* mutant lines, and of wild-type *Arabidopsis* (ecotype Columbia-0 (Col-0)) plants, were sterilized using chlorine gas and post-sterilization, seeds were plated out onto standard *Arabidopsis* plant growth media (half-strength Murashige and Skoog (MS) salts), and stratified for 48 h at 4 °C in the dark. Post-stratification, the sealed plates were transferred to a temperature-controlled growth cabinet (A1000 Growth Chamber, Conviron[®] Australia) and cultivated for an 8-day period under a standard growth regime of 16 h light / 8 h dark, and a day/night temperature of 22 °C / 18 °C. Post this initial 8-day cultivation period, equal numbers of Col-0, *drb1*, *drb2* and *drb4* seedlings were transferred under sterile conditions to either fresh standard *Arabidopsis* plant growth media that contained 1.0 mM of PO₄ (P⁺ plants; non-stressed controls) or to *Arabidopsis* plant growth media where the PO₄ had been replaced with an equivalent molar amount (1.0 mM) of potassium chloride (KCl) (P⁻ plants; PO₄ stress treatment). Post seedling transfer, the P⁺ and P⁻ plates for each plant line were returned to the temperature-controlled growth cabinet for an

additional 7-day cultivation period. For the tissue-specific analyses performed here, namely the root tissue assessments, additional Col-0, *drb1*, *drb2* and *drb4*, 8-day old seedlings were treated exactly as outlined above, except for the 7-day treatment period, where P⁺ and P⁻ plates were orientated for vertical growth. Unless stated otherwise, all the phenotypic and molecular analyses reported here were conducted on 15-day old plants.

4.2. Phenotypic and Physiological Assessments

The fresh weight of 8-day old Col-0, *drb1*, *drb2* and *drb4* whole plants germinated and cultivated on standard *Arabidopsis* plant growth media was initially determined to establish the effect of loss of DRB1, DRB2 or DRB4 activity on *Arabidopsis* development. The fresh weight of 15-day old Col-0, *drb1*, *drb2* and *drb4* plants was also determined to establish the effect of the 7-day PO₄ stress treatment on the development of each plant line. The area of the rosette and the length of the primary root of 15-day old Col-0, *drb1*, *drb2* and *drb4* plants was determined via the assessment of photographic images using the ImageJ software. The same photographic images were also used to establish the number of lateral roots formed by P⁺ and P⁻ Col-0, *drb1*, *drb2* and *drb4* plants post the 7-day stress treatment period.

A standard methanol:HCl (99:1 v/v) extraction method was applied to extract anthocyanin from P⁺ and P⁻ plants, and post extraction, anthocyanin content was determined using a spectrophotometer (Thermo Scientific, Australia) at an absorbance wavelength of 535 nanometers (A₅₃₅). The 99:1 (v/v) methanol:HCl extraction buffer was used as the blanking solution and the A₅₃₅ of each sample was next divided by the fresh weight of the sample to calculate the relative anthocyanin content per gram of fresh weight (A₅₃₅/g FW).

For chlorophyll *a* and *b* content quantification, rosette leaves of 15-day old P⁺ and P⁻ Col-0, *drb1*, *drb2* and *drb4* plants were sampled and incubated in 80% acetone for 24 h in the dark. Post incubation, rosette leaf tissue was clarified via centrifugation at 15,000 × *g* for 7 min at room temperature. The resulting supernatants were immediately transferred to a spectrophotometer and the absorbance of these solutions assessed at wavelengths 646 nm (A₆₄₆) and 663 nm (A₆₆₃) using 80% acetone as the blanking solution. The chlorophyll *a* and *b* content of each sample was then determined using the Lichtenthaler's equations exactly as outlined in [57], and these initially determined values were subsequently converted to micrograms per gram of fresh weight (µg/g FW).

The shoot and root tissue of 15-day old P⁺ and P⁻ Col-0, *drb1*, *drb2* and *drb4* plants were carefully separated from each other and then ground into a fine powder under liquid nitrogen (LN₂). One milliliter (1.0 mL) of 10% acetic acid (v/v in H₂O) was added to the ground powder and the powder thoroughly resuspended via vigorous vortexing. The resulting resuspension was then centrifuged at 15,000 × *g* for 5 min at room temperature, and post centrifugation, 700 µL of the resulting supernatant was mixed with an equivalent volume of Ames Assay Buffer (6 parts 0.5% ammonium molybdate (v/v in H₂O) to 1 part of 2.5% sulphuric acid (v/v in 10% acetic acid)) and incubated at room temperature for 1 h in the dark. The absorbance of each solution was determined using a spectrophotometer at wavelength 820 nm (A₈₂₀) and the Pi content (µmol/gFW) of each sample subsequently determined via the construction of a Pi standard curve.

4.3. Total RNA Extraction for Quantitative Molecular Assessments

For each molecular assessment reported here, total RNA was extracted from four biological replicates (each biological replicate contained tissue sampled from eight individual plants) of 15-day old P⁺ and P⁻ Col-0, *drb1*, *drb2* and *drb4* plants using TRIzolTM Reagent according to the manufacturer's (InvitrogenTM) instructions. The quality of the extracted total RNA was visually assessed via a standard electrophoresis approach on a 1.2% (w/v) ethidium bromide stained agarose gel and the quantity of total RNA extracted determined using a NanoDrop spectrophotometer (NanoDrop[®] ND-1000, Thermo Scientific, Australia).

For the synthesis of a miR399-specific complementary DNA (cDNA), 200 nanograms (ng) of total RNA was treated with 0.2 units (U) of DNase I (New England Biolabs, Australia) according to the

manufacturer's instructions. The DNase I-treated total RNA was next used as template for cDNA synthesis with 1.0 U of ProtoScript® II Reverse Transcriptase (New England Biolabs, Australia) and the cycling conditions of 1 cycle of 16 °C for 30 min; 60 cycles of 30 °C for 30 s, 42 °C for 30 s, and 50 °C for 2 s, and; 1 cycle of 85 °C for 5 min.

A global, high molecular weight cDNA library for gene expression quantification was constructed via the initial treatment of 5.0 µg of total RNA with 5.0 U of DNase I according to the manufacturer's protocol (New England Biolabs, Australia). The DNase I-treated total RNA was next purified using an RNeasy Mini Kit (Qiagen, Australia) and 1.0 µg of this preparation used as template for cDNA synthesis along with 1.0 U of ProtoScript® II Reverse Transcriptase (New England Biolabs, Australia) and 2.5 mM of oligo dT₍₁₈₎, according to the manufacturer's instructions.

All generated, single-stranded cDNAs were next diluted to a working concentration of 50 ng/µL in RNase-free H₂O prior to their use as a template for the quantification of the abundance of either the miR399 sRNA or of gene transcripts. In addition, all RT-qPCRs used the same cycling conditions of 1 cycle of 95 °C for 10 min, followed by 45 cycles of 95 °C for 10 s and 60 °C for 15 s, and the GoTaq® qPCR Master Mix (Promega, Australia) was used as the fluorescent reagent for all performed RT-qPCR experiments. miR399 abundance and gene transcript expression was quantified using the 2^{-ΔΔCT} method with the small nucleolar RNA, *snoR101*, and *UBIQUITIN10 (UBI10; AT4G05320)* used as the respective internal controls to normalize the relative abundance of each assessed transcript. The sequence of each DNA oligonucleotide used in this study either for the synthesis of a miR399-specific cDNA, or to quantify transcript abundance via RT-qPCR is provided in Supplemental Table S1.

Supplementary Materials: The following are available online at <http://www.mdpi.com/2223-7747/8/5/124/s1>, Table S1: Sequences of the DNA oligonucleotides used in this study for the synthesis of miRNA-specific cDNAs and the RT-qPCR based quantification of miRNA abundance, miRNA target gene expression, or the assessment of standard gene expression.

Author Contributions: J.L.P., C.P.G. and A.L.E. conceived and designed the research. J.L.P. and J.M.O. performed the experiments and analyzed the data. J.L.P., C.P.G., J.M.O. and A.L.E. authored the manuscript and, J.L.P., C.P.G., J.M.O. and A.L.E. have read and approved the final version of the manuscript.

Funding: This research received no external funding.

Acknowledgments: The authors would like to thank fellow members of the Centre for Plant Science at the University of Newcastle for their guidance with plant growth care and RT-qPCR experiments.

Conflicts of Interest: The authors declare no conflict of interest.

References

1. Abel, S.; Ticconi, C.A.; Delatorre, C.A. Phosphate sensing in higher plants. *Planta* **2002**, *115*, 1–8. [[CrossRef](#)]
2. Hammond, J.P.; Bennett, M.J.; Bowen, H.C.; Broadley, M.R.; Eastwood, D.C.; May, S.T.; Rahn, C.; Swarup, R.; Woolaway, K.E.; White, P.J. Changes in Gene Expression in *Arabidopsis* Shoot during Phosphate Starvation and the Potential for Developing Smart Plants. *Society* **2003**, *132*, 578–596. [[CrossRef](#)] [[PubMed](#)]
3. Raghothama, K.G. Phosphate transport and signaling. *Curr. Opin. Plant Biol.* **2000**, *3*, 182–187. [[CrossRef](#)]
4. Hackenberg, M.; Shi, B.J.; Gustafson, P.; Langridge, P. Characterization of phosphorus-regulated miR399 and miR827 and their isomirs in barley under phosphorus-sufficient and phosphorus-deficient conditions. *BMC Plant Biol.* **2013**, *13*, 214. [[CrossRef](#)]
5. Chiou, T.J.; Lin, S.I. Signaling network in sensing phosphate availability in plants. *Annu. Rev. Plant Biol.* **2011**, *62*, 185–206. [[CrossRef](#)] [[PubMed](#)]
6. Wu, P.; Ma, L.; Hou, X.; Wang, M.; Wu, Y.; Liu, F.; Deng, X.W. Phosphate Starvation Triggers Distinct Alterations of Genome Expression in *Arabidopsis* Roots and Leaves. *Plant Physiol.* **2003**, *132*, 1260–1271. [[CrossRef](#)] [[PubMed](#)]
7. Lin, S.I.; Chiang, S.F.; Lin, W.Y.; Chen, J.W.; Tseng, C.Y.; Wu, P.C.; Chiou, T.J. Regulatory network of microRNA399 and PHO2 by systemic signaling. *Plant Physiol.* **2008**, *147*, 732–746. [[CrossRef](#)] [[PubMed](#)]
8. Jones, D.L. Organic acids in the rhizosphere – A critical review. *Plant Soil* **1998**, *205*, 25–44. [[CrossRef](#)]
9. Poirier, Y.; Thoma, S.; Somerville, C.; Schiefelbein, J. Mutant of *Arabidopsis* deficient in xylem loading of phosphate. *Plant Physiol.* **1991**, *97*, 1087–1093. [[CrossRef](#)]

10. Stefanovic, A.; Arpat, A.B.; Bligny, R.; Gout, E.; Vidoudez, C.; Bensimon, M.; Poirier, Y. Over-expression of PHO1 in *Arabidopsis* leaves reveals its role in mediating phosphate efflux. *Plant J.* **2011**, *66*, 689–699. [[CrossRef](#)]
11. Wang, Y.; Ribot, C.; Rezzonico, E.; Poirier, Y. Structure and Expression Profile of the *Arabidopsis* PHO1 Gene Family Indicates a Broad Role in Inorganic Phosphate Homeostasis 1. *Plant Physiol.* **2004**, *135*, 400–411. [[CrossRef](#)]
12. Delhaize, E.; Randall, P.J. Characterization of a Phosphate-Accumulator Mutant of *Arabidopsis thaliana*. *Plant Physiol.* **1995**, *107*, 207–213. [[CrossRef](#)]
13. Dong, B.; Rengel, Z.; Delhaize, E. Uptake and translocation of phosphate by *pho2* mutant and wild-type seedlings of *Arabidopsis thaliana*. *Planta* **1998**, *205*, 251–256. [[CrossRef](#)]
14. Park, B.S.; Seo, J.S.; Chua, N.H. Nitrogen Limitation Adaptation recruits PHOSPHATE2 to target the phosphate transporter PT2 for degradation during the regulation of *Arabidopsis* phosphate homeostasis. *Plant Cell* **2014**, *26*, 454–464. [[CrossRef](#)]
15. Aung, K. *pho2*, a Phosphate Overaccumulator, Is Caused by a Nonsense Mutation in a MicroRNA399 Target Gene. *Plant Physiol.* **2006**, *141*, 1000–1011. [[CrossRef](#)]
16. Nilsson, L.; Müller, R.; Nielsen, T.H. (2007). Increased expression of the MYB-related transcription factor, PHR1, leads to enhanced phosphate uptake in *Arabidopsis thaliana*. *Plant Cell Environ.* **2007**, *30*, 1499–1512. [[CrossRef](#)]
17. Rubio, V.; Linhares, F.; Solano, R.; Mart'ın, A.C.; Iglesias, J.; Leyva, A.; Paz-Ares, J. A conserved MYB transcription factor involved in phosphate starvation signaling both in vascular plants and in unicellular algae. *Genes Dev.* **2001**, *15*, 2122–2133. [[CrossRef](#)]
18. Fujii, H.; Chiou, T.J.; Lin, S.I.; Aung, K.; Zhu, J.K. A miRNA involved in phosphate-starvation response in *Arabidopsis*. *Curr. Biol.* **2005**, *15*, 2038–2043. [[CrossRef](#)]
19. Hsieh, L.C.; Lin, S.I.; Shih, A.C.C.; Chen, J.W.; Lin, W.Y.; Tseng, C.Y.; Li, W.H.; Chiou, T.J. Uncovering small RNA-mediated responses to phosphate deficiency in *Arabidopsis* by deep sequencing. *Plant Physiol.* **2009**, *151*, 2120–2132. [[CrossRef](#)]
20. Buhtz, A.; Springer, F.; Chappell, L.; Baulcombe, D.C.; Kehr, J. Identification and characterization of small RNAs from the phloem of *Brassica napus*. *Plant J.* **2008**, *53*, 739–749. [[CrossRef](#)]
21. Pant, B.D.; Buhtz, A.; Kehr, J.; Scheible, W.R. MicroRNA399 is a long distance signal for the regulation of plant phosphate homeostasis. *Plant J.* **2008**, *53*, 731–738. [[CrossRef](#)]
22. Wang, Y.-H.; Garvin, D.F.; Kochian, L.V. Rapid induction of regulatory and transporter genes in response to phosphorus, potassium, and iron deficiencies in tomato roots. Evidence for cross talk and root/rhizosphere-mediated signals. *Plant Physiol.* **2002**, *130*, 1361–1370. [[CrossRef](#)]
23. Shin, R.; Berg, R.H.; Schachtman, D.P. Reactive oxygen species and root hairs in *Arabidopsis* root response to nitrogen, phosphorus and potassium deficiency. *Plant Cell Physiol.* **2005**, *46*, 1350–1357. [[CrossRef](#)]
24. Kant, S.; Peng, M.; Rothstein, S.J. Genetic regulation by NLA and microRNA827 for maintaining nitrate-dependent phosphate homeostasis in *Arabidopsis*. *PLoS Genet.* **2011**, *7*, e1002021. [[CrossRef](#)] [[PubMed](#)]
25. Liang, G.; He, H.; Yu, D. Identification of Nitrogen Starvation-Responsive MicroRNAs in *Arabidopsis thaliana*. *PLoS ONE* **2012**, *7*, e48951. [[CrossRef](#)] [[PubMed](#)]
26. Doerner, P. Phosphate starvation signaling: A threesome controls systemic Pi homeostasis. *Curr. Opin. Plant Biol.* **2008**, *11*, 536–540. [[CrossRef](#)]
27. Bari, R.; Pant, B.D.; Stitt, M.; Golm, S.P. PHO2, MicroRNA399, and PHR1 Define a Phosphate-Signaling Pathway in Plants. *Plant Physiol.* **2006**, *141*, 988–999. [[CrossRef](#)] [[PubMed](#)]
28. Berkowitz, O.; Jost, R.; Kollehn, D.O.; Fenske, R.; Finnegan, P.M.; O'Brien, P.A.; Hardy, G.E.S.J.; Lambers, H. Acclimation responses of *Arabidopsis thaliana* to sustained phosphite treatments. *J. Exp. Bot.* **2013**, *64*, 1731–1743. [[CrossRef](#)] [[PubMed](#)]
29. Chiou, T.J.; Aung, K.; Lin, S.I.; Wu, C.C.; Chiang, S.F.; Su, C.L. Regulation of phosphate homeostasis by MicroRNA in *Arabidopsis*. *Plant Cell* **2006**, *18*, 412–421. [[CrossRef](#)] [[PubMed](#)]
30. Huang, T.K.; Han, C.L.; Lin, S.I.; Chen, Y.J.; Tsai, Y.C.; Chen, Y.R.; Chen, J.W.; Lin, W.Y.; Chen, P.M.; Liu, T.Y.; et al. Identification of downstream components of ubiquitin-conjugating enzyme PHOSPHATE2 by quantitative membrane proteomics in *Arabidopsis* roots. *Plant Cell* **2013**, *25*, 4044–4060. [[CrossRef](#)]

31. Rouached, H.; Arpat, A.B.; Poirier, Y. Regulation of phosphate starvation responses in plants: Signaling players and cross-talks. *Mol. Plant* **2010**, *3*, 288–299. [[CrossRef](#)] [[PubMed](#)]
32. Martin, A.C.; Del Pozo, J.C.; Iglesias, J.; Rubio, V.; Solano, R.; De La Peña, A.; Leyva, A.; Paz-Ares, J. Influence of cytokinins on the expression of phosphate starvation responsive genes in *Arabidopsis*. *Plant J.* **2000**, *24*, 559–567. [[CrossRef](#)] [[PubMed](#)]
33. Franco-Zorrilla, J.M.; Valli, A.; Todesco, M.; Mateos, I.; Puga, M.I.; Rubio-Somoza, I.; Leyva, A.; Weigel, D.; García, J.A.; Paz-Ares, J. Target mimicry provides a new mechanism for regulation of microRNA activity. *Nat. Genet.* **2007**, *39*, 1033–1037. [[CrossRef](#)] [[PubMed](#)]
34. Mallory, A.C.; Bouché, N. MicroRNA-directed regulation: To cleave or not to cleave. *Trends Plant Sci.* **2008**, *13*, 359–367. [[CrossRef](#)] [[PubMed](#)]
35. Han, M.H.; Goud, S.; Song, L.; Fedoroff, N. (2004). The *Arabidopsis* double-stranded RNA-binding protein HYL1 plays a role in microRNA-mediated gene regulation. *Proc. Natl. Acad. Sci. USA* **2004**, *101*, 1093–1098. [[CrossRef](#)]
36. Eamens, A.L.; Smith, N.A.; Curtin, S.J.; Wang, M.B.; Waterhouse, P.M. The *Arabidopsis thaliana* double-stranded RNA binding protein DRB1 directs guide strand selection from microRNA duplexes. *RNA* **2009**, *15*, 2219–2235. [[CrossRef](#)]
37. Eamens, A.L.; Kim, K.W.; Curtin, S.J.; Waterhouse, P.M. DRB2 is required for microRNA biogenesis in *Arabidopsis thaliana*. *PLoS ONE* **2012**, *7*, e35933. [[CrossRef](#)]
38. Eamens, A.L.; Kim, K.W.; Waterhouse, P.M. DRB2, DRB3 and DRB5 function in a non-canonical microRNA pathway in *Arabidopsis thaliana*. *Plant Signal. Behav.* **2012**, *7*, 1224–1229. [[CrossRef](#)]
39. Rajagopalan, R.; Vaucheret, H.; Trejo, J.; Bartel, D.P. A diverse and evolutionarily fluid set of microRNAs in *Arabidopsis thaliana*. *Genes Dev.* **2006**, *20*, 3407–3425. [[CrossRef](#)]
40. Péliissier, T.; Clavel, M.; Chaparro, C.; Pouch-Péliissier, M.N.; Vaucheret, H.; Deragon, J.M. Double-stranded RNA binding proteins DRB2 and DRB4 have an antagonistic impact on polymerase IV-dependent siRNA levels in *Arabidopsis*. *RNA* **2011**, *17*, 1502–1510. [[CrossRef](#)]
41. Lu, C.; Fedoroff, N. A mutation in the *Arabidopsis* HYL1 gene encoding a dsRNA binding protein affects responses to abscisic acid, auxin, and cytokinin. *Plant Cell* **2000**, *12*, 2351–2366. [[CrossRef](#)]
42. Curtin, S.J.; Watson, J.M.; Smith, N.A.; Eamens, A.L.; Blanchard, C.L.; Waterhouse, P.M. The roles of plant dsRNA-binding proteins in RNAi-like pathways. *FEBS Lett.* **2008**, *582*, 2753–2760. [[CrossRef](#)]
43. Luo, Q.J.; Mittal, A.; Jia, F.; Rock, C.D. An autoregulatory feedback loop involving PAP1 and TAS4 in response to sugars in *Arabidopsis*. *Plant Mol. Biol.* **2012**, *80*, 117–129. [[CrossRef](#)]
44. Williamson, L.C.; Ribrioux, S.; Fitter, A.H.; Leyser, H.M.O. Phosphate availability regulates root system architecture in *Arabidopsis*. *Plant Physiol.* **2001**, *126*, 875–882. [[CrossRef](#)]
45. Schachtman, D.P.; Reid, R.J.; Ayling, S.M. Phosphorus Uptake by Plants: From Soil to Cell. *Plant Physiol.* **1998**, *116*, 447–453. [[CrossRef](#)]
46. Yang, X.J.; Finnegan, P.M. Regulation of phosphate starvation responses in higher plants. *Ann. Bot.* **2010**, *105*, 513–526. [[CrossRef](#)]
47. Remy, E.; Cabrito, T.R.; Batista, R.A.; Teixeira, M.C.; Sá-Correia, I.; Duque, P. The Pht1;9 and Pht1;8 transporters mediate inorganic phosphate acquisition by the *Arabidopsis thaliana* root during phosphorus starvation. *New Phytol.* **2012**, *195*, 356–371. [[CrossRef](#)]
48. Vazquez, F.; Vaucheret, H.; Rajagopalan, R.; Lepers, C.; Gascioli, V.; Mallory, A.C.; Hilbert, J.L.; Bartel, D.P.; Crété, P. Endogenous *trans*-acting siRNAs regulate the accumulation of *Arabidopsis* mRNAs. *Mol. Cell* **2004**, *16*, 69–79. [[CrossRef](#)]
49. Kurihara, Y.; Takashi, Y.; Watanabe, Y. The interaction between DCL1 and HYL1 is important for efficient and precise processing of pri-miRNA in plant microRNA biogenesis. *RNA* **2006**, *12*, 206–212. [[CrossRef](#)]
50. Jiang, C.; Gao, X.; Liao, L.; Harberd, N.P.; Fu, X. Phosphate starvation root architecture and anthocyanin accumulation responses are modulated by the gibberellin-DELLA signaling pathway in *Arabidopsis*. *Plant Physiol.* **2007**, *145*, 1460–1470. [[CrossRef](#)]
51. Shin, H.; Shin, H.S.; Dewbre, G.R.; Harrison, M.J. Phosphate transport in *Arabidopsis*: Pht1;1 and Pht1;4 play a major role in phosphate acquisition from both low- and high-phosphate environments. *Plant J.* **2004**, *39*, 629–642. [[CrossRef](#)] [[PubMed](#)]

52. Reis, R.S.; Hart-Smith, G.; Eamens, A.L.; Wilkins, M.R.; Waterhouse, P.M. Gene regulation by translational inhibition is determined by Dicer partnering proteins. *Nat. Plants* **2015**, *1*, 14027. [[CrossRef](#)]
53. Yang, L.; Wu, G.; Poethig, R.S. Mutations in the GW-repeat protein SUO reveal a developmental function for microRNA-mediated translational repression in *Arabidopsis*. *Proc. Natl. Acad. Sci. USA* **2012**, *109*, 315–320. [[CrossRef](#)] [[PubMed](#)]
54. Xu, M.; Hu, T.; Zhao, J.; Park, M.Y.; Earley, K.W.; Wu, G.; Yang, L.; Poethig, R.S. Developmental Functions of miR156-Regulated *SQUAMOSA PROMOTER BINDING PROTEIN-LIKE (SPL)* Genes in *Arabidopsis thaliana*. *PLoS Genet.* **2016**, *12*, e1006263. [[CrossRef](#)]
55. Adenot, X.; Elmayan, T.; Laussergues, D.; Boutet, S.; Bouché, N.; Gascioli, V.; Vaucheret, H. DRB4-Dependent *TAS3* *trans*-Acting siRNAs Control Leaf Morphology through AGO7. *Curr. Biol.* **2006**, *16*, 927–932. [[CrossRef](#)] [[PubMed](#)]
56. Nakazawa, Y.; Hiraguri, A.; Moriyama, H.; Fukuhara, T. The dsRNA-binding protein DRB4 interacts with the Dicer-like protein DCL4 in vivo and functions in the *trans*-acting siRNA pathway. *Plant Mol. Biol.* **2007**, *63*, 777–785. [[CrossRef](#)] [[PubMed](#)]
57. Lichtenthaler, H.K.; Wellburn, A.R. Determination of total carotenoids and chlorophylls *a* and *b* of leaf extracts in different solvents. *Biochem. Soc. Trans.* **1983**, *11*, 591–592. [[CrossRef](#)]



© 2019 by the authors. Licensee MDPI, Basel, Switzerland. This article is an open access article distributed under the terms and conditions of the Creative Commons Attribution (CC BY) license (<http://creativecommons.org/licenses/by/4.0/>).

Appendix 2

Solutions and Mediums

A.2 Solutions and Mediums

A.2.1 Solutions

All reagents used to make the following solutions (**A.2.1.1- A.2.1.8**) were sourced from Sigma-Aldrich, Australia. All autoclaving was conducted in a Pratika B20 (20L) Basic steriliser, Siltex, Australia.

A.2.1.1 *MS Macro (20X)*

NH₄NO₃	33 g
KNO₃	38 g
KH₂PO₄	3.4 g
MgSO₄.7H₂O	7.4 g
CaCl₂.2H₂O	8.8 g

Make up to 1000 mL with MQ-H₂O. Store at 4°C.

A.2.1.2 *MS Micro (100X)*

MnSO₄.4H₂O	11.15 g
Na₂MoO₄.2H₂O	0.125 g
H₃BO₃	3.11 g
ZnSO₄.7H₂O	4.3 g
CuSO₄.5H₂O	0.0125 g
CoCl₂.6H₂O	0.0125 g
KI	0.115 g

Make up to 500 mL with MQ-H₂O. Store at 4°C.

A.2.1.3 *MS Vitamins (100X)*

Nicotinic acid	0.05 g
Pyridoxine HCL	0.05 g
Thiamine HCL	0.01 g
Glycine	0.2 g

Make up to 1000 mL with MQ-H₂O. Store at 4°C.

A.2.1.4 *MS Iron + EDTA (200X)***Na₂EDTA** 6.7 g**FeCl₃·6H₂O** 5.4 g

Make up to 1000 mL with MQ-H₂O. Store at 4°C.

A.2.1.5 *0.5 M EDTA (pH 8.0)***EDTA** 186 g

Add 800 mL of MQ-H₂O. Gradually add NaOH pellets and stir to dissolve EDTA powder. Make up to 1 L with MQ-H₂O and autoclave. Store at 22°C.

A.2.1.6 *10X TBE***TRIS powder** 108 g**Boric acid** 55 g**0.5 M EDTA** 40 mL

Make up to 1000 mL with MQ-H₂O and autoclave. Store at 22°C.

A.2.1.7 *0.1 M CaCl₂ (*or 0.1 M CaCl₂ +15% glycerol)***CaCl₂** 1.10 g

Dissolve CaCl₂ in 100 mL of MQ-H₂O and filter sterilise. Stored at 22°C. *Note to produce 0.1 M CaCl₂ +15% glycerol, mix 85 mL of 0.1M CaCl₂ with 15 mL of 100% glycerol, Store at 22°C.

A.2.1.8 *Tris-EDTA (TE) buffer (1X)***0.5M EDTA** 1 mL**1M Tris-HCl** 200 µL

Make up to 100mL with MQ-H₂O. Store at 22°C.

A.2.2 *Mediums*

All reagents used to make the following mediums (**A.2.1.1- A.2.1.4**) were sourced from Sigma-Aldrich, Australia. All autoclaving was conducted in a Pratika B20 (20L) Basic steriliser, Siltex, Australia.

A.2.2.1 *Murashige and Skoog (MS) Plant Growth Medium*

MS Macro	50 mL
MS Micro	1 mL
MS Vitamins	10 mL
MS iron + EDTA	5 mL
Sucrose	30 g
Myoinositol	0.1 g

Make up to 800 mL with MQ-H₂O. Adjust pH to 5.7 with 1M KOH. Make up to 1 L with MQ-H₂O. Add 8 g of Bacto agar and autoclave.

A.2.2.2 *Luria-Bertani (LB) Liquid Medium*

Tryptone	10 g
Yeast extract	10 g
NaCl	5 g

Make up to 1000 mL with MQ-H₂O. Adjust pH to 7.0 with 1M NaOH and autoclave. *Note: to make solid media add 15 g Bacto agar prior to autoclaving.

A.2.2.3 *Yeast Extract Peptone (YEP) Liquid Medium*

Yeast extract	10 g
Peptone	10 g
NaCl	5 g

Make up to 1000 mL with MQ-H₂O. Adjust pH to 7.0 with 1M NaOH and autoclave.

A.2.2.4 *Super Optimal Broth with Catabolite Repression (SOC)*
Liquid Medium

Yeast extract	5 g
Tryptone	20 g
NaCl	0.584 g
KCl	0.186 g
MgSO₄	2.4 g

Make up to 1000 mL with MQ-H₂O. Adjust pH to 7.5 with 1M NaOH and autoclave. After medium is cooled below 50°C add 20 mL of filter sterilised glucose (20%) solution.

Appendix 3

Standardised Reaction Programs

A.3.1 PCR and qPCR Cycling Conditions

A.3.1.1 Genotyping PCR

Table A.3.1 PCR cycling conditions used for genotyping PCRs. *Optimal annealing temperatures (X°C)

Cycle Number	Step Number	Temperature (°C)	Time (min)
1	1	95	2
2-35	1	94	0.5
	2	X*	0.5
	3	68	0.75
36	1	68	5
	2	16	5

A.3.1.2 cDNA Synthesis

Table A.3.2 PCR cycling conditions used to synthesis cDNA.

Cycle Number	Step Number	Temperature (°C)	Time (min)
1	1	50	60
1	1	70	20

A.3.1.3 miRNA-Specific cDNA Synthesis

Table A.3.3 PCR cycling conditions used to synthesis miRNA-specific cDNA.

Cycle Number	Step Number	Temperature (°C)	Time (min)
1	1	16	30
2-35	1	30	0.5
	2	42	0.5
	3	50	0.25
36	1	85	5
	2	16	5

A.3.1.4 *quantitative PCR*

Table A.3.4 qPCR cycling condition. *Temperature of the melt cycle is increase 1°C every minute, beginning at 72°C and completing at 94°C.

Cycle Number	Step Number	Temperature (°C)	Time (min)
1	1	95	10
2-46	1	95	0.16
	2	60	0.25
47	1	72-94*	23

A.3.1.5 *Colony PCR screen*

Table A.3.5 PCR cycling conditions for screening for +/- bacterial colonies.

Cycle Number	Step Number	Temperature (°C)	Time (min)
1	1	95	5
2-35	1	95	0.5
	2	59	0.6
	3	68	1
36	1	68	5
	2	4	5

A.3.1.6 *Amplification of Gene Fragments PCR*

Table A.3.6 PCR cycling conditions used for amplifying gene fragments for cloning.

Cycle Number	Step Number	Temperature (°C)	Time (min)
1	1	95	2
2-35	1	95	0.5
	2	59	0.5
	3	68	3
36	1	72	10
	2	16	5

Appendix 4

Primer Sequences

A.4.1 Primer Sequences

All primers were ordered from Integrated DNA Technologies (IDT; Coralville, Iowa) and resuspended in TE buffer (1X; **Appendix 2.1.8**).

A.4.1.1 Genotyping Related Primers

Table A.4.1 The nucleotide sequence of all primers used in this study pertaining to the genotyping of *Arabidopsis* DRB-KO mutant plant lines investigated.

Primer Name	Primer Sequence (5'-3')
DRB1 TDNA FP	CTTCTTGGAAATTGGATTGCAGTG
DRB1 TDNA RP	GCCCCCTAACGTATTCTCACAGC
DRB2 TDNA FP	GCTAAACCCTCCAACGATTTTCC
DRB2 TDNA RP	GAGATCTCAGCACCGACCCTAATAAG
DRB4 TDNA FP	CCCTAGATCATTGAGTCTGACCAATTC
DRB4 TDNA RP	CAACTTTAGCAGCGCTCATTTCAGCCAAC
GABI	CGCTGCGGACATCTACATTTTTG
SALK	GATGGTTCACGTAGTGGGCCATCGC

A.4.1.2 Cloning Related Primers

Table A.4.2 The nucleotide sequence of all primers utilised in the molecular cloning methodologies of this study.

Primer Name	Primer Sequence (5'-3')
MIM399 FP	CTCGAGAGACTGCAGAAGGCTGATT
MIM399 RP	GGATCCCCTCACACAAAGAACACAC
miR399C-SL FP	CTCGAGGTCCATGAATAACCAACCAGC
miR399C-SL RP	AAGCTTGCCAGAGAGACCAATTCTCTATC
pBART genotype FP	CATCGAGACAAGCACGGTCA
pBART genotype RP	AAACCCACGTCATGCCAGTT

A.4.1.3 *qPCR Related miRNA Primers*

Table A.4.3 The nucleotide sequence of all primers used in this study pertaining to SL-RT-qPCR analyses of miRNAs.

microRNA	Primer	Primer sequence (5'-3')
miR156	SL-RT	GTCGTATCCAGTGCAGGGTCCGAGGTATTTCGCACTGGATACGACGTGCTC
	SL-FOR	CGCCTGACAGAAGAGAGTGAGCAC
miR160	SL-RT	GTCGTATCCAGTGCAGGGTCCGAGGTATTTCGCACTGGATACGACTGGCAT
	SL-FOR	GCCTGGCTCCCTGTATGCC
miR163	SL-RT	GTCGTATCCAGTGCAGGGTCCGAGGTATTTCGCACTGGATACGACATCGAA
	SL-FOR	GCGCTTGAAGAGGACTTGGAACCTCG
miR167	SL-RT	GTCGTATCCAGTGCAGGGTCCGAGGTATTTCGCACTGGATACGACTAGATC
	SL-FOR	CGCTGAAGCTGCCAGCATGATCTA
miR169	SL-RT	GTCGTATCCAGTGCAGGGTCCGAGGTATTTCGCACTGGATACGACCGGCAA
	SL-FOR	AGTGAGCCAAGGATGACTTGCCG
miR319	SL-RT	GTCGTATCCAGTGCAGGGTCCGAGGTATTTCGCACTGGATACGACAAGGAG
	SL-FOR	GCTTGGACTGAAGGGAGCTCCTT
miR395	SL-RT	GTCGTATCCAGTGCAGGGTCCGAGGTATTTCGCACTGGATACGACGAGTTC
	SL-FOR	GCGCTGAAGTGTTTGGGGGAACTC
miR396	SL-RT	GTCGTATCCAGTGCAGGGTCCGAGGTATTTCGCACTGGATACGACAAGTTC
	SL-FOR	GCGCGTTCCACAGCTTTCTTGAAC
miR397	SL-RT	GTCGTATCCAGTGCAGGGTCCGAGGTATTTCGCACTGGATACGACCATCAA
	SL-FOR	GCGCTCATTGAGTGCATCGTTGATG
miR399	SL-RT	GTCGTATCCAGTGCAGGGTCCGAGGTATTTCGCACTGGATACGACCAGGGC
	SL-FOR	GCATGCCAAAGGAGATTTGCCCTG
miR400	SL-RT	GTCGTATCCAGTGCAGGGTCCGAGGTATTTCGCACTGGATACGACGTGACT
	SL-FOR	GCGCGGGCGTATGAGAGTATTATAAGTCAC
miR408	SL-RT	GTCGTATCCAGTGCAGGGTCCGAGGTATTTCGCACTGGATACGACCATGCT
	SL-FOR	ACGACAGGGAACAAGCAGAGCATG
miR773	SL-RT	GTCGTATCCAGTGCAGGGTCCGAGGTATTTCGCACTGGATACGACGAGACA
	SL-FOR	GGCGTTTGCTTCCAGCTTTTGTCTC
miR778	SL-RT	GTCGTATCCAGTGCAGGGTCCGAGGTATTTCGCACTGGATACGACCGGTGT
	SL-FOR	GGCGTGGCTTGTTTATGTACACCG
miR839	SL-RT	GTCGTATCCAGTGCAGGGTCCGAGGTATTTCGCACTGGATACGACGGGAAC

	SL-FOR	AGCGTACCAACCTTTCATCGTTCCC
miR855	SL-RT	GTCGTATCCAGTGCAGGGTCCGAGGTATTCGCACTGGATACGACTTCCTT
	SL-FOR	GGCGGAGCAAAAAGCTAAGGAAAAGG
miR857	SL-RT	GTCGTATCCAGTGCAGGGTCCGAGGTATTCGCACTGGATACGACATACAC
	SL-FOR	GGCGGCGTTTTTGTATGTTGAAGGTG
miR858	SL-RT	GTCGTATCCAGTGCAGGGTCCGAGGTATTCGCACTGGATACGACAAGGTC
	SL-FOR	GGCGTTTCGTTGTCTGTTTCGACCTT
miR869.2	SL-RT	GTCGTATCCAGTGCAGGGTCCGAGGTATTCGCACTGGATACGACGTC AAC
	SL-FOR	GCGCCTCTGGTGTGAGATAGTTGAC
snoR101	FP	CTTCACAGGTAAGTTCGCTTG
	RP	AGCATCAGCAGACCAGTAGTT

A.4.1.4 *qPCR Related mRNA Primers*

Table A.4.4 The nucleotide sequence of all primers used in this study pertaining to RT-qPCR analyses of target gene mRNAs and miRNA production machinery investigated.

<i>GENE (Locus Number)</i>	<i>Primer</i>	<i>Primer sequence (5'-3')</i>
<i>DCL1 (AT1G01040)</i>	FP	AATGGGCATCAGCCGTTTACGAGA
	RP	AAATCTCTTTGCATGAGCCGGTCC
<i>DRB1 (AT1G09700)</i>	FP	ATGACCTCCACTGATGTTTCC
	RP	TGCTAATTCCCGGAGAGC
<i>DRB2 (AT1G09700)</i>	FP	ATGTATAAGAACCAGCTACAAGAGTTG
	RP	CAGCAGCAGAGTGTTTCAGC
<i>DRB4 (AT3G62800)</i>	FP	AAATGGGAACTCGAACCAGA
	RP	CCACCTTGGAAGAAGGTTGA
<i>PXMT1 (AT1G66700)</i>	FP	ACGTCTTTGTATTCTCCCCTATCC
	RP	TGATGATACTATGGAAGCTTGTTTG
<i>SUVH6 (AT2G22740)</i>	FP	TTGCAGTTGCAAACCGAGG
	RP	TCCTTCACCAA ACTCTCGGC
<i>PHO2 (AT2G33770)</i>	FP	ACCGTTTCTCATCAAGGCGT
	RP	GTGCCCGTCCACCATAAGAA
<i>LAC3 (AT2G30210)</i>	FP	CCGTTTCGACAACACAACCAC
	RP	GACTGGGAAAACAGGAGCGA

<i>NFYA5 (AT1G54160)</i>	FP	ACCAAATCCAAAGCACCAAAGT
	RP	AGGCATTGAGTTTCCCAAGA
<i>GRF7 (AT5G53660)</i>	FP	CATCCCCACCGTTAGATCG
	RP	TGCTTCCATGCTTCCGACAT
<i>ATPS1 (AT3G22890)</i>	FP	ATCTCCGGCACTAAGATGCG
	RP	ACCTGGGCACATAAAACCGT
<i>LAC2 (AT2G29130)</i>	FP	TGGGTTGTTTTGGACGGTGA
	RP	GGCGTTGGATCGGTCATAGT
<i>PPR1 (AT1G06580)</i>	FP	GATTGCGTTAACGGCGAAGG
	RP	CTCGGGAATTGCAAATGCGT
<i>DNMT2 (AT4G14140)</i>	FP	TGCATGTTTTGTGTAACAAGGTGT
	RP	ACCGTTGCTTCAGGATGGTT
<i>SPL9 (AT2G42200)</i>	FP	TTTTGGCCCGATGACGGTTA
	RP	AATACCCAAGGCGGGTTCAG
<i>LAC7 (AT3G09220)</i>	FP	ACACACCTTCAACGTACAAAACCT
	RP	ACCCTCCTTGACGCGTATTG
<i>UBQ (AT4G05320)</i>	FP	GGCCTTGATAATCCCTGATGAATAAG
	RP	AAAGAGATAACAGGAACGGAAACATA
<i>P5CS1 (AT2G39800)</i>	FP	GTTTTTGAATCCCGACCTGA
	RP	TTACCCCCAACAGTCTCTGG
<i>GRF1 (AT2G22840)</i>	FP	CGTCGCATAAACAAGCCTCG
	RP	ATTTTCAGCTCTTCGGGCCAA
<i>GRF2 (AT4G37740)</i>	FP	CTTGGCCTGAAGAGCTGACA
	RP	GTGTGTGGAGGAAGGGGATG
<i>GRF3 (AT2G36400)</i>	FP	CCATACGAGTCCCACATCGG
	RP	CTGAGCTCATGGGGCTTGAA
<i>GRF8 (AT4G24150)</i>	FP	GCTGCTGTGACTGTAGCAGA
	RP	CTCATGCCATTGAGCTTCGC
<i>GRF9 (AT2G45480)</i>	FP	CTCACATGAGAATGCCGGGT
	RP	ATCAGAAACTCGGGGCAGTG

Appendix 5

Bacterial Cloning Materials

A.5.1 Transgene Sequences

Table A.5.1 Transgene sequences used in this study. Some transgenes were ordered as gBlock gene fragments from Integrated DNA Technologies (IDT; Coralville, Iowa). The other transgene fragments were amplified from *Arabidopsis* (Col-0) genomic DNA with appropriate primer pairs as indicated.

Transgene/ Length	Sequence (5' to 3')
MIM396	GGTACCCTCGAGAAGTTCAAGAATAAGCTGTGGAATGCATCTTTGA GAGAGATTAGCATCCCTATGTGTGGATTTTGCTTGCACGAGTGTGCA CAGTTCAAGAATAAGCTGTGAAAAGCTTGGTACC
miR396-SL	GGTACCCTCGAGACCATCTCTTATCTTGAATCTTGATGAATCCCTAG GCTAGGCAGGCATTTGCATATCCACCCCTCTTCTTGGAGCTCAATCT TCCTCGTTCTAGCTCTTTCTGTTTTCCCTTTTCCGATCTGATCACCTG GGTAATTGCATGTCTATTGGATCTACATGAGTAGATGGCCCTCTTT GCGATCTTCCACAGCTTTCTTGAAGTCTGCGTGAATTCGAAGTGGC AGAACAGATTGCTTGGGTTCCAGCCGAGATCTACCGATCGAGCAGT TCAATAAAGCTGTGGGAAATTGCAAAGAGAGACCAATTGATCAGCGT TCTGCATCGGAGAAGATTATGTGGTGCCCGGAGGCACGGATGGGC GAGCAAAATGATGGATCTATATCATCTGTGCGCTGCATCACAACAAG GTACAATTTTCTTTCTGGTTAGGTTTATGAATGTACGTATATATGTGT AAAGCTTGGTACC
MIM399 (IPS1)	Primer pairs listed in Table A.4.2
miR399c-SL	Primer pairs listed in Table A.4.2

A.5.2 Competent Cells

Table A.5.2 Competent cell host lines used in this study.

Strain	Reference
<i>Escherichia coli</i> - DH5 α	Hanahan, 1983
<i>Agrobacterium</i> - AGL1	Lazo <i>et al.</i> , 1991

A.5.3 Plasmid DNA Vectors

Table A.5.3 Plasmid DNA vectors used in this study.

<i>Plasmid</i>	<i>Plasmid Features of Interest</i>	<i>Reference</i>
<i>pGEM-T Easy</i>	<ul style="list-style-type: none"> • Linearised plasmid • Thymine overhangs • Ampicillin resistance 	Promega, Australia
<i>pART7</i>	<ul style="list-style-type: none"> • Ampicillin resistance • 35S promoter • OcsT terminator • Necessary restriction digest sites: - <i>BAMHI</i>, <i>HINDIII</i>, <i>NOTI</i>, <i>XHOI</i> 	Gleave, 1992
<i>pBART</i>	<ul style="list-style-type: none"> • Spectinomycin resistance • Necessary restriction digest sites: - <i>NOTI</i> 	Gleave, 1992

A.5.4 Antibiotics and Herbicides

Table A.5.4 Working antibiotic concentration. Used for transformant selection in liquid culture and on agar media petri dishes used in this study. *Timentin was used to prevent *agrobacterium* contamination during putative transformant seedling selection.

Antibiotic	Working Concentration (µg/mL)
Ampicillin	100
Spectinomycin	50
Rifampicin	50
Timentin*	150

Table A.5.5 Working herbicide concentration. Used for *in planta* selection of mutant *Arabidopsis* lines .

Herbicide	Working Concentration (µg/mL)
Glufosinate ammonium (PPT)	10

Appendix 6

Additional Results

A.6.1 RT-PCR Based Genotyping of DRB knockout Plant Lines

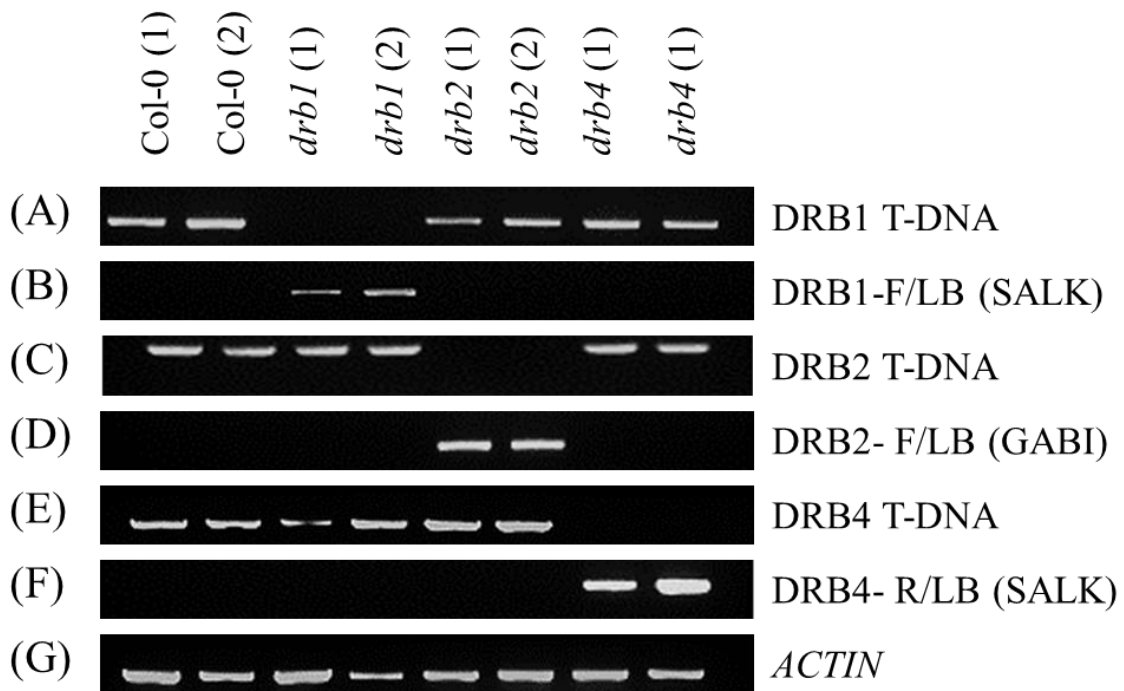


Figure A.6.1: Genotyping of wild-type *Arabidopsis* plants and *drb* knockout insertion mutant lines. PCR-based genotyping with gene-specific primer pairs that flank the respective *DRB1* (A), *DRB2* (C) and *DRB4* (E) T-DNA insertions. A subsequent PCR-based assessment using T-DNA left border-specific primers with either the gene-specific forward or reverse primer (depending on the orientation of the T-DNA insert) was conducted to confirm the presence of the respective T-DNA insertions in the *DRB1* (B), *DRB2* (D) and *DRB4* (F) loci. PCRs were run for 35 cycles and visualised on a 1.0% agarose gel. For each gDNA sample assessed by PCR genotyping, an *ACTIN* PCR was also conducted and used as an internal control (G).

A.6.2 sRNA Sequencing Raw Read Count

Table A.6.1 Raw miRNA reads and the Log2 fold change in abundance of each *Arabidopsis* miRNA sRNA detected via high throughput sRNA sequencing.

miRNA	<i>Arabidopsis</i> Line/ Treatment														
	Col-0				drb1				drb2				drb4		
	Control	Heat	Mannitol	Salt	Control	Heat	Mannitol	Salt	Control	Heat	Mannitol	Salt	Control	Heat	Mannitol
MIR156a	4901	4496	17203	8912	756	1790	1146	619	3952	1950	9649	6512	2986	5806	8833
MIR156b	3224	4990	13996	8087	1115	3996	2657	1395	3566	2422	7559	5595	2344	6929	6742
MIR156c	3939	4160	15082	7661	407	942	636	415	3487	1929	8144	5870	2448	5596	7535
MIR156d	3060	3399	11644	6657	260	862	416	432	3143	1759	5970	5476	1818	5692	5499
MIR156e	1757	1725	8646	3752	204	666	382	236	1895	960	4274	3188	1081	3157	3789
MIR156f	1855	1727	8812	3762	203	670	354	235	1911	965	4345	3190	1107	3160	3853
MIR156g	52	100	219	86	10	40	14	13	64	39	113	59	34	161	84
MIR156h	8	45	16	6	1	35	0	3	11	30	9	23	4	53	7
MIR156i	2	0	4	2	1	2	2	4	1	0	6	5	0	5	7
MIR156j	7	5	35	8	1	10	1	0	22	16	36	20	5	26	34
MIR157a	4512	6652	25207	9606	395	1758	673	331	6075	3300	11971	7097	3630	12635	12061
MIR157b	4513	6643	25214	9604	397	1755	669	329	6079	3304	11978	7092	3631	12632	12059
MIR157c	1814	3447	8181	4911	811	2237	763	544	3484	2137	4844	4431	1522	5232	4222
MIR157d	37	68	179	112	13	52	7	6	64	93	104	127	33	215	92
MIR158a	93924	111812	271986	185555	32968	30686	11547	19931	126789	80557	128641	171339	63599	209875	123113
MIR158b	873	8904	2830	2519	589	3301	383	507	1573	5933	1482	2186	802	16338	1519
MIR159a	25272	41137	95303	44185	1066	4088	2021	1027	22853	17067	52199	37521	9841	41865	40234
MIR159b	28317	42855	85495	44948	3155	10173	4416	1984	24978	19279	46982	37196	10879	44647	36917

MIR159c	2292	4746	11472	4839	159	924	352	163	3148	2915	7183	5647	1297	6189	5073
MIR160a	204	438	710	351	129	233	198	56	285	189	326	232	100	493	281
MIR160b	234	380	646	267	64	106	85	25	301	204	343	242	135	485	355
MIR160c	401	1125	1339	1325	194	592	289	217	579	494	724	681	295	1329	699
MIR161	92819	85868	153129	117690	11295	15816	6458	6479	72918	36252	54170	59276	37486	99385	54548
MIR162a	8042	6261	12887	10759	223	219	190	91	13584	2898	5995	6984	5226	7767	5898
MIR162b	8248	7003	13248	10919	231	241	172	86	14012	3476	6199	7140	5386	9085	6040
MIR163	1569	1256	2573	619	392	345	201	123	775	557	1383	482	640	1298	1181
MIR164a	94	460	364	193	48	216	153	33	159	250	283	249	67	592	260
MIR164b	677	1498	752	341	164	393	203	60	654	1045	590	429	570	1665	643
MIR164c	175	473	578	337	65	171	111	30	219	237	385	403	106	614	376
MIR165a	3567	5693	8410	4668	308	420	511	161	3223	1725	4093	3281	1673	5830	4018
MIR165b	4401	5898	9193	5033	446	561	713	196	3556	1678	4953	3584	1867	5301	4553
MIR166a	4806	5665	10678	6513	1768	2940	3070	1176	3964	1975	4650	4125	1943	6431	4099
MIR166b	3882	4509	8799	5290	1583	2600	2720	1050	3137	1507	3681	3188	1563	5055	3303
MIR166c	3167	3336	6779	3761	1224	2090	2484	902	2312	1136	3018	2471	1165	3575	2625
MIR166d	3101	3266	6670	3687	1198	2035	2437	882	2263	1081	2912	2396	1132	3483	2535
MIR166e	4640	4929	9798	5461	1766	2919	3508	1270	3319	1658	4625	3484	1867	5166	4056
MIR166f	4546	4681	9353	5298	1732	2843	3487	1256	3194	1572	4466	3372	1778	4860	3883
MIR166g	4539	4650	9325	5287	1725	2828	3473	1258	3183	1549	4447	3365	1772	4824	3871
MIR167a	3229	5956	9467	5473	1552	3780	2047	1341	4108	2725	5540	5160	2597	8277	5337
MIR167b	2896	5285	8521	4959	1510	3527	1852	1261	3791	2519	4965	4739	2299	7521	4641
MIR167c	1326	961	3071	1628	366	220	221	184	1076	326	1478	1154	544	886	1542
MIR167d	1890	2843	5913	3631	849	1657	1297	878	2136	1110	3332	2865	1486	4511	3444
MIR168a	2566	5231	5921	5026	2008	6271	3746	1878	2490	2310	2794	3620	2017	7787	3575

MIR168b	1322	2397	4133	3046	856	2568	1823	995	1632	1148	1945	2286	905	3532	2281
MIR169a	40	23	51	30	5	21	12	9	23	6	16	20	47	37	51
MIR169b	33	9	28	11	0	0	0	0	17	7	17	10	45	38	58
MIR169c	1	0	2	0	0	0	0	0	0	0	1	2	1	1	2
MIR169d	211	13	375	28	3	3	1	2	139	5	191	39	43	38	166
MIR169e	207	24	293	10	0	1	2	0	152	4	142	20	37	47	155
MIR169f	263	24	538	76	1	3	4	1	253	7	327	68	46	24	171
MIR169g	214	13	378	23	3	2	1	3	138	3	187	39	44	28	162
MIR169h	14	2	31	2	0	0	1	0	13	0	18	7	12	1	12
MIR169i	19	6	49	18	1	0	0	0	12	5	19	12	8	2	22
MIR169j	4	1	12	2	0	2	1	0	7	3	2	2	3	2	10
MIR169k	4	1	10	2	0	0	0	0	5	0	8	4	2	0	5
MIR169l	8	0	11	1	0	0	0	0	4	1	2	2	4	3	1
MIR169m	7	2	17	0	0	1	0	0	8	0	9	5	1	2	8
MIR169n	6	1	10	1	0	0	0	1	6	3	2	0	4	2	3
MIR170	256	380	481	312	75	153	44	47	197	159	223	253	153	482	296
MIR171a	405	572	793	547	179	429	180	115	321	237	369	442	243	700	462
MIR171b	102	205	165	82	14	7	2	3	120	75	71	59	64	254	105
MIR171c	122	162	132	99	41	40	4	8	116	62	55	62	81	148	64
MIR172a	68	207	59	49	33	55	7	9	94	137	42	57	56	282	41
MIR172b	91	326	93	118	42	97	12	18	149	189	70	106	96	473	64
MIR172c	6	12	8	5	6	26	1	4	9	8	8	10	5	31	5
MIR172d	13	11	15	10	14	12	2	4	14	9	8	10	7	31	5
MIR172e	24	131	48	55	14	45	4	4	53	68	31	54	32	217	27
MIR173	19410	15084	28368	18831	982	590	167	329	16821	5634	9506	8284	9825	18347	11446

MIR1886	52	70	75	85	3	1	0	1	63	43	52	48	31	96	57
MIR1888a	74	55	125	49	37	27	6	13	86	28	52	35	67	125	81
MIR1888b	48	44	52	58	19	30	4	11	33	20	24	40	55	189	50
MIR2111a	2	67	9	28	20	440	13	18	1	62	5	18	2	55	5
MIR2111b	3	47	8	43	6	257	6	21	3	40	6	12	4	53	8
MIR2112	2	10	10	10	0	3	0	1	8	9	6	14	2	42	11
MIR2933a	94	134	115	84	109	195	123	150	159	137	142	221	38	64	48
MIR2933b	70	108	84	63	85	143	89	98	128	110	107	139	30	52	38
MIR2934	0	0	0	0	0	2	0	0	0	0	0	0	0	1	0
MIR2936	32	39	52	43	35	40	70	39	38	30	40	79	31	50	50
MIR2937	3	1	6	4	1	4	2	2	2	6	4	0	2	6	1
MIR2938	0	0	1	0	0	0	0	0	0	0	0	1	0	0	0
MIR2939	1	1	1	0	1	0	0	0	1	0	8	2	1	0	0
MIR319a	2287	2714	3403	2090	900	1112	476	207	2396	1700	1718	1630	1064	3743	1329
MIR319b	1187	2961	2168	1630	466	1678	239	203	1485	1987	1117	1370	621	4992	859
MIR319c	8729	2906	11432	4893	387	273	108	74	4788	1085	3573	1953	3293	2970	3867
MIR3434	245	439	420	301	13	23	8	4	306	240	198	202	794	2716	847
MIR3440b	11	24	24	27	10	42	3	14	13	9	14	20	28	78	39
MIR390a	520	839	955	725	180	553	269	109	859	328	475	542	391	1219	528
MIR390b	331	599	537	503	158	463	236	92	517	206	265	344	225	772	343
MIR391	82	203	468	146	31	12	49	7	62	71	99	53	81	261	268
MIR3932a	56	17	48	54	15	10	2	8	41	10	13	18	135	37	89
MIR3932b	2516	110	1408	1153	110	19	14	19	1566	64	456	476	1910	334	1059
MIR3933	0	4	29	1	0	3	0	0	0	1	18	0	0	20	23
MIR393a	53	172	170	75	16	47	5	19	61	101	86	71	33	400	88

MIR393b	784	3644	2076	1707	810	2117	307	592	948	1549	878	1005	659	4880	1251
MIR394a	101	260	324	180	87	305	87	64	115	137	177	177	61	317	174
MIR394b	118	280	379	205	159	305	117	68	130	138	188	181	85	328	208
MIR395a	29	2217	82	521	9	3137	7	7	105	1938	43	484	46	3097	39
MIR395b	36	350	42	177	4	567	2	8	71	179	19	156	34	508	19
MIR395c	36	344	41	173	3	558	2	9	73	175	20	157	33	511	20
MIR395d	17	1166	39	390	4	2310	3	3	54	864	14	236	33	1485	21
MIR395e	29	2206	79	518	7	3131	7	7	105	1919	41	482	52	3096	40
MIR395f	28	338	31	166	3	541	2	7	75	178	14	142	32	494	17
MIR396a	4316	10849	12785	8549	1078	2830	897	1127	6480	5104	7623	8694	2750	13108	6324
MIR396b	7784	19808	21346	12346	5840	16645	5372	6067	9630	9106	12862	10322	4293	25977	10211
MIR397a	7	56	11	30	21	46	1	16	20	36	2	28	28	91	4
MIR397b	8	41	1	20	21	36	1	6	16	23	1	29	20	75	2
MIR398a	457	1080	717	664	185	187	91	41	624	495	169	354	494	958	274
MIR398b	10077	25333	14693	17800	3865	4955	2461	1387	14688	11030	3513	11560	11924	22151	5971
MIR398c	10072	25318	14698	17763	3841	4919	2464	1372	14678	11015	3503	11522	11906	22089	5953
MIR399a	386	3263	1306	2997	104	2773	66	268	210	2390	326	1109	317	2373	605
MIR399b	322	485	999	550	96	298	40	35	237	283	215	290	120	402	311
MIR399c	341	529	1020	579	98	252	34	30	240	300	231	317	126	425	305
MIR399d	8	140	33	58	1	98	0	0	12	110	18	48	9	98	20
MIR399e	4	9	11	10	0	11	0	0	1	11	4	6	3	7	3
MIR399f	25	119	56	94	7	136	4	7	18	104	30	66	18	119	44
MIR400	758	213	636	479	86	30	4	34	383	91	186	156	173	175	173
MIR401	43	92	65	40	75	118	62	35	165	136	117	109	28	71	42
MIR402	42	205	124	84	2	4	0	2	55	99	75	68	34	412	85

MIR403	7799	9768	15811	12392	2337	1749	727	1768	10312	5567	9493	11498	4762	13501	8714
MIR404	40	55	35	21	46	94	29	55	65	51	51	33	12	20	19
MIR405a	88	109	127	81	105	187	142	106	173	102	158	125	34	64	70
MIR405b	24	20	34	14	18	23	16	15	25	14	40	22	5	13	16
MIR405d	11	11	25	5	10	19	5	7	22	10	20	16	11	12	6
MIR406	95	39	64	37	124	72	9	53	121	54	69	40	19	26	20
MIR407	115	90	125	81	137	115	50	97	192	78	147	111	37	49	46
MIR408	2242	15808	4828	12273	2436	23384	4377	4180	4322	7522	1791	8881	2657	21889	2475
MIR413	0	0	0	0	0	0	0	0	0	0	0	0	0	1	0
MIR414	4	6	7	1	3	9	3	4	5	4	9	8	1	11	5
MIR415	0	0	1	0	0	0	0	0	1	0	1	0	1	2	0
MIR416	14	17	21	8	13	21	10	10	17	24	6	4	4	3	15
MIR419	1	0	1	1	0	0	1	2	0	0	0	1	0	1	0
MIR4221	12	33	12	7	0	1	0	0	11	17	7	7	10	51	11
MIR4227	0	0	1	0	0	0	0	0	0	0	0	0	0	0	0
MIR4228	82	178	77	93	56	408	156	76	58	118	73	52	71	344	80
MIR4239	1	3	6	0	0	3	5	3	0	3	4	6	1	4	1
MIR4240	0	0	0	0	0	0	0	0	0	2	0	0	0	8	0
MIR4243	1	0	3	0	4	3	0	0	0	1	0	0	0	1	0
MIR4245	475	452	537	424	98	22	7	44	514	306	307	249	331	463	315
MIR426	3	6	0	2	2	0	0	1	1	1	0	0	4	0	1
MIR447a	488	666	890	649	27	83	15	45	510	354	504	440	442	1469	792
MIR447b	59	62	89	48	9	12	0	9	65	36	36	30	59	218	71
MIR447c	1	3	11	6	5	1	1	3	3	2	7	2	2	9	6
MIR472	221	517	637	539	53	186	64	47	257	261	333	415	199	779	351

MIR5012	37	85	136	89	2	2	1	0	80	58	72	71	75	248	151
MIR5013	2	0	5	0	1	1	6	1	3	1	5	4	0	0	0
MIR5014a	63	17	46	16	36	25	11	17	57	26	34	20	26	67	32
MIR5014b	254	73	222	76	204	85	26	61	313	78	151	86	197	70	132
MIR5015	1	1	3	1	1	0	0	0	3	3	5	8	1	10	4
MIR5016	2	0	1	1	1	0	0	0	0	1	0	1	1	7	1
MIR5017	1	0	5	1	0	1	0	0	1	0	1	1	1	7	1
MIR5018	0	2	2	0	1	1	0	0	0	0	0	2	4	1	1
MIR5019	0	5	1	1	0	0	0	1	0	4	2	1	1	11	0
MIR5020a	35	4	30	30	24	18	9	14	24	13	17	15	14	10	21
MIR5020b	106	13	37	22	14	28	10	10	43	16	27	18	238	11	174
MIR5020c	4	4	5	3	7	14	6	6	12	5	2	7	8	5	15
MIR5021	3	0	0	0	0	0	0	0	1	0	0	0	0	2	
MIR5023	1	3	2	7	1	1	1	0	0	0	4	1	1	5	5
MIR5024	45	93	113	90	20	50	11	9	52	46	57	46	258	895	425
MIR5025	0	0	0	0	0	0	0	0	0	0	0	1	1	0	0
MIR5026	4861	2392	6738	22173	9107	8700	1360	9490	4701	1214	2524	8311	24465	25334	22457
MIR5027	10	5	21	9	2	2	6	3	9	3	13	3	10	9	7
MIR5028	4	115	17	17	0	6	1	2	3	45	13	17	4	200	13
MIR5029	8	13	10	11	18	23	7	15	31	14	18	23	8	13	2
MIR5595a	171	290	231	202	46	37	4	40	141	116	85	110	100	413	127
MIR5628	5	3	25	7	5	5	2	2	8	2	13	6	18	22	41
MIR5629	26	99	46	83	21	207	15	34	25	46	23	55	181	1429	335
MIR5630a	8	5	5	5	5	2	1	4	4	5	4	1	5	5	4
MIR5630b	11	1	2	2	4	3	1	4	6	3	2	5	5	8	1

MIR5631	1	2	6	4	3	3	0	0	2	1	5	2	3	2	5
MIR5632	7	20	6	27	1	12	0	5	5	15	5	10	53	245	99
MIR5633	10	14	16	14	4	11	2	7	14	9	10	19	11	7	5
MIR5634	5	8	6	5	0	0	1	0	5	2	15	0	3	14	4
MIR5635a	592	492	697	308	562	626	304	401	799	535	765	493	265	498	390
MIR5635b	411	249	354	218	413	317	163	224	576	276	369	309	160	193	176
MIR5635c	203	164	237	141	234	212	148	162	309	172	290	201	77	148	128
MIR5635d	394	312	439	254	422	436	240	276	551	301	442	315	178	332	231
MIR5636	7	5	11	4	0	1	0	3	6	0	5	9	1	12	4
MIR5637	28	76	122	130	7	78	10	21	53	41	53	110	50	225	122
MIR5638a	13	12	38	14	20	20	16	8	21	15	20	15	9	24	39
MIR5638b	4	8	11	7	9	9	6	3	13	17	6	7	7	12	14
MIR5639	6	13	6	3	5	21	5	3	20	11	12	9	33	91	51
MIR5640	64	60	99	48	17	19	15	21	65	24	28	26	64	175	102
MIR5641	21	20	47	41	16	31	9	15	24	25	19	29	8	34	20
MIR5642a	3830	4683	4376	5711	3571	5929	4609	4923	4936	4291	3826	5505	3522	5893	3625
MIR5642b	961	1383	1467	2233	1011	2321	1545	1893	2039	1521	1413	2806	680	1891	933
MIR5643a	166	161	145	95	177	165	35	62	337	173	177	134	42	118	49
MIR5643b	153	74	93	47	143	124	35	47	246	86	110	81	32	46	30
MIR5644	696	237	481	267	600	164	168	196	612	151	303	189	120	71	101
MIR5645a	461	234	418	214	470	272	126	297	597	191	398	271	268	237	325
MIR5645b	405	189	318	164	442	240	104	223	546	165	332	196	152	131	155
MIR5645c	73	61	52	69	70	103	22	47	89	67	67	52	75	113	127
MIR5645d	243	136	191	113	266	187	102	138	322	109	198	133	111	98	130
MIR5645e	90	86	93	62	122	84	63	69	155	79	109	83	118	153	217

MIR5645f	315	188	301	164	301	238	95	196	415	176	315	231	168	155	175
MIR5646	2	0	0	2	1	4	1	0	1	4	2	2	0	0	0
MIR5647	35	99	59	64	32	170	21	36	46	76	47	56	36	219	55
MIR5648	4	2	5	1	0	2	0	0	5	4	2	2	5	20	16
MIR5649a	3	0	4	0	1	0	0	2	0	0	2	0	0	1	1
MIR5649b	2	1	3	0	2	0	0	2	2	0	0	0	0	2	1
MIR5650	127	41	149	90	6	5	0	2	66	16	39	35	439	238	501
MIR5651	91	97	200	94	43	79	11	30	136	71	98	93	42	100	63
MIR5652	300	166	735	420	53	15	16	55	273	108	362	354	30	40	115
MIR5653	1219	1143	1599	911	1423	2310	1908	1040	2066	1049	1559	1390	422	776	751
MIR5654	292	363	693	334	264	499	309	265	263	174	519	238	140	437	352
MIR5655	4	55	8	15	2	51	1	5	6	40	0	8	5	259	16
MIR5656	26	26	51	44	14	19	6	6	33	11	28	36	119	417	238
MIR5657	41	89	68	69	82	66	56	63	53	87	37	40	68	143	73
MIR5658	1	2	2	2	0	9	2	1	1	1	1	5	1	4	2
MIR5659	89	34	71	37	79	45	45	29	126	27	91	39	9	19	29
MIR5660	3	4	2	0	0	5	4	3	3	2	2	5	1	13	5
MIR5661	1	5	3	1	0	5	3	1	2	5	2	1	3	9	2
MIR5662	492	183	356	196	382	182	106	142	543	125	305	167	116	76	117
MIR5663	87	138	178	156	1	9	4	5	74	77	76	109	168	437	300
MIR5664	41	60	49	24	58	86	13	54	25	59	30	12	10	118	41
MIR5665	290	133	266	138	297	119	83	119	352	131	240	144	108	74	93
MIR5666	2	2	3	0	6	2	1	1	1	4	2	2	1	1	2
MIR5995b	55	54	32	31	35	28	2	28	36	28	20	22	24	72	30
MIR5996	623	320	491	879	221	313	41	242	561	212	325	686	6586	3953	7732

MIR5997	6	2	13	6	0	3	0	2	11	3	5	11	51	35	42
MIR5998a	0	4	1	0	0	0	0	0	0	2	1	1	0	2	0
MIR5998b	1	4	1	0	0	0	0	2	0	3	1	0	0	2	1
MIR5999	0	0	3	0	1	0	0	0	2	0	0	1	1	0	1
MIR771	4	2	97	14	0	0	0	0	17	9	42	5	12	10	23
MIR773a	230	203	1068	802	50	36	102	72	301	115	545	645	271	389	787
MIR773b	6	26	58	43	14	29	9	10	24	37	27	20	30	76	78
MIR774a	0	1	4	3	0	0	0	0	1	1	1	1	1	6	1
MIR775	495	1190	1528	771	49	67	30	16	637	668	858	480	410	2115	765
MIR776	1	0	1	2	3	5	1	1	2	2	5	1	0	2	0
MIR777	0	0	1	2	1	2	0	0	0	0	0	0	0	1	2
MIR778	1	13	7	32	0	19	0	2	1	19	3	22	3	59	16
MIR779	205	730	577	349	12	16	6	10	328	388	316	311	187	1064	339
MIR780	6	6	12	3	1	1	0	1	9	2	13	3	4	8	9
MIR781a	92	155	152	212	3	7	0	1	73	109	77	179	129	441	200
MIR781b	75	160	146	167	2	11	1	4	73	110	76	134	119	426	172
MIR782	0	0	0	0	0	2	0	0	1	1	0	0	0	0	0
MIR8121	66	99	91	60	102	134	46	82	99	79	129	77	20	63	44
MIR8165	72	39	100	39	91	49	85	58	124	28	119	53	35	12	34
MIR8166	202	146	224	112	154	242	100	97	194	128	214	154	55	74	81
MIR8167a	115	60	118	64	79	76	86	60	140	52	98	80	32	28	42
MIR8167b	115	62	113	65	77	85	80	62	139	46	103	75	29	25	53
MIR8167c	108	61	114	72	78	79	81	65	140	55	93	73	36	33	49
MIR8167d	112	56	116	74	83	77	90	60	144	47	87	80	29	26	44
MIR8167e	116	66	119	76	90	71	83	61	138	44	97	88	36	31	48

MIR8167f	119	64	118	63	77	70	82	58	139	48	91	81	30	35	59
MIR8168	34	52	54	22	30	36	13	33	56	19	18	36	8	35	13
MIR8169	278	101	153	76	161	122	48	81	268	140	154	72	46	42	25
MIR8170	24	12	37	22	4	1	2	3	19	4	10	11	35	20	19
MIR8171	138	99	106	93	137	148	105	53	136	110	128	66	28	56	65
MIR8172	383	221	372	198	344	281	84	219	516	228	374	279	109	111	128
MIR8173	128	255	131	96	122	310	80	84	138	147	89	53	5	28	9
MIR8174	112	48	75	31	62	30	24	15	87	35	44	21	25	12	25
MIR8175	173	133	211	217	119	330	228	187	120	147	127	230	125	203	115
MIR8176	41	63	44	81	49	87	116	65	31	48	46	90	17	47	60
MIR8177	99	42	89	31	108	51	37	39	160	33	86	42	30	21	44
MIR8178	97	68	62	67	73	59	10	37	59	45	27	42	2374	4309	1582
MIR8179	7	8	14	12	0	5	0	1	4	6	3	10	43	137	83
MIR8180	285	303	311	179	395	397	227	263	517	318	396	378	148	185	156
MIR8181	0	6	1	3	1	2	3	0	0	1	1	5	2	1	4
MIR8182	6	6	14	10	0	0	0	0	5	3	2	10	1	6	6
MIR8183	18	37	42	20	12	16	8	9	11	12	7	3	12	39	12
MIR8184	0	4	1	4	1	0	0	0	0	3	0	0	1	9	1
MIR822	714	612	1582	1822	2145	1139	890	2352	860	348	934	1537	397	602	490
MIR823	160	331	376	507	30	100	12	49	161	155	209	325	79	492	177
MIR824	303	1122	1093	916	36	94	25	19	283	629	737	922	145	1045	565
MIR825	125	109	176	92	11	9	8	6	129	46	86	61	68	159	109
MIR826a	7	8	6	32	0	1	0	0	5	3	3	3	1	41	4
MIR826b	0	0	0	1	0	0	0	0	0	3	0	0	0	2	0
MIR827	318	929	738	1338	157	1292	46	403	410	704	305	1065	295	1298	323

MIR828	1	9	1	4	2	0	0	0	2	10	4	16	0	3	0
MIR829	168	1001	309	337	27	81	10	26	242	653	195	293	178	1669	289
MIR830	8	6	6	6	3	7	1	1	2	2	1	4	9	6	1
MIR831	43	20	74	337	17	23	3	30	38	8	29	54	23	65	32
MIR832	0	0	0	0	0	0	0	0	0	1	0	0	0	2	0
MIR833a	76	96	205	216	45	63	27	52	59	28	150	160	262	449	745
MIR833b	18	16	41	51	15	15	2	6	25	7	18	32	63	156	132
MIR834	0	1	2	1	0	0	0	0	3	0	0	0	0	4	0
MIR835	86	200	225	301	85	189	51	263	97	111	118	174	197	822	380
MIR836	70	41	67	32	3	5	1	0	42	6	22	11	41	43	46
MIR837	69	109	223	131	11	27	5	13	103	93	142	180	723	2305	2421
MIR838	22	64	60	43	2	9	3	4	23	41	41	40	18	110	32
MIR839	25	24	37	30	31	35	38	69	18	19	31	32	35	128	78
MIR840	117	408	450	570	491	2660	737	1675	163	220	230	343	19	152	44
MIR841a	243	192	330	500	131	257	52	164	264	87	155	377	1312	2319	1838
MIR841b	238	107	202	214	90	118	43	60	177	103	112	183	888	1193	1032
MIR842	12	24	39	39	15	29	16	12	11	12	30	24	4	28	18
MIR843	70	33	113	59	61	25	28	24	118	31	45	41	98	89	95
MIR844	31	39	63	44	10	10	5	4	16	21	37	22	9	56	27
MIR845a	559	333	774	1638	583	190	162	336	412	144	304	364	820	1885	508
MIR845b	15	48	16	42	7	5	5	19	2	17	4	20	10	121	3
MIR846	1717	2750	4303	2159	504	395	81	209	2007	1685	2376	2078	821	3511	2299
MIR847	18	154	66	13	2	7	3	1	41	42	37	18	24	257	49
MIR848	407	370	358	385	29	56	4	9	265	164	171	185	225	367	194

MIR849	16	20	18	28	15	10	4	7	15	17	15	17	14	55	15
MIR850	314	156	521	1142	671	422	928	732	402	78	277	606	321	647	399
MIR851	2	2	61	0	0	3	5	1	23	4	24	2	15	8	48
MIR852	42	70	57	173	3	23	2	8	27	33	29	99	140	323	265
MIR853	39	90	72	37	1	1	0	2	48	48	21	23	25	147	29
MIR854a	13	16	19	45	23	18	12	50	71	31	43	102	15	12	19
MIR854b	16	17	24	49	31	18	6	43	89	31	45	97	15	30	12
MIR854c	20	12	19	43	19	13	6	39	63	21	36	97	13	20	10
MIR854d	16	22	15	41	35	13	7	38	89	35	39	111	13	18	7
MIR854e	14	20	25	51	25	16	10	48	86	29	42	110	18	22	11
MIR855	52	39	63	46	85	57	20	28	105	50	56	59	33	29	23
MIR856	3	1	2	3	1	3	0	0	4	4	1	0	2	1	2
MIR857	11	161	4	107	27	135	0	42	18	100	6	121	12	257	7
MIR858a	79	389	301	146	101	224	34	73	82	274	162	194	46	376	181
MIR858b	4	44	27	13	7	43	2	12	7	23	10	13	3	51	15
MIR859	5	57	17	34	0	4	0	1	8	35	10	26	2	80	15
MIR860	11	20	22	28	5	10	4	5	19	6	7	11	94	309	181
MIR861	67	50	103	57	32	79	53	35	45	19	42	28	34	83	56
MIR862	25	13	51	27	9	9	5	0	25	8	27	23	187	406	208
MIR863	5829	1569	5875	12391	698	326	60	678	4425	710	2356	5764	13158	11890	15795
MIR864	2	48	5	4	0	7	0	1	7	26	2	3	3	80	3
MIR865	197	309	315	73	232	298	46	78	189	191	125	84	76	410	135
MIR866	102	558	335	920	117	517	57	575	105	350	130	319	112	2150	158
MIR868	0	2	8	7	0	0	1	0	2	3	3	5	1	8	2
MIR869	398	68	247	87	4	6	4	3	216	7	80	8	445	91	344

MIR870	14	15	21	6	36	31	5	16	12	11	7	11	10	15	11
Library size	30635847	26189325	30060261	28816378	25029006	26815937	26700561	27130057	25439093	23104941	25889615	27181829			
Total # reads	463778	604592	1101705	750255	130824	236083	105033	100664	497031	312417	526700	558189			
% of Library	1.5	2.3	3.7	2.6	0.5	0.9	0.4	0.4	2.0	1.4	2.0	2.1			

A.6.3 Developmental and Reproductive Phenotype of Col-0 Plants, and miR396 and miR399 Altered Plants

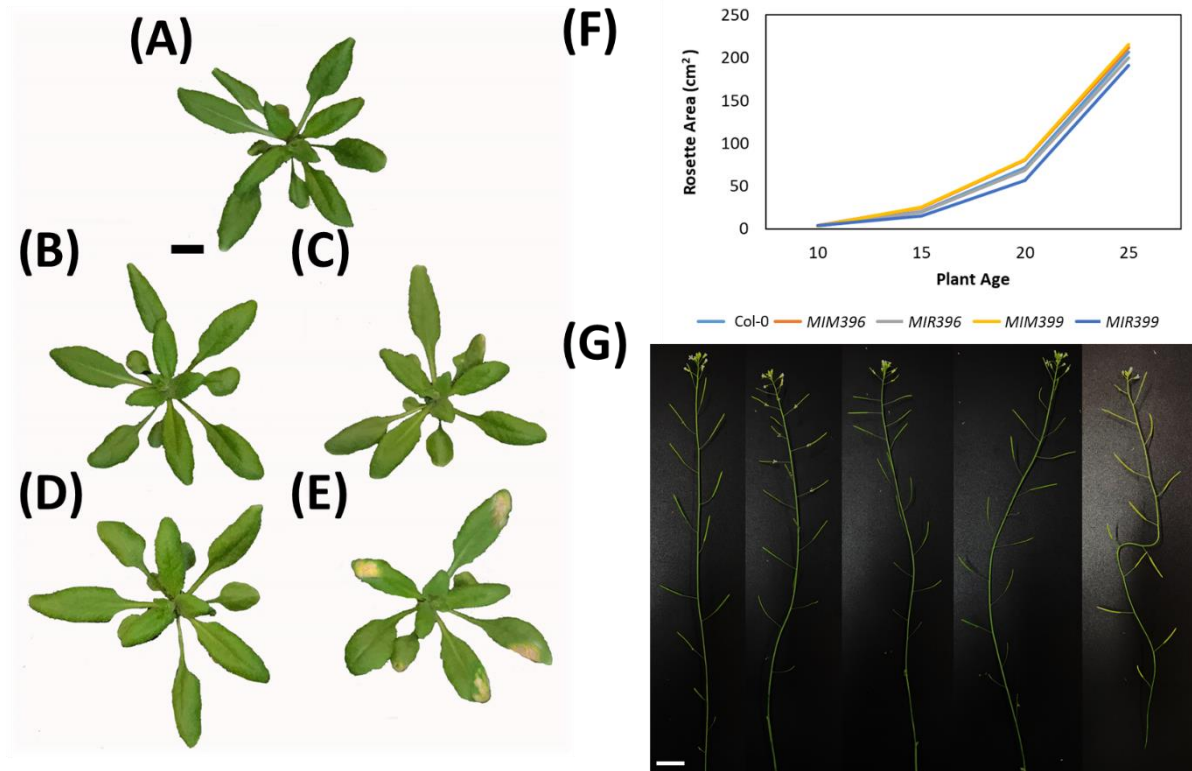


Figure A.6.2 Developmental and reproductive phenotype of Col-0 plants, and miR396 and miR399 altered plants. The representative phenotype of (A) Col-0 (B) *MIM396* (C) *MIR396* (D) *MIM399* and (E) *MIR399*, at 25 d of age (prior to plant bolting), with the scale bar indicative of 1 cm. (F) The average rosette area of each plant line at 10, 15, 20 and 25 d of age is shown. (G) The representative phenotype of the main inflorescence stem is presented for Col-0, *MIM396*, *MIR396*, *MIM399* and *MIR399* (left to right) at 40 d of age, with the scale bar indicative of 2 cm.

References

- Abdel-Ghany, S. E., and Pilon, M.** (2008). MicroRNA-mediated systemic down-regulation of copper protein expression in response to low copper availability in *Arabidopsis*. *J Biol Chem.* **283**(23), 15932-15945.
- Achard, P., Herr, A., Baulcombe, D. C., and Harberd, N. P.** (2004). Modulation of floral development by a gibberellin-regulated microRNA. *Development*, **131**(14), 3357-3365.
- Ahmadi, J., Noormohammadi, N., and Ourang, S. F.** (2014). Identification of Conserved Domains and Motifs for GRF Gene Family. *World Academy of Science, Engineering and Technology, International Journal of Biological, Biomolecular, Agricultural, Food and Biotechnological Engineering*, **8**(12), 1323-1326.
- Akula, R., and Ravishankar, G. A.** (2011). Influence of abiotic stress signals on secondary metabolites in plants. *Plant signaling and behavior*, **6**(11), 1720-1731.
- Aroca, R., Porcel, R., and Ruiz-Lozano, J. M.** (2011). Regulation of root water uptake under abiotic stress conditions. *Journal of experimental botany*, **63**(1), 43-57.
- Ashraf, M. F. M. R., and Foolad, M.** (2007). Roles of glycine betaine and proline in improving plant abiotic stress resistance. *Environmental and experimental botany*, **59**(2), 206-216.
- Aung, K., Lin, S. I., Wu, C. C., Huang, Y. T., Su, C. L., and Chiou, T. J.** (2006). *pho2*, a phosphate overaccumulator, is caused by a nonsense mutation in a microRNA399 target gene. *Plant physiology*, **141**(3), 1000-1011.
- Axtell, M. J., and Meyers, B. C.** (2018). Revisiting criteria for plant microRNA annotation in the era of big data. *The Plant Cell*, **30**(2), 272-284.
- Bao, M., Bian, H., Zha, Y., Li, F., Sun, Y., Bai, B., and Han, N.** (2014). miR396a-mediated basic helix-loop-helix transcription factor bHLH74 repression acts as a regulator for root growth in *Arabidopsis* seedlings. *Plant and Cell Physiology*, **55**(7), 1343-1353.
- Barciszewska-Pacak, M., Milanowska, K., Knop, K., Bielewicz, D., Nuc, P., Plewka, P., Pacak AM., Vazquez F., Karlowski W., Jarmolowski A., and Szweykowska-Kulinska, Z.** (2015). *Arabidopsis* microRNA expression regulation in a wide range of abiotic stress responses. *Frontiers in plant science*, **6**, 410.
- Bari, R., Pant, B. D., Stitt, M., and Scheible, W. R.** (2006). PHO2, microRNA399, and PHR1 define a phosphate-signaling pathway in plants. *Plant physiology*, **141**(3), 988-999.

- Beltramino, M., Ercoli, M. F., Debernardi, J. M., Goldy, C., Rojas, A. M., Nota, F., Alvarez, M.E., Vercruyssen, L., Inzé, D., Palatnik, J.F., and Rodriguez, R. E.** (2018). Robust increase of leaf size by *Arabidopsis thaliana* GRF3-like transcription factors under different growth conditions. *Scientific reports*, **8**(1), 1-13.
- Bennett, E. M., Carpenter, S. R., and Caraco, N. F.** (2001). Human impact on erodable phosphorus and eutrophication: a global perspective: increasing accumulation of phosphorus in soil threatens rivers, lakes, and coastal oceans with eutrophication. *BioScience*, **51**(3), 227-234.
- Berry, J., and Bjorkman, O.** (1980). Photosynthetic response and adaptation to temperature in higher plants. *Annual Review of plant physiology*, **31**(1), 491-543.
- Björn, L. O., Papageorgiou, G. C., and Blankenship, R. E.** (2009). A viewpoint: why chlorophyll *a*? *Photosynthesis research*, **99**(2), 85-98.
- Boudet, A. M.** (2000). Lignins and lignification: selected issues. *Plant Physiology and Biochemistry*, **38**(1-2), 81-96.
- Casati, P.** (2013). Analysis of UV-B regulated miRNAs and their targets in maize leaves. *Plant signaling & behavior*, **8**(10), e26758.
- Chalker-Scott, L.** (1999). Environmental significance of anthocyanins in plant stress responses. *Photochemistry and photobiology*, **70**(1), 1-9.
- Che, R., Tong, H., Shi, B., Liu, Y., Fang, S., Liu, D., and Zhao, M.** (2015). Control of grain size and rice yield by GL2-mediated brassinosteroid responses. *Nature plants*, **2**, 15195.
- Chiou, T. J., Aung, K., Lin, S. I., Wu, C. C., Chiang, S. F., and Su, C. L.** (2006). Regulation of phosphate homeostasis by microRNA in *Arabidopsis*. *The Plant Cell*, **18**(2), 412-421.
- Choi, M., and Davidson, V. L.** (2011). Cupredoxins—a study of how proteins may evolve to use metals for bioenergetic processes. *Metallomics*, **3**(2), 140-151.
- Choi, W. G., Toyota, M., Kim, S. H., Hilleary, R., and Gilroy, S.** (2014). Salt stress-induced Ca²⁺ waves are associated with rapid, long-distance root-to-shoot signaling in plants. *Proceedings of the National Academy of Sciences*, **111**(17), 6497-6502.
- Christidis, N., Stott, P. A., and Brown, S. J.** (2011). The role of human activity in the recent warming of extremely warm daytime temperatures. *Journal of Climate*, **24**(7), 1922-1930.

- Chung, P. J., Park, B. S., Wang, H., Liu, J., Jang, I. C., and Chua, N. H.** (2016). Light-inducible miR163 targets PXMT1 transcripts to promote seed germination and primary root elongation in *Arabidopsis*. *Plant physiology*, **170**(3), 1772-1782.
- Claeys, H., Van Landeghem, S., Dubois, M., Maleux, K., and Inzé, D.** (2014). What is stress? Dose-response effects in commonly used in vitro stress assays. *Plant physiology*, pp-113.
- Cohu, C. M., and Pilon, M.** (2010). Cell biology of copper. In *Cell biology of metals and nutrients* (pp. 55-74). Springer, Berlin, Heidelberg.
- Cordell, D., Drangert, J. O., and White, S.** (2009). The story of phosphorus: global food security and food for thought. *Global environmental change*, **19**(2), 292-305.
- Curtin, S. J., Watson, J. M., Smith, N. A., Eamens, A. L., Blanchard, C. L., and Waterhouse, P. M.** (2008). The roles of plant dsRNA-binding proteins in RNAi-like pathways. *FEBS letters*, **582**(18), 2753-2760.
- Dai, Z., Tan, J., Zhou, C., Yang, X., Yang, F., Zhang, S., Sun, S., Miao, X., and Shi, Z.** (2019). The OsmiR396–Os GRF 8–OsF3H-flavonoid pathway mediates resistance to the brown planthopper in rice (*Oryza sativa*). *Plant biotechnology journal*, **17**(8), 1657-1669.
- Dennison, C.** (2005). Investigating the structure and function of cupredoxins. *Coordination Chemistry Reviews*, **249**(24), 3025-3054.
- Denver, J. B., and Ullah, H.** (2019). miR393s regulate salt stress response pathway in *Arabidopsis thaliana* through scaffold protein RACK1A mediated ABA signaling pathways. *Plant signaling & behavior*, **14**(6), 1600394.
- Ding, Y. F., and Zhu, C.** (2009). The role of microRNAs in copper and cadmium homeostasis. *Biochemical and biophysical research communications*, **386**(1), 6-10.
- Donat, M. G., Alexander, L. V., Yang, H., Durre, I., Vose, R., Dunn, R. J. H., and Hewitson, B.** (2013). Updated analyses of temperature and precipitation extreme indices since the beginning of the twentieth century: The HadEX2 dataset. *Journal of Geophysical Research: Atmospheres*, **118**(5), 2098-2118.
- Dong, Z., Han, M. H., and Fedoroff, N.** (2008). The RNA-binding proteins HYL1 and SE promote accurate in vitro processing of pri-miRNA by DCL1. *Proceedings of the National Academy of Sciences*, **105**(29), 9970-9975.
- Dong, J., Kim, S. T., and Lord, E. M.** (2005). Plantacyanin plays a role in reproduction in *Arabidopsis*. *Plant Physiol.* **138**, 778-789.

- Du, Q., Wang, K., Zou, C., Xu, C., and Li, W. X.** (2018). The PILNCR1-miR399 regulatory module is important for low phosphate tolerance in maize. *Plant physiology*, **177**(4), 1743-1753.
- Duan, L., Dietrich, D., Ng, C. H., Chan, P. M. Y., Bhalerao, R., Bennett, M. J., and Dinneny, J. R.** (2013). Endodermal ABA signaling promotes lateral root quiescence during salt stress in *Arabidopsis* seedlings. *The Plant Cell*, **25**(1), 324-341.
- Eamens, A. L., Curtin, S. J., and Waterhouse, P. M.** (2011). The *Arabidopsis thaliana* double-stranded RNA binding (DRB) domain protein family. In *Non Coding RNAs in Plants* (pp. 385-406). Springer Berlin Heidelberg.
- Eamens, A. L., Kim, K. W., Curtin, S. J., and Waterhouse, P. M.** (2012a). DRB2 is required for microRNA biogenesis in *Arabidopsis thaliana*. *PLoS one*, **7**(4), e35933.
- Eamens, A. L., Smith, N. A., Curtin, S. J., Wang, M. B., and Waterhouse, P. M.** (2009). The *Arabidopsis thaliana* double-stranded RNA binding protein DRB1 directs guide strand selection from microRNA duplexes. *RNA*, **15**(12), 2219-2235.
- Eamens, A. L., Wook Kim, K., and Waterhouse, P. M.** (2012b). DRB2, DRB3 and DRB5 function in a non-canonical microRNA pathway in *Arabidopsis thaliana*. *Plant signaling and behavior*, **7**(10), 1224-1229.
- Elser, J., and Bennett, E.** (2011). Phosphorus cycle: a broken biogeochemical cycle. *Nature*, **478**(7367), 29.
- Felippes, F. F., and Weigel, D.** (2009). Triggering the formation of tasiRNAs in *Arabidopsis thaliana*: the role of microRNA miR173. *EMBO reports*, **10**(3), 264-270.
- Feng, Z. T., Deng, Y. Q., Fan, H., Sun, Q. J., Sui, N., and Wang, B. S.** (2014). Effects of NaCl stress on the growth and photosynthetic characteristics of *Ulmus pumila* L. seedlings in sand culture. *Photosynthetica*, **52**(2), 313-320.
- Fischer, E. M., and Knutti, R.** (2015). Anthropogenic contribution to global occurrence of heavy-precipitation and high-temperature extremes. *Nature Climate Change*, **5**(6), 560.
- Franco-Zorrilla, J. M., Valli, A., Todesco, M., Mateos, I., Puga, M. I., Rubio-Somoza, I., Leyva, A., Weigel, D., García, J.A., and Paz-Ares, J.** (2007). Target mimicry provides a new mechanism for regulation of microRNA activity. *Nature genetics*, **39**(8), 1033.
- Fujii, H., Chiou, T. J., Lin, S. I., Aung, K., and Zhu, J. K.** (2005). A miRNA involved in phosphate-starvation response in *Arabidopsis*. *Current Biology*, **15**(22), 2038-2043.

- Fukudome, A., Kanaya, A., Egami, M., Nakazawa, Y., Hiraguri, A., Moriyama, H., and Fukuhara, T.** (2011). Specific requirement of DRB4, a dsRNA-binding protein, for the in vitro dsRNA-cleaving activity of Arabidopsis Dicer-like 4. *RNA*, **17**(4), 750-760.
- Gamborg, O. L., Murashige, T., Thorpe, T. A., and Vasil, I. K.** (1976). Plant tissue culture media. *In Vitro Cellular & Developmental Biology-Plant*, **12**(7), 473-478.
- Gao, J. P., Chao, D. Y., and Lin, H. X.** (2007). Understanding abiotic stress tolerance mechanisms: recent studies on stress response in rice. *Journal of Integrative Plant Biology*, **49**(6), 742-750.
- Gao, F., Wang, K., Liu, Y., Chen, Y., Chen, P., Shi, Z., and Li, S.** (2015). Blocking miR396 increases rice yield by shaping inflorescence architecture. *Nature plants*, **2**, 15196.
- Gascioli, V., Mallory, A. C., Bartel, D. P., and Vaucheret, H.** (2005). Partially redundant functions of Arabidopsis DICER-like enzymes and a role for DCL4 in producing trans-acting siRNAs. *Current Biology*, **15**(16), 1494-1500.
- Gleave, A. P.** (1992). A versatile binary vector system with a T-DNA organisational structure conducive to efficient integration of cloned DNA into the plant genome. *Plant molecular biology*, **20**(6), 1203-1207.
- Gou, J. Y., Felippes, F. F., Liu, C. J., Weigel, D., and Wang, J. W.** (2011). Negative regulation of anthocyanin biosynthesis in Arabidopsis by a miR156-targeted SPL transcription factor. *The Plant Cell*, **23**(4), 1512-1522.
- Gray, W. M., Östin, A., Sandberg, G., Romano, C. P., and Estelle, M.** (1998). High temperature promotes auxin-mediated hypocotyl elongation in Arabidopsis. *Proceedings of the National Academy of Sciences*, **95**(12), 7197-7202.
- Guan, Q., Lu, X., Zeng, H., Zhang, Y., and Zhu, J.** (2013). Heat stress induction of miR398 triggers a regulatory loop that is critical for thermotolerance in Arabidopsis. *The Plant Journal*, **74**(5), 840-851.
- Guo, H. S., Xie, Q., Fei, J. F., and Chua, N. H.** (2005). MicroRNA directs mRNA cleavage of the transcription factor NAC1 to downregulate auxin signals for Arabidopsis lateral root development. *The Plant Cell*, **17**(5), 1376-1386.
- Hackenberg, M., Shi, B. J., Gustafson, P., and Langridge, P.** (2013). Characterization of phosphorus-regulated miR399 and miR827 and their isomirs in barley under phosphorus-sufficient and phosphorus-deficient conditions. *BMC plant biology*, **13**(1), 214.
- Hajyzadeh, M., Turktas, M., Khawar, K. M., and Unver, T.** (2015). miR408 overexpression causes increased drought tolerance in chickpea. *Gene*, **555**(2), 186-193.

- Hamburger, D., Rezzonico, E., Petétot, J. M. C., Somerville, C., and Poirier, Y.** (2002). Identification and characterization of the *Arabidopsis* PHO1 gene involved in phosphate loading to the xylem. *The Plant Cell*, **14**(4), 889-902.
- Hamza, N. B., Sharma, N., Tripathi, A., and Sanan-Mishra, N.** (2016). MicroRNA expression profiles in response to drought stress in *Sorghum bicolor*. *Gene Expression Patterns*, **20**(2), 88-98.
- Hanahan, D.** (1983) Studies on transformation of *Escherichia coli* with plasmids. *J. Mol. Biol.* 166, 157.
- Hasanuzzaman, M., Nahar, K., Alam, M., Roychowdhury, R., and Fujita, M.** (2013). Physiological, biochemical, and molecular mechanisms of heat stress tolerance in plants. *International journal of molecular sciences*, **14**(5), 9643-9684.
- He, Y., Wu, J., Lv, B., Li, J., Gao, Z., Xu, W., Baluška, F., Shi, W., Shaw, P.C., and Zhang, J.** (2015). Involvement of 14-3-3 protein GRF9 in root growth and response under polyethylene glycol-induced water stress. *Journal of experimental botany*, **66**(8), 2271-2281.
- Hewezi, T., and Baum, T. J.** (2012). Complex feedback regulations govern the expression of miRNA396 and its GRF target genes. *Plant signaling & behavior*, **7**(7), 749-751.
- Hiraguri, A., Itoh, R., Kondo, N., Nomura, Y., Aizawa, D., Murai, Y., and Fukuhara, T.** (2005). Specific interactions between Dicer-like proteins and HYL1/DRB-family dsRNA-binding proteins in *Arabidopsis thaliana*. *Plant molecular biology*, **57**(2), 173-188.
- Horiguchi, G., Kim, G. T., and Tsukaya, H.** (2005). The transcription factor AtGRF5 and the transcription coactivator AN3 regulate cell proliferation in leaf primordia of *Arabidopsis thaliana*. *The Plant Journal*, **43**(1), 68-78.
- Howitz, K. T., and Sinclair, D. A.** (2008). Xenohormesis: sensing the chemical cues of other species. *Cell*, **133**(3), 387-391.
- Hsieh, L. C., Lin, S. I., Shih, A. C. C., Chen, J. W., Lin, W. Y., Tseng, C. Y., Li, W.H., and Chiou, T. J.** (2009). Uncovering small RNA-mediated responses to phosphate deficiency in *Arabidopsis* by deep sequencing. *Plant physiology*, **151**(4), 2120-2132.
- Hu, B., Wang, W., Deng, K., Li, H., Zhang, Z., Zhang, L., and Chu, C.** (2015). MicroRNA399 is involved in multiple nutrient starvation responses in rice. *Frontiers in plant science*, **6**, 188.
- Huang, J., Xu, C. C., Ridoutt, B. G., Wang, X. C., and Ren, P. A.** (2017). Nitrogen and phosphorus losses and eutrophication potential associated with fertilizer application to cropland in China. *Journal of Cleaner Production*, **159**, 171-179.

- Huang, T. K., Han, C. L., Lin, S. I., Chen, Y. J., Tsai, Y. C., Chen, Y. R., Chen, J.W., Lin, W.Y., Chen, P.M., Liu, T.Y., and Chen, Y. S. (2013). Identification of downstream components of ubiquitin-conjugating enzyme PHOSPHATE2 by quantitative membrane proteomics in *Arabidopsis* roots. *The Plant Cell*, **25**(10), 4044-4060.
- Intergovernmental Panel on Climate Change (2018). Special Report on Global Warming of 1.5 °C. <https://www.ipcc.ch/sr15/>
- Jian, H., Wang, J., Wang, T., Wei, L., Li, J., and Liu, L. (2016). Identification of rapeseed microRNAs involved in early stage seed germination under salt and drought stresses. *Frontiers in plant science*, **7**, 658.
- Jiang, C., Gao, X., Liao, L., Harberd, N. P., and Fu, X. (2007). Phosphate starvation root architecture and anthocyanin accumulation responses are modulated by the gibberellin-DELLA signaling pathway in *Arabidopsis*. *Plant physiology*, **145**(4), 1460-1470.
- Jones-Rhoades, M. W., and Bartel, D. P. (2004). Computational identification of plant microRNAs and their targets, including a stress-induced miRNA. *Molecular cell*, **14**(6), 787-799.
- Jovanović, Ž., Stanisavljević, N., Mikić, A., Radović, S., and Maksimović, V. (2014). Water deficit down-regulates miR398 and miR408 in pea (*Pisum sativum* L.). *Plant physiology and biochemistry*, **83**, 26-31.
- June, T., Evans, J. R., and Farquhar, G. D. (2004). A simple new equation for the reversible temperature dependence of photosynthetic electron transport: a study on soybean leaf. *Functional Plant Biology*, **31**(3), 275-283.
- Kantar, M., Lucas, S. J., and Budak, H. (2011). miRNA expression patterns of *Triticum dicoccoides* in response to shock drought stress. *Planta*, **233**(3), 471-484.
- Kearse, M., Moir, R., Wilson, A., Stones-Havas, S., Cheung, M., Sturrock, S., Buxton S., Cooper A., Markowitz S., Duran C., and Thierer, T. (2012). Geneious Basic: an integrated and extendable desktop software platform for the organization and analysis of sequence data. *Bioinformatics*, **28**(12), 1647-1649.
- Khraiweh, B., Zhu, J. K., and Zhu, J. (2012). Role of miRNAs and siRNAs in biotic and abiotic stress responses of plants. *Biochimica et Biophysica Acta (BBA)-Gene Regulatory Mechanisms*, **1819**(2), 137-148.
- Kim, J. H., Choi, D., and Kende, H. (2003). The AtGRF family of putative transcription factors is involved in leaf and cotyledon growth in *Arabidopsis*. *The Plant Journal*, **36**(1), 94-104.

- Kim, J. H., and Kende, H.** (2004). A transcriptional coactivator, AtGIF1, is involved in regulating leaf growth and morphology in *Arabidopsis*. *Proceedings of the National Academy of Sciences of the United States of America*, **101**(36), 13374-13379.
- Kim, J. S., Mizoi, J., Kidokoro, S., Maruyama, K., Nakajima, J., Nakashima, K., and Yoshizumi, T.** (2012). *Arabidopsis* GROWTH-REGULATING FACTOR7 functions as a transcriptional repressor of abscisic acid–and osmotic stress–responsive genes, including DREB2A. *The Plant Cell*, **24**(8), 3393-3405.
- Kim, J. Y., Kwak, K. J., Jung, H. J., Lee, H. J., and Kang, H.** (2010a). MicroRNA402 affects seed germination of *Arabidopsis thaliana* under stress conditions via targeting DEMETER- LIKE Protein3 mRNA. *Plant and cell physiology*, **51**(6), 1079-1083.
- Kim, J. Y., Lee, H. J., Jung, H. J., Maruyama, K., Suzuki, N., and Kang, H.** (2010b). Overexpression of microRNA395c or 395e affects differently the seed germination of *Arabidopsis thaliana* under stress conditions. *Planta*, **232**(6), 1447-1454.
- Kim, V. N., Han, J., and Siomi, M. C.** (2009). Biogenesis of small RNAs in animals. *Nature reviews Molecular cell biology*, **10**(2), 126.
- Kim, W., Ahn, H. J., Chiou, T. J., and Ahn, J. H.** (2011). The role of the miR399-PHO2 module in the regulation of flowering time in response to different ambient temperatures in *Arabidopsis thaliana*. *Molecules and cells*, **32**(1), 83-88.
- Kinoshita, N., Wang, H., Kasahara, H., Liu, J., MacPherson, C., Machida, Y., and Chua, N. H.** (2012). IAA-Ala Resistant3, an evolutionarily conserved target of miR167, mediates *Arabidopsis* root architecture changes during high osmotic stress. *The Plant Cell*, **24**(9), 3590-3602.
- Kohli, A., Sreenivasulu, N., Lakshmanan, P., and Kumar, P. P.** (2013). The phytohormone crosstalk paradigm takes center stage in understanding how plants respond to abiotic stresses. *Plant cell reports*, **32**(7), 945-957.
- Koini, M. A., Alvey, L., Allen, T., Tilley, C. A., Harberd, N. P., Whitelam, G. C., and Franklin, K. A.** (2009). High temperature-mediated adaptations in plant architecture require the bHLH transcription factor PIF4. *Current Biology*, **19**(5), 408-413.
- Kovinich, N., Kayanja, G., Chanoca, A., Otegui, M. S., and Grotewold, E.** (2015). Abiotic stresses induce different localizations of anthocyanins in *Arabidopsis*. *Plant signaling & behavior*, **10**(7), e1027850.
- Kruszka, K., Pacak, A., Swida-Barteczka, A., Nuc, P., Alaba, S., Wroblewska, Z., Karlowski, W., Jarmolowski, A., and Szweykowska-Kulinska, Z.** (2014). Transcriptionally and post-transcriptionally regulated microRNAs in heat stress response in barley. *Journal of experimental botany*, **65**(20), 6123-6135.

- Laufs, P., Peaucelle, A., Morin, H., and Traas, J.** (2004). MicroRNA regulation of the CUC genes is required for boundary size control in *Arabidopsis* meristems. *Development*, **131**(17), 4311-4322.
- Lazo, G. R., Stein, P. A., and Ludwig, R. A.** (1991). A DNA transformation-competent *Arabidopsis* genomic library in *Agrobacterium*. *Biotechnology*, **9**(10), 963.
- Li, S., Fu, Q., Huang, W., and Yu, D.** (2009). Functional analysis of an *Arabidopsis* transcription factor WRKY25 in heat stress. *Plant cell reports*, **28**(4), 683-693.
- Li, S., Liu, L., Zhuang, X., Yu, Y., Liu, X., Cui, X., Ji, L., Pan, Z., Cao, X., Mo, B., and Zhang, F.** (2013). MicroRNAs inhibit the translation of target mRNAs on the endoplasmic reticulum in *Arabidopsis*. *Cell*, **153**(3), 562-574.
- Liang, G., He, H., Li, Y., Wang, F., and Yu, D.** (2014). Molecular mechanism of microRNA396 mediating pistil development in *Arabidopsis*. *Plant physiology*, **164**(1), 249-258.
- Lichtenthaler, H. K., and Wellburn, A. R.** (1983). Determinations of total carotenoids and chlorophylls *a* and *b* of leaf extracts in different solvents. *Biochemical Society Transactions*. **11**, 591-592.
- Lin, S. I., Chiang, S. F., Lin, W. Y., Chen, J. W., Tseng, C. Y., Wu, P. C., and Chiou, T. J.** (2008). Regulatory network of microRNA399 and PHO2 by systemic signaling. *Plant physiology*, **147**(2), 732-746.
- Lin, J. S., Kuo, C. C., Yang, I. C., Tsai, W. A., Shen, Y. H., Lin, C. C., and Lai, H. M.** (2018). MicroRNA160 modulates plant development and heat shock protein gene expression to mediate heat tolerance in *Arabidopsis*. *Frontiers in plant science*, **9**, 68.
- Liu, D., Song, Y., Chen, Z., and Yu, D.** (2009). Ectopic expression of miR396 suppresses GRF target gene expression and alters leaf growth in *Arabidopsis*. *Physiologia plantarum*, **136**(2), 223-236.
- Liu, D., and Yu, D.** (2009). MicroRNA (miR396) negatively regulates expression of ceramidase-like genes in *Arabidopsis*. *Progress in Natural Science*, **19**(6), 781-785
- Liu, H. H., Tian, X., Li, Y. J., Wu, C. A., and Zheng, C. C.** (2008). Microarray-based analysis of stress-regulated microRNAs in *Arabidopsis thaliana*. *RNA*, **14**(5), 836-843.
- Liu, T. Y., Lin, W. Y., Huang, T. K., and Chiou, T. J.** (2014). MicroRNA-mediated surveillance of phosphate transporters on the move. *Trends in plant science*, **19**(10), 647-655.

- Liu, Q., Kasuga, M., Sakuma, Y., Abe, H., Miura, S., Yamaguchi-Shinozaki, K., and Shinozaki, K.** (1998). Two transcription factors, DREB1 and DREB2, with an EREBP/AP2 DNA binding domain separate two cellular signal transduction pathways in drought- and low-temperature-responsive gene expression, respectively, in *Arabidopsis*. *The Plant Cell*, **10**(8), 1391-1406.
- Luo, Q. J., Mittal, A., Jia, F., and Rock, C. D.** (2012). An autoregulatory feedback loop involving PAP1 and TAS4 in response to sugars in *Arabidopsis*. *Plant molecular biology*, **80**(1), 117-129.
- Ma, C., Burd, S., and Lers, A.** (2015). miR408 is involved in abiotic stress responses in *Arabidopsis*. *The Plant Journal*, **84**(1), 169-187.
- Mallory, A. C., Bartel, D. P., and Bartel, B.** (2005). MicroRNA-directed regulation of *Arabidopsis* AUXIN RESPONSE FACTOR17 is essential for proper development and modulates expression of early auxin response genes. *The Plant Cell*, **17**(5), 1360-1375.
- Mallory, A. C., Dugas, D. V., Bartel, D. P., and Bartel, B.** (2004a). MicroRNA regulation of NAC-domain targets is required for proper formation and separation of adjacent embryonic, vegetative, and floral organs. *Current Biology*, **14**(12), 1035-1046.
- Mallory, A. C., Reinhart, B. J., Jones-Rhoades, M. W., Tang, G., Zamore, P. D., Barton, M. K., and Bartel, D. P.** (2004b). MicroRNA control of PHABULOSA in leaf development: importance of pairing to the microRNA 5' region. *The EMBO journal*, **23**(16), 3356-3364.
- Manetas, Y.** (2006). Why some leaves are anthocyanic and why most anthocyanic leaves are red? *Flora-Morphology, Distribution, Functional Ecology of Plants*, **201**(3), 163-177.
- Marko, D., Puppel, N., Tjaden, Z., Jakobs, S., and Pahlke, G.** (2004). The substitution pattern of anthocyanidins affects different cellular signaling cascades regulating cell proliferation. *Molecular nutrition & food research*, **48**(4), 318-325.
- Marschner, H.** (2011). Marschner's mineral nutrition of higher plants. *Academic press*.
- Masliyah, G., Barraud, P., and Allain, F. H. T.** (2013). RNA recognition by double-stranded RNA binding domains: a matter of shape and sequence. *Cellular and Molecular Life Sciences*, **70**(11), 1875-1895.
- Meloni, D. A., Oliva, M. A., Martinez, C. A., and Cambraia, J.** (2003). Photosynthesis and activity of superoxide dismutase, peroxidase and glutathione reductase in cotton under salt stress. *Environmental and Experimental Botany*, **49**(1), 69-76.

- Millar, A. A., and Gubler, F.** (2005). The *Arabidopsis* GAMYB-like genes, MYB33 and MYB65, are microRNA-regulated genes that redundantly facilitate anther development. *The Plant Cell*, **17**(3), 705-721.
- Min, S. K., Zhang, X., Zwiers, F. W., and Hegerl, G. C.** (2011). Human contribution to more-intense precipitation extremes. *Nature*, **470**(7334), 378.
- Mittal, D., Madhyastha, D. A., and Grover, A.** (2012). Genome-wide transcriptional profiles during temperature and oxidative stress reveal coordinated expression patterns and overlapping regulons in rice. *PLoS one*, **7**(7), e40899.
- Montgomery, T. A., Howell, M. D., Cuperus, J. T., Li, D., Hansen, J. E., Alexander, A. L., Chapman, E.J., Fahlgren, N., Allen, E., and Carrington, J. C.** (2008). Specificity of ARGONAUTE7-miR390 interaction and dual functionality in TAS3 trans-acting siRNA formation. *Cell*, **133**(1), 128-141.
- Moura, J. C. M. S., Bonine, C. A. V., de Oliveira Fernandes Viana, J., Dornelas, M. C., and Mazzafera, P.** (2010). Abiotic and biotic stresses and changes in the lignin content and composition in plants. *Journal of integrative plant biology*, **52**(4), 360-376.
- Munns, R.** (2002). Comparative physiology of salt and water stress. *Plant, cell & environment*, **25**(2), 239-250.
- Mutum, R. D., Balyan, S. C., Kansal, S., Agarwal, P., Kumar, S., Kumar, M., and Raghuvanshi, S.** (2013). Evolution of variety-specific regulatory schema for expression of osa-miR408 in indica rice varieties under drought stress. *The FEBS journal*, **280**(7), 1717-1730.
- Nakazawa, Y., Hiraguri, A., Moriyama, H., and Fukuhara, T.** (2007). The dsRNA-binding protein DRB4 interacts with the Dicer-like protein DCL4 in vivo and functions in the trans-acting siRNA pathway. *Plant molecular biology*, **63**(6), 777-785.
- Omidbakhshfard, M. A., Fujikura, U., Olas, J. J., Xue, G. P., Balazadeh, S., and Mueller-Roeber, B.** (2018). GROWTH-REGULATING FACTOR 9 negatively regulates *Arabidopsis* leaf growth by controlling ORG3 and restricting cell proliferation in leaf primordia. *PLoS genetics*, **14**(7), e1007484.
- Omidbakhshfard, M. A., Proost, S., Fujikura, U., and Mueller-Roeber, B.** (2015). Growth-regulating factors (GRFs): a small transcription factor family with important functions in plant biology. *Molecular plant*, **8**(7), 998-1010.
- Ouyang, X., Hong, X., Zhao, X., Zhang, W., He, X., Ma, W., Teng, W., and Tong, Y.** (2016). Knock out of the PHOSPHATE 2 gene TaPHO2-A1 improves phosphorus uptake and grain yield under low phosphorus conditions in common wheat. *Scientific reports*, **6**, 29850.

- Pajoro, A., Madrigal, P., Muiño, J. M., Matus, J. T., Jin, J., Mecchia, M. A., and Ó'Maoiléidigh, D. S.** (2014). Dynamics of chromatin accessibility and gene regulation by MADS-domain transcription factors in flower development. *Genome biology*, **15**(3), 1.
- Palatnik, J. F., Allen, E., Wu, X., Schommer, C., Schwab, R., Carrington, J. C., and Weigel, D.** (2003). Control of leaf morphogenesis by microRNAs. *Nature*, **425**(6955), 257.
- Pandey, N., Ranjan, A., Pant, P., Tripathi, R. K., Ateek, F., Pandey, H. P., and Sawant, S. V.** (2013). CAMTA 1 regulates drought responses in *Arabidopsis thaliana*. *BMC genomics*, **14**(1), 216.
- Pasternak, T., Rudas, V., Potters, G., and Jansen, M. A.** (2005). Morphogenic effects of abiotic stress: reorientation of growth in *Arabidopsis thaliana* seedlings. *Environmental and Experimental Botany*, **53**(3), 299-314.
- Peleg, Z., and Blumwald, E.** (2011). Hormone balance and abiotic stress tolerance in crop plants. *Current opinion in plant biology*, **14**(3), 290-295.
- Pélissier, T., Clavel, M., Chaparro, C., Pouch-Pélissier, M. N., Vaucheret, H., and Deragon, J. M.** (2011). Double-stranded RNA binding proteins DRB2 and DRB4 have an antagonistic impact on polymerase IV-dependent siRNA levels in *Arabidopsis*. *RNA*, **17**(8), 1502-1510.
- Perkins, S. E., Alexander, L. V., and Nairn, J. R.** (2012). Increasing frequency, intensity and duration of observed global heatwaves and warm spells. *Geophysical Research Letters*, **39**(20).
- Pilon, M.** (2017). The copper microRNAs. *New Phytologist*, **213**(3), 1030-1035.
- Piya, S., Liu, J., Burch-Smith, T., Baum, T. J., and Hewezi, T.** (2020). A role for *Arabidopsis* growth-regulating factors 1 and 3 in growth–stress antagonism. *Journal of experimental botany*, **71**(4), 1402-1417.
- Poirier, Y., and Bucher, M.** (2002). Phosphate transport and homeostasis in *Arabidopsis*. *The Arabidopsis book/American Society of Plant Biologists*, **1**.
- Poirier, Y., Thoma, S., Somerville, C., and Schiefelbein, J.** (1991). Mutant of *Arabidopsis* deficient in xylem loading of phosphate. *Plant physiology*, **97**(3), 1087-1093.

- Pouch-Pélissier, M. N., Pélissier, T., Elmayan, T., Vaucheret, H., Boko, D., Jantsch, M. F., and Deragon, J. M.** (2008). SINE RNA induces severe developmental defects in *Arabidopsis thaliana* and interacts with HYL1 (DRB1), a key member of the DCL1 complex. *PLoS genetics*, **4**(6), e1000096.
- Qi, X., Wu, Z., Li, J., Mo, X., Wu, S., Chu, J., and Wu, P.** (2007). AtCYT-INV1, a neutral invertase, is involved in osmotic stress-induced inhibition on lateral root growth in *Arabidopsis*. *Plant molecular biology*, **64**(5), 575-587.
- Qin, L. X., Li, Y., Li, D. D., Xu, W. L., Zheng, Y., and Li, X. B.** (2014). *Arabidopsis* drought-induced protein Di19-3 participates in plant response to drought and high salinity stresses. *Plant molecular biology*, **86**(6), 609-625.
- Raghothama, K. G.** (1999). Phosphate acquisition. *Annual review of plant biology*, **50**(1), 665-693.
- Raghothama, K. G.** (2000). Phosphate transport and signaling. *Current opinion in plant biology*, **3**(3), 182-187.
- Rahmstorf, S., and Coumou, D.** (2011). Increase of extreme events in a warming world. *Proceedings of the National Academy of Sciences*, **108**(44), 17905-17909.
- Rajagopalan, R., Vaucheret, H., Trejo, J., and Bartel, D. P.** (2006). A diverse and evolutionarily fluid set of microRNAs in *Arabidopsis thaliana*. *Genes & development*, **20**(24), 3407-3425.
- Raventós, D., Skriver, K., Schlein, M., Karnahl, K., Rogers, S. W., Rogers, J. C., and Mundy, J.** (1998). HRT, a novel zinc finger, transcriptional repressor from barley. *Journal of Biological Chemistry*, **273**(36), 23313-23320.
- Ray, D. K., Mueller, N. D., West, P. C., and Foley, J. A.** (2013). Yield trends are insufficient to double global crop production by 2050. *PloS one*, **8**(6), e66428.
- Reinhart, B. J., Weinstein, E. G., Rhoades, M. W., Bartel, B., and Bartel, D. P.** (2002). MicroRNAs in plants. *Genes & development*, **16**(13), 1616-1626.
- Reis, R. S., Hart-Smith, G., Eamens, A. L., Wilkins, M. R., and Waterhouse, P. M.** (2015). Gene regulation by translational inhibition is determined by Dicer partnering proteins. *Nature Plants*, **1**(3).
- Ren, L., and Tang, G.** (2012). Identification of sucrose-responsive microRNAs reveals sucrose-regulated copper accumulations in an SPL7-dependent and independent manner in *Arabidopsis thaliana*. *Plant Sci.* **187**, 59-68.

- Rizhsky, L., Liang, H., Shuman, J., Shulaev, V., Davletova, S., and Mittler, R.** (2004). When defense pathways collide. The response of *Arabidopsis* to a combination of drought and heat stress. *Plant physiology*, **134**(4), 1683-1696.
- Rouached, H., Arpat, A. B., and Poirier, Y.** (2010). Regulation of phosphate starvation responses in plants: signaling players and cross-talks. *Molecular Plant*, **3**(2), 288-299.
- Rubio, V., Linhares, F., Solano, R., Martín, A. C., Iglesias, J., Leyva, A., and Paz-Ares, J.** (2001). A conserved MYB transcription factor involved in phosphate starvation signaling both in vascular plants and in unicellular algae. *Genes & development*, **15**(16), 2122-2133.
- Sage, R. F., and Kubien, D. S.** (2007). The temperature response of C₃ and C₄ photosynthesis. *Plant, cell & environment*, **30**(9), 1086-1106.
- Sakuma, Y., Maruyama, K., Qin, F., Osakabe, Y., Shinozaki, K., and Yamaguchi-Shinozaki, K.** (2006). Dual function of an *Arabidopsis* transcription factor DREB2A in water-stress-responsive and heat-stress-responsive gene expression. *Proceedings of the National Academy of Sciences*, **103**(49), 18822-18827.
- Schachtman, D. P., Reid, R. J., and Ayling, S. M.** (1998). Phosphorus uptake by plants: from soil to cell. *Plant physiology*, **116**(2), 447-453
- Schwab, R., Palatnik, J. F., Riester, M., Schommer, C., Schmid, M., and Weigel, D.** (2005). Specific effects of microRNAs on the plant transcriptome. *Developmental cell*, **8**(4), 517-527.
- Semenov, M. A., and Shewry, P. R.** (2011). Modelling predicts that heat stress, not drought, will increase vulnerability of wheat in Europe. *Scientific reports*, **1**, 66.
- Seo, P. J., Xiang, F., Qiao, M., Park, J. Y., Lee, Y. N., Kim, S. G., and Park, C. M.** (2009). The MYB96 transcription factor mediates abscisic acid signaling during drought stress response in *Arabidopsis*. *Plant Physiology*, **151**(1), 275-289
- Shen, J., Xie, K., and Xiong, L.** (2010). Global expression profiling of rice microRNAs by one-tube stem-loop reverse transcription quantitative PCR revealed important roles of microRNAs in abiotic stress responses. *Molecular Genetics and Genomics*, **284**(6), 477-488.
- Shukla, D., Rinehart, C. A., and Sahi, S. V.** (2017). Comprehensive study of excess phosphate response reveals ethylene mediated signaling that negatively regulates plant growth and development. *Scientific reports*, **7**(1), 1-16.

- Smil, V.** (2000). Phosphorus in the environment: natural flows and human interferences. *Annual review of energy and the environment*, **25**(1), 53-88.
- Solfanelli, C., Poggi, A., Loreti, E., Alpi, A., and Perata, P.** (2006). Sucrose-specific induction of the anthocyanin biosynthetic pathway in *Arabidopsis*. *Plant physiology*, **140**(2), 637-646.
- Song, J. B., Gao, S., Sun, D., Li, H., Shu, X. X., and Yang, Z. M.** (2013). miR394 and LCR are involved in *Arabidopsis* salt and drought stress responses in an abscisic acid-dependent manner. *BMC plant biology*, **13**(1), 210.
- Song, Z., Zhang, L., Wang, Y., Li, H., Li, S., Zhao, H., and Zhang, H.** (2018). Constitutive expression of miR408 improves biomass and seed yield in *Arabidopsis*. *Frontiers in plant science*, **8**, 2114.
- Sperdouli, I., and Moustakas, M.** (2012). Interaction of proline, sugars, and anthocyanins during photosynthetic acclimation of *Arabidopsis thaliana* to drought stress. *Journal of plant physiology*, **169**(6), 577-585.
- Strizhov, N., Ábrahám, E., Ökrész, L., Blickling, S., Zilberstein, A., Schell, J., and Szabados, L.** (1997). Differential expression of two P5CS genes controlling proline accumulation during salt-stress requires ABA and is regulated by ABA1, ABI1 and AXR2 in *Arabidopsis*. *The Plant Journal*, **12**(3), 557-569.
- Sudhir, P., and Murthy, S. D. S.** (2004). Effects of salt stress on basic processes of photosynthesis. *Photosynthetica*, **42**(2), 481-486.
- Sun, F., Zhang, W., Hu, H., Li, B., Wang, Y., Zhao, Y., and Li, X.** (2008). Salt modulates gravity signaling pathway to regulate growth direction of primary roots in *Arabidopsis*. *Plant physiology*, **146**(1), 178-188.
- Sunkar, R., Kapoor, A., and Zhu, J. K.** (2006). Posttranscriptional induction of two Cu/Zn superoxide dismutase genes in *Arabidopsis* is mediated by downregulation of miR398 and important for oxidative stress tolerance. *The Plant Cell*, **18**(8), 2051-2065.
- Sunkar, R., Li, Y. F., and Jagadeeswaran, G.** (2012). Functions of microRNAs in plant stress responses. *Trends in plant science*, **17**(4), 196-203.
- Sunkar, R., and Zhu, J. K.** (2004). Novel and stress-regulated microRNAs and other small RNAs from *Arabidopsis*. *The Plant Cell*, **16**(8), 2001-2019.
- Syers, J. K., Johnston, A. E., and Curtin, D.** (2008). Efficiency of soil and fertilizer phosphorus use. *FAO Fertilizer and plant nutrition bulletin*, **18**(108).

- Szabados, L., and Savoure, A.** (2010). Proline: a multifunctional amino acid. *Trends in plant science*, **15**(2), 89-97.
- Székely, G., Ábrahám, E., Cséplő, Á., Rigó, G., Zsigmond, L., Csiszár, J., and Koncz, C.** (2008). Duplicated P5CS genes of *Arabidopsis* play distinct roles in stress regulation and developmental control of proline biosynthesis. *The Plant Journal*, **53**(1), 11-28.
- Teixeira, E. I., Fischer, G., van Velthuisen, H., Walter, C., and Ewert, F.** (2013). Global hot-spots of heat stress on agricultural crops due to climate change. *Agricultural and Forest Meteorology*, **170**, 206-215.
- Tester, M., and Davenport, R.** (2003). Na⁺ tolerance and Na⁺ transport in higher plants. *Annals of botany*, **91**(5), 503-527.
- Thatcher, S. R., Burd, S., Wright, C., Lers, A., and Green, P. J.** (2015). Differential expression of miRNAs and their target genes in senescing leaves and siliques: insights from deep sequencing of small RNAs and cleaved target RNAs. *Plant, cell & environment*, **38**(1), 188-200.
- Treich, I., Cairns, B. R., De Los Santos, T., Brewster, E., and Carlson, M.** (1995). SNF11, a new component of the yeast SNF-SWI complex that interacts with a conserved region of SNF2. *Molecular and Cellular Biology*, **15**(8), 4240-4248.
- Turlapati, P. V., Kim, K. W., Davin, L. B., and Lewis, N. G.** (2011). The laccase multigene family in *Arabidopsis thaliana*: towards addressing the mystery of their gene function(s). *Planta*, **233**(3), 439-470.
- Urano, K., Maruyama, K., Ogata, Y., Morishita, Y., Takeda, M., Sakurai, N., and Yamaguchi-Shinozaki, K.** (2009). Characterization of the ABA-regulated global responses to dehydration in *Arabidopsis* by metabolomics. *The Plant Journal*, **57**(6), 1065-1078.
- Valenzuela, C. E., Acevedo-Acevedo, O., Miranda, G. S., Vergara-Barros, P., Holuigue, L., Figueroa, C. R., and Figueroa, P. M.** (2016). Salt stress response triggers activation of the jasmonate signaling pathway leading to inhibition of cell elongation in *Arabidopsis* primary root. *Journal of experimental botany*, **67**(14), 4209-4220.
- Vance, C. P., Uhde-Stone, C., and Allan, D. L.** (2003). Phosphorus acquisition and use: critical adaptations by plants for securing a nonrenewable resource. *New phytologist*, **157**(3), 423-447.
- Van der Knaap, E., Kim, J. H., and Kende, H.** (2000). A novel gibberellin-induced gene from rice and its potential regulatory role in stem growth. *Plant physiology*, **122**(3), 695-704.

- Vasseur, F., Pantin, F., and Vile, D.** (2011). Changes in light intensity reveal a major role for carbon balance in *Arabidopsis* responses to high temperature. *Plant, Cell & Environment*, **34**(9), 1563-1576.
- Vazquez, F., Gasciolli, V., Crété, P., and Vaucheret, H.** (2004). The nuclear dsRNA binding protein HYL1 is required for microRNA accumulation and plant development, but not posttranscriptional transgene silencing. *Current Biology*, **14**(4), 346-351.
- Veneklaas, E. J., Lambers, H., Bragg, J., Finnegan, P. M., Lovelock, C. E., Plaxton, W. C., Price, C.A., Scheible, W.R., Shane, M.W., White, P.J., and Raven, J. A.** (2012). Opportunities for improving phosphorus-use efficiency in crop plants. *New Phytologist*, **195**(2), 306-320.
- Vidal, E. A., Araus, V., Lu, C., Parry, G., Green, P. J., Coruzzi, G. M., and Gutiérrez, R. A.** (2010). Nitrate-responsive miR393/AFB3 regulatory module controls root system architecture in *Arabidopsis thaliana*. *Proceedings of the National Academy of Sciences*, **107**(9), 4477-4482.
- Wahid, A., Gelani, S., Ashraf, M., and Foolad, M. R.** (2007). Heat tolerance in plants: an overview. *Environmental and experimental botany*, **61**(3), 199-223.
- Wang, F., Deng, M., Xu, J., Zhu, X., and Mao, C.** (2018). Molecular mechanisms of phosphate transport and signaling in higher plants. In *Seminars in cell & developmental biology* (Vol. 74, pp. 114-122). Academic Press.
- Wang, H., Cao, G., and Prior, R. L.** (1997). Oxygen radical absorbing capacity of anthocyanins. *Journal of agricultural and Food Chemistry*, **45**(2), 304-309.
- Wang, J. W., Wang, L. J., Mao, Y. B., Cai, W. J., Xue, H. W., and Chen, X. Y.** (2005). Control of root cap formation by microRNA-targeted auxin response factors in *Arabidopsis*. *The Plant Cell*, **17**(8), 2204-2216.
- Wang, L., Gu, X., Xu, D., Wang, W., Wang, H., Zeng, M., and Cui, X.** (2010). miR396-targeted AtGRF transcription factors are required for coordination of cell division and differentiation during leaf development in *Arabidopsis*. *Journal of experimental botany*, **62**(2), 761-773.
- Wang, T., Chen, L., Zhao, M., Tian, Q., and Zhang, W. H.** (2011). Identification of drought-responsive microRNAs in *Medicago truncatula* by genome-wide high-throughput sequencing. *BMC genomics*, **12**(1), 367.
- Wang, Y., Li, K., and Li, X.** (2009). Auxin redistribution modulates plastic development of root system architecture under salt stress in *Arabidopsis thaliana*. *Journal of plant physiology*, **166**(15), 1637-1645.

- West, G., Inzé, D., and Beemster, G. T.** (2004). Cell cycle modulation in the response of the primary root of *Arabidopsis* to salt stress. *Plant physiology*, **135**(2), 1050-1058.
- Wintz, H., Fox, T., Wu, Y. Y., Feng, V., Chen, W., Chang, H. S., and Vulpe, C.** (2003). Expression profiles of *Arabidopsis thaliana* in mineral deficiencies reveal novel transporters involved in metal homeostasis. *Journal of Biological Chemistry*, **278**(48), 47644-47653.
- Wu, H. C., and Jinn, T. L.** (2012). Oscillation regulation of Ca²⁺/calmodulin and heat-stress related genes in response to heat stress in rice (*Oryza sativa* L.). *Plant signaling & behavior*, **7**(9), 1056-1057.
- Wu, M. F., Tian, Q., and Reed, J. W.** (2006). *Arabidopsis* microRNA167 controls patterns of ARF6 and ARF8 expression, and regulates both female and male reproduction. *Development*, **133**(21), 4211-4218.
- Xie, Z., Allen, E., Wilken, A., and Carrington, J. C.** (2005). DICER-LIKE 4 functions in transacting small interfering RNA biogenesis and vegetative phase change in *Arabidopsis thaliana*. *Proceedings of the National Academy of Sciences of the United States of America*, **102**(36), 12984-12989.
- Xie, Z., Kasschau, K. D., and Carrington, J. C.** (2003). Negative feedback regulation of Dicer- Like1 in *Arabidopsis* by microRNA-guided mRNA degradation. *Current Biology*, **13**(9), 784-789.
- Xin, M., Wang, Y., Yao, Y., Xie, C., Peng, H., Ni, Z., and Sun, Q.** (2010). Diverse set of microRNAs are responsive to powdery mildew infection and heat stress in wheat (*Triticum aestivum* L.). *BMC plant biology*, **10**(1), 123.
- Xinbin Dai, Zhaohong Zhuang and Patrick X. Zhao** (2018). psRNATarget: a plant small RNA target analysis server (2017 release). *Nucleic Acids Research*.
- Yamaguchi, K., Takahashi, Y., Berberich, T., Imai, A., Miyazaki, A., Takahashi, T., Michael, A., and Kusano, T.** (2006). The polyamine spermine protects against high salt stress in *Arabidopsis thaliana*. *FEBS letters*, **580**(30), 6783-6788.
- Yamaguchi-Shinozaki, K., and Shinozaki, K.** (2006). Transcriptional regulatory networks in cellular responses and tolerance to dehydration and cold stresses. *Annu. Rev. Plant Biol.*, **57**, 781-803.
- Yamasaki, H., Hayashi, M., Fukazawa, M., Kobayashi, Y., and Shikanai, T.** (2009). SQUAMOSA promoter binding protein-like7 is a central regulator for copper homeostasis in *Arabidopsis*. *Plant Cell*. **21**, 347-361.

- Yoshiba, Y., Nanjo, T., Miura, S., Yamaguchi-Shinozaki, K., and Shinozaki, K.** (1999). Stress-responsive and developmental regulation of Δ 1-pyrroline-5-carboxylate synthetase 1 (P5CS1) gene expression in *Arabidopsis thaliana*. *Biochemical and biophysical research communications*, **261**(3), 766-772.
- Yu, S. M., Lo, S. F., and Ho, T. H. D.** (2015). Source–sink communication: regulated by hormone, nutrient, and stress cross-signaling. *Trends in plant science*, **20**(12), 844-857.
- Zawoznik, M. S., Groppa, M. D., Tomaro, M. L., and Benavides, M. P.** (2007). Endogenous salicylic acid potentiates cadmium-induced oxidative stress in *Arabidopsis thaliana*. *Plant Science*, **173**(2), 190-197.
- Zhang, H., Zhao, X., Li, J., Cai, H., Deng, X. W., and Li, L.** (2014). MicroRNA408 is critical for the *HY5-SPL7* gene network that mediates the coordinated response to light and copper. *The Plant Cell*. **26**(12), 4933-4953.
- Zhang, D. F., Li, B., Jia, G. Q., Zhang, T. F., Dai, J. R., Li, J. S., and Wang, S. C.** (2008). Isolation and characterization of genes encoding GRF transcription factors and GIF transcriptional coactivators in Maize (*Zea mays L.*). *Plant science*, **175**(6), 809-817.
- Zhao, C., Liu, B., Piao, S., Wang, X., Lobell, D. B., Huang, Y., and Durand, J. L.** (2017). Temperature increase reduces global yields of major crops in four independent estimates. *Proceedings of the National Academy of Sciences*, **114**(35), 9326-9331.
- Zhou, L., Liu, Y., Liu, Z., Kong, D., Duan, M., and Luo, L.** (2010). Genome-wide identification and analysis of drought-responsive microRNAs in *Oryza sativa*. *Journal of Experimental botany*, **61**(15), 4157-4168.
- Zhu, J., Park, J. H., Lee, S., Lee, J. H., Hwang, D., Kwak, J. M., and Kim, Y. J.** (2020). Regulation of stomatal development by stomatal lineage miRNAs. *Proceedings of the National Academy of Sciences*, **117**(11), 6237-6245.